CR 137648

SALES NO.
23267-6001-RU-00

SATURN URANUS ATMOSPHERIC ENTRY PROBE MISSION SPACECRAFT SYSTEM DEFINITION STUDY

FINAL REPORT

JULY 15, 1973

Prepared under Contract No. NAS2-7297

By

TRW Systems Group
Redondo Beach, California

For

AMES RESEARCH CENTER
National Aeronautics and Space Administration

TRW
SYSTEMS GROUP

SALES NO.
23267-6001-RU-00

SATURN URANUS ATMOSPHERIC ENTRY PROBE MISSION SPACECRAFT SYSTEM DEFINITION STUDY

FINAL REPORT

JULY 15, 1973

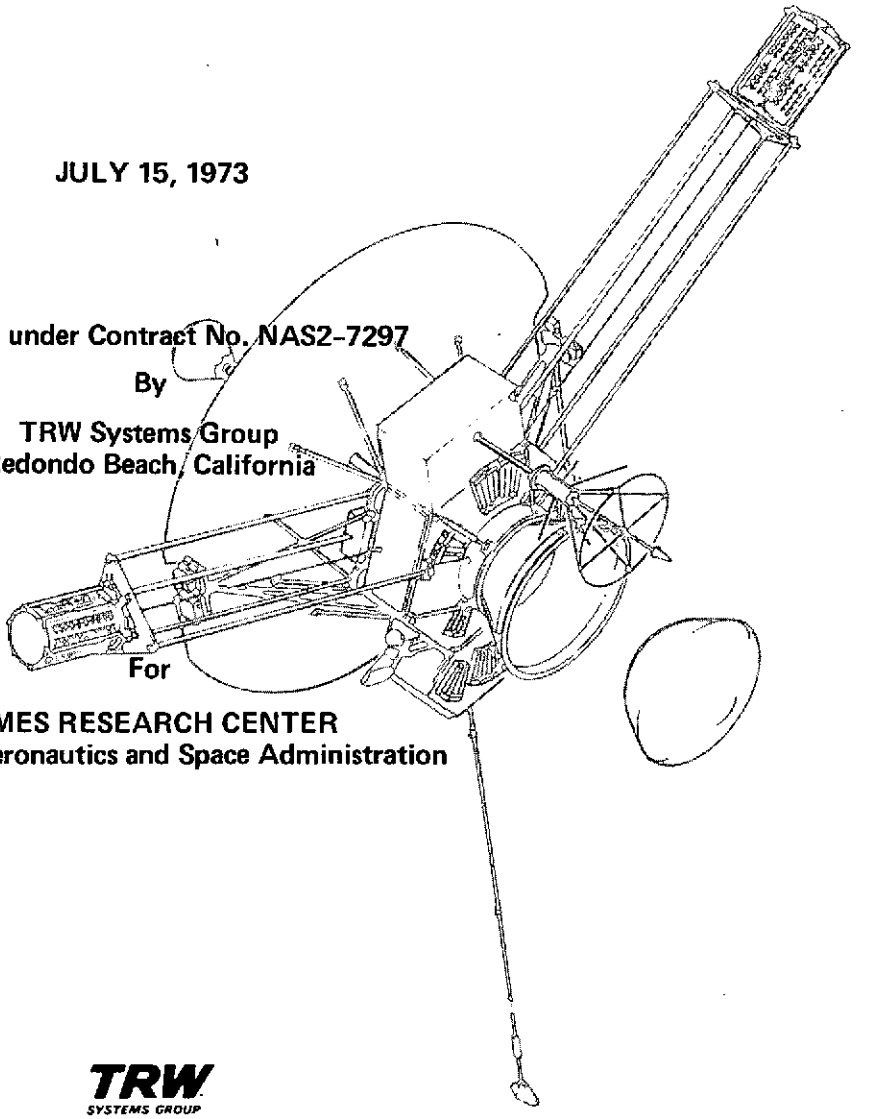

Prepared under Contract No. NAS2-7297

By

TRW Systems Group
Redondo Beach, California

For

AMES RESEARCH CENTER
National Aeronautics and Space Administration

TRW
SYSTEMS GROUP

CONTENTS

CONTENTS (Continued)

CONTENTS (Continued)

CONTENTS (Continued)

CONTENTS (Continued)

CONTENTS (Continued)

CONTENTS (Continued)

ILLUSTRATIONS

ILLUSTRATIONS (Continued)

ILLUSTRATIONS (Continued)

ILLUSTRATIONS (Continued)

ILLUSTRATIONS (Continued)

TABLES

TABLES (CONTINUED)

TABLES (CONTINUED)

TABLES (CONTINUED)

NOMENCLATURE

1. ABBREVIATIONS

AC	Alternating current
ACS	Attitude control subsystem
AGC	Automatic gain control
ARC	Ames Research Center
AU	Astronomical unit
BOL	Beginning of life
CDU	Command distribution unit
CEA	Control electronics assembly
c. g.	Center of gravity
c. m.	Center of mass
CSP	Conscan signal processor
CTRF	Central transformer rectifier filter
DC	Direct current
DDU	Digital decoder unit
DHS	Data handling subsystem
DSA	Despin sensor assembly
DSL	Duration and steering logic
DSN	Deep Space Network
DSS	Deep Space Station
DSU	Data storage unit
DTU	Digital telemetry unit
EGSE	Electrical ground support equipment
EJU	Earth-Jupiter-Uranus
EMC	Electromagnetic compatibility
EOL	End of life
EPS	Electrical power subsystem
ESU	Earth-Saturn-Uranus
ETG	Electrically-heated thermoelectric generator
FOV	Field of view
FSA	Fueled Sphere Assembly

GFE	Government furnished equipment
GHE	Ground handling equipment
GSE	Ground support equipment
HPG	High-power generator
IR	Infrared
JPL	Jet Propulsion Laboratory
LHA	Line heater assembly
MGSE	Mechanical ground support equipment
MHW	Multihundred watt
MU	Memory unit
NRZ	Non return to zero
PAD	Plutonium aerodynamic disc
PCM	Pulse code modulated
PCU	Power control unit
PFG	Pioneer F/G
PLL	Phase lock loop
PMC	Plutonia molybdenum cermet
PMT	Photomultiplier tube
PSA	Propellant supply assembly
PSE	Program storage and execution
R_S	Radius of Saturn (equatorial), 59,800 km
R_U	Radius of Uranus (equatorial), 27,000 km
RCP	Right hand circularly polarized
RF	Radio frequency
RHU	Radioisotope heater unit
RTG	Radioisotope thermoelectric generator
SCT	Spin control thruster
SPC	Sensor and power control
SPSG	Spin period sector generator
SRA	Stellar reference assembly
SSA	Sun sensor assembly

STG Star telemetry gate

SUAE Saturn Uranus atmospheric entry

TCA Thruster cluster assembly

TCXO Temperature controlled crystal oscillator

TGS Terminal guidance sensor

TWT Traveling wave tube

TWTA Traveling wave tube amplifier

UV Ultraviolet

VCO Voltage controlled oscillator

VPT Velocity precession thruster

VRT Velocity radial thruster.

2. MISSION AND STUDY

The Saturn Uranus Atmospheric Entry Probe Mission has been abbreviated SUAE mission. (The P for Probe has been omitted to avoid confusion between "probe" as the title of the mission, and "probe" as an element of the flight vehicle.) This study, the Spacecraft System Definition Study for the SUAE mission is referred to as the SUAE spacecraft study. The parallel study, the Probe System Definition Study, is referred to as the SUAE probe study.

3. ORGANIZATION OF THE FLIGHT VEHICLE

The flight vehicle is the term designating everything that leaves the launch pad. The physical organization and names of its elements are indicated in the chart on the next page.

4. PREVIOUS PIONEERS

Letters (e.g., Pioneer A, Pioneer A-E, Pioneer F/G) refer to a spacecraft program, a spacecraft design, or to a specific spacecraft before it is launched. Numbers (e.g., Pioneer 6, Pioneers 10 and 11) are assigned only after a successful launch, and refer to specific spacecraft after launch. Pioneers F and G have become Pioneers 10 and 11, respectively, after their successful launches in March, 1972, and April, 1973.

Elements of the Saturn Uranus Atmospheric Entry Flight Vehicle

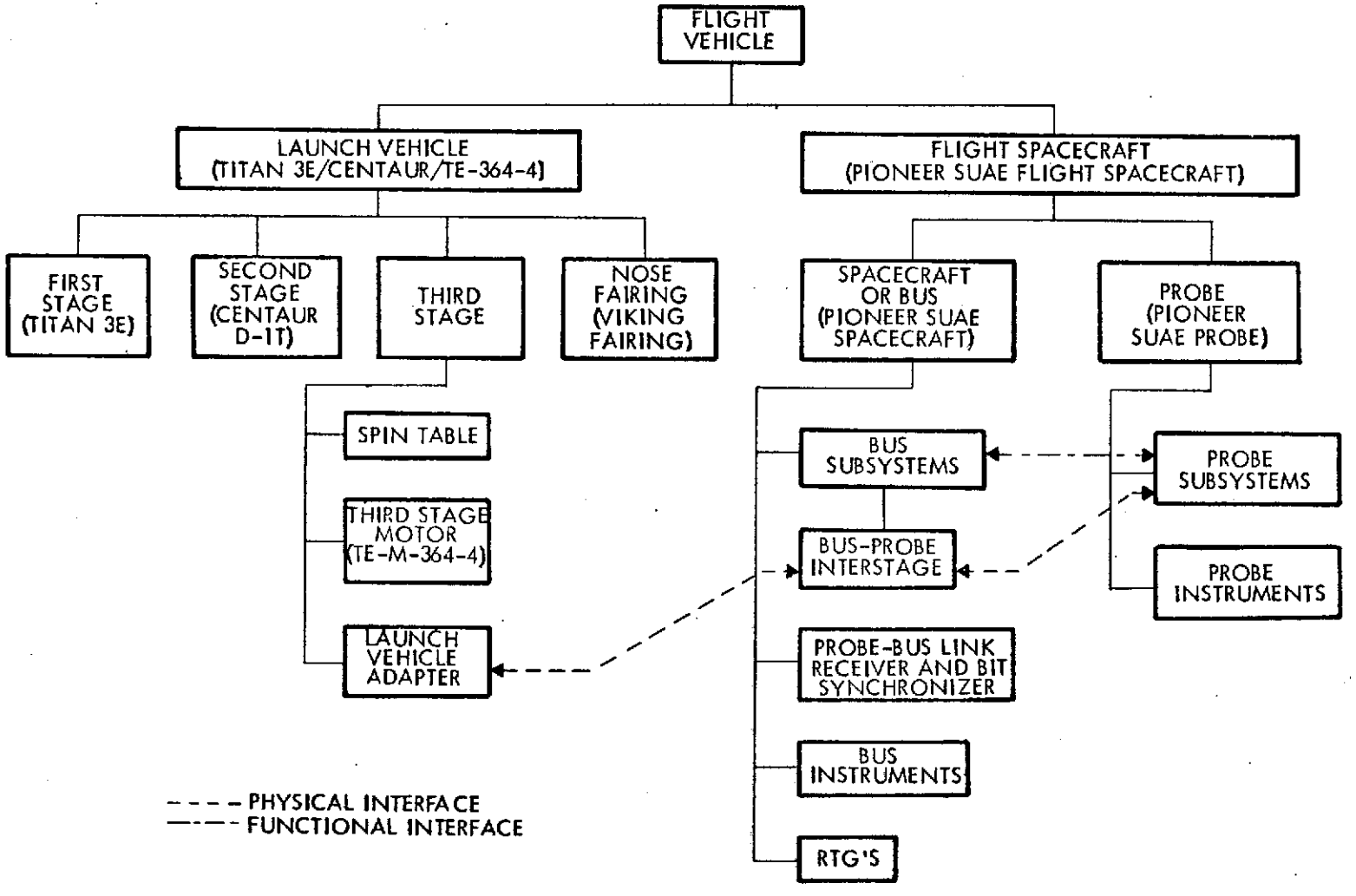

1. INTRODUCTION

This document reports the results of the Spacecraft System Definition Study for the Saturn Uranus Atmospheric Entry Probe Mission. This study was performed by TRW Systems Group under Contract No. NAS2-7297 for the Ames Research Center of the National Aeronautics and Space Administration from November 7, 1972 through June, 1973.

The purpose of the study is to determine the modifications required of the Pioneer F/G spacecraft design for it to deliver an atmospheric entry probe to the planets Saturn and Uranus.

The conclusion of the study is that it is feasible to conduct such a mission within the constraints and interfaces defined in the Statement of Work. The spacecraft required to perform the mission is indeed closely derived from the Pioneer F/G design, and the modifications required are generally routinely conceived and executed. The entry probe, the subject of a parallel study, is necessarily a more wholly new design, although it draws heavily on the technology of past, present, and imminent programs of planetary atmospheric investigations.

1.1 MISSION DESCRIPTION

The Saturn Uranus Atmospheric Entry Probe Mission, or SUAE mission as it is abbreviated in this study, (see "Nomenclature" for terms employed in describing elements of the mission and hardware employed) involves the injection of three Pioneer flight spacecraft by three Titan 3E/Centaur D-IT/TE-M-364-4 launch vehicles onto interplanetary trajectories directed toward an encounter with the planet Saturn.

Each flight spacecraft consists of a spacecraft, or bus, based on the Pioneer F/G design, and a probe which is able to withstand entry into the atmosphere of Saturn or Uranus and descent to the 10-bar (10 atmospheres) pressure level within 70 minutes after entry.

The first flight spacecraft is launched in November, 1979, and its probe is earmarked for delivery at Saturn in April, 1983, 3.4 years later. The second and third flight spacecraft are launched in the next Saturn opportunity, November-December, 1980, on trajectories which swing past Saturn in January 1984 toward Uranus, where they will arrive in

November, 1987, 6.9 years after launch. Each probe of the second and third launches can be delivered to either Saturn or Uranus, and the decision can be made as late as about two months prior to Saturn encounter -- and therefore after the results of the first encounter at Saturn are know.

The three flight spacecraft are to be the same in design and interchangeable. Thus a probe intended for the second launch could serve as a flight spare for the first launch, and the same is true of all components of the bus.

In the launch and interplanetary cruise phases of the mission, the probe is carried by the spacecraft, which provides thermal control throughout this period as well as electrical power and signals for periodic probe health assessment and probe battery charge/discharge cycles.

At the time of separation of the probe (nominally 30 days or 500 R_S before Saturn, and 20 days or 1000 R_U before Uranus) the spacecraft has provided proper trajectory control, orientation, and spin rate for the probe's approach and entry to the planetary atmosphere.

After separation, the spacecraft is deflected by a propulsive maneuver to a new trajectory. The probe and spacecraft approach and encounter trajectories are designed jointly to provide reasonably low entry angles, low probe angles of attack, and a profile of aspect angles and communications ranges for 70 minutes after probe entry which optimizes the transmission of data obtained on the probe to the spacecraft. The selected nominal trajectories must also exhibit tolerance to the expected magnitude of guidance inaccuracies.

The spacecraft, in addition to relaying probe scientific data to earth, carries a complement of instruments itself, and their data -- particularly near the time of encounter -- contribute to the total return of the mission.

It is appropriate to note that with both Saturn and Uranus as target planet, it is Uranus which imposes the more stringent requirements on design. The major areas so affected are mission lifetime, communications capability, propellant requirements, and onboard navigation requirements. (A brief look at the design resulting if Saturn is the only target planet given in Appendix D.)

The position of the planets Saturn and Uranus is appropriate to the dual nature of this mission for launches in 1979 and 1980. The targeting requirements at Saturn are very similar, whether catering optimally to a Saturn probe entry, or embarking on a swingby to Uranus. Thus, it is possible to perform meaningful encounter science by bus instruments while swinging past Saturn en route to probe delivery at Uranus. Conversely it is possible for the spacecraft to deliver the probe to Saturn and carry out all probe relay communications requirements, and still depart Saturn on a trajectory to Uranus to perform a flyby scientific mission at Uranus.

1.2 MISSION OBJECTIVES, CONSTRAINTS, AND SCHEDULES

1.2.1 Mission Objectives

The scientific objectives of the mission (as given in the Statement of Work) are to explore the atmospheres of Saturn and Uranus, the near space environment of these planets and the interplanetary space between Earth and Uranus.

1.2.1.1 Atmospheric Entry Probe

The specific scientific objectives for the exploratory atmospheric entry probes for Saturn and Uranus are as follows:

a. Measure the structure and composition of the atmospheres to a depth corresponding to a pressure of at least 10 bars.

b. Determine location and composition of clouds.

c. Obtain science and engineering data to enhance future missions.

The science payload for the probe is based on the exploratory payload suggested by the Outer Planets Science Advisory Group.

1.2.1.2 Spacecraft Bus

The specific scientific objectives for the spacecraft bus for the Saturn/Uranus probes are as follows:

a. Determine the characteristics (particularly in relation to particles and fields) of interplanetary space between Earth and Uranus and of the near environments of Saturn and Uranus by in situ measurements with instruments based on the Pioneer F/G scientific payload.

b. Make remote measurements of the characteristics of the atmospheres of Saturn and Uranus and the rings and satellites by occultation of the spacecraft communication link from earth by these bodies and with instruments based on the Pioneer F/G scientific payload.

1.2.2 Mission Constraints

The dominant mission constraints are:

a. The selection of launch opportunities and target planets, as outlined in Section 1.1.

b. The use of the Titan 3E/Centaur/TE-364-4 launch vehicle, and Cape Kennedy as the launch site.

c. The use of the JPL Deep Space Network as the ground terminal.

The guideline of the Pioneer F/G program as the technology base leads to such characteristics as spin stabilization, RTG power, and a monopropellant hydrazine system for attitude and trajectory control; however this influence is felt more as a positive guide than a negative constraint.

1.2.3 Schedules

Sections 1.1 and 3.1 identify launch dates in 1979 and 1980, Saturn encounter dates in 1983 and 1984, and Uranus encounter dates in 1987. These dates determine when operational resources and scientific data reduction and interpretation efforts must be utilized.

Section 8 identifies tasks appropriate in 1974 and 1975, and suggests the spacecraft hardware contract phase should begin in January, 1977, to meet the launch dates. The overall program must combine these inputs with the requirements for the probes, the RTG's, the scientific instruments, the launch vehicles, and for operating personnel and facilities, which are beyond the scope of this study.

1.3 MISSION OPTIONS AND ALTERNATIVES

Options and alternatives at the mission level which have surfaced during the course of the study are not numerous. The mission which considers Saturn as the only target planet has already been mentioned.

Another alternate mission which alleviates the tight launch window in 1980 involves Jupiter as an intermediate planet, rather than Saturn, for launches which may be dedicated to Uranus. Trajectory characteristics of Earth-Jupiter-Uranus missions launched in 1980 are treated briefly in Section 3.1, but otherwise are not considered in this study.

1.4 STUDY OBJECTIVES AND PRIORITIES

The primary study objectives relate to the modification of the Pioneer F/G design necessary for the Saturn Uranus spacecraft. The results of the study are not only to identify these design changes, they are also to serve as the basis for subsequent feasibility test and verification projects. To this end emphasis is placed on identifying the tests which are appropriate candidates for such projects and development of information which is necessary for the conduct of such tests.

Other areas which traditionally receive significant emphasis have been reduced in relative priority in this study. These include:

- Mission analysis, in which the identification of interplanetary trajectories has been accomplished by Ames Research Center, and the navigation analyses have been performed by the Jet Propulsion Laboratory. (The material presented in Section 3 draws heavily on the results of these studies.)

- Science requirements analysis, because a) the primary scientific objectives pertain to the probe instruments, which are not directly involved in the spacecraft design, b) the Statement of Work provides a list of sample instruments for the bus, and c) these instruments, being largely derived from Pioneer F/G instruments, require very little modification of bus subsystems, in comparison with modifications responsive to the presence of the probe and to the extension from Jupiter to the more distant planets.

1.5 RELATED STUDIES

Other studies pertaining to this mission have been in progress during the course of this study, and TRW acknowledges contributions derived from those efforts, both directly and indirectly:

Study	Performer	Receipt of Information
Mission Analysis	Ames Research Center	Presentations November 16, 1972 and subsequent[1]
Navigation Analysis	Jet Propulsion Laboratory	Presentations December 1972 to May 1973[2]
Probe Definition Study (Contract NAS2-7328)	McDonnell Douglas Corporation	Numerous interface meetings, November 1972 to March 1973

1.6 APPROACHES TO COST ECONOMY

The necessary duration of the operational phases of this mission (Section 1.1), the number of flight vehicles, the development span, the technology to be involved for successful entry of the atmosphere of the giant planets will all contribute to the cost of SUAE mission.

However, this study points out definite areas of cost economy within the framework of the mission definition. First and foremost is the basing of the spacecraft design approach on the Pioneer F/G spacecraft. This report necessarily dwells on the modifications necessary to the spacecraft hardware and operations to conduct the SUAE mission, but one should not lose sight of the applicability of the fundamental attributes of the Pioneer F/G spacecraft and program:

- The Pioneer spin stabilization, spin rate and earthline orientation are all ideal for establishing the spin rate and attitude of the probe.
- The Pioneer has been qualified for the Titan 3E/Centaur/TE-364-4 launch vehicle.
- The Pioneer has demonstrated an ability to operate from RTG power sources, necessary at Saturn and Uranus distances.

(1) Results published in NASA TMX-2824, "Mission Planning for Pioneer Saturn Uranus Atmosphere Probe Mission," B. L. Swenson, E. L. Tindle, L. A. Manning.
(2) Results published in JPL Report No. 760-88, "Navigation Analyses for Advanced Pioneer Outer Planet Probe Missions," C. K. Paul, R. K. Russell.

- Pioneer has performed long-range communications to earth stations, and this capability can be increased using the same high-gain antenna reflector by going from S- to X-band.

- The data handling formats of Pioneer can accommodate data received from the probe.

- Pioneer has demonstrated a capability for long-life operation in interplanetary space and in the outer solar system environment, including the asteroid belt and the thermal environment which applies in this mission.

Other areas in which cost economy is instituted are evident in the implementation planning recommended in Section 8.2. The maximum multiple use of both test and flight hardware is outlined, to minimize co: while meeting product assurance objectives. The duration recommended for the C/D phase, 34 months from start to first launch, is adequate to encompass the multiple use test program, but short enough to minimize overall project cost.

2. SUMMARY OF RESULTS

This section summarizes the results of the study by presenting a description of the Pioneer F/G spacecraft design, the modifications to that design necessary for the SUAE spacecraft, the definition of the major interfaces which must be satisfied by the spacecraft, the particular demands of the SUAE mission, and brief treatments of mission operations and spacecraft reliability.

2.1 EVOLUTION OF SPACECRAFT CONFIGURATION

The Saturn Uranus atmospheric entry mission is a natural and logical extension of the Pioneer F/G Jupiter flyby mission. The technology of the probe which enters and descends in the atmosphere is not derived from this program, but is based on other atmospheric entry programs, such as manned earth programs, PAET, Viking, and Pioneer Venus. But the spacecraft which carries the probe is strongly based on the Pioneer F/G spacecraft so its description is made with greatest facility in terms of the modifications from the Pioneer F/G design.

2.1.1 Pioneer F/G Spacecraft

Launch dates and pre-Jupiter orbital characteristics for Pioneers F and G (designated Pioneers 10 and 11 after launch) are given in Table 2-1, and pictured in Figure 2-1. The launch vehicle was the Atlas/Centaur/TE-364-4. The post-encounter trajectory depends on the targeting at Jupiter encounter. Pioneer 10 is targeted to pass Jupiter in a near-equatorial, posigrade pass, with a minimum altitude of 1.83 radii of Jupiter (R_J). This will lead to a post-encounter trajectory which is accelerated by Jupiter's gravity beyond solar escape velocity. It will pass Saturn's orbit in 1976, Uranus' in 1979, and Neptune's in 1983, although it will not come close to any of these planets, as they are all on the opposite side of the sun.

Currently Pioneer 11 is on a path which would lead to a similar post-encounter trajectory after an even closer passage of Jupiter. However, there are opportunities after Pioneer 10's encounter at which Pioneer 11 may (and likely will) be commanded to alter its trajectory to different encounter targeting and therefore a different post-encounter trajectory.

Table 2-1. Pioneer 10 and 11 Orbital Characteristics

Designation	Launch Date	Jupiter Encounter Date	Orbit About Sun			Orbit Subsequent to Encounter	Weight	
			Perihelion (AU)	Aphelion (AU)	Inclination (Deg)		Spacecraft (LB)	Experiments (LB)
Pioneer 10 1972 12A	03/03/72	12/04/73	0.99	5.96	2.1	Escape from solar system	565	66.0
Pioneer 11 1973	04/06/73	12/05/74	1.00	6.16	3.1	Depends on final encounter targeting	570	67.4

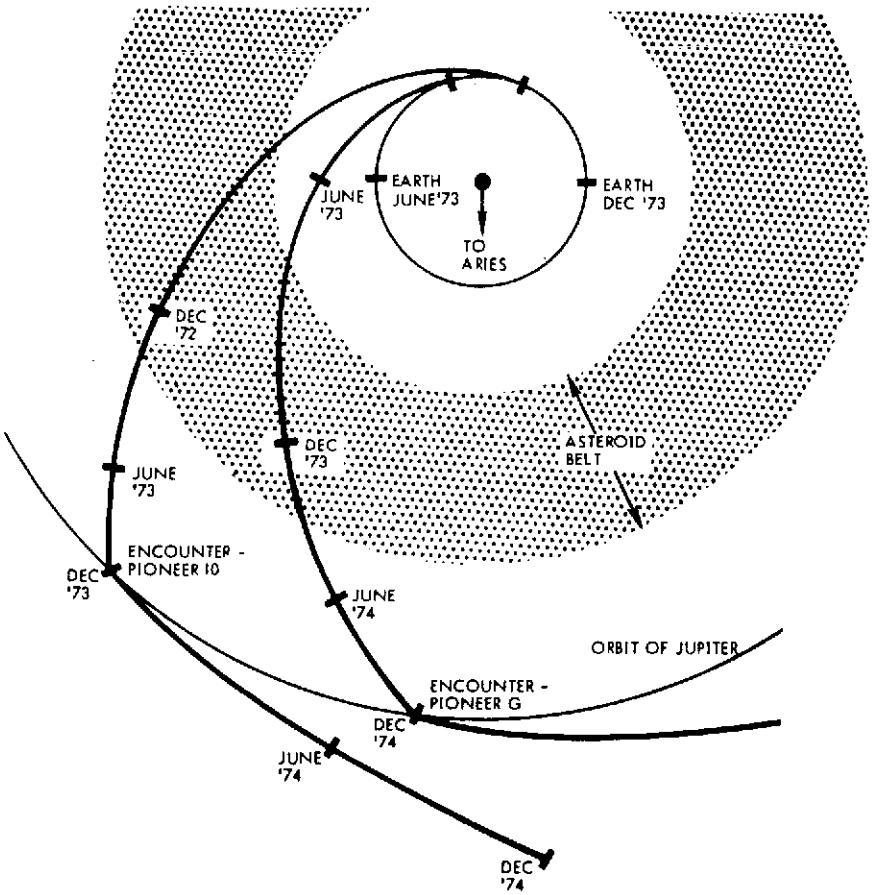

Figure 2-1. Pioneer 10 and 11 Trajectories

2.1.1.1 Physical Description

The Pioneer F and G spacecraft are illustrated in Figures 2-2 and 2-3. Spin stabilization is the basic attitude control mode. High desired antenna gain calls for a large reflecting paraboloidal dish, with its pencil beam lying along the spin axis which is directed toward the earth for nearly the entire mission. The nominal spin rate is 4.8 rpm.

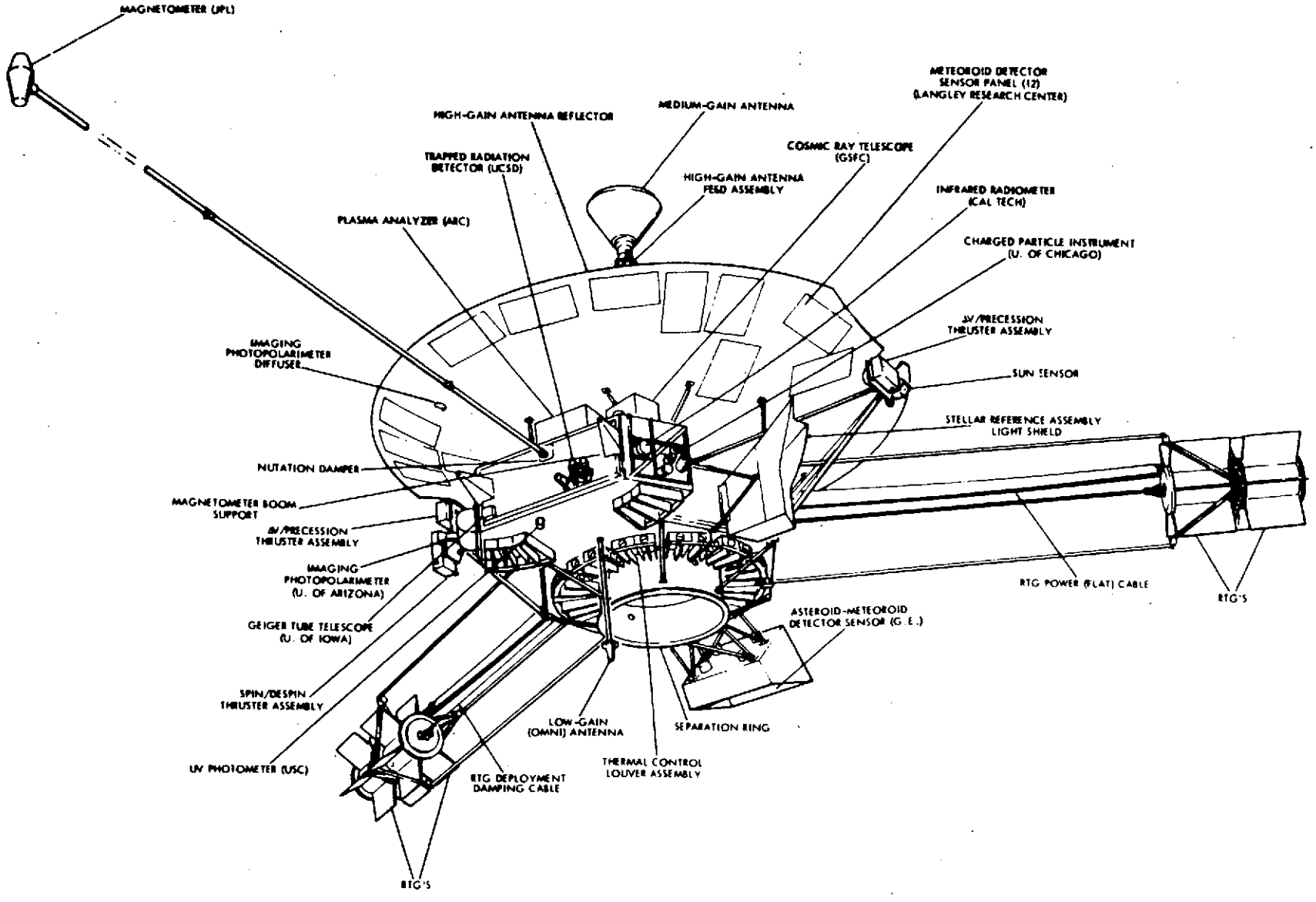

Figure 2-2. Pioneer F and G Spacecraft

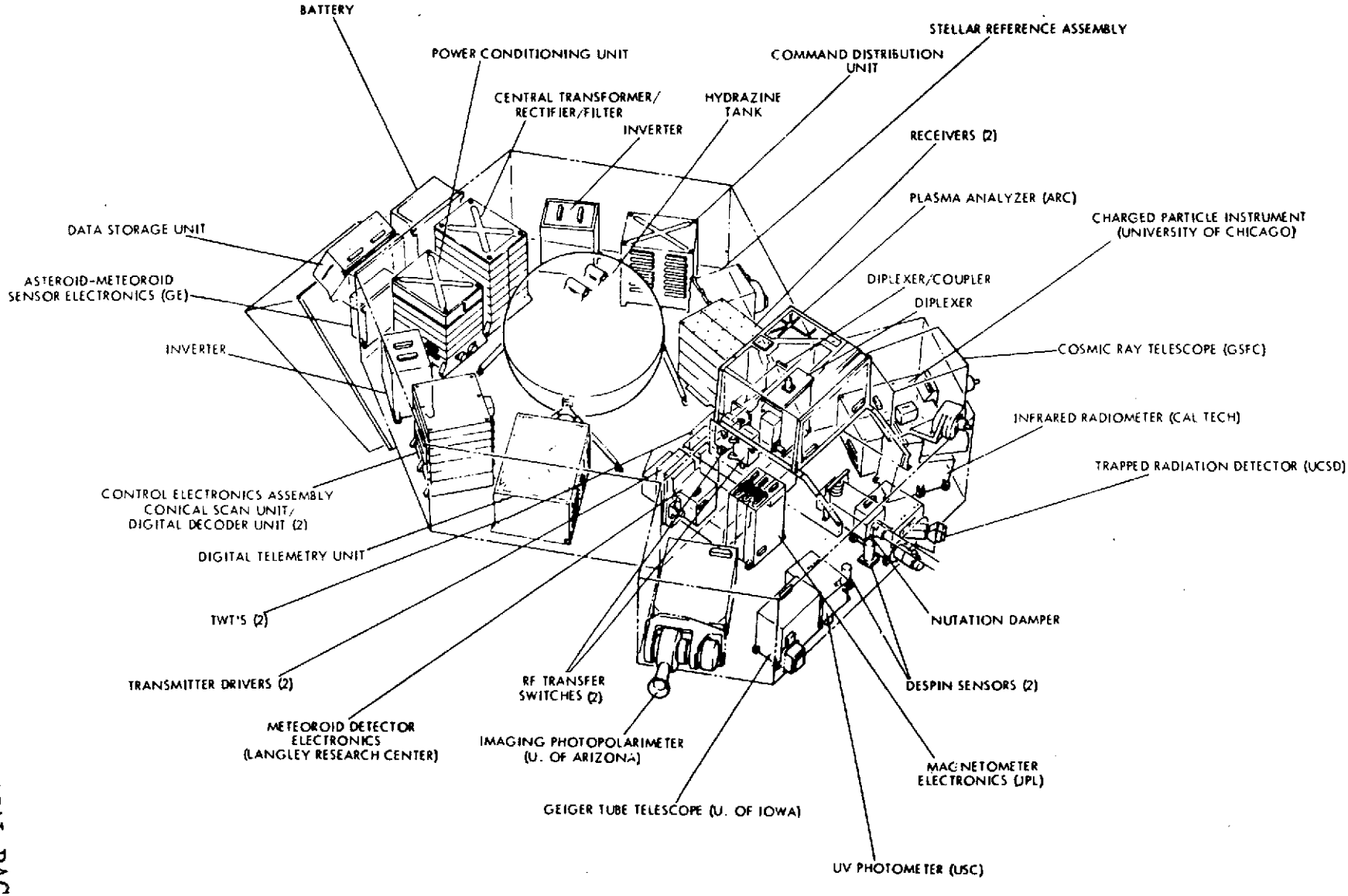

Figure 2-3. Pioneer F and G Equipment Compartment

The promiment physical features in Figure 2-1 include the high-gain antenna reflector and feed, and medium-gain antenna on the same feed tripod. Deployable appendages support the magnetometer sensor and the four 40-watt SNAP-19 radioisotope thermoelectric generators (RTG's) which supply electrical power. Six 1-pound hydrazine thrusters are located near the perimeter of the dish. Four thrust parallel to the spin axis for precession and velocity control, and two act tangentially for spin control. The thrusters are grouped in oppositely directed pairs mounted in clusters, one of which is shown with the cover removed in Figure 2-4.

External optical sensors (and their light shields) are visible as well as ports for most of the instruments. Some instrument sensors are externally located: meteoroid detector panels on the back of the antenna dish; a plasma analyzer and cosmic ray detector; and the optical asteroid-meteoroid detector.

The temperature-controlled equipment compartment (Figure 2-3), a hexagonal box with an additional hexagonal experiment bay, contains the spherical hydrazine propellant tank, the spacecraft subsystem electronic units, and the remaining instrument sensors and electronics.

The primary structural features of the spacecraft provide the support of these external components from the equipment compartment, the support of internal components by the equipment compartment, and the carrying of the loads of all these components during the launch phase via struts and a 25-inch diameter cylinder to the separation ring — the interface with the launch vehicle adapter.

The spacecraft are 9-feet diameter by 9.5 feet in the launch configuration. The deployed RTG's extend to 10 feet radius, the magnetometer to 20 feet.

2.1.1.2 Functional Description

The major performance characteristics of the spacecraft subsystems are shown in Table 2-2. A unique characteristic of the spacecraft is the use of RTG's as the primary source of electrical power. Each of the four SNAP-19 RTG's converts about 6 percent of the heat released from plutonium dioxide fuel to electrical power, using a series-parallel array of TAGS 85/2N thermoelectric converter elements. RTG power is

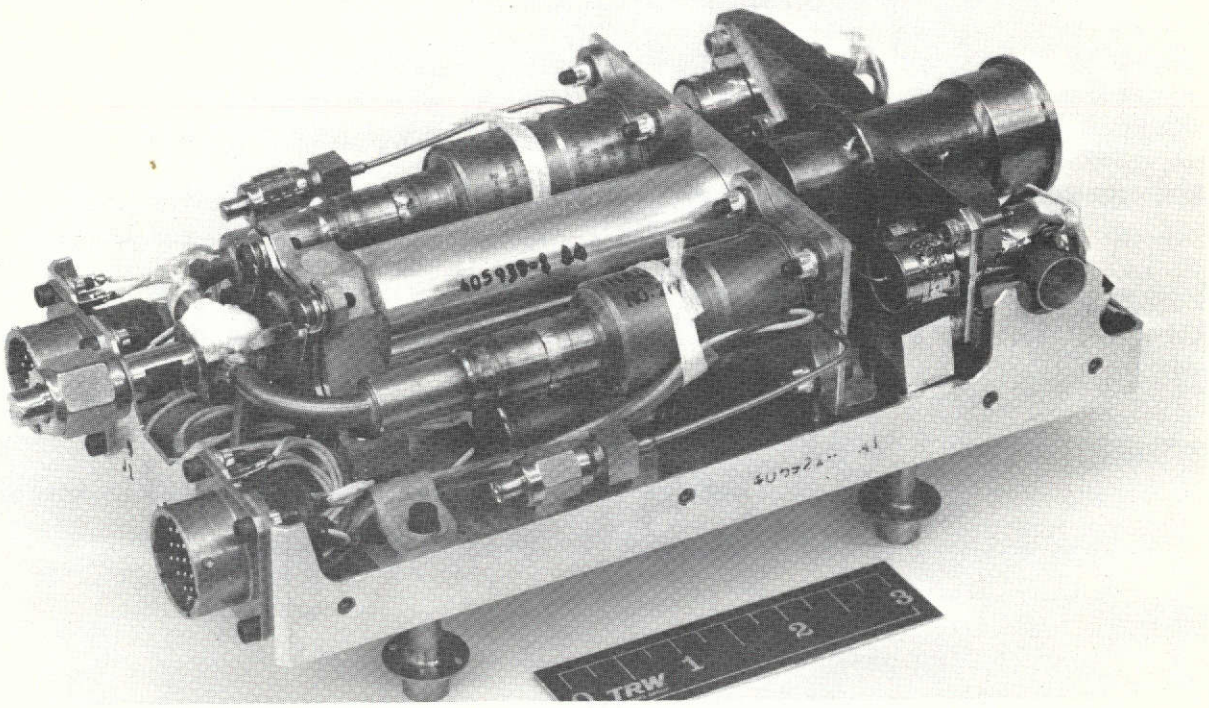

Figure 2-4. Thruster Cluster Assembly

greatest at 4.2V; and inverter boosts this to 28V for distribution. The bus voltages are maintained by shunt dissipation of excess power. A pair of prototype RTG units is shown in Figure 2-5. The power output of the four units of Pioneer '10 is shown in Figure 2-6. (The minor wiggles reflect telemetry round off.) Extrapolation indicates adequate power will be available long after Jupiter encounter, considering that the spacecraft steady load, all units on, is 108W.

The periodic maintaining of the earth-pointing attitude is also a unique feature. On command an on-board digital phase processor (the conscan signal processor) synchronously demodulates (at the 0.08 Hz spin rate) the signal received by a conically scanning antenna. The antenna may be either the permanently tilted medium-gain antenna or the high-gain antenna whose beam is tilted 1 degree by commanding the feed to be translated to an offset position. The processor abstracts phase information to determine the direction of the pointing error and amplitude information to determine its magnitude. It can also control

Table 2-2. Pioneer F and G Subsystem Summary

Power

- Four radioisotope thermoelectric generators — 4.2 volts
  - Maximum (at launch) — 160 watts
  - Minimum (after 2.5 Years) — 120 watts
- Internal distribution — 28 VAC, 28 VDC

Stabilization, Propulsion

- Spin-stabilized 4.8 rpm
- Spin axis directed at earth (cruise)
- References
  - Sun and star (optical)
  - Earth (RF)
- Precession
  - Open-loop to and from earth pointing
  - Closed-loop (conscan) earth tracking (uplink RF)
- Six hydrazine thrusters (one pound)
  - Pulsed - precession, spin control
  - Continuous - ΔV for trajectory Correction

Communications

- Antennas (up and downlink)
  - Nine-foot parabolic reflector (33 dB)
  - 16-inch horn (13 dB)
  - Log conical spiral (aft hemisphere)
- S-band frequencies
- Eight-watt TWT amplifiers
- 1024 bps telemetry capability at Jupiter

Data

- Bit rates, 16 to 2048 bps (powers of two)
- Data formats (192 bits/frame)
  - Two science main frames
  - One science subcommutated
  - Four eng'g main frames (or subcommutated)
  - Sixteen special (combined) science main frames

Commands

- 255 discrete commands available
  - Up to five stored
- One bps command rate
- 22-bit command message
- Hamming (15, 11) coded

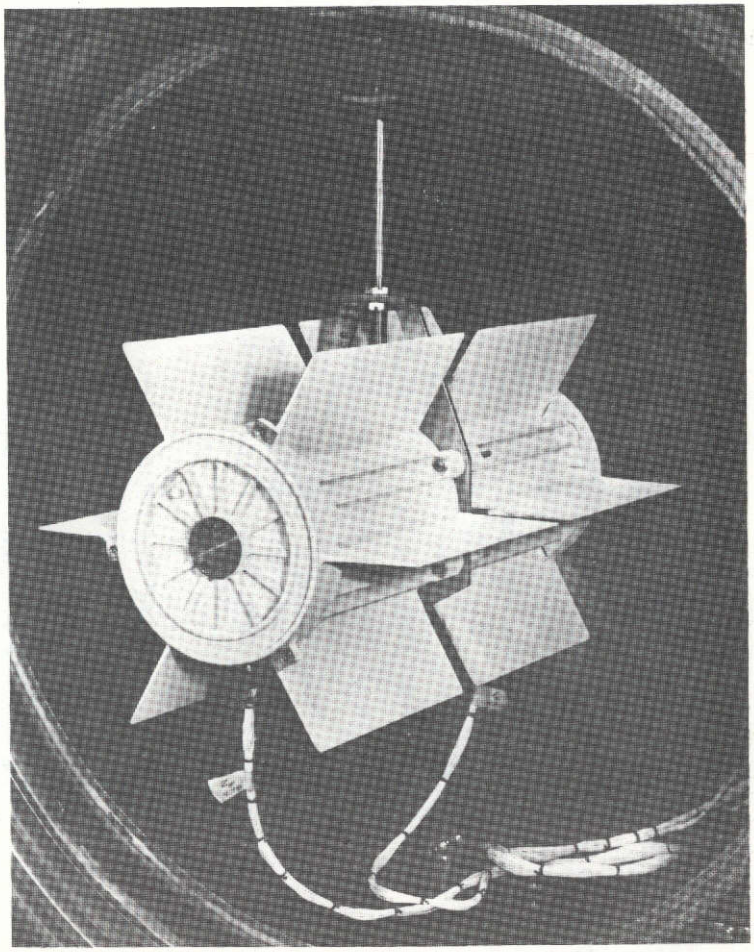

Figure 2-5. Prototype SNAP-19 Radioisotope Thermoelectric Generators

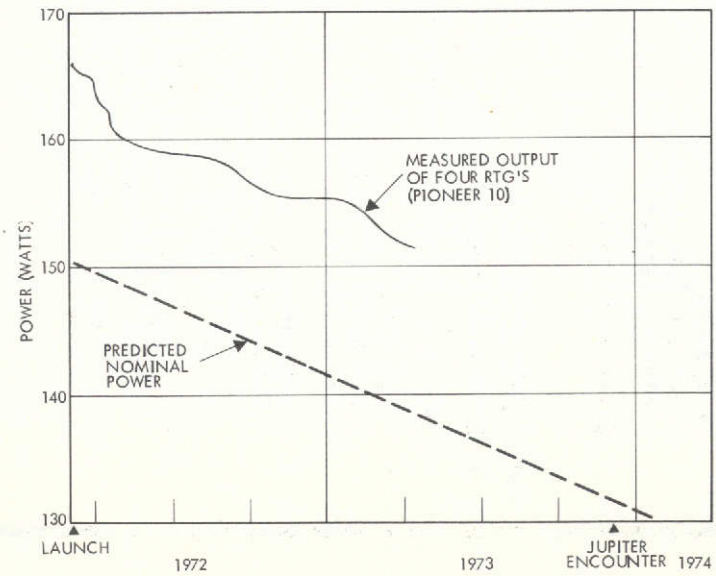

Figure 2-6. RTG Power Output

precession thrusters to correct the pointing error. Because the rotation of the spacecraft-earthline in space is very gradual during the mission, this precession maneuver is required less than once a week. The movable high-gain antenna feed is seen just below the apex of the tripod in Figure 2-7; the tilted medium-gain horn is above.

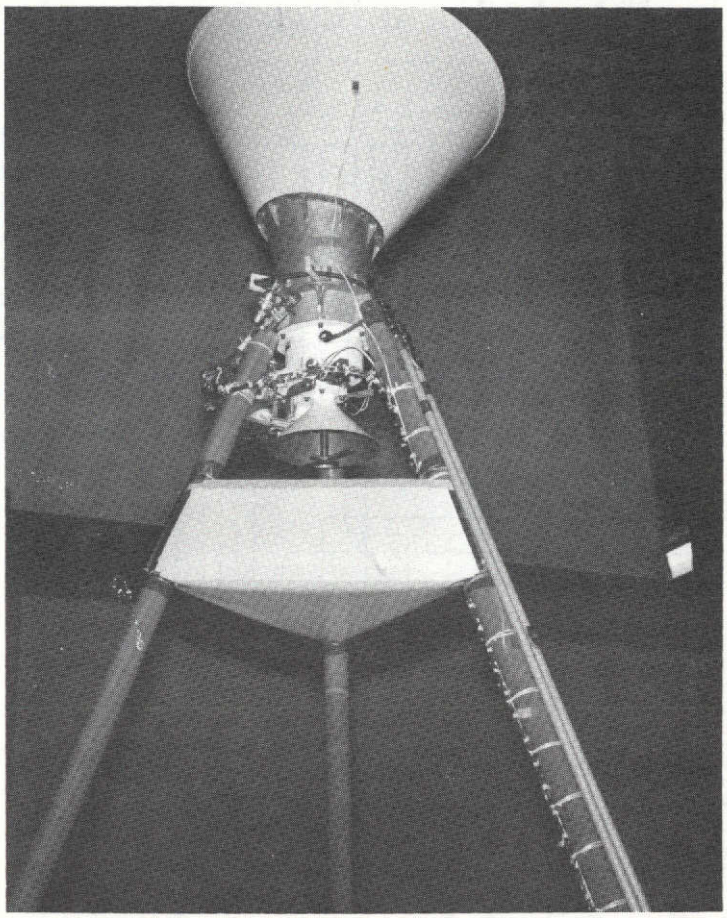

Figure 2-7. Medium-Gain Antenna, and Movable High-Gain Feed

2.1.2 SUAE Spacecraft (Modifications of Pioneer F/G)

Figure 2-8 traces the evolution of design modifications, starting with the nature and characteristics of the SUAE mission, and identifying influences on the spacecraft system design and on the subsystems.

There are two general classes of influence on the bus design. The first arises from the fact that this mission involves a trajectory from the earth to Saturn and Uranus. This has implications arising from the extended duration of such a mission, from the distance from the earth and

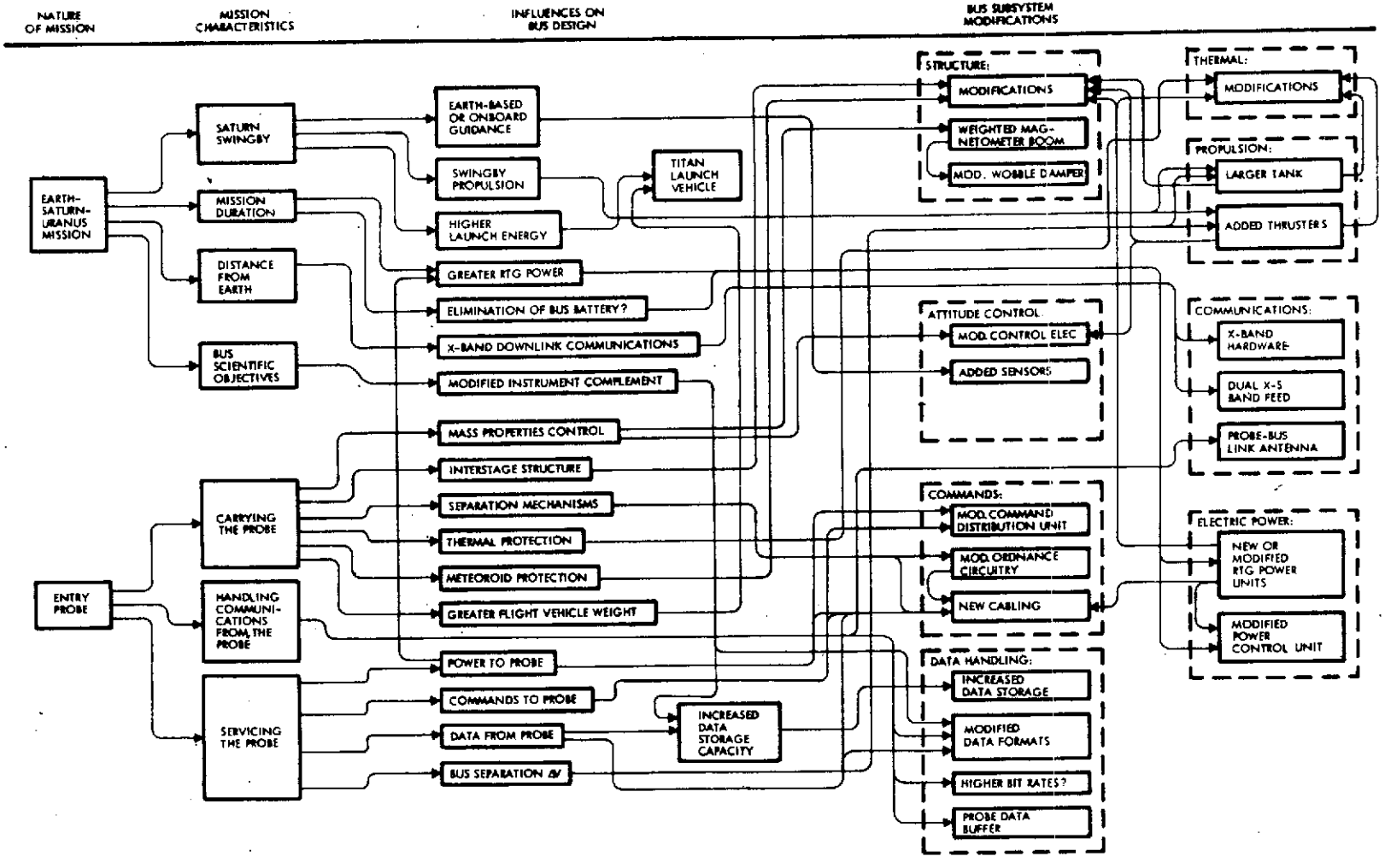

Figure 2-8. Evolution of Spacecraft (Bus) Modifications

and sun (20 AU at Uranus), and from the scientific objectives to be attained by the spacecraft bus and its complement of instruments. It also entails guidance and propulsion requirements for the mission in which the spacecraft swings by Saturn on its way to Uranus.

The second general class of influence on the spacecraft design arises from the presence of the entry probe; the requirements for the physical accommodation of the probe on the spacecraft, servicing the probe with electrical power and command signals, and the receipt of RF communications from the probe before and after it has separated from the spacecraft.

These influences on bus design propagate into modifications to individual components and units of the spacecraft, which are tabulated in the following sections.

2.1.2.1 Propulsion

a) Propellant tank	Must be enlarged to satisfy the requirement for increased propellant. Increased from 16.5 to 22.25 inches in diameter.
b) Thrusters	A pair of radial thrusters is added to the six already present, to permit ΔV maneuver components normal to the spin axis at long distances from the earth.
c) Propellant lines and heaters	Modified and added to accommodate larger tank and added thrusters.

2.1.2.2 Thermal Control

Insulation, louvers, and heaters	New insulation and heaters on probe adapter to control probe temperatures.
	New insulation and louvers for externally located power shunt regulator.
	Modified louver complement for equipment compartment.

2.1.2.3 Structure

a) Probe adapter	New spacecraft-probe adapter structure to carry spacecraft loads around probe to launch vehicle adapter, and to pick up probe loads.
	Modification of spacecraft separation ring.

	New hold-down, release, and separation fittings for the probe.
b) Launch vehicle adapter	Modification of standard 37 inch diameter by 31 inch adapter, to allow single separation joint.
c) Propellant tank accommodation	New tank support structure.
	Cutout for tank in equipment mounting platform.
d) Magnetometer boom	Added deployment counterweight (~24 pounds)
	Modified and strengthened boom and fittings, to accommodate counter weight and simultaneous deployment.
	Modified deployment damper.
e) RTG support structure	Modified RTG mounting structure to accommodate MHW RTG's.
	Relocation of RTG guide rods.
f) Wobble damper	Modified to change damping constant.
g) Equipment compartment	Add -X compartment.

2.1.2.4 Attitude Control

a) Star mapper	Stellar reference assembly is replaced by V-slit star mapper to provide both roll reference pulses and on-board optical navigation measurements.
b) Control electronics	Modified to accommodate star mapper and added thrusters.
c) Despin sensors	Relocated to operate at different spin rate.

2.1.2.5 Communications (Bus-Earth Link)

a) X-band hardware	New drivers, transmitters, waveguide, switch.
b) High-gain antenna feed	Replace offsettable S-band feed by fixed, dual S-X band feed; add X-band waveguide.

c) Low-gain S-band antenna	Remount on new pedestal.
d) S-band receiver	Modified to bring out coherent drive for X-band

2.1.2.6 Communications (Probe-Bus Link)

a) Probe-bus antenna	New unit, operating at 400 MHz, mounted on same pedestal as S-band low-gain antenna.
b) Receiver	Receiver-bit synchronizer unit (furnished by probe contractor) added.

2.1.2.7 Data Handling

a) Digital telemetry unit	Modified to install new formats to accommodate probe data.
b) Data storage unit	Enlarged to accommodate probe data and line-scan imaging data.
c) Probe data buffer	New unit to accept probe data into spacecraft data handling system, from probe-link receiver.

2.1.2.8 Command Distribution

a) Command distribution unit	Modified to accommodate: • commands destined to the attached probe • commands to cut probe cable and to separate the probe • increased ordnance - actuated events • commands associated with the reception of probe data by RF link.
b) Cable harness	New

2.1.2.9 Electrical Power

a) RTG's	Higher power units are required. Two modified MHW RTG's are identified for the SUAE mission, replacing the four SNAP-19 generators of the Pioneer F/G design.

b) Inverter assemblies	Present 4.2-volt-input inverters operating from RTG outputs are replaced by an 28-volt-input inverter unit serving only the CTRF.
c) Battery	Deleted. Pulse loads to be supplied out of RTG power margin.
d) Power control unit	Modified to accommodate higher range of shunt power.
	Modified to replace spacecraft battery charge/discharge circuitry by probe battery charge/discharge circuitry.
e) Shunt regulator	Modified to handle greater shunt power.
	Relocated outside of equipment compartment, to facilitate thermal control.
f) Shunt radiator	Enlarged

2.1.2.10 Summary of Modifications

The completion of this study has confirmed what was predicted at its inception: that although the above list of modifications affects all the subsystems and most units of the Pioneer F/G design, the impact on the basic spacecraft design is relatively minor, in terms of fundamental changes in philosophy or the introduction of concepts of uncertain feasibility. The majority of the modifications can be accomplished routinely by normal processes of mechanical or electrical design.

In fact several areas which at first were considered possible feasibility questions have proven, as a result of the study effort devoted to them, to be resolved with less effort and more confidence.

An example of this is an aspect of mass properties control, the maintenance of satisfactory moment-of-inertia ratios of the flight spacecraft to insure a satisfactory dynamic stability margin. While the moment-of-inertia ratio is significantly greater than 1.0 (and therefore satisfactory) if deployed appendages are considered rigidly attached to the spacecraft, the concern was that realistic accounting for the flexibility with which these appendages are actually tied to the spacecraft would dangerously reduce the margin. Analysis accounting for the flexibility effects has been performed, and the results (reported in

Section 5.5) are that the stability margin is excellent, provided only that the RTG guide rods are fully latched at the completion of deployment, that their tie to the spacecraft effectively has enough stiffness to approach the rigid attachment assumption.

A second example is in the area of thermal control. It was initially felt the increase in the range of power to be dissipated within the equipment compartment and the blockage on heat rejection imposed by the presence of the probe would strain the capability of the spacecraft louvers. However, the design approach which evolved during the study (Section 6.2) actually reduced the variability of heat rejection necessary, making the spacecraft considerably less dependent on louver action, and therefore less influenced by blockage. The approach uses two factors: the X-band transmitter need not be turned on until that portion of the mission when the equipment compartment is shaded from the sun by the nine-foot dish; and a decision to relocate the shunt regulator of the power supply outside the equipment compartment.

Conversely, however, some aspects of the spacecraft design may have engendered somewhat less confidence in ultimate satisfactory performance than existed at the beginning of the study. One area involves the use of a deployment counterweight on the magnetometer boom, to compensate for the first mass moment shift in the -X direction when the RTG's are deployed. This counterweight weighs about 24 pounds. While it restores the spacecraft center of gravity to the Z axis after RTG's and magnetometer boom are all deployed, there can be significant transient c.g. excursion accompanied by induced nutation. To minimize these effects, all these appendages will be released simultaneously, rather than sequentially as in Pioneer F/G. Even so the deployment dynamics involve substantially greater nutation than in Pioneer F/G, a matter which makes advance analysis and deployment tests more critical, and which may feed back to affect the structural design of the deployment mechanizations. Also, the combination of the heavy counterweight on the magnetometer boom and its release at a higher spin rate puts a much greater load on the magnetometer boom structure, both during launch and during deployment, and the F/G boom design may have to be altered to strengthen it adequately without an excessive weight penalty. See Sections 5.5 and 6.1.

Another area is the extension of the use of the Pioneer F/G ordnance-firing circuitry to activate mechanisms toward the end of the mission, possibly 6.9 years after launch. The Pioneer F/G design uses tantalum capacitor banks in the command distribution unit which are charged from the 28-volt line when "arm" is commanded, and discharged by silicon-controlled rectifiers into the squib igniters when actuation is commanded. They were used in the first day of the Pioneer 10 and 11 flights to actuate bolt cutters to deploy the RTG's, to actuate a strap cutter to release the magnetometer, and to actuate a pin puller to free the antenna feed movement mechanism. The concern is over the ability of these components to perform reliably after 6.9 years storage in space. There is no evidence that they will lack reliability; but it is not possible to prove with high confidence that they will operate reliably. This is strictly a matter of component life, and attention is centered on the tantalum capacitors, the SCR's, and the ordnance devices themselves.

In both of these areas we have recommended in Section 8 that interim test programs be initiated to verify that the designs chosen or suitable alternates constitute feasible solutions to the engineering requirements.

2.1.2.11 Summary of Tradeoff Study Results

Several tradeoff studies were identified in the work statement, most of which impinge on the design of the probe as well as the bus, and in which the choice depends on effects in both elements of the flight spacecraft. These choices are reported briefly here, and in more detail elsewhere in this report.

a) Probe-Link Antenna on Bus. One study compared, for the probe-bus communications link, a despun antenna on the bus with an axisymmetric (non-despun) antenna. The despun antennas considered provide gains of 10-13 dB compared with axisymmetric antenna gains of 2.6 dB (Lindenblad -- switchable) and 0.6 dB (loop-vee). This gain advantage could support higher data rates, reduce transmitter power, or accrue to the benefit of other mission parameters. However, the despun antenna mechanizations imposed significant penalties on the spacecraft in terms of weight, power, and reliability. In addition, space limitations restricted consideration of despun antennas to frequencies of 900 MHz or greater. The decision was to utilize the axisymmetric antenna on the spacecraft. (See Appendix A).

A second study compared two axisymmetric antennas, exemplified by an array of three Lindenblad antennas and a loop-vee antenna. The Lindenblad approach gave a 30-degree beam width, a gain at the beam edge of 2.1 to 3.1 dB, and a need to switch via phase shifters according to whether the probe is dropped at Saturn or Uranus. The loop-vee produces a 50-degree beam width which encompasses the aspect angle range at both planets without switching and a gain at the beam edge of 0.1 to 1.1 dB. The loop-vee antenna being smaller could be mounted farther from the equipment platform, and therefore does not require a jettisoning of the probe adapter after probe separation, as does the Lindenblad. Again, the selection favored simplicity over performance, and the loop-vee antenna approach was selected for incorporation into the spacecraft design.

b) Probe-Bus Link Frequency. With the selection of the axisymmetric antenna for the spacecraft terminal of the link, it was possible and desirable to reduce the link frequency to 400 MHz. This is the frequency which gives most efficient communications, and it was adopted.

c) Charging Provisions for the Probe Battery. The question was whether to locate circuitry for providing probe battery charging current on the probe or on the spacecraft. If on the probe, it would simplify the electrical interface to a single power line pair at 28V DC, and simplify the interface description as well. If on the spacecraft, it would relieve the probe of carrying components it has no use for after separation from the spacecraft. Although the design of the probe battery(ies) and its (their) charging requirements changed several times during the study, the decision was made early that charging provisions would be located on the spacecraft and it is a part of the spacecraft electrical power subsystem.

d) Optimum Time of Probe Separation. This trade can involve a number of facets of the spacecraft and probe design and operation. However, from the spacecraft point of view, it became a trade between early separation favoring a reduced propellant requirement and late separation providing better guidance accuracy. The tradeoff was conducted only for approach to Uranus, which, rather than a Saturn target, sizes propellant and requires on-board guidance. For the star mapper of nominal design suggested by TRW (threshold: magnitude 4.0; accuracy: 0.05 to

0.1 milliradians) the separation time originally suggested by ARC mission analysts -- 20 days or 1000 R_U before encounter -- was confirmed as the optimum time, but with little navigational margin on both parameters, sensitivity and accuracy of the sensor. (See Section 3.7).

2.2 MAJOR INTERFACE DEFINITION

2.2.1 Entry Probe

The interfaces between the bus and the probe are described in detail in the Interface Specification contained in Appendix B. The principal features are summarized below. Further details may be found in Section 6.

2.2.1.1 Mechanical

The probe envelope and three-point mount are described in Figure 2-9 which is a McDonnell-Douglas drawing modified to provide sloping clearance near the tiedown points. The nominal center of gravity of the installed probe is on the spin (Z) axis, and as close as possible to the maximum probe diameter. Access to the probe after mating with the spacecraft will be required for the probe-bus electrical cabling, test connectors, ordnance installation, and inspection/thermal closeout of the probe. Separation is via three ordnance-actuated ball lock devices (see Section 6.1.6.1).

2.2.1.2 Thermal

The probe must be designed to survive a long journey (20-30 days) after separation from the bus. It relies on internal radioisotope heating units (RHU's) plus effective insulation to maintain acceptable internal temperatures. When attached to the probe, the bus and probe adapter block most of the probe radiating area, and the tendency will be for the probe temperature to rise. Thus, the basic interface is a requirement by the probe on the bus to accept heat from the probe to maintain the probe temperature within limits to insure survival of the NiCad bootstrap batteries. The excess RHU heat (not lost by leakage through the probe insulation) will be conducted and/or radiated to the probe adapter structure and subsequently radiated to space. Some elevation of the battery temperature (above $32^{\circ}F$) may be encountered during the early mission

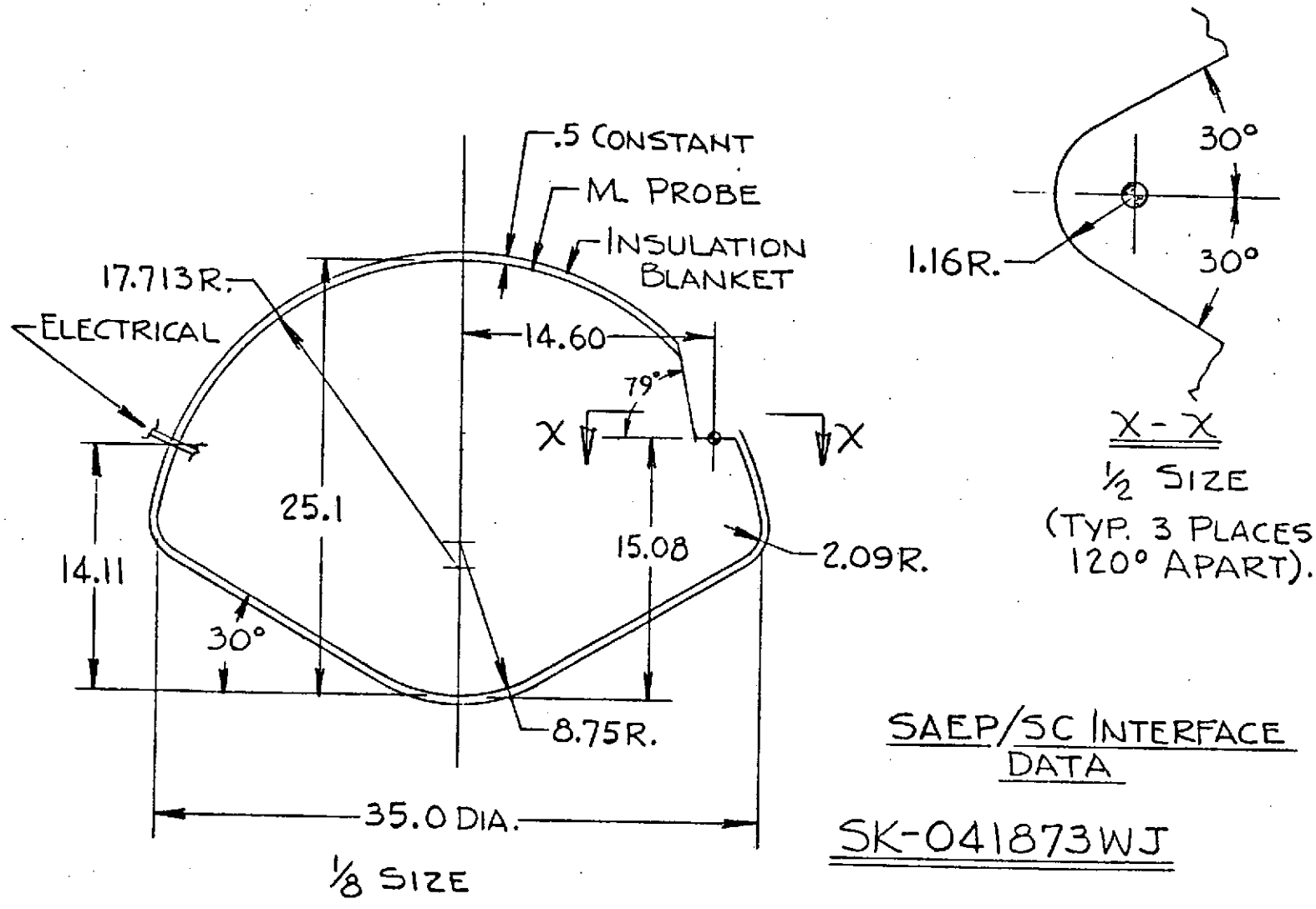

Figure 2-9. Probe Mechanical Interface

phase or during maneuvers due to side-sun (solar insolation). The proposed configuration for thermal control of the probe while attached to the bus is shown in Figure 2-10.

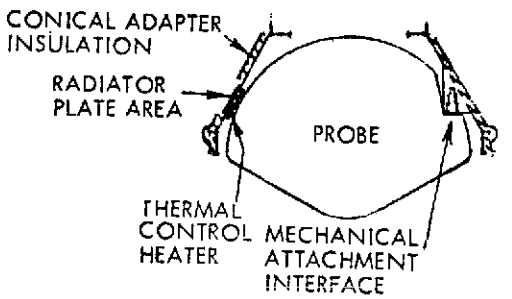

Figure 2-10. Attached Probe Thermal Control Concept

2.2.1.3 Electrical

The probe will be designed to conform to the EMC requirements defined for the Pioneer F/G spacecraft. Some relaxation in the magnetic cleanliness requirements for the probe will be necessary to permit the use of a NiCad battery in the probe. However, the remanent magnetic field at the magnetometer with the probe detached will be comparable to the Pioneer F/G field levels. All electrical signals between the probe and the bus shall be via one cable bundle. The signal and power interfaces are defined on Figure 2-11. At separation, this cable bundle will be severed by an ordnance-actuated guillotine device. Grounding and shielding need not be compatible with Pioneer F/G practices because of the restricted time periods in the mission when the probe is electrically active. Power returns may be grounded in the probe, along with command returns. Detailed EMC requirements will be worked out in compatibility tests, and magnetometer interference will be tolerated for the brief active periods.

2.2.1.4 Communications

The probe contains a 400 MHz transmitter to relay data to the spacecraft. This transmitter is activated when a probe-mounted accelerometer senses a deceleration level of -6 g (decreasing). The bus must receive this signal following blackout, extract the probe data from the carrier, and retransmit these data to the earth. Key characteristics of the probe data are summarized as:

- Symbol bit rate: 88 bps
- Encoding: 2:1 convolutional coding

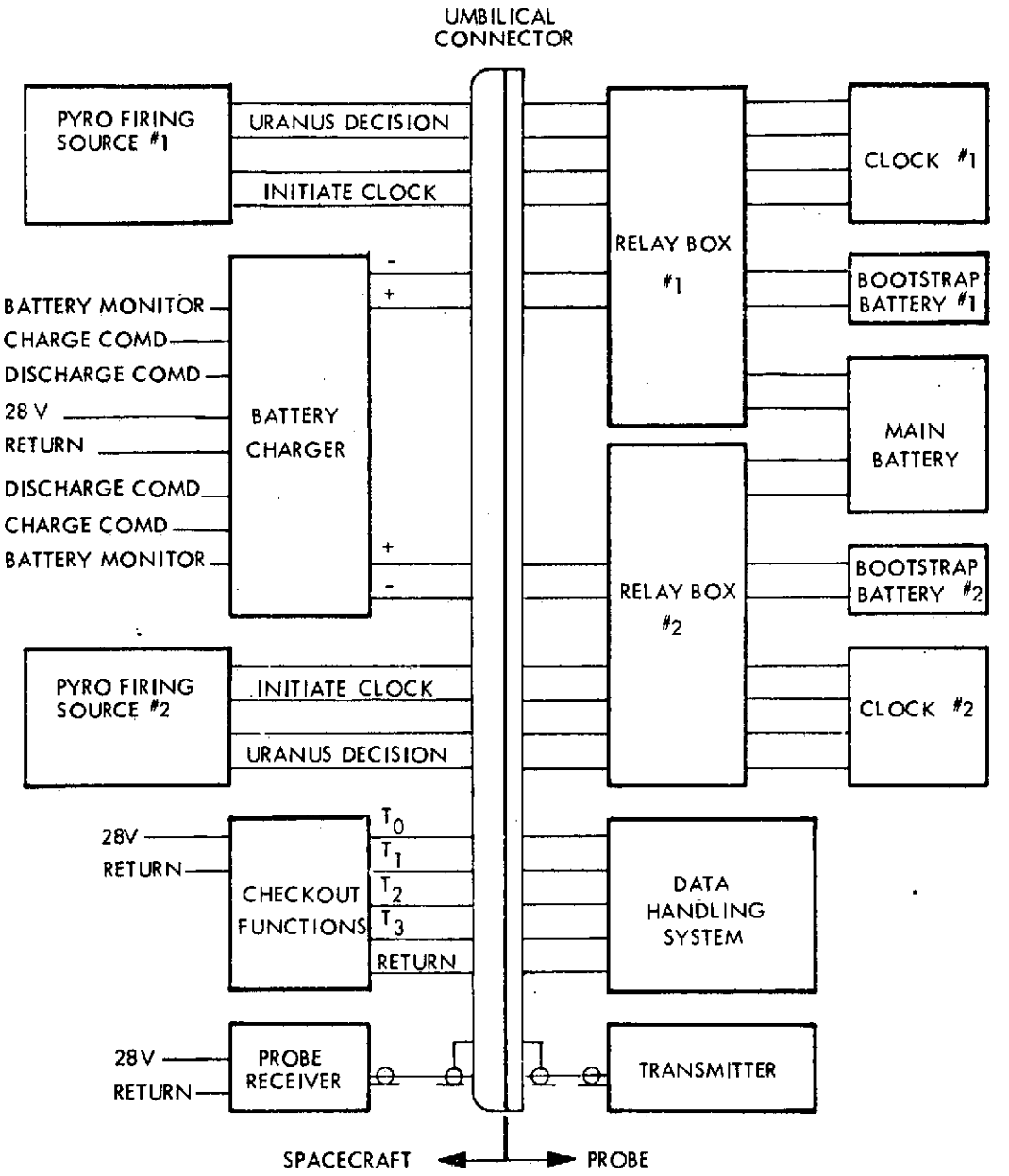

Figure 2-11. Probe to Bus Electrical Interfaces

Geometric parameters involved in this communication link are described in Figure 2-12. The major elements of the link which are located on the bus are shown in Figure 2-13. The receiver and data synchronizer, although physically located on the bus, will be provided by the probe contractor. Further details on the bus-probe data link may be found in Section 6.9.

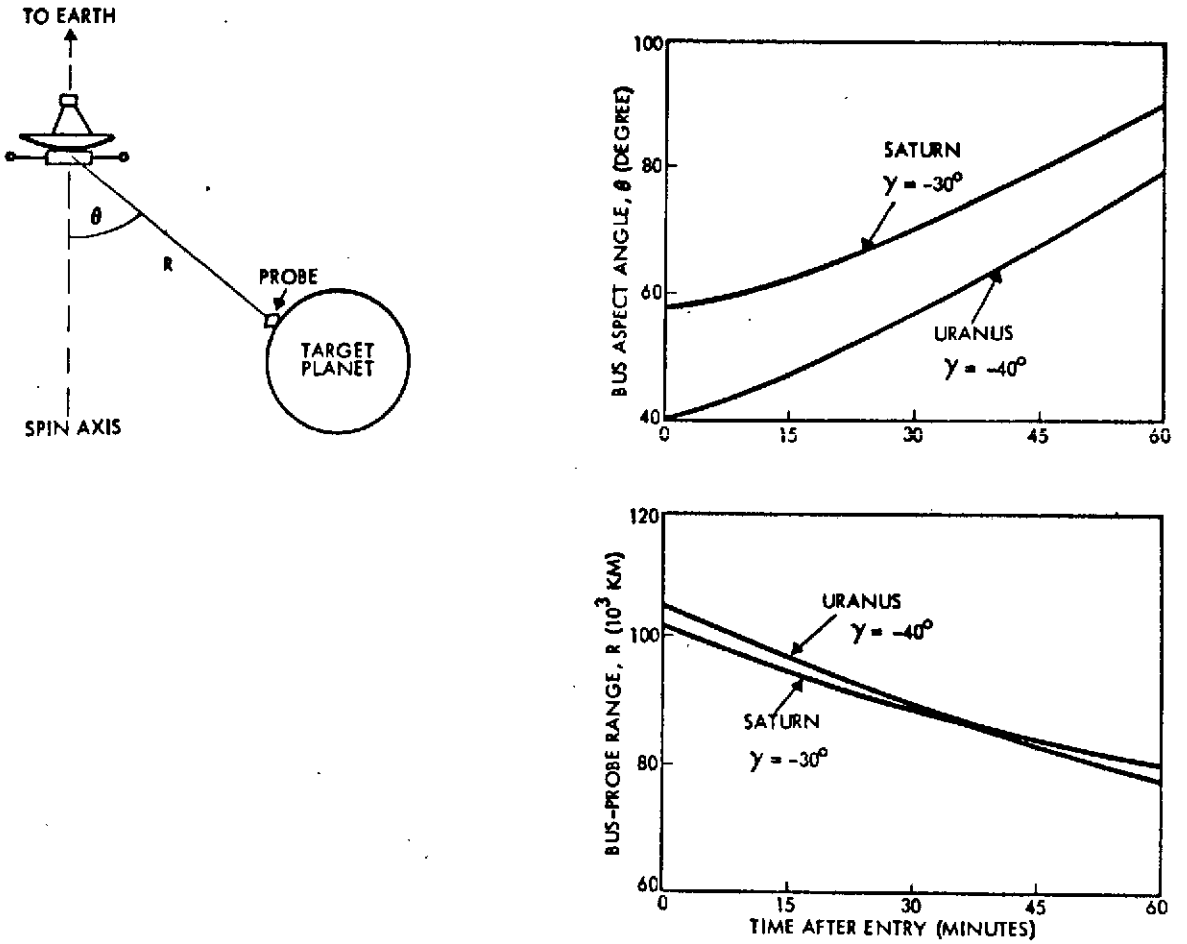

Figure 2-12. Probe-Spacecraft Communication Link Geometry

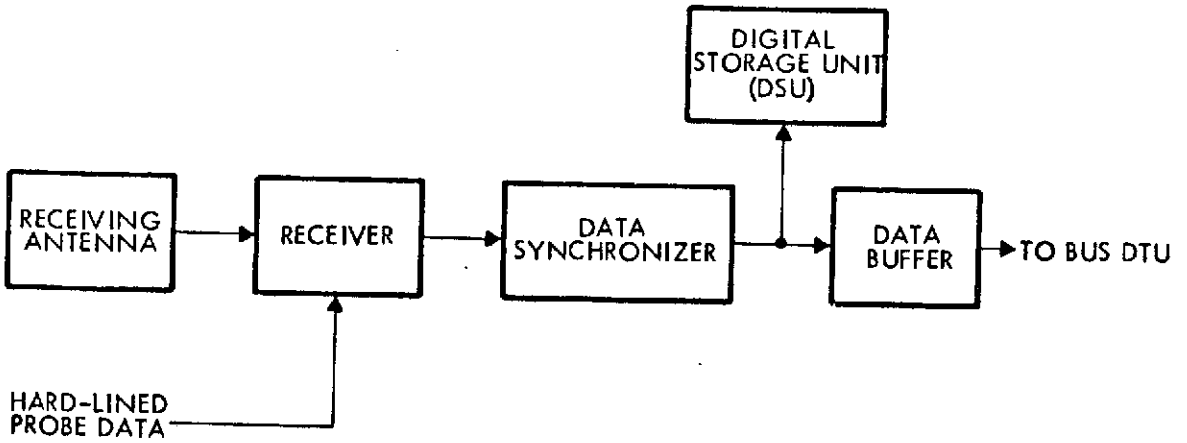

Figure 2-13. Probe-Spacecraft Communication Link (Spacecraft-Mounted)

2.2.1.5 Data Handling and Storage

As shown in Figure 2-13, probe data may be introduced into the bus receiver via the RF link or, while the probe is still attached, via the hardlined coax. In either case, a digital bit stream will be produced by the data synchronizer. (Note that on-board decoding of probe data is not part of the synchronizer functions.) This probe data leaves the synchronizer as a steady stream at 88 bps. Since this bit rate is asynchronous with the spacecraft DTU bit rate, some form of storage or buffering of the probe data is required prior to folding the probe data into the bus format.

In addition to the quasi real-time transmission of probe data via the bus telemetry link, the bus must store the entire probe message for subsequent retransmission in case of problems with the real-time data. This establishes a requirement for a digital storage unit (DSU) with a capacity of 88 bps times 4600 seconds or 404,800 bits.

2.2.2 Launch Vehicle

The launch vehicle for the SUAE mission is the Titan 3E/Centaur D-1T/TE-M-364-4. The launch vehicle for the Pioneer 10 and 11 spacecraft was the Atlas SLV-3C/Centaur D-14/TE-M-364-4. Thus the launch vehicle has a new first stage, a modified second stage, and the same third stage, as the previous Pioneers for Jupiter.

2.2.2.1 Nose Fairing and Envelope

The Viking nose fairing is to be used with the launch vehicle for this mission. While the 10-foot diameter fairing for Pioneers 10 and 11 (based on the OAO fairing) attaches to the forward end of the Centaur, the 14-foot diameter Viking fairing encloses the Centaur and attaches to the forward end of the Titan.

The dynamic envelope available for the spacecraft is increased from 109 inches to 150 inches in diameter. However, because the spacecraft design is not changed from the Pioneer F/G design except where necessary, the SUAE flight spacecraft does not occupy any space outside the 109-inch limit.

2.2.2.2 Payload Capability

The weight which can be sent to Saturn by the launch vehicle for the SUAE mission is discussed in Section 3.

2.2.2.3 Coast Capability

For launches to the outer planets in the months August to December, the departure from earth is at northerly declinations. With the launch site at Cape Canaveral, Florida, and with launch azimuths restricted to the usual ranges of about 90 to 110 degrees, these departures require long coast times (~50 minutes) in parking orbit. The Centaur D-1T stage will have this capability.

2.2.2.4 Mechanical Environment

The acoustic and vibration environment of the launch vehicle, while greater in some frequency bands than the Atlas, falls within the envelope specified for the qualification and acceptance testing of the Pioneer F and G spacecraft in Specfication PC210.03, Pioneer F and G Spacecraft Specification.

2.2.2.5 Launch Vehicle Adapter

The adapter connecting the flight spacecraft to the TE-M-364-4 stage is a modification of the standard 37-inch diameter by 31-inch adapter. The modification (a) lengthens the adapter to 36.38 inches so the probe will have adequate clearance from the third-stage igniter safe-and-arm device, and (b) moves the separation springs radially outward to require only one separation, i.e., the flight spacecraft from the launch vehicle, before the time of separation of the probe from the bus.

2.2.2.6 Umbilical

Because of the use of RTG's as the spacecraft electrical power source, and because RF communications with the spacecraft are used for inserting commands and monitoring results, no umbilical cable is necessary for spacecraft operations from RTG installation — normally about 30 hours before the launch window of the first launch day — until separation from the launch vehicle.

However, ground power (at 28 VDC) is required to support all spacecraft test operations on the launch vehicle prior to RTG installation.

Access to the electrical connectors of the probe will be available on the launch stand, but necessity for this access also ceases at some time well before launch.

2.2.3 Deep Space Network

The NASA Deep Space Network (DSN), utilizing stations at several longitude bands of the world, comprises the ground terminal for flight operations of the SUAE mission.

At the time this mission is flown there will be complete networks of three or more stations (approximately 120-degree spacing) with both 26- and 64-meter antennas, with these capabilities:

Antenna Diameter	Locations	Uplink	Downlink
26 meters	California Australia Spain South Africa	S-Band, up to 10 kW	S-band
64 meters	California Australia Spain	S-band up to 400 kW	S- and X-band

The performance characteristics of these stations are discussed in Section 6.6.

2.2.4 RTG's

The RTG's identified for the SUAE mission are modified versions of the multihundred watt (MHW) RTG which is currently under development for the LES 8 and 9 spacecraft to be launched in 1974 and is designated for use on the Mariner Jupiter Saturn spacecraft to be launched in 1977.

The RTG unit to be employed weighs 70 pounds and has a diameter of 15.7 inches and a length of 21 inches. It contains $Pu^{238}O_2$ as the heat source, producing 2000 watts of thermal power. A shell containing a matrix of silicon-germanium thermocouples converts 120 watts (soon after launch) into electric power which is delivered at 28 volts. A more detailed description of the RTG characteristics is given in Section 7.1.

2.2.4.1 Physical Arrangement

Two units are to be carried on each flight spacecraft, one on each side. The RTG units are in a stowed position, just outboard of the equipment compartment side panel, during launch. Soon after the spacecraft is separated from the launch vehicle, the RTG's are released to deploy some seven feet radially to their location for the remainder of the mission.

This remote location (a) minimizes accumulated interaction between the radioisotope and the components and instruments aboard the spacecraft, (b) establishes a favorable moment of inertia figure for the spacecraft – both the bus with the probe and the bus alone, and (c) virtually eliminates a thermal interaction between the RTG's and the other elements of the spacecraft.

2.2.4.2 Mechanical Interface

The RTG unit is attached to an RTG mounting plate by three bolts. The mounting plate is attached to the equipment compartment by bolts, when stowed; at deployment these bolts are severed by bolt cutters, and the mounting plate is connected to the equipment compartment by guide rods.

2.2.4.3 Thermal Interface

The thermal interface of the RTG with the spacecraft is significant only until deployment. Before launch, cooled air appropriately directed within the shroud keeps the RTG below vacuum operating temperatures, and keeps adjacent spacecraft temperatures low.

From liftoff to deployment (about 1.5 hours) temperatures of both will rise. Internal RTG temperatures are kept low by delaying the venting of the inert fill gas until after deployment. Adjacent spacecraft surfaces may have to withstand temperatures approaching 450°F. Appropriate coatings and kapton insulation will be applied as necessary.

2.2.4.4 Electrical Interface

Power is transferred from the RTG's at 28 Vdc via a cable which is drawn out of a slack box as the RTG is deployed. The spacecraft maintains the bus voltage at this value by dissipating excess power in a shunt circuit.

2.2.4.5 Nuclear Radiation

The nuclear radiation of the RTG's is composed primarily of gamma-ray photons in the energy range, 10 to 1000 keV and neutrons in the energy range, 1.5 to 5 MeV.

The only significant impact of the gamma rays is the potential interference with scientific instruments sensitive to radiation at this energy. This sort of interference, affecting instruments measuring intermediate-energy nuclear particle fluxes at low intensities, has been resolved on Pioneer F/G; the interfering flux levels are increased less than 50 percent on the SUAE Pioneer.

Neutron radiation should be examined for potential damage to components and materials. On the SUAE mission the longer duration and greater isotope weight will raise total neutron fluences at typical equipment compartment locations from 1.7×10^{10} to 7×10^{10} n/cm^2. However, for components utilized, 10^{12} or 10^{13} n/cm^2 would be the threshold of concern, so no impact is foreseen.

2.2.5 Bus Scientific Instruments

The instruments identified in the Statement of Work as a tentative bus payload complement are listed in Table 2-3.

Six of these instruments are identical to, or only slightly modified from the corresponding instruments carried by Pioneer 10 and 11. Their interface requirements with the spacecraft system also remain essentially unchanged.

Three instruments, the IR spectrometer, the line-scan image system, and the RF noise detector are new. Of these only the image system imposes new interfacing requirements that have an appreciable impact on system design as will be discussed below.

Table 2-3. Scientific Instrument Complement for the Spacecraft Bus*

Instrument	Pioneer F/G Type Instrument	Weight (Pounds)	Power (Watts)	Volume (In^3)	Samples per Minute	Bits per Sample	Bits per Second	Special Requirements
Magnetometer	X	5.5	3.0	240	30	24	12	Boom mounted sensor. Spacecraft magnetic constraints like Pioneer F/G
Solar Wind Analyzer	X	6.0	3.0	300	.5	120	10	Solar viewing 20° x 140°
Charged Particle Detector	X	6.0	3.0	240	5	140	12	90° clear FOV - point 90° to spin axis
I.R. Radiometer	X	7.5	3.0	320	5	60	5	20° clear FOV - point 45° off spin axis
I.R. Spectrometer		12.0	4.0	400	5	180	15	20° clear FOV - point 45° off spin axis
U.V. Photometer	X	6.0	2.5	180	10	32	6	45° clear FOV - point 45° off spin axis
Multispectral Line Scan Camera		14.0	10.0(1)	400	(1)	2×10^5	(1)	2° IFOV, 180° clear pointing FOV
R.F. Noise Detector		1.0	0.5	.80	10	24	4	1/4 wave whip antenna length ~ 24 inches
Micrometeoroid Detector	X	3.5	1.0	100	2	10	0.4	~12 penetration panels like Pioneer F/G
Dual Frequency R.F. Occultation	-	-	-	-	-	-	-	Uses S & X band transmitters. No special on-board instrumentation required
Total		61.5	30				64.4(3)	

(1) Time share with other instruments. Imaging on command. Requires on-board storage. Time-share readout of stored data or interleave with other science data.

(2) This experiment uses S-band and X-band channels on spacecraft (no extra payload equipment).

(3) Excluding the image system.

* Tentative list, as specified in NASA/ARC's Statement of Work

Table 2-4 gives a summary of these instrument's functional and physical interface requirements relevant to the design of the spacecraft. The magnetic cleanliness requirements imposed by the magnetometer are identical to those of the Pioneer F/G instrument.* Mounting and clear-field-of-view requirements are also like those in Pioneer F/G for the corresponding instruments. Most of them can be accommodated in the payload compartment dedicated to science instruments on Pioneer F/G or by the same external mounting provisions (e.g., magnetometer, meteoroid sensors). Weight requirements are comparable to Pioneer F/G, but conservative estimates may lead to a higher total than 61.5 pounds, the current tentative estimate. Power requirements, at 30 watts, are about 20 percent higher than for the Pioneer F/G payload.

The multispectral line scan image system presents some interface requirements of a special type, viz.

- High data rate requirements, typically 133 bps if 2 frames of 200 by 200 picture elements are obtained per hour.
- High data buffer storage capacity, i.e., 240 kb per 200 x 200 cell frame, 0.96 megabits for 400 x 400 cells.
- Rotational mount for the camera or a gimballed mirror to vary the cone angle is required.
- Careful selection of mounting area on spacecraft to avoid stray light effects and to provide a wide pointing field of view. (110 degree range of cone angles).
- Comparably high power requirement for camera and gimbal actuator (10 to 15W).
- Mode switching for multispectral options.
- Special provisions required to shield the camera and sensor elements against inadvertent exposure to sun and to protect objective lens against long exposure to potential micrometeoroid damage.

Some of the image system interface requirements are not unlike the requirements imposed by the Imaging Photo-Polarimeter (IPP) of

*However, these requirements are not imposed on the probe design, or if they are, at a lower priority than other probe design criteria.

Table 2-4. Summary of Payload Interface Aspects

Instrument	Interface Aspects
Magnetometer Solar Wind Analyzer Charged Particle Detector I.R. Radiometer	• No change from Pioneer F/G
I.R. Spectrometer	• Potential weight problem (> 12 pounds), requires development
U.V. Photometer	• No change from Pioneer
Multispectral Line Scan Camera	• Requires gimbal mounted camera or mirror • Attention to stray light interference necessary • High data volume and bit rate accommodated without increasing system capacity (time-sharing) • Physical protection necessary during long dormant periods
R. F. Noise Detector Micrometeoroid Detector	• Minor change • No change from Pioneer F/G
Dual Frequency RF Occultation	• Uses available S-band and X-band channels

Pioneer F/G which is not included in the SUAE mission payload. The mode switching, line-of-sight rotation, and clear field-of-view requirements of the two instruments are similar.

Actually some interface aspects of the line-scan camera are less demanding than those of the IPP. The instrument is inoperative except for periods of a few days at the time of the Saturn and Uranus encounters. It does not require the sequence of frequent cone angle changes necessary for the IPP, and less complex data processing is required on the ground to reconstruct image frames.

In summary, the interface requirements of the proposed science payload do not impose unique design problems on the spacecraft and its subsystems; in most cases the interface aspects are the same as with the payload of Pioneer F/G. Telemetry and data storage resources to be allocated to the line-scan image system are comparable to, and can be time-shared with those required to support the entry probe data relay requirements.

2.3 ENVIRONMENT

Some design features and operational modes of the SUAE spacecraft, different from those of Pioneer F/G, are dictated by the changed environment in which this spacecraft must operate. These environmental conditions are discussed below with emphasis on major differences from the Jupiter flyby mission environment.

2.3.1 Launch Environment

The Titan III E/Centaur/TE-364-4 acoustic and vibration environment is included in the specification PC 210.03 to which Pioneer F/G was developed and qualified. Thus, no requalification of the spacecraft for the new launch vehicle is necessary. However, the increased mass moments of the longer and much heavier SUAE flight spacecraft introduces greater structural/dynamic loads on the launch vehicle and third-stage adapter. This subject is discussed in Section 6.1 and Appendix F.

The vehicle follows a launch and injection sequence different from Pioneer 10 and 11 since a 50-minute coast in parking orbit is required prior to the interplanetary injection burn. This is followed by a possible

delay of appendage deployment to permit verification and control of deployment events from the ground. Prolonged (up to 80 minutes) thermal radiation of the stowed RTG units on adjacent portions of the flight vehicle can be of some concern, but adverse effects are avoided by selecting an appropriate RTG deployment and venting sequence (see Section 6. 2. 3).

2. 3. 2 Thermal Environment

The only concern with an adverse thermal environment in this mission arises from the possible exposure of the probe interstage adapter and the protruding probe entry cone to a side-sun condition during the first 50 days after launch, if the flight spacecraft is maintained in an earth-pointing mode for medium and high-gain communication coverage. However, to minimize the thermal load on the probe, a compromise with communication requirements can be made during this initial mission phase where omni-antenna coverage still provides adequate telemetry rates.

This flexibility in pointing requirements is illustrated in Figure 2-14. The graph shows the angular variation of the spacecraft-earth and spacecraft-sunlines versus time from launch. A second scale on the abscissa gives the earth spacecraft distance. It can be seen that during the first 50 days of the mission the entry probe would be exposed to continuous side-sun heating if the spin axis were fully oriented to the earth. A zone of ± 28 degrees is shown on both sides of the sunline which corresponds to spacecraft orientations that assure probe shading. This zone is overlapped by another zone (slanting downward to the right) in which communication coverage by the medium- and low-gain antennas could be interrupted because of nulls in the combined antenna pattern. The null-zone can be avoided by orienting the spin axis either closer to or further from the earthline. A family of constant bit rate contours (64, 256, and 1024 bps) also plotted in the graph indicate the decrease in telemetry data rate with increasing communication distance and offset angle from the earthline. The curves show that large offsets can be used initially to protect the probe against solar heating without loss of telemetry coverage.

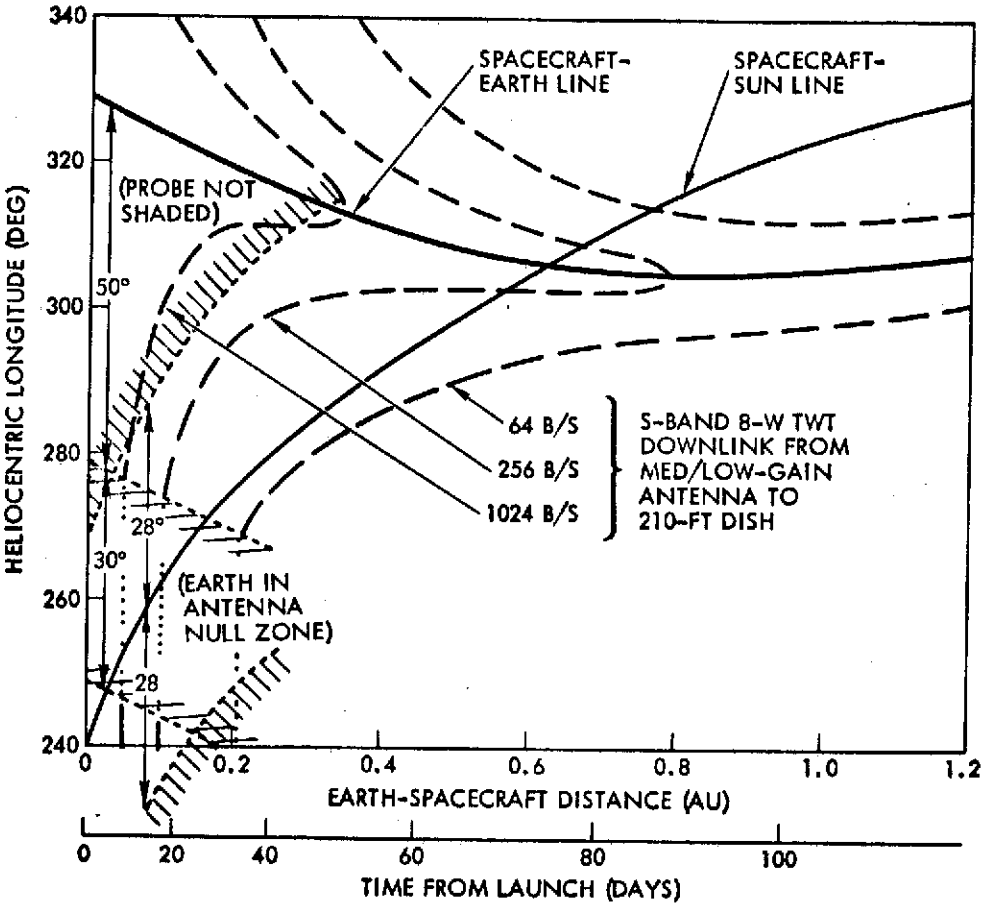

Figure 2-14. Early Mission Orientation to Shade Probe

Reorientation of the spacecraft for the initial midcourse correction and trim maneuvers may also expose the probe to direct solar heating, depending on the required thrust direction. However, since such maneuvers can be completed within a few hours even in the worst case no significant probe heating effects will be experienced.

For the remainder of the mission the thermal environment does not present problems that differ in principle from those experienced by Pioneer 10/11. Conditions that exist at solar distances up to 20 AU (Uranus) and beyond can be met by provision of appropriate thermal insulation and local heaters.

2.3.3 Meteoroids and Saturn Ring Particles

Exposure of the spacecraft to micrometeoroid impact in interplanetary space and in the vicinity of the large outer planets, especially to impacts sustained in crossing the plane of Saturn's rings at distances

of 2.3 and 2.75 planet radii (see the nominal Earth-Saturn and Earth-Saturn-Uranus mission profiles in Section 3.2), is a matter of concern regarding spacecraft survival.

Without further analysis it is apparent that the meteoroid hazard is not serious, even for a seven-year exposure in the ESU mission, when extrapolating from the low impact rates experienced during the first 18 months of the Pioneer 10 mission. The spacecraft, designed to survive the originally estimated relatively high flux density of the asteroid belt, ($N = 10^{-13}$ particles per m^3 of mass $\geq 10^{-3}$ at 2.5 AU), actually encountered a flux density which was several orders of magnitude lower than anticipated.

With regard to particle impacts on the spacecraft during the instant of crossing the plane of Saturn's rings, a preliminary estimate of an upper bound of the integrated flux of particles of various sizes was obtained based on the current model of particle flux density in Saturn's rings, as defined in NASA SP-8091.* Upper bounds were calculated for the cumulative number density of particles of various sizes at the perimeter of the outer ring (A), at $R = 2.30\ R_S$. The vehicle's relative velocity (11.4 km/sec) is inclined relative to the ring particles' velocity vector such that the particles strike the vehicle from the rear, at an angle of about 45 degrees from the -Z axis. Estimated upper bounds of hits sustained by the equipment bay and the area of the propellant tank not shielded by the equipment mounting platform are given in Table 2-5. The exposed equipment bay area is about 1.5 m^2 and the exposed area of the propellant tank is 0.12 m^2.

Figure 2-15 shows a plot of the calculated upper bounds (solid curves) of impacts versus particle size and mass. A less conservative assumption of impact is given by the dashed curves in Figure 2-15. It is estimated that particles of 10^{-2} grams (i.e., of radius $r_i = 0.3$ cm, assuming a density $\phi_P = 1$ gram/cm^3) would cause 0.3 hits on the equipment bay and only 0.025 hits on the exposed propellant tank area. This may be interpreted as a hit probability of 30 and 2.5 percent, respectively.

*Space Vehicle Design Criteria (Environment); the Planet Saturn (1970), Section 3.6.4.

Table 2-5. Upper Bound of Number of Hits Sustained by the Spacecraft Equipment Bay and Propellant Tank during Saturn Ring Plane Crossing (Earth-Saturn Mission)

Number of Hits N_i		By Particles of	
Equipment Bay	Propellant Tank	Radius r_i (cm) or larger	Mass m_i (grams) or larger
4.7	0.38	0.1	4.2×10^{-3}
3.1	0.24	0.133	0.01
0.96	0.08	0.287	0.1
0.31	0.02	0.62	1.0

Results based on: Ring crossing at 2.3 Saturn radii; relative velocity: 11.4 km/sec; velocity component ⊥ to ring plane: 8 km/sec; intercept angle relative to spacecraft -Z axis: 4.5 degrees. Exposed equipment bay area: ~1.5 m^2, exposed propellant tank area: 0.12 m^2; assumed particle density: 1 gram/cm^3.

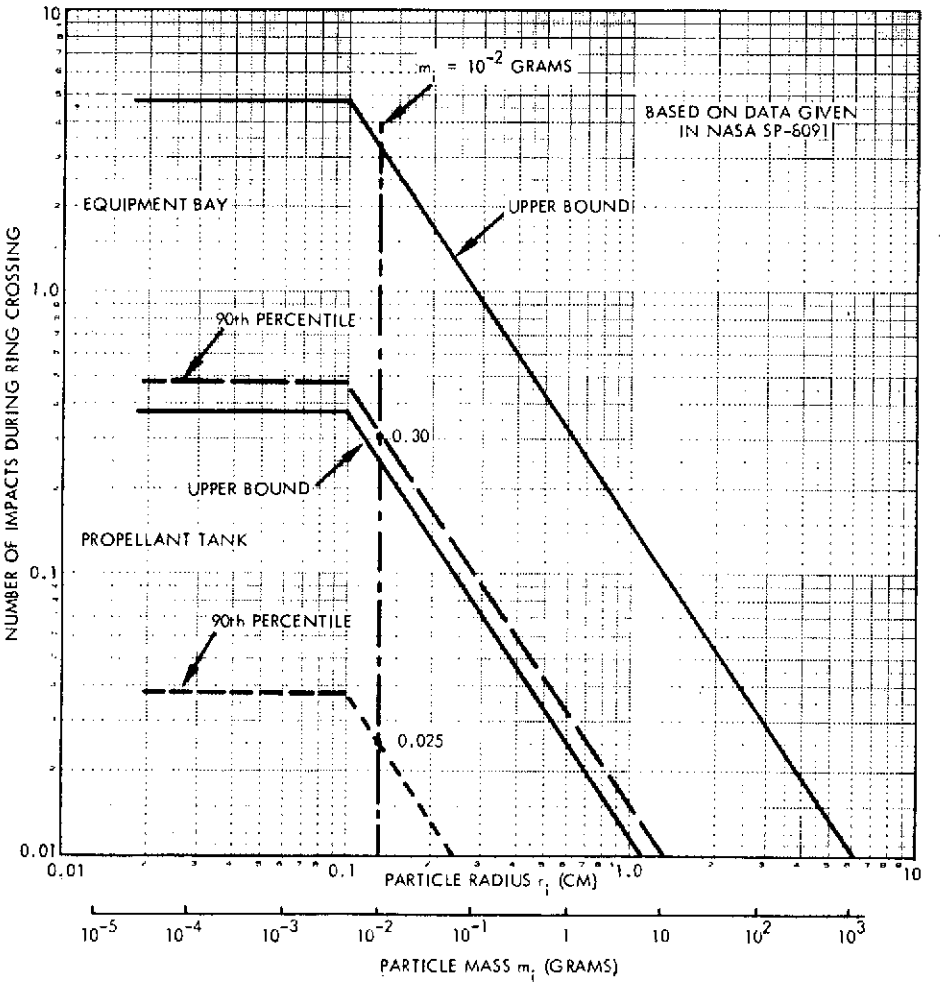

Figure 2-15. Estimated Impacts Sustained During Saturn Ring Crossing

We note that just inside the perimeter of ring A or R = 2.29 R_S i.e., 600 km closer to the planet) the estimated particle number density in NASA's model is six times greater than at 2.30 R_S. In the ESU mission the ring plane crossing occurs at a larger distance (R = 2.75 R_S) than in the ES mission, but according to NASA's model the integrated flux density is assumed to be unchanged at this location. The nominal trajectory crosses the ring plane at a steeper angle thus increasing the particle approach angle relative to the -Z axis to 67 degrees. Comparing the ES and ESU missions it should be noted that in the former the entry probe is no longer carried by the bus at the time of the ring plane crossing so that the propellant tank is partly exposed. In the ESU mission the probe is protected on the exposed side by the insulation blanket and heat shield. Other portions of the probe are enclosed by the interstage adapter cone which provides effective shielding.

Actually, the results obtained indicate that unless a more severe particle environment in the outer ring area is established by the current series of DSIF radar observations of Saturn, the probability of damage during ring crossing is reasonably small.

2.3.4 Radiation Environment of Saturn and Uranus

The existence of radiation belts at Saturn and Uranus has been postulated based on the observation of UHF radio emission from these planets and on the assumption that the mechanism of producing radiation belts in the presence of strong magnetic fields is similar to that at Jupiter. However, as discussed in the Design Criteria Documents NASA SP-8091 and SP-8103 it is plausible that the number density, flux and energy of radiation belt particles are much weaker than at Jupiter. With large spacecraft flyby distances of 2.3 to 2.75 Saturn radii and 4.0 Uranus radii, respectively, it is unlikely that radiation belt exposure should present a significant hazard to the spacecraft. However, from a scientific standpoint observation of charged particle flux and energy during closest approach is definitely an important objective. An approximate analysis of quantitative characteristics of the radiation belt environment experienced by the spacecraft based on the referenced upper-limit estimates is given in Section 2.6.3.

It is of interest to note that existing models of Saturn's radiation belt predict that the presence of ring particles tends to depopulate the radiation belt at distances below 2.3 R_S. At the nominal periapsis distances of 2.3 R_S and 2.75 R_S and during approach and departure the spacecraft traverses regions where trapped particle characteristics should be measurable.

In the case of the Uranus encounter observability of trapped particles is probably reduced, not only because of the larger relative distances of the flyby trajectory, but also because of the orientation of the planet's magnetic field. The spacecraft will arrive at Uranus at a time when its geographic pole and, therefore, probably also its magnetic dipole axis are pointing nearly in the direction of the sun. The mechanism believed to produce radiation belts of trapped solar wind particles is therefore weakened in that time period. However, residual belts may still be present from a period of more favorable orientations of the magnetic field with respect to the solar wind as mentioned in SP-8103. The Uranian radiation belt could possibly also be populated by charged particles of galactic rather than solar origin.

2.4 MISSION REQUIREMENTS

Principal mission requirements that differ from those of the Pioneer 10 and 11 Jupiter flyby missions are listed below, and their impact on spacecraft design and operations is summarized.

Launch via Parking Orbit. This launch mode which includes a 50-minute coast period is dictated by the large northern declination of the departure asymptote (see Section 3.3). This necessitates control of the injection burn from a remote ground station such as the Guam STDN facility or a ship stationed in that region of the Pacific. It may also cause delays in the deployment sequence until the spacecraft can be monitored and commanded by a ground station located further East (e.g., Hawaii).

Trajectory Corrections in the Earth-Pointing Mode. Almost all major trajectory corrections, some of them with large ΔV components normal to the earthline, must be executed in the earth-pointing mode to

assure uninterrupted communications coverage by the high-gain antenna. This requires the use of lateral thrust, usually in combination with axial thrust (see Section 3. 5). A pair of radial thrusters are provided for this purpose. Since radial thrust can only be exercised in a series of short (1 to 2 second) pulses, the ΔV maneuver will usually extend over many hours. Precession coupling must be compensated by intermittent use of the axial precession thrusters, and time-consuming intermittent ground verification of this process is necessary (see Section 3. 6).

Approach Navigation and Guidance. Unlike the Pioneer 10 and 11 Jupiter flyby missions which can be controlled with sufficient accuracy by radio-guidance from Earth, a mission to Uranus via Saturn would be too inaccurate without the use of an added onboard sensor. This sensor uses stars and bright satellites of the target planet for optical navigation fixes (see Section 3. 7). The navigational data thus obtained are used by the ground station, in addition to radio tracking data, for updating the trajectory relative to the target planet and for determining the required correction maneuver. For a mission to Saturn only this requirement is not critical. However, for the ESU mission optical navigation fixes are essential (1) at Saturn to minimize the post-swingby trajectory correction, and (2) at Uranus to eliminate the effect of that planet's very large ephemeris uncertainty.

Trajectory Deflection of the Bus Spacecraft After Entry Probe Separation. System analysis and capability tradeoffs performed early in the study led to selection of a mission profile where the spacecraft bus delivers an inert entry probe on a direct planet intercept trajectory. The bus then executes a deflection maneuver to retarget its own approach trajectory. Thus, the bus achieves a flyby altitude and arrival time compatible with the requirement of functioning as relay communication link for entry probe telemetry data (see Section 3. 5). The alternative of delivering a maneuverable entry probe was ruled out in the interest of probe design simplicity. Since the magnitude of the required deflection ΔV depends strongly on the time of execution prior to the planetary encounter it is essential that the probe separation take place as early as possible, 20 to 30 days before arrival.

Thus, timing of the terminal guidance maneuver which must precede probe separation also becomes critically important. This in turn requires that the target satellite be acquired early and the navigational fix be completed shortly thereafter. These time constraints indicate that performance characteristics of the navigation sensor (namely sensitivity and angular resolution) have a direct influence on the amount of propellant to be carried by the bus. Sensor performance can be traded against an increase in propellant mass.

Bus Science Objectives and Operations. Bus spacecraft scientific objectives during the cruise and planet encounter phases are basically similar to those of Pioneer 10 and 11 (see Section 4). However, with planetary atmosphere exploration by the entry probe a principal mission objective, some restriction of the bus science payload and operational capability is necessary to keep the total program cost within current NASA budget planning guidelines. An important consideration in that context is the performance envelope of the Titan III E/Centaur class of boosters which limits the gross weight of the SUAE flight spacecraft at the required injection energy (C_3 = 142 km^2/sec^2) for the ESU mission to 1050 pounds. This permits a weight allocation of about 60 pounds to bus science, slightly less than in the case of Pioneer 10 and 11 (see Sections 4 and 5). The proposed bus payload includes six instruments of the Pioneer 10 and 11 payload, plus three new instruments, one of them a high-resolution multi-spectral line-scan imaging system which will replace the spot-scanning imaging photopolarimeter carried by Pioneer 10 and 11 (see Section 4).

The bus science payload can be operated during the planetary encounter, which includes the approach phase and the occultation phase following the probe entry phase, without interfering with the priority requirements of the relay telemetry and data handling support functions to be provided to the probe. This may necessitate interruption of image data acquisition during the probe entry phase. The mission profiles also include planetary encounters without probe delivery, viz. Saturn flyby in the case of the ESU mission, and Uranus flyby following the probe mission to Saturn, such that bus planetary science observations are unconstrained by probe support functions.

Probe Data Relay Requirements. The data relay requirement dictates the choice of the bus spacecraft encounter trajectory, i. e., position and time of arrival relative to the probe entry time, (see Section 3). The relay link geometry in turn governs the selection and location of the link antenna onboard the bus spacecraft.

In addition to transmitting probe telemetry data in real time during the 1 to 1.2 hours of the probe's atmospheric entry phase, the bus will also be required to store and retransmit the probe data as a safeguard against downlink contingencies that may cause data loss. This process will be repeated until stopped by ground command.

Due to the long communication round trip delay time involved the rebroadcasting of probe data may have to be extended until after the occultation phase following the planet flyby. During this time interval the storage and telemetry of probe data takes priority over the handling of bus science data.

Ground Verification of Critical Events Subject to Long Communications Time Delay. The communications round trip time at planet encounter is two to four times larger than in the Pioneer 10 and 11 Jupiter flyby. This imposes a significant constraint on command and verification sequences, that must be carefully considered in flight operations planning (see Section 3.6 and 3.7). The delay is 2.6 hours at Saturn and 5.4 hours at Uranus. Flight operations that are inconvenienced particulary by the long round trip delay include conscan procedures with ground verification, precession, spin correction and ΔV maneuvers, navigation fixes, probe checkout and pre-separation procedures, probe data relay and bus science operations at planet encounter.

The delay time can also interfere with routine calibration and verification procedures, and will make troubleshooting and mode switching in the case of system malfunctions more time consuming. This requires provision of various automatic backup modes in attitude control, data handling and storage, command sequencing, telemetry, and power system operation (see Section 6).

2.5 SUMMARY OF FLIGHT OPERATIONS

Mission requirements and their effect on flight operations have been discussed in the preceding section. The sequence of major events from launch to flyby at the target planet is given in Table 2-6. Flight operations that are critical to mission success are listed below.

1. Launch and Spacecraft Deployment

   - Must safeguard against dynamic instability and high structural loads during deployment
   - Detailed deployment sequence differs from Pioneer 10 and 11 (e. g. , simultaneous release of appendages).

2. Precession Maneuvers

   - Required throughout mission, initially at frequent intervals due to higher earth-line rotation rate
   - Conscan technique determines angular offset and correction requirement

3. ΔV Maneuvers

   - Initial midcourse maneuver and trim maneuver performed with spacecraft reoriented for desired thrust direction (axial thrusting)
   - All other maneuvers, e. g. , planet approach, guidance corrections, and retargeting maneuver after probe separation in earth-pointing mode
   - Radial thrust maneuvers require compensation of unintended precession effects; extended maneuver sequences

4. Planet Approach Navigation

   - Essential at Uranus because of large (10, 000 km) ephemeris uncertainty
   - Also required on Saturn approach of ESU mission to minimize post-flyby ΔV maneuver
   - Early acquisition of target satellite by optical navigation sensor required
   - Star references give accurate indication of spin axis pointing and of target offset angles in terms of spacecraft cone and clock angles

Table 2-6. Summary Mission Sequence of Events

A. NEAR EARTH

NO.	TIME AFTER LAUNCH	EVENT	REMARKS
1	0	LIFTOFF TO INJECTION	
2	1 - 6 HOURS	SEQUENCER-INITIATED EVENTS ON SPACECRAFT	INCLUDES DESPIN, DEPLOYMENT OF APPENDAGES, AND INITIAL ORIENTATION
3	4 DAYS, AND PERIODICALLY THROUGHOUT MISSION	EARTH POINTING (MAY HOLD CLOSER TO SUN POINTING FOR 50 DAYS TO SHADE PROBE FROM SUN)	OPEN-LOOP OR CLOSED-LOOP (CONICAL SCANNING) PRECESSION
4	5 DAYS	FIRST TRAJECTORY CORRECTION MANEUVER	PRECESSION, ΔV, AND RETURN PRECESSION MANEUVERS
5	20 DAYS	SECOND TRAJECTORY CORRECTION MANEUVER	

B. NEAR SATURN (ON SWINGBY TO URANUS)

NO.	TIME FROM SATURN ENCOUNTER	EVENT	REMARKS
1	-20 TO -10 DAYS	TERMINAL GUIDANCE SENSING	USE ONBOARD STAR MAPPER
2	-8 DAYS	APPROACH TRAJECTORY CORRECTION MANEUVER	ΔV IN EARTH-LINE MODE
3	-10 TO +10 DAYS	ENCOUNTER SCIENCE	
4	+20 DAYS	DEPARTURE GUIDANCE SENSING	USE STAR MAPPER
5	+40 DAYS	DEPARTURE TRAJECTORY CORRECTION MANEUVER	ΔV IN EARTH-LINE MODE

C. NEAR TARGET PLANET

NO.	TIME FROM SEPARATION*	EVENT	REMARKS
1	-20 TO -3 DAYS	TERMINAL GUIDANCE SENSING	USE STAR MAPPER
2	-2 DAYS	APPROACH TRAJECTORY CORRECTION MANEUVER	ΔV IN EARTH-LINE MODE
3	-2 DAYS	CHECKOUT PROBE OPERATION	
4	-2 DAYS	CHARGE PROBE BATTERY	
5	0 DAYS	DISCONNECT PROBE ELECTRICAL CONNECTOR	ORDNANCE EVENTS INITIATED BY SPACECRAFT
6	0 DAYS	SEPARATE PROBE FROM SPACECRAFT	
7	+1 DAY	SPACECRAFT TRAJECTORY CHANGE MANEUVERS	ΔV IN EARTH-LINE MODE PLACES SPACECRAFT ON APPROPRIATE FLYBY TRAJECTORY
	TIME FROM ENCOUNTER		
8	-10 DAYS	SPACECRAFT TRAJECTORY TRIM MANEUVER (IF NECESSARY)	
9	0	ENTRY PHASE OF PROBE	PEAK DECELERATION AND ENTRY HEATING
10	+1 MINUTE	ESTABLISH PROBE-BUS COMMUNICATIONS	AFTER BLACKOUT
11	+60 MINUTES (APPROXIMATELY)	END OF PROBE DESCENT PHASE	PROBE IS BELOW 10-BAR LEVEL
12	+70 MIN (SATURN) +100 MIN (URANUS)	SPACECRAFT IS AT PERIAPSIS	$R_p \cong 2.25\ R_S,\ 4\ R_U$
13	+3 TO +6 HOURS (SATURN) +7 TO +10 HOURS (URANUS)	SPACECRAFT OCCULTATION BY TARGET PLANET	

*SEPARATION IS NOMINALLY 32 DAYS BEFORE ARRIVAL AT SATURN, 20 DAYS BEFORE ARRIVAL AT URANUS.

- Spacecraft orbit determination performed by ground station based on telemetered navigation fixes and radio tracking data
- Required approach guidance maneuvers executed on ground command

5. Planetary Departure Navigation (at Saturn)

- Required to minimize midcourse maneuver at start of Saturn-to-Uranus cruise
- Saturn's satellites sufficiently bright for navigation fixes even under unfavorable aspect angles

6. Probe Checkout, Pre-separation and Separation Procedures

- Bus initiates commands to probe checkout circuits via umbilical
- Bus telemeters probe engineering data
- Bus actuates pre-separation ordnance firing sequence on probe
- Bus actuates ordnance for umbilical cable cutter and release of retention bolts, initiating probe release

7. Relay Telemetry of Probe Entry Data

- Bus receives probe entry data on 400 MHz relay link and retransmits to earth in real time
- Bus also stores probe data and retransmits to earth after probe expiration

8. Bus Science Operations

- Cruise science operations as in Pioneer 10 and 11. Extended beyond Uranus if possible
- Encounter science operations as in Pioneer 10 and 11, except as required by new payload instruments
- Gimballed line-scan imaging system pointed at planet and operated on ground command, at most two frames per hour
- Imaging system pointed at observable satellites and operated on ground command
- Imaging operations discontinued during probe data relay operation if inadequate data storage capacity available
- Dual frequency (S-/X-band) occultation experiment conducted at planet (and if possible, at satellite) occultation. Also during Saturn's ring occultation periods.

2.6 RELIABILITY

The primary concern of reliability in the SUAE spacecraft compared with the Pioneer F/G spacecraft, is the lifetime extension from 2.5 to 7 years. This concern is mitigated by several factors:

- Integrated exposure to solar originating environments is not increased, because of inverse square-law effects
- There is no exposure to the Jovian radiation belts
- In terms of thermal extremes and anticipated meteoroid flux, the extended part of the mission entails the more benign environment
- Anomalies not related to depletion or wear-out factors would be expected at a lower incidence rate during the extended part of the mission.

For operational reasons, certain components of the spacecraft are in line (in the reliability sense) at later times in the SUAE mission than their counterparts in the Pioneer F/G mission, and redundancy has been implemented accordingly. Examples are attitude reference sensors and spin control thrusters.

2.6.1 Fail-Safe Design Policy

For the SUAE mission the following fail-safe policy is proposed and observed:

> The spacecraft should be designed with appropriate redundancy, workarounds and backup capabilities which will eliminate as many electronic, mechanical, and electromechanical failure modes as sources of spacecraft failure as practical. When redundancy or backups are employed, circuits, interfaces between units, and switching circuits should be designed with fault isolation so that a failure inone unit does propagate into, or does not interfere with the operation of, the redundant units or backup modes.
>
> Electrical or electromechanical random single-point failures should be eliminated from equipment which must successfully operate at a high duty cycle throughout the mission, and from equipment which is especially critical to the success of the mission. For the purposes of this single-point failure criteria, failure or degradation from predictable wearout shall not be regarded as random, and the design should be capable of surviving a single-random failure in addition to expected wearout failures.

The spacecraft should be designed so that it can survive failures occurring when the spacecraft is not being monitored by the ground, since those that occur in deep space require long periods for telemetry detection, problem diagnosis and corrective command transmission.

The above policy is intended to be a firm guideline to the spacecraft design, but is not intended to be inviolate or inflexible. In implementing the policy in specific cases, competing factors – such as cost, practicality, schedule, weight, redesign or repackaging of existing equipment, possible introduction of higher probability failures, increased risks of operator errors, etc. – should be taken into account and possibly weigh heavier than the above reliability policy.

However, it should carry more influence in establishing the spacecraft design than numerical reliability calculations, because the assumptions underlying numerical calculations – exponential probability of failure – have questionable applicability to this class of mission.

2.6.2 Single-Point Failures

The following single-point failure considerations apply in the SUAE spacecraft:

a) Spin Control. As in the Pioneer F/G design, the primary control of spin rate is in two non-redundant thrusters – one to spin up, and the other to spin down. In Pioneer F and G, no backup thrusters were provided, because, in the normal mission, spin rate changes are not required after 20 days (the second midcourse maneuver).

   In the SUAE mission, however, because ΔV maneuvers must be performed late in the mission (after probe separation at the target planet), spin coupling of ΔV thrusters could require spin rate corrections. The SUAE spacecraft does not add redundant spin control thrusters, but the two radial thrusters added for lateral ΔV maneuvers are canted slightly so that they can act to backup the spin control thrusters. This backup can be effected with no cost in propellant if it is done during a lateral ΔV maneuver (when it would most be needed); but it can be done anytime if propellant reserves permit an inefficient mode.

b) Deployment Dampers. Each deployed appendage — two RTG's and the magnetometer boom — has a single rotary viscous damper to restrain the rate of deployment. As in Pioneer F/G, this component is nonredundant. This is justified by the fact that the component is used only once, and only on the first day of the mission. Also, because the three appendages should be matched in their deployment times, a redundant damper in actual use would upset this balance.

c) Propulsion System. As noted above the radial thrusters serve as a redundant backup to the spin control thrusters. They are also redundant to each other. In fact, with operational penalties, the spin control thrusters can perform the function of the radial thrusters (lateral ΔV). As on Pioneer F/G, the four velocity precession thrusters are a redundant set; any one thruster could fail, and all required functions could be performed.

The propellant tank, including its bladder and pressure gauge, is nonredundant. This single-point failure possibility is tolerable primarily because of the great weight and space penalty which would be incurred to attain true redundancy.

d) Conscan Signal Processor. This unit is nonredundant, as it is in the Pioneer F/G design. The function is twofold: to determine, by use of the spacecraft's offset antenna pattern and reception of uplink transmission, the magnitude and direction of the pointing error of the spin axis from the earthline; and to control precession thrusters which will correct this pointing error.

On Pioneers 10 and 11 the conscan unit has been used often for attitude determination, but only infrequently for controlling the correction maneuver. (Mostly, attitude has been controlled directly by open-loop precession commands.)

However, there is an operational mode in which the pointing error is determined from the downlink transmission by similarly processing on the ground the signal received at the DSN station. The SUAE spacecraft, having a permanently offset S-band antenna feed, is less likely to have either the primary or backup modes of attitude determination unavailable because of spacecraft equipment failure.

2.6.3 Radiation Environment

Table 2-7 summarizes the fluences of radiation by nuclear particles for Pioneer F/G and for the SUAE spacecraft, and the estimated tolerances of the Pioneer F/G design to this radiation.

Table 2-7. Radiation Fluences and Tolerance

	Species					
	Neutrons(1)		Electrons		Protons	
	Fluence	Energy	Fluence	Energy	Fluence	Energy
Pioneer F/G:						
• RTG's	$1.7 \cdot 10^{10}$	1-5 MeV				
• Jovian radiation belts ($R_p=3R_J$):						
Specification (2)			$5 \cdot 10^{10}$	5-100MeV	$5 \cdot 10^{10}$	0.1-4 MeV
Maximum estimate(3)					$5 \cdot 10^{13}$	20 MeV equivalent
SUAE Mission:						
• RTG's	$7 \cdot 10^{10}$	1-5 MeV				
• Saturnian radiation belts ($R_p=2.3R_S$):						
Maximum estimate based on SP-8091(4)			$1.5 \cdot 10^{11}$	1-10 MeV	$3 \cdot 10^{10}$	2-100 MeV
Threshold of concern over damage (Pioneer F/G design)	10^{12}-10^{13}	1-5 MeV	10^{11}	5-100 MeV	10^{11}	20 MeV equivalent

Notes:

All fluences are in particles/cm^2

(1) Neutron fluences are estimated for typical locations in the equipment compartment for 2.5 years (Pioneer F/G) and for 7 years (SUAE).

(2) Integration of fluxes given in PC210.02, Pioneer F/G Spacecraft Specification, 1969.

(3) Integration of maximum fluxes given by Brice, Kennel, Thorne, Coroniti, JPL Workshop on Jovian radiation belts, July 1971.

(4) Integration of maximum fluxes given in SP-8091.

The neutron radiation is entirely that due to the radioisotopes aboard, of which the RTG power sources are by far the greatest contributor. This effect has been discussed in Section 2.2.4.

The electron and proton environments indicated are entirely due to planetary trapped radiation belts – Jupiter for the Pioneer F/G spacecraft and Saturn for the SUAE spacecraft. The environments shown are based on models giving particle fluxes as a function of near-planetary geometry: the Pioneer F/G spacecraft specification and the 1971 workshop, in the case of Jupiter and NASA publication SP-8091 in the case of Saturn. It is emphasized that these latter two estimates are maximum levels, with uncertainties ranging downward through three orders of magnitude at Jupiter, and all the way to zero at Saturn. Fluences were determined by integrating fluxes along hyperbolic flyby trajectories approaching to 3 R_J or 2.3 R_S from the planet centers, respectively.

It is concluded that while the integrated exposure to neutrons is up a factor of four, it is still far below the threshold of concern in terms of damage to spacecraft components.

The maximum fluences of electrons and protons at Saturn may be slightly higher than the design (or specification) fluences at Jupiter, but they are two or more orders of magnitude below the maximum fluences at Jupiter. Thus it would appear at this time that there is no justification for concern over the radiation environment for the SUAE mission, at least not to instigate protective design measures beyond those of Pioneer F/G.

2.6.4 Long-Term Ordnance Storage

In the Pioneer F/G design, ordnance device squibs are fired by current released from wet slug tantalum capacitor banks by silicon-controlled rectifiers. The same circuitry is proposed in the SUAE spacecraft. On Pioneers 10 and 11, no ordnance devices were used (or intended to be used) after the first day of flight; but on the SUAE spacecraft, ordnance activated events occur at the end of the mission (probe separation).

No problems are anticipated for the mechanical portion of the squib or for the pyrotechnic charge itself. However, long-term storage for

these devices is currently under study in several NASA contracts at other contractors, the results of which will be available later this year.

The capacitor has three concerns. The first is susceptibility to the radiation environment, but as noted above, the anticipated environment is not increased enough to have any effect. The second concern is over the integrity of the hermetic seal. No data are available which will substantiate the intregity of the hermetic seal after six or seven years of storage in a vacuum; however, experience has been very good with shorter storage times since only negligible increases in leakage current have been observed. (Note that discharge of the acid electrolyte would be a serious failure on Pioneer 10 and 11 even after all ordnance events were complete, because of corrosive action on other components.) A third phenomena which would occur in long storage (ignoring the radiation environment) is an electrolytic disassociation into H_2SO_4 and H_2O. The only impact, however, is that a charge time of 12 to 24 hours should be used to insure reassociation of the electrolyte to optimize the capacitor's operation.

A replacement of the wet slug tantalum capacitors with solid tantalum capacitors would preclude problems due to leaks or radiation damage. There would, however, be a weight and space penalty.

In Section 8 we recommend the initiation of a life test program to evaluate the Pioneer F/G ordnance-firing circuits for this mission.

2.6.5 Wearout Life

Since most of the equipment on the spacecraft comes from the Pioneer F and G program, whose mission time was 900 days, it is necessary to review that equipment for its ability to survive the longer SUAE mission. The spacecraft must be designed with all expendables and known wearout phenomena sized for seven years.

The fact that most of the equipment was used on a 900-day mission must not be construed as necessarily meaning that their lifetime is limited to that period. Indeed, many of the potentially life-limited equipment (or similar equipment) have been used on spacecraft with five- or seven-year missions.

Table 2-8 lists the equipment currently identified as potential sources of wearout, a description of their wearout phenomena, the circumstances of their use on the SUAE mission, and possible provisions which could be implemented where necessary.

While there are some unanswered questions which require additional study, there do not appear to be an unmanageable problems at this time.

2.6.6 Reliability Analysis

A top level reliability assessment was made for the SUAE spacecraft, with the following results, for a seven-year mission:

Subsystem	Reliability
Structures and ordnance	0.996
Thermal	0.998
Propulsion	0.937
Attitude control	0.858
Data handling	0.710
Antennas	0.977
Communications	0.831
Electrical power	0.959
Command distribution	0.843
System	0.372

This assessment is generally based on Pioneer F/G reliability models, with extensions at the same failure rates to seven years.

This extension is probably unduly pessimistic, because failure rates reflect data based on shorter missions, including a number of earth-orbiting spacecraft programs. Thus infant failures and failures in the temperature-cycling earth-orbit environment tend to produce failure rates which are too high for the long mission with its unchanging environment.

Therefore the 0.37 figure is not a realistic estimate of the probability of mission success. Nevertheless, the calculations point out those portions of the spacecraft design where reliability augmentation would be comparatively most effective.

Table 2-8. Life-Limited or Time-Variable Components

Equipment	Aging Phenomena	Comments
Traveling wave assemblies	Cathode depletion	State-of-the-art theoretical barium exhaustion times are currently in excess of 100,000 hours (11.5 years). Redundant TWTA's are provided.
	Degradation of insulation in high-voltage power supply causing arcing	State-of-the-art packaging and insulation concepts permit seven-year lifetimes to be achieved.
Star mapper	Lens fogging from long-term space radiation	Integrated solar radiation and electron and proton fluences are lower than Pioneer F/G, or earth orbiters with one year life. No problems anticipated.
	Photomultiplier tube emitter degradation	Seven-year life appears to be within state of the art of star tubes.
Thruster assemblies	Degradation of seal and seating integrity	Thrusters have demonstrated 500,000 pulses life without leakage. SUAE mission worst case thruster requirement is 5-10,000 pulses. Proper thermal control will provide assurance of seal/seat integrity.
	Catalyst bed degradation from cold starts	The catalyst bed has a design life of 150 cold starts which falls within SUAE mission requirements. The catalyst bed is maintained at temperatures high enough to alleviate the cold start problem.
Thermal coatings	Long-term aging and discoloration of thermal surfaces	Integrated UV and particulate radiation is reduced. No problems anticipated.
Sun sensors	Degradation of sun sensing devices	Not required beyond first year of mission.
Ordnance charge	Shelf-life degradation	Ordnance has been successfully stored on the ground for ten years.

Before reviewing specific areas, note that the above tabulation includes only the parts of the flight spacecraft considered to be the responsibility of the spacecraft contractor. RTG's, scientific instruments, and the probe are excluded.

The possibility of failing due to meteoroids has not been included above. A probability of sustaining no catastrophic failure from meteoroids of 0.96 was calculated for Pioneer F/G. However, Pioneer 10's measurements out to 4.3 AU show such a small Asteroid Belt population at damage-producing sizes that the risk is well below 0.01. The passage through Saturn's ring plane (outside the visible ring diameter) is similarly dependent on an uncertain environment – See Section 2.3 for further discussion.

The following paragraphs review the major areas which limit spacecraft reliability.

Propulsion. The 0.937 reliability largely reflects the possibility of failure of the thrusters to fire, accounting for the many redundant modes cited above. Note that internal thruster redundancy (dual valve seats) protects against a thruster failing to turn off, and the redundancy of multiple thrusters protects against a thruster failing to fire.

Attitude Control. The 0.858 reliability shown reflects the possibility of two different failure processes: the star mapper and the DSL (duration and steering logic) circuitry. The star mapper is proposed with a single optical train and a single gimballed assembly, but with dual photomultiplier tube detectors and dual electronics. While the gimbal drive motor and bearings are indicated nonredundant, they could be made redundant at some weight penalty, increasing the subsystem reliability to 0.890.

The Control Electronics Assembly has nonredundant PSE (Program Storage and Execution) circuitry, with many electronic components (λ=4308 failures per 10^9 hours). This could degrade mission reliability significantly, except that, as in Pioneers 10 and 11, this circuitry is considered critical to the mission only for 40 days (through all midcourse corrections). All subsequent maneuvers, being performed

in the earthline mode, could be performed by direct command if the PSE circuitry failed. Thus the PSE circuits do not degrade mission reliability significantly.

On the other hand, the DSL circuitry, with comparable complexity (λ=4500 failures per 10^9 hours), is necessary for all maneuvers, and is redundant in both the Pioneer F/G and SUAE spacecraft designs. Even though it is redundant, the seven-year requirement makes the DSL the portion of attitude control electronics most responsible for the low indicated reliability.

Data Handling. Two portions of the data handling subsystem contribute to its low indicated reliability. The data storage capability (three units, each with 245,760 bits capacity) alone has an indicated reliability of 0.897, even though advantage has been taken of very flexible on-board restructuring ability to effect triple redundancy and a lower standby (power-off) failure rate has been assumed for the long cruise phase of the mission. It should be noted that the proposed C-MOS memory circuitry which promises impressive performance in areas of weight, power, and cost, does not yet have a data base which permits accurate reliability extrapolation for a seven-year mission.

The second portion is the dual multiplexing circuitry of the DTU which gates data into the telemetered bit stream. This function is considered critical for the entire mission, and its reliability of 0.801 reflects the long mission duration.

Communications. Regarding X-band downlink transmission as critical for the entire mission (even though partial mission success can result from S-band only) the dual X-band transmitter is one contributor to decreased reliability (0.935). The dual S-band receiver, necessary to get commands into the spacecraft, is the other significant contributor (0.889).

Command Distribution. Continuing the command link, the DDU's (Digital Decoder Units) and command distribution circuitry of the CDU, both dually redundant, combine to decrease reliability.

3. MISSION ANALYSIS

This section summarizes the results of mission analyses for the Pioneer Saturn Uranus mission, with primary emphasis on the requirements of the bus spacecraft. The purpose is to identify mission characteristics and requirements as necessary for the design of the spacecraft and its subsystems, and for an understanding of spacecraft operations.

This section draws from material presented in Appendix C as well as from the results of analyses performed by Ames Research Center personnel in conjunction with this study. Results of the parallel study of the Pioneer Saturn Uranus probe mission performed by McDonnell Douglas, and of related navigation and guidance studies performed by JPL are also reflected in this section. (See references cited in Section 1.)

3.1 INTERPLANETARY TRAJECTORIES

3.1.1 Mission Profile Types

The study calls for consideration of the launch opportunities in 1979 for a probe mission to Saturn and in 1980 for a probe mission to Uranus via Saturn swingby. An additional flight, launched in 1980, is also considered which will provide two options: 1) delivery of a probe to Saturn as a backup for the 1979 mission, or (2) as a backup to Uranus, if the first probe mission to Saturn is completed successfully.

The two 1980 missions will be launched at about the same date and along nearly identical trajectories toward Saturn. The decision as to the ultimate probe destination in the backup Saturn/Uranus mission can be made as late as a few months prior to arrival at Saturn and requires only a minor retargeting maneuver. The option of continuing to Uranus after delivering the probe at Saturn is available through appropriate targeting of the Saturn encounter.

Figures 3-1 and 3-2 show typical trajectories of a 1979 Saturn and a 1980 Saturn Uranus mission, projected into the ecliptic plane. These mission profiles are assumed as nominal for purposes of this study. Their characteristics are presented in detail in Appendix C. Communication ranges, pointing requirements, and other geometrical properties of

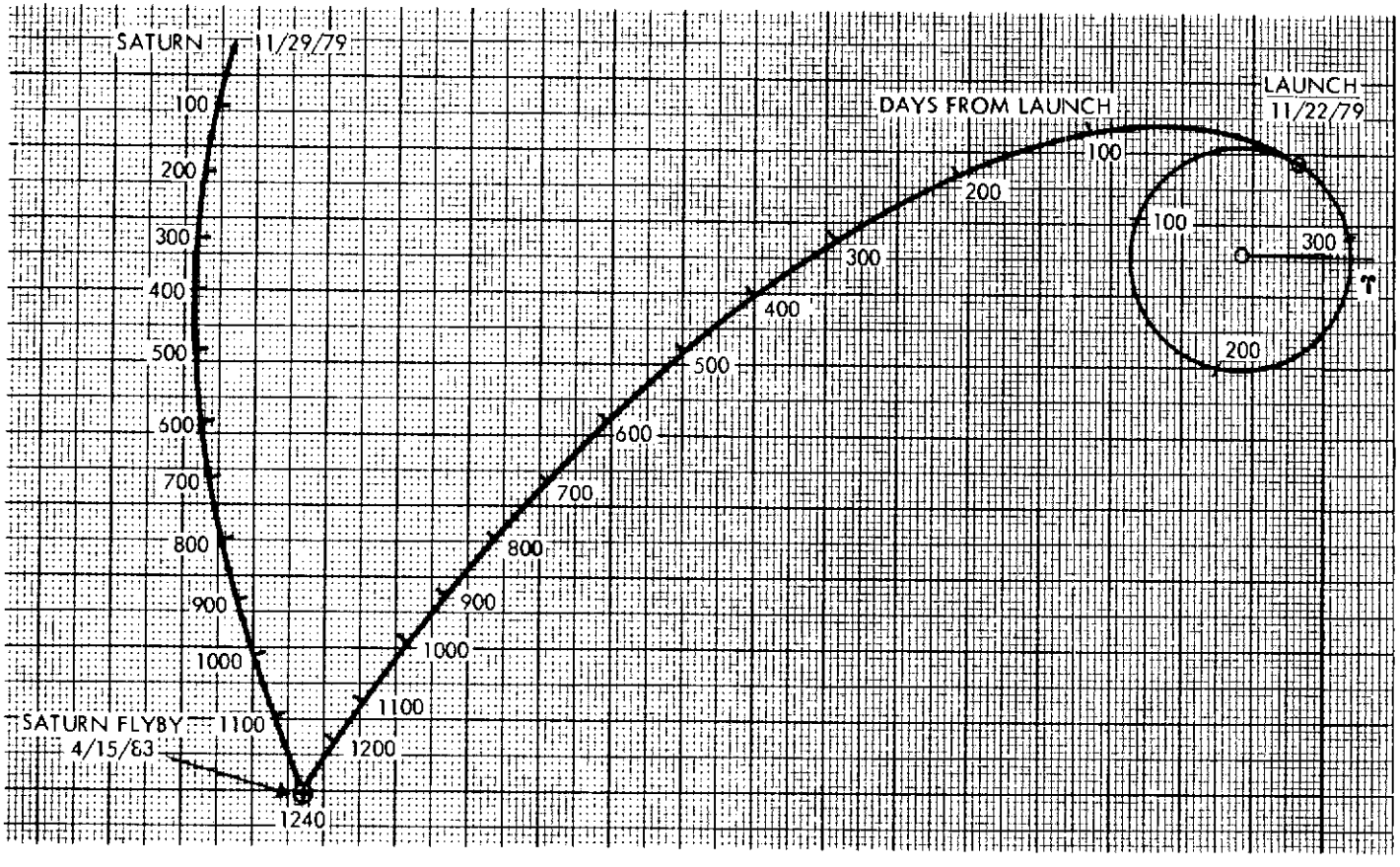

Figure 3-1. Nominal 1979 Earth-Saturn Trajectory

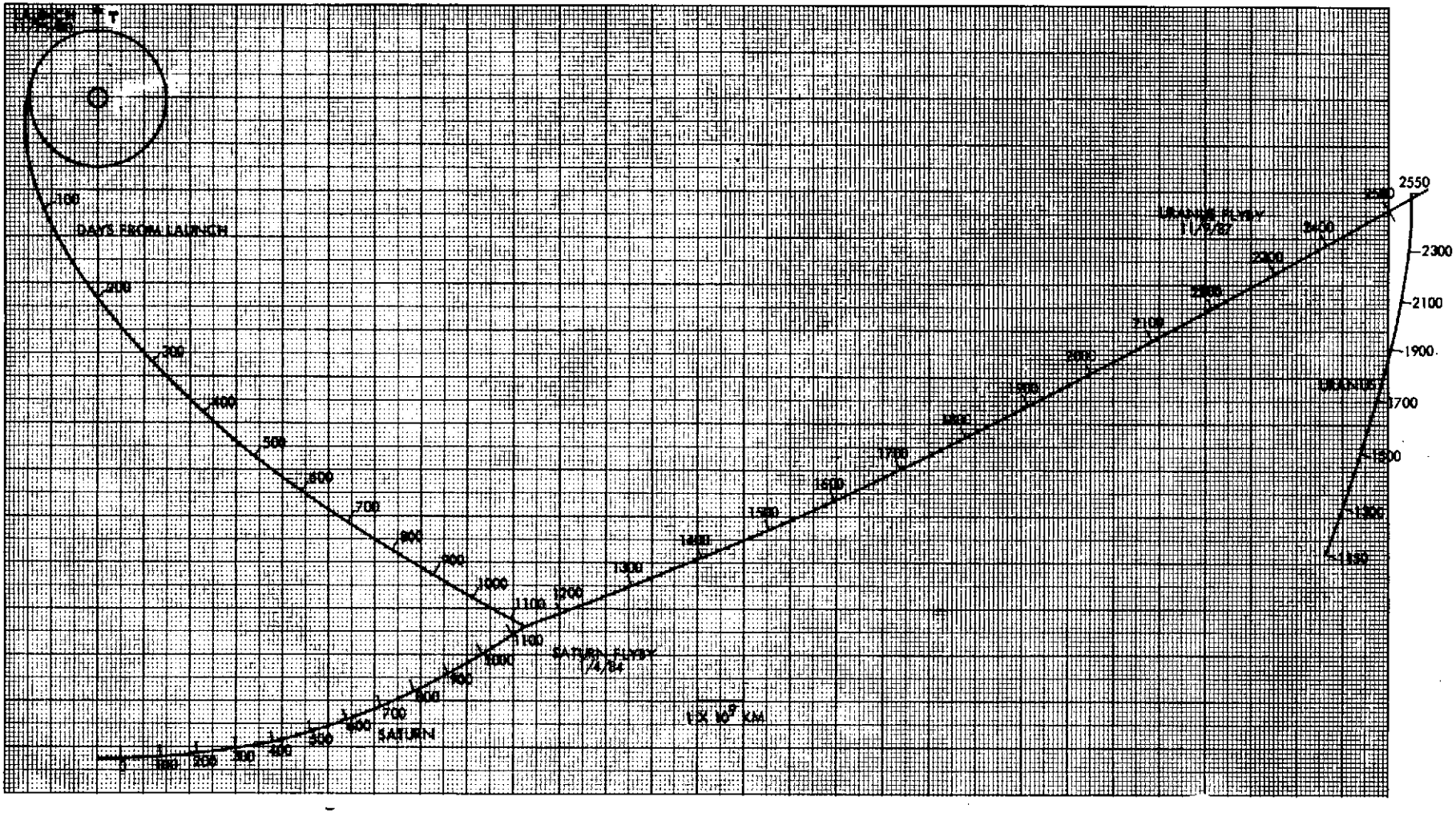

Figure 3-2. Nominal 1980 Earth-Saturn-Uranus Trajectory

these nominal mission profiles are used in the remainder of this report to illustrate spacecraft and subsystem operating characteristics.

3.1.2 Trajectory Characteristics

Table 3-1 summarizes principal earth launch and planetary arrival/departure characteristics of the nominal trajectories.* Launch conditions for the two missions are quite similar. However, the 1979 mission to Saturn, launched on 22 November 1979 with an injection energy $C_3 = 134\ km^2/sec^2$ ($V_\infty = 11.6$ km/sec) has a trip time of 1240 days to Saturn which is 105 days longer than the first leg of the 1980 Saturn-Uranus mission launched 25 November 1980 with $C_3 = 144\ km^2/sec^2$ ($V_\infty = 12$ km/sec). The total trip time to Uranus is 2540 days.

The nominal payload weight capability of the Titan 3E/Centaur D-1T/TE-364-4 booster, as defined by Ames Research Center for purposes of this study, is shown in Figure 3-3. At $C_3 = 142\ km^2/sec^2$ a gross spacecraft weight of 1050 pounds can be injected. This is used as reference weight in the remainder of our study.

Table 3-1. Nominal Trajectory Data (In Planetocentric Equatorial Coordinates)(1)

	1979 Mission		1980 Mission			
	Depart Earth 11-22-79	Arrive Saturn 4-15-83	Depart Earth 11-25-80	Arrive Saturn 1-4-84	Depart	Arrive Uranus 11-9-87
V_∞ (km/sec)	11.62	10.55	11.97	10.52		13.79
RA of V_∞	149.8	180.3	171.3	193.2	281.8	25.0
Declination of V_∞	32.7	-2.3	26.94	8.6	-29.1	-67.8
RA of planet's axis(2)		38.4		38.4		76.8
Declination of planet's axis(2)		83.3		83.3		14.9
Aim angle(3)		-18.25		-28.7		-64.2
Probe entry angle		-30.0				-40.0
Bus periapsis radius		$2.25R_S$		$2.73R_S$		$4.0R_U$

All quantities (except V_∞) in degrees).

NOTES:

1) These coordinates are analogous to celestial coordinates at earth, making use of a redefined planetary "vernal equinox" as reference.

2) RA and declination of planet's rotation axis are given in conventional, earth celestial coordinates.

3) Aim angle is orientation of aim point vector $\bar{B}$ in R, T plane, measured clockwise from T-axis.

*All data in this analysis and elsewhere in this section were obtained on the basis of a Uranus equatorial radius of 2.35×10^4 km, before it was redefined to 2.7×10^4 km, in accordance with NASA SP-8103.

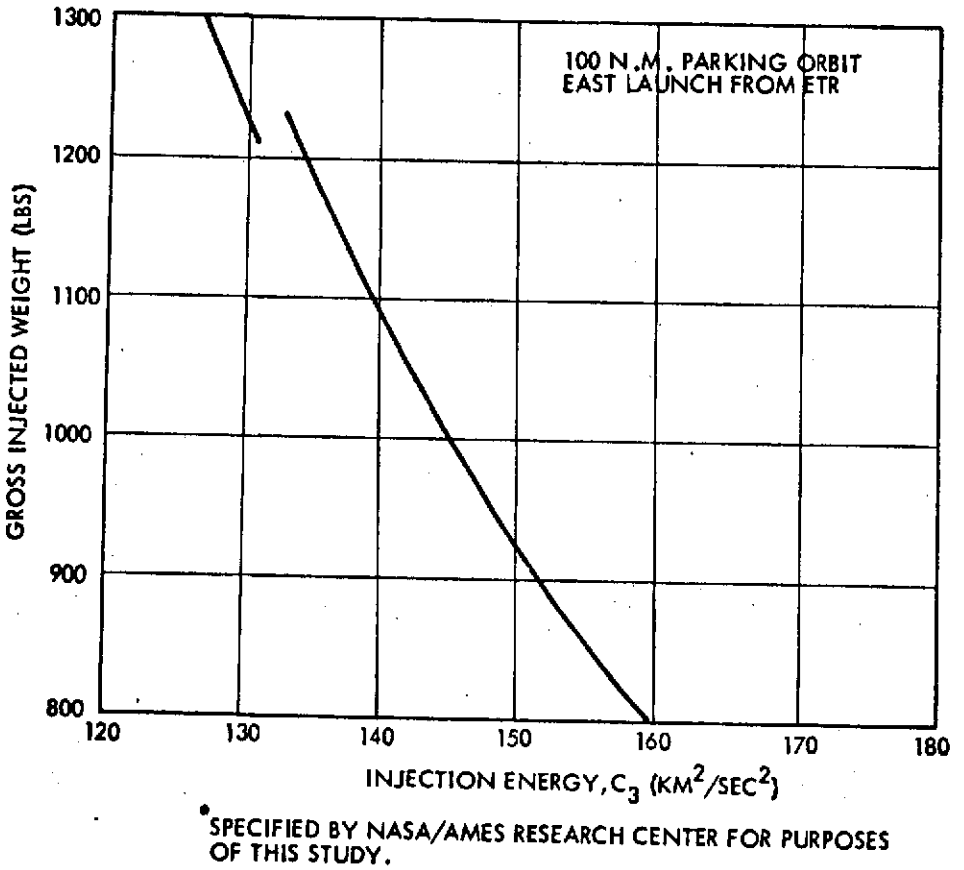

Figure 3-3. Nominal Injection Energy Performance of Titan III E/Centaur/TE-364-4*

Figure 3-4 (a) and (b) show contours of injection energy and injected gross weight for the two missions, in terms of earth departure and target planet arrival dates. The shortest trip times are obtained for launch dates in late November 1979 and early December 1980. Because of Saturn's orbital motion of 12 degrees/year, similar Earth-to Saturn trajectories can be obtained if they are launched one year and two weeks apart.

The mission maps shown in Figure 3-4 also indicate arrival dates at which conjunction of earth and target planets would occur. These dates are to be excluded in mission planning in order to avoid disruption of spacecraft communications on arrival. For the same reason, arrival during the weeks following the conjunction date should be excluded because of the critical events that precede encounter: approach navigation

*Injected weight shown excludes spacecraft adapter (assumed to be 56 pounds).

A. 1979 SATURN MISSION

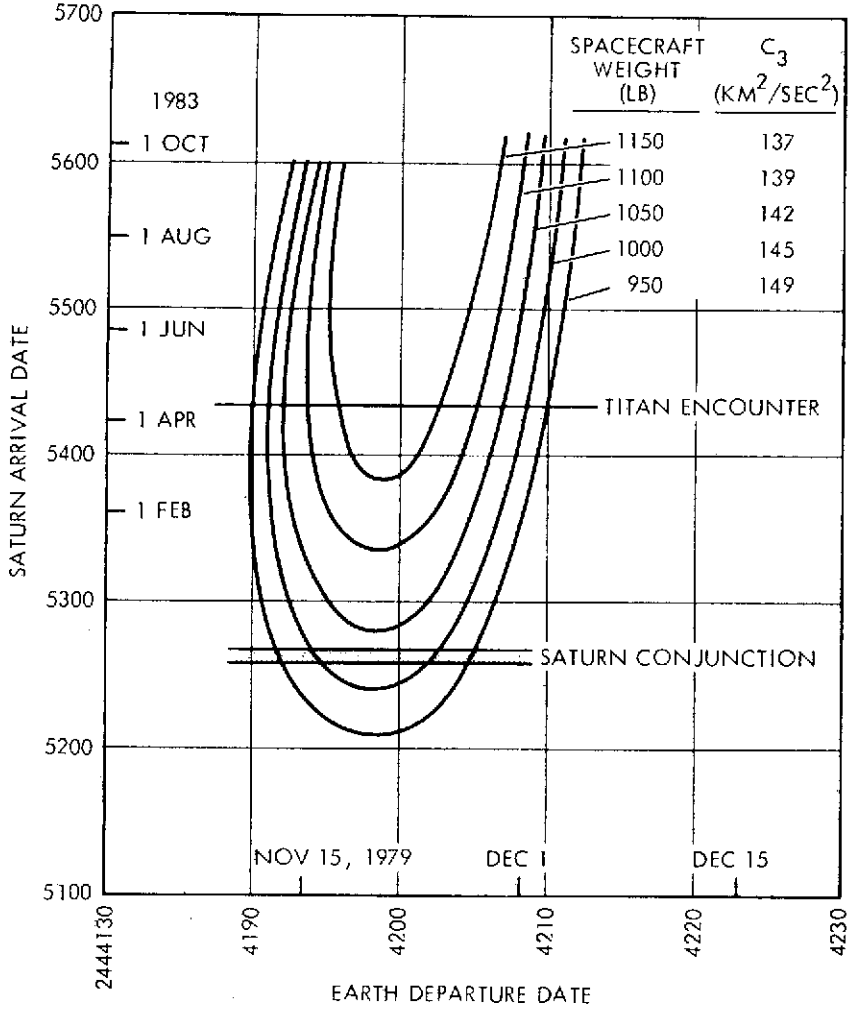

B. 1980 SATURN/URANUS MISSION

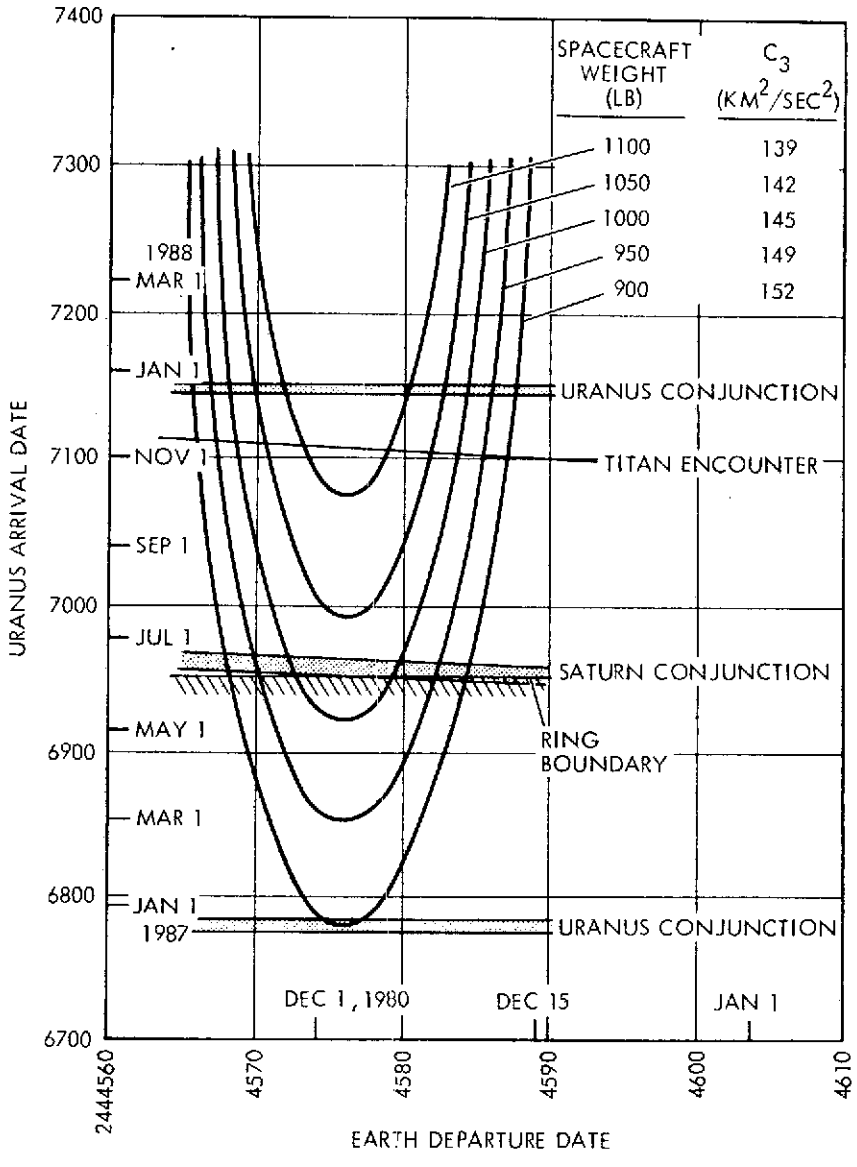

Figure 3-4. Injection Energy and Spacecraft Weight Contours

fixes, terminal guidance corrections, probe separation, and spacecraft deflection maneuvers. All of these events occur over a period of 15 to 30 days before encounter (see Section 3.2).

The mission maps show that for the nominal arrival dates of 8 April 1983 at Saturn in the first mission, and 4 January 1984 and 9 November 1987, respectively, at Saturn and Uranus in the second mission (or the backup mission), a launch window of at least 11 days is available. Conjunctions prior to and at the encounters are avoided. In the case of the 1979 Saturn mission, a small change of the nominal arrival date would permit a close encounter of the satellite Titan, although this is not a specified mission objective.

Geometrical characteristics of the two reference missions are presented in Appendix C. Of principal concern from a system design standpoint are the solar distance, earth distance, and earth-spacecraft-sun angle which are shown in Figure 3-5 for the 1980 Earth-Saturn-Uranus mission. Because of the similarity of trajectories the data for the first 1200 days of this graph also characterize the conditions for the 1979 Earth-Saturn mission.

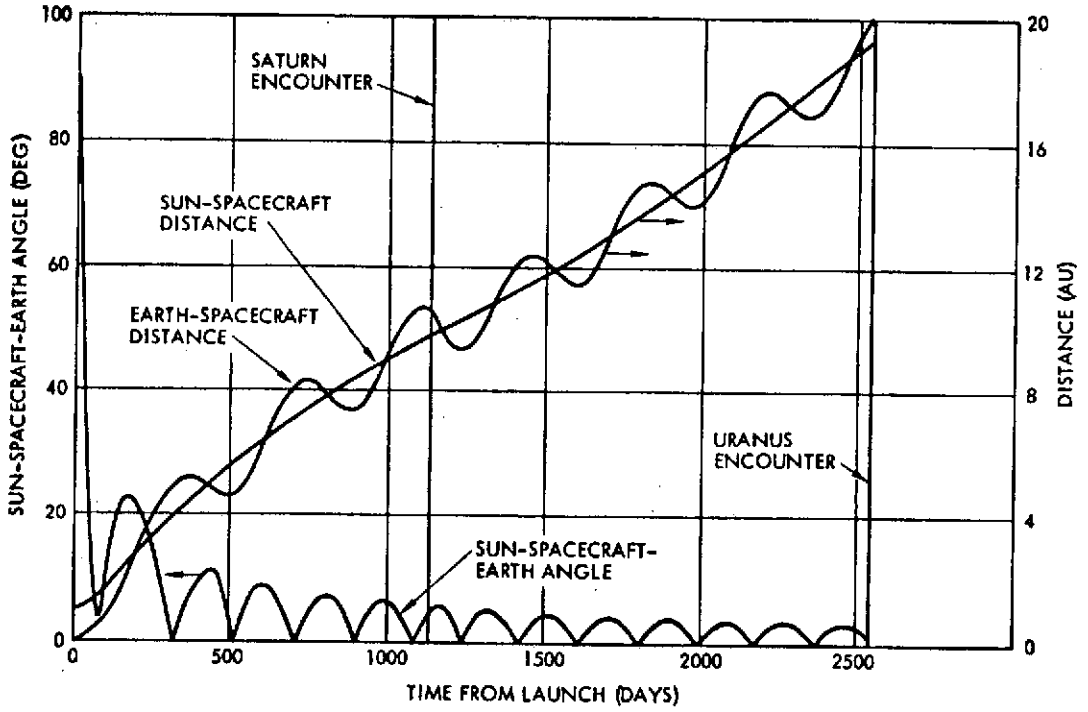

Figure 3-5. Solar Distance, Earth Distance and Earth-Spacecraft-Sun Angle for the Nominal Earth-Saturn-Uranus Mission

The earth-spacecraft-sun angle that is of principal concern to telemetry, thermal control, and optical sensor operation has maxima of less than 20 degrees after the first six months of the mission. The maximum excursions are 6 degrees toward the end of the Earth-Saturn mission phase, and 3 degrees toward the end of the Saturn-Uranus phase. The rate of rotation of the earth line of sight is at most 0.2 degree per day during the year preceding the Saturn encounter, and at most 0.1 degree per day for several years preceding the Uranus encounter. This means that spacecraft precession maneuvers to keep the spin axis, and hence the high-gain antenna beam, earth-pointed within ±0.5 degree for X-band telemetry need to be performed at most every five or ten days under these conditions. For S-band telemetry such maneuvers would be required about three times less often.

3.1.3 Alternate Mission Options

As an alternate mission option to Uranus a swingby of Jupiter rather than Saturn is a possibility. This mission mode does not permit delivery of an atmospheric probe at Saturn as a backup to the 1979 Saturn mission, but it has the advantage of a much shorter total trip time to Uranus; five rather than seven years. This is apparent from the alignment of the planets in the early 1980's as shown in Figure 3-6.

The Earth-Jupiter-Uranus (EJU) mission mode also has the advantage of avoiding the potential hazard of a Saturn ring passage quite close to the planet, at 2.75 R_S, which might be encountered in the Earth-Saturn-Uranus (ESU) mode. In the EJU mission mode the closest approach to Jupiter is in the range of 10 to 20 Jupiter radii, thus avoiding hazards due to the trapped radiation environment at that planet.

In addition, with Jupiter's ephemeris more accurately known than Saturn's, and with a less critical swingby geometry from a guidance accuracy standpoint, the pre-encounter and post-encounter trajectory corrections in the EJU mission are likely to be much smaller than at Saturn in the case of the ESU mission.

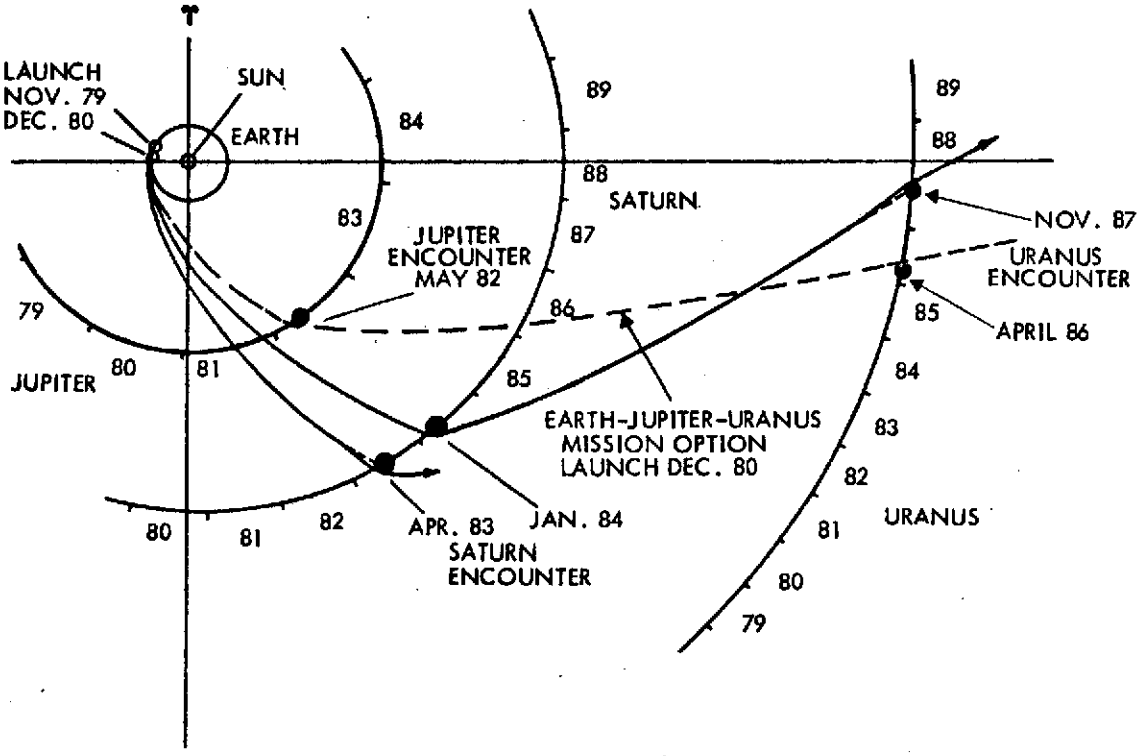

Figure 3-6. Relative Planet Alignment in Early 1980's and Alternate Mission Options

Figure 3-7* shows payload weight contours of the 1980 EJU mission (at left) and a comparison of the 1050-pound payload contours of the 1980 EJU and ESU missions (at right). Minimum trip times differ by about 650 days. An interesting possibility is the use of a combined 23-day launch window of the two mission modes to Uranus opening in late November and closing in late December 1980, as indicated in the mission maps.

It should be emphasized however, that further consideration of the EJU alternative is not within the scope of this study, particularly so because it does not provide the desired Saturn probe backup option.

3.2 PLANETARY APPROACH AND ENCOUNTER

3.2.1 Constraints

The principal trajectory requirements for the target planet encounter are dictated by the objectives of

*Data furnished by Ames Research Center.

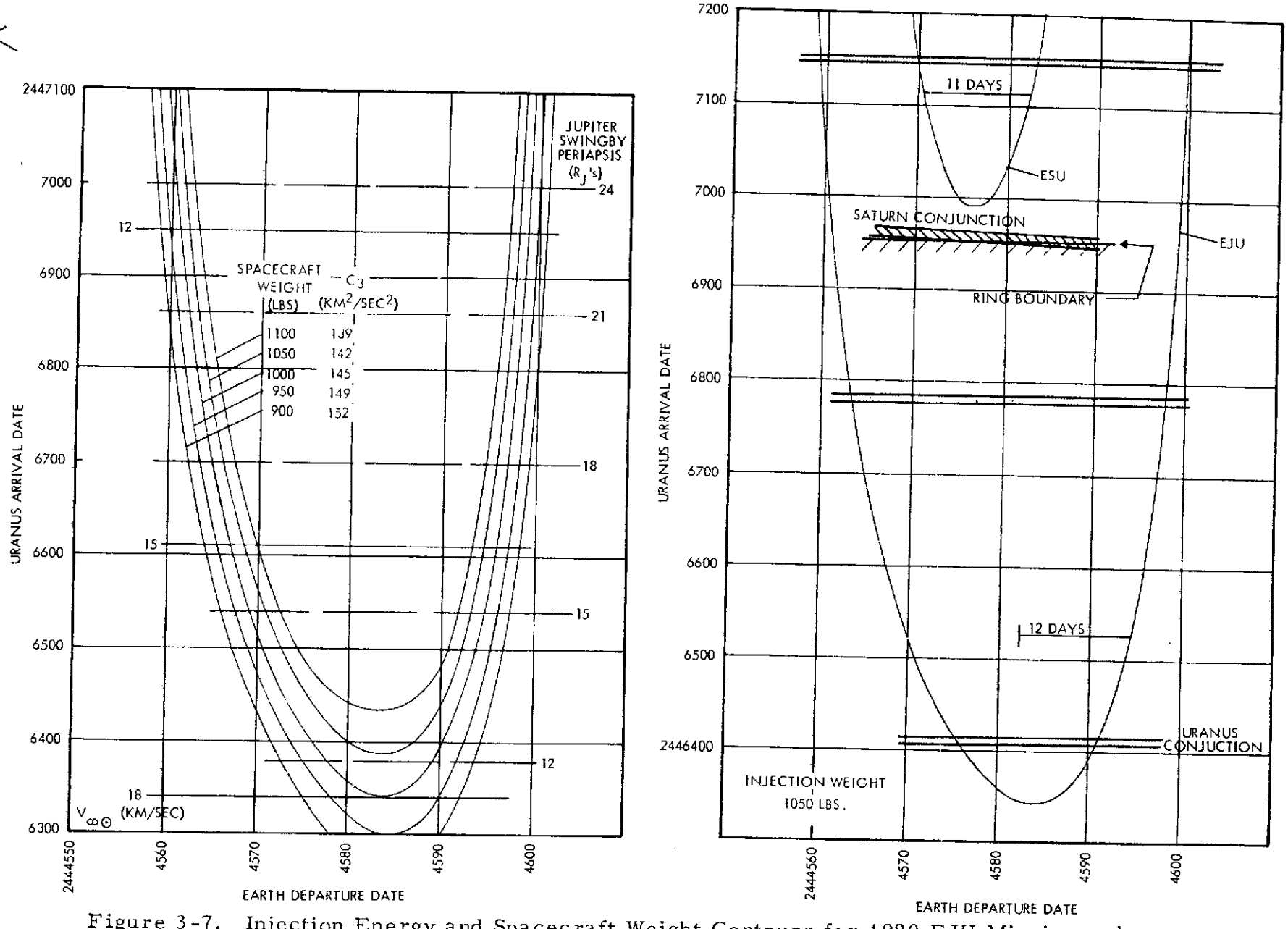

Figure 3-7. Injection Energy and Spacecraft Weight Contours for 1980 EJU Mission and Combined Launch Opportunities for 1980 EJU and ESU Missions

- achieving accurate entry probe delivery to the specified target area with entry conditions that the probe is designed to withstand,
- providing a relative geometry between bus and probe positions at the time of overflight such that the bus can function effectively as communications relay for data transmitted by the probe after entry.

To meet these requirements, terminal guidance corrections are necessary before probe separation to control the dispersion of the probe entry point.

Secondly, the bus must perform a deflection maneuver soon after probe separation to achieve passage of the probe entry area at an altitude and timing that optimize the relay link geometry. Without this deflection maneuver the bus would, of course, also enter the planet's atmosphere. These sequences are illustrated schematically in Figure 3-8. The timing of the bus deflection maneuver is constrained primarily by consideration of maneuver propellant economy and probe delivery accuracy.

These factors tend to impose conflicting requirements. The velocity increment for achieving a desired bus trajectory offset is inversely proportional to the distance from the planet at which the maneuver is performed. Thus, in the interest of propellant economy the maneuver should occur early in the planetary approach. On the other

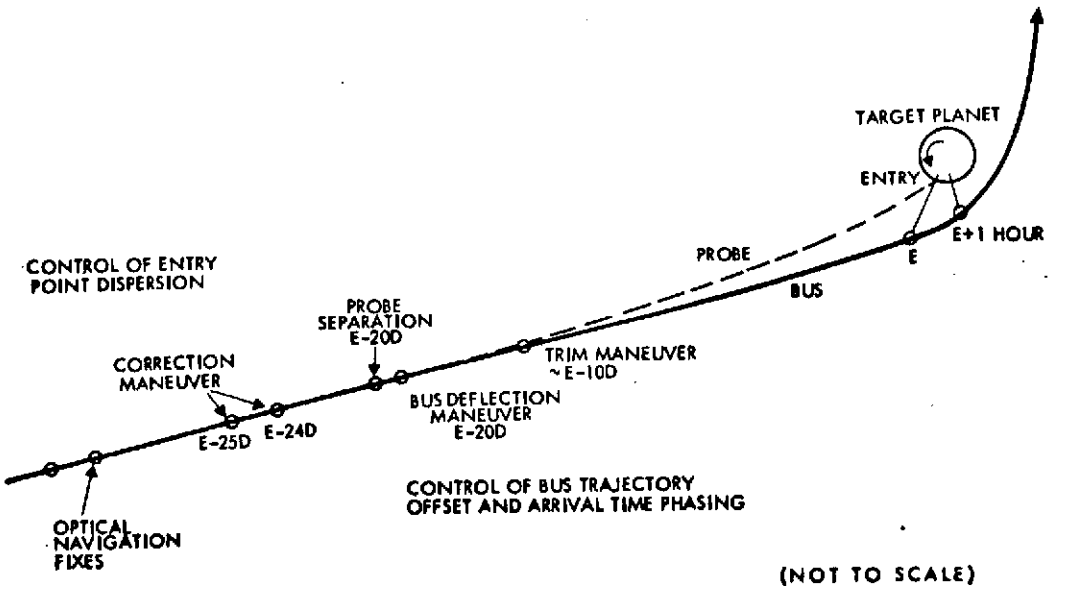

Figure 3-8. Control of Approach and Encounter Conditions

hand, the terminal navigation fixes and guidance corrections are the more effective the closer to the planet they are being performed. A reasonable compromise between these constraints leads to selection of probe separation points at a distance of about 500 planet radii (3×10^7 km) at Saturn and 1000 radii (2.35×10^7 km) at Uranus.* Considering the approach velocities of 10.6 km/sec at Saturn, and 13.8 km/sec at Uranus, these ranges correspond to separation times of 33 and 20 days, respectively, before planet encounter.

Characteristics of the deflection maneuver are further explained by data presented in Figures 3-9, 3-10, and 3-11. Figure 3-9 shows velocity vectors before and after the maneuver under conditions typical for the approach to Saturn. The velocity increment is expressed in terms of

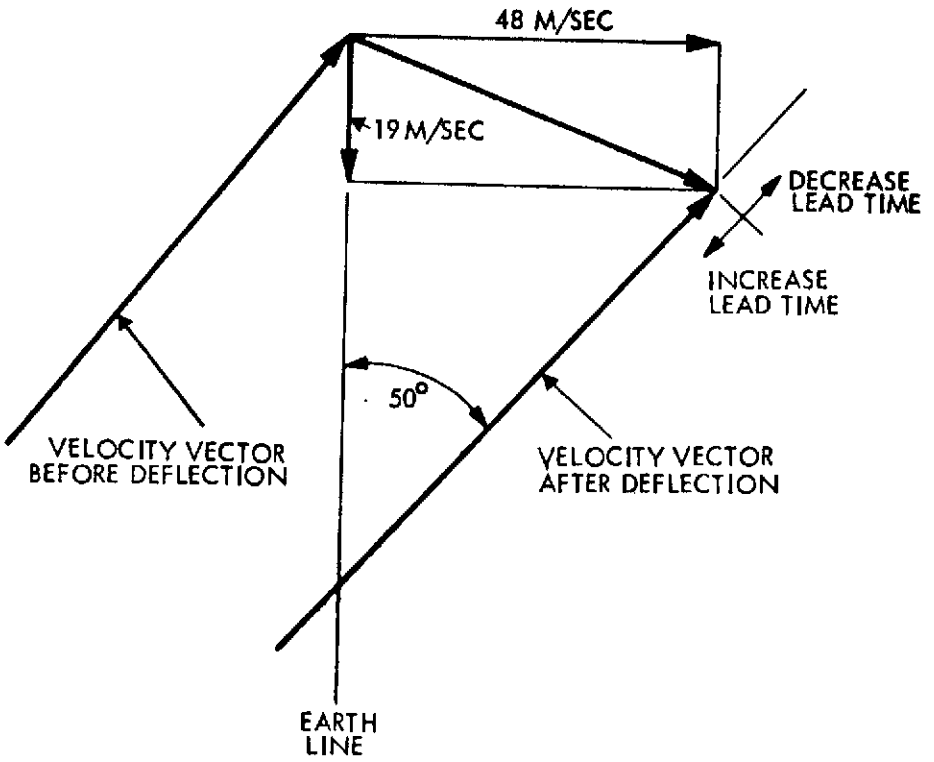

Figure 3-9. Deflection and Phasing Maneuver Velocities

*These data are results of mission analyses performed at Ames Research Center and furnished to TRW Systems.

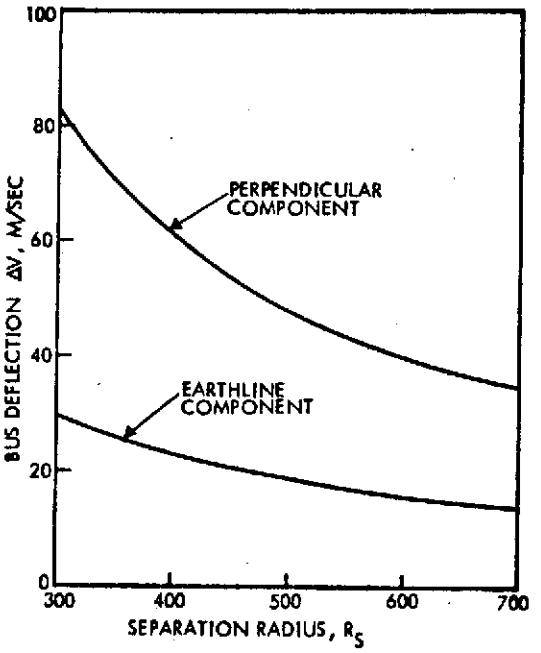

Figure 3-10. Deflection/Phasing ΔV Requirements for 1979 Saturn Mission Phased Overhead at Entry Plus One Hour; γ_E = -30 Degrees, Periapsis 2.25R_S

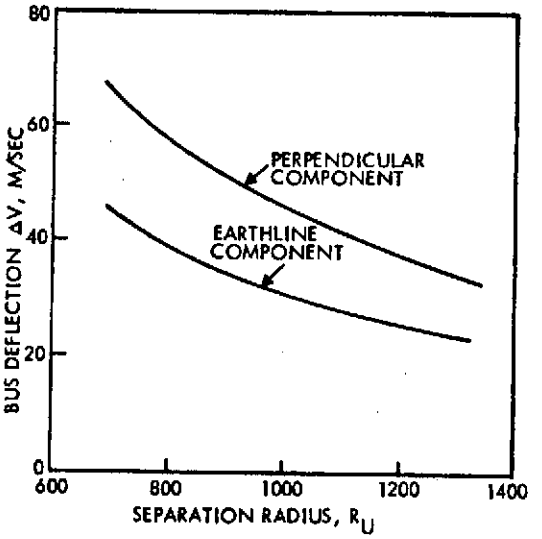

Figure 3-11. Deflection/Phasing ΔV Requirements for 1980 Uranus Mission γ_E = -40 Degrees; Retrograde Entry; 4.0 R_U Periapsis

components parallel to and perpendicular to the earthline in accordance with the thrust directions available on the earth-oriented Pioneer spacecraft. The time phasing of the spacecraft's passage over the probe entry site can be controlled by variation of these components without changing the trajectory deflection angle as indicated in the diagram. Figure 3-10 shows the two ΔV components as functions of planet distance for an entry angle of -30 degrees at Saturn. Figure 3-11 shows the corresponding ΔV components for the Uranus mission where the nominal entry angle is -40 degrees. These curves show that the required offset maneuver velocity at Saturn is 70 m/sec if the maneuver is performed at 500 R_S. Algebraic rather than vectorial addition of the two maneuver components is appropriate in the case of Pioneer where separate thrusters are used to provide the velocity increments parallel and perpendicular to the earthline.

The tradeoffs involving propulsion requirements versus terminal navigation and guidance capabilities will be further discussed in Sections 3.5 and 3.7.

3.2.2 Encounter Trajectories

Figure 3-12 shows the bus and probe trajectories at Saturn for the nominal 1979 mission. The bus trajectory is offset to pass the planet at a periapsis radius of 2.25 R_S. Probe entry occurs about 1.2 hours before the bus passes periapsis. As shown in the trajectory plot the bus arrives at a position vertically above the probe at the time of entry (E). This geometry is favorable for probe-to-bus relay communication since due to Saturn's axial rotation the probe, while descending into the atmosphere, travels at approximately the same angular rate as the bus above it. Thus, the probe aspect angle, i.e., the angle between the probe-to-bus line of sight and the probe's spin axis, remains nearly constant during the entire entry phase. This simplifies probe antenna design requirements. However, due to the line-of-sight rotation relative to the earth-line (which is also the orientation of the spacecraft's spin axis) some variation of the bus aspect angle during the probe entry phase is inevitable.

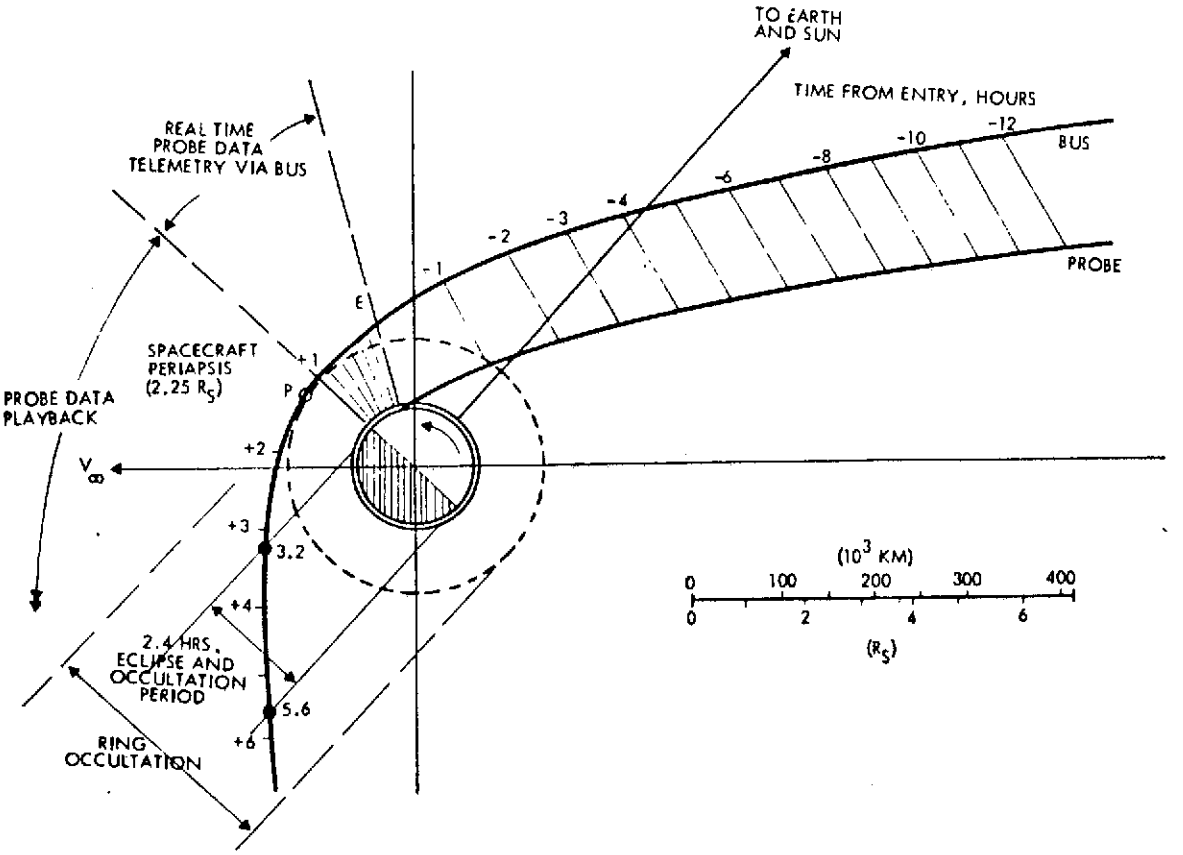

Figure 3-12. Bus and Probe Trajectories Near Saturn (Arrival 15 April 1983)

Figure 3-13 shows the time variation of the bus aspect angle and the communication distance during the entry phase for both the nominal Saturn and Uranus encounter conditions. As shown in these curves, the aspect angle variations are small enough to avoid receiver antenna design problems on the bus spacecraft (see Section 6.6).

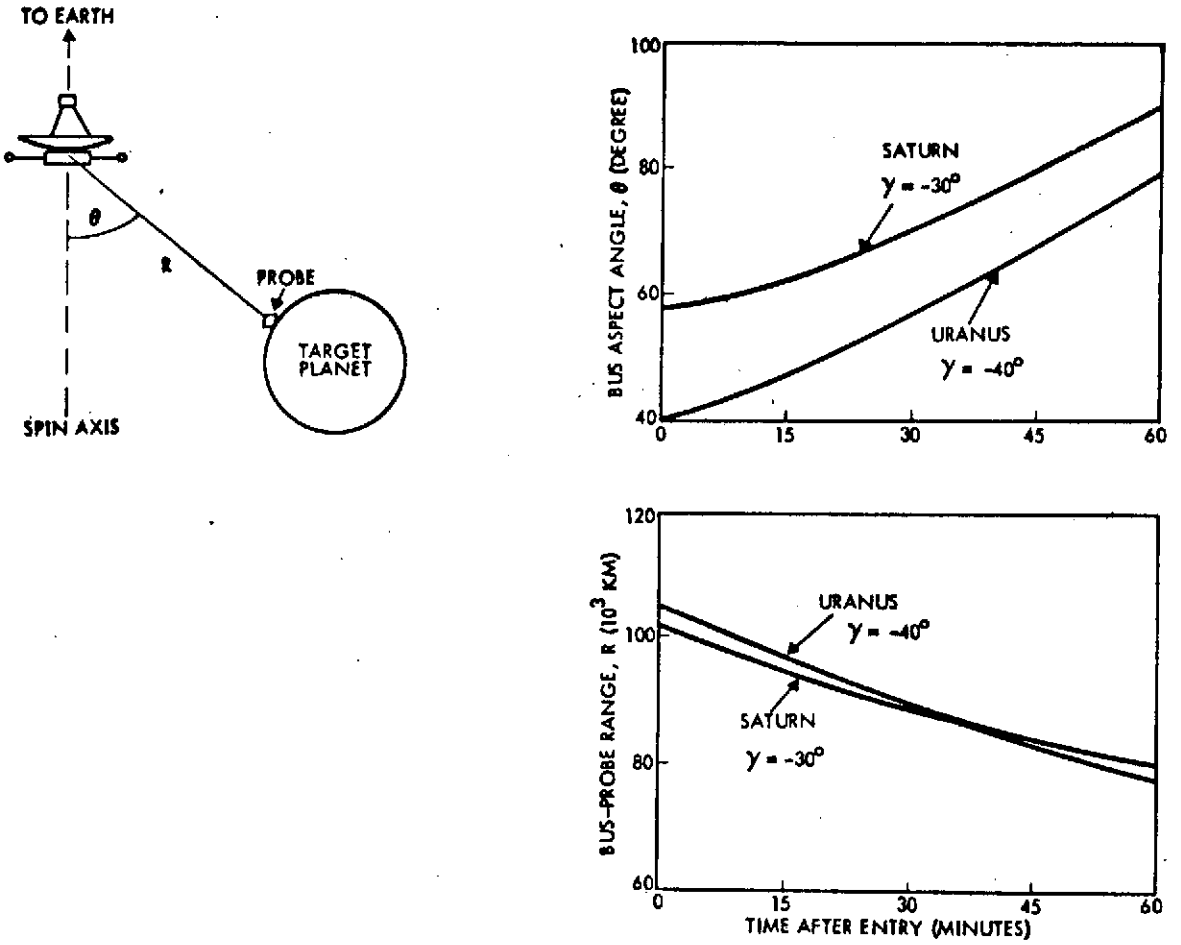

Figure 3-13. Relay Link Geometry

Figure 3-14 shows nominal bus and probe encounter trajectories at Uranus for the 1980 Earth-Saturn-Uranus mission. In contrast to the Saturn encounter, a retrograde encounter and probe entry mode has been selected here. This choice is made primarily to avoid unduly large angles of attack at probe entry under the aim point constraint that the planet encounter must also include an earth occultation phase for the bus spacecraft in order to meet secondary planet science objectives of the mission.

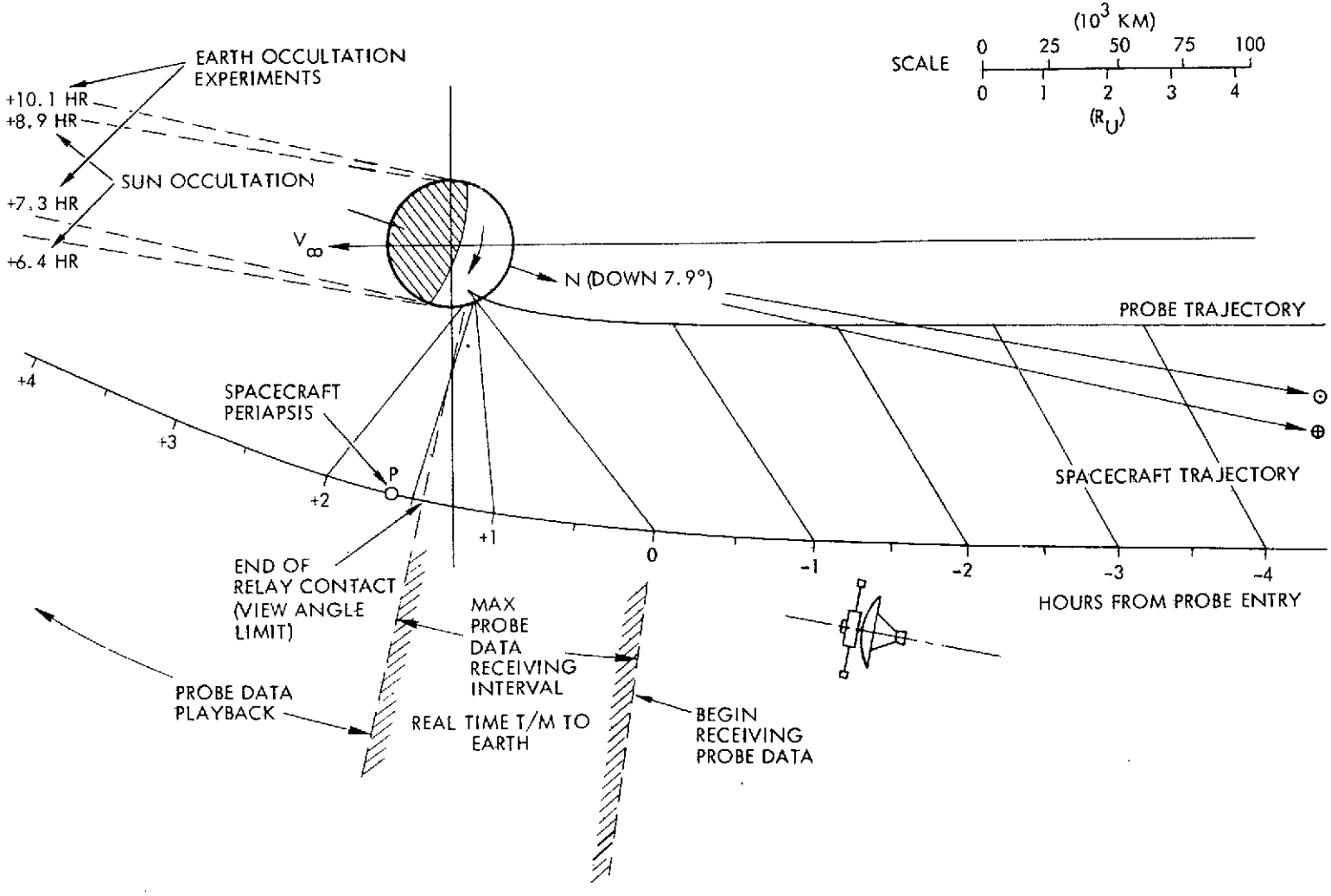

Figure 3-14. Uranus Encounter Trajectory, Arrival 1 November 1987

If posigrade entry were selected, the angle of attack would be 20 to 30 degrees larger than for retrograde entry in the range of inertial entry angles, -30 to -60 degrees, that are consistent with probe survival. The variation of angle of attack as function of entry angle is shown in Figure 3-15 for posigrade as well as retrograde encounter modes. The large differences are explained by the respective orientations of the entry velocity vectors relative to the earthline orientation which is also the orientation of the probe spin axis by virtue of the delivery mode by the spacecraft bus.

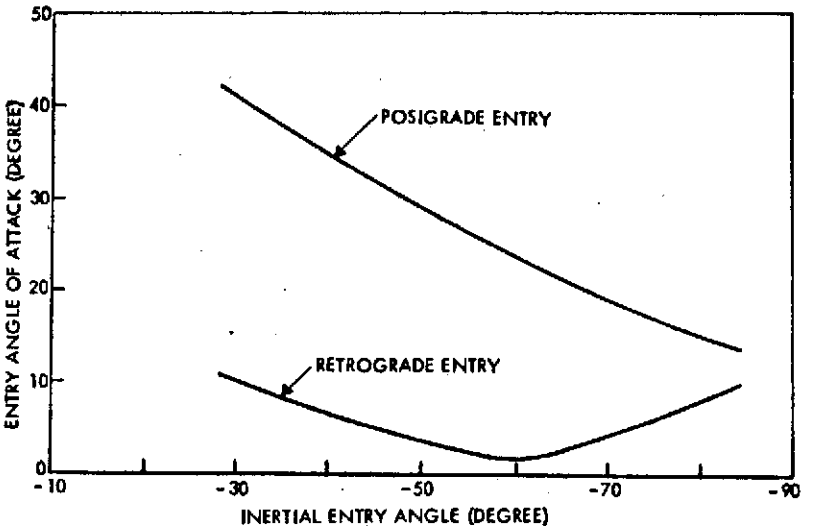

Figure 3-15. Entry Angle of Attack 1980 Saturn/Uranus at Uranus Diametric Occultation (Data furnished by Ames Research Center)

The equatorial plane of Uranus is tilted by about 98 degrees relative to the ecliptic, and the north pole is pointing nearly in the direction of the incoming spacecraft in the season during which this encounter will occur. This makes the relative motion of bus and probe during the overflight interval in the case of Uranus significantly different from that previously discussed for the Saturn encounter where the planet's rotation actually alleviates aspect angle problems. In the case of Uranus, the axial tilt is such that the planet's rotation causes the probe after entry to move normal to the spacecraft's plane of motion, traversing an angle of 34 degrees during the nominal one-hour entry and descent period. To achieve the best relay link geometry, the bus spacecraft is targeted to overfly a point 17 degrees east of the probe entry point. Thus, the probe on its eastward motion crosses the spacecraft track just when the spacecraft passes vertically overhead. With this sequence of relative positions, achieved

through appropriate probe and bus targeting, any aspect angle problems of the bus or probe that are due to the peculiarity of Uranus' axial tilt can be readily avoided.

3.2.3 Saturn Flyby on Uranus Probe Mission

Encounter conditions during Saturn flyby on the 1980 Uranus probe mission are similar to those that would be selected if the probe were to be delivered at Saturn instead of Uranus. Both are similar to the encounter conditions illustrated in the preceding section for the 1979 Saturn mission. The differences between these cases involve the selection of the Saturn encounter aim point and the pre-encounter maneuvers, which depend on whether the probe is to be delivered at Saturn or to be carried on to Uranus. In the first case the spacecraft (bus) is targeted to a periapsis of 2.25 R_S, in the second case to 2.73 R_S.

The navigation and guidance requirements also are different in the flyby and the probe delivery modes. In the flyby mode it is anticipated that trajectory corrections will be necessary before and after the Saturn encounter to achieve the highest possible precision of the Saturn-to-Uranus departure velocity and thus to minimize subsequent midcourse corrections. Repeated navigational fixes by an onboard optical sensor will probably be required to achieve the desired guidance accuracy. This is further discussed in Section 3.7.

3.2.4 Saturn Ring Encounter

The question of whether the spacecraft or probe will come close to or penetrate Saturn's rings in the various Saturn encounter modes of the 1979 and 1980 Saturn/Uranus missions is of importance from the standpoint of

- hazard avoidance
- scientific observation.

The nature and dimensions of the rings, and the particle size and spatial density are highly uncertain. The outer perimeter of the rings as observed by telescope from earth is thought to be of radius 2.3 R_S. However, radar echoes received recently by means of the 64-meter DSIF antenna at Goldstone, although not yet conclusively interpreted, appear

to provide evidence that the extent of the outermost ring material may be several Saturn radii larger than has been previously assumed on the basis of visual observations.*

In any case, it is quite possible that crossing the ring plane at distances of 2.3 to 2.7 R_S as envisioned in the nominal mission profiles may present a definite hazard to spacecraft survival.

Figure 3-16 shows a perspective view, as seen from Earth, of the 1979 Saturn encounter trajectory. The figure also shows a projection of the trajectory into Saturn's equatorial plane to illustrate important encounter events. On approaching the planet the spacecraft bus would be a considerable distance "above", i.e., to the north of the rings. It crosses the ring plane about 30 degrees beyond the periapsis passage, at $r = 2.35\ R_S$. The closest approach phase could be hazardous if ring particles of sufficient size and numbers are found much beyond the targeted periapsis distance.

The entry probe will be targeted to an entry at northern latitudes ranging from 17 to 30 degrees. This means it will not be in danger of penetrating the rings prior to entry.

Overflight by the bus also occurs north of the ring plane. The mission plan is predicated on the expectation that the spacecraft survives long enough to transmit real-time probe data and subsequently a complete set of recorded data. Thus, in a mission dedicated primarily to delivering a probe to Saturn, the main objective is achieved even in the event the bus should be subsequently damaged on crossing the ring plane.

If the probe mission is to be continued to Uranus the larger periapsis offset of 2.75 R_S selected for this case should increase the probability of safe passage.

Evidently these mission plans could be strongly affected by results of future radar echo experiments at Goldstone tracking station which are projected to be repeated during the 1973 Saturn opposition. The mission profile could be modified if necessary by increasing the periapsis range, however, this would tend to increase the flight time to Uranus. Use of

*Communication from Dr. L. Friedman, of Jet Propulsion Laboratory.

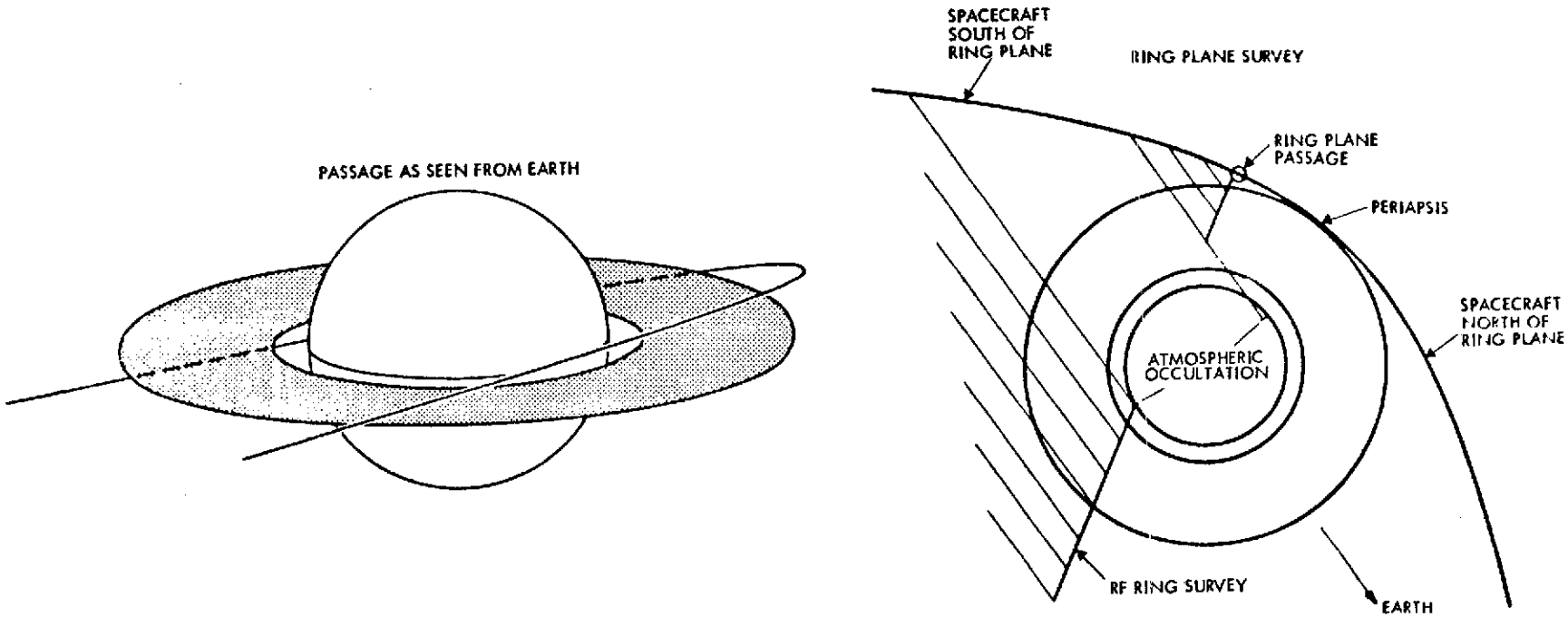

Figure 3-16. Saturn Ring Encounter (1979 Mission)*

*Data furnished to TRW Systems by Ames Research Center.

the Jupiter-Uranus mission profile instead of Saturn-Uranus may also have to be reconsidered.

3.2.5 Summary of Saturn and Uranus Transfer Trajectory and Encounter Conditions

Table 3-2 lists the key mission parameters that characterize the nominal heliocentric trajectories, targeting options, entry conditions, separation characteristics and communication relay geometry data, summarizing the conditions previously discussed. This compilation is from Ames Research Center's mission analysis notes, furnished to TRW.

Table 3-2. Summary of Transfer Trajectory and Encounter Characteristics

Mission	Heliocentric Trajectory	Targeting/Options	Entry Conditions	Separation/ Communications
1979 Saturn Probe Mission	15-day launch window (1050 lbs) 3.4-year trip time Titan encounter (150,000 km)	Saturn emphasis: 2:2 R_S periapsis Post-encounter to Uranus: 2.20 R_S periapsis	17 to 30 degrees north latitude 5 to 12 degrees angle of attack	500 R_S separation 70 m/sec velocity requirement 80 to 100,000 km communications range Bus aspect angle <90 degrees Probe aspect angle <10 degrees
1980 Saturn/ Uranus Mission (probe delivery at Saturn)	11-day launch window (1050 lbs) 3.1-year trip to Saturn 7-year trip to Uranus Titan encounter (300,000 km)	Saturn emphasis: 2.30 R_S periapsis Swingby to Uranus: 2.73 R_S periapsis	19 to 27 degrees north latitude 4 to 14 degrees angle of attack	500 to 700 R_S separation 70 m/sec velocity requirement 110 to 130,000 km communications range Bus aspect angle <90 degrees Probe aspect angle <10 degrees
1980 Uranus Mission via Saturn and Saturn/ Uranus Mission (probe delivery at Uranus)		Retrograde diametrical occultation 4.0 R_U periapsis	45 to 70 degrees north latitude 3 to 7 degrees angle of attack	1000 R_U separation 75 m/sec velocity requirement 80 to 100,000 km communications range Bus aspect angle <70 degrees Probe aspect angle <15 degrees

3.3 LAUNCH PHASE ANALYSIS

3.3.1 Nominal Launch Phase Characteristics

Nominal characteristics of the launch phase, including geocentric and heliocentric orientations of the launch asymptote, launch azimuths, coast angles and coast times in parking orbit are listed in Table 3-3 for the 1979 and 1980 mission opportunities. Because of the almost identical launch dates in both years and the similar trajectories flown, any differences in launch characteristics are minor.

Table 3-3. Launch Phase Characteristics

	Mission 1	Mission 2
Launch date	22 November 1979	25 November 1980
Departure asymptotic velocity (km/sec)	11.62	11.97
Inclination of interplanetary trajectory (deg)	5.3	6.0
Declination of launch asymptote (deg)	32.7	26.9
RA of launch asymptote (deg)	149.8	171.3
Launch azimuth (deg)	107.0	90.0
Heliocentric latitude of launch asymptote (deg)	19.1	21.2
Heliocentric longitude of launch asymptote (deg)	142.7	162.6
Powered flight angle (deg)	25.0	25.0
Free flight angle from injection burn to V_∞ (deg)	104.8	103.8
Coast angle to injection burn (deg)	201.8	214.8
Coast time in parking orbit (min)	49.4	52.4

The relatively large inclinations with respect to the ecliptic of both interplanetary trajectories are due to the selected Saturn arrival dates in 1983 and 1984, a time when the planet is close to its maximum northern heliocentric latitude. These arrival dates are dictated of course by the objective, applying to at least two of the three missions, of a Uranus intercept following the Saturn swingby.

For a trajectory inclination of 5 to 6 degrees a large inclination of the departure velocity vector $\overline{V}_\infty$ is required, i.e., about 20 degrees north relative to the ecliptic and 30 degrees north relative to the equator. The large out-of-plane angle of the departure velocity vector explains

the high launch energy (134 and 144 km^2/sec^2) in these missions compared to minimum energies of less than 120 km^2/sec^2 for favorable launch opportunities in missions to Saturn only.

With the given northerly declinations of the launch asymptote the use of an orbital rather than the direct ascent mode used in the Pioneer 10 and 11 missions becomes necessary. At these declination angles coast times of 49.4 and 52.4 minutes in the parking orbit are required.

The Centaur stage, originally restricted to orbital coast times of less than 25 minutes, has been modified to permit coast times of up to one hour or longer in future missions. Increased coast capability is provided by additional thermal insulation of the propellant tanks, to reduce boil-off, and by increased attitude control propellant capacity. The total payload weight penalty accruing from these modifications is about 70 pounds in the injection velocity range of interest in the Pioneer Saturn Uranus missions.* However, this payload penalty is already reflected in the reference Titan III E/Centaur/TE-364-4 performance curve (Figure 3-3) defined by Ames Research Center for purposes of this study.

3.3.2 Launch Azimuth Requirements Related to Launch Window Duration

The launch azimuths of 107 and 90 degrees listed in Table 3-3 correspond to conditions for attaining the desired launch asymptote declination (DLA) (32.7 and 26.9 degrees north) without consideration of a daily launch window. For a launch window of one hour's duration a range of launch azimuths must be provided as illustrated in Figure 3-17. Somewhat different launch azimuth requirements apply in the cases of missions of type 1 and 2 since, in the first case, the DLA is larger and in the second case it is smaller than 28.3 degrees, the largest declination that can be accommodated by a due east launch from ETR. To achieve a daily launch window of up to one hour in the first case, an increase of the launch azimuth to 108 degrees is necessary (see Figure 3-17a). In the second case (see Figure 3-17b) a change of at most 9 degrees north or

*Information received from Mr. W. Glunt of Convair Aerospace Division.

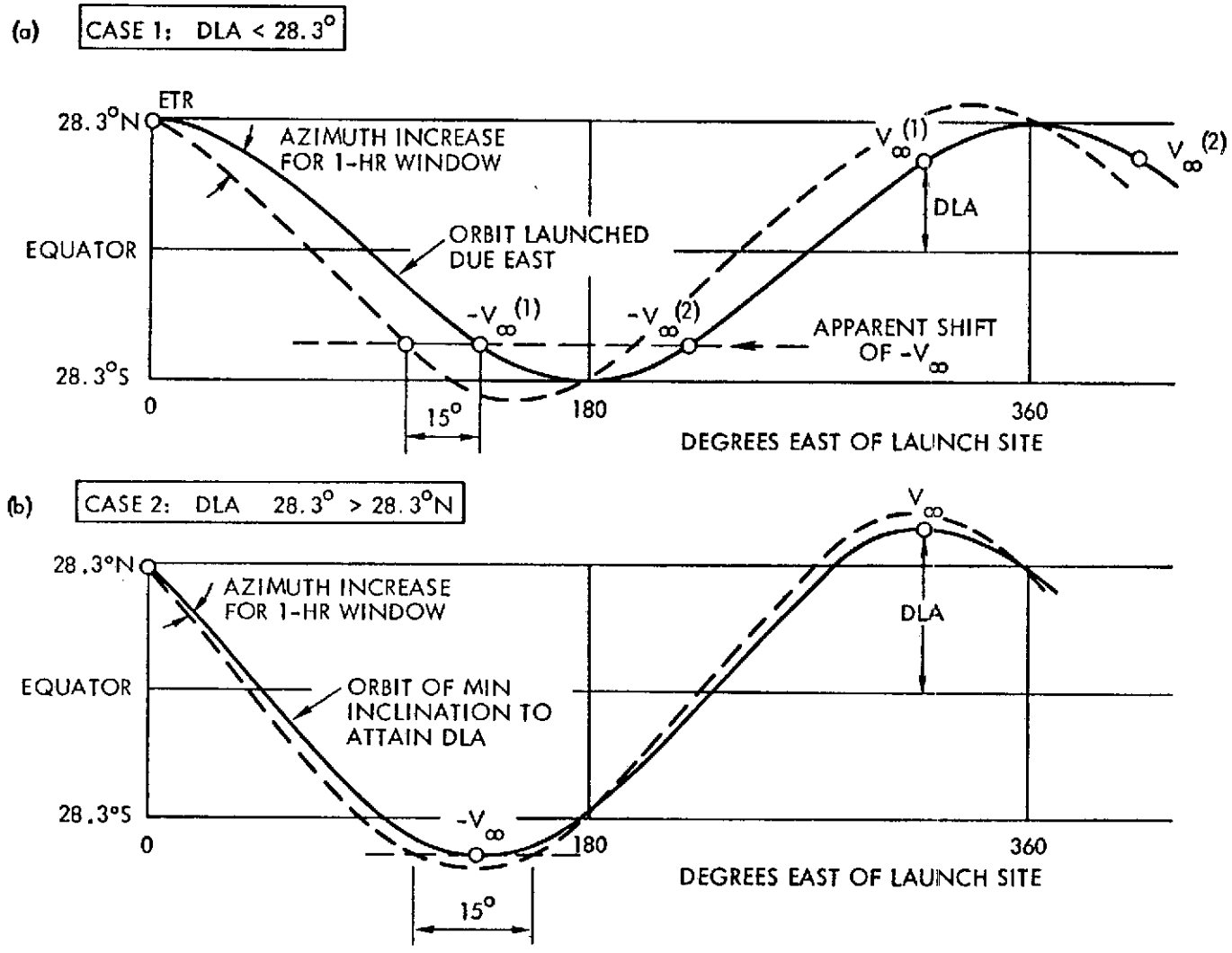

Figure 3-17. Relationship Between Launch Asymptote Declination, Orbit Inclination, Launch Azimuth and Daily Launch Window (Not to scale)

south of due east would be required. In general, launch azimuth angles in the sector from 90 to 114 degrees are routinely permitted under the range safety restrictions at ETR. Thus, to avoid northerly azimuths (angles less than 90 degrees) a one-hour launch window can also be attained by launching at azimuths of 90 to 103 degrees. Weight penalties associated with these deviations from due east are very small. Table 3-4 lists the azimuth requirements for missions 1 and 2, and shows that the launch velocity penalties are only 20.1 and 10.4 m/sec, respectively. The injected weight penalties are only 9 and 4 pounds. A daily launch window of more than one hour can thus be readily allowed if necessary, particularly in the case of mission 2.

Table 3-4. Launch Azimuth Requirements for One-Hour Daily Launch Window

		Mission 1	Mission 2
Declination of launch asymptote	(deg)	32.7	26.9
Launch azimuth required for zero launch window	(deg)	107.0	90.0
Increased launch azimuth for 1-hour launch window	(deg)	108.0	103.0
Injection velocity penalty, ΔV_C, for off-east launch	(m/sec)	20.1	10.4
C_3 - penalty, ΔC_3	(km^2/sec^2)	0.46	0.24
Injection weight sensitivity $\frac{\partial W_o}{\partial C_3}$	($lb/km^2/sec^2$)	20.0	16.0
Azimuth weight penalty ΔW_o	(lb)	9.0	4.0

3.3.3 Ground Station Coverage of Injection Burn Phase

Preliminary analysis of ground station coverage shows that the injection burn could occur within the range of the Honeysuckle or Carnarvon (Australia) or the Guam STDN stations. The required southerly launch azimuths of 103 and 108 degrees have the effect of

shifting the ground track by 26 and 34 degrees, respectively, to the west relative to the ground track obtained with a due east launch. Actually, a shift nearly as large as this is necessary to bring the spacecraft orbit within the range of the Guam STDN station for observation of the injection phase. If the injection burn phase cannot be observed conveniently by an existing ground station, a ship can be stationed at the desired location for this purpose as was done for Pioneer 10 and 11.

3.3.4 Other Characteristics

The acoustic and vibration environment of the Titan III E/Centaur/TE-364-4 is included in the envelope to which the Pioneer F/G spacecraft was developed and qualified as per Specification PC 210.02. Thus no requalification of the SUAE spacecraft for the new launch vehicle is required.

3.4 DISPERSION OF SPACECRAFT BUS AND MIDCOURSE CORRECTION REQUIREMENTS

Results of a concurrent study by JPL of Pioneer Saturn Uranus navigation and guidance characteristics* were excerpted and are presented in this section to summarize spacecraft dispersion and midcourse maneuver requirements.

3.4.1 Launch Vehicle Injection Errors and Spacecraft Correction Maneuvers

Injection errors and midcourse maneuvers previously determined for several classes of Pioneer missions to Jupiter are not applicable in the case of the Saturn Uranus mission, although the same launch vehicle upper stages are to be used, because of the much larger injection velocity of this mission. The following results were obtained for the first midcourse maneuver from the JPL navigation and guidance study (see Table 3-5).

* This JPL study was under the cognizance of L. A. Manning of Ames Research Center, who furnished results to TRW.

Table 3-5. Midcourse Maneuver Five Days After Injection (m/sec)

Mean velocity correction	32.7
1σ velocity correction	15.8
Probable velocity correction (99%)	80.1

Figure 3-18 shows the probability of requiring a maneuver of magnitude ΔV as a function of ΔV for the given values of the mean and standard deviation, evaluated by the Hoffman-Young method. The results are to be considered as conservative.

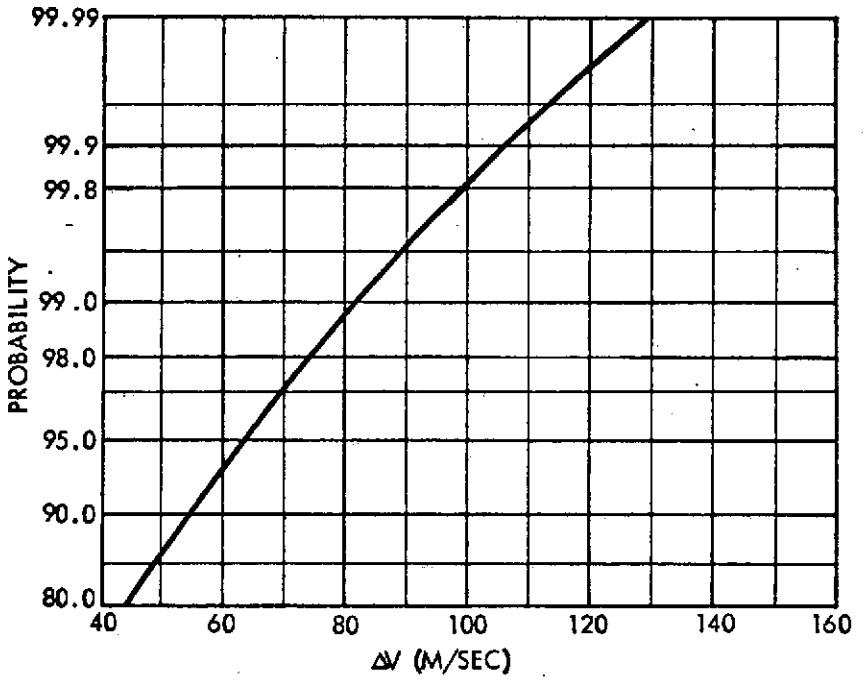

Figure 3-18. Probability of Maneuver of Magnitude ΔV as Function of ΔV

Execution errors of this maneuver cause dispersions at Saturn, mapped as an error ellipse with semi-major axis of 2,422 km and semi-minor axis of 606 km. The orientation of the error ellipse is 20 degrees from the T axis in the R-T coordinates of the impact plane. Actually, the uncertainty of Saturn's ephemeris ($1\sigma \cong 1000$ km in the direction of right ascension) is not reflected in these data and must be added in an RMS sense to obtain the overall spacecraft dispersion errors relative to the planet.

3.4.2 Trajectory Errors and Correction Maneuvers on Saturn-Uranus Leg of Mission

Two cases have been considered in the JPL study:

a) navigation on the Saturn-Uranus leg using radio tracking data only

b) navigation using radio and optical sensor data.

The maneuver requirements for a post-Saturn guidance correction, 50 days after encounter, and the resulting dispersion ellipse dimensions mapped at Uranus are listed in Table 3-6.

Table 3-6. Post-Saturn Maneuver Requirements and Dispersions at Uranus

	Radio Tracking Only	Radio Plus Optical Sensor
1. ΔV requirements (m/sec) (at Saturn +50 days)		
Mean velocity correction	48.1	8.8
1σ velocity correction	30.4	4.8
Probable velocity correction (99%)	139.3	23.2
Mean ΔV component along earthline	0.2	--
1σ component along earthline	12.8	3.8
Mean ΔV perpendicular to earthline	45.9	8.0
1σ component perpendicular to earthline	31.0	4.8
Probable total velocity correction (99%) when added algebraically(1)	177.5	33.8
2. Dispersions at Uranus (km)(2)		
Semi-major axis	8017	1357
Semi-minor axis	882	149

(1) Algebraic addition is appropriate for Pioneer thruster implementation (see also Section 3.5).
(2) These dispersions do not reflect errors due to Uranus' ephemeris uncertainty.

The correction maneuver requirement for radio tracking only is prohibitively large, although by using quasi-very-long baseline interferometry it would be less than the figure (177.5 m/sec) given in the table. With the aid of an optical navigation sensor the maneuver requirement is reduced to 33.8 m/sec. The dispersion ellipse at Uranus has a semi-major axis of 1357 km which is oreinted approximately in the spacecraft orbit plane. Again, the uncertainty of Uranus' ephemeris has to be added to this dispersion. Uranus' position uncertainty, $1\sigma \sim 10,000$ km

in the direction of right ascension, dominates the spacecraft trajectory error relative to Uranus. Thus, to achieve a Uranus encounter with adequate probe delivery accuracy, as well as to reduce the velocity requirements of the post-Saturn maneuver the optical navigation sensor becomes indispensable in this mission (see Section 3.7). However, for the 1979 Earth-Saturn mission, onboard guidance is not necessary to provide adequate probe delivery accuracy; radio tracking alone will suffice.

3.5 PROPULSION REQUIREMENTS

3.5.1 Types of Maneuvers

Propellant requirements can be estimated based on all ΔV maneuvers to be performed in the course of the mission, with allowance for additional trim maneuvers that may become necessary. A margin for contingencies such as maneuver efficiency loss in certain thruster failure modes must also be included. In addition, the total spin control and precession during the mission must be estimated and included in the total propellant weight. The principal $\overline{\Delta V}$ maneuver requirements include:

1) correction of launch dispersion (plus trim if necessary)
2) approach guidance correction at target planet
3) spacecraft bus deflection maneuver (plus trim if necessary)
4) post-encounter midcourse maneuver (plus trim) at Saturn if mission continues to Uranus.

Since all but the first midcourse correction and trim maneuver are to be performed in the earth-pointing mode which is less efficient than a maneuver mode with the spacecraft spin axis oriented in the desired ΔV orientation an additional weight allowance must be made. This will be discussed below.

3.5.2 Maneuvers in the Earth-Pointing Mode

In the interest of maintaining an uninterrupted command and telemetry capability at large earth-spacecraft distances, the spacecraft must remain earth-oriented at all times. Off-earth-pointing for maneuver purposes is therefore not permitted, except for the initial midcourse maneuver(s) to be performed right after launch where the omni-antenna provides adequate coverage.

Consequently, the spacecraft must be equipped with an off-axis thrust capability, so as to be able to execute ΔV-maneuvers in any desired direction, while keeping the spin axis earth-oriented.

Alternate approaches to effect off-axis thrusting are either to use the circumferential spin/despin thrusters or a radial thruster in a pulsed thrust mode. These alternatives are examined in detail in Appendix E. The use of the spin/despin thrusters in the Pioneer F/G configuration has the disadvantage of causing large unintended precession torques around the Y-axis as a by-product of the trajectory correction. This would require cancellation by the axial precession thrusters and result in operational complexity as well as extra propellant expenditure, typically an increase of 25 percent. Thus, the addition of radial thrusters is the preferred approach. These thrusters are mounted in the equipment bay extension, with line of thrust acting through the center of mass of the spacecraft bus, i.e., the axial location to which the c.m. moves when the entry probe is separated. This alignment is preferable because it reduces operational complexity, i.e., compensation of precession effects, at a critical time in the mission profile. It may also save propellant.

Lateral ΔV maneuvers, or combinations of lateral and axial maneuvers involve a loss in propulsive efficiency for these reasons:

- Pulsed operation reduces I_{sp} compared to continuous operation of axial thrusters.
- Cosine losses are incurred when the firing pulse lasts over a significant portion of the spin cycle.
- Combination of axial and radial thrust components to exercise thrust in arbitrary direction relative to spin axis results in vector addition losses.
- Unwanted residual precession effects due to radial thrust vector misalignment must still be compensated by axial thrust.

Figure 3-19 shows the composite efficiency of pulsed lateral ΔV thrusting. For large pulse durations the cosine loss effect dominates,

while for short pulse durations the loss is mainly due to a reduction of effective I_{sp}. The losses due to these effects are minimized when the pulse length is 1 to 1.5 seconds, corresponding to a firing arc of 30 to 45 degrees.

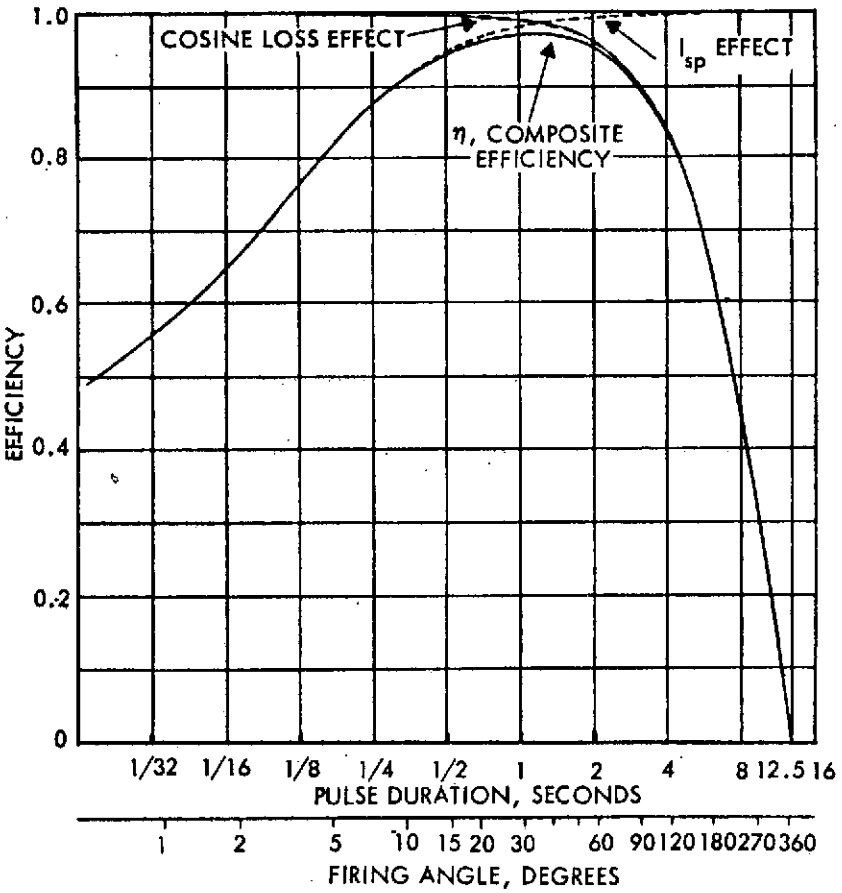

Figure 3-19. Composite Efficiency of Pulsed Lateral ΔV Thrusting

Figure 3-20 explains the character of the vector addition losses. (A more complete analysis is presented in Appendix E.) On the left is a vector diagram of the achievable $\overline{\Delta V}$ resulting from the addition of radial and axial components $\overline{\Delta V}_R$ and $\overline{\Delta V}_A$. The diagram shows the locus of the resulting $\overline{\Delta V}$ vectors, a triangle with its apex 90 degrees from the spin axis. The efficiency loss due to pulsed operation is taken into account. In the example shown, the efficiency η is 0.8 (solid triangle). The case of $\eta = 1.0$ is also illustrated (dashed triangle). The relative ΔV-loss is the segment between the circle of radius 1 and the resultant $\overline{\Delta V}$-vector,

as shown for a given orientation θ from the spin axis. The smallest off-axis thrusting loss occurs for $\theta = 90$.

The sketch at the right in Figure 3-20 illustrates the three-dimensional surface that defines the effectiveness of combined axial and radial thrust in arbitrary clock angle directions rather than only in one plane. This surface consists of two cones having a common base, the tips pointing in opposite directions along the spin axis. One can visualize this by letting the triangle in the diagram at the left rotate with the spacecraft. The reference circle of radius 1 thus becomes the unit sphere.

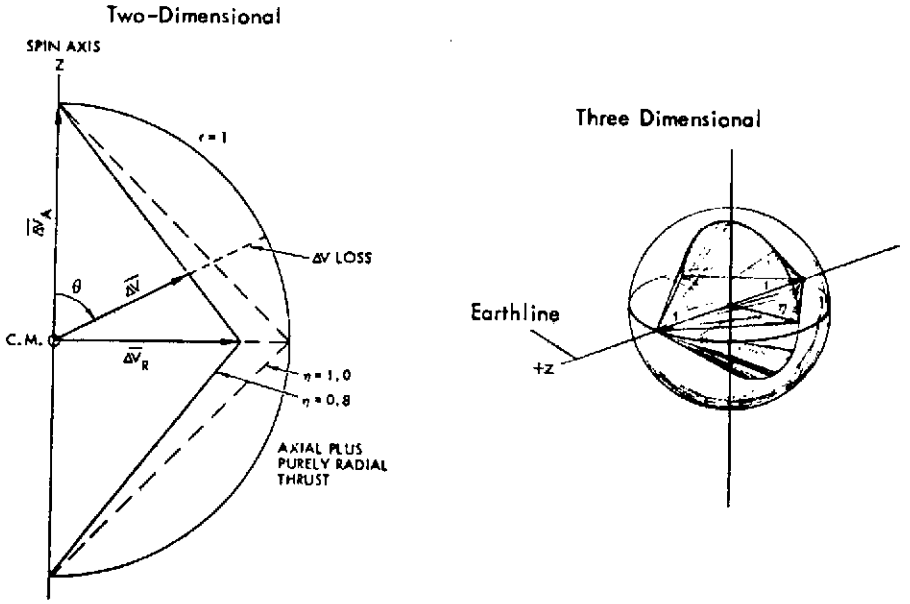

Figure 3-20. Vector Addition Losses

If maneuvers are considered where thrust orientations are assumed to be equally likely in any direction, an average thrust effectiveness coefficient μ can be defined which takes into account the relatively higher percentage of thrust requirements in radial directions compared to those in axial directions. This implies averaging over all orientations on a sphere rather than over the cone angle only.

Figure 3-21 shows the average thrust effectiveness μ as a function of thrust efficiency η. This parameter includes only the pulsed thrust losses (I_{sp} and cosine losses, e.g., $\eta = 0.97$ for a one-second thrust arc). It may also include the penalty for precession correction propellant. We conclude from this discussion that combined ΔV losses of 25 to 30 percent are typical under the conditions assumed here.

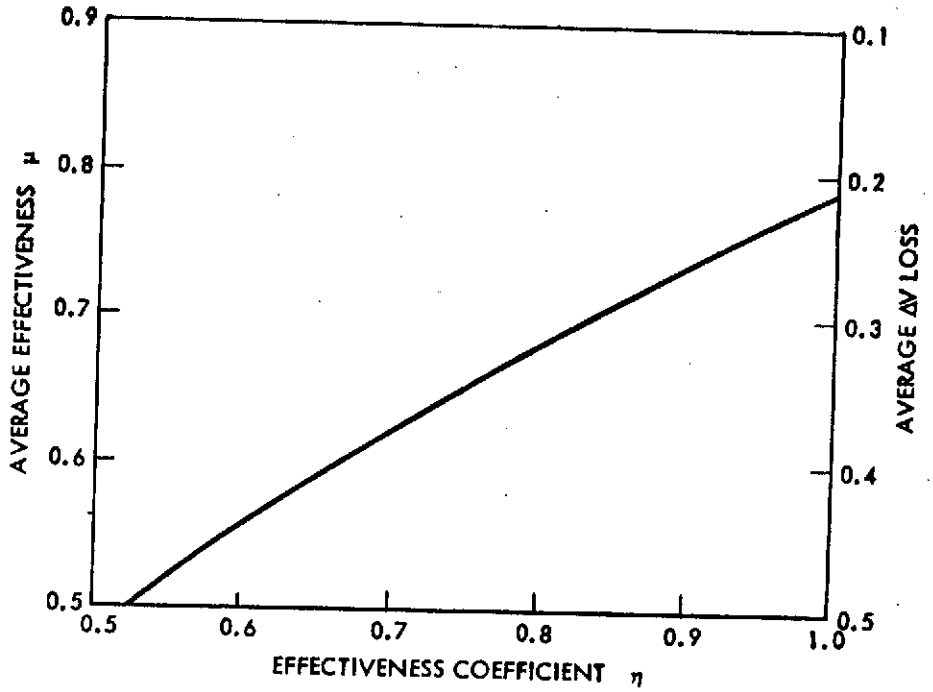

Figure 3-21. Average Thrust Effectiveness for Combined Axial and Radial Thrust

3.5.3 Maneuver Requirements and Propellant Budget

Propulsive maneuver requirements and propellant budgets have been evaluated for both the Earth-Saturn and the Earth-Saturn-Uranus missions. Table 3-7 lists maneuver requirements for the Earth-Saturn-Uranus mission in terms of ΔV maneuvers including spin and precession control. For each ΔV maneuver event the time of occurrence, the mode and direction of thrusting, and the estimated ΔV requirements are stated. Spin and precession control requirements that account for only a small portion of the total propellant budget are stated more summarily.

The required ΔV (column 5) is translated into an "equivalent ΔV" value (column 9) by taking into account any losses due to off-axis thrust operations. Thus, propulsive efficiencies of less than 100 percent

Table 3-7. Propulsive Maneuver Requirements for Earth-Saturn-Uranus Mission

A. ΔV REQUIREMENTS

TIME	MANEUVER	PROBE	MODE	ΔV M/SEC	DIRECTION	EFFICIENCY	EFFECTIVE I_{SP} (SEC)	EQUIVALENT ΔV M/SEC AT I_{SP} = 225 SEC	
E+5	LAUNCH VEHICLE CORRECTION NO. 1	ON	NORMAL	85*	ANY	1	225	85	
E+20	LAUNCH VEHICLE CORRECTION NO. 2	ON	NORMAL	3	ANY	1	225	3	
S-8	SATURN APPROACH TRIM	ON	EARTH LINE	5	⊥ EARTH LINE	0.85(1)	191	6	143.0 (PROBE ON)
S+40	SATURN DEPARTURE CORRECTION	ON	EARTH LINE	30	ANY	0.71(1)	160	42	
U-22	URANUS APPROACH TRIM	ON	EARTH LINE	5	ANY	0.71(1)	160	7.0	
U-20	SPACECRAFT DEFLECTION	OFF	EARTH LINE	30**	∥ EARTH LINE	1	225	30.0	80.0 (PROBE OFF)
				46**	⊥ EARTH LINE	0.97(2)	218	47.5	
U-10	URANUS APPROACH TRIM	OFF	EARTH LINE	2	ANY	0.65(2)	191	2.5	

(1) BASED ON $\eta = 0.85 = 0.97 \div 1.14$
(2) BASED ON $\eta = 0.97$

* NOMINAL TRAJECTORY: $\mu + 3\sigma$ = 81.1 M/SEC (99%)
** MISSION ANALYSIS PRESENTATION, NOVEMBER 16, 1972

B. SPIN CONTROL REQUIREMENTS

APPENDAGES	ΔN (RPM)	I_{SP} (SEC)
STOWED	60	225 (CONTINUOUS)
DEPLOYED	18	160 (PULSED)

C. PRECESSION REQUIREMENTS

ANGLE PRECESSED THROUGH: $\Delta\theta$ = 1500 DEG
SPECIFIC IMPULSE: I_{SP} = 150 SEC
SPIN RATE: N = 4.8 RPM

(column 7) reflect in a proportional reduction of effective specific impulse (column 8). For propellant weight calculations based on the nominal I_{sp} value of 225 seconds the equivalent ΔV (column 9) must be used which is obtained from the actual ΔV requirement through division by the efficiency factor.

The first two maneuvers, performed right after launch, can use the normal thrust mode with the spacecraft oriented in the required direction, generally off-earth. These maneuvers can therefore be performed with 100 percent efficiency. The lowest propulsive efficiency is assigned to the Saturn departure correction, at S + 40 days, and the Uranus approach trim, at U -22 days. The low efficiency value (0.67) used here reflects both the average loss for a composite maneuver in arbitrary direction (see Figures 3-20 and 3-21), and the extra propellant expenditure of about 23 percent per unit velocity change that is required to compensate for unintended precession effects due to radial-thrust-line offset from the center of mass. This 23 percent penalty only applies to maneuvers performed with the probe onboard the spacecraft, since after probe separation the thrust vector offset goes to zero.

Some of the assumed ΔV requirements are on the conservative side. The values of 85 m/sec and 30 m/sec assumed for the first and fourth maneuver reflect ΔV estimates that will not be exceeded with 99 percent probability. Actually, the algebraic sum of the two maneuver allocations, each based on 99th percentile requirements, is much greater than the 99th percentile of the combined maneuvers. Thus the actual total equivalent ΔV requirements of this mission are likely to amount to only 220 m/sec rather than 246.5 m/sec as listed in Table 3-7.

Table 3-8 summarizes the corresponding actual and equivalent ΔV requirements and the spin and precession control requirements of the Earth-Saturn mission. The total equivalent ΔV requirement is 166.5 m/sec, 80 m/sec less than for the ESU mission. The spin and precession control requirements do not differ significantly.

The propellant budget for the ESU mission is summarized in Table 3-9 based on the sequence of propulsive maneuvers listed in Table 3-7. Mass characteristics used in obtaining these results correspond to the case of a 250 lbm separated probe mass and an interstage

Table 3-8. Propulsive Maneuver Requirements for Earth-Saturn Mission

A. ΔV Requirements

Time	Maneuver	ΔV (m/sec)	Equivalent ΔV (m/sec)	
E + 5	Launch vehicle correction no. 1	85	85	
E + 20	Launch vehicle correction no. 2	3	3	
S - 26	Saturn approach trim	5	7.5	
S - 24	Spacecraft deflection ΔV			166.5
	∥ Earthline	19	19	
	⊥ Earthline	48	49.5	
S - 10	Saturn approach trim	2	2.5	

B. Spin Control Requirements

Appendages	ΔN (rpm)	I_{sp} (sec)
Stowed	60	225 (continuous)
Deployed	14	160 (pulsed)

C. Precession Requirements

Angle precessed through:	$\Delta\theta$ = 1400 deg
Specific impulse:	I_{sp} = 150 sec
Spin rate	N = 4.8 rpm

Table 3-9. Summary of Propellant Budget for ESU Mission

Assumed Sequence of Maneuvers	Weight (lbs)
Initial weight	1039.5
Spin control	3.4
ΔV maneuvers (probe on)	65.1
Precession control	17.6
Probe removal	250.0
ΔV (probe off)	25.1
Final dry weight (1)	678.3
Total usable propellant weight	111.2
Minimum tank diameter (2) (inches)	20.4

(1) Includes 4.0 lbm of unusable propellant and pressurant.

(2) Assumes the same ratio of usable propellant to ullage volume as for Pioneer F/G propellant tank.

adapter that remains attached to the bus. (The case previously considered in the study where the adapter was jettisoned after probe separation resulted in nearly the same propellant mass.) The total usable propellant mass required for this mission is 111.2 lbm.

The proposed spacecraft design uses the existing 22.25-inch Lockheed P-95 propellant tank to save development and cost rather than the minimum tank size (20.4 inches) that would be required for the above propellant load. This also has the advantage of providing a margin for a propellant load increase should mission requirements be modified at a later time.

Figure 3-22 shows the change in propellant mass allocations that would correspond to a variation of spacecraft dry mass in the ESU mission: the total propellant mass varies by only ±3.3 pounds for a ±30 pound variation in spacecraft dry mass.

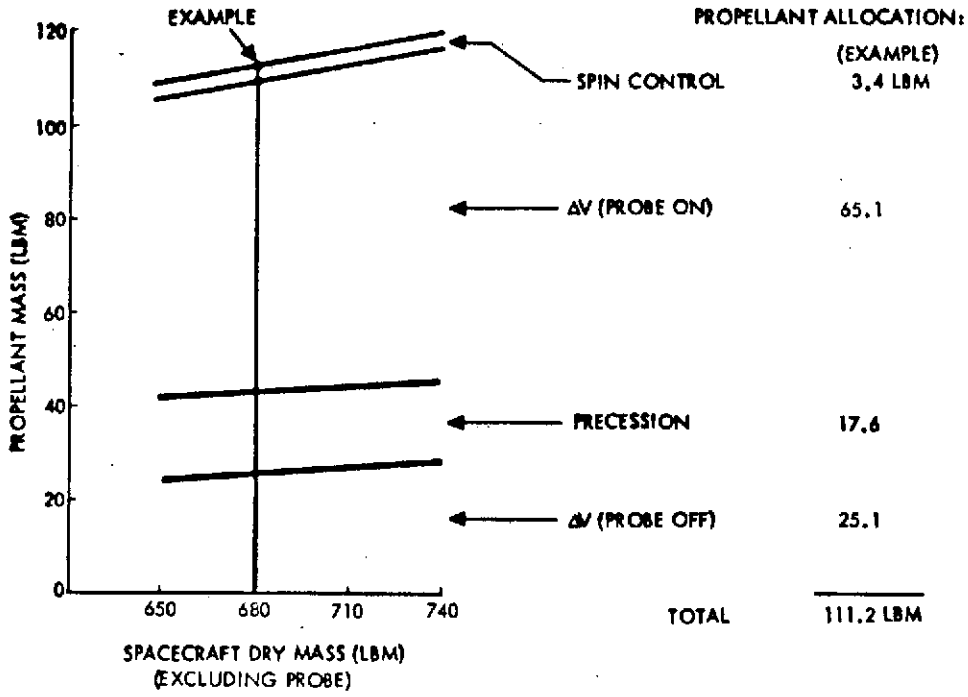

Figure 3-22. Propellant Requirements for Earth-Saturn-Uranus Mission

3.5.4 Propulsion Tradeoffs and Alternatives

Since the propellant mass for the ESU mission is nearly twice as large as for the Pioneer F/G Jupiter missions it is worth examining some possible approaches to achieve propellant savings.

The largest individual ΔV requirements are for correction of launch dispersion, correction of Saturn swingby velocity error, and trajectory deflection at Uranus. The latter two, being performed in the earth-pointing thrust mode, are penalized by efficiency losses discussed in Section 3.5.2.

The total ΔV penalty of thrust operations performed in the earth-pointing mode is 41.5 m/sec corresponding to about 21 lbm of propellant. The weight saving alternative of reorienting the spacecraft for thrusting in the normal mode would increase operational complexity and introduce unacceptable risks due to interruption of communication coverage at large earth distance. However, this mode may still provide a potential propellant reserve under contingencies where propellant consumption would be much higher than expected, for example, as a result of excessively large launch dispersion or unforeseen delay of entry probe separation at the target planet.

Propulsion requirements for the correction of velocity errors at Saturn swingby and for bus trajectory deflection at the target planet are subject to reduction through improved accuracy and sensitivity of the optical navigation sensor. The potential weight savings can be significant because more than half of the total propellant mass of 112.6 pounds is provided to meet these ΔV requirements. This tradeoff between propellant mass and navigation capability will be further discussed in Section 3.7.

3.6 SEQUENCE OF EVENTS

The sequence of events during the Pioneer Earth-Saturn and Earth-Saturn-Uranus mission is similar to the Pioneer 10 and 11 Jupiter flyby missions from the injection into transfer orbit by the launch vehicle through the interplanetary cruise phases between Earth and Saturn and between Saturn and Uranus. The principal differences, emphasized in this discussion, involve events before arrival at Saturn and Uranus and during the planetary encounter(s).

3.6.1 Summary of Event Sequence

Table 3-10 gives a summary of the event sequence in the ES and ESU missions, except that in the case of the ES mission the events listed under B are not applicable with Saturn itself being the target planet. A brief description of principal operations during each mission phase is given below.

3.6.2 Description of Events

Launch and Injection Sequence. This sequence differs from the Pioneer 10/11 launch only in terms of the ascent mode. While Pioneer 10 and 11 were launched by direct ascent, the Saturn Uranus missions use a parking orbit with a 50-minute coast period, because of the northerly declination of the launch asymptote of about 30 degrees dictated by the launch dates.

Using the same second and third booster stages as Pioneer 10 and 11, the Pioneer Saturn Uranus spacecraft will go through essentially the same acceleration profile and staging events.

Separation from Launch Vehicle and Spacecraft Deployment. Spin-up and separation from the third booster stage, TE-364-4, are essentially the same as for Pioneer 10 and 11. The despin maneuver following separation, the deployment sequence of appendages, establishment of the desired spin rate and orientation to cruise attitude are also unchanged.

First Midcourse Maneuvers. The main midcourse maneuver for correction of injection errors takes place about five days after launch on ground command. The spacecraft is reoriented in the desired thrust direction to perform this maneuver. This and the subsequent trim maneuver, about 20 days after launch, are the only ΔV maneuvers of the mission that use the same thrust pointing mode as Pioneer 10 and 11 since at an earth distance of less than 20 million km adequate omni-antenna coverage is available for both uplink and downlink communications. All subsequent ΔV maneuvers are performed in the earth-pointing mode to ensure uninterrupted communications coverage.

Earth-to-Saturn Cruise. During the cruise the spacecraft operates in the same mode as Pioneer 10 and 11. Scientific observations of

Table 3-10. Summary Mission Sequence of Events

A. NEAR EARTH

NO.	TIME AFTER LAUNCH	EVENT	REMARKS
1	0	LIFTOFF TO INJECTION	
2	1 - 6 HOURS	SEQUENCER-INITIATED EVENTS ON SPACECRAFT	INCLUDES DESPIN, DEPLOYMENT OF APPENDAGES, AND INITIAL ORIENTATION
3	4 DAYS, AND PERIODICALLY THROUGHOUT MISSION	EARTH POINTING (MAY HOLD CLOSER TO SUN POINTING FOR 50 DAYS TO SHADE PROBE FROM SUN)	OPEN-LOOP OR CLOSED-LOOP (CONICAL SCANNING) PRECESSION
4	5 DAYS	FIRST TRAJECTORY CORRECTION MANEUVER	PRECESSION, ΔV, AND RETURN PRECESSION MANEUVERS
5	20 DAYS	SECOND TRAJECTORY CORRECTION MANEUVER	

B. NEAR SATURN (ON SWINGBY TO URANUS)

NO.	TIME FROM SATURN ENCOUNTER	EVENT	REMARKS
1	-20 TO -10 DAYS	TERMINAL GUIDANCE SENSING	USE ONBOARD STAR MAPPER
2	-8 DAYS	APPROACH TRAJECTORY CORRECTION MANEUVER	ΔV IN EARTH-LINE MODE
3	-10 TO +10 DAYS	ENCOUNTER SCIENCE	
4	+20 DAYS	DEPARTURE GUIDANCE SENSING	USE STAR MAPPER
5	-40 DAYS	DEPARTURE TRAJECTORY CORRECTION MANEUVER	ΔV IN EARTH-LINE MODE

C. NEAR TARGET PLANET

NO.	TIME FROM SEPARATION[1]	EVENT	REMARKS
1	-20 TO -3 DAYS	TERMINAL GUIDANCE SENSING	USE STAR MAPPER
2	-2 DAYS	APPROACH TRAJECTORY CORRECTION MANEUVER	ΔV IN EARTH-LINE MODE
3	-2 DAYS	CHECKOUT PROBE OPERATION	
4	-2 DAYS	CHARGE PROBE BATTERY	
5	0 DAYS	DISCONNECT PROBE ELECTRICAL CONNECTOR	ORDNANCE EVENTS INITIATED BY SPACECRAFT
6	0 DAYS	SEPARATE PROBE FROM SPACECRAFT	
7	+1 DAY	SPACECRAFT TRAJECTORY CHANGE MANEUVERS	ΔV IN EARTH-LINE MODE PLACES SPACECRAFT ON APPROPRIATE FLYBY TRAJECTORY
	TIME FROM ENCOUNTER		
8	-10 DAYS	SPACECRAFT TRAJECTORY TRIM MANEUVER (IF NECESSARY)	
9	0	ENTRY PHASE OF PROBE	PEAK DECELERATION AND ENTRY HEATING
10	+1 MINUTE	ESTABLISH PROBE-BUS COMMUNICATIONS	AFTER BLACKOUT
11	~60 MINUTES (APPROXIMATELY)	END OF PROBE DESCENT PHASE	PROBE IS BELOW 10-BAR LEVEL
12	~70 MIN (SATURN) ~100 MIN (URANUS)	SPACECRAFT IS AT PERIAPSIS	R_P 2.75 R_S, 4 R_U
13	~5 TO ~6 HOURS (SATURN) +7 TO +10 HOURS (URANUS)	SPACECRAFT OCCULTATION BY TARGET PLANET	

[1] SEPARATION IS NOMINALLY 32 DAYS BEFORE ARRIVAL AT SATURN, 20 DAYS BEFORE ARRIVAL AT URANUS.

particles and fields phenomena are made using similar instruments (except for the asteroid/meteoroid sensor which will not be included in the payload). The nominal time of flight to Saturn is 3.4 years in the ES mission and 3.1 years in the ESU mission.

For routine telemetry operations S-band provides adequate bit rates, e.g., 32 bps to a distance of 6 AU on the 26-meter DSS antenna, 256 bps at Saturn on the 64-meter antenna. If higher bit rates are required during special events the telemetry link is switched to X-band. The use of S-band rather than X-band telemetry during normal cruise operations reduces the number of periodic pointing update maneuvers and avoids dependence on the 64-meter antenna stations during the early part of the mission. Initially the spacecraft orientation must be updated as often as twice per week, but toward the end of this phase only once every other week when operating on S-band, and only if close earth-pointing is necessary.

Saturn Approach and Encounter (on Swingby to Uranus). Operations here differ from the Pioneer 10 and 11 missions since accurate control of the flyby distance is essential to a reduction of the first post-encounter midcourse ΔV requirement. To this end the optical navigation sensor will be used to determine relative trajectory errors (largely due to Saturn ephemeris uncertainty) to within less than 100 km. This involves pointing the instrument in the direction of a navigational reference target such as the satellite Titan, acquiring the target and measuring its position relative to several reference stars.

This sequence takes place 10 to 20 days before encounter. All operations are performed on ground command. The navigational fixes are telemetered by the spacecraft to earth where they are interpreted and used for improved orbit determination relative to Saturn.

An approach trajectory correction is commanded and executed about eight days before encounter, with the spacecraft performing the maneuver in the earth-pointing mode.

The sequence is repeated after the flyby with navigation fixes occurring about 20 days, and the departure trajectory correction about 40 days after encounter.

Scientific observations of Saturn are conducted during the interval of -10 to +10 days from encounter. Of particular interest are atmospheric occultation and ring occultation observations by dual frequency RF measurements.

Saturn-to-Uranus Cruise. The same operational modes apply as in the Earth-to-Saturn cruise, (see discussion above), with telemetry bit rates of 64 (to 14 AU) and 32 bps (to Uranus) on S-band, using the 64-meter DSS antennas, or 1024 bps to Uranus on X-band. Periodic pointing update maneuvers are required every five to ten days if on X-band, and only every 15 to 30 days if on S-band. The total Saturn-to-Uranus cruise time is 3.8 years.

Scientific observations of interplanetary particles and fields phenomena include, in particular, the detection of an increase in galactic influences coupled with a gradual decrease of solar wind influence. The spacecraft will be traveling in the direction toward the nearest boundary of the heliosphere while Pioneers 10 and 11 move in the opposite direction owing to their 1972/73 launch dates.*

Approach to Target Planet (Saturn or Uranus). On approaching the target planet the spacecraft must carry out the following operations as commanded from earth (timing of these events as given in Table 3-10):

- Prepare for terminal navigation observation: aim star mapper, transmit angle data on reference stars scanned; stars are identified and accurate spin axis orientation determined by ground operations.
- Acquire navigational reference object (i.e., a bright satellite of the target planet) and transmit angle data to earth; ground operations updates trajectory and determines terminal maneuver requirement.
- Execute approach trajectory correction maneuver as commanded from earth.
- Checkout entry probe operation and charge probe battery.
- Separate probe (events as listed in Table 3-10).

*For Pioneer 11 this will be true only if targeted to a posigrade Jupiter swingby to a solar system escape.

- Perform trajectory deflection maneuvers as commanded from earth; main maneuver followed by trim maneuver if necessary.

The planet approach phase involves events of critical importance. Accurate performance of all steps listed in this sequence is essential to mission success. The time constraints of probe separation and bus trajectory deflection are dictated by the sensitive dependence of ΔV requirements on planet range at which the maneuver is performed. In planning and executing this sequence the long round-trip signal delay (2.6 hours at Saturn, 5.4 hours at Uranus) on command and telemetry communications must be taken into account. Typically, each critical command received must be verified by the spacecraft before the go-ahead signal is transmitted from earth. This requires at least 1.5 round-trips per operation. The terminal navigation and guidance sequence, in particular, is subject to large delays due to repeated interchanges that are necessary between ground station and spacecraft, and the possible requirement of iterated maneuvers.

Target Planet Encounter Phase. All events occurring during the encounter phase are critical for achieving ultimate mission success, i.e., obtaining data on the planetary environment and the physics of the planet itself. The events that involve primarily the spacecraft bus during this mission phase, rather than both bus and probe, and their time of occurrence are those listed in Table 3-10(c).

With the geometry and phasing of bus arrival over the probe entry site appropriately controlled during the approach phase by bus deflection and trim maneuvers, ranges and aspect angles for probe-to-bus communication are established that permit the relay link to function. Incorrect time-phasing would tend to curtail or degrade relay link operation.

In order to avoid any possible risk of probe data not being received at earth after being transmitted in real-time via the probe-bus relay link, it is necessary to allow for repeated transmission by the bus, using the bus data storage unit (DSU) as backup. The bus will therefore repeatedly transmit the stored data, i.e., up to one hour's worth of probe-to-bus communications, until informed from earth that the complete set of data have been received intact. Only at this time will erasure of stored probe data from the DSU be permissible.

Under worst-case conditions, at Saturn as well as Uranus, the long communications delay to and from earth precludes verification of successful probe data telemetry until after the bus emerges again from occultation behind the planet. This means that probe data may have to remain stored on the bus DSU through the occultation period. Thus, DSU capacity dedicated to probe data storage cannot be counted on to serve other data storage needs, for example storage of image system data. Allocation of this segment of DSU to probe data begins at the time of entry when probe data are first received.

Observation of planetary characteristics by bus science instruments is an essential part of the overall scientific mission objectives, although not of the same priority as the observations by the entry probe. Any bus science operations that permit unconstrained performance of the relay link function by the spacecraft subsystems can be continued through the encounter. The only significant restriction on bus science operations are those imposed by data handling and storage limitations, starting with the time of probe entry. The bus science instruments affected by this restriction are the TV image system and possibly those instruments that would normally operate through the occultation/eclipse phase of the encounter.

Post-Encounter Phase. After completion of the target planet encounter the spacecraft will resume normal cruise operations and extend its mission as far as possible to the outer regions of the heliosphere; e.g., three years after passing Uranus it will reach the distance of 30 AU. Theoretically, it can continue to transmit data at bit rates of at least 16 bps to distances of the order of 80 AU. The extended final phase of the mission can thus provide important scientific data on interplanetary phenomena much beyond the range of the primary target, and explore heliospheric/galactic interactions.

3.6.3 Critical Spacecraft Operations

Flight operations critical to mission success were listed in Section 2.5. These include:

- Launch and spacecraft development
- Precession maneuvers
- ΔV maneuvers
- Planet approach navigation
- Planet departure navigation (at Saturn)
- Probe checkout and separation procedures
- Relay telemetry of probe entry data
- Bus science operations.

Examples of ΔV maneuver operations and planet encounter operations have been analyzed in greater detail and are discussed below.

3.6.3.1 Thrust Operations Before and After Probe Separation

Timing of the maneuver sequence before and after probe separation strongly affects the magnitude of the bus spacecraft deflection maneuver that is required to achieve the appropriate encounter geometry for probe data relay operations. The sequence of thrust operations for these maneuvers is given in Table 3-11 for the case of probe delivery at Uranus. Because of the long communication round trip time delay at Uranus (5.4 hours) this case is presented as a worst-case example.

To verify that the complex radial thrust sequence (necessary to achieve the ΔV maneuvers in the earth-pointing mode) can actually be carried out in the available time, a detailed analysis of the thrust execution procedure was performed. Principal factors in this sequence are:

a) The large number of pulsed radial thrust increments required per unit ΔV increment

b) The unintended precession effects due to c.m. offset of the radial thrust vector that must be compensated by periodic precession control pulses

c) The constraint of maintaining the spin axis pointed at earth within the 3 dB antenna

Table 3-11. Thrust Operation Sequences Before and After Probe Separation (At Uranus)

DAYS		
E - 26*		• FIRST NAVIGATIONAL DATA OBTAINED FROM TITANIA
E - 25	24 HOURS	• CHANGE OCTANTS (2X), GIMBAL ANGLE (1X), UPDATE NAVIGATIONAL DATA
	6 HOURS	• LOAD CORRECTION MANEUVER ΔV (5 M/SEC) – LATERAL THRUST, VERIFY DATA
	6 HOURS	• EXECUTE FIRST PART, CORRECT ANTENNA POINTING (ERROR ±0.6 DEGREE)
E - 24	CONTINUE FOR 12 HOURS	• RE-EXECUTE PROGRAM, SECOND PART, INTERRUPTED BY CONSCAN CORRECTION AFTER FIRST 10 GROUPS OF RADIAL -AXIAL THRUST PATTERNS. ACTUAL ΔV-TIME 5.3 HOURS
E - 22	2 DAYS	• VERIFY CORRECTED TRAJECTORY (RADIO + OPTICAL NAVIGATION)
E - 20		• COMPLETE CHECKOUT OPERATIONS, COMMAND AND EXECUTE PROBE SEPARATION
E - 19	24 HOURS	• ΔV CALIBRATION
	6 HOURS	• LOAD DEFLECTION MANEUVER ΔV (46 M/SEC) AND VERIFY
	6 HOURS	• EXECUTE FIRST PART, CORRECT ANTENNA POINTING
E - 16	3 DAYS	• EXECUTE SECOND PART (46 M/SEC), INTERRUPTED BY CONSCAN CORRECTIONS
E - 14	2 DAYS	• DETERMINE RESIDUAL TARGETING ERROR
E - 13	8 HOURS	• COMMAND AND EXECUTE TRIM MANEUVER

*E = ENTRY TIME

beamwidth, which limits the permissible maximum precession angle buildup

d) The 5.4-hour communication round trip time delay.

Figure 3-23 shows the timeline of radial thrust ΔV maneuver execution at Uranus. The upper diagram presents the gross operational sequence, indicating in particular the time lost due to ground command and verification steps. Initial calibration is required to determine the actual precession effects of a radial thrust pulse sequence. Another round trip light time (RTLT) delay occurs to perform a second conscan attitude determination and correction via earth command at an intermediate point in the sequence. The lower diagram shows a detailed sequence of the precession buildup due to radial thrust pulses and the required compensation steps by the axial precession control thrusters.

With S-band communications used during these maneuvers the angular tolerance for precession buildup is ± 0.8 degree, determined by the 3 dB half-beamwidth of the high-gain antenna. For X-band this tolerance would be prohibitively small.

The low telemetry data rate available with S-band at Uranus (32 bps) imposes additional constraints on spacecraft operations (engineering, probe data, and bus science data telemetry) during the days required to complete the maneuver sequences.

Referring again to the lower diagram in Figure 3-23, the elements of the thrust maneuver sequence are 13 precession steps, two compensation steps and a total of 12 commands which are required to reload program storage and execution (PSE) after each cycle, to reset the sequence and to command the next cycle. The total cycle which requires 468 seconds in the example shown is referred to as a pulse group. A block of ten groups is assumed between ground checks, conscan, and drift correction operations. Seventy eight groups ($\sim$ eight blocks) of thrust sequences are required to execute a total lateral ΔV maneuver of 10 m/sec at a total elapsed time of 43.2 hours, including eight RTLT's.

The following assumptions on pulse length, thrust level, thrust offset, precession effects, etc., were made in this analysis of the maneuver timeline:

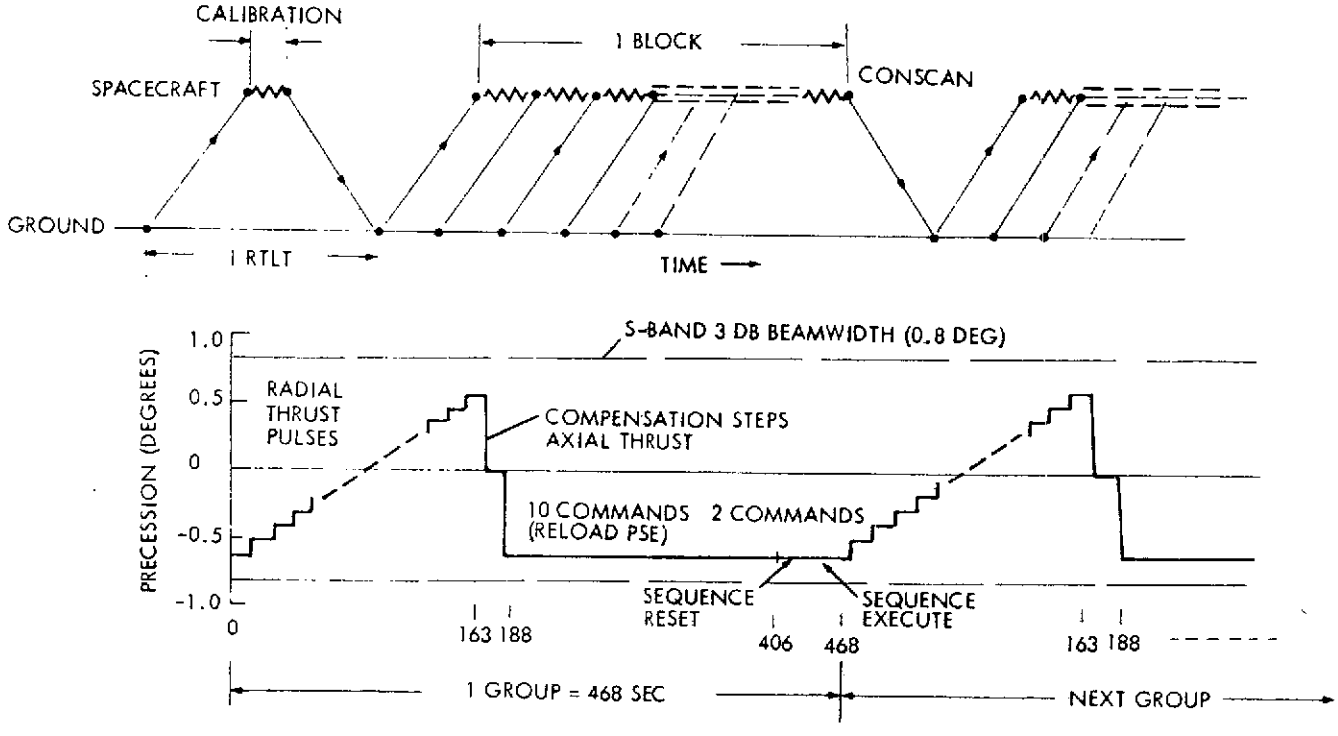

1 GROUP = 13 PRECESSION STEPS + 2 COMPENSATION STEPS + 12 COMMANDS = 468 SEC
10 GROUPS = 1 BLOCK, BETWEEN GROUND CHECKS AND CONSCAN TO CORRECT DRIFT
78 GROUPS ~ 8 BLOCKS REQUIRED TO EXECUTE ΔV = 10 M/SEC
TOTAL TIME ELAPSED ~ 8 RTLT = 43.2 HOURS ~ 2 DAYS

*RTLT = ROUND TRIP LIGHT TIME = 5.4 HOURS TO URANUS (2.6 HOURS TO SATURN)

Figure 3-23. Execution of Radial Thrust ΔV Maneuver (Example: 10 m/sec Approach Correction at Uranus)

Pulse length	0.5 sec
Thrust level (two thrusters)	2 lbf
Thrust offset	8 inches
Precession increment per ΔV pulse	0.095 degree
Precession correction per pulse	1.2 degrees
Accumulated drift per group	0.035 degree
Accumulated drift per block (= 10 groups)	0.35 degree
ΔV increment per pulse	0.00978 m/sec
Required number of pulses to deliver ΔV = 10 m/sec	1022
Command execution time	22 to 30 seconds
Time elapsed per group (188 sec for pulses, 280 sec for command execution)	468 sec

The above analysis is overly conservative with respect to required ground verification steps. Actually, since these operations would consume the major part of the elapsed time, a carefully designed and initially verified thrust sequence can reduce the number of RTLT's required to two. Secondly, the actual ΔV requirement estimated for the approach guidance maneuver is 5 rather than 10 m/sec, thus only four blocks of ten pulse groups are required to complete the maneuver. As a result the total maneuver execution time, after initial preparations, reduces to 12 hours as indicated in Table 3-11 (24 days before planet encounter).

The much larger deflection maneuver (46 m/sec) to be executed after probe separation can be carried out on an accelerated basis. Because of the changed center-of-mass location the thrust misalignment torque and hence the unintended precession effects are at least ten times less than what was assumed in the computation of the previous maneuver sequence. As a result the total pulsed ΔV maneuver sequence can be executed in less than three days. Completion of this maneuver is estimated to occur 14 days prior to encounter.

We conclude that the critical sequence of propulsion events occuring during the last 14 to 25 days before arrival at Uranus can be performed with adequate time margin for possible trim maneuver requirements and other delays and contingencies.

3.6.3.2 Encounter Operations at Saturn

The sequence of events during Saturn flyby serves as an example of rapid changes of the physical environment and functional requirements to which the spacecraft must be adapted by ground command. Scientific observations of the planet and its rings, and effective relay telemetry of probe entry data must be accommodated to meet the mission objectives.

Referring to the Saturn encounter trajectory shown in Figures 3-12 and 3-16 it is noted that the following events occur in rapid sequence during a period of only a few hours:

- Probe entry (start of real-time relay telemetry)
- Probe expiration (start of relay playback telemetry)
- Terminator crossing (end of planet imaging objectives)
- Ring plane crossing (potential hazard of impact damage; end of ring imaging objectives)
- Entry and exit of occultation zone (occultation experiments)
- Post-encounter navigation fix preparation

Table 3-12 summarizes these events, the time of occurrence, and the spacecraft operations to be performed.

With regard to probe data relay operations, real-time transmission by the bus spacecraft extends over a period of 1 to 1.2 hours. The probe data are also stored by the spacecraft DSU during this period and are subsequently retransmitted to earth to assure safe reception in the event that the downlink is inoperative for some reason at the time of real-time relay transmission.

Owing to the 2.6-hour round trip communications delay the spacecraft would enter the occultation phase at E + 3.2 hours before ground verification of intact probe data reception can reach it. Therefore, the spacecraft must continue to transmit probe data repeatedly until occultation and after resumption of telemetry is again possible following occultation. A command to discontinue probe data telemetry can reach the spacecraft at this time at the earliest.

Table 3-12. Encounter Operations at Saturn

NOMINAL SEQUENCE (X-BAND TELEMETRY AT 2048 BPS). IF ON S-BAND (256 BPS) CURTAIL BUS SCIENCE AFTER PROBE ENTRY.

TIME	
UNTIL E*	• PERFORM PLANETARY OBSERVATIONS, INCLUDING IMAGING (~2 FRAMES/HOUR)
E	• START RECEIVING PROBE DATA, START REAL-TIME TELEMETRY AND RECORDING OF DATA
E + 1 HOUR TO E + 1.2 HOURS	• END RECEIVING PROBE DATA, START PLAYBACK OF RECORDED DATA, CONTINUE TO TRANSMIT UNTIL COMMANDED TO STOP
	• CONTINUE BUS SCIENCE OBSERVATIONS (INCLUDING IMAGING UNTIL RING CROSSING)
E + 65 MINUTES	• PASSAGE OF TERMINATOR
E + 2 HOURS	• RING PLANE CROSSING, MAXIMUM POTENTIAL HAZARD**
	• BEGIN RING PLANE SURVEY AND RF RING OCCULTATION
E + 3.2 HOURS	• ENTER OCCULTATION AND ECLIPSE, PERFORM RF OCCULTATION EXPERIMENT
	• PERFORM DARK SIDE OBSERVATION
E + 5.6 HOURS	• EXIT OCCULTATION AND ECLIPSE, PERFORM RF OCCULTATION EXPERIMENT
E + 5.6 HOURS	• RESUME BUS AND PROBE DATA TELEMETRY
E + 5.6 HOURS	• CONTINUE OBSERVATION OF PLANET ENVIRONMENT, INCLUDING RING PLANE SURVEY
	• PREPARE FOR AND CONDUCT POST-ENCOUNTER NAVIGATIONAL FIXES

*E = ENTRY TIME

**DURATION OF CROSSING ~ 0.1 SECOND IF THICKNESS = 1 KILOMETER

As a second contingency, the possibility of damage to the spacecraft at the time of ring plane crossing (E + 2 hours) must be considered. Thus, the time interval between the end of real-time probe data telemetry and the ring crossing event (0.8 hour in the worst case) should be used for probe data relay telemetry at the highest available bit rate to increase the probability of safe reception at Earth. If a data rate of 512 bps is allocated to probe data replay three to four complete cycles of probe data can be transmitted before the ring crossing event.

Commands to be transmitted to the spacecraft (involving operations listed in Table 3-12) during the encounter and post-encounter phase typically include those shown in Table 3-13.

The examples in Table 3-13 show that the spacecraft operations, while requiring several mode changes within a 6-hour period, can follow the desired command sequence in a routine manner. However, unlike other critical event sequences, these operations must be performed without benefit of ground verification and correction, because of the rapid execution necessary and the long time delay in effect at the encounter.

Table 3-13. Commands Transmitted to Spacecraft

Time of Command Reception	Command Message
E*	• Start probe data telemetry in real time (provided data are being received, beginning at probe entry time)
E	• Store probe data in DSU
E + 1 hour	• Discontinue probe data telemetry in real time and start playback telemetry (provided probe data are no longer received)
E + 1 hour	• Reduce image data frame rate by switching to alternate DTU format (prior to initiating probe data replay telemetry)
Between E and E + 2 hours	• Repoint image system per commanded sequence to view bright side of planet, terminator region and rings (about four exposures)
E + 2 hours	• Discontinue image system operation (ring plane crossing)
E + 2 hours	• Secure optical navigation sensor and image system mirror against ring particle impact (rotate away from impact direction)
Before E + 3.2 hours	• Change bus science data flow to DSU for storage during occultation phase • Change telemetry format to occultation phase format • Change S-/X-band communications to noncoherent mode for dual frequency RF occultation experiment
After E + 5.6 hours	• Resume communications in coherent mode • Start replay telemetry of stored bus science data
Undetermined after E + 5.6 hours	• Discontinue probe data replay telemetry • Discontinue telemetry of stored bus data • Resume cruise mode
E + 1 day	• Prepare for post-encounter navigation fix (start of navigation fix series)

*E = Probe entry time.

3.7 TERMINAL NAVIGATION

This section addresses terminal navigation and accuracy of probe delivery at the target planet. Results of concurrent navigation and guidance studies by JPL (see also Section 3.4) will be summarized and the implementation of the preferred navigation technique will be discussed. The principal alternatives are:

1) Navigation by radio-tracking only
2) Navigation by radio-tracking combined with optical measurement of target location relative to celestial references.

3.7.1 Radio Navigation versus Radio Plus Optical Navigation

The JPL study* established that navigation on the basis of radio-tracking alone meet mission requirements for probe delivery at Saturn if "tight" station location errors are assumed. The semi-major axis of the 1σ error ellipse at Saturn is of the order of 1000 km or less.

The key to sufficient accuracy of radio-navigation in this case is the relatively accurate knowledge of Saturn's ephemeris, with uncertainties of the order of 1000 km in azimuth direction. This uncertainty must be added in an RSS sense to the radio navigation error. The total delivery accuracy is still within acceptable limits such that neither the entry flight path angle nor the entry angle of attack vary by more than a few degrees with the dispersion of the entry point.

Radio plus optical data provides navigation accuracies of the order of 200 km (1σ). This is based on a navigation sensor with threshold sensitivity of fourth magnitude and accuracy of 0.1 milliradian. Since this navigational accuracy is unnecessarily high it was concluded that, for purposes of a probe mission to Saturn only, optical navigation can be omitted.

Results obtained for probe delivery at Uranus, on the other hand, showed that the total radio navigation error is completely dominated by

*The study was performed by J. Ellis and K. Russell. Preliminary data were furnished by L. D. Friedman, JPL Study Manager. Results will be published in JPL Technical Memorandum No. 391-441.

the large ephemeris uncertainty of this planet, ~10,000 km (1σ) in azimuth direction.

With trajectory errors of this magnitude and a planetary radius that is less than half of Saturn's, probe delivery conditions can vary between these two extremes: (a) The probe misses the planet altogether, or (b) arrives at a prohibitively large entry angle. Probe survival at entry angles greater than 60 degrees is doubtful, and even in the event of a successful probe entry the large dispersion would tend to interfere with effective relay communication.

An alternative aim point selection has been proposed by McDonnell-Douglas in their concurrent Entry Probe Definition Study* to minimize entry point dispersion along the track by accepting a larger cross-track dispersion (see Figure 3-24). This approach may provide successful probe deliveries, with radio-navigation only, especially if the ephemeris uncertainty of Uranus were reduced by a stepped-up earth-based observation and orbit determination effort in advance of the mission. However, when aim points are selected, as shown in Figure 3-24, that are located about ± 90 degrees from the nominal (retrograde) aim point, the bus spacecraft trajectory does not satisfy the objective of passing through Uranus' earth occultation zone after the encounter.

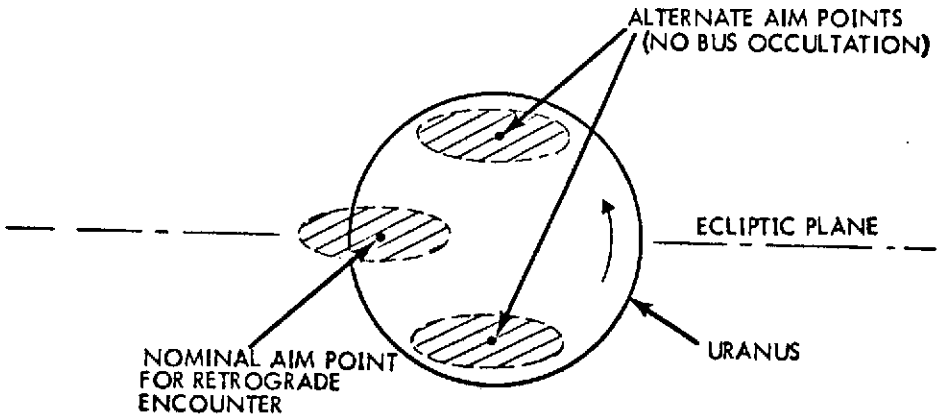

Figure 3-24. Uranus Aim Point Alternatives*
(Not to Scale)

*"System Level Definition Study of a Saturn/Uranus Atmospheric Entry Probe," McDonnell Douglas Final Study Report (in preparation).

The JPL study established that radio-plus-optical navigation can achieve terminal accuracies adequate for the Uranus mission, i.e., both for the control of probe entry point location and relay link geometry. By tracking the satellite Titania (the brightest satellite of Uranus) until 20 days prior to encounter, at a range of 1000 R_U, a 1σ dispersion of only about 1500 km can be attained. By continued tracking until E -14 days at 700 R_U range, the dispersion would be reduced to about 1000 km. (These values are the semi-major axes of the dispersion ellipses in the B-plane).

On the basis of these results it is apparent that an optical onboard navigation sensor is essential to accomplishing the Uranus probe mission. As previously discussed in Section 3.4, the navigation sensor also serves the important purpose of improving the Saturn encounter accuracy and thus, reducing the post-encounter midcourse maneuver requirement.

The JPL study also recommends that a refinement of Uranus' ephemeris be undertaken prior to implementing mission plans, in order to make the mission less critically dependent on optical navigation. Reduction of the ephemeris uncertainty to ~3000 km is believed feasible by coordinated observations over a period of no more than one year.*

3.7.2 Implementation of Optical Navigation

The optical navigation concept adopted for this mission uses a scanning star sensor that is compatible with the spinning Pioneer spacecraft. The method of operation is illustrated in Figure 3-25. The star scanner detects a satellite of the target planet and determines its location relative to selected reference stars. As the sensor field of view scans an annular region of the celestial sphere, images of the stars and the target pass the slits of a V-shaped reticle located at the focal plane, and are detected by a photomultiplier. A sequence of pulse pairs is thus generated, as illustrated at the bottom of Figure 3-25. The timing of these pulses indicates the position of the target relative to the reference stars. The mean time and the pulse separation of each pair give the

*Communication received from L. D. Friedman, JPL.

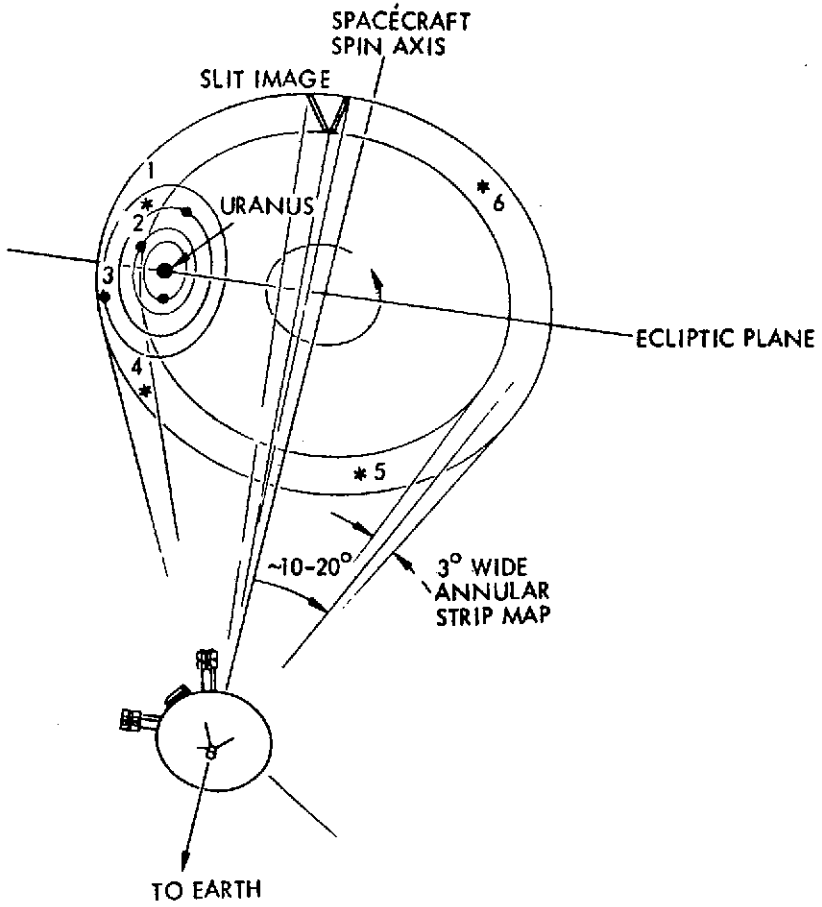

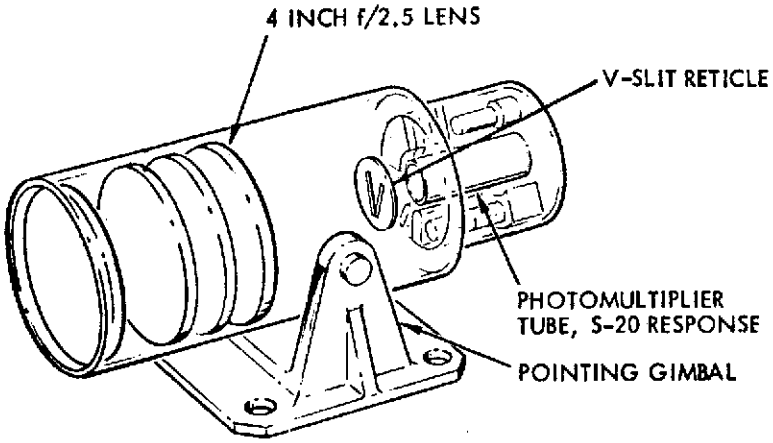

- MINIMUM NUMBER OF REFERENCE STARS IS TWO
- STAR PATTERN IDENTIFIED IN ADVANCE OF TARGET DETECTION
- STAR MAPPER ALSO ACCURATELY DETERMINES SPIN AXIS POINTING ON CELESTIAL SPHERE
- PLANET'S SATELLITES ARE PREFERABLE AS NAVIGATIONAL REFERENCES: SMALLER IMAGE SIZE; MASS CENTER DETERMINATION SIMPLIFIED
- INTERFERENCE BY BRIGHT PRIMARY IMAGE TO BE AVOIDED

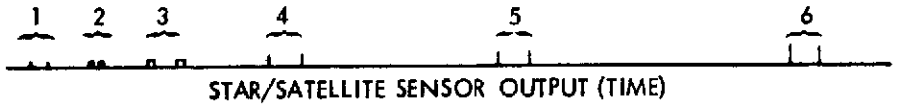

Figure 3-25. Terminal Navigation Sensor Operation

clock and cone angles of the object, respectively. The sensor is gimballed so that the angle of the optical axis to the spacecraft spin axis can be adjusted to include the target in the 3-degree annulus. (See also discussion of sensor characteristics in Section 6.3.) Interpretation of the pulse sequence permits:

- Identification of the reference stars
- Verification of the target satellite after it is detected by the sensor
- Determination of the target's clock and cone angles
- Compensation for uncertainty in spin axis orientation and gimbal angle.

This terminal navigation sensor has been previously proposed and analyzed for other advanced Pioneer applications where precision planetary guidance is essential. Several versions of the instrument have been developed and tested. Concurrently with this study a laboratory demonstration of a V-slit star sensor is being undertaken by TRW Systems under NASA/Ames study contract* to verify its performance characteristics under simulated star scanning conditions. If requirements on detection sensitivity and angular precision of the instrument are held to a reasonable level, problems of a major new technology development can be avoided.

The block diagram shown in Figure 3-26 defines the functions of terminal navigation and guidance that are assigned to the spacecraft and the ground facility. To minimize the complexity of onboard operations the signals generated by the star scanner are telemetered to the ground for processing and interpretation. The spacecraft only acquires the data and executes guidance maneuvers as commanded from the ground. The ground facility automatically

- Screens the incoming star sensor signals and identifies the reference stars
- Detects and verifies the target satellite by its time-varying brightness and parallax

*"Feasibility Test of a V-Slit Mapper for Pioneer Terminal Navigation," under NASA Contract NAS2-7592.

- Performs orbit determination and updates the position and velocity of the spacecraft relative to the target planet, using the optical sensor data in combination with radio tracking data
- Determines desired trajectory corrections, and
- Transmits maneuver commands to the spacecraft.

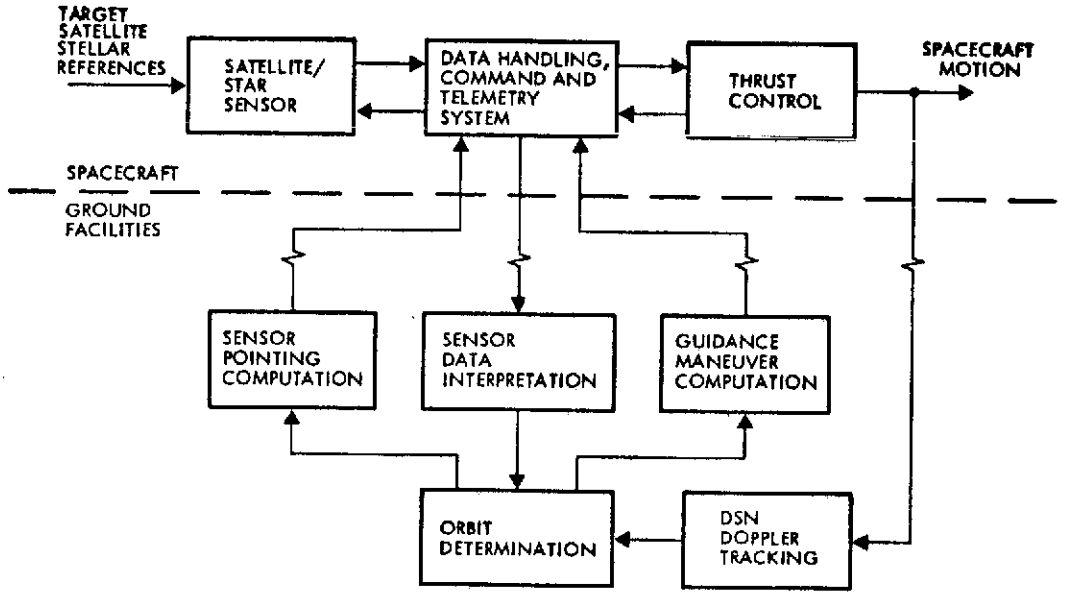

Figure 3-26. Navigation and Guidance Functional Block Diagram

Time losses must be minimized to complete the approach correction maneuver as early as possible consistent with probe separation timing. The navigation and guidance operations can be expedited as follows:

1) The star scanner is commanded to point in the desired direction well in advance of the predicted target acquisition time. This permits identification of reference stars in the annular region scanned by the sensor, ahead of time, and speeds up the subsequent determination of the target's relative position.

2) Ground-based data interpretation, orbit determination and guidance command computations are fully automated to minimize

the turnaround time between acquisition of navigational fixes and guidance maneuver execution.

3) The guidance maneuvers are executed without a spacecraft reorientation.

3.7.3 Target Acquisition and Viewing Conditions

Figure 3-27 shows the visual magnitude of Saturn and Uranus and their satellites as function of spacecraft distance. For a given sensor acquisition magnitude, i.e., $M_V = 4$ for the proposed instrument, the distances of first detection of the various satellites can be directly

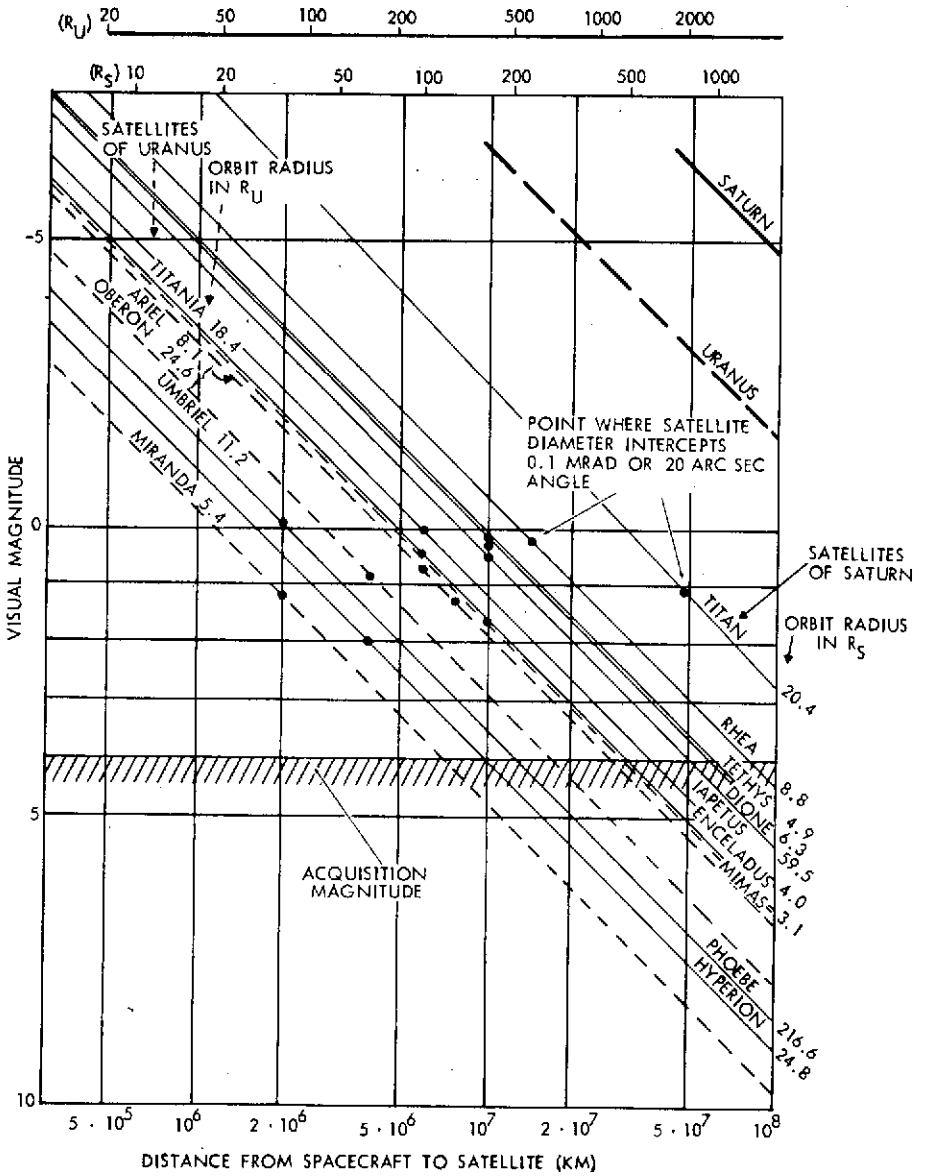

Figure 3-27. Acquisition Ranges of Saturn, Uranus and Their Satellites

determined from this graph. Most of Saturn's satellites are sufficiently bright for early acquisition with respect to the desired probe separation distance of 3×10^7 km. Three of Uranus' satellites, Titania, Oberon, and Ariel, are bright enough to permit early acquisition to meet the constraint of probe separation at $R = 2.7 \times 10^7$ km. Thus, from a standpoint of acquisition distance the assumed instrument sensitivity is adequate.

However, in addition to the satellite's detectibility as a single source, its apparent separation from the primary is also important for successful operation of the sensor. If the angular separation is too small the sensor will be exposed to illumination by the much brighter primary. This not only makes acquisition more problematic, it also tends to interfere with the cone and clock angle measurements by the sensor. Figure 3-28 shows representative locations of Titan, Titania, and Oberon relative to their primaries. The separation angle is particularly small in the case of Uranus' satellites, and an offset of the V-slit scanner becomes necessary to exclude the planet from the field of view. This will place the target satellite close to the inner or outer rim of the field of view and may cause some degradation of angle measurement accuracy.

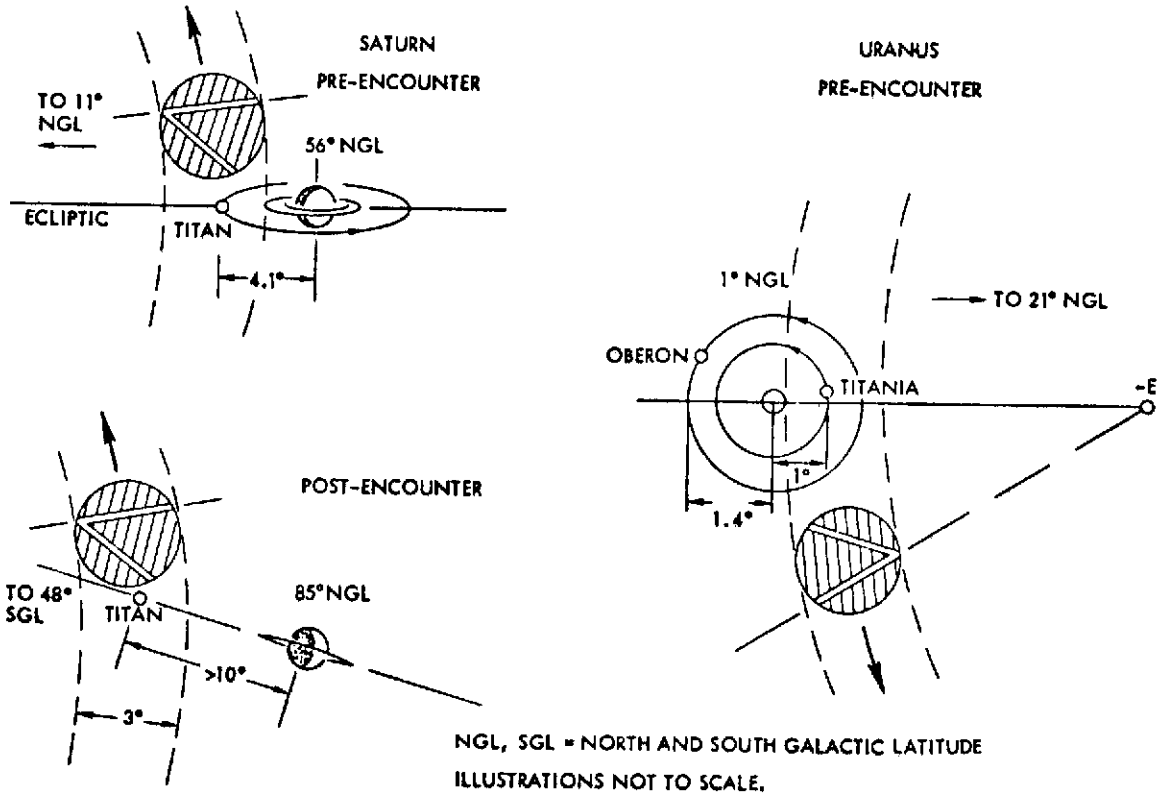

Figure 3-28. Star Mapper Viewing Geometry

Regardless of the difference in the aspect angle of the satellites' orbit plane at Saturn and Uranus, the best measurements can be performed only during about half of the satellite's orbit period when the separation of satellite and primary, in terms of cone angle differences seen by the sensor, are near a maximum. Measurements are degraded in accuracy or prevented as the cone angle difference approaches zero.

Careful planning of the arrival data of Uranus is required to avoid problems due to inaccessibility of Titania for navigational fixes. With an orbital period of 8.7 days, accessibility problems occur in four-day cycles. Use of Oberon or Ariel as alternative targets is possible although both are less bright than Titania by 0.3 magnitude and would therefore be acquired about three days later than Titania. Also, the usefulness of Ariel is marginal since its orbital radius (and its separation from Uranus) is less than half of Titania's. Its short orbit period of 2.5 days causes more frequent interruptions of accessibility. In the case of Saturn approach navigation this problem does not occur because the large number of potential bright backup satellites to Titan, and their generally much larger angular separation from the primary.

The JPL study points out that in principle the satellites with a small orbit radius permit orbital determination and navigation fixes with greater accuracy than more distant satellites because of their shorter orbital period. However this advantage is offset by the viewing difficulties explained above.

Table 3-14 summarizes the differences in viewing geometry during the Saturn and Uranus encounters, as illustrated by Figure 3-28, and their effect on star sensor use. Table 3-15 gives a quantative comparison of star mapper operation conditions at these planets.

It is interesting to note that, based on average densities of stars of magnitude four and brighter, about the same number of reference stars should be available as navigational references in the Saturn and Uranus approach navigation phases, although the angular region swept out by the star mapper is much smaller in the case of the Uranus encounter. This is explained by the fact that in the latter case the star mapper swath is located closer to the galactic equator. Actually the number of bright

reference stars visible within the path of the star mapper is even greater as determined by the concurrent JPL navigation and guidance study, i.e., five stars of magnitude three or brighter at Saturn and eight to ten stars of this brightness at Uranus. The minimum number of reference stars required is two.

Table 3-14. Effect of Viewing Geometry on Star Mapper Use

SATURN ENCOUNTER	
PRE-ENCOUNTER NAVIGATION	• SATELLITE ORBITS SEEN EDGEWISE • MAXIMUM ANGLE SEPARATION FROM PLANET TITAN 4.1 DEG (8 DAYS BETWEEN ELONGATIONS) IAPETUS 11.8 DEG (40 DAYS BETWEEN ELONGATIONS) • PLANET (WITH RINGS) IMPRACTICAL FOR DIRECT NAVIGATION FIXES. GIBBOUS EFFECT $\sim 10^4$ KM, 1/6 OF PLANET RADIUS
POST-ENCOUNTER NAVIGATION	• PLANET AND SATELLITES ARE VIEWED AT ~110 DEGREES PHASE ANGLE, AT CONE ANGLE OF ~70 DEGREES (NEAR SENSOR VIEW ANGLE LIMIT) • LARGE SATELLITE ANGLE SEPARATION FOR NAVIGATION FIXES • MANY ALTERNATE SATELLITES AVAILABLE
URANUS ENCOUNTER	
PRE-ENCOUNTER NAVIGATION	• SATELLITE ORBITS SEEN NEARLY FROM POLE • ONLY TITANIA BRIGHT ENOUGH FOR TIMELY ACQUISITION (6 DAYS TO SEPARATION) • SEPARATION ~1 DEGREE • PLANET IMAGE INTERFERENCE AVOIDANCE DURING 2/3 OF 8.7 DAY ORBIT PERIOD OF TITANIA • PLANET AVAILABLE AS EARLY ALTERNATE NAVIGATION REFERENCE: NEAR-CIRCULAR DISK, ONLY 350 KM GIBBOUS EFFECT (10-DEGREE PHASE)

Table 3-15. Comparison of Star Mapper Operating Conditions at Saturn and Uranus

CONDITIONS	SATURN	URANUS	REMARKS
STAR MAPPER OPERATING CONDITIONS:			
• MAXIMUM ANGULAR SEPARATION OF PLANET AND SATELLITE	TITAN 4.1° IAPETUS 11.8°	TITANIA 1° OBERON 1.4°	SENSOR AIMING BIAS REQUIRED TO EXCLUDE PLANET INTERFERENCE
• TIME FROM FIRST SATELLITE ACQUISITION TO NOMINAL PROBE SEPARATION	175 DAYS (TITAN)	6 DAYS (TITANIA)	MARGINALLY SHORT FOR URANUS
• PLANET PHASE ANGLE	40°	10.5°	URANUS DISK NEARLY CIRCULAR
• CONE ANGLE	140°	169.5°	SENSOR ACCURACY DEGRADED FOR URANUS
• AREA OF STAR MAPPER SWATH	700 DEG^2	190 DEG^2	SMALL SWATH AREA NO PROBLEM FOR URANUS
• SCAN CIRCLE GALACTIC LATITUDES	11 TO 56°N	1 TO 21°N	
• AVERAGE NUMBER OF REFERENCE STARS (MAGNITUDE 4 OR BRIGHTER)	FOUR	FOUR	

3.7.4 Sensor Operational Requirements

Principal operating modes of the star sensor and functional requirements and constraints that govern its application in various mission phases are briefly described as follows:

1) Preparations for the target acquisition and terminal navigation sequence are started at least two days in advance of the projected acquisition time. The sensor is pointed at the desired cone angle, and star data are transmitted to earth for identification and selection of reference stars. The exact aim point of the spin axis and the exact cone angle of the sensor's optical axis can be determined at this time.

2) Since a high-telemetry bit rate is available, details of star mapper signals can be transmitted to the ground to expedite early target detection and discriminate against false alarms. Actually, the probability of false alarms is extremely small under normal conditions (10^{-8}) and is not of much concern in this application.

3) Under typical encounter conditions and for distances greater than 10 million km, the target line-of-sight rotation per day and its position uncertainty are a small fraction of a degree. Since the FOV is 3 degrees, resetting of the sensor cone angle is generally unnecessary during the initial acquisition and navigation phase. However, as target range decreases, reorientation of the sensor may be required.

4) During navigational observations any residual spacecraft wobble must be held to less than 0.1 millirad. Precession maneuvers, to keep the high-gain antenna pointed at earth, are ruled out during that time. Such maneuvers can be performed before or after the navigation phase.

5) The instrument serves the dual function of navigation sensor and star reference assembly. During normal cruise operation the gimbal angle of the sensor is set to a selected reference star, e.g., Canopus, and adjusted periodically to follow the star's apparent motion. The same signal processing as in the navigation mode can be used to generate the roll reference signal, except the second star pulse is ignored. The threshold setting is raised to discriminate against stars fainter than the selected reference star.

3.7.5 Navigational Accuracy at Uranus

The accuracy achievable by the combined radio-optical navigation technique depends on the star sensor accuracy (i.e., bias and noise errors), the sampling rate, the distance from encounter at which the navigational observations are completed, and the algorithm used in orbit determination. Since most of the target satellites have ephemeris uncertainties of thousands of kilometers (the uncertainty in the case of Titan is ±40, 000 km) it is essential that the target by observed over an extended period in order to obtain an improved estimate of its position relative to the planet, as a prerequisite to obtaining accurate characteristics of the spacecraft trajectory.

Results of the JPL navigation study show that at Uranus the major part of the initial trajectory uncertainty is removed in the first four to six days of navigational observations. Extension of the data arc to about ten days before encounter would further reduce the trajectory error but is not practical under the constraint of early probe separation. Of the two orbit determination algorithms investigated the method of estimating the navigation sensor bias on the basis of observations yields more accurate results than considering a given sensor bias. In the case of bias estimation the resulting error is inversely proportional to the sample rate, in the second case it is relatively insensitive to sampling rate. By using Titania as a target and employing the most effective estimation technique the residual navigation error is 1200 km (1σ) 20 days before encounter if the sampling rate is four samples per day. At 24 samples per day the error reduces to 500 km.

3.7.6 Sensor Capability Tradeoff

The star mapper performance characteristics of principal interest are threshold sensitivity and accuracy. The proposed sensor specifications are:

- Detection sensitivity: 4th magnitude
- Accuracy in single-point source measurement: Bias 2.3 arc sec, noise 4-9 arc sec
- Accuracy in determination of target direction from two or more sensors: Bias 10 arc, noise 15-25 arc sec

A conservative estimate of target direction errors (bias plus noise) is 20 arc sec, or 0.1 millirad. Actually, the JPL study results using a sensor of the above specification shows that the best trajectory estimates are obtainable that correspond to effective errors of 0.05 millirad or less if aim point errors were directly scaled to observation errors.

The principal tradeoff in navigation performance involves sensitivity and accuracy of the sensor versus propellant requirements for the bus spacecraft deflection maneuver. This is illustrated in Figure 3-29. Dashed lines in this graph show the star mapper sensitivity (upper curve) required to acquire the satellite Titania six days before probe separation, and the accuracy (lower curve) required to achieve a 1500 km approach accuracy in the B-plane, both quantitites plotted as functions of time and location of probe separation. Late probe separation implies a reduction in sensitivity and accuracy requirements (i.e., increase in permissible sensor error). The solid lines show the required propellant mass. The propellant mass allocated to the deflection maneuver is 22 lbm if probe separation occurs at the nominal separation distance of 1000 R_U, 20 days before arrival at Uranus. A delay of probe separation by eight days would double this propellant allocation but a less accurate (0.12 milliradians) and less sensitive (star magnitude three) instrument would be sufficient. Since there is little or no weight margin in the spacecraft (see Section 5.4) this tradeoff of sensor capability, although attractive in terms of potentially lower development cost and complexity is not feasible. A tradeoff in the other direction saves too little propellant weight to be of interest.

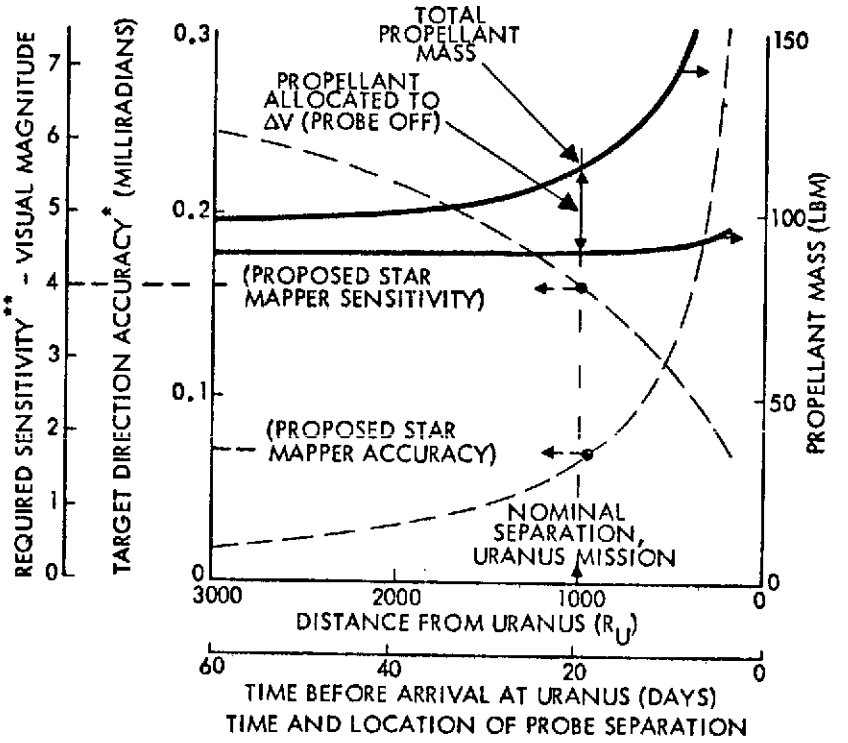

*TARGET DIRECTION ACCURACY (1σ) OF STAR MAPPER FOR 1500 KM (1σ) APPROACH ACCURACY ($\delta\bar{B}$)

**SENSITIVITY THRESHOLD REQUIRED OF STAR MAPPER TO ACQUIRE THE SATELLITE TITANIA SIX DAYS BEFORE PROBE SEPARATION

Figure 3-29. Propellant Mass and Optical Sensor Requirements vs Separation Time

4. BUS SPACECRAFT SCIENCE

This section discusses the objectives of scientific observations to be performed by the spacecraft bus and their implementation by means of a complement of payload instruments, defined for purposes of this study by NASA/Ames Research Center (see Statement of Work). Only a few of the specified instruments differ from those on Pioneer F/G.

4.1 STUDY SCOPE

In accordance with the study guidelines the following tasks are of principal concern in performing the science payload study:

- Review instrument accommodation requirements and establish compatibility with spacecraft subsystems (particularly for those instruments not on Pioneer F/G).
- Define an arrangement of the instruments and their sensors on the spacecraft bus that meets the instrument mounting, orientation and viewing requirements.
- Verify that the planned trajectories and operational sequences will provide measurement opportunities such that the scientific objectives can be accomplished with the proposed instrument complement.

In addition, the payload study must address questions of compatibility of payload operations with the principal requirements of the entry probe, namely, accurate delivery to the designated target area and use of the bus data handling and communication subsystems for probe entry data relay. In effect, these requirements constrain bus science operations (1) during the planetary approach phase, when terminal navigation fixes and guidance maneuvers must be carried out, and (2) during the encounter phase, when spacecraft telemetry, data handling, and data storage capabilities must be allocated to probe data relay operations on a priority basis.

Descriptions of bus science instruments and measurement procedures are omitted from this section except for the new line-scan imaging system. This instrument affects subsystem design and spacecraft operations more strongly than all others, especially in terms of its inherently large data acquisition capacity, and thus requires special attention.

Some of the tradeoffs involving bus payload performance and scientific data acquisition capability versus system simplicity, cost economy and weight constraints are discussed in this section but will be covered more broadly in Sections 5, 6, and 7.

4.2 SCIENTIFIC MISSION OBJECTIVES AND PRIORITIES

Scientific objectives of the mission are exploration of the atmospheres of Saturn and Uranus, the near-space environment of these planets, and the interplanetary space between Earth and Uranus. Exploration of interplanetary phenomena beyond Uranus and interaction with galactic phenomena at increasing distances from the sun is a secondary objective, predicated on the spacecraft's continued functioning after the seven years that are required to reach Uranus.

While atmospheric exploration at Saturn and Uranus is primarily the mission objective of the entry probe it is also included among the objectives of the spacecraft bus. These have been defined as follows:

a) Observation of phenomena in interplanetary space, i. e., especially particles and fields phenomena, and of the near-environments of Saturn and Uranus by in situ measurement with instruments based on the Pioneer F and G scientific payload.

b) Remote measurement of the atmospheres and other characteristics of Saturn and Uranus, their satellites, including the rings in the case of Saturn, by instruments partly based on the Pioneer F and G scientific payload and by occultation experiments using the spacecraft-to-earth communication link.

The scientific objectives and the observations to be conducted by the bus payload instruments are summarized in Table 4-1.

The visual imaging system has the objectives of providing global views of the planet during the approach phase and partial views at higher resolution during the encounter phase. It will also be used to observe physical features of satellites that are encountered at close enough range during the flyby, and to provide views of Saturn's rings at a variety of aspect and illumination angles.

Table 4-1. Principal Bus Science Objectives and Experiments

Phenomena	Experiment
Planetary	
Planet, satellite (and Saturn ring) physical features	Imaging
Atmospheric temperature and energy balance	IR radiometer
Atmospheric composition	UV photometer
Atmospheric structure and composition	IR spectrometer
Atmosphere and ionosphere	Radio occultation
Magnetic fields (magnetosphere)	Magnetometer
Radio emissions	RF noise detector
Trapped radiation	Charged particle detector
Planetary/Interplanetary	
Solar wind interaction with planet	Solar wind analyzer
Micrometeoroids	Impact detectors
Planet ephemeris and mass (celestial mechanics)	Radio tracking
Interplanetary	
Particles and fields	Magnetometer
Solar wind/galactic influence	Solar wind analyzer
	Charged particle detector
Micrometeoroids	Impact detectors

Together with data obtained from infrared radiometry and spectrometry and ultraviolet photometry, close-up images of the planet's atmosphere and cloud features provide an extension of data obtained by in situ measurements made by the entry probe. Combination of the data acquired by the bus and probe serves to accomplish the interrelated objectives:

1) Correlation of local atmospheric characteristics observed by the entry probe with conditions in the surrounding atmosphere and the planetary atmosphere as a whole as observed by the bus instruments;

2) Calibration of remote observations made by the bus instruments against quantitative characteristics measured in situ by the probe instruments.

Thus the scientific value and accuracy of observations made separately by the bus and probe will be enhanced by interpretation of the combined observations.

Assignment of relative priorities to individual experiments or experiment groups is likely to be controversial. However, in the event that not all of the desired bus payload instruments can be accommodated for reasons of development status, cost, complexity, weight requirements, and demands on spacecraft resources (such as power, telemetry, and data storage), some of the proposed instruments may have to be selected over others.

These questions are in part a matter of policy and as such outside the scope of this study. Informal conversation with Ames representatives in the course of the study indicated that particles and fields sensors and the IR radiometer and UV photometer, being part of the Pioneer F/G payload, would exhibit an advantage over a new imaging system and IR spectrometer. Factors in this selection would be cost economy, weight savings, and simpler accommodation.

A priority argument can be made for those instruments of the bus payload that do not tend to duplicate in situ atmospheric measurements made by the entry probe but observe phenomena inaccessible to probe measurement. On this basis the imaging system ranks high in priority, especially regarding the diversity of features that it can observe, in spite of the greater difficulty and cost of accommodating such an instrument as part of the bus payload.

4.3 PROPOSED SCIENCE PAYLOAD COMPLEMENT

Table 4-2 lists the complement of scientific instruments as specified in the Statement of Work. Included are estimated weight, volume, power, and data rate requirements for each instrument. The last column lists special requirements such as instrument pointing and field-of-view characteristics, location on the spacecraft, etc.

Table 4-2. Scientific Instrument Complement for the Spacecraft Bus*

Instrument	Pioneer F/G Type Instrument	Weight (Pounds)	Power (Watts)	Volume (In^3)	Samples per Minute	Bits per Sample	Bits per Second	Special Requirements
Magnetometer	X	5.5	3.0	240	30	24	12	Boom mounted sensor. Spacecraft magnetic constraints like Pioneer F/G
Solar Wind Analyzer	X	6.0	3.0	300	5	120	10	Solar viewing 20° x 140°
Charged Particle Detector	X	6.0	3.0	240	5	140	12	90° clear FOV - point 90° to spin axis
I.R. Radiometer	X	7.5	3.0	320	5	60	5	20° clear FOV - point 45° off spin axis
I.R. Spectrometer		12.0	4.0	400	5	180	15	20° clear FOV - point 45° off spin axis
U.V. Photometer	X	6.0	2.5	180	10	32	6	45° clear FOV - point 45° off spin axis
Multispectral Line Scan Camera		14.0	10.0(1)	400	(1)	2×10^5	(1)	2° IFOV, 180° clear pointing FOV
R.F. Noise Detector		1.0	0.5	80	10	24	4	1/4 wave whip antenna length ~24 inches
Micrometeoroid Detector	X	3.5	1.0	100	2	10	0.4	~12 penetration panels like Pioneer F/G
Dual Frequency R.F. Occultation	-	-	-	-	-	-	-	Uses S & X band transmitters. No special on-board instrumentation required
Total		61.5	30				64.4(3)	

(1) Time share with other instruments. Imaging on command. Requires on-board storage. Time-share readout of stored data or interleave with other science data.

(2) This experiment uses S-band and X-band channels on spacecraft (no extra payload equipment).

(3) Excluding the image system.

* Tentative list, as specified in NASA/ARC's Statement of Work

Six of the instruments are of the type carried by Pioneer 10 and 11 and require little or no modification. The IR spectrometer, multispectral line-scan camera and RF noise detector are new additions. Five instruments of the Pioneer 10 payload have been omitted: the imaging photo-polarimeter, asteroid/meteoroid detector, cosmic ray telescope, trapped radiation telescope, and Geiger-tube telescope.

By omission of these instruments the weight and power requirements of the proposed payload are kept within the same brackets as the Pioneer 10/11 payload. However, the weight requirements of the IR spectrometer and the line-scan camera must be further evaluated as these instruments become more firmly defined. The power for the line-scan camera (estimated as 10 watts) can be time-shared with other payload instruments if necessary.

The pointing requirements of the fixed-orientation instruments listed in Table 4-2 are dictated by planet view angles and are comparable to those of Pioneer F/G. The range of camera pointing directions is specified as 0 to 180 degrees in cone angle, i. e., a full view of the forward and rear hemisphere.

Actually, pointing the camera at angles close to the center of the forward hemisphere (which means close to the sunline at the time of the Saturn and Uranus encounters) is not considered a firm requirement. As will be discussed in Section 4. 5, it would be impractical to cover cone angles less than about 70 degrees because of (1) field-of-view obscuration by the high-gain antenna and (2) stray light interference. Camera orientations in the range of 70 to 180 degree cone angles are sufficient to meet essentially all planetary observation objectives.

The dual-frequency RF occultation experiment listed in Table 4-2 can be performed by means of the dual X-S band communication system carried by the spacecraft, without requiring added equipment. X-band communication capability has been added to the S-band communication system of Pioneer F/G to meet the increased telemetry performance requirements at the larger distances occuring in this mission (see also Sections 2. 1 and 6. 6). Simultaneous use of two RF frequencies for the

occultation experiment permits improved isolation of earth ionospheric influences on the received signal characteristics, and thus a better resolution of the planetary atmospheric phenomena measured.

In addition to the RF occultation experiment, the celestial mechanics experiment (not listed in Table 4-2) also uses the spacecraft-to-earth communication link without requiring onboard instrumentation. As with Pioneer 10 and 11, this experiment will be conducted to improve the knowledge of the target planets' ephemeris and gravity.

4.4 CHARACTERISTICS OF THE IMAGE SYSTEM

4.4.1 Imaging by a Line-Scan System

The proposed imaging system* consists of a linear array of a large number of solid-state photo detectors which are swept in push-broom fashion across the visual scene being observed. The line elements describe concentric circles around the spin axis, the radii of these circles being determined by the cone angle at which the optical axis of the instrument is pointed. The sweep rate varies with the sine of the cone angle. Viewing of objects at cone angles near 180 degrees should be avoided because of the deterioration of the imaging process. (Cone angles near zero degree are excluded in any case, as discussed before.)

The preference for a line-scan image system in this application is based on the following considerations:

- A point scan image system such as the imaging photopolarimeter used on Pioneer F and G requires more complex data processing in composing images from successive scans, particularly during rapid changes of the scene close to the planet.

- Conventional image forming (vidicon) TV systems are penalized by the 5-rpm Pioneer spin rate without further state-of-technology advances. The short exposure times necessary to avoid smear call for increased optics size.

*See "The Application of Linear Arrays of Silicon Phototransistors to Multispectral Imaging of Earth Resources," TRW Report by N. P. Laverty dated November 15, 1972.

- The solid-state line scan photodetector, developed originally for near-earth applications, is compatible with the spinning Pioneer spacecraft, offers high geometric accuracy, long life, compact design and has a low power requirement.

A laboratory demonstration of a line-scan system is currently being conducted by TRW Systems under NASA/Ames Research Center study contract to verify its applicability to the SUAE mission and other outer planet missions by the Pioneer spacecraft.

4.4.2 Performance Criteria for Line-Scan Image System

The image system is limited in resolution in the direction normal to the sensor array, i.e., the spin scan direction, by the required minimum exposure time of each detector cell. The present state of technology requires at least 0.1 msec, which for a 5 rpm spin rate translates into about 0.05 milliradians of image smear. Resolution along the sensor array is determined at least geometrically by the field of view (FOV) and the number of cells, although other characteristics of the optical system should also be considered in a more rigorous analysis.

Based on the geometrical model, Figure 4-1 presents performance criteria of the line-scan image system in terms of resolution along the sensor array versus resolution normal to the sensor array. The design point indicated in the graph corresponds to a 3-degree FOV and 195 sensor cells. An exposure time of 0.5 msec would permit equal resolution of 0.3 mrad in both directions.

The shaded square at the lower left in Figure 4-1 marks the resolution that would be desired if the sensor were also to be used for optical navigation fixes, such as the Mariner Mars Orbiter vidicon camera. We note that a resolution of 0.1 mrad cannot be achieved unless the FOV is decreased or the number of cells increased, and unless the minimum cell exposure time or the spacecraft spin rate is reduced, by about a factor of 3. Since none of these alternatives is practical for the SUAE mission, the use of the sensor for navigation purposes is essentially ruled out.

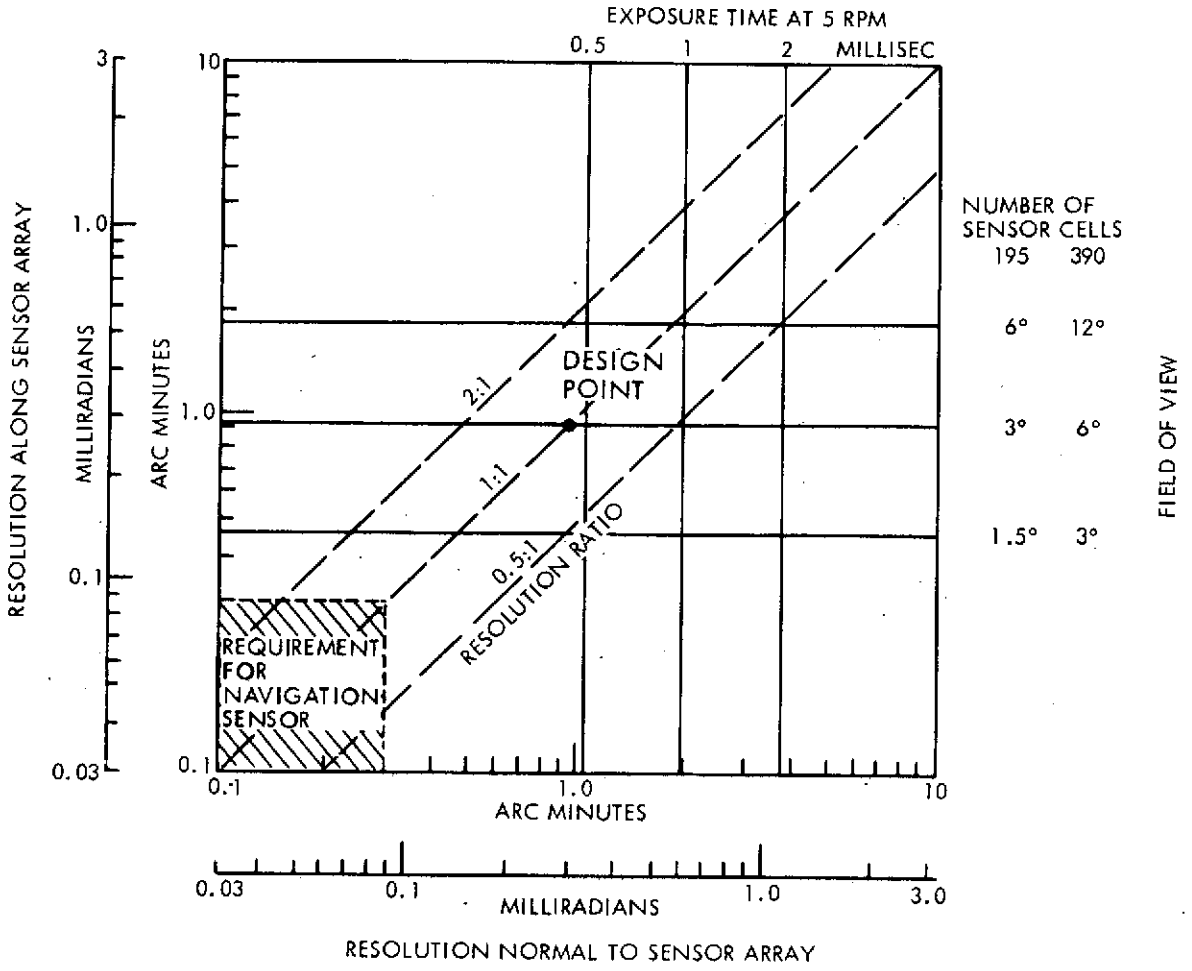

Figure 4-1. Performance Criteria for Line-Scan Image System

4.4.3 Description of the Solid-State Photodetector Array

The large scale array (LSA) shown in Figure 4-2 consists of 195 phototransistors, fabricated by triple-diffusion in silicon on a single chip. The array consists of two rows of phototransistors containing 97 and 98 elements, respectively. This configuration provides sufficient spacing between adjacent elements along the array to prevent crosstalk due to penetration of the incident radiation into the base material. The size of the photosensitive area of each phototransistor is 0.7×10^{-3} by 0.9×10^{-3} inches, and the pitch spacing determines the limiting spatial resolution of the array.

In addition to the 195 phototransistor elements, the LSA chip contains an equal number of individual amplifiers, a shift register and multiplexer. The multiplexer is used to commutate the outputs of the

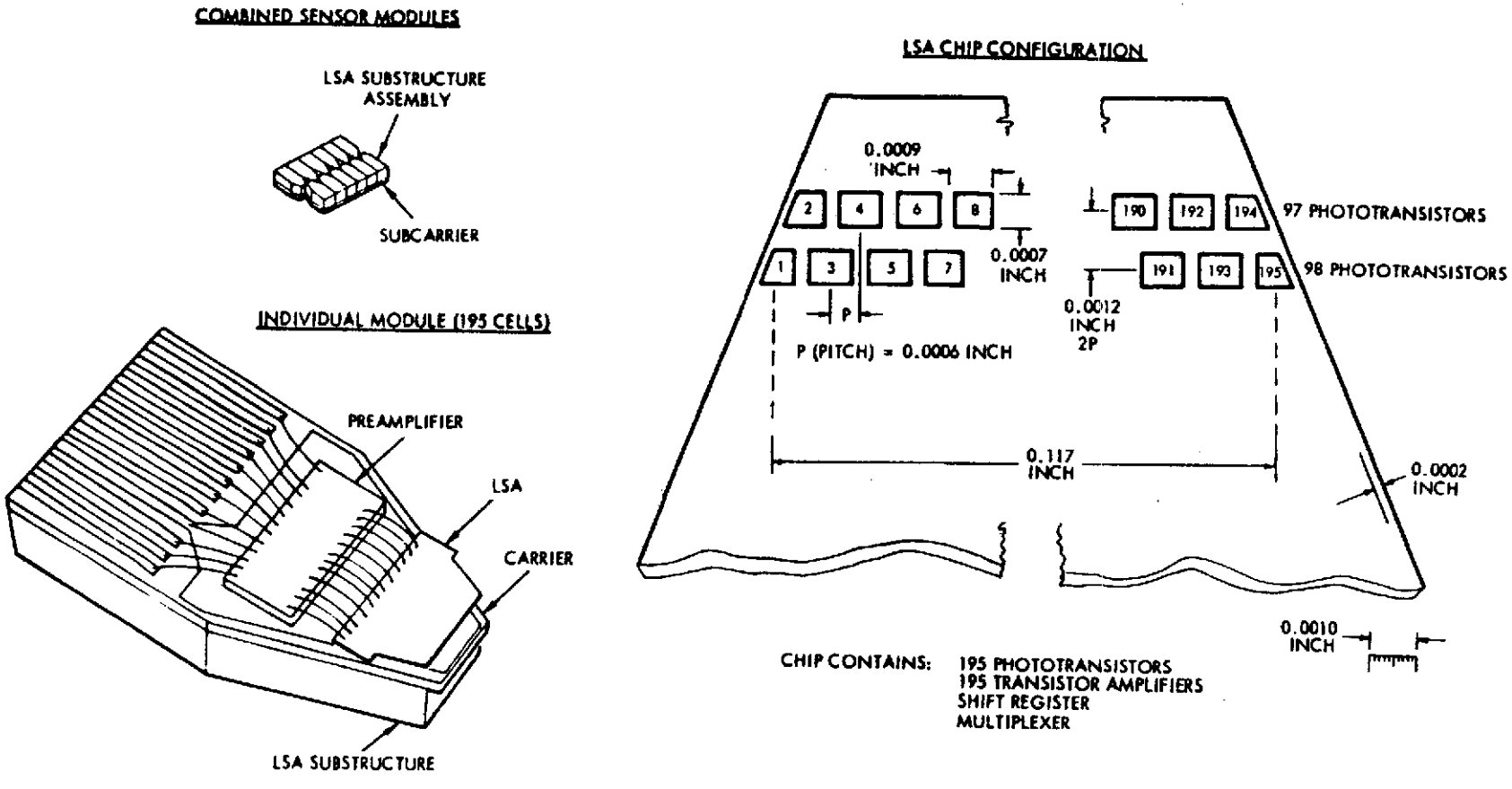

Figure 4-2. Solid State Photodetector Array

195 preamplifiers onto five signal leads, each containing the serial output of 39 preamplifiers. These five signal leads are hard-wired to a second chip, containing five signal conditioning electronics (SCE) amplifiers, that further amplify the five serial signals prior to digital processing of the signals.

The equivalent circuit of the LSA, illustrated in Figure 4-3, consists of a phototransistor and preamplifier transistor. After bias is applied to the base-collector capacitance of the phototransistor through terminal V_{CC}, the base-collector capacitance is charged to a specified value. Light incident on this junction generates hole-electron pairs that discharge the initial bias applied to the junction, proportionally to the amount of energy absorbed during the exposure. The voltage change of the base-collector capacitance is amplified by the preamplifier.

EQUIVALENT CIRCUIT

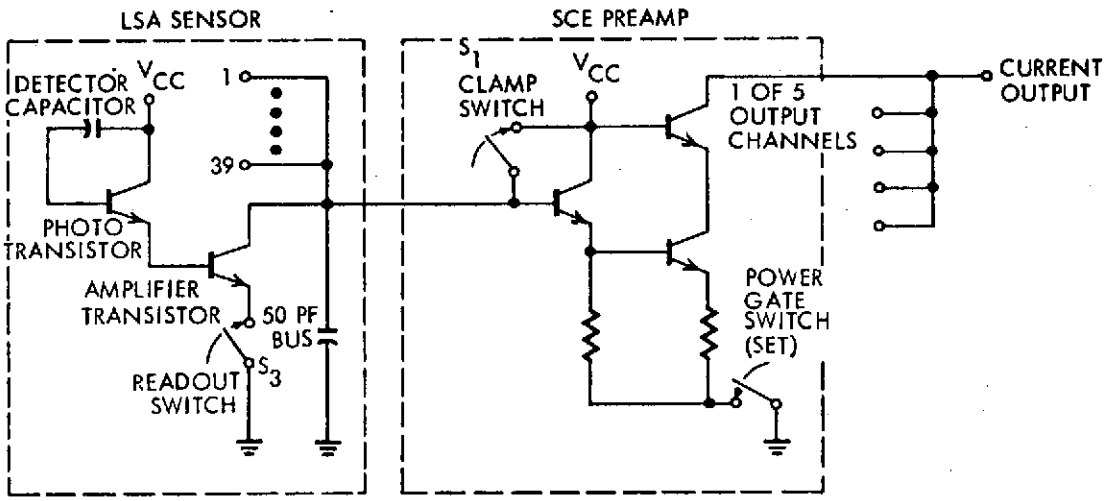

OPERATING CYCLE

TIMING SEQUENCE OF LSA CHIP-DETECTOR

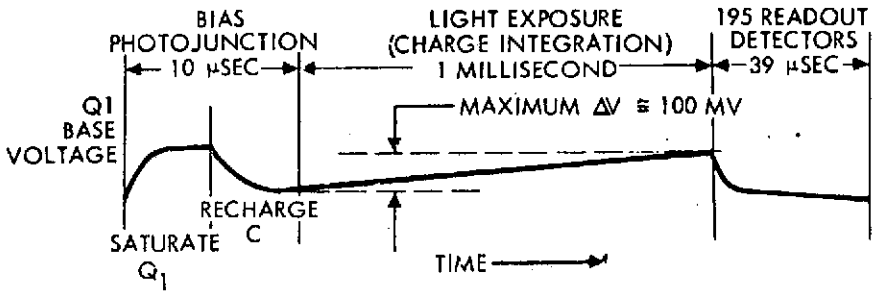

Figure 4-3. LSA Phototransistor Circuit and Operating Cycle

The 195 signals from the phototransistors are commutated in five groups of 39. Readout is accomplished by closing of the readout switches (S3), in sequence. This switching is actually accomplished by individual transistors under control of a shift register. The readout, or sampling, of the output of each preamplifier is accomplished in 2 μsec, thus 78 μsec are required for serial sampling of each group of 39. After this sampling, the photojunctions of the phototransistors are again biased, and the cycle is repeated.

The SCE preamplifier consists of two stages of gain, with five parallel groups being contained on a single chip to amplify the five multiplexed signals. The clamp switch, S1, is used to reset the signal to a reference level between each of the 39 serial samples from the LSA sensor. The power gate switch is used only to apply power to the SCE preamplifier to initiate operation.

4.4.4 Representative Sensor Design and Performance Characteristics

The optical design and system characteristics of a representative image system are summarized in Table 4-3. For this configuration a 3 x 3 degree field of view and a linear array of 390 phototransistor cells (i.e., two LSA chips) was assumed. The number of data bits per frame is 0.913×10^6 bits. For purposes of the SUAE application this data volume is actually larger than can be accommodated by the data handling and storage system (see Section 6.7).

A field of view reduction to 2 x 2 degrees and a reduction of phototransistor cells to 195 (= 1 LSA chip) would leave the optical characteristics and resolution almost unchanged, but reduces the required data storage capacity to 228 Kbits per image frame.

Figure 4-4 shows the performance of the sample spin-scan system (3 x 3 degrees FOV, 395 transistor cells) under conditions representative for image taking at Saturn and Uranus, for two spacecraft spin rates, 5 rpm (dashed lines) and 1 rpm (solid lines). The performance is expressed in terms of signal-to-noise current and power ratios as function of spatial frequency at the image plane. The performance varies with the modulation contrast of the scene as shown parametrically for values from 5 to 100 percent contrast. The signal-to-noise ratio drops with

Table 4-3. Representative Imaging System Characteristics

SENSOR	LINEAR ARRAY OF 390 SILICON PHOTOTRANSISTORS
OPTICAL SYSTEM	CASSEGRAIN, 4.7-IN. FOCAL LENGTH, f/1.0
INSTANTANEOUS FIELD OF VIEW	0.150 X 50 MILLIRADIANS
ANGULAR SIZE OF IMAGE	50 X 50 MILLIRADIANS (3 X 3 DEG)
SCAN PATTERN	390 TV LINES
LINE EXPOSURE TIME	0.127 MILLISECONDS (S/C ω = 5 RPM) 0.550 MILLISECONDS (S/C ω = 1 RPM)
FRAME SCAN TIME	0.495 SECONDS (S/C ω = 5 RPM) 2.14 SECONDS (S/C ω = 1 RPM)
DYNAMIC RANGE OF SENSOR	1000/1
DATA SAMPLES/TV LINE	390
ENCODING LEVEL	6 BITS/SAMPLE
DATA BITS/FRAME	0.913×10^6 BITS
WEIGHT	
OPTIC, ARRAY, PREAMPLIFIERS, MULTIPLEXER	6 LB
SIGNAL PROCESSING ELECTRONICS	5 LB
MIRROR AND POINTING MECHANISM	6 LB
POWER	
ARRAY, PREAMPLIFIERS, MULTIPLEXER AND ELECTRONICS	5 W
A/D CONVERTERS (5)	8 W
MIRROR POINTING CONTROL SYSTEM	5 W
VOLUME	
OPTIC AND ARRAY	0.15 FT^3
SIGNAL PROCESSING ELECTRONICS	0.12 FT^3
MIRROR AND POINTING MECHANISM (SWEPT VOLUME)	0.4 FT^3

increasing spatial frequency and decreasing scene contrast. At a spatial frequency of 32.8 line pairs per mm for the given focal length and cell array size a sharp degradation of imaging capability occurs due to coincidence of image feature and photocell spacing. In the performance graphs this singularity is indicated as resolution limit.

The data shows that images with very satisfactory signal-to-noise ratios (ranging from 8 to 15) are obtainable by this system even at low values of the modulation contrast. However, at Uranus the signal-to-noise ratio is two to three times lower than at Saturn for a given modulation contrast as might be expected.

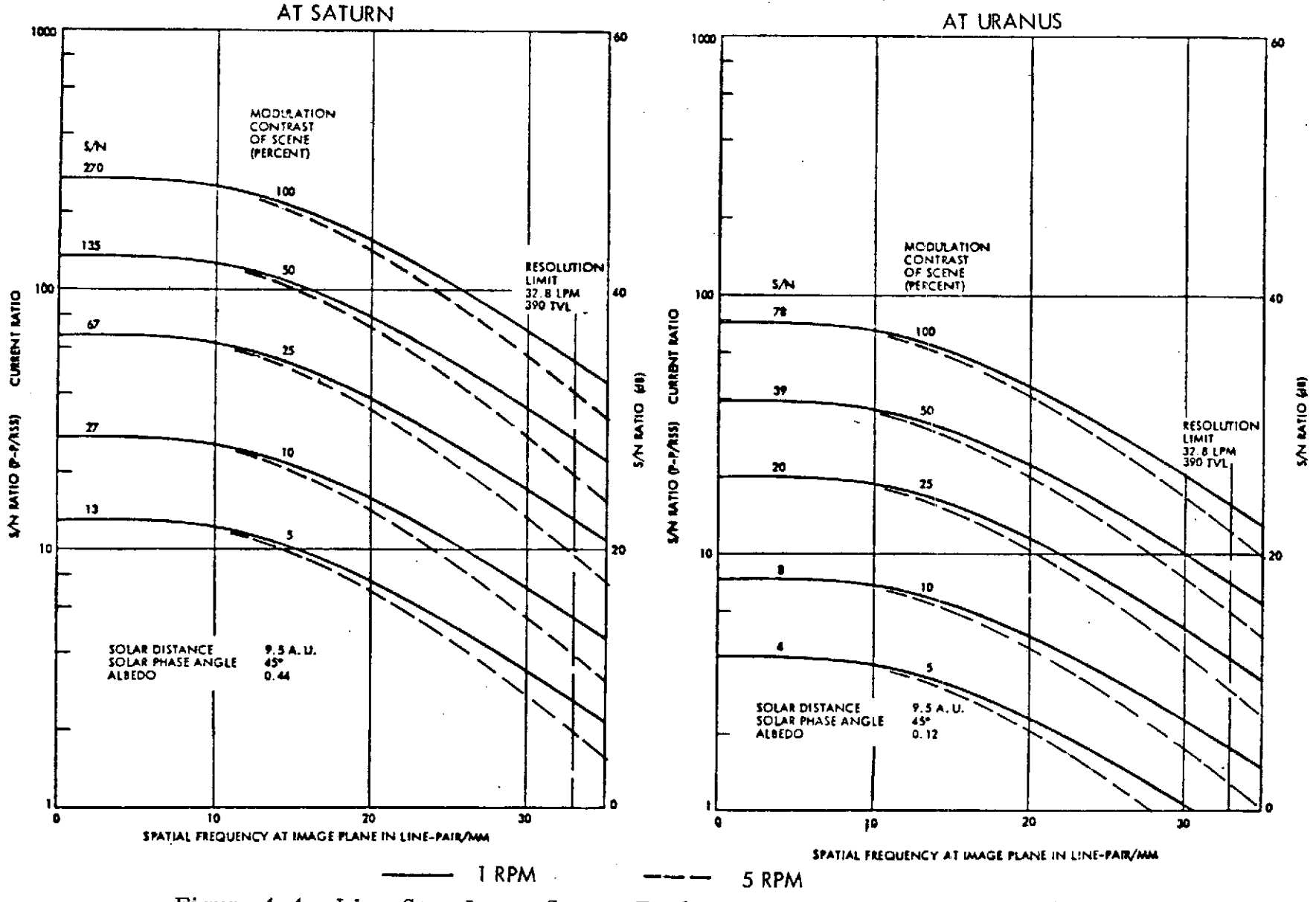

Figure 4-4. Line-Scan Image Sensor Performance at Saturn and Uranus (4.7-Inch Optics, f/1.0, Exposure Time 0.55 msec, Spin Rate 1 and 5 rpm)

4.5 ACCOMMODATION OF SCIENCE INSTRUMENTS ON THE BUS SPACECRAFT

4.5.1 Instrument Mounting and Orientation

Figure 4-5 shows the physical arrangement of payload instruments in the equipment bay of the modified Pioneer spacecraft. As in the baseline Pioneer F/G, most of the instruments are housed in the elongated hexagonal payload compartment attached to the +X side of the main structure.

The location of the UV photometer and charged particle detector remain unchanged. The new IR spectrometer is placed at the location formerly occupied by the IR radiometer which is now relocated to the opposite side. The line-scan camera uses the location formerly assigned to the imaging photopolarimeter. An externally mounted rotatable mirror assembly is used to change the camera's field-of-view orientation between cone angles of 70 and 180 degrees. As in Pioneer F/G, the viewing ports for the optical instruments are provided in the compartment's side panels.

The specified orientations and clear field-of-view requirements of the sensors are readily met by the arrangement shown, with the exception of the line-scan camera.

As previously discussed, the camera's view in a forward direction is partially obscured by the antenna dish. However, that limitation is offset by advantages inherent in the selected placement of the camera and mirror:

- Shielding by the antenna dish against direct sunlight and avoidance of a separate less effective light shade
- Thermal protection of the camera inside the payload compartment
- Shielding of the camera against dust impingement during cruise phases and Saturn ring encounter

The plane of the camera's field of view rotation is selected so as to minimize stray light effects from deployed appendages.

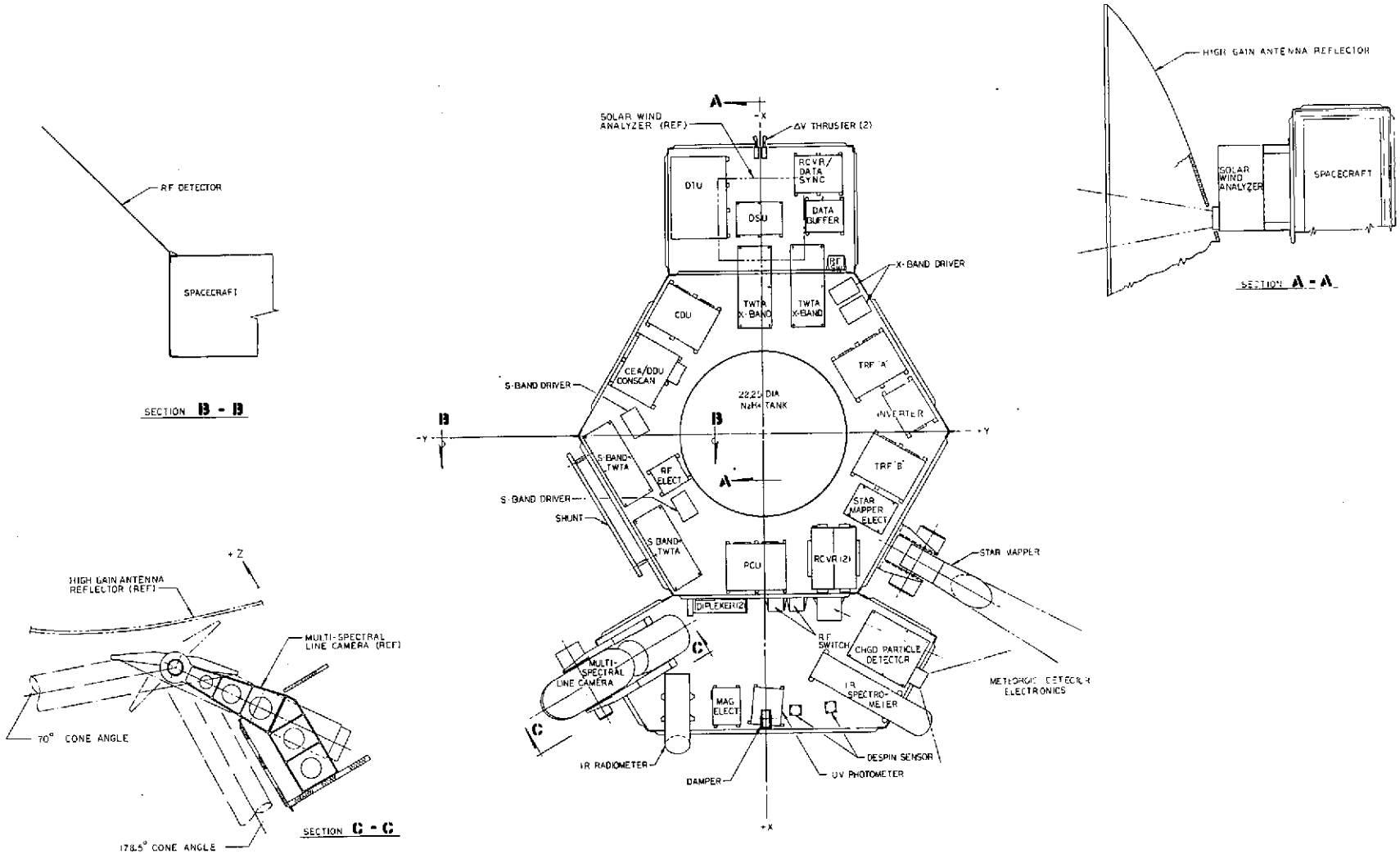

Figure 4-5. Pioneer Saturn Uranus Spacecraft; Equipment Layout

Actually, the cone angle range limitation imposed by the selected camera and mirror arrangement does not restrict planet or satellite viewing significantly. These bodies are to be observed primarily from the sunlit side which means at cone angles greater than 90 degrees. The relative geometry of the Saturn and Uranus encounters permits observation of the planet's bright limbs at cone angles greater than 70 degrees practically to the point of terminator crossing.

The only observation objective that would be restricted is that of obtaining images of Saturn's rings under certain back-lighting conditions.

Instruments not mounted in the payload compartment are the following:

- Solar wind analyzer
- Magnetometer
- Micrometeoroid impact detectors
- RF noise detector.

The solar wind analyzer is relocated to the -X side of the equipment bay, opposite its former position in Pioneer F/G, for reasons of mass balance. A new viewing slot for the instrument is provided in the high-gain antenna dish to permit forward viewing with a 20 by 140 degree field of view.

Externally mounted, and not shown in Figure 4-5, are the magnetometer and the micrometeoroid impact detectors. In its deployed position the magnetometer is at the same location and distance, 19.5 feet from the spacecraft centerline as in Pioneer F/G, thus meeting the same magnetic isolation constraints.

The micrometeoroid detectors remain at the same location on the aft surface of the high-gain antenna dish, as on Pioneer F/G.

The two-foot whip antenna used as an RF noise detector is mounted on a corner of the hexagonal equipment bay and protrudes at an angle of 45 degrees relative to the spacecraft centerline.

In summary, the modified Pioneer spacecraft layout provides ample mounting space and volume for all payload instruments* owing to the addition of an extension bay for new and relocated subsystem components and omission of several instruments of the Pioneer F/G payload.

4.5.2 Payload Weight and Power Allocation

The instrument weights given in Table 4-2 are preliminary estimates only and serve as guidelines. The total of 61.5 pounds, about 5 pounds less than for Pioneer 10, is consistent with the payload weight capacity of the modified Pioneer (see Section 5.4).

The estimated 30 watt power allocation, although 6 watts higher than for Pioneer 10, is consistent with the modified Pioneer capabilities, with 188 watts total RTG output power available at the time of arrival at Uranus (see Section 5.6). The largest individual allocation, i.e., 10 watts for the line-scan image system, can be time-shared with other instruments if necessary.

In case of power shortage due to failure of one RTG during transit, the total power allocation for experiments has to be reduced to 7.3 watts to be used by some of the instruments on a time-shared basis. Use of the image system is not possible in this mode.

4.5.3 Accommodation of Data Handling and Telemetry Requirements

The spacecraft provides telemetry data rates of 2048 and 1024 bps (using X-band) at the time of Saturn and Uranus encounters, respectively. Use of S-band as a backup mode would only permit data rates of 256 and 32 bps, respectively. The total data rate (64.4 bps) of all instruments except the image system can be readily accommodated with X-band telemetry. Storage of the science data during earth occultation can be handled comfortably by the data storage units (DSU) providing a total capacity of 740 Kbits, only 400 Kbits of which is dedicated to probe data.

The main concern is accommodation of the image system data requirements in terms of data handling, data storage, and telemetry. An image system with even a relatively small number of sensor cells

*See also the configuration drawing and layout description in Section 5.2.

requires hundreds of Kbits of buffer storage capacity and a large percentage of the available telemetry bit rate. Multispectral imaging implies an increased number of image frames compared to a single instrument and hence, still greater data handling and telemetry requirements.

Figure 4-6 is a nomograph designed for convenient evaluation and tradeoff of image system data requirements versus capabilities. The chart at the lower left gives the bit rates, required to transmit a desired number of image frames per hour, as a function of the number of sensor cells in the array. The diagonal parametric lines indicate the frame rate as well as the number of spacecraft revolutions between exposures. The lower horizontal scale shows the required buffer storage per frame. A conservative value of 8 data bits per cell is assumed here.

The chart at the upper left indicates the angular resolution obtainable with a given number of cells and a given field-of-view angle. The chart at the upper right converts angular resolution to surface resolution for a given observation distance. It also shows the distances at which Saturn's and Uranus' disk would cover the entire field of view of a 2 x 2 degree image system, and the surface resolution corresponding to these distances.

The illustrative example shown in the chart indicates that for a line scanner with 200 image cells the required buffer storage is 320 Kbits, and a frame rate of two images per hour corresponds to a bit rate of 178 bps. With the less conservative assumption of 6 rather than 8 data bits per cell, the storage requirement would be 240 Kbits and the data rate 134 bps. With a 2 x 2 degree field of view this line scanner achieves an angular resolution of 0.16 milliradian and a surface resolution of 16 km at a distance of 10^5 km, the closest approach distance at both the Saturn and Uranus encounters.

Tradeoff options between data rate requirements and imaging capability can be readily evaluated with the aid of the nomograph. For example, it is evident that doubling the number of line-scan elements for a given FOV-size would unnecessarily improve the surface resolution to 8 km at 10^5 km distance while multiplying the storage and telemetry requirements by a factor of four.

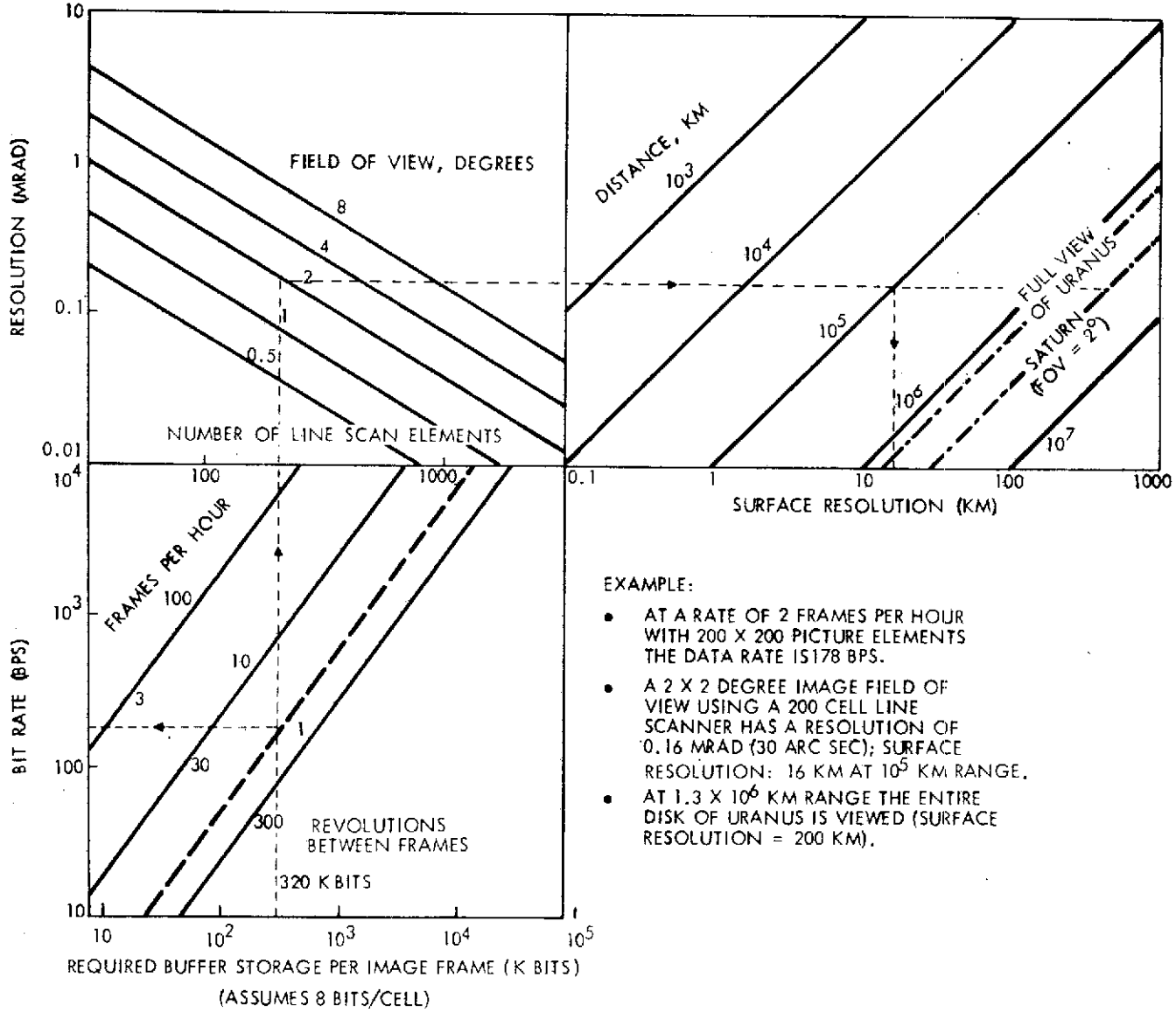

Figure 4-6. Line-Scan Imaging Capabilities and Data Rate Requirements

As another example we consider satellite viewing. An increase in FOV-size from 2 x 2 to 4 x 4 degrees would simplify the task of obtaining satellite pictures if the relative encounter geometry is not known accurately in advance. This can be achieved if the cell number is kept unchanged without burdening the telemetry and storage requirements. Surface resolution would then be 32 km at 10^5 km distance (rather than 16 km). Loss of resolution by a factor of two may be justifiable in exchange for increasing the probability of obtaining satellite images by a factor of four if a close satellite encounter should become a definite objective of the mission.

At X-band telemetry bit rates of 2048 to 1024 bps the acquisition rates determined in this example can be easily accommodated not only before the time of probe entry when imaging operations are unrestricted, but also during the probe data relay phase. Prior to the data relay phase it would be possible to transmit more than two frames per hour if desired, perhaps even as many as 6 to 8 frames per hour at Saturn.

If the communication system is constrained to operate at S-band (as a backup mode), the data rate of 256 bps available at Saturn would permit about one image frame per hour prior to the probe data relay phase. However, during the relay phase telemetry of image data must be discontinued or would be restricted to less than one frame per hour.

Buffer storage of 320 Kbits per frame (or 240 Kbits if 6 data bits per image cell are used) can be accommodated without interfering with probe data storage, since at most 400 Kbits of the total available DSU capacity of 740 Kbits is required. Thus if a high-telemetry bit rate is available, image system operation can continue during the data relay phase. However, in the event of a partial DSU failure with the remaining data storage capacity insufficient to accommodate both probe and image data, the probe data will have priority.

Tentative allocation of data formats in the digital telemetry unit (DTU) to bus science data, and assignment of storage capacity in the DSU's in the cruise mode, pre-encounter mode, data relay mode, and

occultation mode will be discussed in Section 6. Of particular interest is the flexible manner in which image system data can be interleaved with other bus science and engineering data and probe data such that under all conditions not more than half of the available telemetry data rate will be allocated to image system data. This flexibility is provided by the interchangeable DTU formats of the baseline Pioneer communication subsystem that can be directly adapted to the bus science and engineering telemetry needs of the SUAE mission.

4.6 SCIENCE INSTRUMENT OPERATING MODES AND SEQUENCES

4.6.1 Cruise Operations

During the interplanetary cruise phases only the particles and fields detectors (i.e., magnetometer, solar wind analyzer, and charged particle detector) and the micrometeoroid detectors will be in continuous operation. The line-scan camera will be turned on only in the event that a target of opportunity, e.g., an asteroid or comet, is encountered within close range.

Since the data acquisition rate of the cruise science instruments is of the order of 30 bps, and since the instruments only need to be sampled intermittently, it is possible to use the large available DSU data storage capacity to reduce the number of telemetry periods. Thus, if only one hour of science data are recorded per day the intervals between telemetry sessions could be extended up to seven days. Actually, the amount of engineering telemetry that is necessary for routine spacecraft monitoring also has to be considered. Flare events which can be detected at earth would of course call for a change in the sampling and telemetry mode.

S-band communication will be adequate in the cruise mode until well beyond the Saturn encounter. The use of S-band instead of X-band is preferred during this phase since fewer pointing corrections are necessary to maintain the spacecraft spin axis within the 3 dB half-beam width. At the communication distance of about 14 AU (4.6 years after launch) the S-band data rate drops below 128 bps, and it is desirable to switch to X-band telemetry thereby increasing the data rate to 1024 bps.

4.6.2 Encounter Operations

Prior to and during the planetary encounter the bus science activities will be stepped up (1) since all onboard payload instruments will be used during the event and (2) their outputs will require much more frequent sampling. Selected examples of event sequences and instrument operating modes will be discussed in the following paragraphs.

4.6.2.1 Pre-encounter Calibration and Checkout

The instruments which will have remained inoperative during the long cruise phases to Saturn and Uranus require calibration and checkout well in advance of the encounters. If malfunctions are detected sufficient time is required to remedy the conditions if possible, to implement back-up modes, or to revise the observation strategy.

4.6.2.2 Sequence of Major Physical Phenomena and Events Encountered at Saturn and Uranus

Major physical phenomena and events at the planet encounters that govern the sequence of science instrument operations are listed in Table 4-4. Distance from the planet and approximate time to encounter (periapsis passage) are also indicated. Reference is made to Figures 3-12 and 3-14 which show the encounter trajectories near the closest approach to Saturn and Uranus.

With regard to image system utilization it is interesting to note that Saturn and its ring formations will cover the entire width of the camera's field of view (2 degrees) at a range of 7.9×10^6 km. The planet alone will cover the FOV at a range of 3.4×10^6 km. This occurs 8.7 days and 3.8 days before the encounter, respectively. Up to this time it will be adequate to obtain only a few images per day. On closer approach, as surface resolution increases and the phase angle begins to change more rapidly an increase of image frame rate is desired, the maximum of 1 to 2 frames per hour being consistent with spacecraft data handling and telemetry capabilities, as discussed in the preceding section.

For Uranus the distance and time to encounter at which the planet fills the camera's FOV are 1.45×10^6 km and 1.6 days.

Table 4-4. Sequence of Major Physical Phenomena and Events at Saturn and Uranus Encounters

Event	Saturn		Uranus	
	Distance from Planet (km)	Time to Encounter (days/hrs)	Distance from Planet (km)	Time to Encounter (days/hrs)
Spacecraft crosses magnetosphere boundary (estimated maximum distance at Saturn is 240 R_S)*	1.44×10^7	15.9 d	No estimate available	
Planet covers camera FOV (2 x 2 degrees)	3.43×10^6	3.8 d	1.45×10^6	1.6 d
(Saturn plus rings cover FOV width)	(7.90×10^6)	(8.7 d)		
Encounter of Titan (if included in mission)**	1.22×10^6	1.35 d	-	-
Spacecraft passes minimum phase angle point**	3.70×10^5	5.2 h	7.0×10^5	~13 h
Probe entry time	1.60×10^5	1.2 h	1.4×10^5	1.7 h
End of probe entry phase (nominal)	1.40×10^5	0.2 h	1.08×10^5	0.7 h
Terminator passage	1.35×10^5	-4.4 h	1.02×10^6	~0
Periapsis passage	1.38×10^5	0	1.02×10^5	0
Saturn ring plane passage	1.40×10^5	-2.0 h	-	-
Entry of earth occultation zone**	1.80×10^5	-3.0 h	3.9×10^5	-5.6 h
Exit of earth occultation zone**	3.10×10^5	-4.4 h	6.1×10^5	-8.4 h

*See NASA SP-8091 and SP-8103.

**Approximate data.

Other events that are of direct interest to imaging system operations are the passage of the minimum phase angle point and the terminator. The interval between these events marks the most active period of image system operation, as planet aspect angles change at an increasing rate and surface resolution approaches an optimum. Images of the probe entry area will be of particular interest for subsequent interpretation of probe observed phenomena.

Figure 4-7 shows the observation intervals available to some of the payload instruments during the encounter of Saturn. Field-of-view limitations of the sensors relative to the earth-pointing spacecraft (see insert drawing at upper left) restrict the locations along the trajectory from where planet and ring phenomena can be viewed. This reflects in observation intervals of different length for the individual payload sensors as indicated by solid and dashed arc segments along the trajectory. Solid lines represent observability periods of the planet and rings, dashed lines observability of rings only. Corresponding results can be readily derived for Uranus, by using the encounter trajectory given in Figure 3-14

As can be seen in Figure 4-7 the IR radiometer and spectrometer having fields of view of 40 degrees, centered at a cone angle of 135 degrees, are more restricted in their observation capability during the Saturn approach phase than the other sensors. The "blind spot" in sensor coverage at cone angles greater than 155 degrees reflects in a 10-hour gap in planet observation capability. The gap in ring observation capability is only 1.5 hours. The instrument can resume planet observation, during the final approach phase, for a period of 3.5 hours until 0.3 hour before periapsis passage. Ring observation can continue for another 1.5 hours beyond this point.

In the Uranus encounter the gap in IR sensor coverage is considerably longer due to the shallower trajectory angle relative to the earthline, but the final observation period (3.3 hours) is about the same as in the case of Saturn.

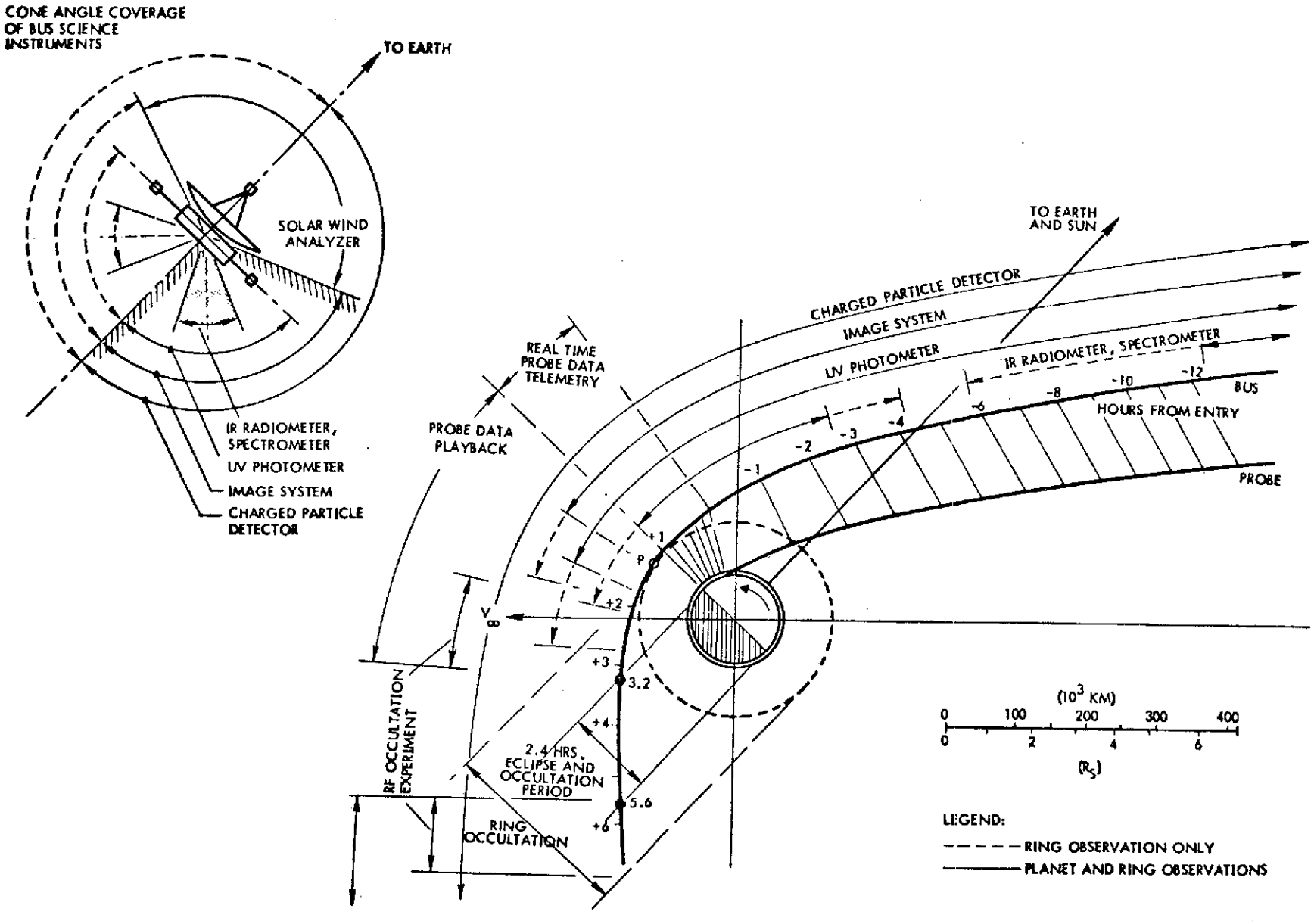

Figure 4-7. Observation Intervals of Bus Science Instruments at Saturn Encounter

The UV photometer, not subject to the same blind spot as the IR sensors can be used uninterruptedly for planet observation until 0.5 hour beyond periapsis passage in both Saturn and Uranus encounters. Saturn ring observation can continue for another hour beyond this point.

The charged particle detector, covering a 180-degree cone angle range, in effect provides omni-directional observation capability and can be used throughout the encounter. The solar wind analyzer also can operate without restriction other than the effects of the solar eclipse which in the case of Saturn starts 2 hours after periapsis passage and lasts for 2.4 hours.*

Planet observation by the image system can be continued until periapsis passage in the case of Saturn, and for 1 hour beyond periapsis in the case of Uranus. Observation of the bright side of Saturn's rings is possible fro about 0.5 hour longer than observation of the planet proper.

To avoid complexity in programming or commanding individual observation sequences for the different payload sensors a common operating mode is adopted whereby all sensors (except the image system) continue to function throughout the encounter phase, even at times when no useful information is acquired. This is acceptable because of their modest data acquisition rate. Image system operations will be sequenced in accordance with the scientific importance of observations at different phases of the encounter, and subject to the constraints of data storage and telemetry capacity with and without concurrent probe data relay requirements.

4.6.2.3 Titan Encounter

The possibility of a close encounter with the satellite Titan during the 1983 or 1984 Saturn flyby missions has also been briefly analyzed. Figure 4-8 shows characteristics of the encounter in terms of distance versus phase angle and time from closest approach. The date of arrival at Saturn in this example is April 8, 1973; a late launch date is assumed.**

*All quantitative data presented above are the result of simple graphical analysis, accurate to about 0.5 hour.

**Data supplied by Ames Research Center.

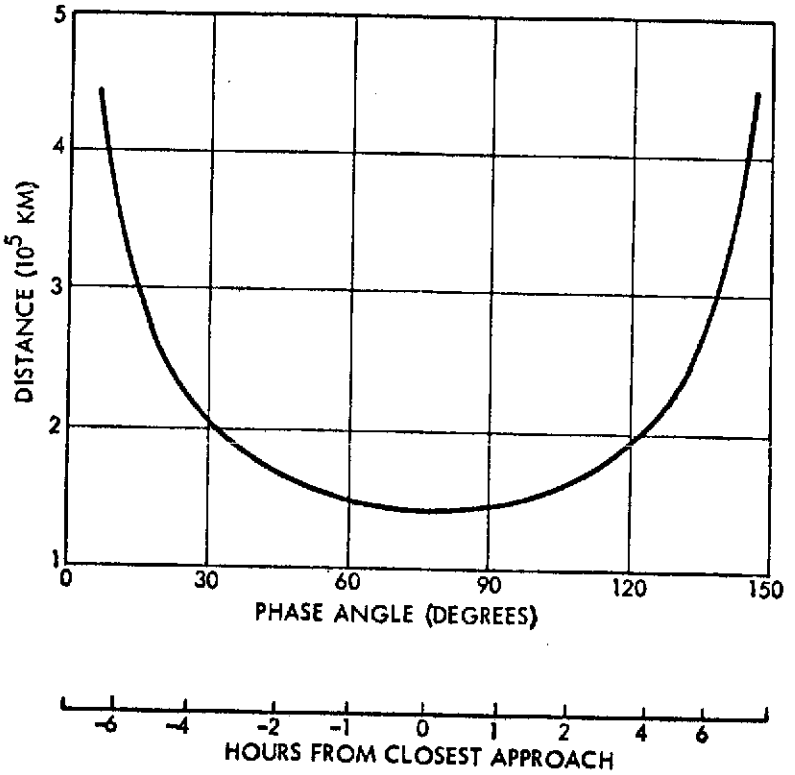

Figure 4-8. Titan Encounter Conditions (Saturn Arrival on April 8, 1983)

The satellite can be viewed for about 7 hours within a distance of 2×10^5 km, that is with the long dimension of its visible disk occupying at least 70 percent of the camera's field of view. At closest approach (1.4×10^5 km) the phase angle is 75 degrees and the length of the gibbous equals the field-of-view width. The spacecraft will be occulted by the satellite for 0.3 hour about 4.5 hours after the encounter, at a range of about 2.5×10^3 km. With a diameter of 4800 km Titan is sufficiently large to make the objective of achieving occultation compatible with predicted terminal guidance capabilities. Observation phases by the various encounter instruments are similar to those depicted in Figure 4-7 for the Saturn encounter (except for the trajectory being essentially a straight line).

4.7 SUMMARY OF SCIENCE PAYLOAD ACCOMMODATION AND OPERATION CAPABILITIES

Table 4-4 summarizes the payload operation and support capabilities of the SUAE spacecraft as detailed in the preceding subsections. In all categories of science payload accommodation listed here the modified Pioneer spacecraft meets or exceeds the requirements dictated by scientific mission objectives.

Table 4-4. Summary of Spacecraft Bus Science Support and Accommodation

1. ADEQUATE WEIGHT AND POWER CAPACITY	• WEIGHT IS 4.5 POUNDS LESS, POWER 6W MORE, THAN FOR PIONEER F/G PAYLOAD • FIVE PIONEER F/G INSTRUMENTS OMITTED, THREE NEW INSTRUMENTS ADDED, HAVE COMPARABLE REQUIREMENTS
2. ADEQUATE DATA STORAGE AND TELEMETRY	• 2048 BPS AT SATURN, 1024 BPS AT URANUS PERMIT SEVERAL HUNDRED BPS TO BE ALLOCATED TO IMAGE DATA TELEMETRY (AT LEAST ONE FRAME PER HOUR) • 3 X 250 KBITS OF DATA STORAGE AVAILABLE. IF ONLY TWO OPERABLE AT ENCOUNTER, IMAGE DATA BUFFER STORAGE DISCONTINUED IN FAVOR OF PROBE DATA STORAGE
3. MOUNTING AREA AND FREE FIELD OF VIEW	• SIMILAR TO PIONEER F/G FOR ALL SIMILAR INSTRUMENTS • AMPLE MOUNTING AREA AVAILABLE FOR THREE NEW INSTRUMENTS (IR SPECTROMETER, LINE-SCAN IMAGE SYSTEM, RF NOISE DETECTOR) • LINE-SCAN IMAGE SYSTEM (REPLACING IMAGING PHOTOPOLARIMETER) USES ROTATABLE MIRROR
4. PRINCIPAL PERIODS OF OPERATION	• INSTRUMENTS OPERATING THROUGHOUT ENCOUNTER (INCLUDING OCCULTATION ZONE): (a) MAGNETOMETER (b) SOLAR WIND ANALYZER (c) CHARGED PARTICLE DETECTOR (d) RF NOISE DETECTOR (e) MICROMETEOROID DETECTORS • IR RADIOMETER AND SPECTROMETER PARTIALLY CONSTRAINED BY 40 DEGREE FOV LIMITATION, BUT CAN FUNCTION WITH INTERRUPTION UNTIL PERIAPSIS PASSAGE • UV PHOTOMETER FUNCTIONS UNCONSTRAINED UNTIL PERIAPSIS PASSAGE • IMAGE SYSTEM OPERABLE AT FRAME RATES UP TO TWO PER HOUR THROUGHOUT PRE-ENCOUNTER PHASE, AT LEAST UNTIL PROBE DATA RELAY INITIATION • IF NO CONFLICT WITH RELAY SUPPORT REQUIREMENTS IMAGE SYSTEM CAN CONTINUE UNTIL END OF OBSERVABILITY, I.E., PERIAPSIS PASSAGE OR RING PLANE CROSSING (AT SATURN)

In summary the baseline Pioneer F/G spacecraft adapted to the SUAE mission provides these design features and operating modes in support of the science payload functional requirements:

a) Payload operations during the cruise and encounter phases are similar to those in Pioneer F/G.

b) Principally the same modes of command, data handling and telemetry are used as in Pioneer F/G.

c) The X-band communications capability added to provide adequate data rates at Saturn and Uranus readily accommodates the high-data volume line-scan image system if modest frame rates are used.

d) The new MOS data storage units with total storage capacity of 740 Kbits is used for purposes of probe data storage, image data buffer storage, and other science data storage during occultation periods. With economy in total storage capacity since requirements are only partially overlapping.

e) Flexible DTU formats of Pioneer F/G are directly adaptable to multi-mode science data handling, interleaving image data at different frame rates, etc.

f) Science support capability has a variety of backup modes to minimize loss of essential data.

g) Prior to probe entry all spacecraft resources are available to support bus science payload.

h) During and after probe entry bus still meets science payload requirements while catering to probe data relay requirements on a priority basis.

i) On encounters with no probe delivery all spacecraft resources are available without constraint to support bus science instruments, e.g., higher image data rates if desired.

5. SYSTEM DESIGN

5.1 SYSTEM DESIGN CRITERIA

This section describes the selected bus spacecraft configuration for the Pioneer Saturn Uranus mission, its design characteristics and its interfaces with the entry probe, from the overall system standpoint. The approach used in arriving at this configuration was guided by the following criteria:

- Minimum configuration change from Pioneer F/G
- Retention of as many subsystem components developed for Pioneer F/G as possible
- Provision of effective functional support to the entry probe before and after its separation from the bus, as dictated by mission requirements, while keeping interfaces as simple as possible
- Effective accommodation of the bus science payload
- Increased system reliability, commensurate with the required long mission life (3.4 years to Saturn flyby, 7.0 years to Uranus)
- Achieving a gross target weight of 1050 pounds (bus and probe) consistent with the launch vehicle performance characteristics specified by Ames Research Center
- Achieving maximum cost economy in system design, implementation and operation.

The evolution of the Pioneer Saturn Uranus spacecraft from the baseline Pioneer F/G configuration, and the principal modifications required for this mission have been summarized previously in Section 2. As discussed in that section, many of the Pioneer F/G design features can be retained intact, while some of the design modifications already contemplated for outer planet missions in general* meet the objectives of the SUAE mission. The description of system and subsystem design characteristics in this and the following section will substantiate this conclusion in greater detail.

*"Outer Planets Pioneer Spacecraft," prepared for NASA/Ames Research Center, under contract NAS2-6859, 23 March 1973.

5.2 CONFIGURATION DETAIL

5.2.1 Configuration Layout

The selected design concept of the Pioneer Saturn Uranus spacecraft is shown in Figure 5-1 and the internal equipment arrangement in Figure 5-2. The side view in Figure 5-1 shows the spacecraft bus and the attached entry probe in stowed configuration, mounted on top of the launch vehicle's third stage, the TE-364-4 solid rocket. The 37-inch diameter launch vehicle adapter is slightly modified from a standard version associated with this third stage, with a 5-inch extension of its cylindrical length to 36 inches, and some structural changes necessitated by the design of the separation mechanism.

The spacecraft is housed within the 14-foot diameter Viking shroud, the standard nose fairing for Titan III E/Centaur class boosters. Actually, with maximum lateral dimensions the same as in Pioneer F/G, as defined by the 9-foot diameter high-gain antenna dish, the vehicle would fit into the Centaur/Pioneer F/G shroud. Thus, the Viking shroud provides more than ample space, both longitudinally and laterally. In fact, a potential weight advantage, estimated as about 100 pounds, would accrue from the use of the smaller Centaur/Pioneer shroud, if this shroud were to be adapted to the Titan III E/Centaur class boosters. However, no such plans are currently under consideration.

The major mechanical changes from Pioneer F and G, evident from the design drawings are:

- Accommodation of the 36-inch diameter entry probe attached to the bus by a 14.5-inch long conical interstage adapter that also transfers the spacecraft load to the launch vehicle.
- Incorporation of a 22.25-inch diameter propellant tank containing 115.2 pounds of hydrazine and associated nitrogen pressurant, in lieu of the 16.5-inch diameter tank of Pioneer F/G, to increase the ΔV capability as required.
- Addition of an equipment bay extension on the -X axis outboard of the main hexagonal compartment, to accommodate new subsystem components as well as equipment displaced from the main compartment by the enlarged propellant tank.

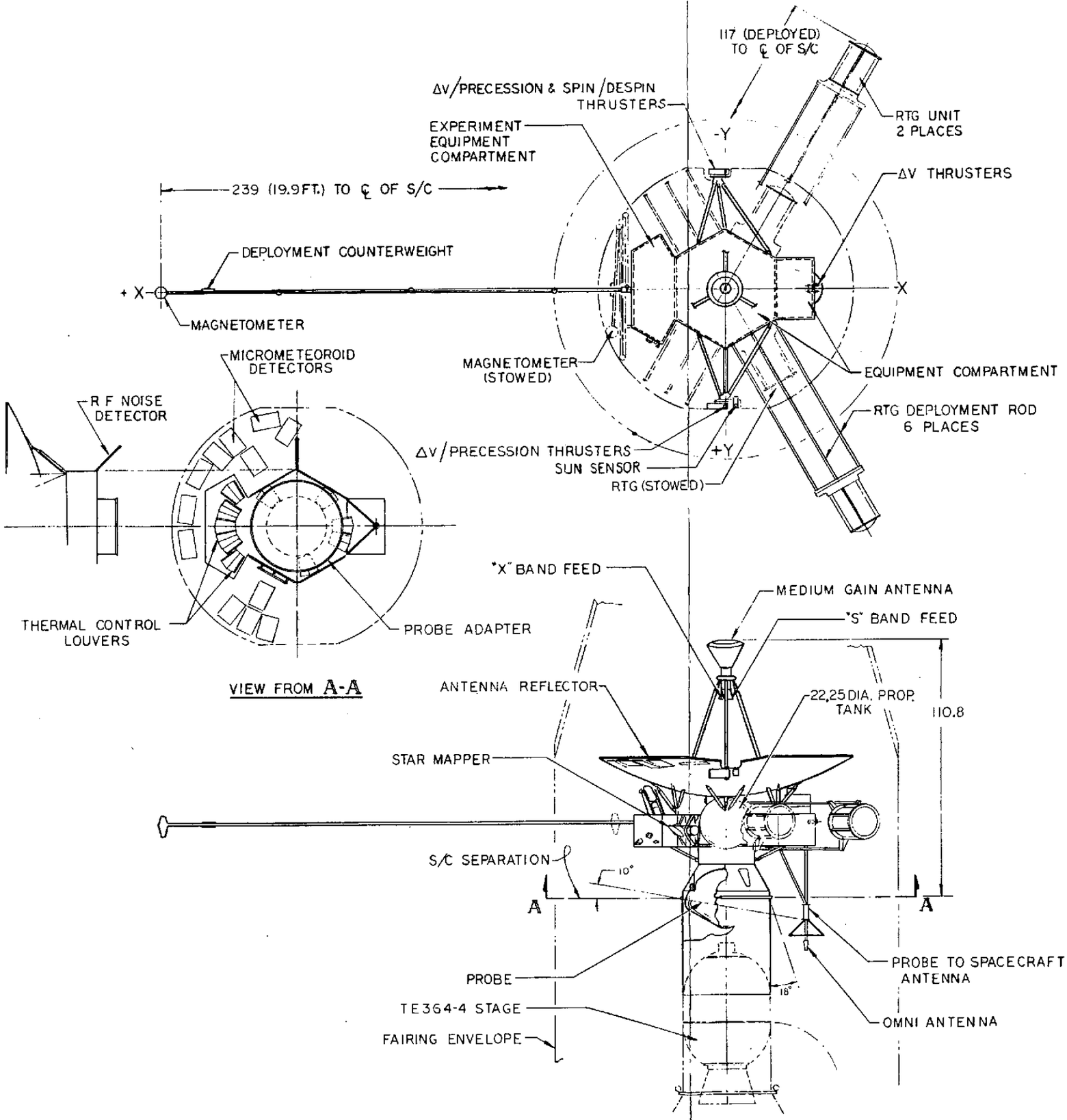

Figure 5-1. Pioneer Uranus Spacecraft, External Configuration

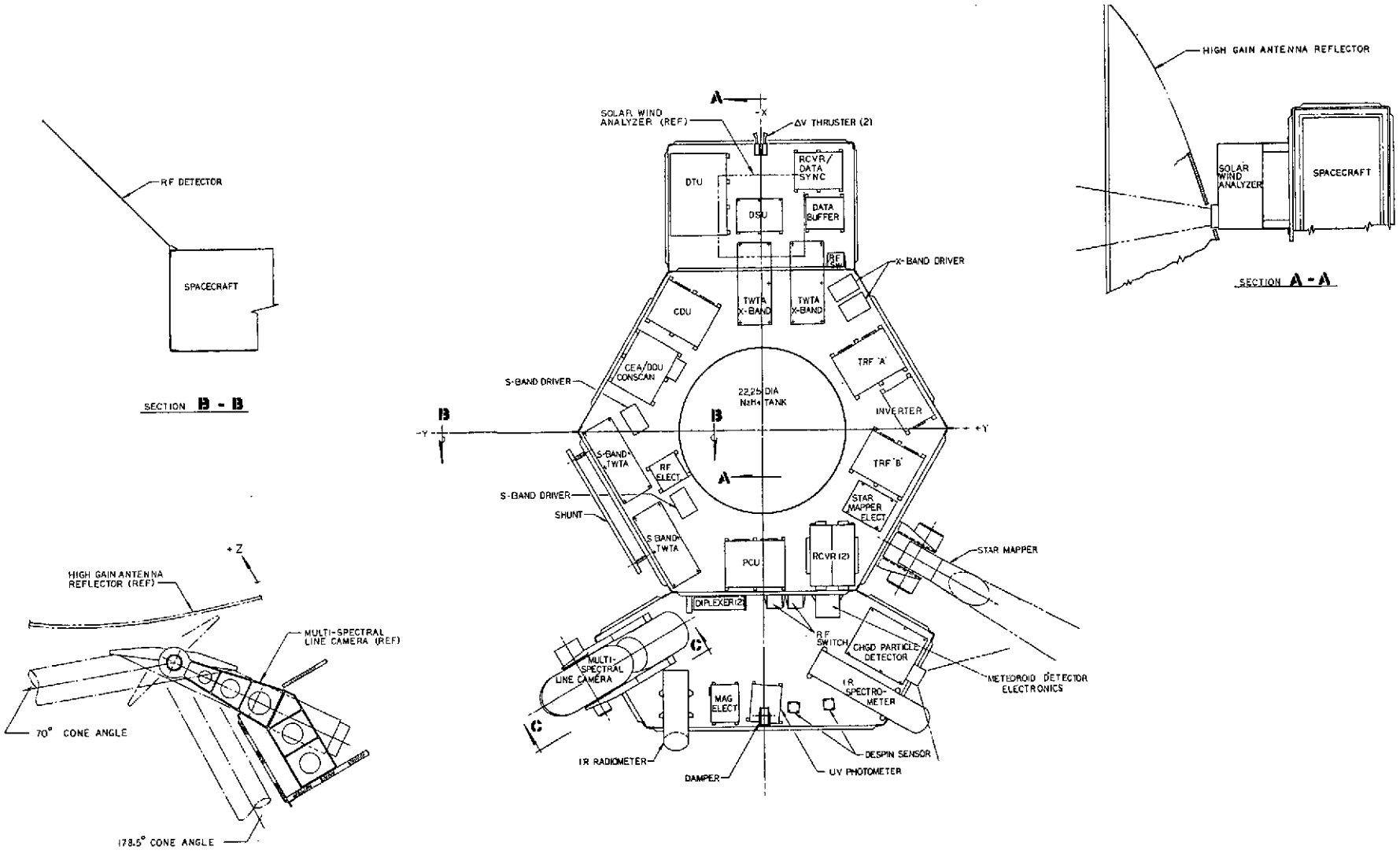

Figure 5-2. Pioneer Saturn Uranus Spacecraft; Equipment Layout

- Relocation of the RTG deployment guide rods and the addition of a clearance hole in the main equipment platform in order to accommodate the larger propellant tank.

- Incorporation of two high-performance MHW RTG's replacing the SNAP-19 RTG's of Pioneer F/G to meet the higher power requirements of the mission.

- Addition of two radial ΔV thrusters with lines of force approximately along the +X axis in the plane containing the bus spacecraft's center of mass. These thrusters are used for lateral ΔV maneuvers while the spacecraft spin axis is kept earth-oriented.

- A revised complement of science instruments including a one-axis gimballed image system.

- Incorporation of a star mapper, serving the dual function of navigational and roll reference sensor, replacing the star reference assembly of Pioneer F/G.

- Addition of a 400 MHz "loop-vee" antenna extending from the aft end of the equipment compartment beyond the conical bus/probe interstage structure, designed with a rotationally-symmetric beam pattern for receiving probe telemetry signals during the entry phase.

5.2.2 Structure and Equipment Compartment

The spacecraft configuration retains the basic structural geometry and load paths of Pioneer F and G. The dimensions, geometry, and physical location of the following main features of the Pioneer F and G spacecraft have been retained intact or almost unchanged:

- Spacecraft separation ring located between equipment bay and probe interstage
- Main hexagonal equipment compartment
- Hexagonal compartment corner support struts
- Science compartment on the +X axis
- Magnetometer boom and support structure

- Basic RTG support structure
- High-, medium- and low-gain antennas and support structures
- Sun sensor and attitude control thruster clusters.

The equipment compartment is located immediately forward of the interstage and is constructed principally of aluminum honeycomb sandwich panels. The aft panel of the compartment is the principal mounting surface for the electronic components. The hexagonal compartment forward cover and certain of the side panels employ semi-monocoque structure to accommodate unique load conditions. The hexagonal compartment corners are reinforced by external boron composite struts attached to the interstage as on Pioneer F and G.

The asymmetric RTG deployment would cause lateral movement of the bus spacecraft c. m. unless compensated. To keep the operational spin axis parallel to the antenna axis and coincident with the spacecraft's geometrical centerline at all times, with the probe onboard the spacecraft or off, a balanced deployment technique is used with a 24-pound deployment counterweight added near the tip of the magnetometer boom to provide mass balance in the stowed as well as the deployed configuration. The three appendages are deployed simultaneously to minimize transient unbalance effects during the transition from the (dynamically unstable) initial configuration to the dynamically stable fully deployed configuration.

As noted earlier, the science compartment at the +X axis is unchanged from that of Pioneer F and G except that the clearance holes for the instrument apertures will be modified to accept the revised science payload.

An additional equipment bay has been added on the -X axis, as shown in Figures 5-1 and 5-2 in order to house new subsystem components as well as equipment displaced from the hexagonal compartment by the physical growth of the propulsion system.

5.2.3 Science

The spacecraft configuration retains the Pioneer F and G science compartment geometry and location at the spacecraft +X axis adjacent

to the hexagonal compartment. The compartment provides the same internal and external equipment mounting surfaces and the same mounting provisions for the stowed and deployed magnetometer boom.

Figure 5-2 shows one possible arrangement for the science equipment which provides all sensors with unobstructed fields of view. The arrangement permits use of the Pioneer F and G thermal louver and ground handling fitting installations with only minor changes.

The charged particle detector looks through one of the diagonal side panels of the compartment, and the magnetometer electronics unit is mounted near the magnetometer boom similar in location as on Pioneer F and G. The IR radiometer and spectrometer and the UV radiometer also view through the compartment's side panels.

As envisioned in this preliminary placement of science instruments, the multi-spectral line-scan camera is mounted inside the compartment, using an externally mounted rotatable mirror to observe target objects at cone angles ranging from 70 to nearly 180 degrees.

5.2.4 Propulsion

The Pioneer F and G 16.5-inch diameter tank which contains 60 pounds of hydrazine and the associated nitrogen pressurant is replaced by a 22.25-inch diameter hydrazine tank (Model Lockheed P95) with 156 pound propellant capacity including pressurant. As in Pioneer F/G the system operates in a simple blowdown mode. Although the ES and ESU missions require a total propellant capacity of only 77 and 115 pounds respectively, the larger tank size was adopted to save development costs. It also provides a possible growth capability.

The propellant tank is mounted to the equipment platform by a full skirt attached to the tank's equator. The skirt is cut out as required to accommodate the propulsion system hardware and to save weight. The tank attachment to the forward surface of the equipment mounting platform is matched to the attachment of the spacecraft interstage to the aft surface so that the tank loads are transferred directly to the interstage with minimum stress induced in the mounting platform.

The arrangement of the 4-axial and 2-circumferential hydrazine thrusters remains unchanged from Pioneer F/G. The new radial thruster pair is mounted on the -X axis sidewall of the add-on equipment bay in the plane containing the center of mass of the bus spacecraft minus entry probe. The thruster lines of force are slightly canted off the X axis such that they pass within 6 inches on both sides of the nominal c. m. location. Small lateral c. m. offsets from the nominal location can be accommodated without a net spin or despin torque effect by using a slightly different total number of pulses from each of the two thrusters to achieve a desired velocity increment.

5.2.5 Thermal

As on Pioneer F and G, the spacecraft is wrapped in thermal blankets and the equipment compartment is thermally isolated from all external appendages by supporting them with nonmetallic materials of low-thermal conductance, to minimize uncontrolled heat loss.

The aft surface of the equipment compartment is provided with active thermal control louvers for rejection of excess heat to space. In spite of higher heat loads and partial blockage of louvers by the conical probe interstage fewer louvers are used. This is permitted by locating the shunt regulator under the equipment compartment and by not turning on the X-band transmitter until side-sun conditions have passed, thereby reducing the variability of the heat to be rejected.

5.2.6 Attitude Control

As shown in Figure 5-2 a gimballed star mapper is used in place of the stellar reference assembly of Pioneer F/G to generate roll reference pulses as well as for use in navigational measurements during planetary approach. The location of this sensor is similar to that of the SRA on Pioneer F/G, providing a clear field of view between cone angles of 70 and 180 degrees with minimum stray light effects from deployed appendages.

The sun sensor and the ΔV/precession and spin/despin thruster cluster installation is like that of Pioneer F and G. The sun sensor and one ΔV/precession thruster cluster are mounted on a bracket at the +Y

spacecraft axis near the periphery of the high-gain antenna reflector. The bracket is supported by three struts anchored to the hexagonal equipment compartment.

The spin/despin and the second ΔV/precession thruster clusters are mounted in a similar manner at the spacecraft -Y axis. The nutation damper is actuated by the magnetometer boom's motion in the X Z plane, exactly as on Pioneer F and G.

5.2.7 Communications

The location and installation of the high-, medium- and low-gain antenna systems are like those of Pioneer F and G. The conical log spiral low-gain antenna is mounted to a mast and located on the +X axis aft of the equipment compartment and separation plane. The mast also carries the loop-vee antenna which is added to the Pioneer F/G antenna complement to serve as receiving antenna for entry probe telemetry signals. It is placed two feet aft of the probe interstage support structure to avoid obstruction of its rotationally symmetric beam pattern during probe-to-bus relay operation. The tip of the low-gain antenna extends another 12 inches beyond the loop-vee antenna location.

As in Pioneer F/G, the high-gain antenna reflector is mounted to the hexagonal equipment compartment by 12 fiberglass struts. The reflector is like that of Pioneer F/G except for relocation of the small viewing slot provided for the solar wind instrument behind the dish.

The medium-gain antenna and high-gain antenna feed assembly are supported by three fiberglass struts mounted to alternate corners of the hexagonal compartment. It is expected that the inclusion of X-band capability to the high-gain antenna feed will have no effect on the basic support structure.

As can be seen in Figure 5-2, the arrangement and locations of the S-band TWTA, diplexer, diplexer/coupler, RF transfer switches, and transmitter drivers, are either the same or similar to those of the Pioneer F/G spacecraft, minimizing physical changes and line losses in the communications and antenna systems. The added X-band transmitter equipment, the added relay link receiver/data synchronizer package,

and the modified DTU and data handling equipment, use portions of the new add-on equipment bay. The aft surface of this compartment provides additional mounting space for thermal control louvers associated with the thermal load contributed by the new communications and data handling equipment.

5.2.8 Electric Power

The Pioneer F and G basic RTG support structure is retained in the new configuration but with a small modification necessitated by the enlarged propellant tank and by the replacement of the four SNAP-19 RTG units by two "short stack" MHW radioisotope generators. The RTG deployment guide rods are relocated, as shown in Figure 5-1 to clear the 22.25-inch diameter propellant tank. The guide rod support fittings are modified as required by this change and the RTG mounting provisions are changed to fit the new RTG's. However, no increase in the stowed and deployed lateral dimensions of the RTG deployment arm assembly is caused by these modifications.

The externally mounted battery of Pioneer F and G has been eliminated since all peak loads can be readily accommodated by the increased power capacity of the new RTG's. The other components of the electric power subsystem – inverter assemblies, power control unit, CTRF, and external shunt – are shown in Figure 5-2 in locations appropriate to the equipment layout of the new configuration.

5.2.9 Bus-Probe Mounting Interface

Figure 5-3 shows the mechanical interface arrangement between spacecraft bus and probe, and the attachment of the spacecraft/probe interstage to the booster third stage adapter. This layout shows the conical interstage structure to which the probe is attached at three equally spaced recess joints. The drawing also shows the bus/probe umbilical cord attachment to the probe at a fourth connecting point.

At the time of probe separation the ball-lock retention bolts holding the probe attached to the interstage are fired to release the probe which then separates by spring action. The separation springs are arranged

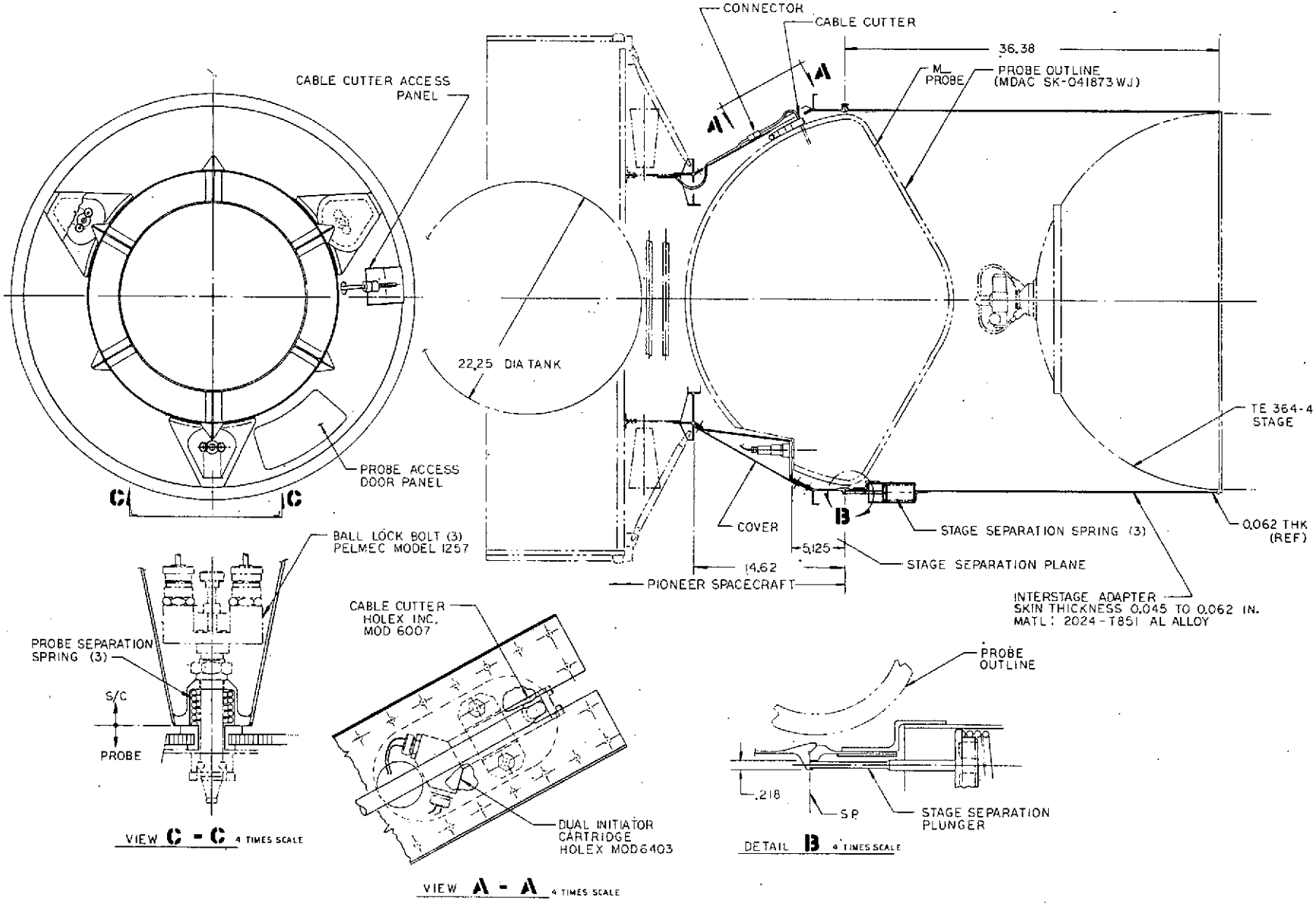

Figure 5-3. Bus/Probe Interface Layout

at the same attach points as the retention bolts. Prior to separation the umbilical connection is severed by an ordnance-actuated cable cutter. This arrangement minimizes tip-off effects.

Additional detail of the bus/probe interstage structure, the separation mechanisms and other mechanical and electrical interface provisions will be presented in Section 6. 1 and in Appendix B.

5. 3 FUNCTIONAL BLOCK DIAGRAM

The functional block diagram shown in Figure 5-4 is similar to that of Pioneer F/G, with the basic electrical design concept essentially unchanged. Required modifications and additions are indicated by cross-hatching.

Principal modifications in individual subsystems are summarized as follows.

The major change in communications and data handling is the adoption of dual-mode S-/X-band telemetry to provide the desired downlink data rates at Saturn and Uranus distance. This design modification has already been adopted for the Outer Planets Pioneer spacecraft*. Addition of the relay communication capability is also indicated in the block diagram.

The digital telemetry unit is changed accordingly, and a high data capacity solid-state data storage system is substituted for the 50 kb core memory of the baseline Pioneer F/G design. This data storage system is used primarily to record entry probe telemetry data for subsequent playback, and as a buffer for bus image system data that are acquired at a rate of 0. 9 Mbps during an exposure of several tenths of a second several times per hour and read out continuously by the telemetry system.

With a different complement of payload instruments, changed observation modes, and the addition of entry probe support functions, the command sequences and command distribution functions must be modified.

*"Outer Planets Pioneer Spacecraft," prepared for NASA/Ames Research Center, under contract NAS2-6859, 23 March 1973.

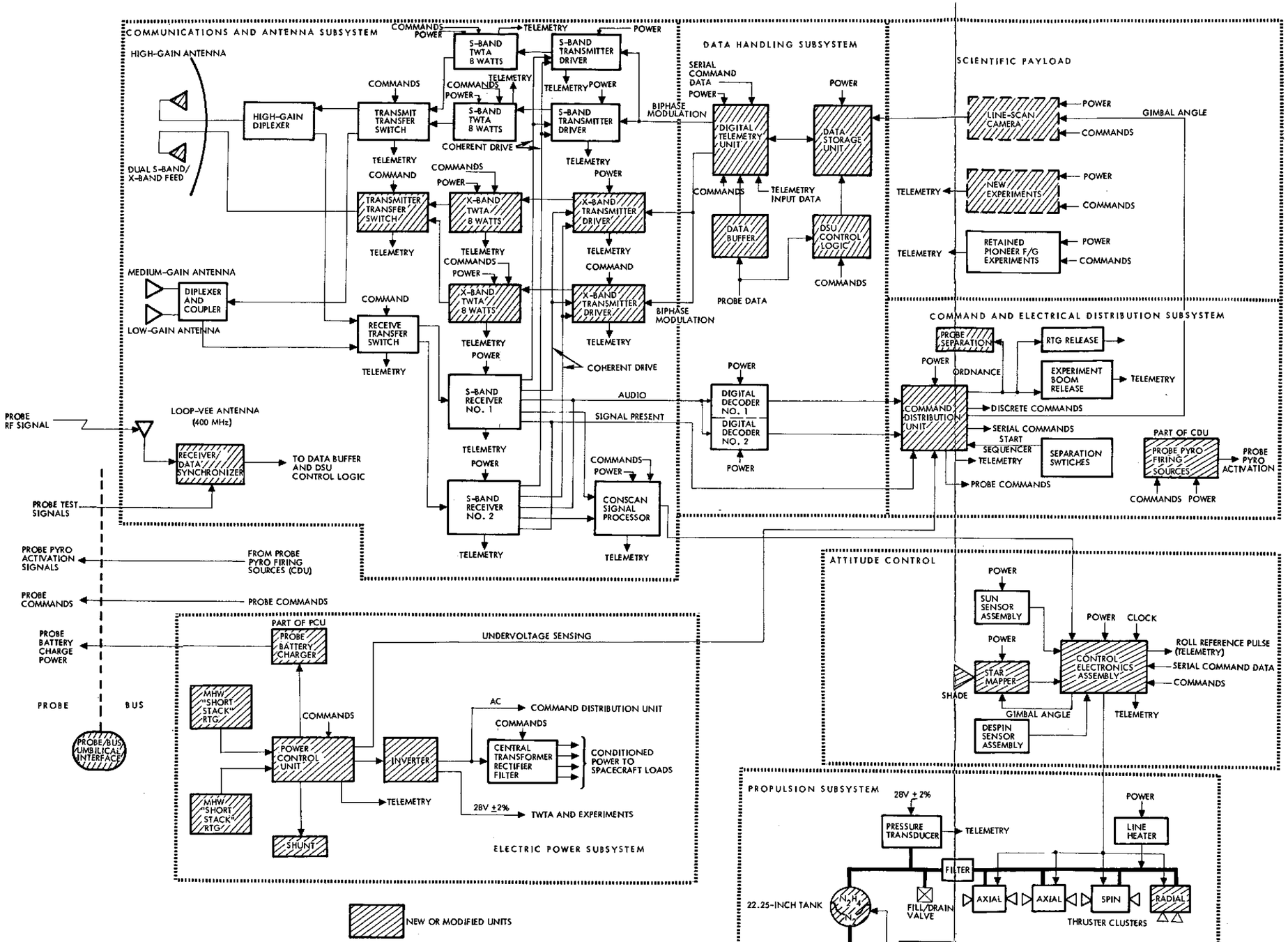

Figure 5-4. Functional Block Diagram

The attitude control system generally uses the same control modes and control sequence logic as the baseline Pioneer F/G system. However, the replacement of the baseline star reference assembly by a gimballed star mapper requires modifications in the control electronics assembly. This sensor must be controlled to provide clock angle reference pulses throughout the mission as well as terminal navigation fixes during the pre-encounter mode. Attitude changes for the first midcourse guidance maneuvers are controlled in the same manner as in Pioneer F/G.

Changes in the electric power subsystem include the replacement of the SNAP-19 RTG's by the higher-powered MHW units. The use of the new RTG's operating at the increased output voltage level of 28 VDC simplifies power processing. Although the requirement for carrying a battery is eliminated in the bus-spacecraft because of the ample power capacity of the new RTG's, the operation of the probe battery must be supported by the power subsystem. This requires the addition of a battery charger.

Modifications of subsystem interfaces occur in several areas of the system as a result of the changes described above. The modifications involve primarily the flow of command signals and telemetry input data. The changes also affect power distribution and control, and modifications in the power subsystem configuration.

Bus/probe interface requirements involving additions to, or modifications of the baseline functional block diagram are indicated at the lower left of Figure 5-4. As discussed above, the electrical interfaces depicted here affect primarily the communications, command and electrical distribution, and the electric power subsystems. Details will be discussed in Section 6 and Appendix B.

5.4 MASS PROPERTIES

Mass properties estimates for the conceptual SUAE spacecraft configuration as described in detail in Section 5.2 are summarized herein. Presented are weight summaries and sequential spacecraft mass properties estimates for various flight conditions.

5.4.1 Weight Summary

The estimated weight of the flight spacecraft above the launch vehicle/spacecraft adapter is 1040.6 pounds including a 28.7 pound contingency allowance. Table 5-1 gives the weight summary of the SUAE spacecraft in comparison with the baseline Pioneer G spacecraft by subsystem groupings and lists individual weight increments. A more detailed weight breakdown is presented in Table 5-2. These weight estimates were obtained by using weight elements of Pioneer F/G as a basis and estimating incremental weight changes due to additions, deletions, and/or modifications of components as a result of the new mission requirements.

The total weight increase is 471.9 pounds. Sources of the various weight increments are listed in Table 5-3.

Of this total, 417.7 pounds are associated with hardware changes and 54.2 pounds are due to additional propellant and pressurant requirements. Of the ~418 pounds increase in the dry spacecraft weight, approximately 273 pounds are due to entry probe related hardware (i.e., 250 pounds for the probe and ~23 pounds for the probe adapter).

The contingency weight allowance is determined by assuming 15 percent contingency on new equipment, 7 percent on modified equipment and 2 percent on existing equipment. Table 5-3a gives a summary of these allowances for the three categories. The contingencies are added to a total of 411.5 pounds of equipment, i.e., the total dry weight less payload instruments, RTG's and entry probe. The resulting allowance, 28.7 pounds, constitutes a conservative estimate.

The total injected weight of 1040.6 pounds, burdened by 3.5 pounds to account for the weight difference between the estimated and the nominal adapter weights (59.5 and 56 pounds, respectively), is 6 pounds below the injected weight target of 1050 pounds assigned for the ESU mission (see Section 3.1).

Table 5-1. SUAE Flight Vehicle Summary

Description	Pioneer G* (Ref.) (lb)	Increment (lb)	SUAE Mission Flight Vehicle (lb)
Electrical power (less RTG's)	39.0	-8.8	30.2
RTG's	120.4	+19.6	140.0**
Communications (bus-earth)	22.5	+15.2	37.7
Communications (probe-bus)	0	+4.2	4.2
Antennas	45.5	+8.0	53.5
Data handling	11.8	+1.6	13.4
Electrical distribution	38.0	+5.1	43.1
Attitude control	12.6	+9.2	21.8
Propulsion (dry)	24.2	+12.5	36.7
Thermal control	16.3	+4.8	21.1
Structure	104.5	+45.3	149.8
Deployment counterweight	0	+23.7	23.7
Balance weights	5.9	+4.1	10.0
Scientific instruments	67.0	-5.5	61.5
Entry probe	0	+250.0	250.0
Weight contingency		+28.7	28.7
Spacecraft (dry)	507.7	+417.7	925.4
Residual propellant and pressurant	1.8	+2.2	4.0
Expendable propellant	59.2	+52.0	111.2
Weight contingency			
Spacecraft gross weight	568.7	+471.9	1040.6
Launch vehicle/spacecraft adapter	30.0	+29.5	59.5
Launch vehicle payload	598.7	+501.4	1100.1

*IOC 8524-73-04, "Pioneer G Mass Properties Based on Final Measurements Prior to Shipment," J. L. Petty to W. F. Sheehan, dated 5 February 1973.

**A revised estimate of 150 pounds for the RTG's was received too late for its effects to be incorporated in Section 5, which is all based on 140 pounds for the RTG's. See Section 7.1.

5.4.2 Estimated Mass Properties

Esimated mass properties for various flight conditions are summarized in Table 5-4. The maximum longitudinal center of mass excursion between beginning-of-life and end-of-life conditions, is 7.8 inches. This is primarily the result of probe separation.

As a prerequisite of long-term spin stability, the roll interia, I_z, should be greater than either of the transverse inertias, I_x and I_y, for all conditions. It should be noted however, that after third stage separation when all the appendages are still stowed the maximum transverse moment of inertia (I_y) is nearly equal to the roll moment of inertia. Dynamic stability implications of this condition will be further discussed in Section 5.5. Due to the mass distribution of the spacecraft bus and the tandem arrangement of the entry probe relative to the bus, the maximum transverse moment of inertia is very sensitive to mass and mass distribution changes. Ideally, the center-of-mass of the spacecraft bus and the probe should be as close together as possible and the spread of the

Table 5-2. SUAE Flight Vehicle Detailed Weight Breakdown

Description	Pioneer G* (lbs)	Increment (lbs)	SUAE Mission Flight Vehicle (lbs)	Comments
Electrical Power	159.4	+10.8	170.2	
RTG's (2)	120.4	+19.6	140.0	New power source using two MHW RTG's.
Power control unit	10.9	-3.6	7.3	(See note, Table 5-1.)
Battery	5.3	-5.3	-	
Inverter assembly	10.2	-5.1	5.1	
Central TRF assembly (2)	11.8	+1.8	13.6	
Shunt regulator assembly	-	+2.2	2.2	
Strip heater assembly (3)	0.8	+1.2	2.0	
Communications	22.5	+19.4	41.9	Added X-band capability from bus to earth and communications from probe to bus
Conscan signal processor	0.8		0.8	
Receivers (2)	10.2		10.2	
TWTA, S-band (2)	8.0		8.0	
TWTA, X-band (2)	-	+12.0	12.0	
Transmitter driver, S-band (2)	2.6		2.6	
Transmitter driver, X-band (2)	-	+2.8	2.8	
Attenuators (2)	0.05		0.05	
Receiver/data synchronizer (probe to bus)	-	+4.2	4.2	
RF cabling and connectors	0.9	+0.4	1.3	
Antennas	45.5	+8.0	53.5	
High-gain antenna assembly	33.4	+0.5	33.9	
Parabolic reflector	(25.5)		(25.5)	
Reflector mount subassembly	(3.7)		(3.7)	
Feed support assembly	(2.9)	(+0.5)	(3.4)	Added X-band feed
Medium-gain antenna	3.7		3.7	
Probe to spacecraft antenna (including supports)	-	+4.2	4.2	New
Low-gain antenna	0.7	-0.4	0.3	Support provided by probe to spacecraft antenna
Diplexer/coupler (2/1)	4.3		4.3	
Switches, S-band (2)	1.3		1.3	
Switch, X-band	-	+2.2	2.2	Added X-band circulator switch
RF cabling and connectors	2.1	+0.2	2.3	Additional coax for probe to spacecraft antenna
Waveguide	-	+1.3	1.3	Waveguide for X-band
Data Handling	11.8	+1.6	13.4	
Digital telemetry unit	6.8		6.8	
Data storage unit (3)	3.3	+0.6	3.9	
Digital decoder unit (2)	1.7		1.7	
Probe data buffer	-	+1.0	1.0	Add item for probe data handling

*IOC 8524-73-04, "Pioneer G Mass Properties Based on Final Measurements Prior to Shipment," J. L. Petty to W. F. Sheehan, dated 5 February 1973.

Table 5-2. SUAE Flight Vehicle Detailed Weight Breakdown (Continued)

Description	Pioneer G* (lbs)	Increment (lbs)	SUAE Mission Flight Vehicle (lbs)	Comments
Electrical Distribution	38.0	+5.1	43.1	
Command distribution unit	8.8	+1.1	9.9	Added circuitry
Cabling and connectors	29.2	+4.0	33.2	Additional cabling to probe and X-band units
Attitude Control	12.6	+9.2	21.8	Changes due to new control scheme and control requirements
Control electronics assembly	5.1	+3.2	8.3	
Stellar reference assembly	2.6	-2.6	-	
SRA light shade	3.4	-3.4	-	
Sun sensor assembly	1.1		1.1	
Star mapper assembly	-	+12.0	12.0	
Despin sensor assembly (2)	0.4		0.4	
Propulsion (Dry)	24.2	+12.5	36.7	
Thruster cluster assembly – Strut mounted (3)	9.0		9.0	
Thruster cluster assembly – Compartment mounted	-	+1.1	1.1	Add item
Propellant tank assembly	8.7	+8.6	17.3	Change to larger capacity tank (~22.25-in. diameter)
Tank support assembly	2.0	+2.8	4.8	Change from strut type to conical frustum
Filter	0.5		0.5	
Temperature transducer	0.2		0.2	
Pressure transducer	0.4		0.4	
Fill and drain valve	0.5		0.5	
Lines, fittings and miscellaneous	1.6		1.6	
Line/heater assembly	1.3		1.3	
Thermal Control	16.3	+4.8	21.1	
Insulation	11.3	+3.2	14.5	Added -X compartment and probe system
Thermal louvers (10)	4.3	-1.2	3.1	Re-evaluation of thermal requirements
RHU and support (sun sensor)	0.6		0.6	
Second surface mirrors	-	+0.9	0.9	Cover louvers
Probe heaters and miscellaneous	0.1	+1.9	2.0	Probe thermal interface requirement
Structure	104.5	+45.3	149.8	
Platform assembly	18.5	+2.3	20.8	Add -X compartment; cut-out under tank assembly
Side panels and interior bulkheads (14)	12.1	+2.7	14.8	Added -X compartment
Cover panels (6)	7.1	+2.0	9.1	Added -X compartment
Frame assembly	8.6	+2.7	11.3	Added -X compartment
Separation assembly	13.9	-1.0	12.9	Modify separation ring to interface with probe adapter
Spacecraft/probe adapter assembly	-	+23.4	23.4	New add item
Thruster support assembly (2)	5.8		5.8	
Magneotometer support assembly	7.6	+7.2	14.8	New
RTG support assembly – fixed items (2)	9.9	+0.8	10.7	Modified to accommodate MHW RTG's
RTG support assembly – deployable (2)	12.5	+2.0	14.5	New RTG support plate design
Wobble damper	1.2		1.2	
Miscellaneous and attach hardware	7.3	+3.2	10.5	Increased due to added compartment, probe adapter, new antenna and larger tankage

*IOC 8524-73-04, "Pioneer G Mass Properties Based on Final Measurements Prior to Shipment," J. L. Petty to W. F. Sheehan, dated 5 February 1973.

Table 5-2. SUAE Flight Vehicle Detailed Weight Breakdown (Continued)

Description	Pioneer G* (lbs)	Increment (lbs)	SUAE Mission Flight Vehicle (lbs)	Comments
Mass Properties Control Weights	5.9	+27.8	33.7	
Deployment counterweights	-	+23.7	23.7	Due to probe/bus mass properties control requirements
Static and dynamic balance weights	5.9	+4.1	10.0	Assumed ~1 percent of total spacecraft weight
Scientific Instruments	67.0	-5.5	61.5	Per statement of work
Magnetometer			5.5	
Solar wind analyzer			6.0	
Charged particle detector			6.0	
IR radiometer			7.5	
IR spectrometer			12.0	
UV photometer			6.0	
Multispectral line-scan camera			14.0	
RF noise detector			1.0	
Micrometeoroid detector			3.5	
Weight contingency allowance		+28.7	28.7	
Entry Probe	-	+250.0	250.0	
• Dry spacecraft	507.7	+417.7	925.4	
Propellant and Pressurant	61.0	+54.2	115.2	
Residual propellant and pressurant	1.8	+2.2	4.0	
Expendable propellant	59.2	+52.0	111.2	
• Spacecraft gross weight	568.7	+471.9	1040.6	
Launch/Vehicle/Spacecraft Adapter	30.0	+29.5	59.5	
• Launch vehicle payload	598.7	+501.4	1100.1	(Including launch vehicle/spacecraft adapter)
			(1044.1)	(Excluding 56 pounds of launch vehicle/ spacecraft adapter weight)

*IOC 8524-73-04, "Pioneer G Mass Properties Based on Final Measurements Prior to Shipment," J. L. Petty to W. F. Sheehan, dated 5 February 1973.

Table 5-3. Weight Increment Sources

Item	Pounds
Modified power system using two MHW RTG's	+10.8
Addition of X-band & probe communications	+27.4
Increased data storage and added probe data buffer	+1.6
Increased electrical distribution cabling due to electronic components changes and addition of probe	+5.1
Attitude referencing and control electronic changes	+9.2
Increased propulsion requirements	+66.7
Added structural and thermal changes (e.g., added -X compartment, added probe adapter, and heavier RTG and magnetometer boom supports)	+50.1
Addition of entry probe	+250.0
Mass properties control weights	+27.8
Decrease in science weight	-5.5
Weight contingency	+28.7
	+471.7

Table 5-3a. Weight Contingency Estimates (Summary)

Type of Equipment	Percent of Total	Estimated Weight (lbs)	Percent Contingency	Contingency Weight (lbs)
Existing	55	223.2	2	4.5
Modified	12	51.5	7	3.6
New	33	136.8	15	20.6
Total	100	411.5	(7% average)	28.7

Table 5-4. SUAE Flight Vehicle Spacecraft Sequential Mass Properties

Condition	Weight (lb)	Center of Gravity (Inches)*			Moment of Inertia (Slug-ft^2)			$\frac{2I_z}{I_x + I_y}$
		$\bar{X}$	$\bar{Y}$	$\bar{Z}$	I_x	I_y	$I_{z\,(roll)}$	
At separation from launch vehicle	1016.7	0	0	22.0	127.9	138.0	139.2	1.05
With RTG's and magnetometer deployed	1016.7	0	0	22.0	386.9	534.1	794.3	1.72
With one-half propellant depleted	960.2	0	0	21.5	385.9	533.1	794.3	1.73
After entry probe separation	710.2	0	0	29.3	343.9	490.8	788.6	1.89
With total propellant depleted	653.8	0	0	29.2	343.9	490.8	788.6	1.89

*Note: 1) $\bar{X}$ and $\bar{Y}$ referenced from the spacecraft centerline.
2) $\bar{Z}$ referenced from the spacecraft/launch vehicle adapter separation plane.
3) X-axis orientation coincident with the deployed magnetometer boom axis.

transverse inertias (I_x and I_y) be minimized. After the appendages (RTG's and magnetometer boom) are deployed, the moment of inertia ratio is substantially greater than 1.0.

In comparison with Pioneer F/G moments of inertia, the SUAE spacecraft moments of inertia are considerably greater. The roll moment of inertia is greater due to the heavier RTG's and due to the added deployment counterweight (~24 pounds) on the magnetometer boom. Likewise, the moments of inertia about the transverse axes are greater due to heavier RTG's and the tandem arrangement of the entry probe. Since the counterweight is deployed along the X-axis, the increased I_x is small, however the increase in I_y is quite pronounced.

5.4.3 Control of the Principal Axes of Inertia

The use of deployment counterweight, to be added near the tip of the magnetometer boom, is dictated by the requirement for maintaining the center of mass on the geometrical centerline of the spacecraft at all times, i.e., during initial spinup; at third-stage separation; during the deployment of appendages; under propellant depletion; and finally, at entry probe separation.

In contrast to the mass center control approach used for Pioneer F/G where a lateral shift of the c.m. was acceptable as long as

the principal spin axis of inertia was maintained parallel to the geometrical centerline (as dictated by antenna pointing requirements) the SUAE spacecraft cannot tolerate a lateral c. m. shift. If such a shift were to occur due to asymmetric appendage deployment, with the probe mass remaining on the centerline, a tilt of the principal axes of inertia could not be avoided.

The approach used in the selected spacecraft configuration is to provide a deployment counterweight such that the deployment of all appendages has no net effect on the c. m. location. This design approach resolves the problem of asymmetrical mass distribution but at the same time introduces not only a significant weight penalty (i. e., 24 pounds of added counterweight) but also a structural load problem for the magnetometer boom that does not occur in the baseline Pioneer F/G configuration. The structural loads of concern are (a) due to launch vibration environment, and (b) due to dynamic loads during magnetometer boom deployment at high-spin rates. These problems and approaches to their solution will be discussed in Section 6.

5.5 DYNAMICS

Spacecraft dynamic characteristics which have a significant effect on system performance are examined in this section. These include:

- Attitude stability and pointing accuracy of the deployed spacecraft
- Deployment dynamics
- Nutation damping
- Wobble due to thrust misalignment
- Probe separation tip-off errors.

Because of the significant change in mass distribution from the original Pioneer F/G design, including some mass increase of the deployed appendages, a new analysis of dynamic characteristics was performed in which the influence of the appendages' structural flexibility had to be taken into account to obtain realistic spin stability criteria.

5.5.1 Attitude Stability and Pointing

The Pioneer F and G scheme of spin stabilization is used to maintain the inertial orientation of the spacecraft's Z axis.

Spin is initially provided by a Centaur-mounted spin table which spins up the spacecraft and third stage to approximately 60 rpm. During the first three minutes after Centaur separation, including 45 seconds of TE-364-4 thrusting and a two minute and 15 second wait period for residual thrusting to decay, the spacecraft is spinning about an axis of minimum moment of inertia. In this configuration, energy dissipation due to propellant sloshing causes nutation to increase. Starting with a nutation angle of 2.5 degrees induced by third stage thrusting this will increase the angle by less than 0.5 degree.

During the interval (23 minutes, Pioneer 11) between third-stage separation and appendage deployment the SUAE spacecraft possesses only marginal spin stability since the three moments of inertia are approximately equal (see Table 5-4). With completion of the RTG and magnetometer deployment the spacecraft attains a stable configuration, and the nutation angle, having increased by several degrees during the interim, begins to decay. The nutation damping time constant is 2 to 3 minutes. Stability characteristics of the undeployed and fully deployed spacecraft/probe configurations have been analyzed in some detail and will be discussed in Section 5.5.4.

In the stability analysis of the combined bus/probe configuration the structural flexibility of the deployed appendages was taken into account since the assumptions involved in the stability of a spinning rigid body as in Pioneer F/G are no longer realistic for the modified spacecraft.

The greatly increased moments of inertia of the center body and the increased tip masses supported by the deployment booms can lead to boom deflections which make the flexible spacecraft less stable than a rigid spacecraft with the same mass distribution. Thus the stability criteria of a rigid body, i.e., the requirement that the spin moment inertia be larger than the two transverse moments of inertia is no longer sufficient to assure stability in the case of a spacecraft with flexible appendages.

Deviations from the dynamic stability of a rigid spacecraft are still greater if, in the limit, the appendages are considered as articulated (hinged) rather than flexible booms.

The analysis was performed parametrically to determine the change of stability boundaries with variations of the following design characteristics:

- Probe mass and location relative to the spacecraft center of mass
- Appendage mass
- Flexural stiffness of magnetometer and RTG booms
- Damping constant of the wobble damper.

Figure 5-5 shows the simplified mathematical model of bus/probe combination with flexible appendages used for purposes of this study. Table 5-5 defines the dimensions, masses and design characteristics used in the analysis and gives their quantitative values. Although these values do not fully reflect the actual design constants of the selected configuration, the results obtained clearly show the trends in stability characteristics that are applicable to this design and can be used to establish available stability margins.

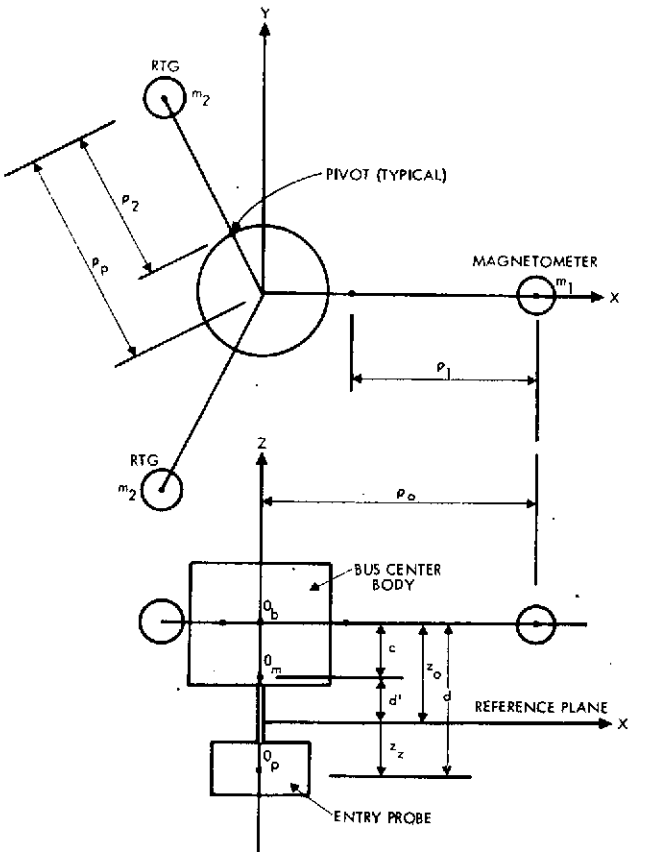

Figure 5-5. Mathematical Model of Spinning Spacecraft with Flexible Appendages and Added Probe Mass

Table 5-5. Nominal Values Assumed in Stability Analysis

Symbol	Description	Value
m_1	Magnetometer weight	29.8 lb
m_2	RTG weight	66.9 lb
m_b	Main body weight (bus only)	438.0 lb
m_p	Probe weight (including associated structure)	300.0 lb
I_x^p	Probe principal moment of inertia about its own c. g.	43052 lb-in.^{2}
I_y^p		44053 lb-in.^{2}
I_z^p		63200 lb-in.^{2}
I_x^b	Main body (without probe) principal moment of inertia about its own c. g.	188000 lb-in.^{2}
I_y^b		261700 lb-in.^{2}
I_z^b		312200 lb-in.^{2}
ρ_o	Distance from Z axis to magnetometer boom c. g.	205.6 inches
ρ_p	Distance from Z axis to RTG tip mass	107.6 inches
ρ_1	Distance from the pivot to magnetometer boom c. g.	166.8 inches
ρ_2	Distance from pivot to RTG tip mass	85.6 inches
S_1	Magnetometer boom damping constant	12 ft-lb-sec/rad
S_2	RTG boom damping constant	(small)
K_1	Spring constant of magnetometer boom	4.0 ft-lb/rad
K_2	Spring constant of RTG boom	548 ft-lb/rad
Ω	Spin rate of the spacecraft	0.503 rad/sec
z_z	Dimensions as indicated in Figure 5-5.	18.1 inches
z_o		18.9 inches
c		15.04 inches
d'		3.86 inches
d		37.0 inches

Influence of Mass and Location of the Entry Probe on Stability Boundary. The addition of a sizable probe mass to the basic Pioneer configuration appreciably alters the stability characteristics. This is shown in Figure 5-6. An increase in the probe mass or in probe distance from the hinge plane of the appendages increases the transverse moment of inertia I_t and ultimately causes the moment-of-inertia ratio I_t/I_s to exceed the stability limit.

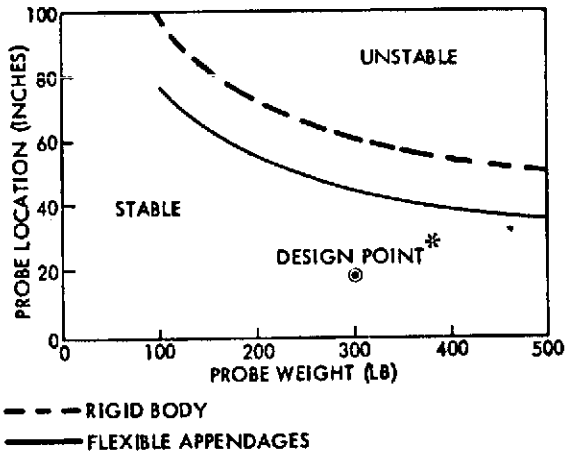

Figure 5-6. Stability Boundary: Probe Location vs Probe Weight

The graph also shows a comparison of the stability boundary for a rigid spacecraft and a body with flexible appendages. The nominal design point* indicated in the diagram is stable for both cases, but the stability margin (expressed in terms of the distance to the location of the boundary for the given probe mass) decreases by about 40 percent (20 inches) for the case of flexible appendages. This comparison demonstrates the importance of using the flexible body rather than the rigid-body dynamics model for stability analysis in this spacecraft design study.

This reduction of the stability margin is quite plausible when one considers the reduced stabilizing effect of the deployed mass on the spinning center body due to the flexibility of its attachment.

Influence of Appendage Mass and Probe Location on Stability Boundary. (Figure 5-7.) The increase in appendage mass enhances the spin inertia (I_s). Consequently, it decreases the I_t/I_s ratio and widens the stability margin. Any increase in appendage mass will thus enhance the spacecraft stability. The stability boundary is plotted in a graph of probe location versus appendage mass, normalized in terms of the design values of the magnetometer boom and RTG boom equivalent end masses, m_1^* and m_2^*.

*This term designates the reference point of the analysis.

Influence of Appendage Stiffness and Probe Location. Any increase in appendage stiffness, in general, enhances the stability boundary. For a relatively stiff appendage (e. g., the RTG), Figure 5-8, the stability boundary can be characterized by a transition zone and a constant zone. Only in the transition zone does the appendage stiffness appreciably influence the location of the stability boundary.

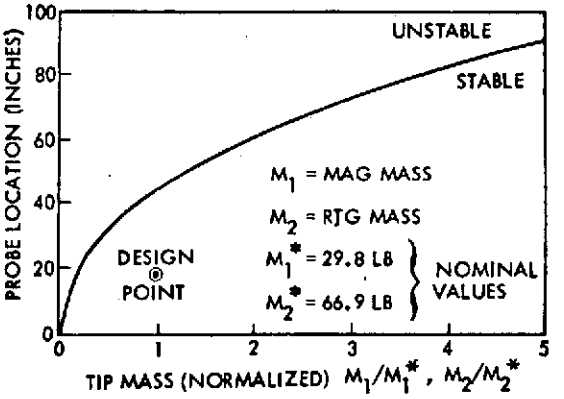

Figure 5-7. Stability Boundary: Probe Location vs Normalized Appendage Mass

For a relatively flexible appendage such as the magnetometer boom, Figure 5-9, the stability boundary gradually reaches a constant value and the effect due to stiffness variation is minimal.

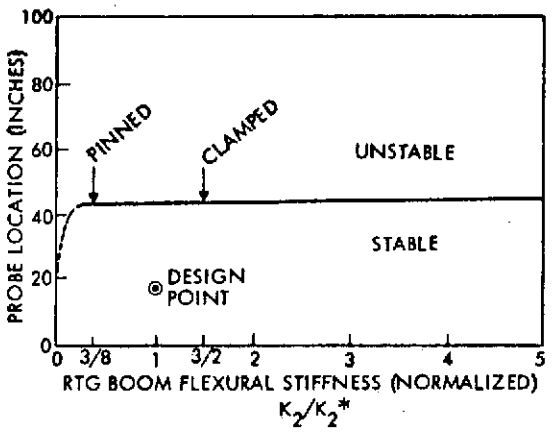

K_2 = RTG BOOM FLEXURAL STIFFNESS

K_2^* = 548 FT-LB/RAD (NOMINAL VALUE)

Figure 5-8. Stability Boundary: Probe Location vs Normalized Flexural Stiffness for Relatively Rigid Appendages

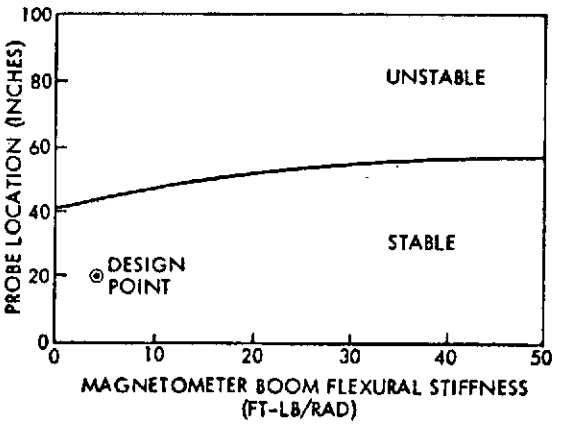

Figure 5-9. Stability Boundary: Probe Location vs Normalized Flexural Stiffness for Relatively Flexible Appendages

Effect of Magnetometer Damping Constant on Nutation Time Constant. The results of the parametric studies demonstrate that damper constant does not alter the stability boundary. However, damping has a strong effect on the nutation decay time constant. Figure 5-10 shows the effect on the damping time constant of changes in the magnetometer damper constant. (The RTG damper constant was set to a small positive value.)

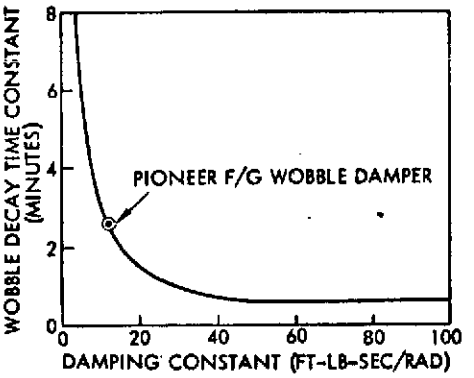

Figure 5-10. Nutation Damping Time Constant vs Damper Constant

In summary the analysis leads to these conclusions:

- The system with flexible appendages has a comfortable stability margin at the given probe location (c. m. 18 inches below Pioneer F/G separation plane) and weight (300 pounds).
- Flexural stiffness variation of the RTG booms has a strong effect on stability in the range of low stiffness. At larger values the system's stability is equivalent to that of a rigid body. Flexural stiffness variation of the magnetometer boom has much less influence on the stability margin. The boom in effect acts as if articulated.
- The increased RTG-mass and magnetometer boom tip mass tends to increase stability margin by about 15 and 65 percent, respectively, compared to a system with the original tip masses.
- An increase in wobble damper constant has no effect on stability margin, but reduces wobble decay time.
- With the probe added the wobble decay time decreases to about 1/3 (2.5 minutes) even without change of wobble damper characteristics.

5.5.2 Spin Axis Misalignment

Alignment of the spin axis with respect to the theoretical centerline is achieved by prelaunch balancing of the stowed, empty spacecraft bus and the bus/probe combination, and by properly locating and aligning the consumables and deployables. The approach for maintaining dynamic balance is based on controlling the combined center of mass of the

deployable appendages such that it remains on the geometrical centerline of the bus/probe combination after deployment. This approach differs from Pioneer F/G where a lateral displacement of the combined c. m. of the deployable arms was permissible. As mentioned before, the required c. m. control of appendages is achieved by adding a deployment counterweight (or weights) near the tip of the magnetometer boom.

Estimates of the sources of principal axis (spin axis) misalignment are listed in Table 5-6, based on data obtained for the Pioneer Outer Planets Spacecraft. Combination of these effects yields an expected (RSS) value of the product of inertia, I_{xz} = 2820 lb-in.^{2} (= 0.61 slug-ft^2).

Table 5-6. Major Sources of Spin Misalignment (X-Z plane product of inertia with full propellant tank and appendages deployed: worst case spin axis misalignment)

Spin Misalignment Source	Product of Inertia (lb-in.^{2})
Balance machine sensitivity	125
0.01 degree misalignment of spacecraft on balance machine	135
Magnetometer boom deployment	2040
0.10 inch vertical c.g. location uncertainty of hydrazine	126
0.22 inch vertical c.g. location uncertainty of RTG's	1940
RSS Total	2820

The values in Table 5-6, and hence the estimated value of I_{xz}, apply to both configurations of the spacecraft, with the probe on or off. This derives from the fact that a change of center of mass along the centerline due to probe separation does not change the product of inertia under conditions that apply here. The relation between the corresponding products of inertia (I_{xz} and I'_{xz}) is given by

$$I'_{xz} = I_{xz} + x_o z_o m$$

where

x_o = lateral offset of the combined c. m. of the deployed masses,

z_o = change of the total spacecraft c. m. along the centerline.

The misalignment sources listed in Table 5-6 only cause a negligible lateral offset x_o, hence the products of inertia remain essentially unchanged.

The spin axis misalignment is determined by

$$\epsilon = 57.3\, I_{xz}/(I_z - I_x)$$

Using the above value of I_{xz} and the moment of inertia difference $I_z - I_x$ (407 slug ft^2 with the probe on, 445 slug ft^2 with the probe off, see Table 5-4) the expected spin axis misalignment is about 0. 07 degree in both configurations. This is well within the tolerance of 0. 15 degree allowed for Pioneer F/G.

5. 5. 3 Nutation Effects due to Injection and Spacecraft Separation

Accuracy of third stage injection is dependent upon mass properties of the combined third stage/spacecraft vehicle, thrust vector misalignment with respect to the vehicle c. m., and spin rate. For the purpose of this analysis it is assumed that the initial spin rate is the same as in Pioneer F/G (60 rpm) and that the mass properties of the combined third-stage/ spacecraft configuration are consistent with spin stability during injection, as in Pioneer F/G.

Computer simulations of injection, in which it is conservatively assumed that a constant, body-fixed, transverse torque of 14, 900 pounds x 0. 10 inch = 1, 490 inch-pounds acts throughout the entire third-stage thrusting duration, indicate that the induced errors will not exceed the following values:

- Angular dispersion of velocity vector = 0. 48 degree
- Reduction in magnitude of velocity vector = negligible
- Nutation angle (from thrust misalignment only) = 2. 5 degrees.

Correction of the velocity vector misalignment is well within the mid-course maneuver capability of the spacecraft.

Following separation of the spacecraft from the third stage, the resultant nutation angle is:

$$\nu = \nu_0 \times \frac{A_2 C_1}{A_1 C_2}$$

where C_1 and A_1 are the spin and transverse moments of inertia of the combined third-stage/spacecraft vehicle and C_2 and A_2 are the spin and transverse moments of inertia of the separated spacecraft. ν_0 and ν are the nutation angles prior to and following separation, respectively. For the SUAE Pioneer configuration, the estimated 3.0 degree wobble angle prior to separation would decrease to 1.8 degrees according to the above equation. Due to tipoff error the angle will actually be somewhat larger.

5.5.4 Despin Maneuver Stability Characteristics

The spinning flight spacecraft is very sensitive to perturbations after separation from the launch vehicle and before the appendages are deployed, since the transverse moment of inertia I_y is almost equal to the roll moment of inertia, I_z (see Table 5-4).

This condition can introduce a significant stability problem during the despin maneuver, since operation of the despin thruster with its line of force offset by 19 inches fr m the center of mass causes a 23-in.-lb precession torque around the pacecraft Y-axis. Due to this precession torque and the unfavorable moment-of-inertia ratios a large wobble angle can build up during the 130 to 140 second time interval required to reduce the spin rate from 60 to 15 rpm prior to appendage deployment.

Analysis of the wobble build-up under various initial conditions shows that prohibitively large wobble angles can occur during this interval. The maximum wobble angle is highly sensitive to the time phasing at the initiation of the despin maneuver. This is illustrated by the conditions listed in Table 5-6a.

Table 5-6a. Effect of Initial Conditions on Final Wobble Angle Due to Despin Precession Torque

Spin Rate Component at Time of Despin Maneuver Initiation (rad/sec) $\omega_x(o)$	$\omega_y(o)$	Maximum Wobble Angle at End of Despin Maneuver (Degrees)
0	0	11.3
0	-0.44	27.0
0	+0.44	9.0
+0.44	0	>34.0
-0.44	0	>34.0

The initial value of 0.44 rad/sec assumed for the ω_x and ω_y components in these examples corresponds to an initial nutation angle of 4 degrees.

Several approaches have been investigated to limit the wobble build-up and thus avoid structural and dynamic problems at the initiation of the subsequent appendage deployment. These include:

1) Control of despin initiation timing such that the component $\omega_x(o)$ is nearly zero at the start of the maneuver, and the $\omega_y(o)$ component is positive.

2) Retention of the expended third stage until completion of the despin maneuver and appendage deployment. The more favorable moment-of-inertia ratios of this configuration reduce the wobble build-up in spite of the larger precession torque by the despin thruster (moment arm = 29 inches).

3) Compensation of the perturbing precession torque contributed by the despin thruster through simultaneous operation of the radial thrusters which exert a precession torque in opposite direction around the Y-axis. The radial thrusters would be operating continuously during the despin maneuver.

The first alternative requires complex time-phasing of the despin maneuver and probably is only marginally effective if the initial nutation angle is large.

Preliminary analysis of the second alternative yields the following results. The moments of inertia of the combined flight spacecraft and burned-out third stage are approximately:

$$I_x = 235 \text{ slug ft}^2$$
$$I_y = 245 \text{ slug ft}^2$$
$$I_z = 151 \text{ slug ft}^2$$

With this mass distribution the configuration is dynamically stable, and the wobble build-up from an initial value of 4 degrees is limited to about 16 degrees, practically independent of maneuver initiation timing. To avoid major tipoff effects after despin, with the flight spacecraft still in the marginally stable configuration it is proposed to perform the deployment of appendages before separation from the third stage. This would require a change from the nominal Pioneer 10/11 separation sequence and would cause intensive radiative heating of the entry probe insulation blanket by the hot TE-364-4 motor case after burnout. To protect the insulation blanket it will probably be necessary to install a heat shield at the upper end of the third stage/flight spacecraft adapter.

The third alternative, namely compensation of the despin precession effect by means of the offset radial thrusters appears to be the simplest and most effective approach. The two radial thrusters, having a moment arm of 7.9 inches produce a precession torque of 19 inch pounds, in opposite direction and nearly equal to the despin thruster precession torque. Effective compensation can be provided if the two torques are made equal by increasing the radial thruster force 20 percent. A change of the nominal thrust force by 10 to 20 percent requires only a relatively minor adjustment effected in thruster manufacture.

One aspect of this technique is the expenditure of about 1.5 pounds of additional hydrazine for 130 seconds of continuous radial thrusting and an unbalanced lateral ΔV increment of about 0.1 m/sec in a direction that depends on start and cut-off timing of the maneuver. Neither of these side-effects are considered significant.

5.5.5 Deployment Dynamics

The potentially larger nutation angles that can develop during the despin and deployment phases and the increased end masses supported by the deployment arms in the case of the Pioneer SUAE spacecraft combine to impose substantially larger structural loads on these arms under worst case conditions than in the case of Pioneer F and G.

A preliminary analysis was conducted (a) to assess requirements for structural reinforcement of the deployment booms and (b) to define alternatives to the sequential deployment technique of Pioneer F and G (where the RTG booms were deployed before the magnetometer boom) to reduce the dynamic loads.

The four deployment concepts analyzed in this study are compared in Table 5-7. The first is the concept used on Pioneer F and G. It is the simplest, but also the least satisfactory, under the dynamic characteristics of the Pioneer SUAE spacecraft configuration.

Table 5-7. Balanced Boom System Deployment Schemes

MODEL	MODE OF OPERATION	ADVANTAGES/DISADVANTAGES
1. SEQUENTIAL	PRESENT PIONEER F/G SCHEME. RTG'S FIRST, THEN MAGNETOMETER BOOM.	LEAST COMPLEX. PERMITS CONSIDERABLE PRINCIPAL AXIS SHIFT AND WOBBLE BUILDUP.
2. SIMULTANEOUS	ALL BOOMS RELEASED SIMULTANEOUSLY.	REDUCED WOBBLE BUILDUP BUT MORE COMPLEX IMPLEMENTATION.
3. "TUNED" SIMULTANEOUS	ALL BOOMS RELEASED SIMULTANEOUSLY; LOCK-UP ACHIEVED AT SAME TIME.	REQUIRES MATCHED DAMPERS
4. SYNCHRONOUS	DEPLOYMENT CONTROLLED TO MAINTAIN PRINCIPAL AXIS PARALLEL TO Z-AXIS CONTINUOUSLY.	BEST CONTROL OF WOBBLE, BUT MOST COMPLEX IN IMPLEMENTATION.

The fourth concept which may require feedback or other complex techniques of implementation, such as operation from a common deployment damper mechanism, obviously would be most effective in eliminating lateral excursions of the center of mass during deployment, and thus would minimize wobble buildup.

The second and third concepts actually involve open-loop control, based on the assumption that simultaneous release of all deployment arms leads to nearly simultaneous deployment. Model 3 ("tuned" simultaneous deployment) is an idealized system calling for damper matching with a precision which cannot actually be realized in practice. It was included among the four analytical models studied to indicate the best performance of Model 2.

Results of this preliminary analysis are briefly summarized here. Simultaneous deployment was found to lead to acceptable control of deployment-induced wobble and bending moments at the root of the deployment booms. Figure 5-11 shows an example of wobble angle time history, comparing simultaneous and "tuned" simultaneous deployment.

Even with highly conservative assumptions on magnitude of initial wobble angles and angular rates the simultaneous deployment concept holds excursion amplitudes to less than 30 degrees. "Tuned" simultaneous deployment does not appear to be much superior to the simpler "untuned" case, even under the assumption that RTG deployment is completed twice as fast as the magnetometer boom deployment.

Figure 5-12 shows corresponding transverse root bending moments introduced by wobble for the case of "untuned" simultaneous deployment, with RTG deployment completed twice as fast as magnetometer boom deployment. These moments also remain in an acceptable range.

From these data it appears that the concept of (untuned) simultaneous deployment is s suitable candidate for use in the Pioneer SUAE spacecraft. However, the significantly increased nutation during deployment will enter into the structural requirements of the modified magnetometer boom (see also Section 6. 1).

5. 5. 6 Nutation due to ΔV and Precession Maneuvers

Pointing and spin rate errors will occur as a result of maneuvers performed by the axial and radial thrusters. Precession maneuvers executed by the axial thrusters, as well as the unintended precession effects resulting from misalignment torques of the radial thrusters, are associated with a buildup of nutation angles. Although this nutation will

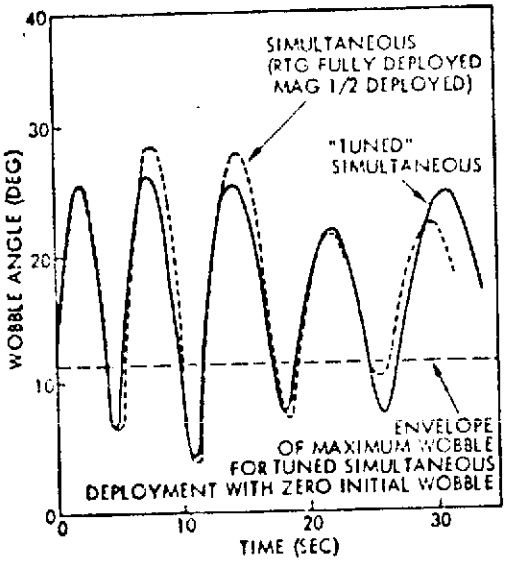

Figure 5-11. Wobble Time History of Simultaneous vs "Tuned" Simultaneous Deployment

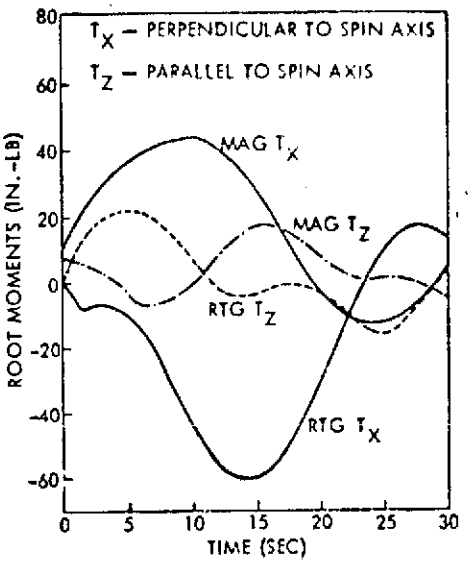

Figure 5-12. Transverse Root Moments vs Time for Magnetometer and RTG Booms (Simultaneous Deployment)

ultimately decay due to wobble damper and other effects, such as propellant sloshing, the peak amplitudes occurring during extended maneuvers are of concern.

Spin rate errors also accrue during these maneuvers due to unavoidable misalignments of the axial and the radial thrusters.

Results of a preliminary analysis of these effects are summarized in the following paragraphs. This analysis was based on a dynamic model of a spacecraft with rigid appendages. Further study is required to determine if structural flexibility would significantly affect these results.

The moment-of-inertia ratios of the spacecraft in the deployed state with probe attached (as per Table 5-4) are:

$$\xi = \frac{I_x}{I_z} = 0.488 \qquad \eta = \frac{I_y}{I_z} = 0.672$$

These ratios affect certain dynamics characteristics of the spacecraft in a manner which may differ slightly from Pioneer F/G behavior.

The nutation frequency (in body coordinates) is K times the spin rate, where K is given by

$$K = \left[\frac{I_z - I_y}{I_x} \cdot \frac{I_z - I_x}{I_y}\right]^{1/2} = \left[\frac{1-\eta}{\xi} \cdot \frac{1-\xi}{\eta}\right]^{1/2} = 0.717$$

This compares with K = 0.86 for Pioneer F/G. The decrease reflects primarily the addition of the entry probe to the basic bus configuration.

After probe separation the corresponding values are $\xi = 0.435$, $\eta = 0.621$ and K = 0.903. The increase in K compared to Pioneer F/G reflects primarily the heavier RTG's and the added deployment counterweight. In this configuration the mass properties are almost identical to those of the Pioneer Outer Planets Spacecraft, (K = 0.91), and the results discussed in the report on that spacecraft are representative of the SUAE bus dynamics.

In pulsed precession maneuvers, nutation can build up to a factor of $|\csc(nK\pi)|$ times the precession step size, where n is the number of spin revolutions between precession pulses. For programmed open-loop precession maneuvers, a pulse is fired every revolution, so with n = 1 the factor is decreased from 2.5 to 1.3 compared to Pioneer F/G when K is reduced from 0.86 to 0.717 (bus plus probe). The factor is increased to 3.3 when K is raised to 0.903 (bus only).

On the other hand, the precession step size is reduced to a factor of 0.55 times its value in Pioneer F/G, because the same thrusters are used but the spin moment of inertia has been increased. Thus the maximum nutation amplitude during such a maneuver is decreased as shown in Table 5-8.

Table 5-8. Nutation Build-up in Precession Maneuver

	Pioneer 10	Outer Planets Pioneer	SUAE Spacecraft	
			Probe On	Probe Off
Coefficient K	0.86	0.91	0.717	0.903
Precession step size (0.125-second pulses)				
Full tank	0.31°	0.17°	0.17°	0.17°
Empty tank	0.12°	0.06°	0.06°	0.06°
Nutation buildup factor	2.5	3.6	1.3	3.3
Maximum nutation				
Full tank	0.78°	0.61°	0.22°	0.56°
Empty tank	0.30°	0.22°	0.09°	0.20°

The table shows a clear trend to smaller nutation amplitudes both in the bus/probe and bus-only configuration, compared to Pioneer F/G. The characteristics of the bus-only configuration are nearly identical to the Outer Planets Pioneer.

Considering the bus/probe combination, for the closed-loop earth-pointing precession maneuver controlled by the conscan signal processor, n = 3, and the factor $|\csc(nK\pi)|$ increases from 1.06 to 2.2. Again, the precession ste e is reduced by a factor of 0.54, so the net effect is to decrease the n num wobble amplitude to 0.48 times its value in Pioneer F/G.

Nutation effects also accompany radial thruster operation when the thrust vector is offset from the c.m. along the Z axis. This is the case in the selected spacecraft configuration with the probe onboard. (Thrust offset in the bus-only configuration is negligible.) These nutation effects are practically of the same magnitude as those produced by the precession thrusters since the incremental impulse is 14 lb-sec-in. for two radial thrusters at 7-inch offset, operating for 1 second, while the incremental impulse for the pair of precession thrusters is 2 x 1 lbf x 0.125 sec x 50 inches = 12.5 lb-sec-in. Thus no additional discussion of this case is necessary.

Nutation buildup may also be of concern during a longitudinal ΔV maneuver, due to possible offset of the resultant axial thrust from the center of mass. Actually, several effects occur together in such a maneuver:

a) The angular momentum vector is displaced from its initial orientation. The amount of this displacement at the termination of thrusting becomes the residual pointing error, after nutation is damped out. The form of this displacement is circular coning at one cycle per revolution, always returning to the initial orientation. The maximum displacement is twice the average displacement.

b) The average pointing error during a long thrusting time is the directional error in the executed ΔV, measured from the initial spin axis orientation.

c) The spacecraft principal axis nutates around the angular momentum vector. Its displacement from the initial orientation represents the pointing error at any particular time during the maneuver. Its displacement from the angular momentum vector at the termination of thrusting becomes the residual nutation amplitude.

Each of the above terms is proportional to the term

$$\tau = M/I_z \omega_s^2$$

where τ is dimensionless, and represents angles in radians if compatible units are used,

M is the disturbing body-fixed, precessing moment
I_z is the spin moment of inertia, and
ω_s is the spin rate.

The constants of proportionality depend on the moment-of-inertia ratios, ξ and η, and on the direction of M relative to body X and Y axes. They approach ∞ as either $\xi \rightarrow 1$ or $\eta \rightarrow 1$.

Not only are the above nutation amplitudes built up by pulsed precession maneuvers or ΔV maneuvers less than in Pioneer F/G, but the lower nutation damping times indicated in Section 5.5.1 insure that their effects will be of shorter duration.

Table 5-9 summarizes the dynamics effects arising from these various inertia parameters. While these parameters are important in the design of the spacecraft, their variation from those characterizing Pioneer F/G does not adversely affect the dynamic behavior of the Pioneer SUAE spacecraft.

Analysis of spin rate changes due to thrust misalignment torques shows that for the small thrust level used in this spacecraft these changes do not exceed 0.02 rpm and therefore present no problem.

5.5.7 Effect of Pointing Errors on Optical Sensor Pointing Accuracy

The question of optical sensor pointing accuracy arises in two areas:

1) Accuracy of navigational fixes by the star mapper
2) Perturbations of spacecraft attitude due to rotation of the optical sensor package.

Table 5-9. Impact of Mass Properties on Spacecraft Design

Parameter	Effect
Center-of-mass location and control	• Launch vehicle interface requirement (avoid degrading injection accuracy) • Thrusting moments • Retain pointing control - Antenna on axis - Knowledge of instrument pointing
Products of inertia	• Main principal axis (spin) parallel to longitudinal axis
Moments of inertia - magnitude	• Precession and spin control propellant requirements
Inertia ratio I_x/I_y	• Introduction of second wobble frequency
Inertia ratios $\frac{I_y}{I_z}, \frac{I_x}{I_z}$	• Stability - Short term - Long term • Nutation buildup - Pulsed precession - ΔV thrusting

The first problem involves holding the observational errors due to residual wobble to a level of less than 0.1 mrad. This can be met by allowing the spacecraft to settle into a steady-state with negligible wobble errors after each attitude perturbation. Residual pointing errors present no problem since they have no influence on the accuracy of the navigational observation; navigational fixes can be obtained after spacecraft orientation is determined with high accuracy from an interpretation of star reference angles.

The second problem involves the effect of angular momentum exchange during large rotations of the gimballed star sensor. (Rotation of the image system mirror package has a much smaller effect by comparison, owing to its smaller moment of inertia). Assuming a moment

of inertia of 100 lb-in.^{2} for the gimballed navigation sensor, including its light shade, the effect of a 60 degree change in sensor cone angle would be a 0.06 milliradian (12 arc sec) precession of the spacecraft spin axis. This is about the level of desired sensor resolution, i.e., 0.1 milliradian. The maximum excursion, including nutation would be 0.12 milliradian. The effect is of little concern since the navigation sensor would rarely be deflected by angles as large as 60 degrees at a time immediately preceding navigational measurements.

5.5.8 Probe Separation Tipoff Errors

An initial requirement, suggested by the probe study contractor, involves three parameters of the separation of the probe from the spacecraft:

- Separation velocity (ΔV) = 0.5±0.05 meters/sec
- Tipoff angle ($\delta\theta$) ≤ 0.2 degree
- Tipoff angular rate ($\dot{\theta}_t$) ≤ 0.3 deg/sec

The separation velocity can be arbitrarily chosen between zero and several meters/sec as far as mission requirements are concerned, although the uncertainty in separation velocity can affect entry geometry errors if it is great enough. (One m/sec uncertainty along the earthline would propagate as follows: from 30 days before Saturn arrival, about 3 minutes in entry time and 1,600 km in B-plane target uncertainty; from 20 days before Uranus arrival, about 2 minutes in entry time and 300 km in B-plane target uncertainty.)

The tipoff angle error will contribute to the uncertainty in the probe angle of attack at entry, but values up to 5 degrees would probably not be an adverse contribution. Related to the tipoff error, and resulting from the same separation dynamic transients is the probe's rigid-body nutation, which will be reduced by damping internal to the probe, for example structural damping or battery electrolyte fluid damping, before the probe enters the planetary atmosphere. This residual nutation, if any, would then be expected to damp out in the supersonic portion of atmospheric entry, and not be a factor in any subsequent probe motion.

Thus it appears that there is considerable margin between the initial requirements and levels which would significantly affect the mission, and this margin was confirmed by conversations with probe study contractor personnel.

For various reasons concerning the design of both the probe and the bus, the preferred separation approach has the separation springs at the three peripherally located tiedown/release points. In this approach, sketched in Figure 5-13(a), the primary cause of tipoff arises from the mismatch of the separation springs. If each spring provides a nominal impulse of (Ft) at separation, with a 3-σ uncertainty of δ (Ft), then the 3-σ offset of the resultant impulse from its nominal axial location in either the x or y direction is ϵ, where

$$\epsilon = \frac{R}{\sqrt{6}} \frac{\delta(Ft)}{(Ft)},$$

and R is 14.5 inches, the radius to the release point. Thus offset and spring impulse mismatch correspond as follows:

Offset of Resultant ϵ (Inch)	Spring Impulse Mismatch δ(Ft)/(Ft) (Percent)
0.01	0.17
0.1	1.7
1.0	17.0

For the seven-year period in the compressed state from launch to separation at Uranus, 3-σ impulse mismatch of five percent will be reasonable, but it will be difficult to expect better performance. Therefore, proposed performance is based on ϵ = 0.3 inch.

The tipoff angle is related to the linear separation velocity increment, as both are caused by the total impulse due to the three springs, 3(Ft) acting on the probe:

$$\Delta V = \frac{3(Ft)}{M} \tag{1}$$

$$\delta\theta = \frac{3(Ft)\epsilon}{I_s \omega_s} \tag{2}$$

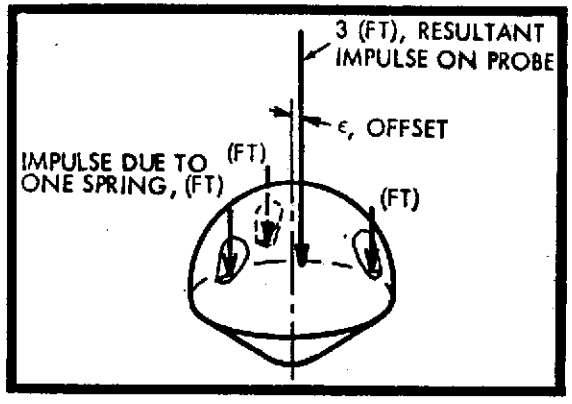

Figure 5-13(a). Resultant Impulse on Probe

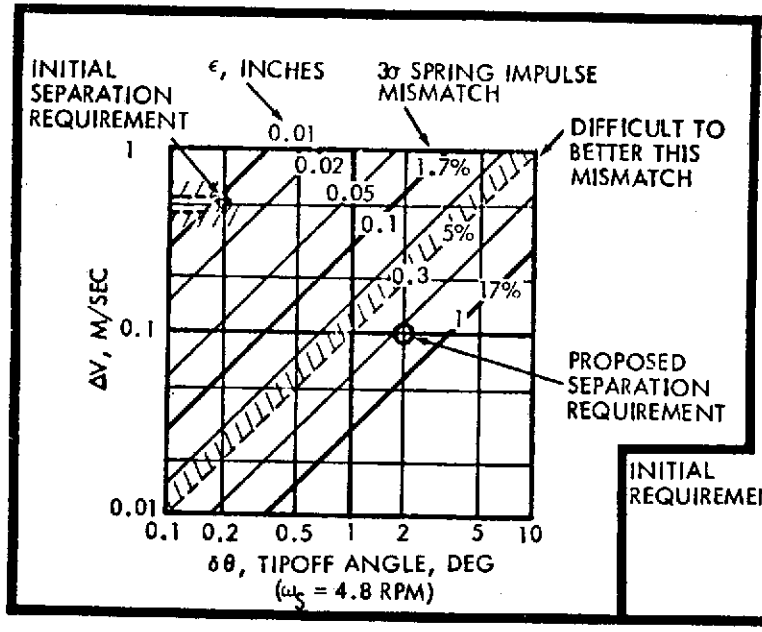

Figure 5-13(b). Probe ΔV, Tipoff Angle and Impulse Offset ϵ

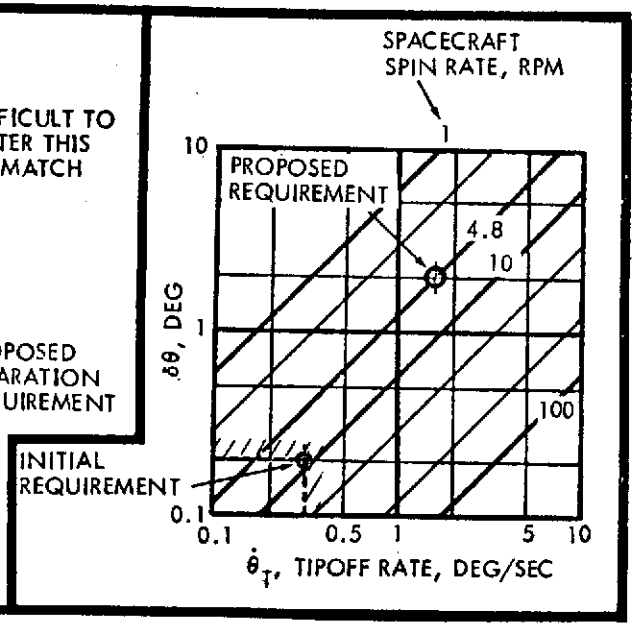

Figure 5-13(c). Tipoff Rate and Tipoff Angle

$$\Delta V = \frac{I_s \omega_s}{M} \frac{\delta\theta}{\epsilon} \qquad (3)$$

Here

M = probe mass (113.4 kg)

ΔV = velocity increment of probe upon separation

$\delta\theta$ = tipoff angle (rotation of probe angular momentum vector)

I_s = probe spin moment of inertia (9.56 kg-m^2)

ω_s = spin rate (4.8 rpm)

Figure 5-13(b) illustrates Equation 3 for the values of M, I_s, and ω_s given above. It can be seen that the initial separation requirement would have required a 3-σ offset, ϵ, no greater than 0.012 inch (0.2 percent spring impulse mismatch). To relate the tipoff angle to the proposed performance (ϵ = 0.3 inch) it is necessary to reduce ΔV, raise ω_s, raise $\delta\theta$, or effect some combination of these.

Probe study contractor personnel wish to retain the 4.8 rpm spin rate, but will accept reduced ΔV and increased $\delta\theta$. Figure 5-13(b) indicates the proposed separation requirement of $\delta\theta \leq 2$ degree at ΔV = 0.1 m/sec. This would tolerate separation spring impulse mismatch about 80 percent greater than the proposed five percent performance.

The tipoff rate $\dot{\theta}_t$ is related to the spin rate and the tipoff angle by a kinematic relation:

$$\delta\theta = \frac{I_t \dot{\theta}_t}{I_s \omega_s} \qquad (4)$$

where

$\dot{\theta}_t$ = component of angular velocity about transverse axis

I_t = probe moment of inertia about transverse axis (6.16 kg m^2)

I_t is assumed the same about transverse axis. Figure 5-13(c) illustrates Equation 4, with I_s as previously stated, and $\delta\theta$, $\dot{\theta}_t$, and ω_s variable.

The initially suggested requirement is indicated, as well as the presently proposed requirement. For the probe inertia ratios, the proposed 2-degree tipoff angle and 4.8-rpm spin rate lead to a tipoff rate of 1.6 degree/second.

In summary, the proposed separation requirements are:

- Separation velocity (ΔV) = 0.1 m/sec
- Tipoff angle ($\delta\theta$) $\leq$ 2.0 degrees
- Tipoff rate (θ_t) $\leq$ 1.6 degrees.

There is no concern over the uncertainty in ΔV. These requirements can be met with comfortable margin with three separation springs having a 3-σ spring impulse mismatch of five percent.

5.6 ELECTRICAL POWER REQUIREMENTS

The electrical power requirements of the Pioneer Saturn Uranus spacecraft bus are listed in Table 5-10 for conditions on the launch stand, during early cruise and during the encounter phase, before and after probe separation. Power requirements that can be met with only one of the two RTG's operating during the encounter phase are listed separately (columns 3 and 5), indicating the minimum system capability available under partial power failure. For convenient reference the nominal power requirements of Pioneer F/G during Jupiter encounter are also listed in the table.

Principal items of increased power requirements in the Saturn Uranus spacecraft include:

- Addition of the X-band transmitter
- Increased experiment power
- Increased digital data storage
- Substitution of a gimballed star mapper for the stellar reference assembly of Pioneer F/G
- Probe battery charging requirement and probe adapter thermal control.

Inverter losses are lower than in the case of Pioneer F/G since the main 28-volt power bus, operating directly from the MHW RTG's provides primary power to subsystems and science experiments without conversion penalties, as will be discussed in Section 6.5.

Table 5-10. Power Requirements

LOAD	LAUNCH		ENCOUNTER			PIONEER F/G
	ON-STAND	EARLY CRUISE	PRIOR TO PROBE SEPARATION		AFTER PROBE SEPARATION	
			1 RTG	2 RTG'S	1 RTG	
SECONDARY DC POWER						
COMMUNICATIONS						
RECEIVERS (2)	3.4	3.4	3.4	3.4	3.4	3.4
DRIVER, S-BAND	-	1.3	1.3	1.3	1.3	1.3
DRIVER, X-BAND	-	2.5	-	2.5	-	-
CONSCAN SIGNAL PROCESSOR	-	1.2	-	1.2	-	1.2
ATTITUDE CONTROL						
CONTROL ELECTRONICS ASSEMBLY	3.2	3.2	3.2	3.2	3.2	2.7
SUN SENSOR ASSEMBLY	0.2	0.2	-	0.2	-	0.2
STAR MAPPER ASSEMBLY	-	5.0	5.0	5.0	5.0	0.3 (i)
COMMAND						
COMMAND DISTRIBUTION UNIT	3.6	3.6	3.6	3.6	3.6	3.1
DIGITAL DECODER UNIT	1.3	1.3	1.3	1.3	1.3	1.3
DATA HANDLING						
DIGITAL TELEMETRY UNIT	4.2	4.2	4.2	4.2	4.2	3.7
DIGITAL STORAGE UNIT	-	-	-	5.0	5.0	0.6
SUBTOTAL (CTRF OUTPUT)	15.7	25.9	22.0	30.9	27.0	17.8
SECONDARY AC POWER						
CTRF LOSSES (66% EFFICIENCY)	8.1	13.3	10.7	15.9	13.9	10.6
SUBTOTAL (INVERTER OUTPUT)	23.8	39.2	32.7	46.8	40.9	28.4
PRIMARY DC POWER						
COMMUNICATIONS						
TWTA, S-BAND (8W)	-	27.8	27.8	27.8	27.8	27.8
TWTA, X-BAND (10W)	-	-	-	36.0	-	-
ATTITUDE CONTROL						
CONTROL ELECTRONICS ASSEMBLY	-	0.4	0.4	0.4	0.4	0.4
COMMAND						
COMMAND DISTRIBUTION UNIT	0.2	0.2	0.2	0.2	0.2	0.2
PROPULSION						
TRANSDUCERS	0.4	0.4	-	0.4	-	0.2
PROPULSION HEATERS	-	8.0	8.0	8.0	-	2.0
ELECTRIC POWER						
POWER CONTROL UNIT	3.0	3.0	3.0	3.0	3.0	7.7
INVERTER LOSSES (85% EFFICIENCY)	3.6	5.9	5.0	7.0	6.1	13.3
EXPERIMENTS						
EXPERIMENTS	-		7.3	30.0	1.0	24.0
PROBE						
HEATERS	-	4.0	4.0	4.0	-	-
DATA LINK	-	-	-	-	10.0	-
BATTERY CHARGING	-	-	(a)	(b)	-	-
SUBTOTAL (28 VDC LOADS)	31.0	88.9	89.4	163.6	89.4	
CABLE LOSSES (SPACECRAFT)	-	0.1	0.1	0.2	0.1	0.6
SUBTOTAL (PRIMARY BUS OUTPUT)	31.0	89.0	89.5	163.8	89.5	104.4
RTG POWER						
RTG CABLE LOSSES	1.0	1.0	0.5	1.0	0.5	4 2
SHUNT REGULATOR (2)	47.0	4.0 (d)	4.0 (d)	4.0 (d)	4.0 (d)	0
SHUNT RADIATOR (2)	46.0	171.1 (e)	0	0	0	0
POWER MARGIN AND PULSED LOADS	-	0.0 (f)	0 (h)	19.2	0 (h)	15.6
TOTAL RTG OUTPUT	125.0 (c)	265.0 (g)	94.0	188.0	94.0	124.0 (k)

(a) 6.0 WATTS TIME SHARED WITH TWTA, S-BAND
(b) 6.0 WATTS TIME SHARED WITH EXPERIMENTS
(c) RTG OUTPUT POWER IS REDUCED AT SEA LEVEL (ARGON FILL GAS)
(d) HEATER POWER FOR EXTERNAL REGULATOR
(e) USE THIS LEVEL TO SIZE RADIATOR AREA
(f) PULSE LOAD POWER INTERCHANGEABLE WITH SHUNT POWER
(g) MAXIMUM ANTICIPATED RTG POWER AT BEGINNING OF LIFE
(h) PULSE LOADS REQUIRE POWER DOWN OF OTHER SUBSYSTEMS (E.G., PROBE DATA LINK, DSU)
(i) PIONEER F/G USES STELLAR REFERENCE ASSEMBLY INSTEAD OF STAR MAPPER
(k) TOTAL RTG POWER OUTPUT OF PIONEER F/G RTG'S AFTER 2.5 YEARS (ESTIMATED PERFORMANCE INTERFACE SPECIFICATION)

During the seven-year lifetime mission, the MHW generator system provides a power margin sufficient to handle all anticipated steady and pulse loads without a battery. An even greater margin is achieved if S- and X-band transmissions are not powered simultaneously. Conversely, in the event that one of the two MHW RTG's fails, alternative operational modes, involving duty cycling of transmitters or experiments, are available to ensure operational flexibility in continuing to meet mission objec- objectives.

The power budget shows that a 10-watt X-band TWTA can be accommodated, leaving an adequate margin of 19.2 watts for pulse loads. It is also evident that use of a 12-watt X-band transmitter, requiring an input power of 43 rather than 36 watts would reduce the power margin to about 10 watts, i.e., a margin insufficient to handle the pulse load requirements unless the image system uses time-shared power. The communication subsystem performance analysis (Section 6.6) indicates that 10-watt transmitter power on X-band gives a sufficient downlink data rate margin for all phases of the ES and ESU missions.

Table 5-11 lists the pulse loads occurring during the mission, based on Pioneer F/G characteristics. With the exception of the battery heater and feed movement mechanism which are deleted, these loads are representative of the SUAE mission requirements. Actually, none of the pulse loads need to overlap since they are all ground commanded and may be sequenced accordingly. The transfer switches, used to interconnect transmitters and receivers with the antennas, would, in general, only be actuated in case of a transmitter or receiver failure. Initiation of this action can be commanded with experiments turned off, if necessary.

As noted in the table, every thruster pair firing event introduces a pulse load of 11.5 watts, i.e., the power required for solenoid actuation, including losses involved in command distribution. The ΔV/ precession thrusters and the spin rate control thrusters operate infrequently, or for short time intervals only. However the radial thruster pair may be required to operate in the pulsed mode, once every 12 seconds, for extended periods as long as 48 hours if large lateral ΔV maneuvers are to be performed. For practical purposes this pulse pattern can be regarded as a steady load during such periods. It can be readily accommodated by the available power margin.

Table 5-11. Pulse Loads (Watts)

Function	Pioneer F/G	Pioneer SUAE Spacecraft
Experiments (command initiated)	3-4	3-4
Transfer switch (command initiated)	14 (50 msec)	14 (50 msec)
Thruster pair (every firing)	11.2	11.2
Spacecraft battery heater (command initiated)	1.6	-
Feed movement mechanism (command initiated)	4.3	-
Experiment ordnance (one-time only; after injection)	6	6
CDU ordnance	0.5	0.5

The power budget given in Table 5-6 is actually quite conservative since not all of the load items in column 4, representing the most critical phase of the mission from the power requirements point of view, need to operate simultaneously. Items in this category are listed in Table 5-12. As mentioned previously they may be duty-cycled or turned off temporarily to reduce the total load, if necessary.

Table 5-12. Items Permitting Temporary Turn-off for Load Reduction

Item in Power Budget	Watts
Star mapper assembly	5.0
S-band or X-band TWTA's	27.8 or 36.0
Propulsion heaters	8.0
Some of the experiments	10 to 30
Probe adapter heater	4.0
	54.8 or 90 Total

5.7 COMMAND, TELEMETRY AND DATA STORAGE REQUIREMENTS

A preliminary review of the command, telemetry and data storage requirements was made to determine what modifications of Pioneer F/G would be necessary to meet the SUAE mission objectives.

5.7.1 Command

Changes in the command subsystem are required primarily as a result of:

- enhanced communications performance of the system, i.e., the addition of X-band communication equipment;
- additional data handling and storage requirements;
- accommodation of probe housekeeping, test and telemetry requirements by the bus; and
- accommodation of the modified bus science payload complement.

Table 5-13 lists the additional command functions accruing from these requirements. These additions are partly offset by elimination of some of the baseline Pioneer F/G equipment from the SUAE spacecraft. These deletions are also listed in Table 5-13.

The required expansion of functions to be performed by the command distribution unit (CDU) is possible without a major design change since the CDU can be tailored to accommodate the specific requirements of the SUAE spacecraft. The CDU is capable of processing 255 discrete commands whereas less than 190 have been implemented on Pioneer F/G. Thirty-four of the unused discretes are available without further modification; the remainder can be made available by the addition of integrated circuits. Cabling harnesses will, of course, require substantial redesign.

The preliminary estimate given in Table 5-13 of 45 additional command (taking the deletions into account) is within the functional capacity of the existing CDU design and still leaves a margin of 20 unused discrete commands.

The specific command requirements of the new bus science instruments are not defined at this point. However, the addition of three new

Table 5-13. Additional Command Requirements (Preliminary)

Subsystem	Command	Number of Commands Added	Number of Commands Deleted
Electrical Distribution	Select register	5	
	Probe separation pyro actuation	6	
	Probe operations pyro actuation	8	
	Probe battery charge	4	
	Probe test commands	4	
Communication	S-band transmitter	4	
	TWTA to high gain antenna	2	
	L-band receiver/data synchronizer on/off	2	
	S-band feed offset		4
Attitude Control	SPSG roll reference input	4	
	Reference set	2	
	SCT pair select	1	
	Pulse length	6	
	Image system gimbal angle register	2	
	Image system gimbal rotation execute	2	
	Star mapper gimbal angle register	2	
	Star mapper gimbal rotation execute	2	
Data Handling	DSU control logic	2	
	Probe data buffer	2	
Propulsion	Radial thruster	6	
Electrical Power	Bus battery control		7
Science	Added instruments (3), estimated	6	
	Deleted instruments (5), estimated		10
	Deleted IPP mode and angle control		6
	Total Added	72	
	Total Deleted	27	
	Net Total Increase	45	

instruments in the list of science experiments specified by Ames Research Center is offset by the elimination of five others of the present Pioneer F payload. This change can be accommodated by redistribution of commands that are now being used in the baseline spacecraft. Six of the present Pioneer F/G instruments can probably be retained with only minor changes.

The command memory feature of the Pioneer F/G CDU, providing the capability of storing up to five command messages and their associated time delay periods for later sequential execution, is retained. The command memory capability may be essential for execution of certain time-dependent functions such as controlling scientific experiments when the spacecraft is occulted by the planet. Other operational procedures such as probe release sequences, instrument calibration and mode selection may be greatly simplified with the command memory.

The existing redundant digital decoder unit (DDU) is capable of demodulating and verifying a maximum of 255 discrete commands. Therefore, no changes to this unit are contemplated.

5.7.2 Communications

To maintain a high data rate capability at earth distances up to 20 AU is a requirement that has already been addressed in the Pioneer Outer Planet Spacecraft design study. The same approach can be taken in the SUAE spacecraft to achieve the highest possible bit rate consistent with retaining as much of the simplicity, reliability, and technology of Pioneer F/G as possible, constrained by the available electrical power. The inclusion of an X-band transmission capability to provide the prime telemetry support is the most straighforward solution within the constraints cited which can provide the desired improvement in link gain.

Retention of an S-band downlink capability is imperative, however, because it:

a) Supports tracking and telemetry operations during launch, ascent, and initial Deep Space Station acquisition phases of the mission.

b) Provides continuous communications during off earth-pointing maneuvers.

c) Permits routine data acquisition from the DSN 26-meter diameter antenna network.

d) Serves as a backup data link (at reduced bit rate) for the X-band system.

e) Provides increased assurance of continuous telemetry coverage in the event that the spacecraft attitude "drifts" beyond the X-band beamwidth.

The communication subsystem configuration of the Outer Planets Pioneer that can be adopted for the SUAE Pioneer differs from Pioneer F/G in the following areas:

a) The existing S-band transmission system has been augmented with an X-band capability comprised of redundant TWTA's (each providing 12 watts RF output) and driver amplifiers. The option for the X-band downlink to be phase coherent with the S-band uplink carrier is implemented by command, just as it is for the S-band downlink on Pioneer F/G.

b) An X-band transfer switch, utilizing waveguide ports, has been included to permit selection, by ground command, of either X-band TWTA/driver pair.

No changes in the maximum bit rate capacity of the existing DTU (2048 bps) is required according to the telemetry budget given in Table 5-14, although a higher bit rate (4096) could be supported by the X-band transmitter at Saturn. Thus, some modifications in the Outer Planets Pioneer communications subsystem design can be avoided here.

Relay communication of probe data to earth via the bus spacecraft is a unique requirement of this mission. It impacts the communication subsystem design primarily in terms of added equipment complexity. However the data rate requirement (88 bps) is sufficiently small to be accommodated comfortably within the capability of X-band communications. Rapid playback of probe data after the critical real time telemetry phase is over can be performed by allocating a larger portion of the telemetry data format to probe data frames.

Table 5-14 summarizes the telemetry allocations based on the data rate capabilities of the modified spacecraft.

Allocation of high data rates to the probe data relay and playback functions has priority and is dictated by the timing aspects of the planetary encounter and the time available after completion of the probe entry phase until ring crossing at Saturn and until bus occultation at Uranus. It is

Table 5-14. Telemetry Budget (Preliminary)

	Earth to Saturn		Saturn to Uranus	
Cruise Phase	S-Band	X-Band	S-Band	X-Band
Available bit rates	2048 - 256	2048	256 - 32	2048 - 1024
Allocation to				
Engineering telemetry	1024 - 128	1024	128 - 16	1024 - 512
Bus science data	1024 - 128	1024	128 - 16	1024 - 512
	Saturn		Uranus	
Pre-encounter Phase	S-Band[a]	X-Band	S-Band[a]	X-Band
Available bit rates	256	2048	32	1024
Allocation to				
Bus engineering telemetry	128	1024	8	384
Probe test data	64	264	8	128
Bus science data	64	760	16	512
Probe Entry Phase				
Allocation to				
Bus engineering telemetry	16	128	8	128
Probe data relay (88 bps)	224[b]	1664[b]	16	768[b]
Bus science data	16	256	8	128
Post Probe Entry Phase				
Allocation to				
Bus engineering telemetry	16	128	8	128
Probe data playback	224[c]	1664[c]	16	768[c]
Bus science data	16	256	8	128

(a) Use of S-band at planet encounter only if X-band unusable
(b) Includes real time probe data relay and recorded data playback
(c) Probe data playback at high rate (6 minutes at Saturn, 12 minutes at Uranus)
NOTE: Table only applies to probe delivery at Saturn or Uranus

anticipated that probe data playback will be started in addition to continued relay operation half-way through the probe entry phase at Saturn to assure several full data playback runs prior to ring plane crossing because of the potential hazards to spacecraft survival at this event. The time interval between probe expiration and Saturn ring crossing is less than a half hour in the nominal mission profile. Rapid probe data playback in the case of the Uranus encounter is not critically important.

5.7.3 Data Storage Requirements

A data storage capacity greater than the 50 kb core memory capacity of Pioneer F/G is dictated primarily by the requirements of:

- Probe data storage during the entry phase, for subsequent playback as a safeguard against possible loss of data during real-time relay link telemetry
- Bus science data storage (a) to serve as buffer for image system data, (b) to record data during earth occulation.

Probe data storage is the priority requirement. At relay link data rates of 88 bps a total of 316 kb must be stored during a maximum of one hour of probe data gathering. A 20 percent margin for additional data volume in case of prolonged probe survival on entry is desirable.

Image system data buffer requirements are actually much higher as discussed in Section 4. The data volume from a 390-cell line scan image system used on a square image frame is 0.9 megabits. A 195-cell array would yield a data volume of 228 kb. Flexibility is desired to use all of the redundant solid state data storage units (see Section 6) so as to provide maximum image data buffer capacity if these units are fully operational during the planetary encounter. However the priority of probe data recording and retention until cleared by earth command curtails the further use of the DSU as image data buffer after the relay operation is initiated. If three redundant segments of 250 kb are available in the DSU then at least one segment could be used to store truncated image frames (i.e., rectangular frames with an aspect ratio of about 1:4). The data rate capability of the X-band telemetry link permits allocation of sufficiently high bit rates to transmit several such frames per hour at no interference with probe data telemetry requirements.

6. SUBSYSTEM DESIGN

6.1 STRUCTURE

The bus structure subsystem carries primary flight loads, provides the physical interface to the launch vehicle, and provides secondary mounting structure for all spacecraft assemblies including the probe. The bus structure must include provisions for meteoroid and thermal protection of critical components. It must incorporate access provisions to facilitate integration, assembly, and maintenance. The structure subsystem includes all deployment and separation mechanisms as well as any required balance weights. The structure must survive the powered-flight environment and other environments as currently apply to the Pioneer F/G spacecraft (see TRW Specification PC-210.02 for further definition of design environments).

6.1.1 Equipment Compartment

The equipment compartment (see Figure 6-1) consists of three sections: a hexagonal center section, rectangular section, and experiment section. The primary structural elements consist of aluminum honeycomb material for the floors and sides tied together with an external box structure employing angle sections and fittings.

The equipment layout shown in Figure 6-2 includes consideration of such factors as static balance, moments of inertia throughout all mission phases, thermal control, sensor fields of view, and additional factors such as ease of assembly and minimum cabling weight. The much larger propellant tank required to perform the Saturn Uranus Mission, the new experiment complement, the new RTG's, and the addition of an X-band downlink have been the major factors in forcing both structural and configuration changes to the Pioneer F/G system design.

In addition to the internal equipment, several components are mounted external to the compartment, including the shunt assemblies, strut-mounted thruster-cluster assemblies, and sun sensor (see Figure 6-3). The equipment compartment also contains or supports various mechanisms (deployment, louver, damper) and interfaces directly with all other major structure elements except the third-stage adapter.

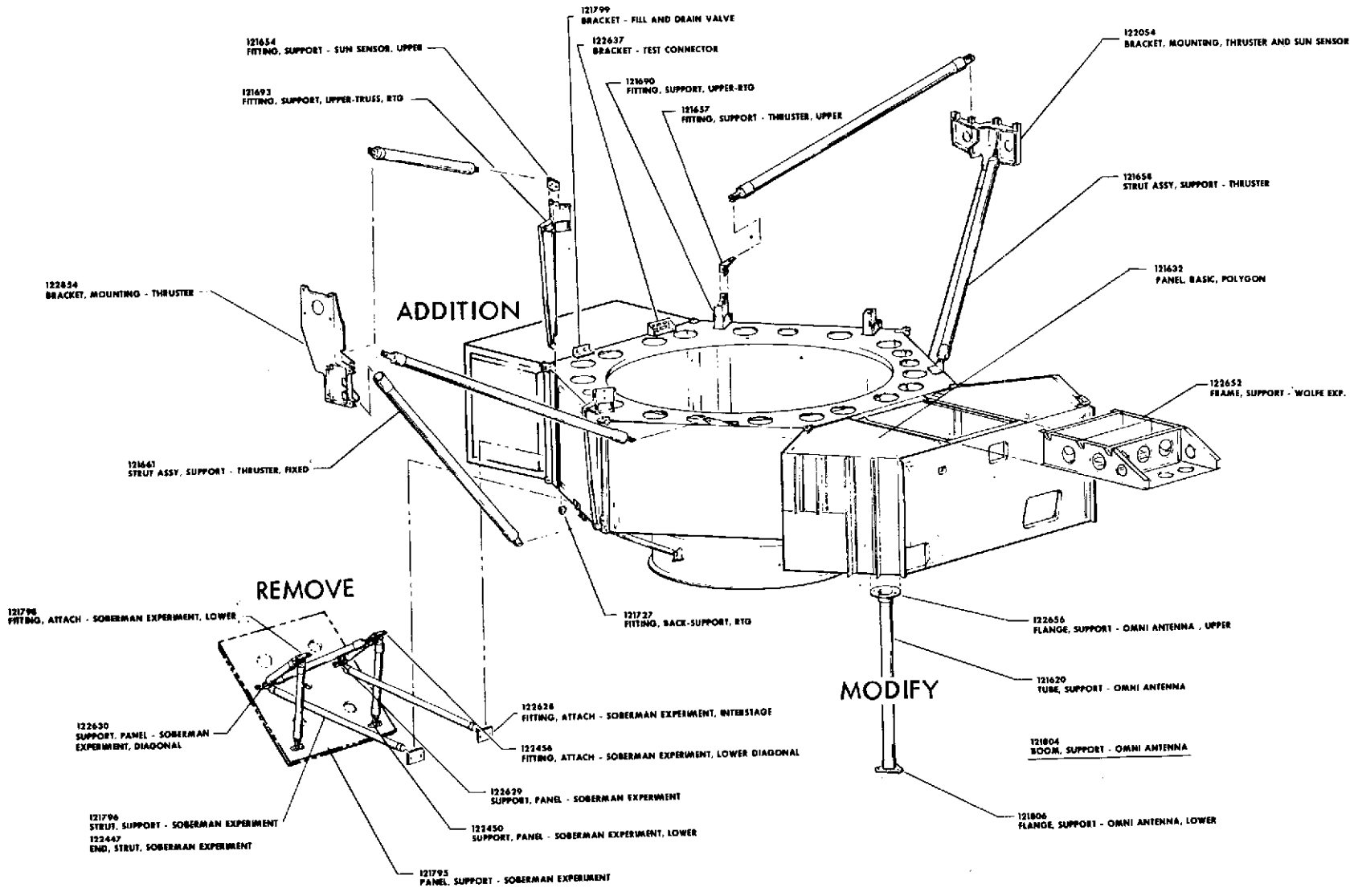

Figure 6-1. Pioneer F/G Equipment Compartment

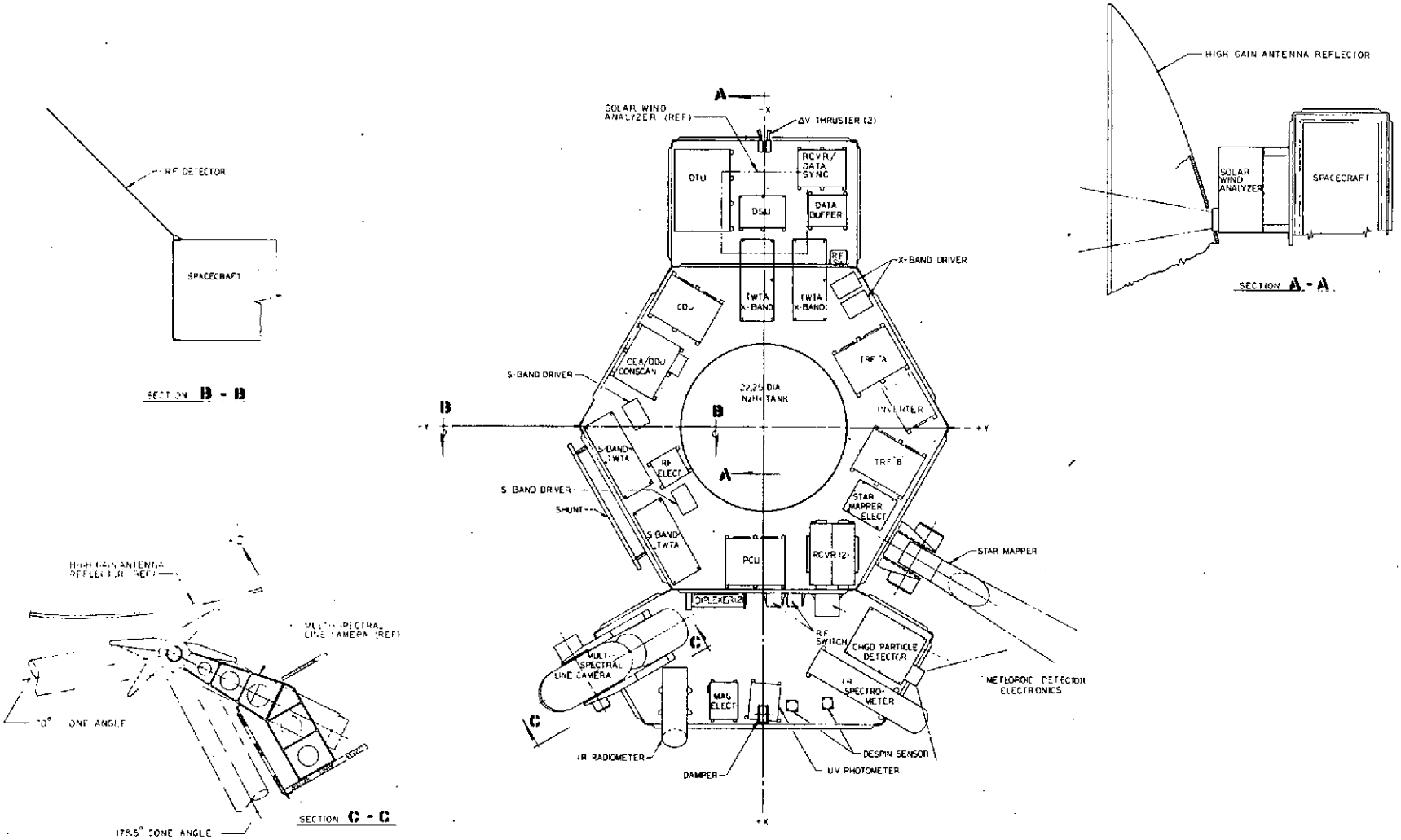

Figure 6-2. SUAE Equipment Layout

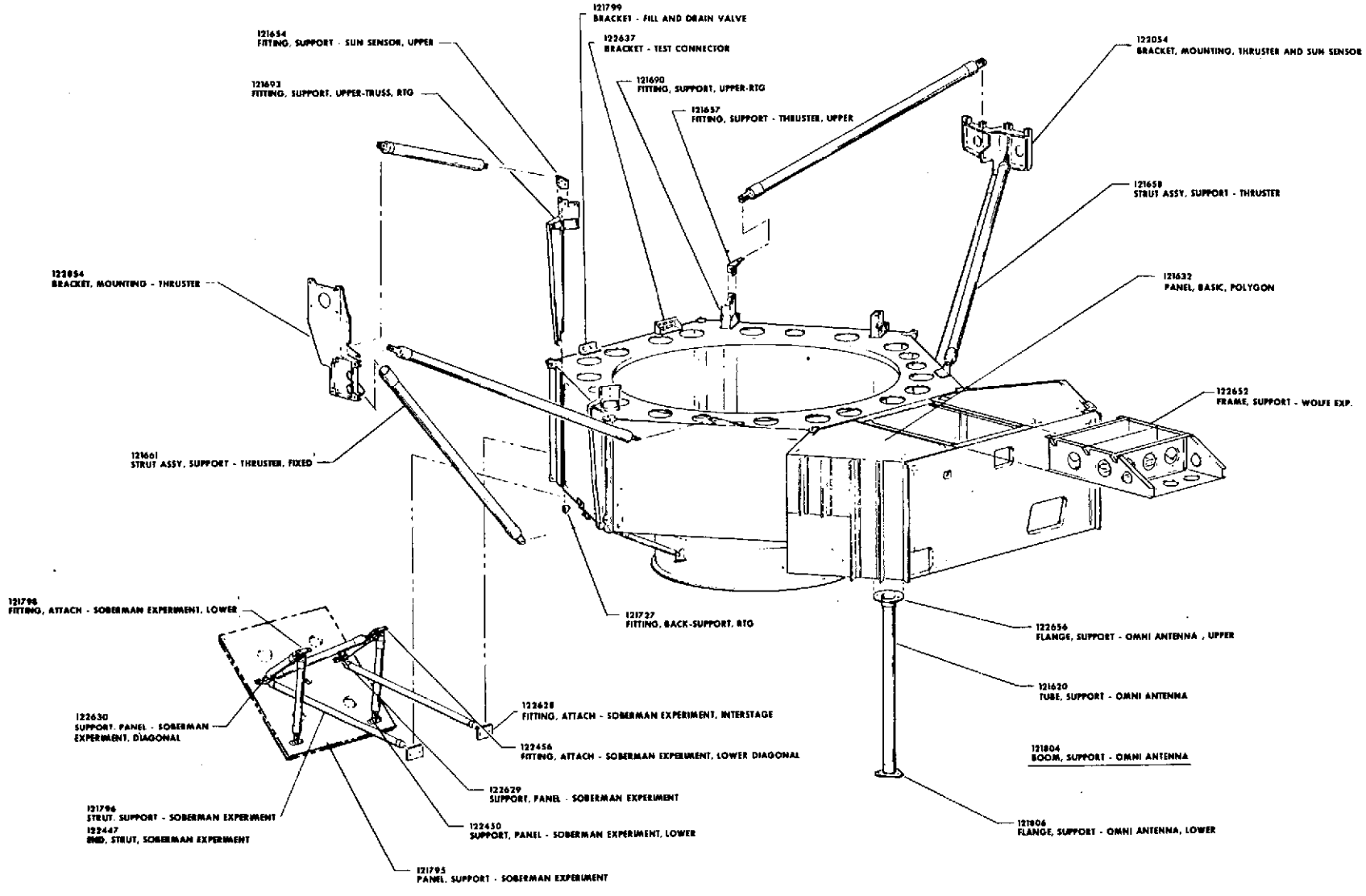

Figure 6-3. Pioneer F/G External Equipment Mounting

The principal modifications to the Pioneer F/G equipment compartment structure are summarized as follows:

1) Cutout hexagonal compartment floor and provides new support struts for larger propellant tanks. (See Figure 6-4.)

2) Provide an additional rectangular compartment on the -X axis to accommodate new mission equipment.

3) Modify internal equipment arrangement to maintain acceptable mass properties and to accommodate new bus science equipment.

4) Modify RTG support fittings to accommodate larger units.

6.1.2 High-Gain Antenna Support

The 9-foot diameter reflector, high-gain antenna feed assembly, and medium-gain S-band antenna are all supported via struts mounted directly to the hexagonal section of the equipment compartment. The strut arrangement, as shown in Figure 6-5, is identical to the Pioneer F/G.

One potential modification is the addition of attach fittings on one of the feed support struts for the new X-band waveguide between the TWT and the feed. Modifications to the feed assembly itself are described in Section 6.6.

6.1.3 Interstage Support Ring

The interstage support ring and strut assembly (Figure 6-6) distributes launch loads to the equipment compartment and serves as a transition section between the probe adapter and the bus.

Modification of this item for the SUAE Mission will be minimal. The clearance holes for one set of RTG rods must be relocated to insure clearance between the rod and the larger propellant tank (Figure 6-7). With the probe/bus interstage adapter retained, it is possible to omit the separation spring brackets and separation switch mounting, required for the Pioneer F/G configuration.

The central cylinder, made of glass-reinforced epoxy laminate, and the equipment compartment attach ring may require modification to

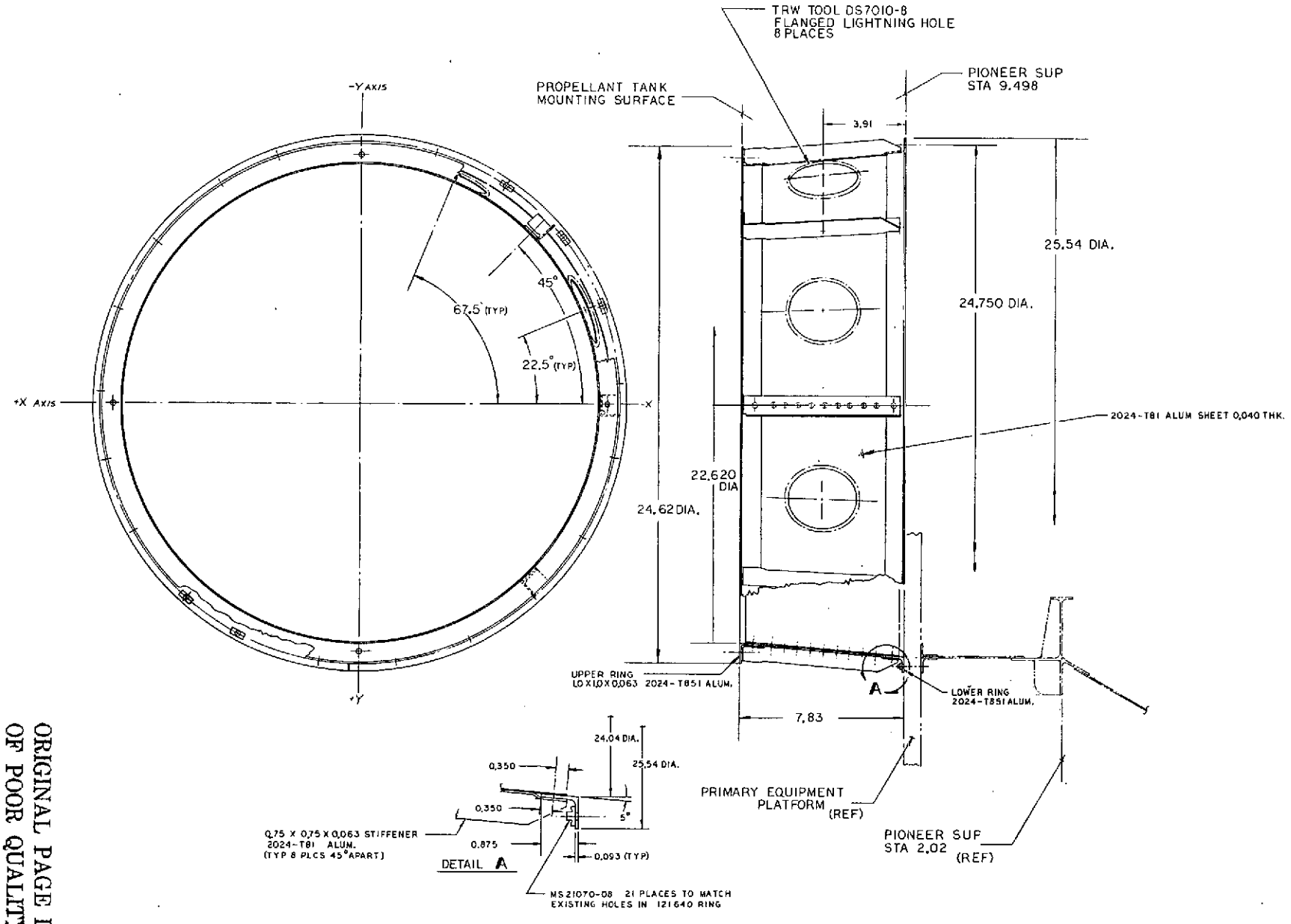

Figure 6-4. SUAE Propellant Tank Support Cone

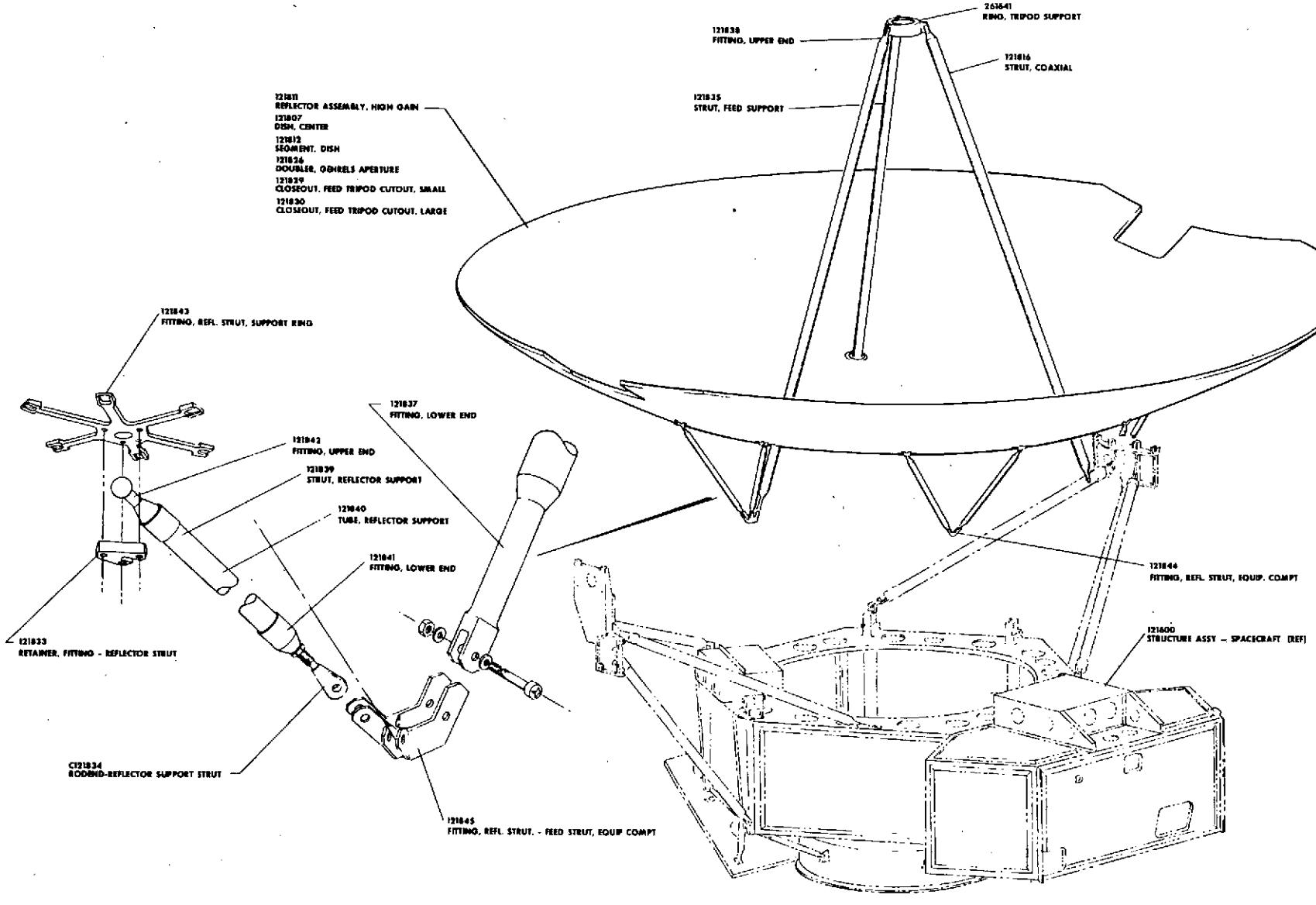

Figure 6-5. High-Gain Antenna Support

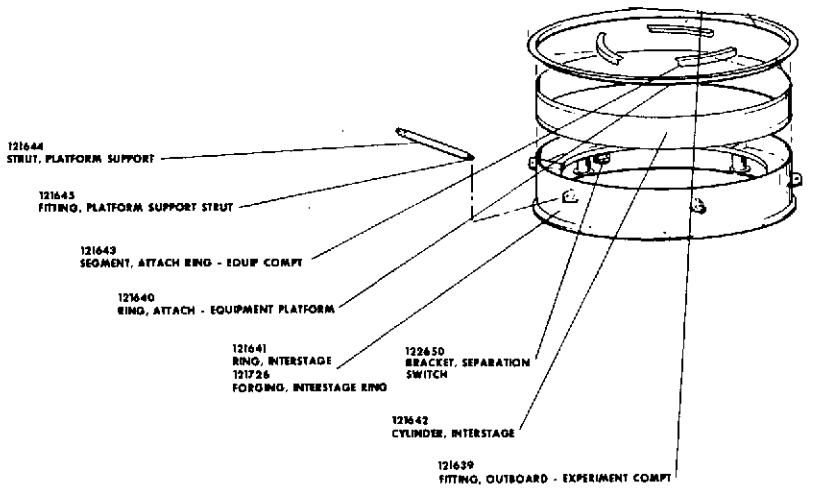

Figure 6-6. Spacecraft Cylindrical Interstage

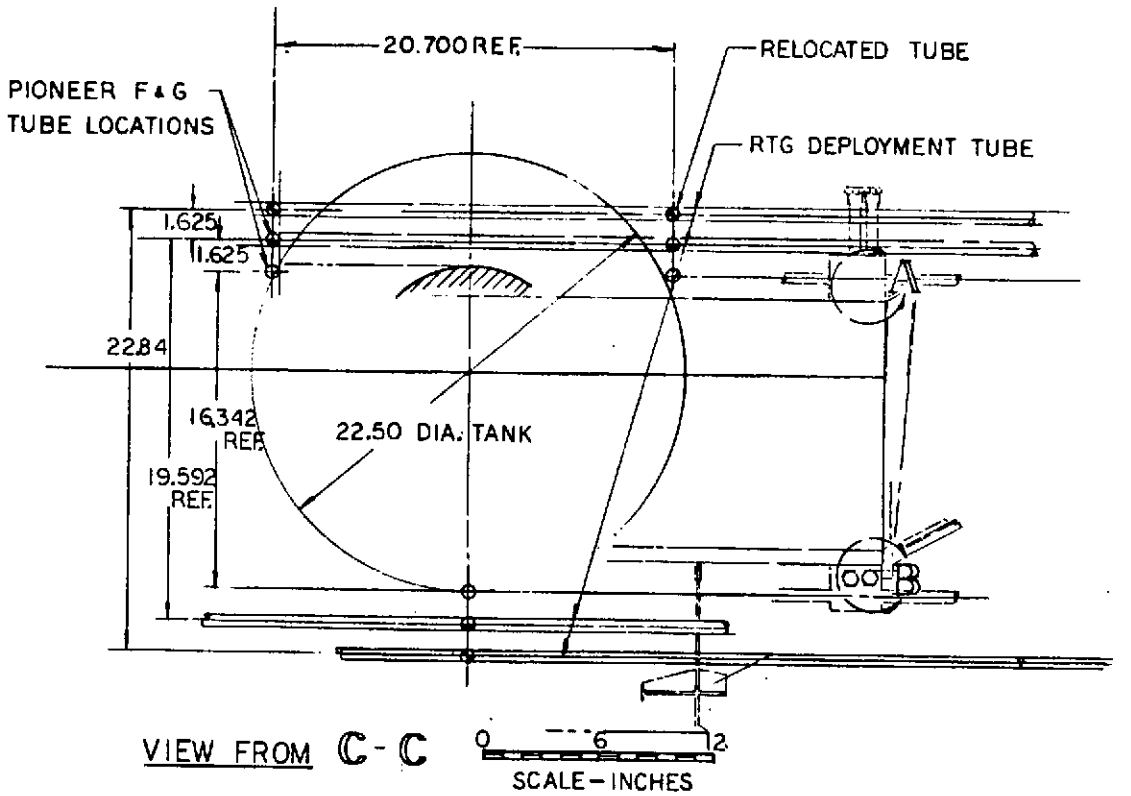

Figure 6-7. RTG Rod Relocation

ORIGINAL PAGE IS
OF POOR QUALITY

accept the higher loads resulting from increasing the spacecraft weight. The same may be true of the struts and their attach fittings. Such modification could also be required to stiffen the structure so that it will perform satisfactorily under vibration. However, a more detailed and thorough dynamics analysis would be required to establish the need for such changes in the structure stiffness.

6.1.4 RTG Support Assembly

The RTG selected for the Saturn/Uranus mission (see Section 7.1), coupled with the larger propellant tank, necessitates some change in the RTG deployment hardware even though the form of deployment is unchanged. The MHW "short stack" complement is 20 pounds heavier than the four SNAP-19 RTG's of the Pioneer F/G spacecraft. The increased weight, the fact that there are two units rather than four, and the changed mounting geometry all lead to a new RTG support structure. Figure 6-8a shows the Pioneer F/G support structure and deployment mechanism. The SUAE spacecraft replaces the bipod truss and the delta mounting fitting by a mounting plate (Figure 6-8b). The relocation of guide rods to clear the larger propellant tank causes modifications to the guide fittings.

6.1.5 Magnetometer Boom Assembly

In section 5.5, various problems and solutions for control of the spacecraft principal axis of inertia were discussed. The selected approach involved the addition of a 24-pound counterweight to the magnetometer boom that is shown as it is in the Pioneer F/G design in Figures 6-9 and 6-10.

A preliminary structural investigation of the present Pioneer F/G magnetometer boom was conducted to determine whether the boom would tolerate the added counterweight. The results of the investigation indicated that although the present design concept may be feasible, the added boom structural weight necessary to withstand the higher loads makes the present design inefficient.

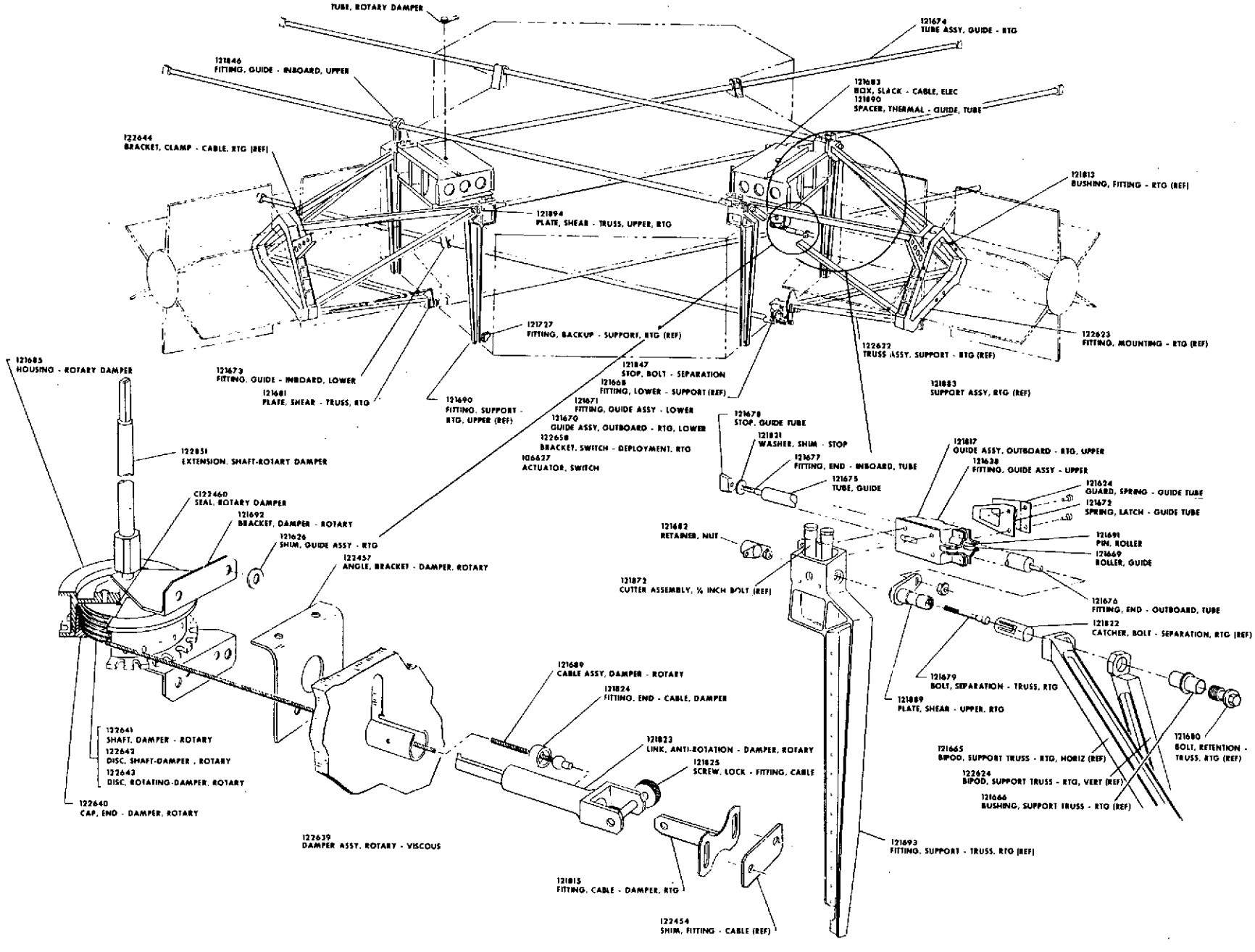

Figure 6-8a. Pioneer F/G RTG Support Structure and Deployment Mechanism

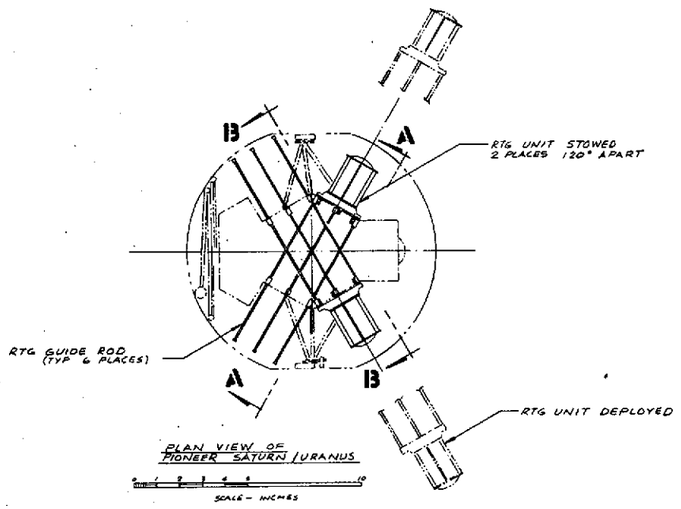

PLAN VIEW OF PIONEER SATURN/URANUS

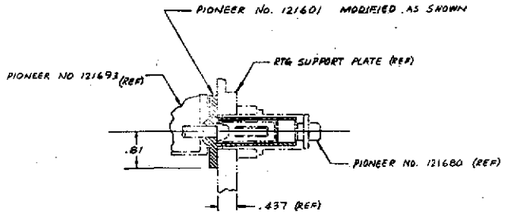

DETAIL C TYP 6 PLACES
4 TIMES SCALE

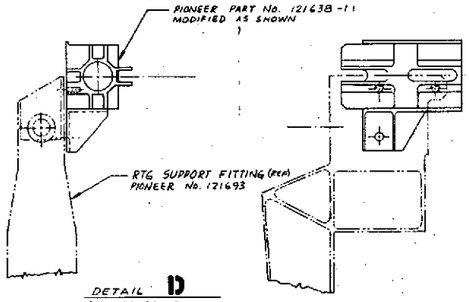

DETAIL D
4 TIMES SCALE

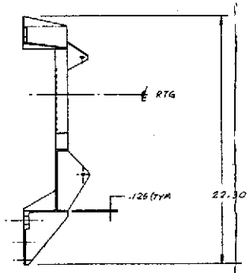

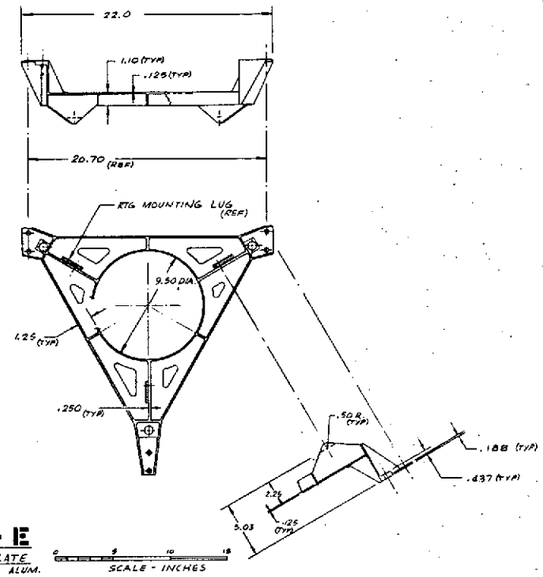

SECTION E - E
RTG SUPPORT PLATE
MAT'L 7075-T6 ALUM.

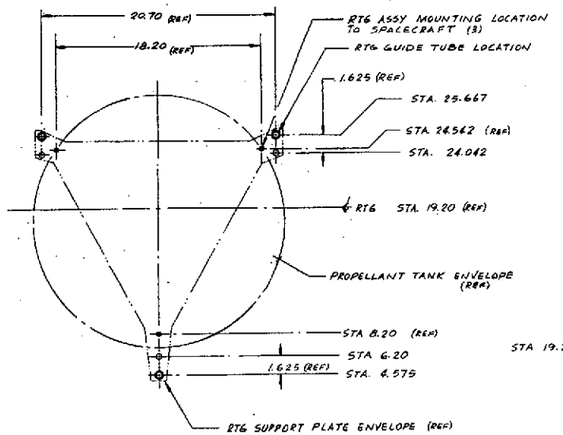

SCHEMATIC SHOWING RTG ATTACHMENT / GUIDE TUBE LOCATIONS
4 TIMES SCALE

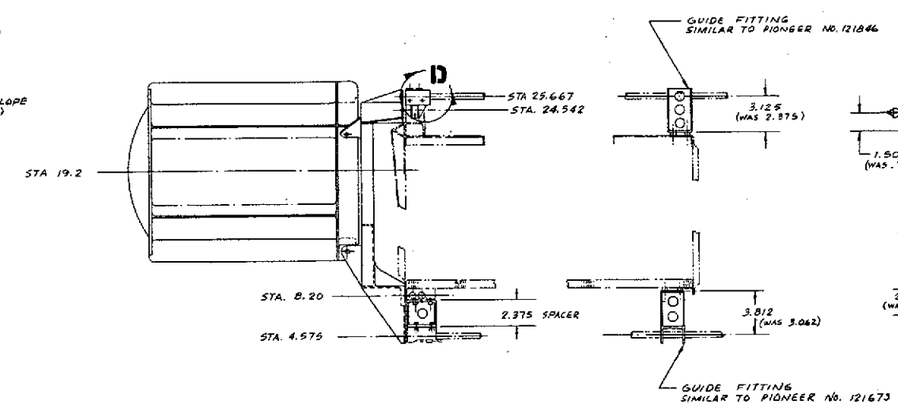

SECTION B - B

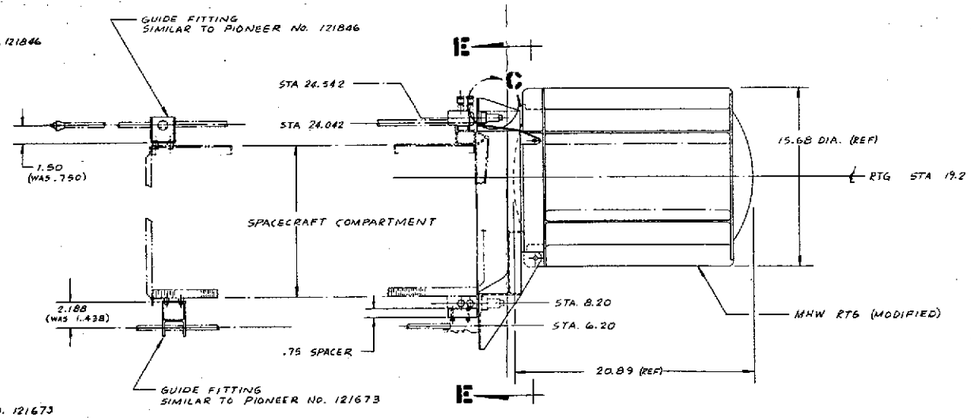

SECTION A - A

Figure 6-8b. RTG Installation

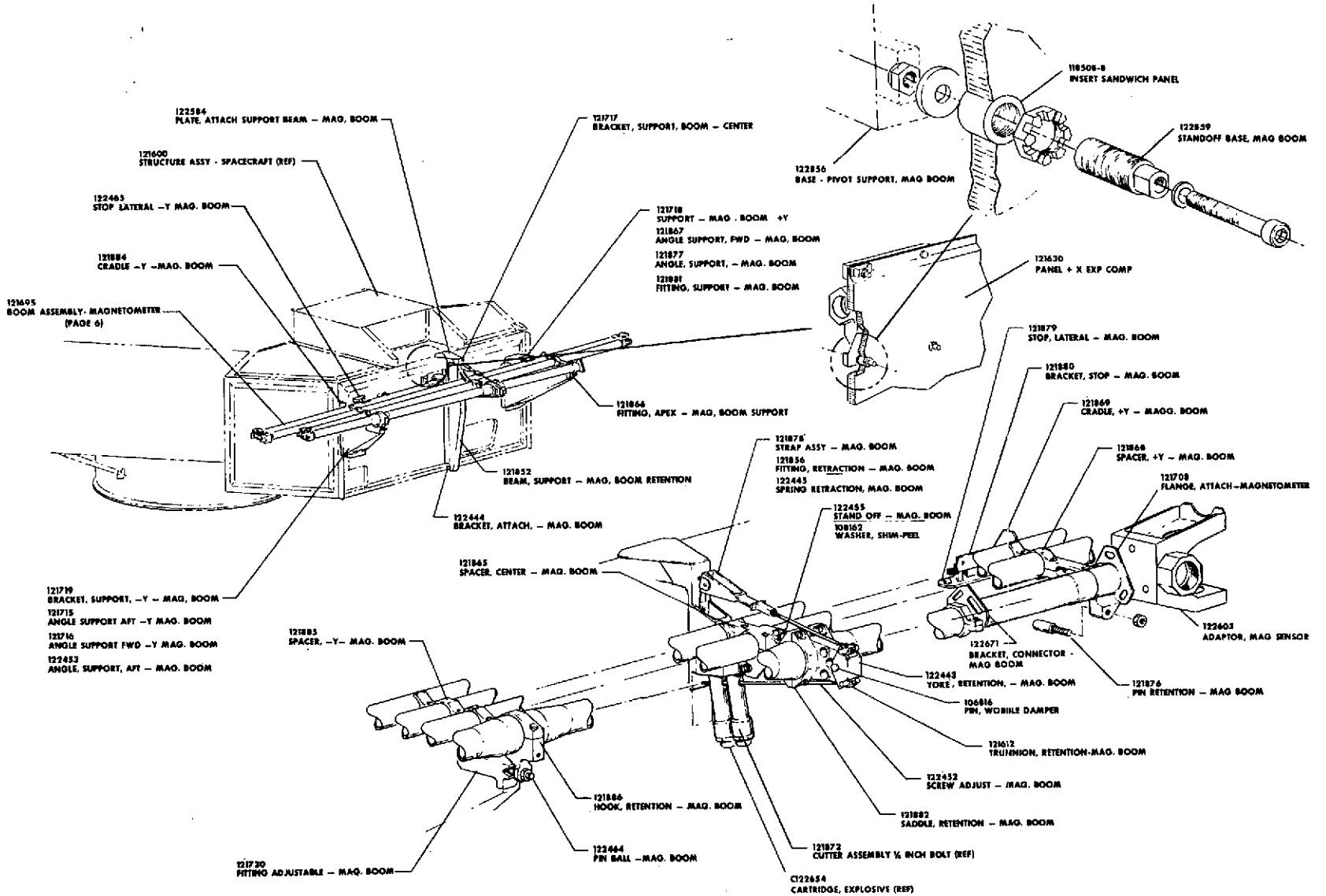

Figure 6-9. Pioneer F/G Magnetometer Boom Installation

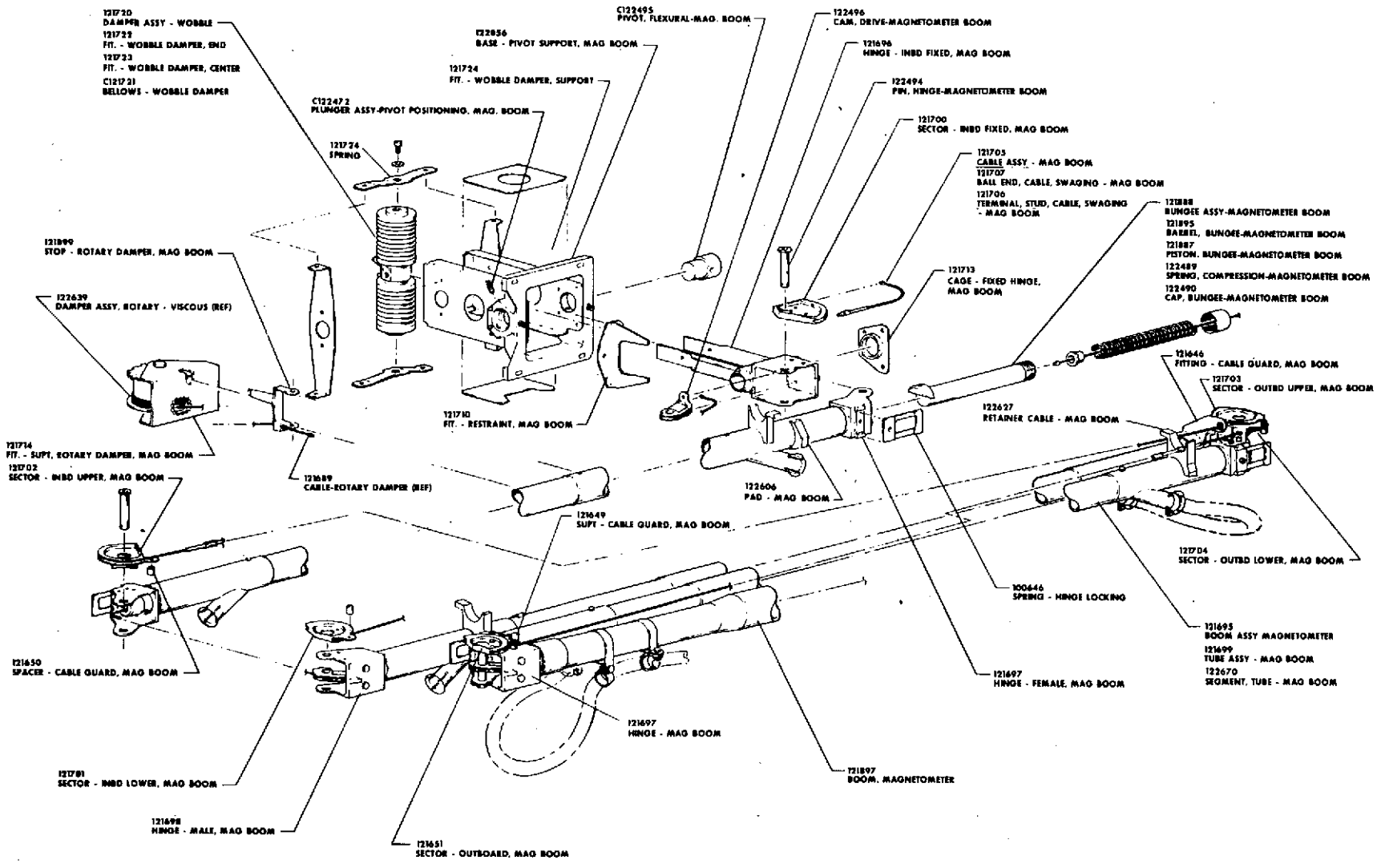

Figure 6-10. Pioneer F/G Magnetometer Boom Details

The investigation of the impact on the present magnetometer boom design for the addition of the 24-pound counterweight and for the initiation of deployment at a higher spacecraft spin rate, showed the following items have to be considered:

- Higher launch loads – vibration – quasi-static acceleration
  - support structure
  - boom structure
- Higher deployment loads
  - deployment damper
  - boom structure
  - release loads
  - centrifugal forces
  - Coriolis forces
  - latch loads
- Higher in-orbit loads
  - boom as cantilever beam damper
  - wobble damper and pivot mechanism.

The primary portions of the magnetometer boom are presently designed from loads experienced at the initiation of deployment. Load portions of the boom (the stowed boom support points) are designed by launch vibration loads.

Structural loads generated at the initiation of boom deployment are from two effects:

1) The energy release due to the preload in the tie-down mechanism, and
2) The centrifugal force on the boom, sensor and counterweight.

The problem arises with the present magnetometer boom design because of the centrifugal force effect. With the addition of a counterweight the loads go up in proportion to the change of weight. The 24-pound counterweight may be compared with the 9.8-pound weight of the entire Pioneer F/G boom, including the sensor. Also, since the magnetometer boom and the RTG's will be deployed simultaneously, the rotational velocity at the initiation of deployment will be greater than that in the

present Pioneer F/G magnetometer boom deployment. The increase in loads at this time is given by another factor equal to $(\omega_{new}/\omega_{old})^2$ with spin rates ω_{new} = 15 rpm, ω_{old} = 6 rpm, this second factor is 6.25.

The net result of a loads increase of this magnitude would be an extensive redesign of the boom components and boom supports and an undesirable weight increase. (Note that increases in weight of the boom's outermost segment inflicts no penalty: merely reduce the counterweight accordingly. But increases in weight of inner segments does inflict a weight penalty, rising to 100 percent of the weight increase if it is on the stationary structure, i.e., support structure on the equipment compartment.)

It is desired to retain as much of the present design concept as possible. One solution to the problem would be to:

1) Release the boom in two stages, i.e., release the preload in the center tie prior to release of the boom from the spacecraft. This would reduce the initiation of deployment loads by the increment contributed by the dynamic response of the system to the preload energy release; and

2) Replace the present deployment damper with one that would tie to the outer boom segment, which incorporates the counterweight. This would tend to unload the boom constraint cables, therefore unloading the booms.

With proper damping characteristics, only minor changes to the boom structure would be anticipated.

A second alternative for a magnetometer boom design revision would be to incorporate a scissors type of boom system as shown in Figure 6-11.

The scissors concept would allow a controlled symmetrical deployment while considerably reducing the loads in the boom tube segments. When the boom is fully deployed it would have the same structural and mechanical characteristics as those of the present design concept. Uncertainties with this concept include the stowage envelope and the weight tradeoff.

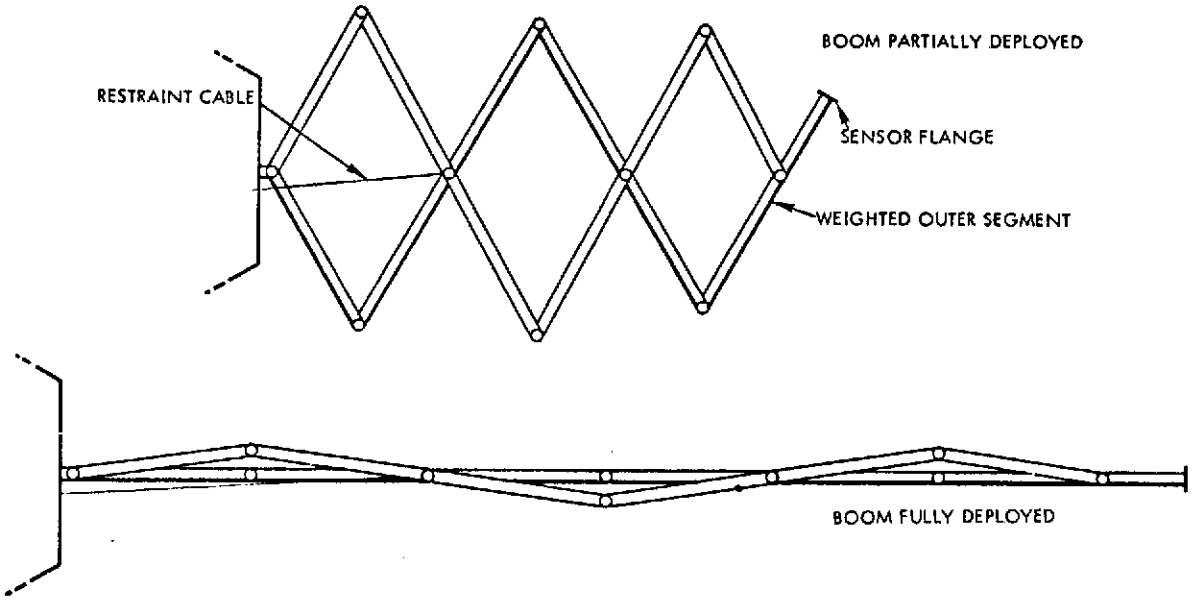

Figure 6-11. Scissors Type Magnetometer Boom

In either concept further study is needed in order to identify the revisions necessary to the stowed boom supports, adjacent spacecraft support structure, preloading mechanism, deployment damper, wobble damper, and the boom elements.

6.1.6 Probe/Bus Interstage

The interstage structure between the launch vehicle adapter and the bus has three principal functions. First, it transfers launch loads from the flight spacecraft to the launch vehicle, and interfaces with the separation joint of the launch vehicle. Second, it provides a mounting and a separation system for the probe. Third, it provides a mount for thermal control elements to maintain the probe temperature within acceptable limits. In addition, the adapter contains mounting brackets for a bus-to-probe cable and a cable separation mechanism (guillotine). Sufficient access to the interior of this adapter must be provided to facilitate assembly and integration of this unit with the other spacecraft segments. Details of this structure element are shown in Figure 6-12. The probe-bus physical interface is defined by Figure 2-9.

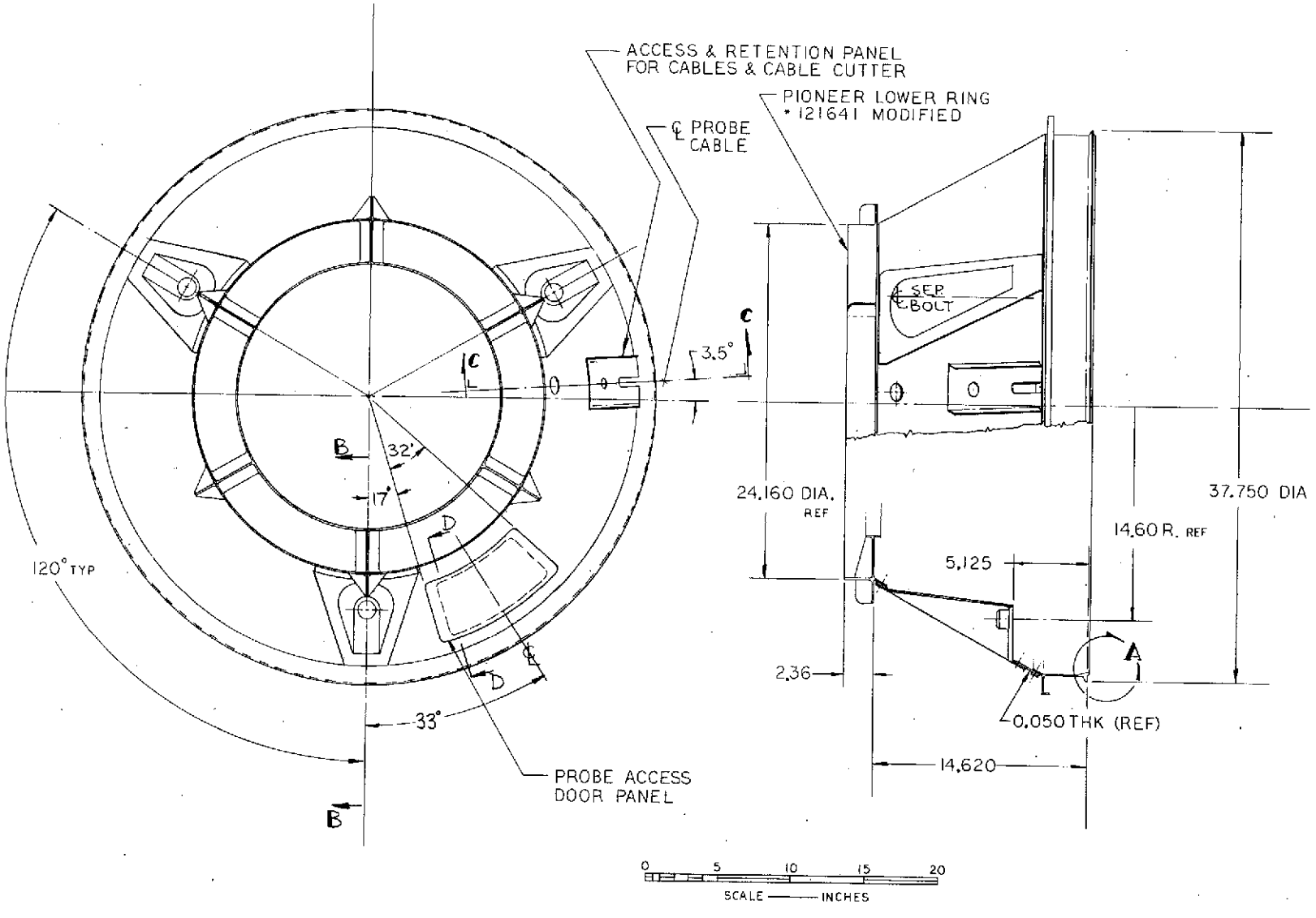

Figure 6-12. SUAE Spacecraft/Probe Adapter

6.1.6.1 Probe Separation Mechanism

Figure 5-3 shows the basic approach selected for separating the probe from the spacecraft. It consists of three equally spaced and fully redundant ball lock bolts (Figure 6-13 shows operating details), each mounted concentric with three carefully matched separation springs. The separation system is required to provide the following initial conditions to the probe following release:

- Relative velocity $0.1 \pm 0.01 \frac{\text{meters}}{\text{sec}}$
- Angular tipoff rate $\leq 1.6 \frac{\text{degrees}}{\text{sec}}$
- Tipoff angle ≤ 2.0 deg

To meet these requirements, three springs, each with the following characteristics, have been selected:

Material	Inconel X
Spring constant	9.6 lbf/in.
Total travel	0.5 in.
Compressed force	4.8 lbf
Number of coils	5
Coil diameter	1.25 in.
Wire diameter	0.91 in.

Several factors are critical in determining the performance of this separation system. This includes temperature, the effects of long storage on spring characteristics, the simultaneity of release of the ball lock devices and any residual drag, the center-of-mass location of the probe and the concentricity of the combined spring forces with this center of mass. Many of these factors can be eliminated by using one central separation spring such as is shown in Figure 6-14. This concept has three serious drawbacks which led to its rejection. First, it requires the addition of a substantial piece of structure on the bus for the spring to push against. Second, the constant (six years) spring pressure on the probe aft heat shield (not a load-carrying structure) would result in some unknown, unpredictable deformation and creep thereby destroying the

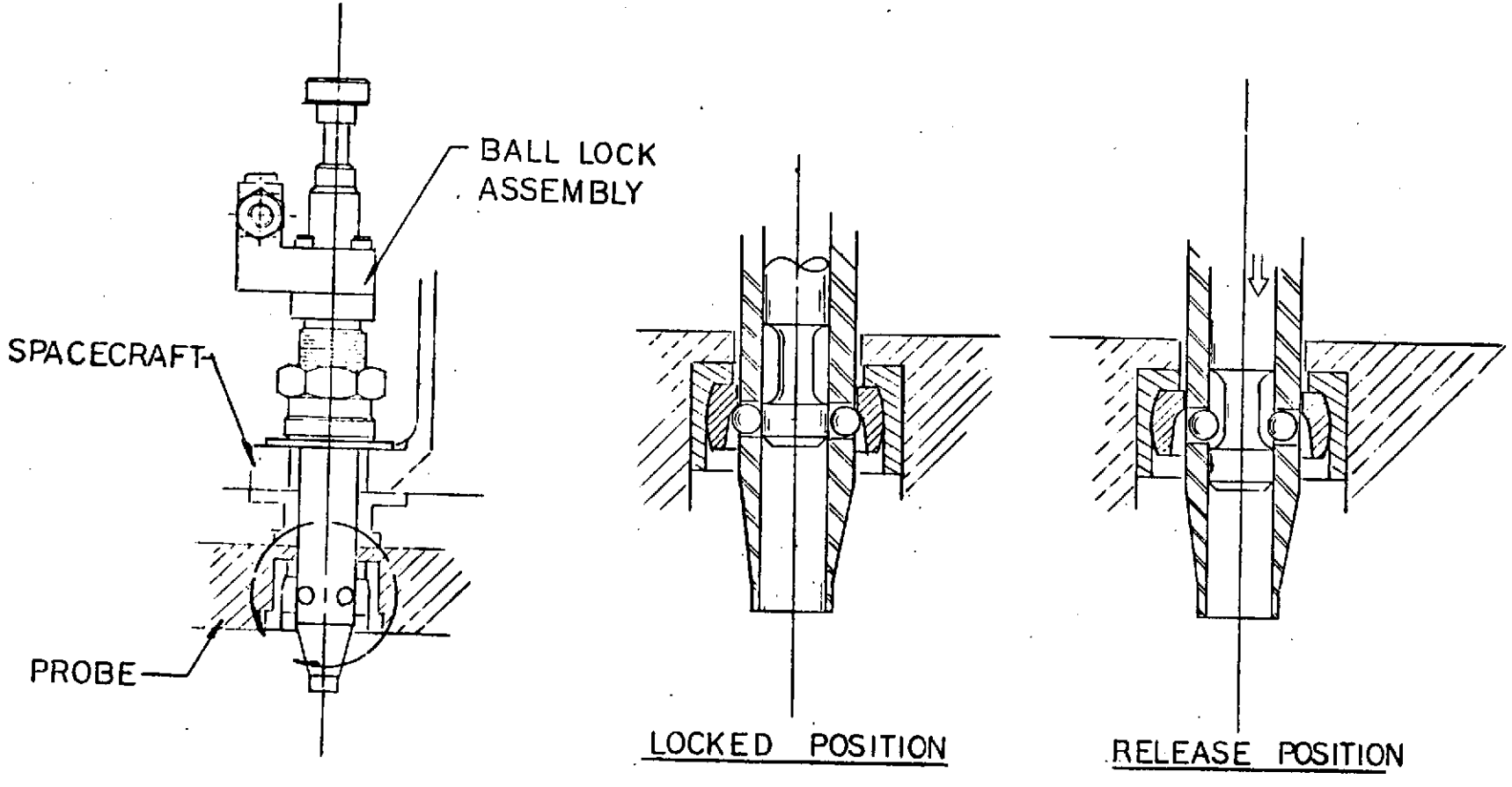

Figure 6-13. Ball-Lock Joint Operation

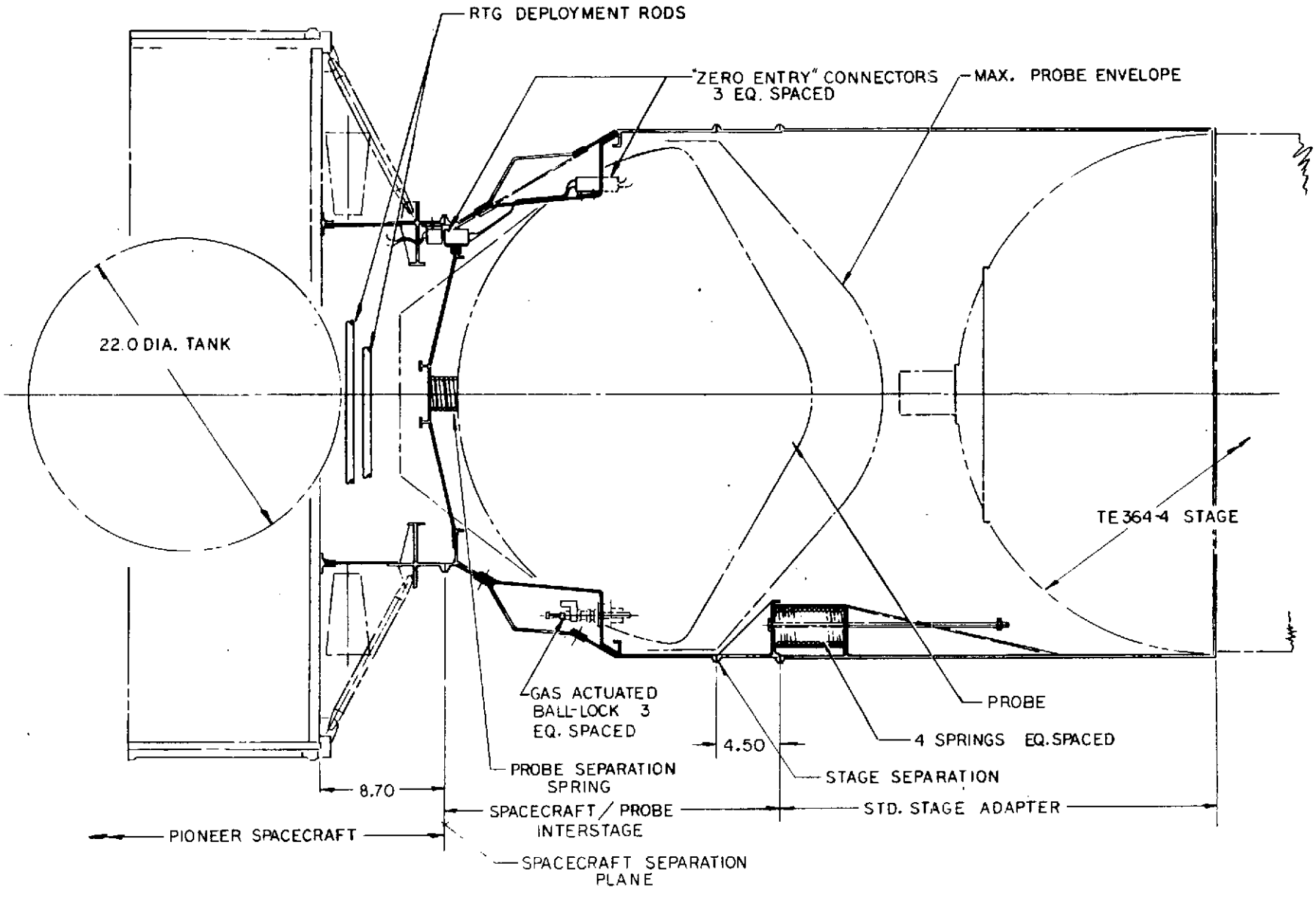

Figure 6-14. SUAE Interface Layout (Standard Adapter)

separation system performance. (Alternatively, a two-stage separation could be used in which spring pressure is not applied to the probe until just before separation.) Third, this location would complicate or preclude the use of a stabilizing chute or anchor which must be deployed along the probe aft centerline.

The probe adapter separation (if necessary) would use a similar set of three springs plus a Marmon-type tension band which is explosively released prior to separation.

As noted above, the adapter must include a thermal control system to insure survival of the probe. This includes multi-layer insulation with a window or cutout, the adapter surface coating, an electrical heater, and a good thermal bond between the probe mounting surface and the adapter structure. Further details of these components are described below in Section 6.2.

6.1.7 Third-Stage Adapter

Figure 6-14 shows the spacecraft to third-stage interface layout based on using the 37-inch diameter by 31 inch "standard stage adapter" provided as part of the launch vehicle. Use of this standard adapter creates two serious interface problems. First, the adapter does not extend far enough to permit separation at the largest probe diameter while still maintaining clearance between the probe nose and the third-stage motor; this requires the addition of a small cylindrical section as shown. Second, the standard adapter separation spring requires some structure to react against, and this structure cannot be on the probe adapter. It is placed on the cylindrical segment, then this segment must also be separated prior to probe release.

The complexity of the separation sequence apparent in the configuration employing the standard adapter can be avoided by using a customized third-stage adapter and separation system such as that shown in Figure 5-3. A single-stage separation plane, located at the probe maximum diameter, will insure a clear probe exit envelope as well as an adequate adapter separation clearance angle. The adapter length has been selected to allow sufficient clearance between the probe nose and the third-stage

igniter assembly should the mass spectrometer probe inadvertently deploy. The three or four separation springs will be selected to provide the same separation characteristics as the standard adapter, namely:

- Axial load factor: -1.5g longitudinal
  ±1.0g lateral
- Shock: 1400 g sawtooth
  0.3 m/sec duration

The springs would act upon the burned-out third-stage motor upon release of the Marmon tension band which joins the third-stage and the probe adapters.

6.2 THERMAL CONTROL

Thermal survival of the Saturn/Uranus flight vehicle from launch to planet flyby involves many variables. There are variations in solar insolation, RTG output (240 to 188 watts no failure, 120 to 94 watts with one RTG failed, variations in component dissipation, and in material and surface properties. During the prelaunch operations there is a substnatial variation in the thermal control mechanism since conduction and convection replace radiative transfer as the predominant processes for thermal control. To accommodate these variations, the spacecraft bus utilizes a combination of passive elements (coatings, insulation), semi-active elements (louvers) and active elements (heaters). The final choice of the various elements involves full-scale model testing, computer modeling, and full-scale qualification testing of flight quality hardware.

The Saturn/Uranus flight vehicle can be described (thermally) in terms of two major segments: the equipment compartment, and the probe. The proposed equipment compartment is similar to the Pioneer F/G unit, whereas the probe is a totally new spacecraft entity.

The equipment compartment is heavily insulated. The side panel blankets adjacent to the stowed RTG's are 22 layers of 1/4-mil aluminized Kapton with 2-mil aluminized Kapton outer layers. The other side panel and forward blankets are of similar construction except made of Mylar. The aft surface blankets consist of 22 layers of 1/4-mil Kapton with 2-mil outer layers.

The Pioneer F/G louver system (Figure 6-15) consists of 30 individually actuated blades or vanes, 24 of which are positioned radially around the interstage adapter and 6 of which are mounted on the aft side of the experiment platform. Each trapezoidal blade is supported on the larger end by a bimetallic spring/actuator housing assembly and on the smaller end by a lexan bearing assembly which, for the two-bladed assemblies, are contained in the interstage ring. Each blade is constructed from 0.156-inch aluminum honeycomb core with 2-mil aluminum face sheets. The overall blade thickness is approximately 0.160 inch. Functionally, the louver system acts to control the heat rejection of the radiating platform by varying the angular position of a set of highly reflective blades or shutters. A bimetallic spring, thermally coupled radiatively to the platform, provides the motive force for altering the angle of each blade. In a closed condition the heat rejection of the platform is minimized by virtue of the "blockage" of the blades while open louvers provide the platform with a nearly unobstructed view of space. The bimetallic spring is thermally connected (radiatively) to the platform and varies the angular setting of the blades according to the platform temperature in its particular sector. A typical louver angle-spring temperature plot is shown in Figure 6-16.

The probe and probe adapter represent a different set of thermal control conditions. Here we have a relatively large mass/volume which must be temperature controlled with a minimum of heating power. Further, the desired temperature is relatively high and narrow in range as dictated by the NiCad battery survival requirements. Thus there is a need to conserve the small amount of probe internal heat provided by radioisotope heating units (RHU's) by heavy insulation around the probe, but in a precise or controlled way to insure proper probe temperature.

6.2.1 Equipment Compartment Thermal Control

The SUAE spacecraft thermal control system is similar to Pioneer F/G (PFG) in most respects. Three major changes have been made to the equipment compartment thermal control system, based on F and G experience, to maximize the ability to handle RTG beginning of life (BOL) to end of life (EOL) power output changes. They are discussed further below.

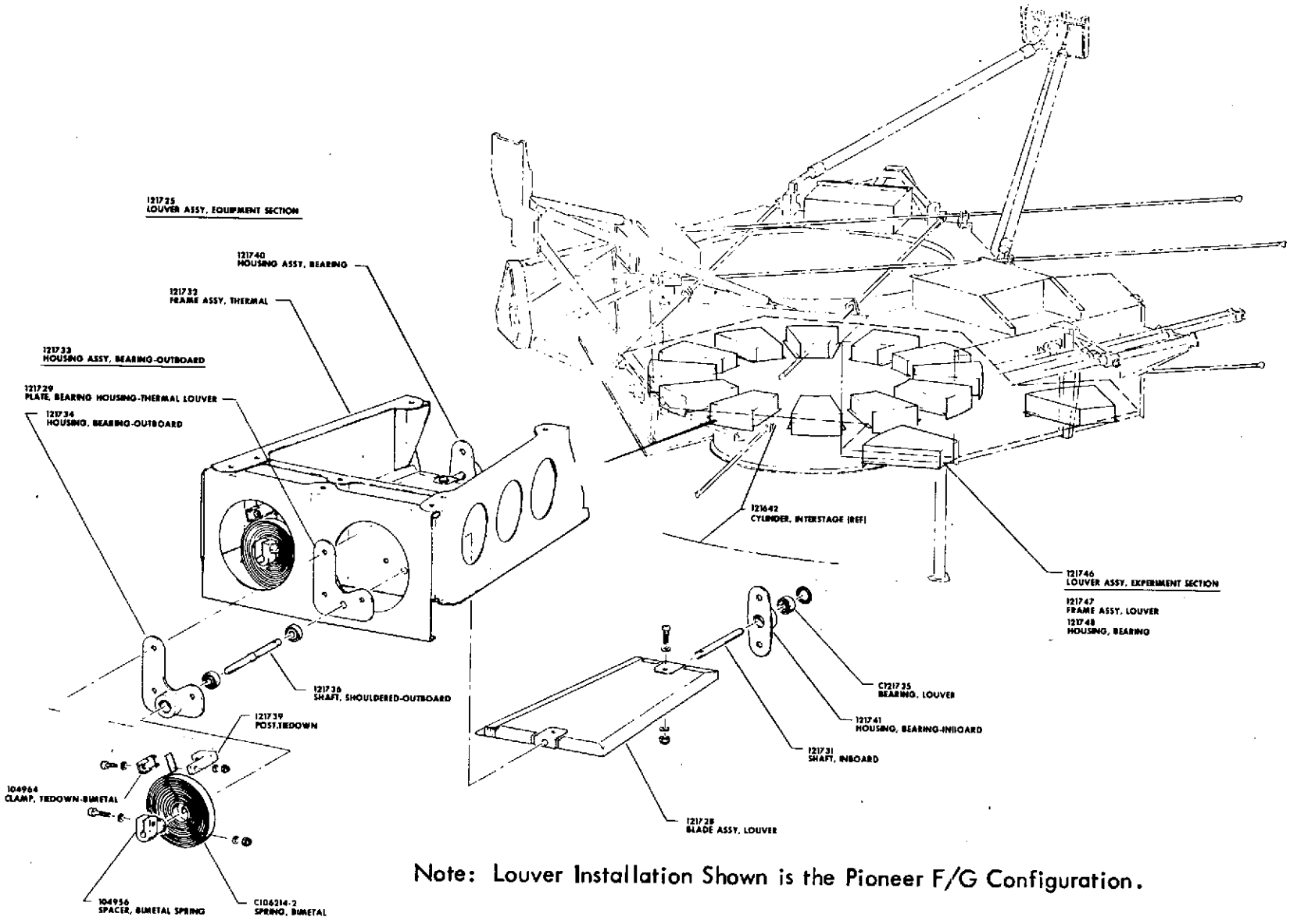

Note: Louver Installation Shown is the Pioneer F/G Configuration.

Figure 6-15. Pioneer F/G Louver Installation

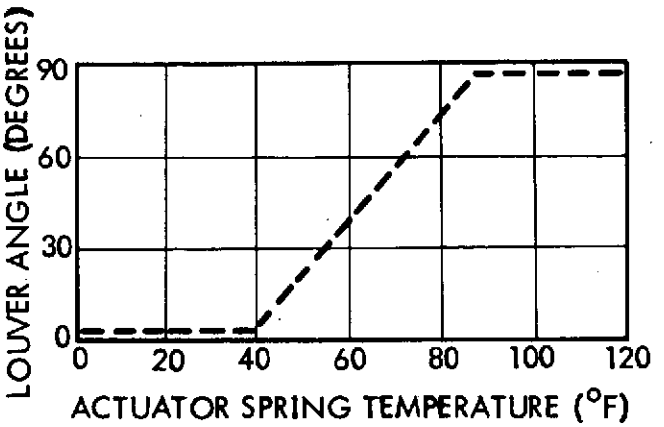

Figure 6-16. Typical Louver Performance Plot

6.2.1.1 Shunt Regulator Relocation

The PFG shunt regulators were located internal to the equipment compartment to maintain them above minimum temperature limits (-70°F) at EOL when their heat dissipation approaches 0. This location causes the PFG equipment compartment internal heat dissipation to vary by 32 watts (16 percent of maximum 1.0 AU side-sun total) from BOL to EOL. The shunt regulator location was chosen early in the program and did not present thermal control problems based on the first estimates of EOL RTG power output (104 watts). Later estimates of possible EOL RTG power output (82 watts) did present thermal control problems because the 22-watt power decrease produces a 22-watt (11 percent of maximum 1.0 AU side-sun total) decrease in PFG equipment compartment internal heat dissipation resulting in lower EOL temperatures. The decrease in EOL temperature was magnified by the fact that the PFG equipment compartment louvers were fully closed and could not control the lower heat rejection with a minimum of temperature change. The decrease in EOL RTG power from 104 watts to 82 watts necessitated the addition of propellant tank and line heaters and insulation late in the program. The temperature sensitivity of the PFG thermal control system with the louvers closed at the 82-watts EOL RTG power level also required several spacecraft thermal-vacuum tests to determine the proper amount and location of propellant system heater power required.

In order to minimize the temperature problems associated with BOL to EOL RTG power changes during the program, the SUAE spacecraft equipment compartment thermal control system incorporates the maximum possible BOL to EOL RTG power change control capability from the beginning. The maximum control capability is achieved by minimizing the change in internal equipment compartment heat dissipation from BOL to EOL. Locating the SUAE shunt regulators external to the equipment compartment eliminates a 62-watt heat dissipation change from BOL to EOL conditions. The SUAE equipment compartment internal electronic heat dissipation remains essentially constant from BOL to EOL even though the RTG power output varies from 240 to 188 watts (two RTG's operative).

The loss of one RTG can be tolerated on the SUAE bus even though the RTG and equipment compartment EOL internal electronic heat dissipation decreases by 50 percent. This large a decrease in RTG power output could not be tolerated if it were not for the fact that the SUAE shunt regulators are located external to the equipment compartment. The SUAE equipment compartment internal electronic heat dissipation would decrease 67 percent rather than 50 percent from BOL (two RTG's) to EOL (one RTG) if the shunt regulators were located inside the PCU as was done on PFG.

Locating the SUAE shunt regulators external to the equipment compartment does require an additional 4-watt thermal control heater for these units. The 4-watt thermal control heater maintains the shunt regulators above the -70°F minimum temperature limit at EOL when the normal unit heat dissipation approaches zero. PFG bimetal actuated louvers are mounted to the shunt regulator radiator plate to minimize EOL thermal control heater power required. The SUAE shunt regulators will be mounted to a radiating plate mounted to the aft surface of the equipment platform. The radiating plate will be conductively and radiatively decoupled from the platform with fiberglass isolators and multilayer insulation, respectively. The shunt regulator radiator plate

aft surface will be painted white and will have two three-bladed and one two-bladed PFG louver assemblies attached to it facing aft to control the heat loss to space. The 4-watt thermostatically controlled heater will evenly distribute the heat across the radiator plate (turn on -60°F, turn off -50°F).

6.2.1.2 1.0 AU Side-Sun Power Decrease

The PFG equipment compartment internal electronic heat dissipation is maintained at maximum levels during 1.0 AU side-sun environmental conditions at BOL to obtain maximum science and engineering data. During 1.0 AU side-sun conditions the PFG equipment compartment absorbs approximately 38 watts of additional solar heat compared to 1.0 AU front-sun conditions. The PFG equipment compartment louvers are sized to handle this additional 38-watt 1.0 AU side-sun heat input. When front-sun conditions are achieved, the PFG equipment compartment net heat input decreases 38 watts (19 percent of 1.0 AU side-sun total) and temperatures decrease approximately 24°F.

In order to maximize SUAE's ability to handle RTG BOL to EOL power output changes, it is recommended that the equipment compartment thermal control system should not be designed (louver area sizing) to 1.0 AU side-sun maximum power conditions. If the SUAE equipment compartment internal electronic heat dissipation can be reduced during 1.0 AU side-sun conditions to offset the increased absorbed solar heat input, the net heat input can be reduced to below 1.0 AU front-sun full power conditions. Designing the equipment compartment (louver area sizing) to full power 1.0 AU front-sun conditions will eliminate the approximate 38-watt decrease (19 percent of 1.0 AU side-sun total) in internal heat input associated with sun angle changes from BOL to EOL.

Turning off the SUAE X-band transmitter during 1.0 AU side-sun conditions (first 50 days of mission) will more than offset the 38-watt increase in absorbed solar heat input compared to 1.0 AU front-sun conditions. The S-band transmitter should be able to handle all engineering and science data requirements during this time period. If additional electronic heat dissipation reductions were required to hold 1.0 AU side-sun temperature below 1.0 AU front-sun maximum design

limit values, some experiments could be turned off, further reducing internal equipment compartment heat dissipation. Actually some of the planetary instruments would not normally be on so this would not be any penalty.

The powered down 1.0 AU side-sun approach is not used on PFG because the shunt regulators are located internal to the equipment compartment. If the PFG transmitter or experiments are turned off under 1.0 AU side-sun conditions, the major portion of the excess power will be dissipated in the shunt regulators in the PCU. The net heat dissipation in the PFG equipment compartment will not be decreased appreciably, only the distribution will change concentrating the heat in the PCU.

6.2.1.3 Increased Propellant Tank and Line Heaters Power

In order to maximize SUAE's ability to handle RTG BOL to EOL power output changes, the propellant tank and line heaters used on PFG should be retained on SUAE. The SUAE propellant tank and line heater power should be increased from PFG power values to take into account larger tank sizes and longer line lengths. The SUAE propellant tank heater budget should be 3 watts and the line heater budget should be 5 watts (3 watts internal to equipment compartment, 2 watts external).

The propellant tank and line heaters will not be required under normal two RTG operating conditions. If one RTG should fail, the equipment compartment internal heat dissipation will drop to levels requiring the propellant heaters to maintain tank and lines above $40^{\circ}F$. The predicted SUAE average equipment compartment temperature for various mission operating conditions is discussed in Paragraph 6.2.3 and summarized in Table 6-1.

6.2.2 Probe/Spacecraft Interface Thermal Control

The SUAE spacecraft thermal control system must maintain the conical adapter in contact with the probe within a specified temperature range (-20 to $+20^{\circ}F$) after launch to probe separation to satisfy probe nickel cadmium bootstrap battery storage temperature requirements (less than $32^{\circ}F$). The probe will dissipate a maximum of 4 watts of heat during the storage cruise time. The spacecraft conical adapter interface

Table 6-1. Predicted SUAE Compartment Temperatures

Bus	Case Number	Mission Time BOL: Beginning of Life EOL: End of Life	Distance From the Sun (AU)	Sun Angle to Spin Axis (Degrees)	Equipment Compartment Louver Area (ft^2)	Total Louver Area (ft^2)	Number of RTG's	RTG Power Output (Watts)	Internal Electrical Heat Dissipation (Watts)	Absolute Solar Heat (Watts)	Total Internal Heat Dissipation (Watts)	Average Equipment Temperature (°F)	Comments
SUAE	1	BOL	1.0	0	2.1	3.0	2	240	142	0	142	85	Sized louver area
(PFG)	(1)	(BOL)	(1.0)	(0)	(4.5)	(4.5)	(4)	(154)	(129)	(0)	(129)	(63)	
SUAE	2A	BOL	1.0	90	2.1	3.0	2	240	142	38	180	110	Must power down
(PFG)	(2A)	(BOL)	(1.0)	(90)	(4.5)	(4.5)	(4)	(154)	(129)	(38)	(167)	(87)	(Sized louver area)
SUAE	2B	BOL	1.0	90	2.1	3.0	2	240	92	38	130	78	X-band off
SUAE	2C	BOL	1.0	90	2.1	3.0	2	240	62	38	100	62	X-band, experiment off
SUAE	3A	EOL	10.0	0	2.1	3.0	2	188	142	0	142	85	Prior to probe separation
SUAE	3A'	EOL	10.0	0	2.1	3.0	2	188	140	0	140	84	Probe battery charge
SUAE	3B	EOL	10.0	0	2.1	3.0	2	188	152	0	152	90	After probe separation
(PFG)	(3B)	EOL	(5.5)	(0)	(4.5)	(4.5)	(4)	(104)	(89)	(0)	(89)	(39)	(Louvers just closed)
SUAE	4A	EOL	10.0	0	2.1	3.0	1	94	80	0	80	49	Prior to probe separation
SUAE	4A'	EOL	10.0	0	2.1	3.0	1	94	69	0	69	38	Probe battery charge
SUAE	4B	EOL	10.0	0	2.1	3.0	1	94	85	0	85	53	After probe separation
(PFG)	(4B)	(EOL)	(5.5)	(0)	(4.5)	(4.5)	(3)	(82)	(68)	(0)	(68)	(9.0)	(Propulsion heaters on)

temperature is maintained within specified limits by establishing a heat balance on the conical adapter. Heat input from the probe, spacecraft, thermal control heater and external environment (direct solar) is balanced by heat losses to space through the conical adapter insulation and radiator plate area. The conical adapter insulation and radiator area are sized to lose 5 watts of heat to space when the adapter is at $0^{\circ}F$. The spacecraft will normally transfer 1 watt of heat to the conical adapter by conduction down the central cylinder. The probe will supply up to 2 watts of heat to conical adapter by conduction across structural interface attachments. The conical adapter commandable thermal control heater will supply 2 watts of heat to maintain the adapter at the desired $0^{\circ}F$.

The conical adapter thermal control heater has a ± 2-watt control capability about the nominal 2-watt value required to compensate for variations in heat losses to space through the insulation and heat gains from the probe and spacecraft central cylinder. The conical adapter is essentially biased cold and maintained in the desired temperature range by the thermal control heater to account for variations in heat losses and gains due to unknowns. The probe/spacecraft structural interface attachments are sized to transfer at 2 watts of heat or more with a $10^{\circ}F$ temperature difference across the attachments. This will cause the probe to track the controlled conical adapter temperature within $10^{\circ}F$. Variations in probe/spacecraft structural thermal conductance are acceptable as long as the conductance is greater than the 0.2 watt/$^{\circ}F$ (2 watts/$10^{\circ}F$) minimum value specified. A higher conductance value will only cause the probe to track the controlled conical adapter temperature more closely.

The thermal control hardware used to maintain the required thermal interface temperature range is located on the adapter. It consists of controlled heat conduction paths from the probe, second surface mirror areas and multilayer insulation on the outside of the adapter, and strip heaters commandable at 1-watt increments on the inside. These components are illustrated in Figure 6-17, and described in Table 6-2.

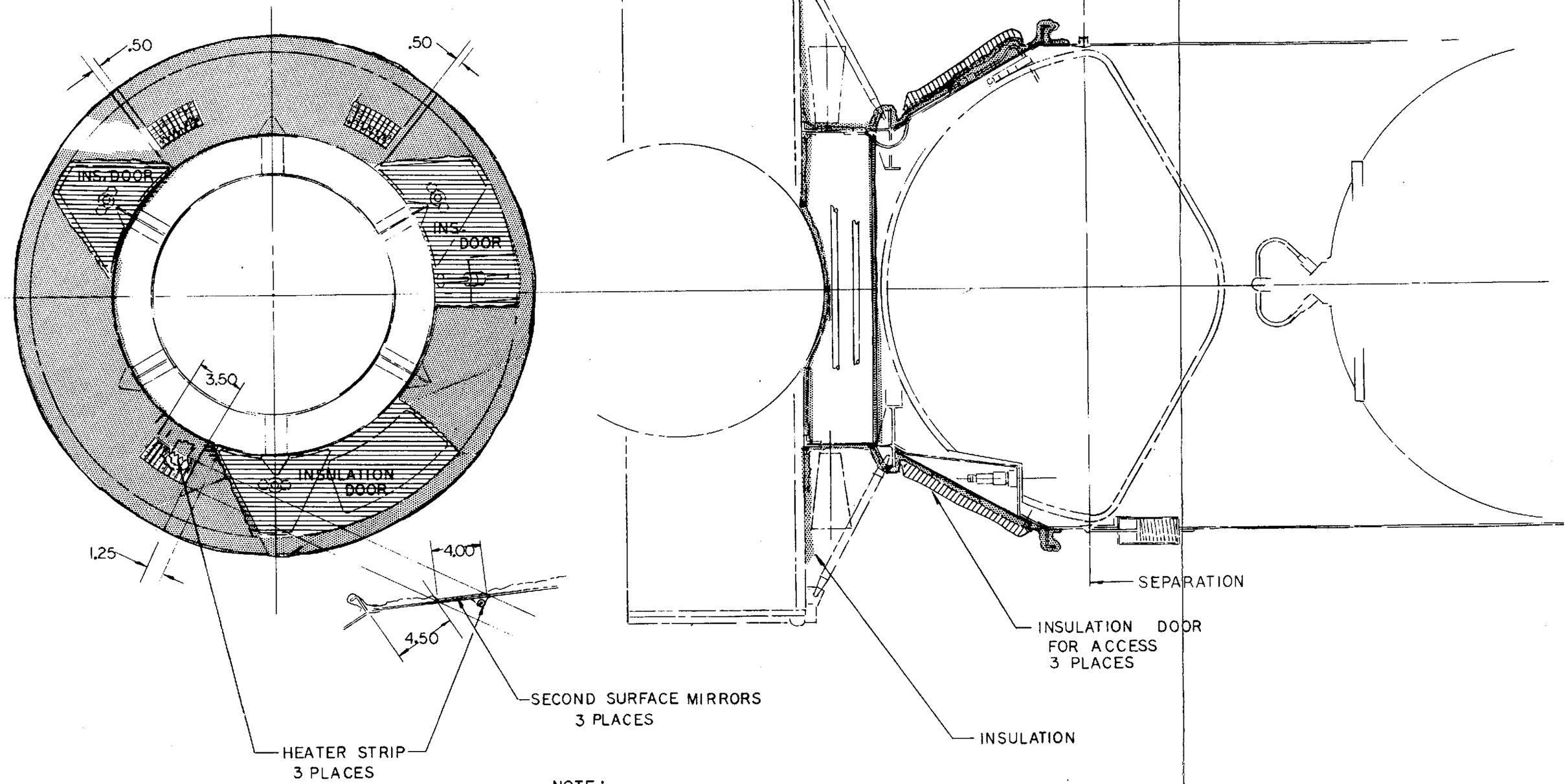

Figure 6-17. Probe Adapter Insulation Arrangement

Table 6-2. Thermal Control Hardware and Power Summary

A. Equipment Compartment and Shunt Regulator Thermal Control Hardware and Power Requirements

Description	SUAE Bus	Pioneer F/G
Two-blade louver units (number)	7.0	12.0
Three-blade louver units (number)	2.0	2.0
Total mounting area (ft^2)	3.0	4.5
Total blade area (ft^2)	2.0	3.0
Louver weight (lbs)	2.7	4.2
Change in weight from F/G (lbs)	(-1.5)	---
Insulation area (ft^2)	65.0	50.0
Insulation weight (lbs)	14.7	11.3
Change in weight from F/G (lbs)	+3.4	---
Thermal control heater requirements (W)	12.0	4.0
Change in heater requirements from F/G (W)	+8.0	---
Total thermal control hardware weight (lbs)	17.4	15.5
Change in weight from F/G (lbs)	+1.9	---

B. Probe/Spacecraft Interface Thermal Control Hardware and Power Requirement

Description	SUAE Bus
Conical adapter insulation area (ft^2) (24-layer aluminum Mylar)	10.0
Insulation weight (lbs)	2.5
Change in weight from F/G (lbs)	+2.5
Radiator plate area (ft^2) (Second surface mirrors-glass)	1.0
Radiator weight (lbs)	0.2
Change in weight from F/G (lbs)	+0.2
Thermal control heater requirements (W) (Commandable 0, 1, 2, 3, 4-watt levels)	4.0*
Change in heater requirements from F/G (W)	+4.0
Total thermal control hardware weight (lbs)	2.7
Change in weight from F/G (lbs)	+2.7

*Probe will require additional 2-watt to heat battery for charging.

The spacecraft thermal control system can satisfy the probe/spacecraft conical adapter interface temperature requirements (-20 to 20°F) to maintain the probe bootstrap battery below 32°F during most of the mission when the angle between the spin axis and solar vector is less than 30 degrees. During 1.0 AU side-sun and transition to front-sun (first 50 days of the mission) the spacecraft thermal control system will maintain the probe thermal interface at a slightly higher temperature range (30 to 70°F) unless non-earth pointing is maintained as discussed in Section 2.3.2. This will cause the probe battery to reach a maximum temperature of 80°F during the 50-day time period. It is desirasle to reserve two months of the probe battery six-month storage capability at <80°F for the first two months of the mission.

If the probe battery must be maintained below 32°F during 1.0 AU side-sun conditions (as well as front-sun), the conical adapter radiator area and thermal control heater power would have to be increased from 4 watts to 9 watts to hold the probe conical adapter interface temperature uniform for side- and front-sun conditions.

Table 6-1 summarizes predicted SUAE average equipment compartment temperatures for various mission phases, sun angles, and RTG power levels. The internal electronic, absorbed solar, and total internal heat dissipation are presented for reference. Average predicted PFG equipment compartment temperatures are presented in parentheses ( ) for similar conditions for comparison purposes. The following paragraphs discuss briefly the contents of Table 6-1. Table 6-3 presents expected SUAE unit acceptance temperature limit requirements for reference based on PFG data. Predicted SUAE average equipment compartment temperatures given in Table 6-1 indicate that the unit temperature limits can be satisfied with margin.

Case 1. BOL-1.0 AU Front-Sun. Case 1 is the BOL design hot case for SUAE. The SUAE equipment compartment louver area (2.1 ft^2) is sized to produce an average temperature of 85°F for this condition. Case 1 is an intermediate case for PFG. PFG Case 2A is used to size the equipment compartment louver area at an average temperature of 87°F.

Table 6-3. Expected SUAE Unit Acceptance Temperature Requirements (Based on PFG Data)

Unit	SUAE Acceptance (1) Temperature Limits	
	Minimum (°F)	Maximum (°F)
EXPERIMENTS	0	90
SUBSYSTEM EQUIPMENT		
Star Mapper Assembly (SMA)	0	75(2)
Despin Assembly	30	90
Propellant Tank	40(3)	140
CEA/CONSCAN	20	105
DSU/DDU/CDU	20	105
Receivers/Xmtr Driver	20	100
TWT	20	125
DTU	20	95
PCU	20	160
TRF	20	140
Inverter	20	145
Shunt*	-250	250
Shunt Regulator*	-70	212

*External to Equipment Compartment

Notes:

1. Table 6-1 predicted SUAE average equipment compartment temperature extremes of 90°F (Case 3B) and 38°F (Case 4B') indicate that units located internal to the compartment will be maintained within their respective acceptance temperature limits.
2. The SUAE SMA temperature will be maintained some 20°F lower (PFG data) than the average equipment compartment temperature (90°F) for hot case 3B conditions to satisfy the maximum temperature limit requirement of 75°F.
3. The SUAE propulsion tank and line heaters (8W) will maintain propellant temperatures above the 40°F minimum temperature limit for cold case 4B' conditions when the average equipment compartment is at 38°F.

Case 2A, 2B, 2C. BOL-1.0 AU Side-Sun. Case 2A predicts an excessively high SUAE average equipment compartment temperature (110°F) at maximum BOL internal electronics heat dissipation conditions. The SUAE average equipment compartment temperature can be decreased to an acceptable 78°F (Case 2B) or 62°F (Case 2C) by turning off the X-band transmitter or S-band transmitter and experiments, respectively. Case 2A is the BOL design hot case for PFG. The PFG equipment compartment louver area (4.5 ft^2) was sized to produce an average temperature of 87°F for this condition.

Case 3A, 3A', 3B. EOL-Front-Sun, No RTG Failed. Case 3A, 3A', and 3B predict SUAE EOL average equipment compartment temperatures (85, 84, 90°F, respectively, very little changed from BOL design temperatures. The SUAE equipment compartment temperature does not change appreciably as the RTG output decreases with life (240 watts to 188 watts) since the shunts and shunt regulators dissipate the variable excess power external to the equipment compartment. The PFG average equipment compartment temperature decreases from 63°F (Case 1) to 39°F (Case 3B) as the RTG power drops from 154 to 104 watts with mission time. The PFG temperature changes appreciably with mission time since the shunt regulators dissipate a large portion of the variable excess power internal to the equipment compartment (PCU).

Case 4A, 4A', 4B. EOL-Front-Sun, One RTG Failed. Cases 4A and 4B predict SUAE EOL one RTG failed average equipment compartment temperatures (49°F and 53°F, respectively) quite a bit lower than SUAE two RTG Case 3A and B temperatures. The SUAE Case 4A and 4B temperature are well above propellant minimum temperature limits (40°F) and thermal control heaters on propellant tank and internal lines would not be activated. During probe battery charge (Case 4A') the energy transferred to the probe reduces the heat dissipated internal to the equipment compartment causing the average temperature to drop to 39°F. Propellant tank and internal line heaters would be activated to maintain the propellant above 40°F under these conditions. The PFG average equipment compartment temperature (Case 4B, 9°F) is much lower than SUAE with one RTG failed.

6.2.3 Spacecraft-RTG Thermal Interaction

A rough preliminary thermal analysis is performed on the spacecraft-RTG interface. Of primary concern is the effect of the stowed RTG's (two) on the adjacent spacecraft insulation, the high-gain antenna dish and the star mapper. Temperature rise of the RTG still containing an inert fill gas before deployment is also of concern due to blockage from the high-gain antenna reducing the RTG's heat dissipation capability.

RTG's for the SUAE spacecraft each generate 2000 watts of heat of which about 120 watts is converted into electrical energy. This is a considerable increase over the Pioneer F/G RTG's which dissipate 650 watts of thermal energy each. Outer case temperature for the RTG is estimated to be from 250°C to 270°C (482°F to 518°F) in vacuum.

It is anticipated that RTG hot junction temperature can be maintained at 800°C before deployment if the inert gas within the RTG is not vented out. Preliminary calculations show average outer case temperature under this condition is approximately 520°F. Therefore to prevent overheating the RTG's hot junctions the inert fill gas is recommended not to be vented out until deployment.

Spacecraft components adjacent to the RTG's are analyzed with the RTG as a constant boundary at 270°C (518°F). Steady-state calculations are made, therefore subsequent temperatures discussed represent maxima that might not be reached before RTG deployment. Refer to Figure 6-18a.

The insulation directly opposite the end of the RTG is calculated to be 455°F. This temperature is rather conservative due to the fact the RTG's end temperature would probably be less than the 518°F assumed. However Kapton sheets can take temperatures up to 500°F and it is recommended 3-mil Kapton be used in the area under the RTG.

Insulation adjacent to the RTG side reaches only 345°F with full sun illumination. This area is not so severe; however, Kapton face sheets should still be used.

The star mapper sensor is assumed to be coated with white paint. Full solar illumination and the effect of the hot RTG can bring this unit

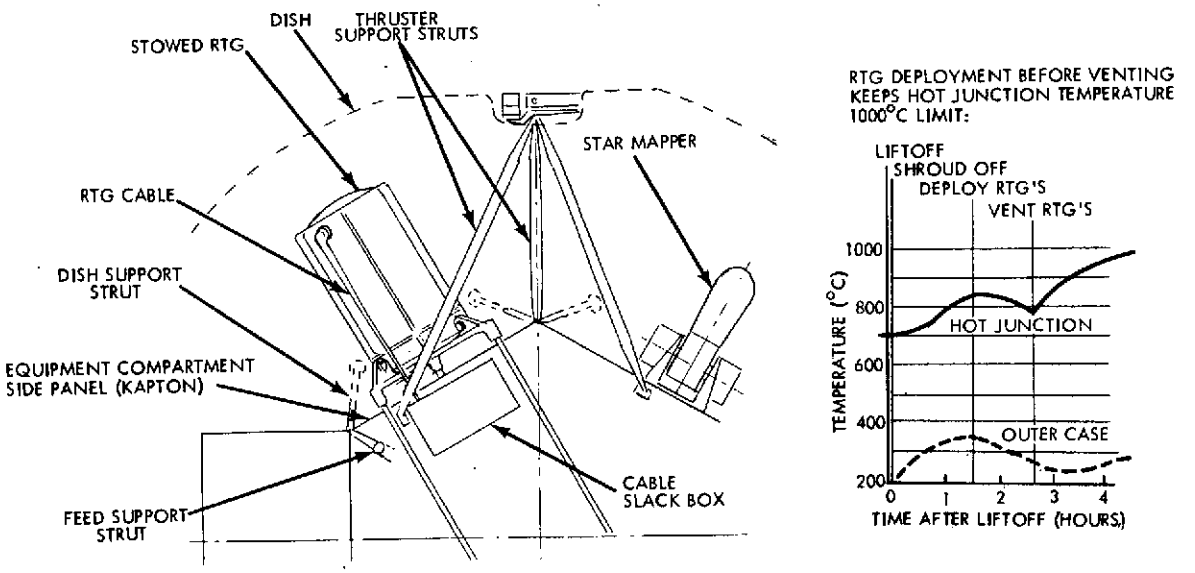

Figure 6-18a. RTG Thermal Interaction

up to its temperature limit of 140°F. This temperature however is influenced more by the solar input than by the RTG. Without solar illumination the effect of the RTG will not cause an over temperature condition for the star mapper.

The high-gain antenna dish, under worst case solar illumination on the front surface, will reach a maximum temperature near 80°F. The maximum temperature the dish can tolerate for structural integrity is 180°F.

Other problems due to the effect of the hot RTG's that require further analyses are the RTG support structure and the support struts for the antenna dish and thruster clusters. These supports will need to be thermally isolated with low-thermal conductivity material and be constructed to minimize heat leaks to the equipment compartments.

Thermal physical properties assumed for this preliminary analysis are listed below:

- RTG outer surface

$$\frac{\alpha}{\epsilon} = \frac{0.2}{0.85}$$

- High-gain antenna

  Back side $\frac{\alpha}{\epsilon} = \frac{0.17}{0.04}$ (polished aluminum)

  Front side $\frac{\alpha}{\epsilon} = \frac{0.21}{0.80}$ (white paint)

- Insulation

  Aluminized Kapton, Kapton side out

  $$\frac{\alpha}{\epsilon} = \frac{0.44}{0.78}$$

- Star mapper

  $\frac{\alpha}{\epsilon} = \frac{0.21}{0.80}$ (white paint)

6.2.4 Thermal Control Subsystem Hardware Comparison

Table 6-2 summarizes SUAE equipment compartment thermal control system hardware changes compared to PFG. Additional thermal control hardware required for probe/spacecraft interface control is also summarized. The following paragraph describes briefly the contents of Table 6-2.

6.2.4.1 Equipment Compartment and Shunt Regulator Hardware and Power Requirement Comparison

The SUAE equipment compartment will require only 2.1 ft^2 of louver mounting area compared to 4.5 ft^2 for PFG because the louvers do not have to reject shunt regulator heat and excess absorbed 1.0 AU side-sun heat as is required for PFG. The SUAE shunt regulators will require 0.9 ft^2 of louver mounting area, however, for the external equipment compartment location. SUAE shunt regulator louver area is minimized by allowing the units to radiate maximum excess power at nearly 212°F compared to 120°F for PFG. The total SUAE louver mounting area required (3.0 ft^2) is 1.5 ft^2 less than that required for PFG (4.5 ft^2). Figure 6-18b locates the SUAE louver area, compared to PFG. The SUAE equipment compartment insulation area (65 ft^2) is increased approximately 15 ft^2 from PFG (50 ft^2) to cover the probe/spacecraft interface electronics porch that was added.

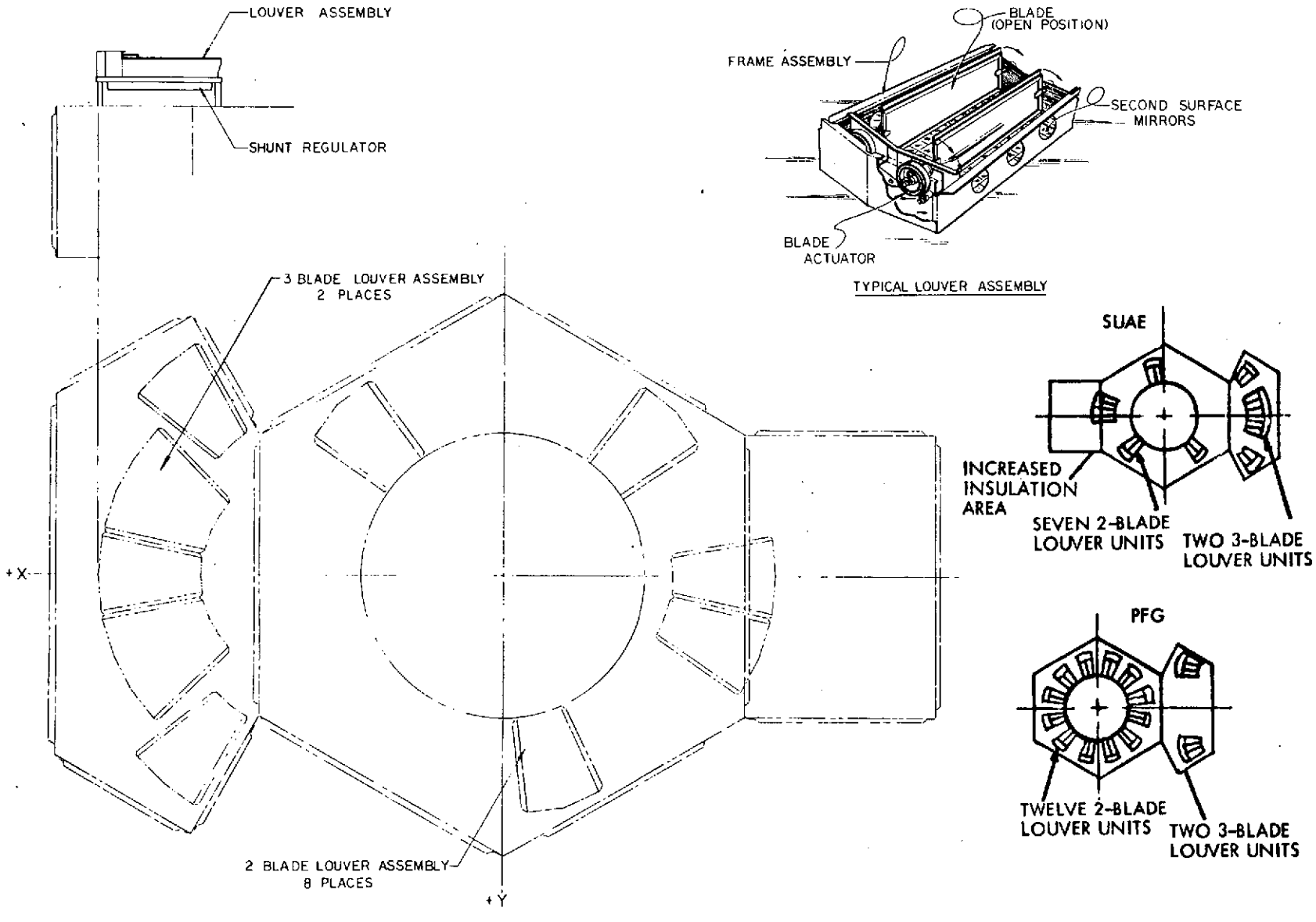

Figure 6-18b. SUAE Louver Configuration

The SUAE propellant tank and line heater power requirements (8.0W) were increased 4.0W from PFG (4.0W) to account for the larger tank size and longer line lengths compared to PFG. Locating the SUAE shunt regulators external to the equipment compartment created an additional requirement for 4.0W of heater power for these units. The total SUAE equipment compartment and shunt regulator thermal control heater power requirements (12.0W) is 8.0W more than the PFG requirement (4.0W).

The total SUAE equipment compartment thermal control hardware weight (17.4 lbs) is only 1.9 lbs more than the PFG (15.5 lbs) weight.

6.2.4.2 SUAE Probe/Spacecraft Interface Hardware and Power Requirements

The SUAE thermal control system must add 10.0 ft^2 of 24-layer aluminized Mylar insulation around the probe/spacecraft conical interface adapter to limit heat leaks to space. A second surface radiation area (approximately 1.0 ft^2) is required to establish the desired heat loss to space. A 4-watt thermal control heater is required to control the conical adapter temperature to the desired $+20^{\circ}F$ to $-20^{\circ}F$ range. The 4-watt heater will be commandable at 0, 1, 2, 3 and 4 watt levels to establish the required heat balance on the adapter. The various command power levels on the heater will allow the thermal control system to adjust for unknowns and changes in heat losses and gains from the probe, spacecraft and conical adapter. The probe battery will require 2 watts of power to warm the battery prior to and during battery charge.

The total probe/spacecraft thermal control hardware weight (2.7 lbs) is a 2.7-lb weight increase compared to PFG.

6.2.4.3 Total Thermal Control Hardware and Power Requirement Comparison

The total SUAE thermal control system hardware weight (17.4 + 2.7 = 20.1 pounds) is 4.6 pounds more than the PFG weight (15.5 lbs). The total SUAE thermal control system heat power requirement (16.0W) is 12.0W more than the PFG power requirement (4.0W). The 12.0W increase in SUAE heater power allows the spacecraft to maintain proper thermal control over greater BOL to EOL RTG power change ranges than PFG.

6.3 ATTITUDE CONTROL

6.3.1 ACS Description

6.3.1.1 General Description

The ACS subsystem consists of a sun sensor, terminal guidance (star) sensor, despin sensor assembly, and control electronics assembly. Except for the terminal guidance sensor, the ACS components are direct adaptations of the Pioneer F and G design. The subsystem units perform the following functions.

a) Sun Sensor Assembly (SSA). Provides sun pulses to establish a reference plane for open-loop precession and as a roll reference for experiments.

b) Terminal Guidance Sensor (TGS). Provides star, planet, or planetary satellite roll pulses and aspect measurements in order to enable proper targeting for the probe and the spacecraft during Saturn and Uranus encounter. Pulses may also serve as roll reference.

c) Despin Sensor Assembly (DSA). Provides a discrete onboard signal when spin speed has been reduced to a level safe for RTG deployment. The despin sensor is redundant and is used only once, during the initial despin maneuver.

d) Control Electronics Assembly (CEA). Processes sensor inputs, input commands and data, and produces outputs to fire the appropriate precession, velocity or spin control thrusters. The CEA controls power to all units within the CEA, provides sensor pulses for the spacecraft and scientific instruments, and processes the telemetry outputs.

The locations of the ACS equipment on the spacecraft are shown in Figures 6-19 and 6-2. The spacecraft coordinates are defined in the figures, with the +Z axis along the axis of symmetry of the high-gain antenna, the +X axis located in the direction of the magnetometer boom, and the +Y axis completing the orthogonal triad. The +Z axis also coincides with the spin axis with spin defined as positive along this axis as given by the right hand rule. The sun sensor is located near the

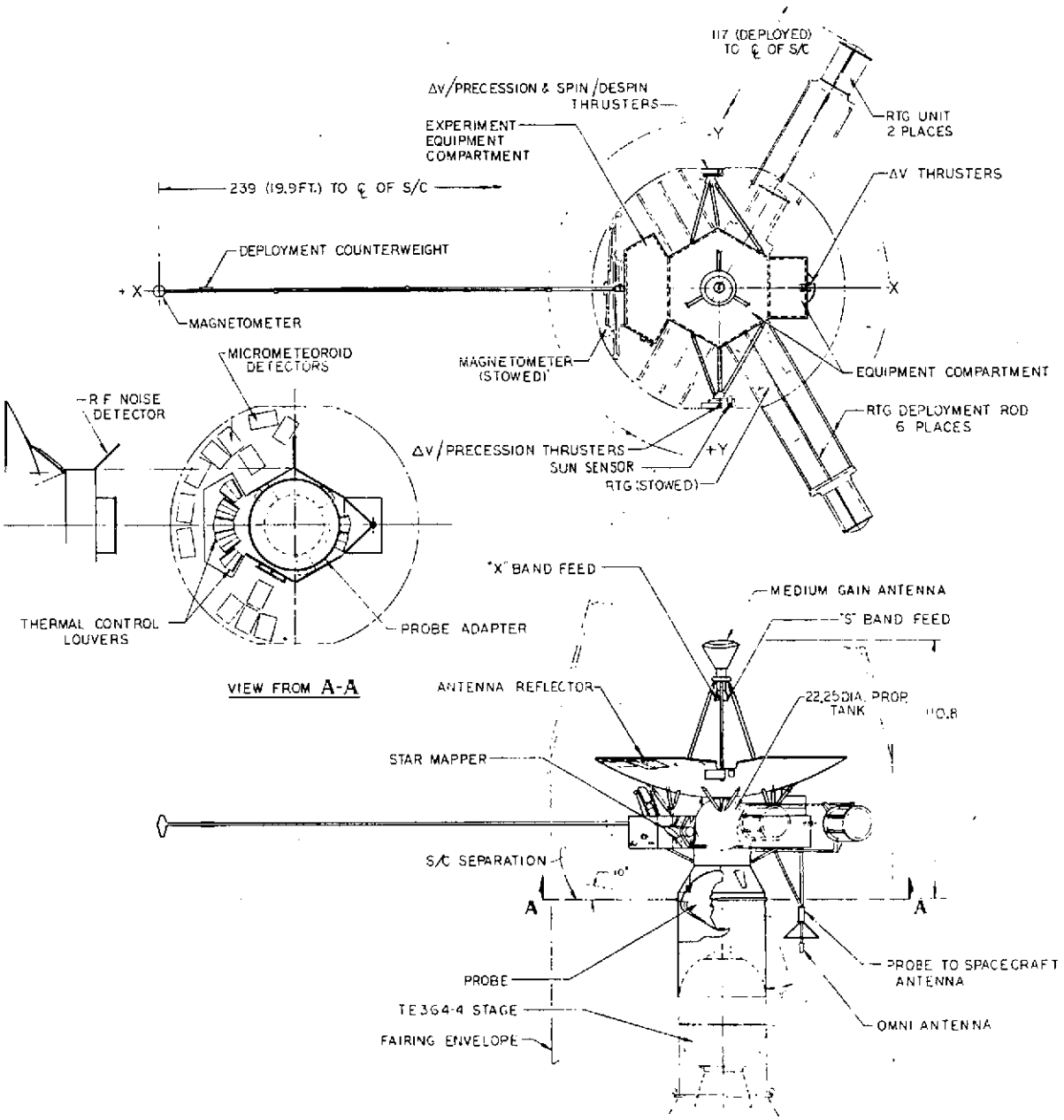

Figure 6-19. Pioneer Saturn Uranus Spacecraft Bus

edge of the high-gain dish nearest the +Y axis and has a field of view which lies in the +Y, ±Y plane. The sun is sensed as a pulse once per spacecraft revolution with the sun between 1 and 165 degrees from the spin axis. The terminal guidance sensor is a gimballed star mapper with a 3-degree field of view. The single gimbal axis is perpendicular to the spin axis such that the field of view sweeps a cone about the spin axis with the cone angle determined by the commanded gimbal angle. The despin sensors are located in the equipment compartment as shown in Figure 6-2, 37 inches from the c. g. of the spacecraft. The CEA is located within the equipment compartment as shown.

Although not part of the ACS subsystem, the eight propulsion thrusters perform an integral function with ACS and are also shown in Figure 6-19.

The four velocity precession thrusters (VPT) all have their line of action parallel to the Z axis and are located in pairs near the edge of the high-gain dish on the +Y and -Y axes. On command, these thrusters can be fired individually or in pairs, pulsed or continuously for precession or ΔV maneuvers.

The spin control thrusters (SCT) are located near the edge of the high-gain dish and on the -Y side. These thrusters can be fired either for spin control, or via alternate firing at 180-degrees intervals, for small ΔV maneuvers. The radial thrusters are located on the -X face of the equipment compartment with a joint line of action parallel to the X axis and through the nominal spacecraft c. g. after probe deployment. The individual lines of action of these thrusters pass 6 inches on either side of the c. g. Although normally used only for lateral ΔV maneuvers after probe release, these thrusters can also be used for spin control.

6. 3. 1. 2 ACS Functional Characteristics

The ACS (in conjunction with the propulsion subsystem) performs seven basic functions.

1) Despin the spacecraft from its high-speed stowed condition to an intermediate speed sufficient to permit RTG and magnetometer deployment.

2) Control the spin speed after deployment in response to ground commands.

3) Provide closed-loop precession pointing of the spin axis toward earth, using pulses from the conscan signal processor of the communications subsystem.

4) Provide control of the duration and direction of the midcourse velocity (ΔV) corrections using either programmed or real-time commands.

5) Provide roll reference signals for referencing the scientific experiments and spacecraft subsystems.

6) Provide star and planetary satellite cone and clock angles for attitude determination and for navigation near planetary encounter.

7) Provide telemetry of ACS functions indicative of unit status.

The processing of information (from sensors, ground commands, and ground data) to perform the functions of the ACS subsystem. The CEA is a single assembly (partially redundant) and is comprised of four subassemblies which are:

1) Program Storage and Execution Subassembly (PSE). The PSE contains the circuitry for storing and executing, upon command, the open-loop precession and velocity programs. The PSE also provides the major telemetry interface between the ACS and the DTU.

2) Sensor and Power Control Subassembly (SPC). The SPC processes the SSA and TGS outputs, provides logic for selecting the desired reference sensor and switches power to the PSE and DSL subassemblies of the ACS. The SPC also provides timing control and clock references to the CEA.

3) Duration and Steering Logic Subassemblies (DSL). Two identical and redundant DSL's (A and B) are employed in the CEA. Each DSL has complete capability, when appropriately commanded, of metering out the proper pulse length and steering the pulse to the appropriate valve drivers for executing any of the required maneuvers.

In addition to the CEA sensor processing, additional logic for gating, thresholding, and telemetry processing also exists in the terminal guidance sensor electronics. The detailed functions performed by the CEA and TGS in providing the desired operations are described in Table 6-4. There are 14 functions implemented in the CEA. These functions are in the subassemblies indicated.

Table 6-4. CEA and TGS Functions

Sensor and power control (SPC)	• Power and clock switching for the CEA • Octant generation and timing derivation • Star gating • Star delay • Sensor selection
Duration and steering logic (DSL)	• Thruster pulse duration selection • Thruster selection • Real-time operations • Conscan operation • Despin operation
Program storage and execution (PSE)	• Program storage • Program loading • Program execution • Telemetry
Terminal guidance sensor electronics (TGS)	• Star threshold selection • Star telemetry gate • Star aspect telemetry

There are four modes of spacecraft control: precession, ΔV, spin, and despin. In each mode, there are a number of ways to provide the stimulus to initiate a particular operation.

1) Precession. A precession can be accomplished four different ways: fixed angle, conscan, real time, and programmed.

a) Fixed Angle. A precession pulse is initiated at one of four fixed angles: 0, 90, 180 or 270 degrees after the roll reference pulse, following each command from the ground.

b) Conscan. The conscan mode is a closed-loop operation. Following a start closed-loop ground command, a precession pair will fire each time a conscan pulse is received and as long as an enable signal is present. Pulses normally will occur each third revolution of the spacecraft.

c) Real time. Real-time firing is initiated by ground command and fires a preselected valve pair for a preselected duration each time a command is received.

d) Programmed precession. A precession pulse is generated once per revolution at a programmed angle for a programmed period of time. A programmed delay period occurs before the precession or before a programmed ΔV.

2) ΔV. There are three ways of achieving a ΔV maneuver.

a) Programmed ΔV. Programmed ΔV is a continuous valve firing. Firing is terminated when one or the other or both signals from redundant counters in the PSE go false.

b) Real-Time ΔV. Real-time firing is initiated by ground command and fires a preselected valve pair for a preselected duration each time a real-time command is received.

c) ΔV/SCT Maneuver. A ΔV/SCT maneuver is enabled by ground command. The command enables the spin selection such that the first ΔV/SCT pulse (0 degree) will fire SCT No. 1 and the second pulse (180 degrees) will fire SCT No. 2 and will continue to alternate as long as ΔV/SCT stored program pulses are present.

d) ΔV Radial Thruster. A minor modification of (c) deletes the 180-degree pulse and controls radial thrusters (either or both) for pulsed, lateral ΔV.

3) Spin. The spin control command enables the selected pulse-width to fire SCT 1 to produce an increase in the spin speed or SCT 2 to produce a decrease.

4) Despin. Despin is initiated either by ground command or by the sequencer in the CDU. The despin stop signal is produced by two redundant despin sensor assemblies (DSA No. 1 and DSA No. 2). This signal is on during the despin operation until the spin speed is reduced to about 21 rpm (Pioneer F/G), and off below 21 rpm. This rpm setting may be changed for the SUAE spacecraft.

6.3.1.3 ACS Operation and Performance

The attitude control system block diagram in Figure 6-20 shows all system elements for providing the required functions given in Section 6.3.1.2. Roll reference signals are provided by the sun sensor and the star mapper; attitude and navigation data is provided by the star mapper, and thruster firing for ΔV, precession and spin control are provided by the CEA. The operation of these units and their interaction is described in the following paragraphs.

Sun Sensor Assembly Description. The sun sensor assembly (SSA) is a single assembly mounted at the edge of the high-gain antenna dish along the +Y axis as shown in Figure 6-21. It operates from 0.9 to 6.0 AU from the sun over a spin speed range of from 2 to 85 rpm, and gives 1 pulse/revolution. The sun sensor detects the sun as it passes through the Z, +Y plane and issues a pulse. The sun sensor consists of three channels with overlapping fields of view as shown in the figure. The sun sensor is internally redundant in channels 2 and 3, that are selectable by command. Each channel is designed using two detectors behind a slit. The sun pulse is derived using the differential photocurrent of the two detectors to eliminate the effect of sun size variation. Channel 1 of the SSA can be modified to operate out to about 10 AU, however, a major redesign will probably be required for a larger operating range. Roll pulses will be provided by the star mapper at Saturn and beyond.

Star Mapper Assembly. The star mapper assembly is the only ACS component requiring a new design. The mapper has a 3-degree field of view with a V-slit mask and a photomultiplier tube (PMT). Star pulses for roll reference are provided by the first slit with time of star crossing

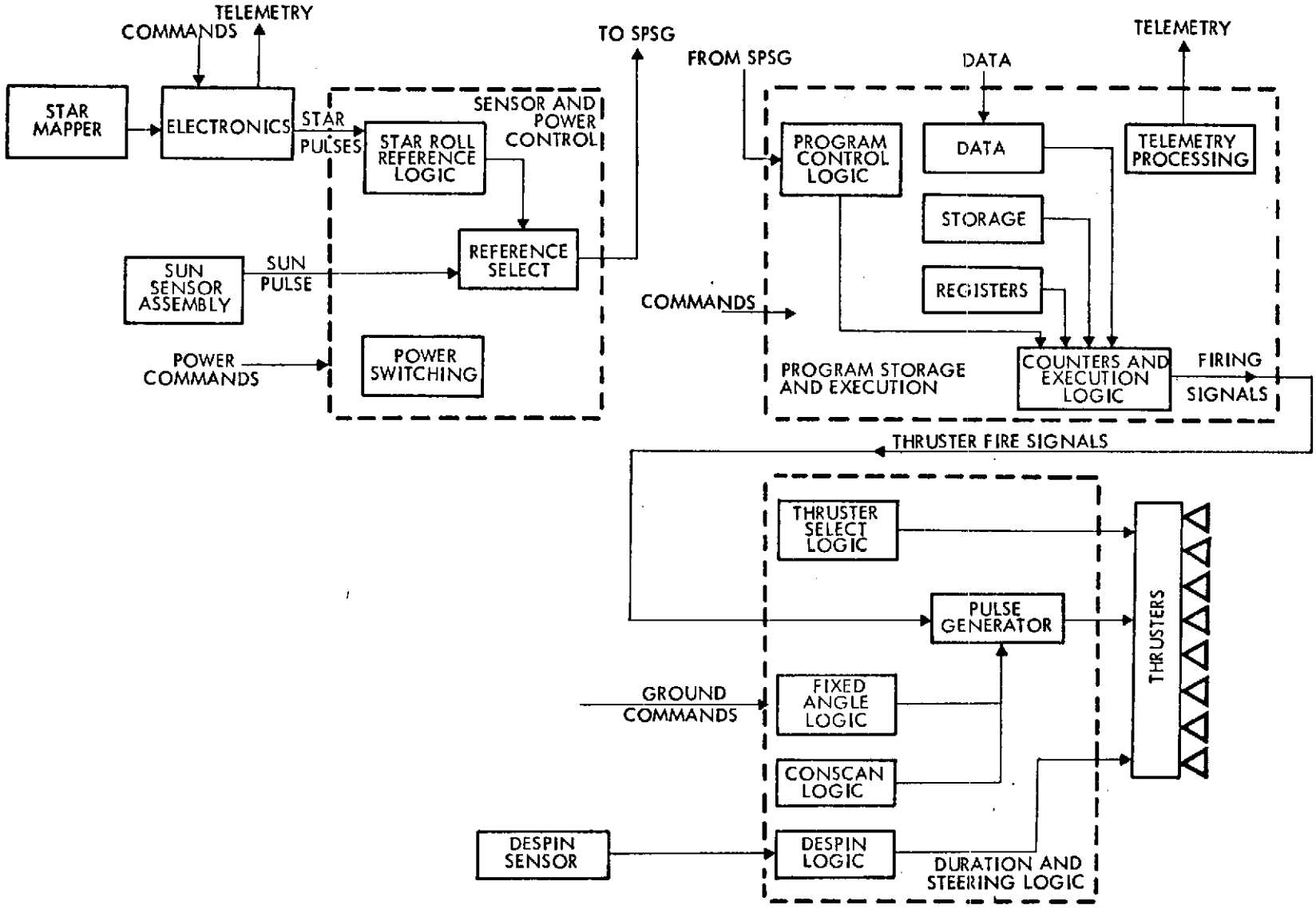

Figure 6-20. Control System Functional Block Diagram

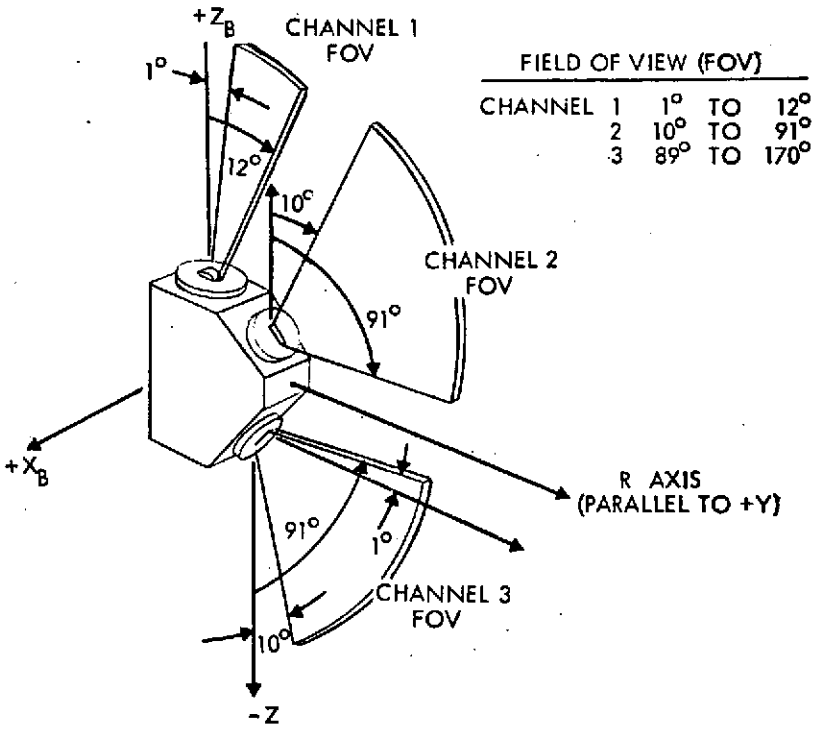

Figure 6-21. Sun Sensor Field of View

between the two slits giving a measure of star aspect. The FOV is gimballed such that the sweep cone can be selected to observe either stars or planetary satellites as required for terminal navigation during planetary encounter and probe deployment. The electronics for the mapper includes a preamplifier, filter circuitry, and telemetry logic. The mapper design is internally redundant with two PMT's behind split fiber optics. All electronics, telemetry circuits and logic is redundant. A detailed description of the new logic is given in Section 6.3.2.

Control Electronics Assembly

1) Sensor and Power Control (SPC). The left hand side of Figure 6-20 shows the SPC functions. The SPC processes star roll reference pulses (from the first slit) to enable a single star to be acquired. The logic includes an angle gate for star selection, a star counter, a star time gate to permit exclusion of all stars except the one desired, a star advance for selecting the next star, star coincidence and location logic

for identification, and star delay for moving the roll reference to the ecliptic plane (or any other plane) for science or attitude roll reference. An "auto star mode" logic also exists which, when enabled, provides a "replacement" pulse if the star roll pulse should not be detected for one revolution. Two successive missed pulses would cause a switch of roll reference to the sun sensor in this mode. Using the above logic elements, a star can be selected at the exclusion of all others, locked onto via the time gate, and maintained as a 1 pulse/revolution roll reference. Either this star reference or the sun pulse reference can be selected as roll reference which is provided to the spin period sector generator (SPSG) in the DTU. The SPSG in turn divides a revolution into 512 equal parts for use by science and the CEA.

The sensor and power control unit also provides power switching to other CEA subassemblies, the PSE and redundant DSL's described further in this section. Undervoltage detection and clock countdown also occurs in the SPC.

2) Program Storage and Execution (PSE). The PSE subassembly is used on the SUAE mission without modification of the Pioneer F/G design. The PSE provides circuitry for the storage and execution of spacecraft precession, velocity, and spin maneuvers. Program storage is accomplished with three sets of registers:

- No. 1 precession angle register
  No. 1 precession primary magnitude register
- Delay register
- ΔV primary magnitude register
- No. 2 precession angle register
  No. 2 precession primary magnitude register

These registers are shown in the CEA block diagram, Figure 6-20, which consists of the block diagrams of the three subassemblies of the CEA; the PSE (center), the SPC (left hand side), and a typical DSL.

Upon sequence initiation, the contents of the above registers are transferred into counters (angle, delay, primary magnitude, and redundant magnitude) in accordance with the occurrence of the following PSE program sequence states.

Sequence State	Function	Command
S0	Reset	ACX4
S1	Delay	ACX1
S2	No. 1 precession	
S3	Delay	
S4	Midcourse ΔV	
S5	Delay	
S6	No. 2 precession	
S7	Program complete	

All stored programs cycle through all eight sequence states unless interrupted by ground command.

The angle and magnitude data are used for a complete open-loop precession maneuver to obtain the proper attitude for the ΔV execution. The angle data enables the selection of an fixed-roll angle relative to the sun or star roll pulse. Precession is performed at this fixed angle for a duration determined by the magnitude data. The path of the spin axis described on a sphere about the spacecraft is that of a rhumb line (a straight line on a Mercator projection) with the length of the rhumb line determined by the magnitude data. The length of the rhumb line is determined by the total impulse of the thrusters which are calibrated both on the ground and in orbit. One method of controlling the thruster impulse is by counting the number of pulses issued during the maneuver; however, the total time for the maneuver is used in the magnitude counters since effects of spin speed coupling are thereby eliminated. Pioneer 10/11 experience has demonstrated that open-loop precession using this technique can obtain maneuver accuracies on the order of two percent of the desired precession magnitude.

Upon commanded initiation of the sequence the program enters state S1 from S0. At this time, the delay word is transferred into the primary magnitude counter. The counter down-counts the delay word at a 1/64 Hz rate, until its magnitude is 0. The sequence then automatically advances to state S2. At this time, the No. 1 primary and redundant

magnitude words are transferred into counter and precession begins. The angle is transferred and counted to fire the thrusters once each spacecraft revolution until the contents of the magnitude register is 0. The sequence then continues to advance to each state. In the ΔV state, S4, the axial thrusters selected are fired continuously for a predetermined time to achieve the ΔV. The program then continues with the second precession used for reorienting the spacecraft to earth pointing. Ground commands can be used to interrupt the program, continue the program from the point inhibited, step the program to the next state, or reset to state 0 for a new program.

The PSE also has a secondary mode for ΔV execution. This mode is called the ΔV/SCT mode where spin control thrusters (SCT's) can be fired alternately at 180 degrees intervals to cause a ΔV perpendicular to the spin axis. By changing thruster selection, this mode can also be used to fire the two radial thrusters simultaneously for ΔV execution. This choice of thrusters is a basic improvement in the Pioneer F/G capability in that precession coupling (significant in Pioneer F/G) has been greatly reduced such that much larger ΔV magnitudes can be executed between corrections for spin and precession coupling error.

Duration and Steering Logic Subassembly (DSL). The CEA contains two identical DSL subassemblies which provide redundant valve driving capability. Power to the DSL's is supplied by the SPC and is an "exclusive or," in that power can only be supplied to one DSL at a time. Each DSL drives one of the redundant valve coils such that either DSL, when powered, can drive the valves. The DSL accepts commands and signals from the CDU, PSE, CSP, SPC, DSA and provides response to these inputs by controlling the duration of firing, selection of valve pairs to be fired and finally by firing the desired valves.

The DSL generates the pulse widths for controlling the duration of the various valve firings, provides valve selection, provides logic to despin the spacecraft continuously until command to stop, and provides logic such that a precession may be made at preselected angles of 0, 90, 180 and 270 degrees relative to the roll pulse.

All functions normally programmable in the PSE can also be performed by individual ground commands in a DSL. Thruster combinations for either precession (VPT's), ΔV (VPT's or both radial thrusters) or spin (SCT's or an individual radial thruster) are first selected. Next one of the five pulse widths is selected; 2, 1, 0.5, 0.125 or 0.03125 seconds. Pulse execution is achieved either by a real-time fire command, or in the case of precession, a fixed-angle command is sent. The 0 and 180 degrees fixed-angle pulses cause precession either toward or away from the sun while 90 and 270 degrees fixed-angle commands cause precession perpendicular to the sunline-spin axis plane. All DSL ΔV commands are real-time pulses.

6.3.2 Changes From Pioneer F/G Design

6.3.2.1 Configuration Changes

The most significant ground rule in obtaining the control subsystem design is that design changes be minimized from the Pioneer F/G baseline. The required changes have been limited to the following:

- Delete Pioneer F/G SRA
- New design for TGS and electronics
- Modify DSP power switching and thruster selection logic
- Add two radial thrusters, two valve drivers and thruster operation logic, two real-time thruster commands, and redundant star reference logic.

Replacement of the SRA with the TGS. The Pioneer F/G SRA was a star pipper which produces only a roll reference. It is replaced by redundant terminal guidance sensors which provide both roll and aspect measurements for stars and planetary satellites, and has a commandable threshold permitting measurements for stars down to 4th visual magnitude. The 3-degree field of view of this sensor is shown in Figure 6-22 which also gives a summary of the sensor characteristics. The primary requirement for the TGS is to provide navigation near planetary encounter by observation of planetary satellites; however, roll reference is also supplied by locking onto a given star.

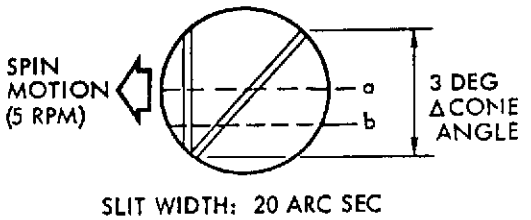

SLIT WIDTH: 20 ARC SEC

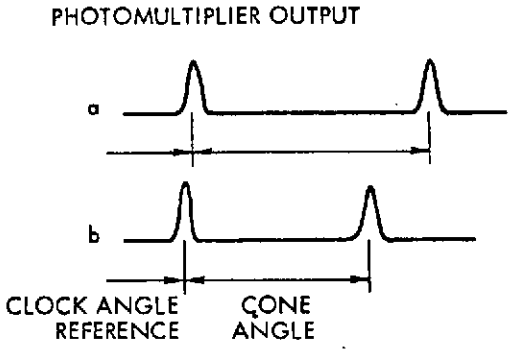

OPTICS

FOCAL LENGTH: 12 IN.

APERTURE DIAMETER: 3.42 IN.

SLIT DIMENSIONS: 3 DEG x 20 ARC SEC

ELECTRONICS

PHOTOMULTIPLIER SPECTRAL SENSITIVITY: S20
(370 nm TO 800 nm)

GAIN: 10^6

BANDWIDTH OF SIGNAL: 2.7 KHz

SENSITIVITY: 4TH MAGNITUDE

AVERAGE NUMBER OF STARS OF 4TH MAGNITUDE OR BRIGHTER IN 3 DEG SWATH, AT 140 DEG CONE ANGLE: 4 - 10

1σ - ACCURACY* (ARC SEC)

SINGLE POINT SOURCE:

	CONE ∢	CLOCK ∢
BIAS	2.3	2.3
NOISE	3.9	9.2

DETERMINATION OF TARGET DIRECTION FROM TWO OR MORE SOURCES:

BIAS	8	10
NOISE	15	25

*APPLIES TO 140 DEG CONE ANGLE. SOME DEGRADATION FOR TARGETS CLOSER TO SPIN AXIS.

Figure 6-22. Preliminary Star Mapper Characteristics

Operation of the TGS is shown in Figure 6-23. Existing Pioneer F/G star logic permits a single star roll pulse to be locked on as a "roll reference" and delayed to the ecliptic or other desired reference plane. All star/satellite outputs are also sent to telemetry, to determine roll and aspect angles relative to the desired roll reference.

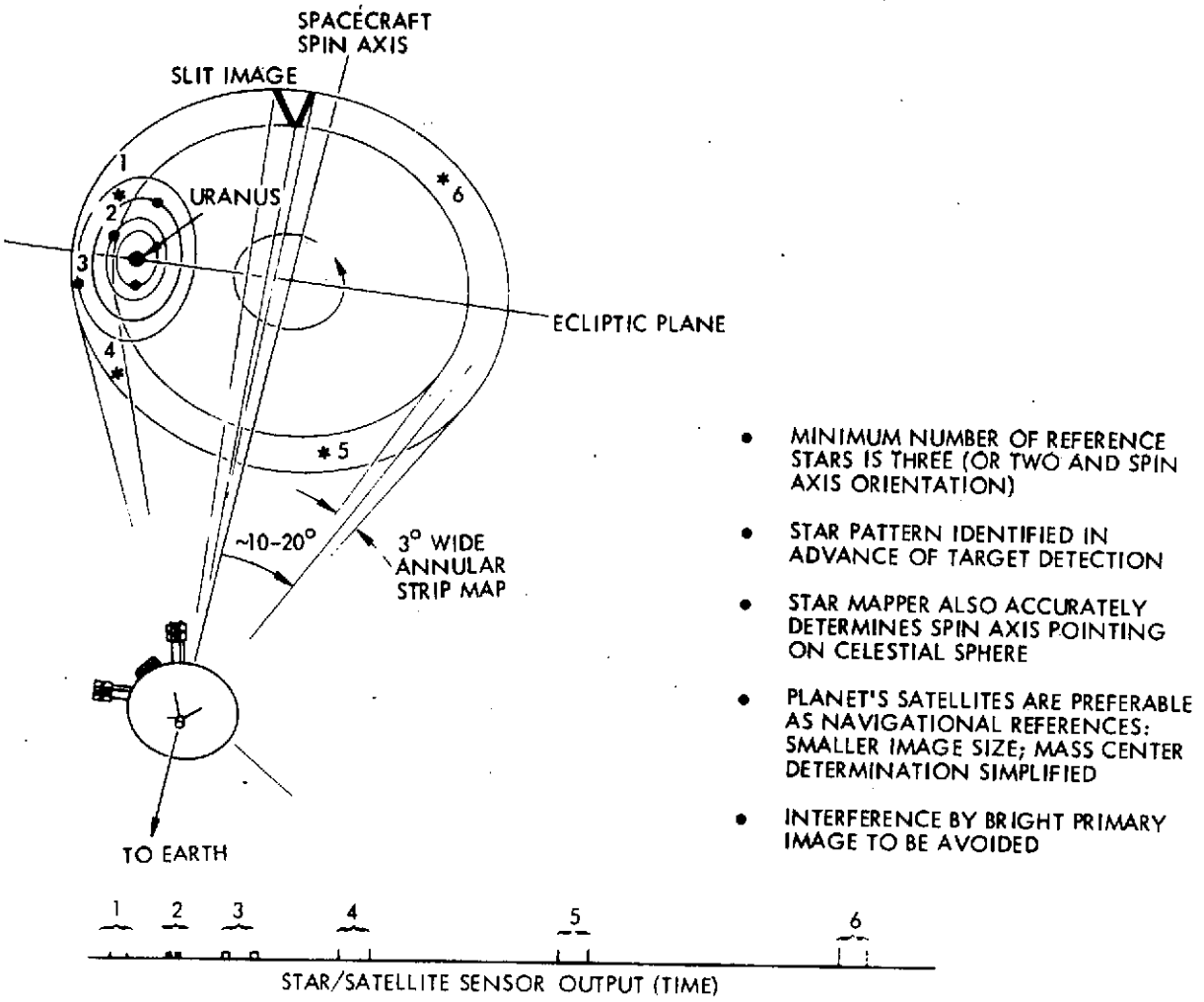

Figure 6-23. Terminal Navigation Sensor Operation

The star/satellite output times must be telemetered for all objects sensed. To limit the required electronics for the case where a large number of objects are observed, specific gating logic is envisioned. A commandable star telemetry gate (STG) has been selected such that only four objects are committed to telemetry. This enables the data to be stored in the DTU data buffer (144 bits) while awaiting the telemetry word gates. This saves storage registers for the roll angle telemetry which requires 19 bits for each star/satellite roll angle and 12 bits for each aspect measurement at a telemetry quantization of 3.1 arc seconds.

The commandable STG operates using the existing octant generator in the Pioneer F/G angle gate logic. The star telemetry gate starts on any selected octant and continues for a commanded number of octants

such that any portion of a revolution can be observed for its star/satellite content. Once the observation octants are selected, the objects in the field of view must be telemetered. One possible implementation of the logic required is shown in Figure 6-24. Operation of the circuit is performed in the following sequence.

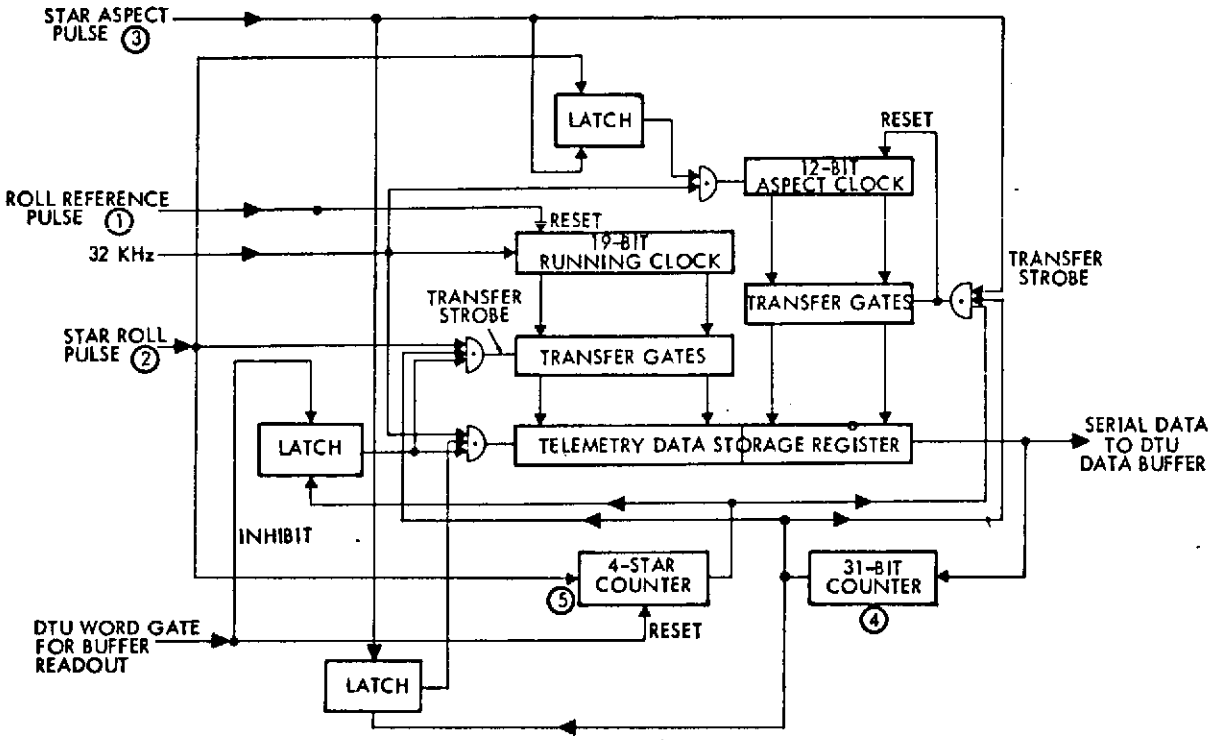

Figure 6-24. Star Mapper Roll Pulse and Aspect Time Measurement Telemetry Logic

1) The roll reference pulse starts a 19-bit running clock which is reset once/revolution of the spacecraft.

2) A star roll pulse causes a parallel transfer of the value in the running clock (T_i) into the telemetry storage register. This same star roll pulse starts the 12-bit star aspect clock. Further data transfer from the 19-bit running clock is inhibited until the data is shifted to the DTU data buffer for telemetry.

3) Arrival of a star aspect pulse from the second slit of the TGS causes transfer of the aspect clock accumulated time into the telemetry register and resets the aspect clock.

4) The star aspect pulse indicates that the 31 bits of star roll and aspect measurement have been transferred into storage. This data is then immediately clocked serially into the DTU buffer. During the clock interval, new star data cannot be taken (inhibited via 31-bit counter) but only 0.95 msec of data is lost.

5) Each star roll pulse is counted as it occurs. After four stars, the buffer is filled such that all data output must be inhibited until the buffer has been read into telemetry. Operation is re-enabled after the next roll reference pulse.

DSL Power Switching Modification. The DSL power switching modification is made to correct a Pioneer F/G design deficiency. Power turn-on of the DSL can possibly result in an inadvertent thruster firing. Separate switching of the 28-volt power to the thruster valve driver will correct this problem.

Thruster Configuration Changes. Two thrusters have been added to improve the lateral ΔV capability and also provide backup spin control. Redundant valve drivers and separate thruster selection logic must also be added. The separate logic would permit individual or combined firing of these thrusters in any of the modes of operation used on Pioneer F/G. These include real-time open loop, fixed-angle firing, or continuous firing via the program storage and execution assembly.

6.3.2.2 Hardware Implications

The configuration changes have direct weight and power requirements which have been obtained by sizing relative to Pioneer 10/11. The changes in weight and power are listed in Table 6-5.

Installation of ACS hardware is shown in Figure 6-2. The sun sensor and CEA are located identically as on Pioneer 10/11. The despin sensors have been moved over slightly, but are at the same radial distance from the c.g. prior to appendage deployment as on Pioneer 10/11. The gimballed star mapper is external to the equipment compartment, but has the same general location of the SRA on Pioneer 10/11.

Table 6-5. ACS Weight and Power Requirements

	Pioneer F/G		Pioneer SUAE	
	Weight	Power	Weight	Power
SSA	1.1	0.17	1.1	0.17
SRA	2.3	0.29	-	-
Shade	2.5			
CEA	6.24	2.70	8.3	3.2
PSE	1.30		1.3	
SPC	1.60		3.0	
DSL	2.06		2.6	
Interconnect and miscellaneous	1.28		1.4	
Star mapper (TGS)	-	-	12.0	5.00
Optics and sensors	-		5.0	
Shade	-		1.5	
Gimbal	-		4.5	
Electronics	-		1.0	
Despin sensor	0.40	-	0.4	-
Total	12.54 lb	3.16W	21.8 lb	8.4W

6.4 PROPULSION

The propulsion subsystem configuration for the SUAE mission is a direct adaptation of the Pioneer F/G design. It is a blowdown system using hydrazine as the propellant and gaseous nitrogen for pressurization. The principal components and their status is given in Table 6-6. The system is shown in Figure 6-25 in block diagram form.

6.4.1 Subsystem Requirements

The propulsion subsystem, in conjunction with the vehicle angular momentum, maintains the spacecraft attitude as required by the Attitude Control Subsystem. The propulsion subsystem not only maintains the magnitude and direction of the spacecraft spin vector, but in addition it can vary the spacecraft linear velocity within narrow limits. These so-called ΔV maneuvers originate from launch vehicle (injection) errors, from perturbations due to uncertainties associated with a flyby of Saturn, from uncertainties in our knowledge of the location of Uranus, and finally from the spacecraft deflection maneuver which is an integral part of the mission profile. Table 6-7 summarizes the nominal propulsion requirements for the Uranus mission. These requirements translate into the following propellant mass requirements:

	lbm
Spin control	3.4
Precession	17.6
ΔV (probe on)	65.1
ΔV (probe off)	25.1
Total propellant required	111.2

By using the same blowdown ratio as the Pioneer F/G, the tank size can be calculated as $\left(\frac{111}{60}\right)^{1/3} \times 16.5$ or a minimum diameter of 20.4 inches. (See also Section 3.5 above for a discussion of propulsion requirements).

The large ΔV maneuvers which are denoted as "$\perp$ earth line" in Table 6-7 are not easily accomplished by the Pioneer F/G thruster complement. A more detailed discussion of this new requirement (and alternate solutions) is presented in Appendix E.

Table 6-6. Propulsion System Modifications

ITEM	SAME AS PIONEER F/G	MODIFIED	REMARKS
PROPELLANT TANK		x	22.25-INCH DIAMETER TANK FROM LOCKHEED P-95 STAGE. REQUIRES REQUALIFICATION FOR HIGHER PRESSURE AND BLOWDOWN RATIO
THRUSTERS AND VALVES: • AXIAL AND CIRCUMFERENTIAL • ADDED RADIAL	x	 x	 --- DERIVED FROM PIONEER F/G, NEW INSTALLATION, ELECTRIC HEATERS
PRESSURE TRANSDUCERS	x		---
FILTERS	x		---
FILL AND DRAIN VALVES	x		---
LINE AND FITTINGS	x		PROPELLANT LINES TO NEW THRUSTER ASSEMBLY ADDED

6.4.2 Propellant Supply Assembly

The PSA consists of the following components.

- Propellant and pressurant tank
- Pressure transducer
- Filter
- Temperature transducer
- Fill and drain valves
- Interconnecting lines

The propellant and pressurant tank is a 22.25-inch diameter titanium sphere containing an elastomeric diaphragm. The tank stores hydrazine fuel on one side of the diaphragm, and contains the gaseous nitrogen used to expel the fuel on the other side.

The tank is loaded with fuel through the hydrazine fill port. At least 99 percent of the fuel loaded may be expelled during the mission.

Figure 6-26A shows the installation of the new PSA in the SUAE spacecraft. Depending on the final definition of spacecraft mission duty cycle requirements, the tank may be off-loaded, providing less than the maximum fuel capacity (Figure 6-26B).

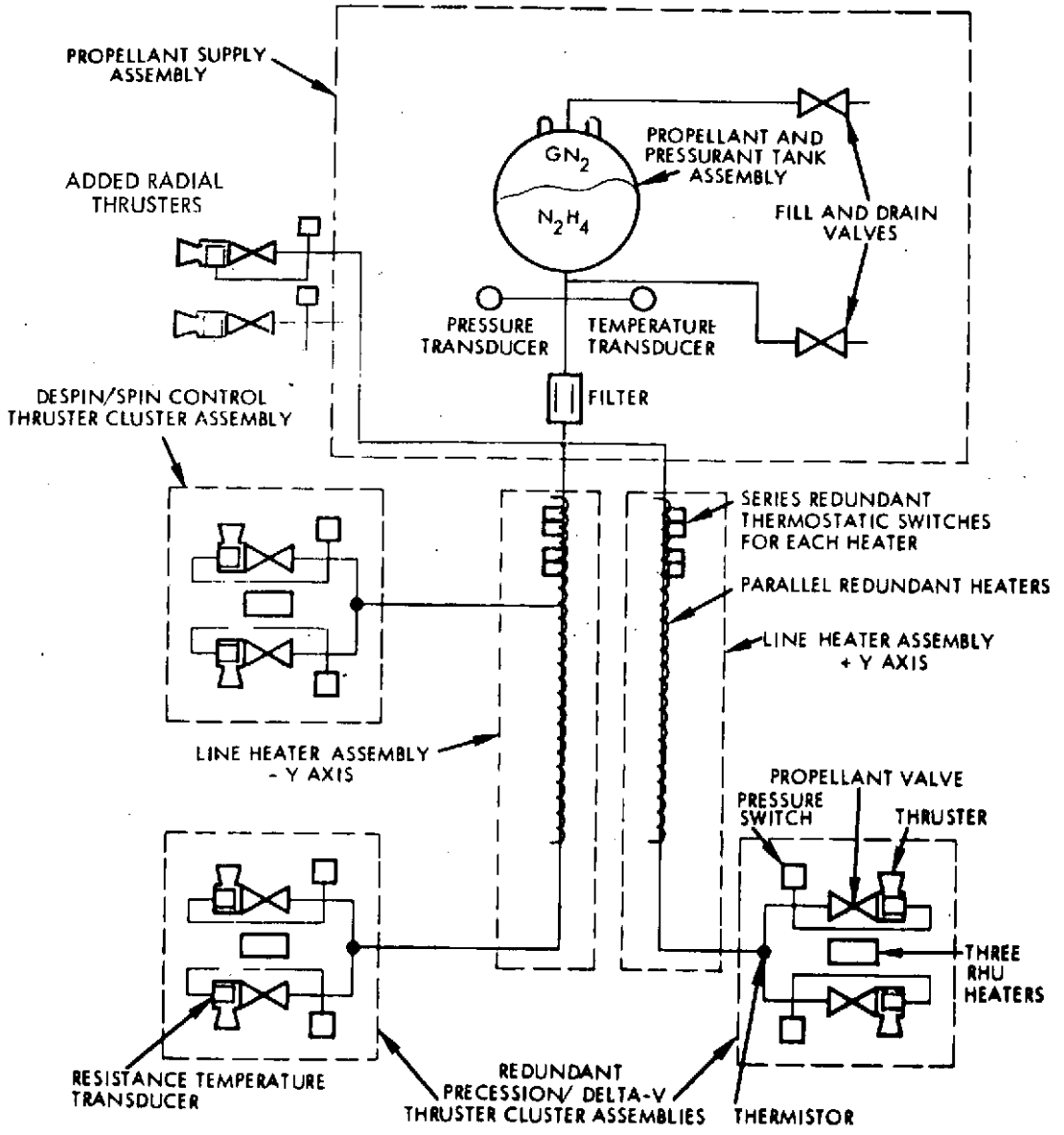

Figure 6-25. Propulsion Subsystem Mechanical Schematic Diagram

The gaseous nitrogen pressurant is loaded through the GN_2 fill port. The loaded pressure will depend on the amount of fuel loaded, but will generally range from 460-550 psia within the 40-110°F allowable temperature range. The pressure and temperature transducers located in the tank propellant outlet line provide a means for telemetry monitoring of subsystem blowdown status and estimating propellant utilization during the mission. A propellant filter in the line is designed to filter out all solid particles larger than 15 microns to preclude contamination and possible subsequent failure of the thrusters.

Table 6-7 . Propulsive Maneuver Requirements

A. ΔV REQUIREMENTS

TIME	MANEUVER	PROBE	MODE	ΔV M/SEC	DIRECTION	EFFICIENCY	EFFECTIVE I_{SP} (SEC)	EQUIVALENT ΔV M/SEC AT I_{SP} = 225 SEC	
E+5	LAUNCH VEHICLE CORRECTION NO. 1	ON	NORMAL	85*	ANY	1	225	85	
E+20	LAUNCH VEHICLE CORRECTION NO. 2	ON	NORMAL	3	ANY	1	225	3	
S-8	SATURN APPROACH TRIM	ON	EARTH LINE	5	⊥ EARTH LINE	0.85(1)	191	6	143.0 (PROBE ON)
S+40	SATURN DEPARTURE CORRECTION	ON	EARTH LINE	30	ANY	0.71(1)	160	42	
U-22	URANUS APPROACH TRIM	ON	EARTH LINE	5	ANY	0.71(1)	160	7.0	
U-20	SPACECRAFT DEFLECTION	OFF	EARTH LINE	30**	∥ EARTH LINE	1	225	30.0	80.0 (PROBE OFF)
				46**	⊥ EARTH LINE	0.97(2)	218	47.5	
U-10	URANUS APPROACH TRIM	OFF	EARTH LINE	2	ANY	0.65(2)	191	2.5	

(1) BASED ON $\eta = 0.85 = 0.97 \div 1.14$
(2) BASED ON $\eta = 0.97$

* NOMINAL TRAJECTORY: $\mu + 3\sigma = 81.1$ M/SEC (99%)
** MISSION ANALYSIS PRESENTATION, NOVEMBER 16, 1972

B. SPIN CONTROL REQUIREMENTS

APPENDAGES	ΔN (RPM)	I_{SP} (SEC)
STOWED	60	225 (CONTINUOUS)
DEPLOYED	18	160 (PULSED)

C. PRECESSION REQUIREMENTS

ANGLE PRECESSED THROUGH: $\Delta\theta$ = 1500 DEG
SPECIFIC IMPULSE: I_{SP} = 150 SEC
SPIN RATE: N = 4.8 RPM

(A)

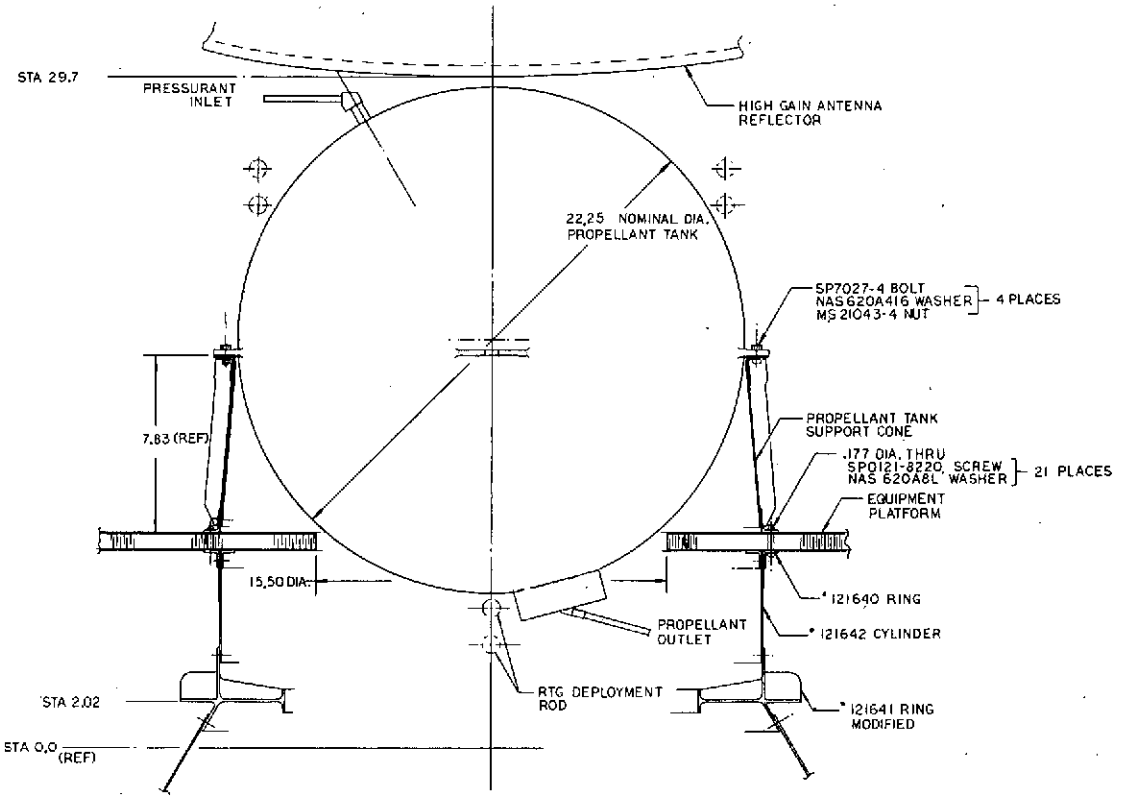

(B)

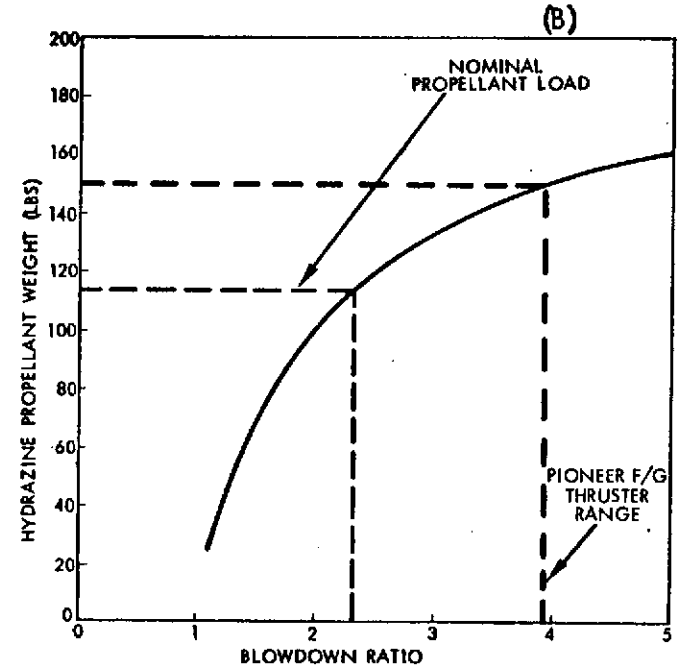

VOLUME: 5580 IN.^{3}
DIAMETER: 22.5 INCHES
WALL THICKNESS: 0.029 + 0.003 INCHES
MATERIAL: 6AL4V TITANIUM T3
STRENGTH: 165-185000 PSI
DIAPHRAGM: EPT-10 RUBBER
EXPULSION EFFICIENCY: 99%
WEIGHT: 13.3 LBS

Figure 6-26. Propellant Tank Loading Characteristics (P-95 Tank)

6.4.3 Thruster Cluster Assembly

All three TCAs used for spacecraft spin/despin, precession and ΔV maneuvers are identical in configuration. The typical TCA shown in Figure 6-27 consists of the following components.

- Two thrusters with 90 degree nozzles aligned in opposition to each other.
- Two propellant valves.
- Three one-watt radioisotope heater units.
- Two pressure switches (one for each thruster).
- Three temperature transducers.
- One baseplate.
- Upper and lower heat shields.

Fuel enters the TCA through a single inlet line to a manifold block which divides the flow to the individual thrusters. Fuel inlet temperature is monitored via telemetry by a thermistor surface mounted on the manifold. On-off control of flow to each thruster is provided by the solenoid operated propellant valve which contains re ındant coils and seats.

The three radioisotope heate_ units (RHUs) provide the thermal energy necessary to prevent freezing of the hydrazine in the TCA during periods of non-operation. Two resistance type temperature transducers, one each surface mounted on the thruster bodies near the catalyst chamber, provide telemetry indication of thruster temperatures. The two pressure switches, one per thruster, sense the buildup in chamber pressure at the initiation of a thruster pulse or steady-state firing and close an electrical circuit used to verify thruster operation. The switch returns to the open position upon thrust termination.

6.4.4 Line Heater Assembly

The two propellant line heater assemblies (LHA) have the dual functions of directing propellant flow from the PSA to the TCAs, and also maintaining the propellant above freezing. The LHA's (shown in Figure 6-28) consists of the following components: propellant line, two electrical heaters, and four thermostats. One of the heaters is used as a primary circuit and

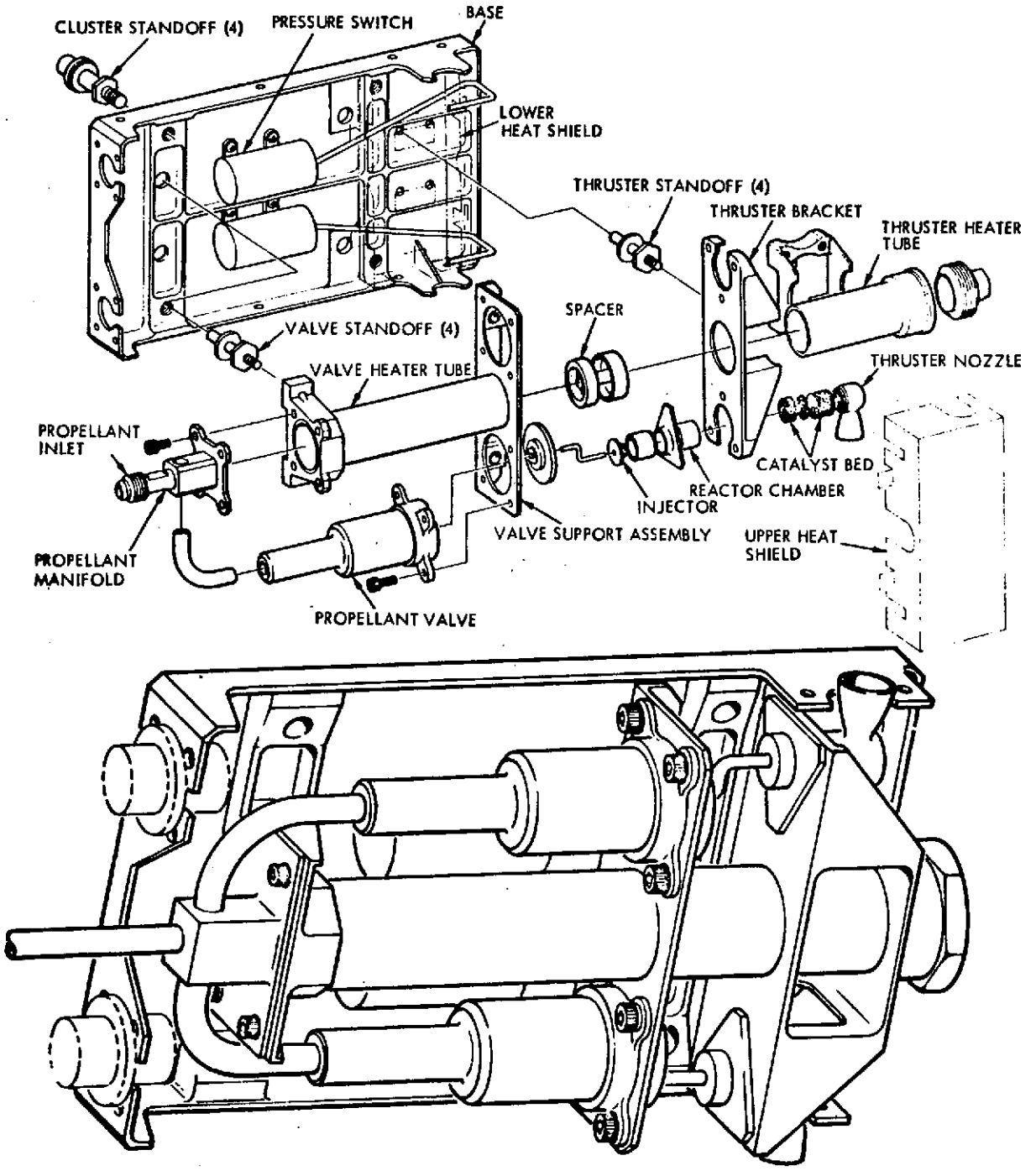

Figure 6-27. Thruster Cluster Assembly

the other is a secondary redundant circuit. The primary (active) heater element controls the propellant temperature from 55-90°F and the secondary (standby) element is set to control between temperatures of 45-90°F. The heaters are controlled on/off by the four thermostats

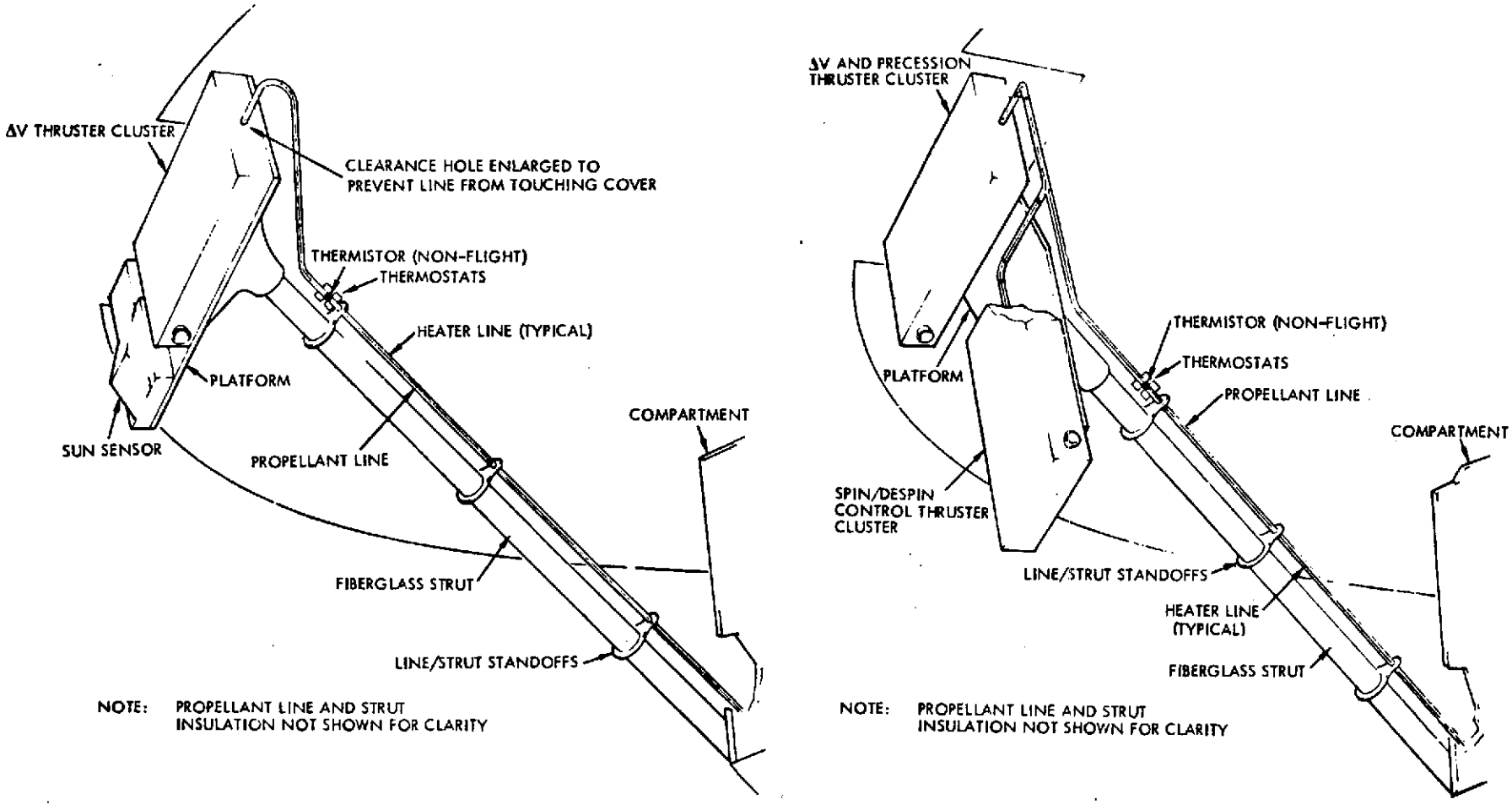

Figure 6-28. External Line Heater Assemblies

(two for each circuit) which are mounted on the propellant line near the PSA.

The entire LHA is wrapped with layers of aluminized mylar insulation. Three high-thermal resistance standoffs made of fiberglass are provided to attach the LHA to platform struts to minimize thermal losses.

6.4.5 Radial Thruster Assembly

Installation of the radial thruster pair is given in Figure 6-29. Each thruster is offset slightly to provide a line-of-force that clears the c.g. thus providing spin/despin capability. The control valve is inside the compartment, and the openings in the compartment will be sealed with insulation. A layer of Kapton may also be required on the external surface to protect the insulation blanket.

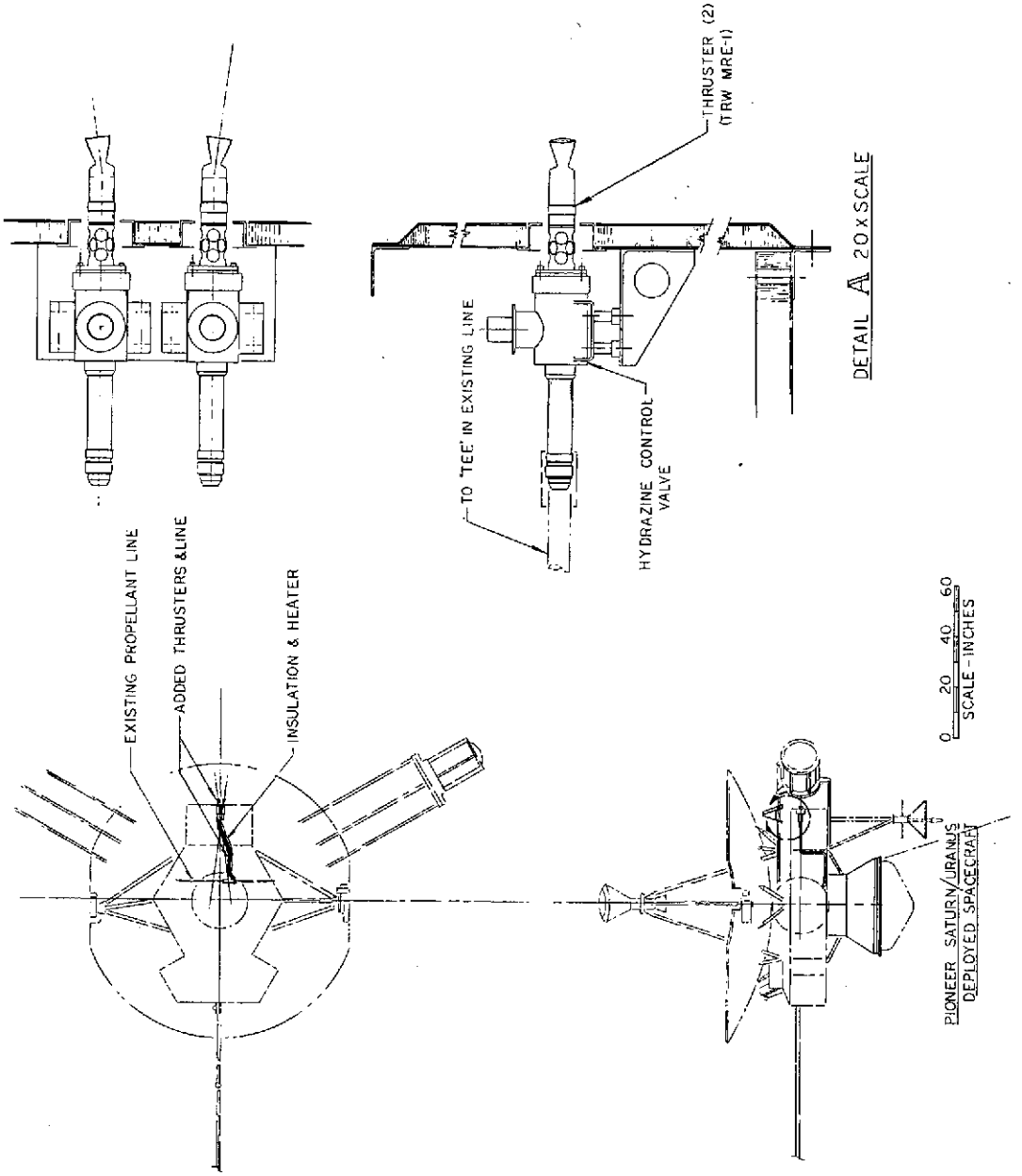

Figure 6-29. Radial Thruster Installation

6.5 ELECTRICAL POWER

6.5.1 Subsystem Description

The electrical power subsystem, as shown in Figure 6-30, consists of two MHW "short stack" RTG's, PCU, inverter assembly, CTRF, a shunt regulator which consists of a shunt regulator assembly in the equipment compartment, and an externally mounted shunt radiator. The PCU, in conjunction with the shunt regulator, regulates the main bus to 28 VDC ±2 percent for all conditions of load as long as RTG power is in excess of load demand at 28 VDC. The PCU also provides cross-strapping of the RTG's, fault isolation for the RTG's and loads, probe battery charging, and certain power system diagnostic telemetry. The inverter assembly, in conjunction with the CTRF, provides conditioned secondary power to the spacecraft loads. All experiment loads are fed from the regulated 28 VDC main bus. Table 6-8 summarizes the functions of these components and shows how they will be modified from the Pioneer F/G design. A comparison of the physical characteristics of these components versus those of Pioneer F/G is given in Table 6-9.

6.5.2 RTG's

The selected RTG for the mission is the MHW "short stack" that has a beginning of life power output of 120W at 25 VDC. Assuming this unit can be designed to provide the same power at 28 VDC; two of these units will be required to support the maximum steady-state encounter load of 168.5 watts plus 18.5 for pulsed loads (see Section 5.6). The characteristics of this source, along with other candidates considered, are given in Section 7.1. The two RTG's are expected to provide a total power of 125W at launch in air (i.e., on the launch stand), 240W at launch in vacuum, and decreasing to 188W seven years after launch.

6.5.3 CTRF

The CTRF contains redundant transformer-rectifier-filters whose outputs are regulated either by series dissipative or switching regulators. Each voltage output of the CTRF (with the exception of two outputs to nonredundant subsystem units) have separate parallel redundant TRF regulators. A combination of automatic or command switching between redundant regulators is provided.

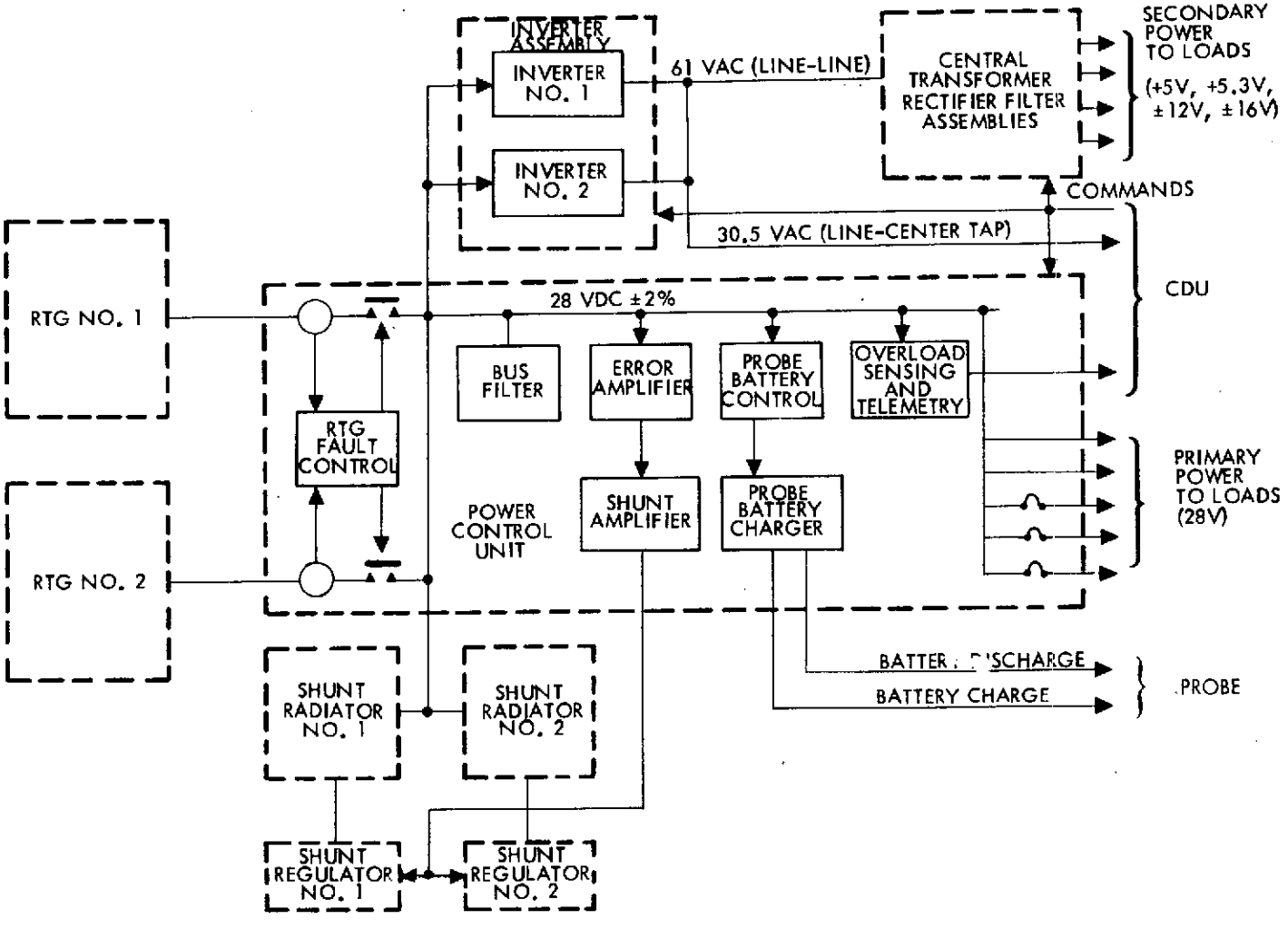

Figure 6-30. Electric Power Subsystem Block Diagram

Table 6-8. Electric Power Subsystem Functional Characteristics

COMPONENT	FUNCTION	MODIFICATION TO PIONEER F/G DESIGN
RTG	GENERATE POWER	REPLACE FOUR 39-WATT, 4.2-VOLT UNITS WITH TWO 120-WATT, 28-VOLT UNITS
POWER CONTROL UNIT	CROSS-STRAP RTG OUTPUTS PROVIDE RTG FAULT ISOLATION DISTRIBUTE PRIMARY DC POWER TO LOADS PROVIDE POWER CIRCUIT PROTECTION REGULATE DC BUS TO 28 VDC ±2% CONTROL DISSIPATION OF EXCESS RTG POWER PROVIDE OVERLOAD SENSING PROVIDE PROBE BATTERY CHARGING CONDITION DIAGNOSTIC EPS TELEMETRY	REMOVE BATTERY CHARGER, BATTERY DISCHARGE REGULATOR REMOVE SHUNT REGULATOR MODIFY CONTROL LOGIC, DC BUS FILTER, TELEMETRY CONDITIONING ADD RTG FAULT CONTROL LOGIC, RTG CROSS-STRAPPING, PROBE BATTERY CHARGER, LOAD DISTRIBUTION CIRCUITS
SHUNT REGULATOR	IN CONJUNCTION WITH SHUNT RADIATOR, DISSIPATE EXCESS RTG POWER	REPACKAGE EXISTING PCU CIRCUIT INTO SEPARATE UNIT
SHUNT RADIATOR	IN CONJUNCTION WITH SHUNT REGULATOR, DISSIPATE EXCESS RTG POWER	INCREASE DISSIPATION CAPABILITY TO 152W
INVERTER ASSEMBLY	INVERT 28 VDC TO 61 VAC, 2.5 KHZ PROVIDE INVERTER FAULT ISOLATION	MODIFY POWER STAGES TO ACCEPT 28 VDC INSTEAD OF 4.2 VDC REDUCE POWER CAPABILITY FROM 160W TO 60 WATTS
CTRF	PROVIDE CONDITIONED AND REGULATED POWER AT SEVERAL VOLTAGES TO SPACECRAFT POWER USERS	INCREASE CAPACITY OF DATA STORAGE UNIT TRF INCREASE CAPACITY OF ATTITUDE CONTROL TRF'S ADD X-BAND TRANSMITTER DRIVER TRF'S ASSEMBLE EXISTING, MODIFIED AND NEW TRF'S TO FORM TWO SEPARATE CTRF'S

A typical CTRF user subsystem power supply is shown in Figure 6-31. The inputs are fused to prevent a low-impedance fault in the CTRF from overloading the AC bus input. Two basic types of regulators are used. The first is a series dissipative regulator and is used for all voltages where the current requirements are less than 100 mA. The second regulator type is a switching regulator and is used for the +5 volt outputs where the current requirements exceed 100 mA. This is done to limit power dissipation and increase efficiency. Each output is current limited by the regulators. This prevents subsystem load faults from propagating back to the inverters and to the main bus.

Table 6-9. Electric Power Subsystem Physical Characteristics

COMPONENT	PIONEER F/G			SATURN URANUS SPACECRAFT		
	NO. OF UNITS	SIZE (IN.)	WEIGHT (LBS)	NO. OF UNITS	SIZE (IN.)	WEIGHT (LBS)
RTG	4	15.7D x 11.1L	30.1 (120.4)	2	15.7D x 21.0L	70.0 (140.0)
POWER CONTROL UNIT	1	6.0 x 8.0 x 9.3H	10.9	1	6.0 x 8.0 x 7.7H	7.3
INVERTER ASSEMBLY	2	4.5 x 6.0 x 7.0H	5.1 (10.2)	1	4.5 x 6.0 x 7.0H	5.1
SHUNT REGULATOR ASSEMBLY				1	6.0 x 8.0 x 1.6H	2.2
SHUNT RADIATOR	1	12.5 x 15.0 x 1.9H	0.8	1	243 $in.^2$	1.0
CENTRAL TRF UNIT A	1	6.0 x 8.0 x 11.3H	11.8	1	6.0 x 8.0 x 6.9H	7.2
CENTRAL TRF UNIT B				1	6.0 x 8.0 x 6.1H	6.4
BATTERY	1	10.0 x 8.2 x 2.7H	5.2			
TOTALS			159.3			169.2

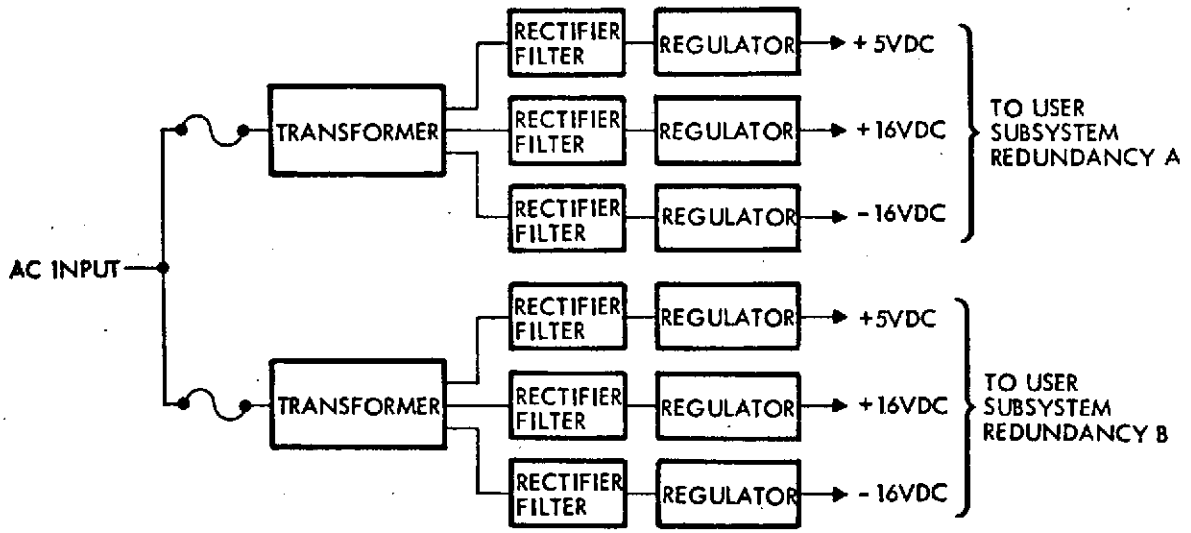

Figure 6-31. CTRF User Subsystem Power Supply

6.5.4 Power Control Unit

The PCU is the heart of the power subsystem. It performs the following functions:

- Combines the two RTG inputs to form a DC bus. This bus is distributed to the TWTA, pulse loads, scientific instruments and heaters.
- Regulates the DC bus to 28 VDC ±2 percent by control of the shunt regulator.

- Charges the probe battery at current and voltage levels determined by battery requirements.
- Dissipates RTG power in excess of load and battery charge requirements in a linear dissipative shunt.
- Provides fault isolation for the RTG's.
- Provides bus overload sensing.
- Conditions subsystem diagnostic telemetry.
- Provides fused branch circuits for scientific instruments.
- Controls the probe battery heater.
- Implements commands.

A simplified block diagram of the PCU is shown in Figure 6-32. Regulation of the 28 volt bus is controlled to ±2 percent by majority voting error amplifiers located in the central control electronics. Bus voltage variations are caused by load changes or RTG source degradation. The majority voting bus voltage sensor generates signals in response to these variations, thus controlling shunt regulator operation.

Shunt regulation is utilized since, as RTG power degradation occurs, the dissipation required by the regulation element continually decreases. This results in minimum shunt losses at that point in the mission when the RTG output power equals the total vehicle load. This also results in maximum power availability thereafter since load power can be maintained equal to or less than the source capability by ground command. This source regulation technique is particularly suited to RTG requirements which necessitate operation near the maximum power point voltage or less.

The excess RTG power is dissipated in the shunt regulator and the remainder is dissipated outside the spacecraft equipment compartment in a resistive shunt radiator. Placing the shunt radiator on the spacecraft exterior surface simplifies spacecraft thermal control design since variations in internal compartment dissipation are minimized. The apportionment of shunt dissipation between the shunt regulator and shunt radiator as a function of shunt current is shown in Figure 6-33.

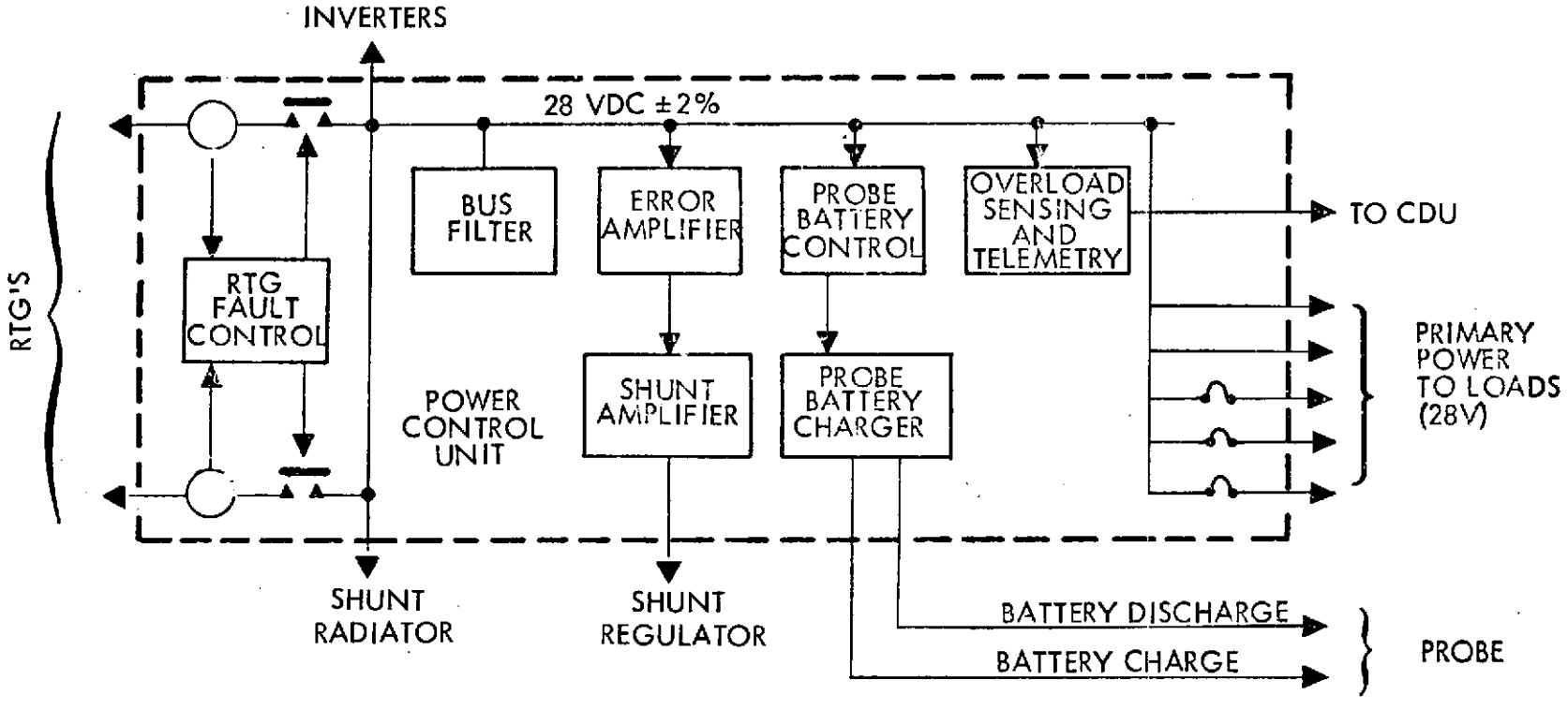

Figure 6-32. PCU Simplified Block Diagram

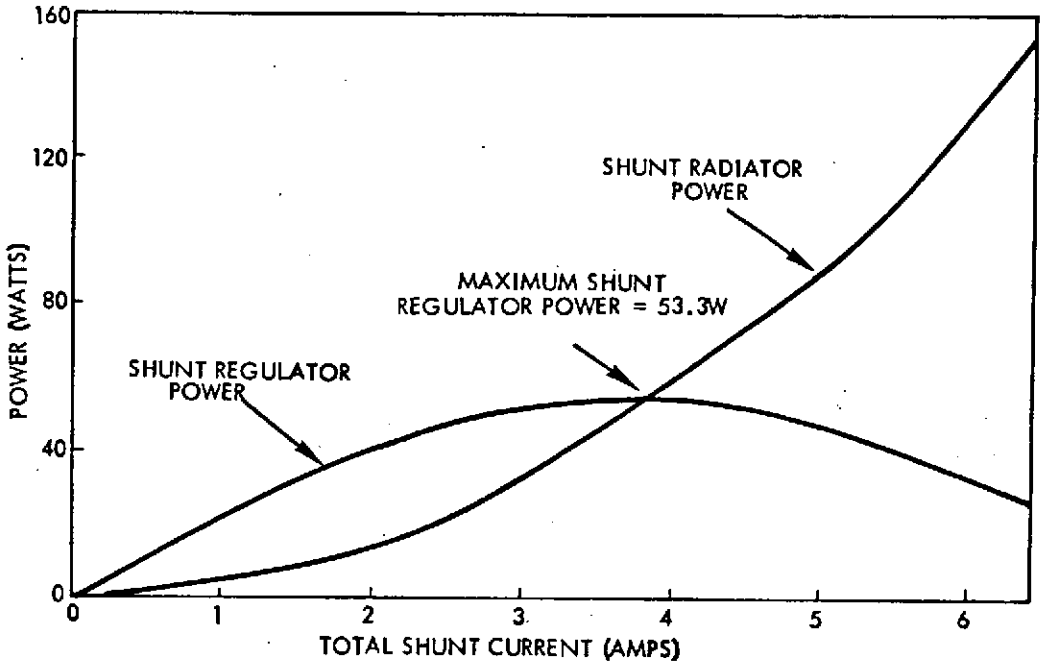

Figure 6-33. Shunt Dissipation as a Function of Shunt Current

If RTG degradation is as predicted, and no RTG or RTG cable failures occur, the power subsystem will operate in the shunting mode for essentially the entire mission. Excess RTG power capability is readily determined from the shunt current telemetry sensor since shunt current multiplied by the known bus regulation voltage of 28VDC is the excess RTG power.

The probe charge regulator that charges the probe battery is located in the PCU. This charge regulator is described in detail in Section 6.5.6.

6.5.5 Inverter Assembly

A block diagram of the inverter assembly is shown in Figure 6-34. The inverter assembly contains two separate inverters that are standby redundant. The output of the prime inverter provides the CTRF with a 30.5V (rms) bus, line-to-center tap, with a nominal frequency of 2.5 kHz. In the event of a failure of the prime inverter, switchover to the redundant inverter is automatic. A fault to ground within the inverter will result in the input fuse blowing and then switchover to the standby inverter.

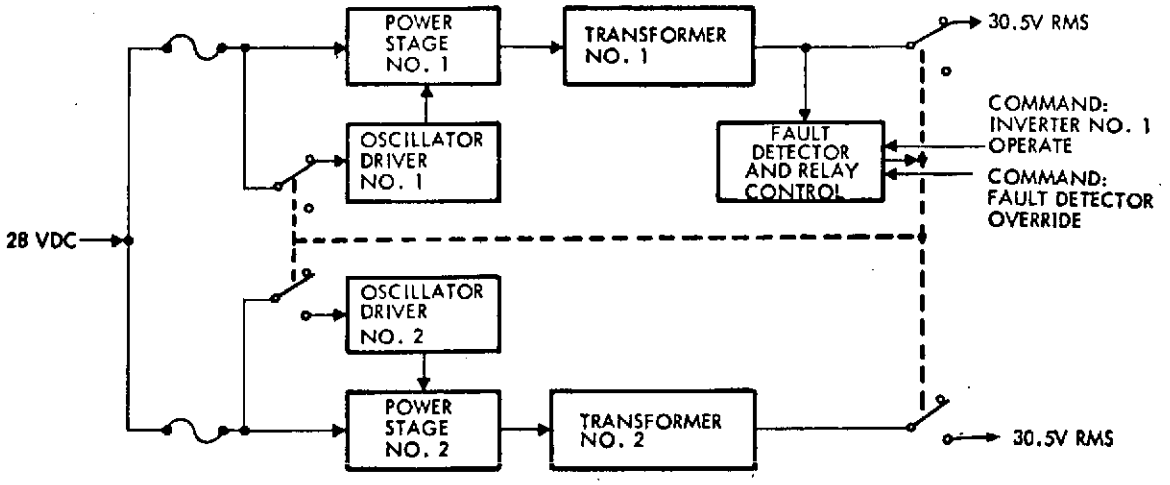

Figure 6-34. Inverter Assembly Functional Block Diagram

6.5.6 Probe Battery Charger

The baseline probe design contains two different battery types – an auto-activated silver-zinc main battery plus redundant nickel-cadmium batteries.* The two small (2 Ampere-hour) NiCad batteries are manually activated prior to launch. They are used by the probe during the 20 to 30 days between separation and planetary entry. During this period, the batteries will provide energy for the redundant probe clocks (20 micro-watts each) plus a series of pyrotechnic events including activation of the main battery. Since battery charging is completed prior to separation, this hardware is of no further use to the probe, and it was agreed that charging would be accomplished from the bus. The charging require-ments are minimal.

The battery load (0.02 Ampere-hours) is only 1 percent of the battery capacity (2 Ampere-hours) and consequently there is no concern related to achieving a high-degree of charge. A simple ground-commanded charge cycle such as 0.2 Ampere for 14 hours should be adequate. The batteries will be stored open-circuited and thermally controlled to approxi-mately 32°F. Every six months these small "boostrap" batteries will be

*"Saturn/Uranus Atmospheric Entry Probe Electrical Power/Energy Source Trade Study," MDAC/SAEP Design Note, SAEP-ES-4, dated 27 February 1973.

charged and then discharged back down to 4.5 volts. To meet these requirements, a charger with the following characteristics is proposed:

- V_{in}: 28 VDC ±2 percent
- V_o: Limited to 8.0 VDC ±1 percent at charger terminals
- I_o: Limited to 0.2A ±10 percent
- Discharge: By command through a 22 ohm resistor
- Vd: Discharge terminated at 4.5 VDC
- Commands: Charger on
  Charger/discharger off
  Discharger on
- Telemetry: Charger output voltage.

The circuit diagram for the probe battery charger is shown in Figure 6-35. It is a simple series dissipative regulator utilizing an integrated circuit voltage regulator (μA 723) as the control element). An external pass transistor, Q1, is required since the current and power dissipation are beyond the capability of the integrated circuit. Resistor R1 sets the current limit and resistors R2 and R3 set the voltage limit. Maximum power dissipation in Q1 will occur at onset of charging and will be 4.6 watts dropping to 3.9 watts when the output voltage has risen to 8 volts. In normal operation, the regulator is current limiting at 0.2A. The 8-volt voltage limit is viewed only as a backup to commanded charge termination.

The charger is activated by the closing of latching relay K1 to apply 28 volts of power to the regulator. K1 is also in the output in order to prevent any discharge of the battery by the charger. Discharge of the battery is through latching relay K2 and R4. R4 is sized to discharge the battery in approximately 10 hours. A common off-command is utilized to terminate either charge or discharge. Alternatively, discharge can be terminated automatically when battery voltage has dropped to 4.5 volts (Vd). The modification to the above circuit (not shown) would sense the battery voltage at the top of R4. Decrease of this voltage to 4.5 volts would (through OR logic) activate the common off command.

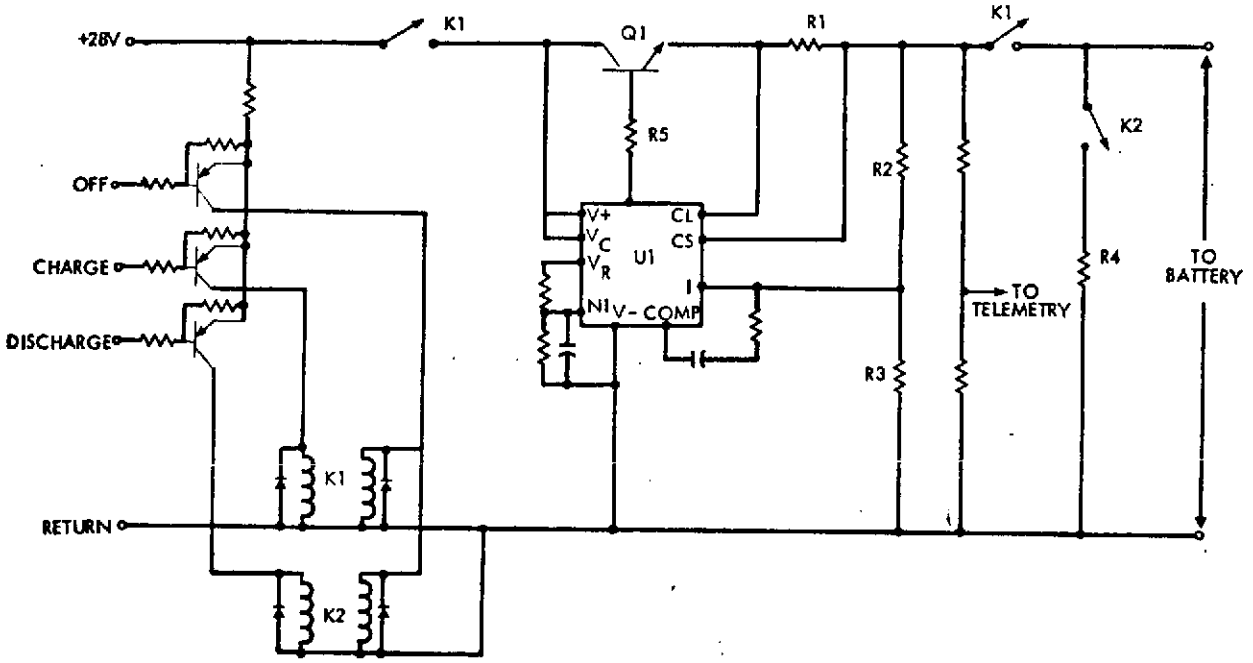

Figure 6-35. Charger Circuit Diagram

A telemetry divider is provided on the charger output to determine when charging or discharging should be terminated. It could be located on the battery side of K1 if it is desired to monitor battery voltage; however, it will then provide a small load to the battery after charge termination, but prior to separation.

6.6 COMMUNICATIONS

Figure 6-36 is a block diagram of the spacecraft bus communication subsystem. It consists of redundant S-band transmitters, S-band receivers, X-band transmitters, a conscan processor, and an assortment of switches, cables, waveguide, and antennas. The principal differences between the Pioneer F/G and the Saturn/Uranus spacecraft are shown enclosed in dotted lines.

Not shown in this block diagram are those communication components associated with the probe-to-bus data link. This link (not a part of Pioneer F/G) will be described in Section 6.9.

6.6.1 Subsystem Requirements

6.6.1.1 Functional Requirements

The communications subsystem must support the telemetry, tracking, and command requirements of the flight vehicle throughout the mission. Specifically, the subsystem performs the following functions:

a) Radiates a noncoherent RF signal with no uplink signal present to permit acquisition of the spacecraft by the Deep Space Stations (DSS).

b) Provides a phase-coherent retransmission after acquisition of an uplink signal such that two-way doppler measurements can be made at the DSS. The frequency translation ratio is 240/221.

c) Receives from the DSS and demodulates commands modulated in a PCM/FSK/PM format on the uplink signal.

d) Modulates and transmits to the DSS scientific and engineering data in a PCM/PSK/PM format utilizing a single subcarrier at 33 kHz.

e) Generates, demodulates, and processes a conical scan error signal on the RF uplink carrier that is utilized by the attitude control subsystem (ACS) to precess the spacecraft spin axis toward earth in a closed-loop attitude control mode.

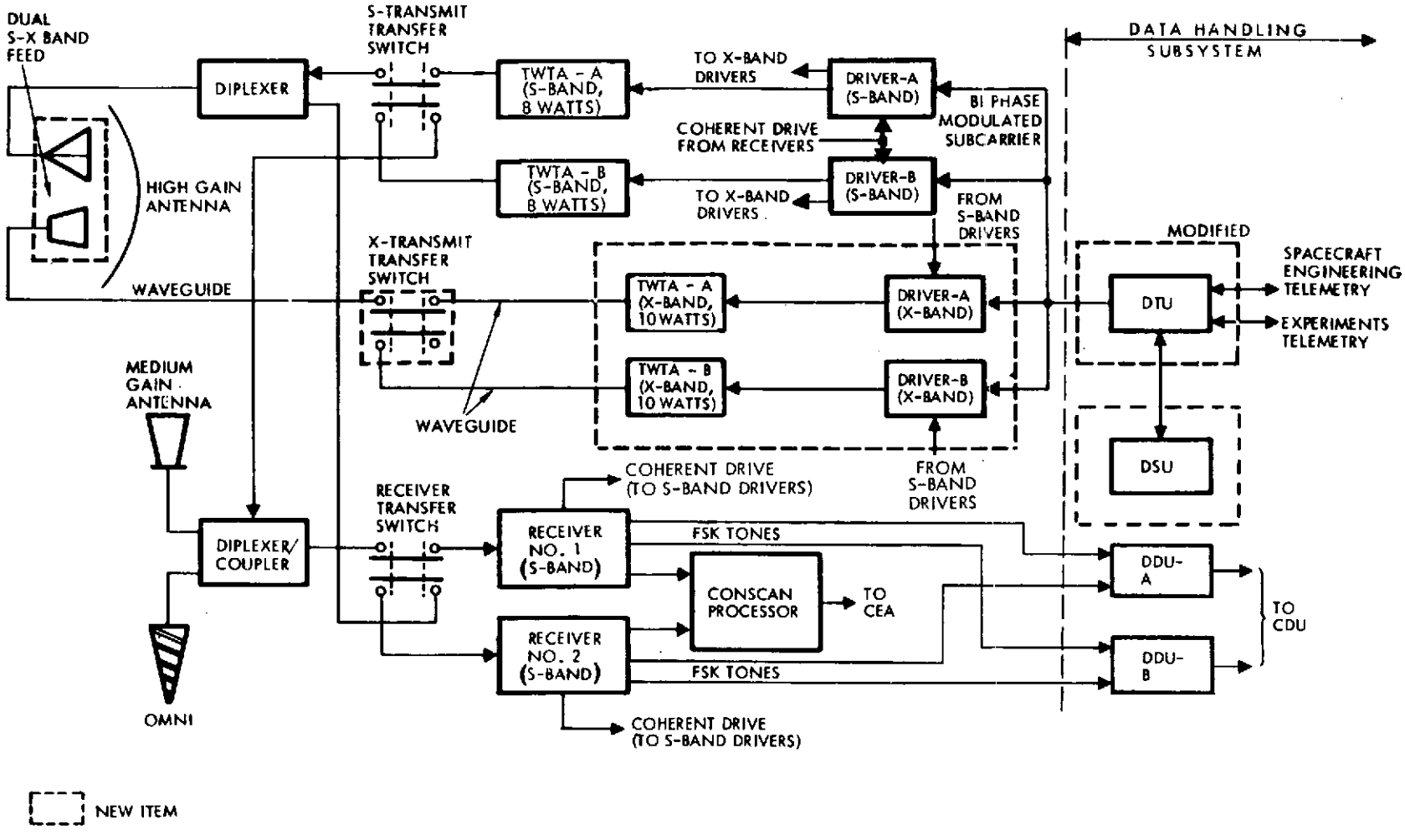

Figure 6-36. Communication Subsystem Functional Block Diagram

f) Simultaneously radiates on two coherently related frequencies (X-band and S-band) in support of an RF occultation experiment.

6.6.1.2 Mission Phases

The communication subsystem must meet the functional requirements identified above during the following phases of the mission:

a) Immediately following separation of the third-stage motor while still in the vicinity of the earth. Here the high-gain antenna will not be pointing to the earth and hence the omni-antenna will normally be earth pointing (see Figure 6-37 for typical orientation angles versus time).

b) Throughout the orientation maneuver when the spin axis is precessed to an earth-pointing attitude. This orientation maneuver is also important to the attitude control subsystem since it provides a calibration of the precession thrusters.

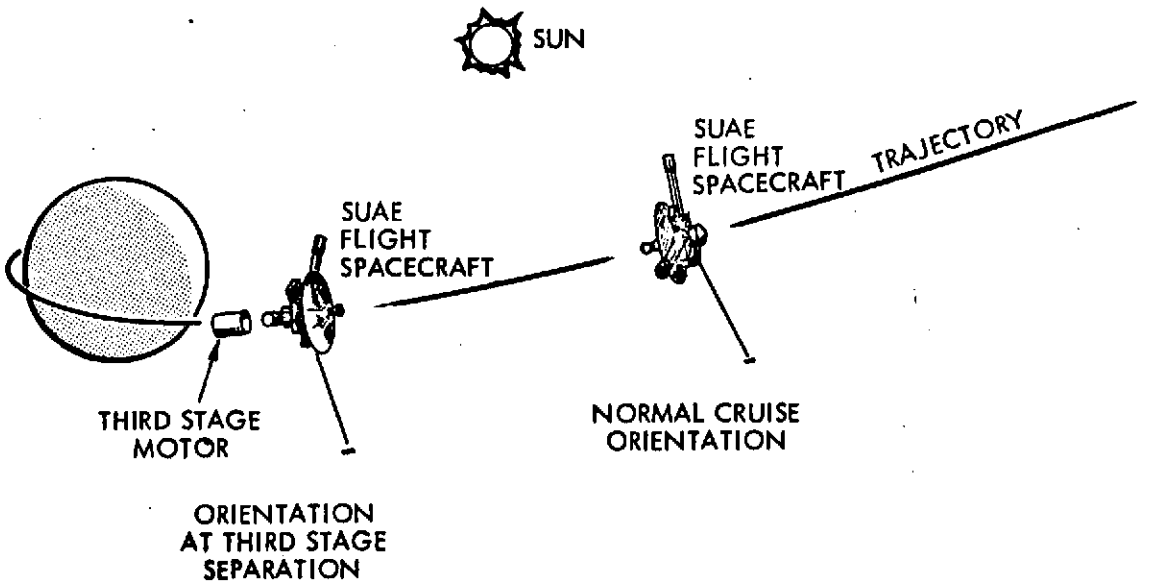

Figure 6-37. Orientations After Launch

c) During the early cruise portion of flight. Normally the mission will not require that the high-gain antenna be earth pointing, and an off-earthline mode using the medium-gain or omni-antenna may be selected to alleviate thermal problems from side-sun.

d) Throughout ΔV correction maneuvers. Early maneuvers to correct launch vehicle errors will be performed by precessing to the necessary off earthline attitude and firing axial thrusters. The medium/low-gain antenna will be required.

Later ΔV maneuvers, for example after Saturn swingby enroute to Uranus, or spacecraft deflection after probe separation, will be done in the earthline mode, using radial thrusters for the lateral component. The high-gain antenna (S- or X-band) will be required.

e) During closed-loop conscan operation. This can be accomplished with either the high- or medium-gain antennas.

f) Throughout the planetary encounter when bus science data is being acquired and during that portion of the encounter when probe data must be received on the bus and relayed to earth. Here also, the high-gain antenna is a mandatory component for successful subsystem operation.

6.6.1.3 Performance Requirements

The subsystem must be compatible with the DSS, must operate in the presence of Doppler, attenuation, noise, and other systematic limitations, and must provide the following:

a) Uplink command signals (S-band only) at a bit rate of not less than one nor more than 20 bps with a bit error rate at the receiver output not to exceed 1 in 10^5 bits at ranges out to Uranus (20 AU).

b) Downlink telemetry data rates consisting of bus science (approximately 70 bps), probe data (approximately 88 bps) and engineering data. The downlink data may be convolutionally coded (optional) in which case the frame deletion rate should not exceed 1 in 10^3. The

telemetry power level for both the X- and S-band transmitters will be selected based on the use of the 64-meter ground station antenna (see Section 6.6.1.4 for DSN interface definition).

c) The receivers shall provide appropriate output signals to control the carrier frequencies of both the X- and the S-band transmitters. The coherency ratio shall be 240/221 times the received uplink frequency for the S-band system and 880/221 for the X-band system. During non-coherent operation (no uplink signal) the S- and X-band transmitter frequencies shall be determined by preselected crystal oscillators.

d) The polarization of all antennas shall be circular and of the same sense for both transmission and reception.

6.6.1.4 DSN Interface

The SUAE mission will require DSN stations which are equipped with 64-meter antennas and X-band receiving capability. The 26-meter antennas with only S-band capability will be inadequate at Saturn and beyond. In establishing the performance capability of the uplink (S-band) and the two downlinks (S- and X-band), certain critical performance parameters related to these ground stations had to be defined. These assumptions are based on data contained in the Pioneer F/G-DSN interface specification PC-222, except as noted in Table 6-10.

Table 6-10. DSN Performance Parameters for SUAE Mission

Parameter	Station Configuration				
	26-Meter Antenna		64-Meter Antenna		
	S-Band Uplink	S-Band Downlink	S-Band Uplink	S-Band Downlink	X-Band Downlink
Frequency range (MHz)	2110-2120	2290-2300	2110-2120	2290-2300	8402-8441
Antenna gain (dBi)	51.8	53.3	60.5 ± 0.6	61.4 ± 0.4	71.5
Antenna beamwidth (deg)	0.36 ± 0.03	0.33 ± 0.03	0.15	0.14	TBD
Polarization	RCP	RCP	RCP	RCP	RCP
Ellipticity (P-P)	1.12 ± 0.4	1.047 ± 0.13	1.18	1.18	1.4
RF power output (kw) maximum	10	-	400	-	-
VCO frequency stability, 12 hour	5 parts in 10^{12}	-	5 parts in 10^{13}	-	-
Carrier phase stability	$\leq 7^{o}$ RMS	-	TBD	-	-
System noise temperature (°K)	-	41	-	25	27

6.6.2 S-Band Receiver

The receiver, shown in block diagram form in Figure 6-38, utilizes a phase-lock loop and a secondary AGC loop to perform all of the necessary receiver functions. This mechanization provides phase and frequency coherent outputs to the transmitter drivers (coherency ratio of 240/221) to allow measurement of two-way Doppler. It provides demodulation for the command tones which are modulated on the uplink carrier. This unit is unmodified from the Pioneer F/G design.

6.6.3 S-Band Transmitter

The S-band transmitter proposed for the SUAE mission consists of two separate units — a transmitter driver and a TWT power amplifier — in a fully redundant configuration (see Figure 6-36). The key characteristics of the units are summarized in Figure 6-39. Except for minor modifications to the driver, the S-band transmitter is the same as that of the Pioneer F/G design.

6.6.3.1 Transmitter Driver

Figure 6-40 is a block diagram of the transmitter driver. The input signal consists of a 32.768 kHz squarewave subcarrier which is biphase modulated by telemetry data from the DTU. The RF input to the modulator is provided (through a resistor summing network) either from a coherent drive signal from the receiver or from a TCXO. Absence of the "signal present" output from either receiver will activate the TCXO. A coherent mode inhibit command can also activate the TCXO. The mdoulator output is buffered, limited, amplified, and finally multiplied in frequency to produce the S-band drive.

The modifications from Pioneer F/G are (1) the use of a buffer amplifier after the RF input summing network to bring out a coherent drive signal for the X-band link, and (2) incorporation of a commandable, 2-state, phase modulation control to provide two modulation index settings of 0.95 and 1.15 radians. The X-band drive is coherent with the S-band downlink, whether the latter is related to the S-band uplink frequency or not. The requirement for the two modulation indexes for S-band transmission is discussed in Section 6.6.8.

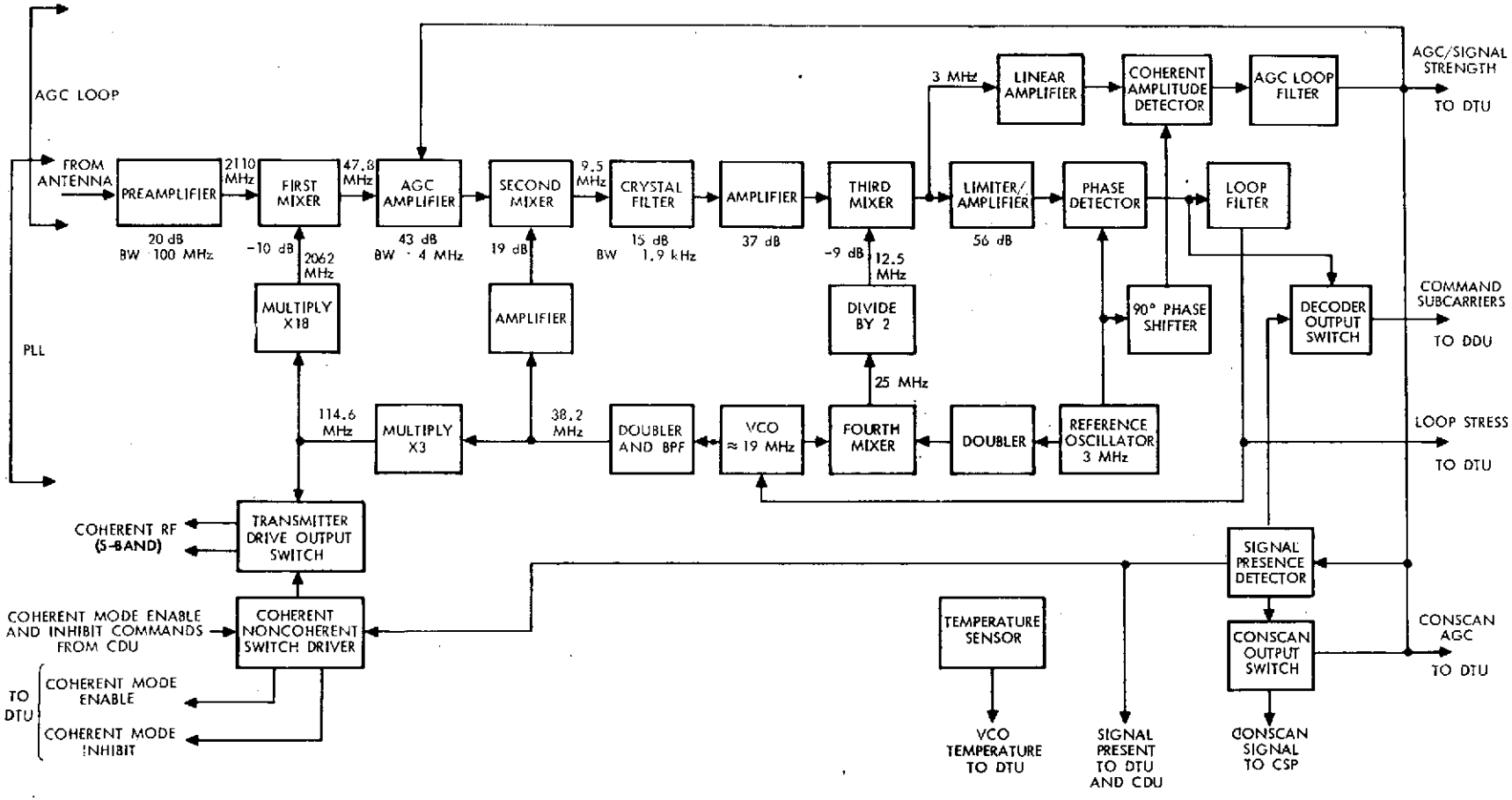

Figure 6-38. Receiver Block Diagram

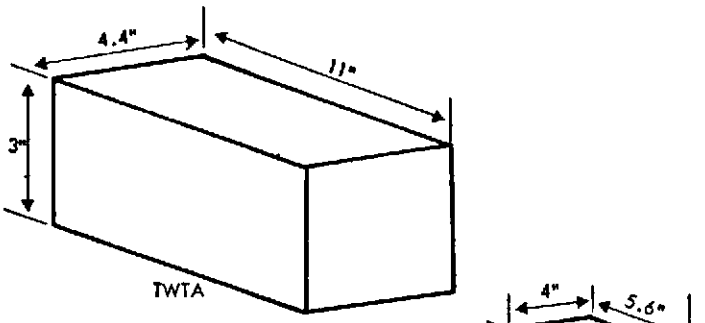

INPUT POWER:
27.8 WATTS AT 28 VOLTS

RF OUTPUT POWER:
8 WATTS NOMINAL
OUTPUT FREQUENCY 2290 TO 2300 MHZ

WEIGHT:
TRANSMITTER DRIVER 1.3 POUNDS
TWTA 4 POUNDS
TOTAL WEIGHT: 5.3 POUNDS

Figure 6-39. S-Band Transmitter

6.6.3.2 Traveling Wave Tube Amplifier

The TWTA is shown in Figure 6-41 in block diagram form. The two major assemblies are the TWT and the power supply. The TWT is derived from the Watkins-Johnson WJ-274 series. Switching of redundant units is accomplished by ground commands.

6.6.4 X-Band Transmitter

The X-band downlink required for the SUAE mission serves three functions:

- Downlink telemetry
- Occultation measurements
- Doppler tracking.

To provide these functions, a traveling wave tube amplifier (TWTA) and a solid-state transmitter driver are selected as the baseline approach. approach.

6.6.4.1 Requirements

The X-band transmitter requirements are:

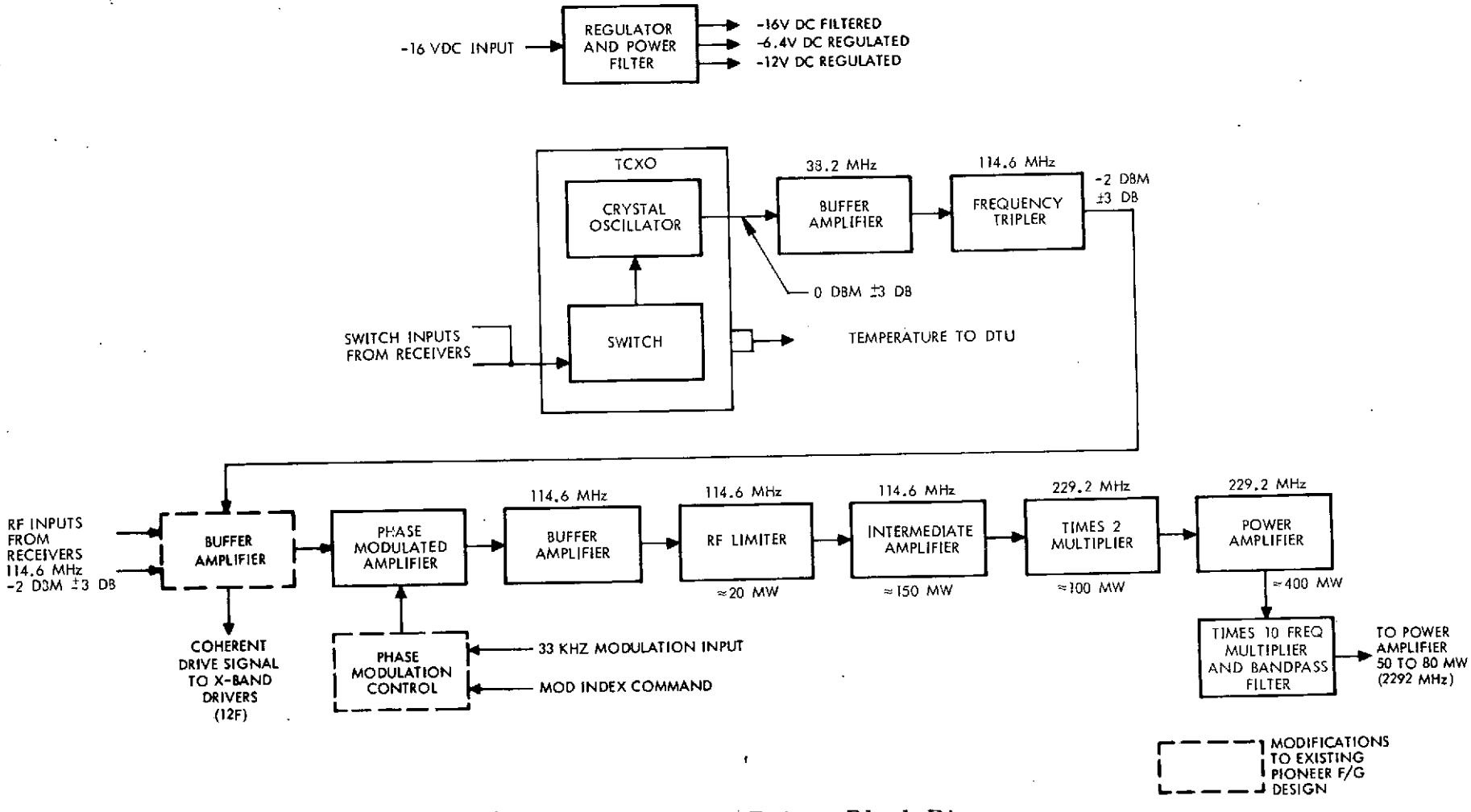

Figure 6-40. Transmitter Driver Block Diagram

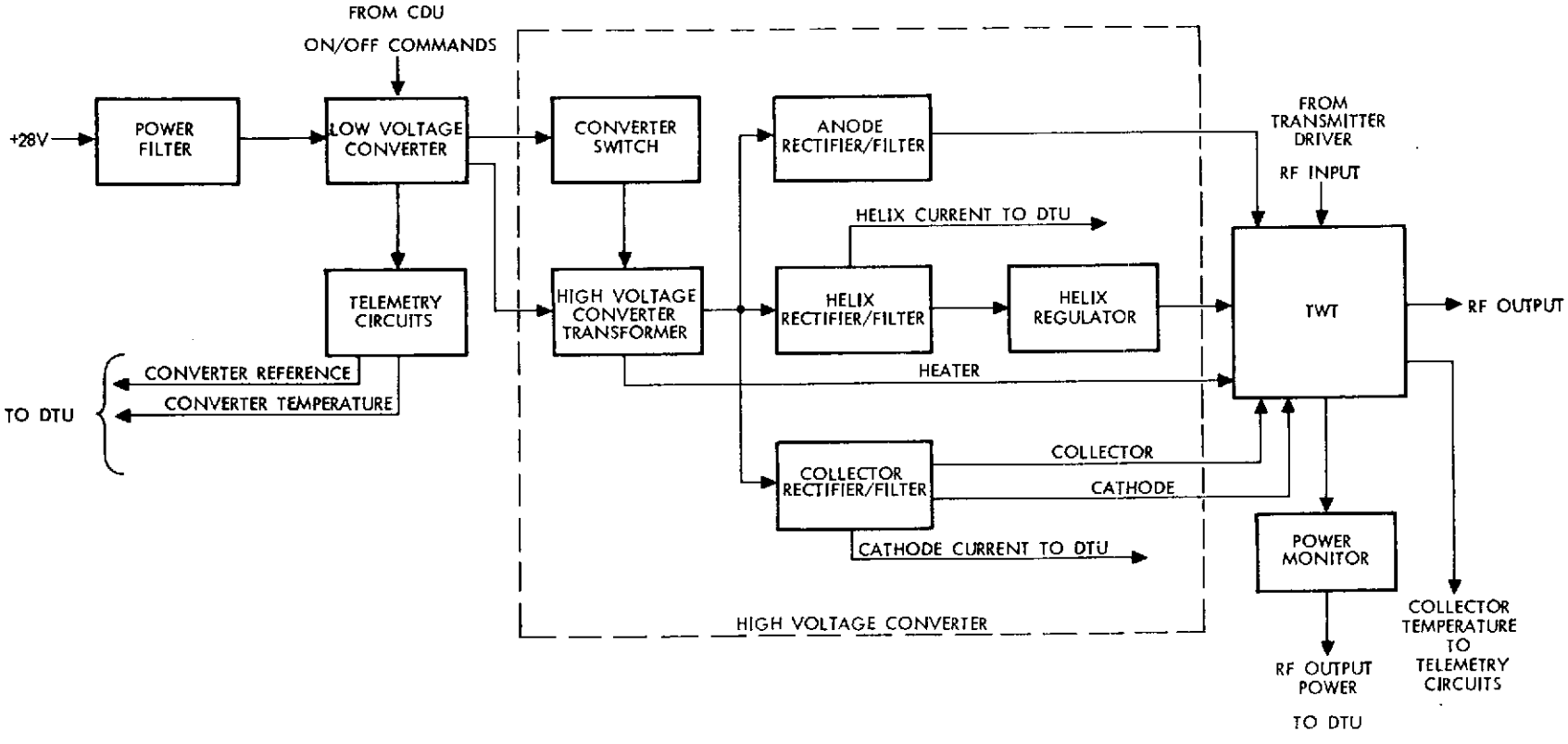

Figure 6-41. TWTA Block Diagram

- Center frequency: 8422 MHz
- Bandwidth: 200 MHz minimum
- Output power: 10W ±2W
- Input level at 12f: 0 dBm (f ≈ 9.55 MHz)
- Modulation index: 1.15 radians
- Coherent mode:
  X-band to received S-band ratio: 880/221
- Noncoherent mode:
  X-band to downlink S-band ratio: 880/221
- Either mode:
  Input drive signal (12f) from S-band drive

6.6.4.2 X-Band Driver

The X-band driver performs the functions of multiplying the coherent drive signal available from the S-band driver and phase modulating the resultant X-band carrier with the 33 kHz telemetry subcarrier. The required power output must be compatible with the input requirements of a 10-watt TWT amplifier. For a TWT gain of 40 dB, this level is of the order of +3 dBm, including isolator losses.

The X-band signal is coherently related to the received S-band by a ratio of 880/221. Several methods of obtaining the X-band signal were considered during the study, arriving at the conclusion that the coherent drive required must be one of the prime numbers in the 880f coherence term, i.e., 2f, 5f, or 11f. The coherent drive presently available from the Pioneer F/G driver is 12f (114.6 MHz). With a minor modification to the existing driver, the X-band and S-band downlink transmissions can be made phase coherent under all operating conditions. This modification contemplates the addition of a buffer amplifier preceding the phase modulated amplifier.

Three different approaches were considered in providing the X-band driver:

- Develop a new design tailored to the specific requirements
- Modify the Motorola X-band transmitter designed for the MVM-73 program
- Modify the TRW Model 35 X-band transmitter.

A new design requires various frequency multiplier and mixer stages to synthesize the desired X-band signal which is coherently related to the S-band receive frequency by the DSN-compatible translation ratio, 880/221. It is assumed that the S-band driver drive signal is available at a frequency of 12f (114.6 MHz).

If the design employs multipliers exclusively, a times eleven (×11) multiplier must be developed, since 11 is a prime factor of the coherence term 880. These high-order multipliers are prone to instability problems and present severe filtering problems. Additional multipliers required are ×2, ×4, and ×5.

Similar devices have been constructed and tested at L- and C-band. A preliminary performance specification for an X-band version includes:

Frequency	8422 MHz
Bandwidth	100 MHz (-0.5 dB)
Required drive power	1 milliwatt
DC power input	1.5 watts
RF power output	20 milliwatts
Baseplate temperature	160°F (maximum allowable)
Construction	Hybrid (discrete components and microstrip)

The X-band transmitter designed by Motorola for the Mariner-Venus-Mercury 1973 mission offers another possible approach to meeting the driver requirement. Figure 6-42 illustrates a block diagram of this existing qualified design. It develops 200 milliwatts output power and consumes 12 watts of DC power. For the Saturn-Uranus mission application, these levels must be reduced by approximately a factor of ten. This can be accomplished by deleting the final power amplification stage (7 dB gain) and redesigning the following ×5 multiplier to operate at the lower level. In addition an input frequency divider (÷6) is required to achieve compatibility with the existing 2f requirement.

The revised performance parameters are 4 watts of input power and 40 milliwatts RF output power.

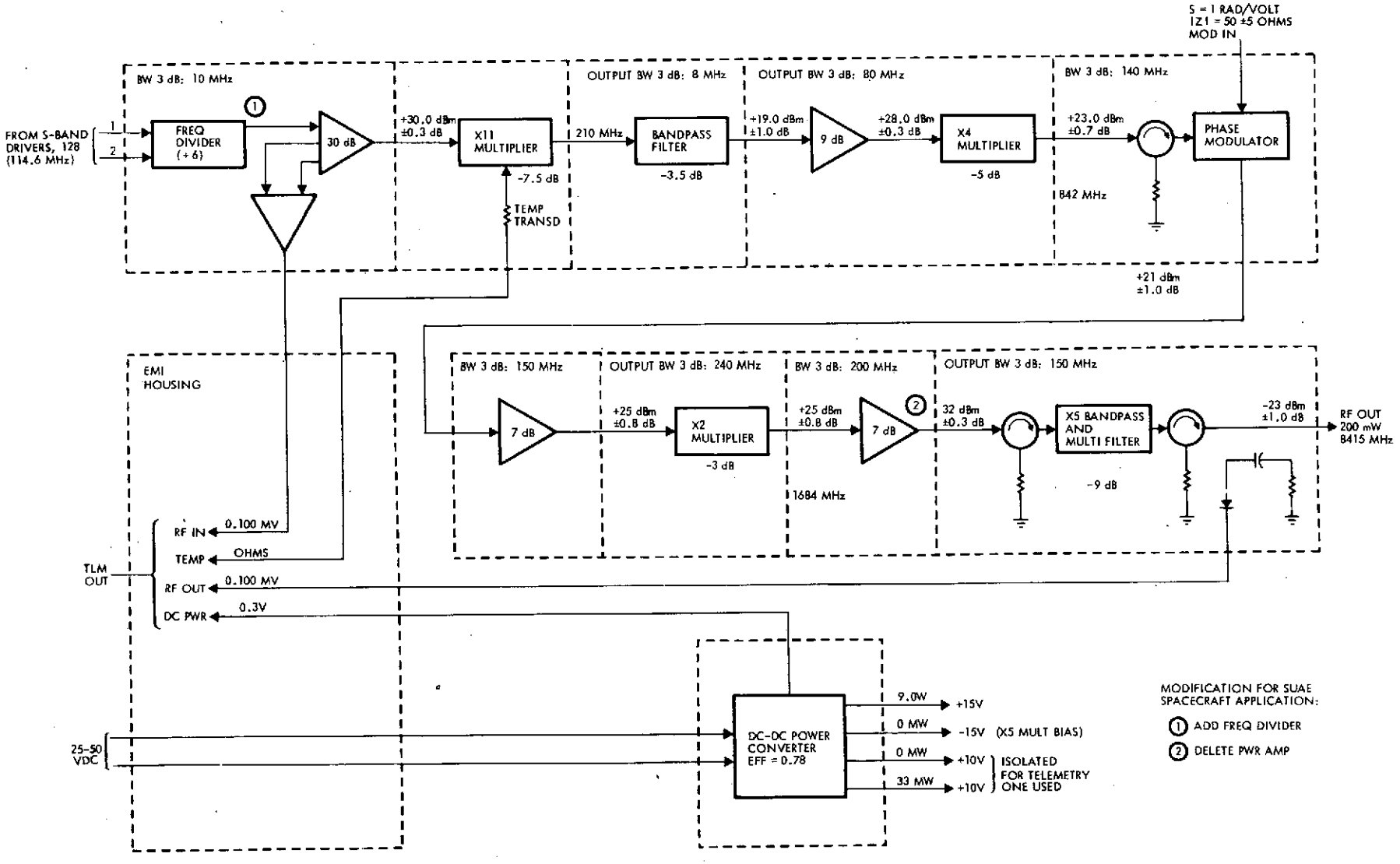

Figure 6-42. Block Diagram of Motorola X-Band Driver

A third approach involves a relatively simple modification of the TRW Model-35 S-band transmitter, depicted functionally in Figure 6-43. The modification consists of adding a frequency divider, mixer, and three multipliers (X5, X2, and X4), as illustrated by the subassemblies in dashed lines. A balanced varactor quadrupler multiplies the S-band signal to X-band.

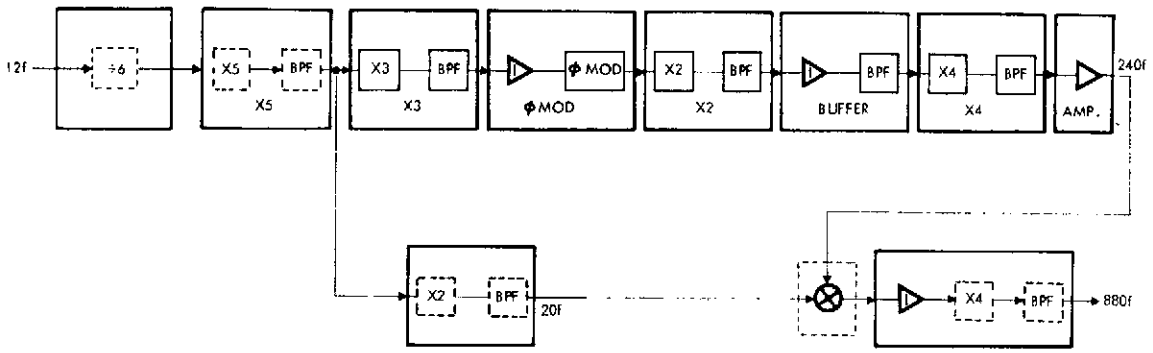

NOTE: DASHED LINES INDICATE MODIFICATIONS.

Figure 6-43. Modified Model 35 Transmitter Driver

The mixer provides a coherent signal at a frequency of 220f, eliminating the requirement for the X11 multiplier. Minor retuning of the final stage of amplification, from 240f to 220f, may be required to improve its performance as a driver for the new quadrupler.

Table 6-11 summarizes the key performance characteristics of the latter two approaches, reflecting the modifications which have been described.

The Model-35 transmitter is recommended for the Saturn-Uranus mission for the following reasons: development cost and risk is significantly less than for an entirely new design. Secondly, stringent weight and power limitations favor using the Model-35 approach compared to the MVM 73.

6.6.4.3 X-Band Power Amplifier

The high-power requirements at X-band precludes, at the present time, consideration of solid-state devices such as high-level varactor diodes and avalanche diode amplifiers. The TWT is better suited to microwave systems because of its inherent ability to provide the highest gain-bandwidth product, low-noise capability and high efficiency. A survey summary of space-qualified X-band TWT tubes is shown in Table 6-12.

Table 6-11. Application of Existing X-Band Transmitter Drivers

	Modified Motorola VNM 1973	Modified Model 35
Input frequency	114.6 MHz (12f)	114.6 MHz (12f)
Drive power required	0 dBm ± 2 dB	0 dBm ± 1 dB
Input power	4 watts	2.5 watts
Output frequency	8415 MHz (880f)	8415 MHz (880f)
Output power	40 mW (min)	20 mW (min)
Modulation	Linear PM (not required)	Linear PM
Size	2 x 6.9 x 8 inches	1.52 x 4.52 x 4.53 inches
Weight	4 pounds	2 pounds
EMI		
Harmonics of 19.125 MHz	-30 dB	-40 dB
Spurious	-50 dB	-60 dB
Transmitter driver modifications required	Add mixer, 3 multipliers (x5, x2, x4), and ÷6 frequency divider	Add ÷6 circuit. Delete power amplifier stage

The Watkins-Johnson tube, Model WJ-3703, was originally designed for JPL TOPS. At the present time the development is being carried out on company funds with expected completion in 1973. This tube weighs 1 to 1.5 pounds. This manufacturer does not have any tube for 10 watts of output power.

The Electron Dynamics Division of Hughes has the largest variety of TWT's for X-band. There are two candidate tubes for the present application. One is Model 285H which can be scaled down to produce an output power of 10 watts. The second choice is a tube being developed for Sylvania for space applications and the range of 11.7 to 12.2 GHz with a 10-watt output. Hughes would prefer to modify the frequency response of their Sylvania tube under development rather than to lower the power of tube 285H. The Sylvania tube is expected to have an efficiency of 30 percent at X-band with a life expectancy of ten years. The cost of this modified tube is larger than the modified tube 285H.

It is recommended that tube 285H be used in this application because of lower cost and higher efficiency. Figure 6-44 indicates the DC power requirement of the TWTA as a function of output power. The conservative baseline efficiency assumed downgrades vendor projections to account for VSWR mismatch, end-of-life performance, etc.

Table 6-12. Survey of Space-Qualified TWT for X-Band

	Manufacturer and Number						
	Watkins-Johnson WJ-3703	Hughes Modified 285H	Watkins-Johnson 231	Hughes 240H	Hughes 265H	Hughes 219H	Hughes 285H
TWT Parameters							
Frequency range	X-band	X-band	6-8 GHz	6-9 GHz	7-9 GHz	7.5-8.5 GHz	8.4 GHz
Power output	25W	10W	35W	16W	22W	20W	22W
Efficiency including heaters	45%	40%	29%	33%	33%	33%	43%
Saturated gain	35 dB	-	41 dB	40 dB	46 dB	40 dB	37 dB
Development status	Under development	-	Space qualified	Space qualified	Space qualified	Developed for NASA Langley; general qualification	Under development for JPL Mariner Jupiter-Saturn mission
Previous usage	New	Modified	*	TAC SAT	777	None	None
Power Supply							
TWT power supply efficiency	86%	-	85% (estimated)	-	-	85% (Gaulton Industries)	85% (estimated)
Driver Parameters							
Power output	-	-	2.8 MW	-	-	2 MW	5 MW
Efficiency	-	-	10%	-	-	15%	-
Previous usage	-	-	None - requires new design	-	-	None - requires new design	None - requires new design
Composite Efficiency (TWT, driver, power supply)	-	-	24.5%	-	-	28%	36%

*Nine tubes life tested two years — no failures.

BASELINE RF POWER OUTPUT

η \ P_o	8W	10W	12W
28% ← BASELINE EFFICIENCY	29	36	43
30%	27	33	40
34% ← VENDOR PROJECTION	24	30	35

Figure 6-44. Projected TWTA Power Requirements

6.6.4.4 Phase Stability

Although no requirement has yet been specified, the phase stability of the X-band transmitter is an important performance parameter. For the baseline system, the phase stability of the coherent output, with the receiver locked to an unmodulated strong input signal, is expected to cause no more than 12 degrees rms or 36 degrees peak phase error. This phase error must be measured with a phase-coherent test set of double side noise bandwidth ($2B_L$) of 12 Hz, and a post-detection video filter with a high-frequency cutoff of 1 kHz or more.

6.6.5 Antennas

The spacecraft carries four distinct antennas (see Figure 6-36):

- High-gain antenna (9-foot dish)
- Medium-gain antenna (a corrugated conical horn and a transition mount)
- Omni-antenna (truncated conical log spiral)
- Probe data-link antenna (loop-vee)

All of the above except the loop-vee antenna are derived from the Pioneer F/G; the loop-vee is described in Section 6.9. The major modifications of the Pioneer design required for the SUAE mission include a change in the high-gain antenna feed assembly to accommodate X-band, plus relocation of the omni element.

The high-gain S-band feed for the Pioneer F/G had a mechanism to allow it to be moved off the spacecraft spin axis approximately one inch. The purpose of this offset was to provide a pointing error signal so that the spin axis could be maintained pointed at the ground station (earthline). Operation of this "conscan" system can be explained by referring to Figure 6-45. Note that as long as the antenna feed (pattern) is coincident with the spin axis there is no change in the antenna gain even though the spin axis is not along the line-of-sight to the ground station antenna.

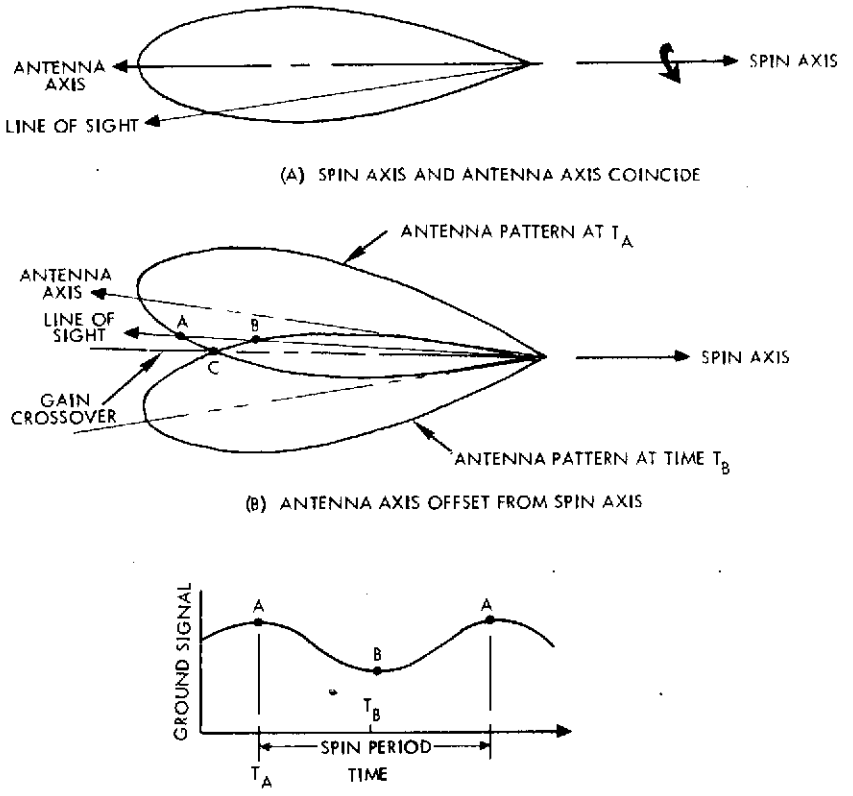

Figure 6-45. Conscan Operation

However, if the antenna feed centerline is moved off the spin axis, and if the spin axis is not earth-pointed, the antenna gain then varies as the antenna rotates. This results in a sinusoidal variation in the received signal level. Measuring the phasing of this signal relative to some reference will provide sufficient data to permit realignment of the spin axis with the earthline. Note that when the spin axis is pointing toward the earth (point C) the resultant antenna gain is lower by 1 dB than the peak gain. This is an undesirable feature of the conscan system.

Since X-band is used for downlink only, there is no requirement for an offset antenna pattern. Therefore, the X-band feed should be located on the spin axis.

Most spacecraft designs incorporate an omnidirectional or "omni" antenna to guarantee command access to the spacecraft regardless of the vehicle attitude. On Pioneer this was accomplished by combining the medium-gain horn and the conical log spiral by means of a diplexer coupler as shown in Figure 6-46.

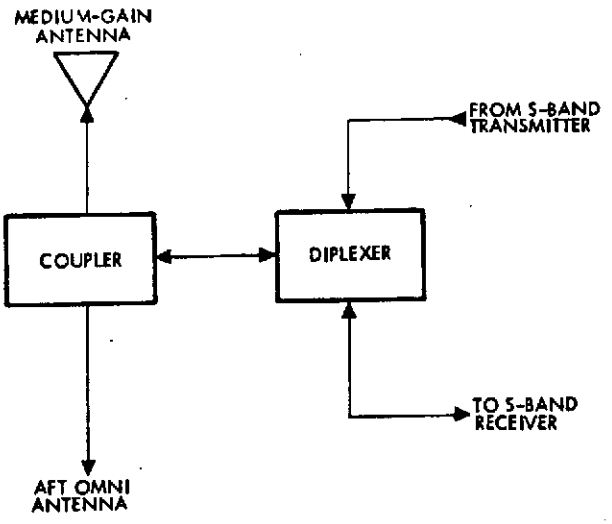

Figure 6-46. Omni-Antenna Schematic

The resultant antenna pattern is given in Figure 6-47. There are interference null regions from 60 to 80 degrees where reliable communications cannot be maintained. This is a common problem in attempting to provide omni coverage without resorting to sophisticated techniques such as polarization or frequency diversity, and is generally considered an acceptable mission risk. The relocation of the omni element and the presence of the probe adapter will affect the antenna pattern given here, but the change will not be significant.

The high-gain antenna consists of a 9-foot diameter reflector with a feed system mounted on a tripod support. The modification of the Pioneer F/G configuration is shown in Figure 6-48.

Here we see that the Pioneer F/G high-gain antenna S-band feed and associated feed movement mechanism is replaced with a fixed dual S- and X-band feed. Ridged waveguide horns are used for this application. The S-band horn is permanently offset from the reflector focal point to squint the beam and produce a -1dB gain crossover. The X-band horn is positioned in one of the S-band waveguide ridges and is coincident with the focal plane axis.

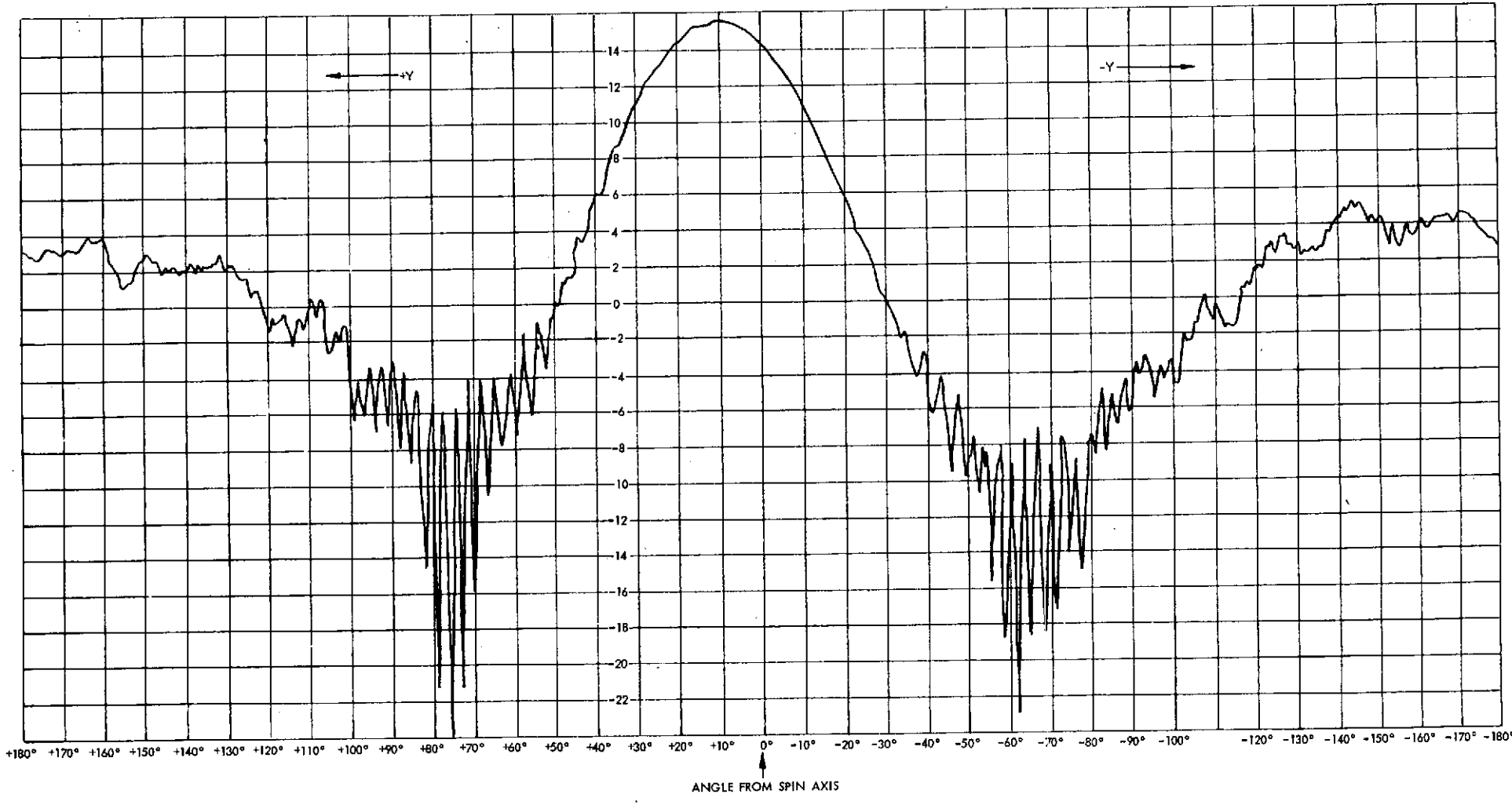

Figure 6-47. Uplink Medium-Gain/Omni-Antenna Pattern

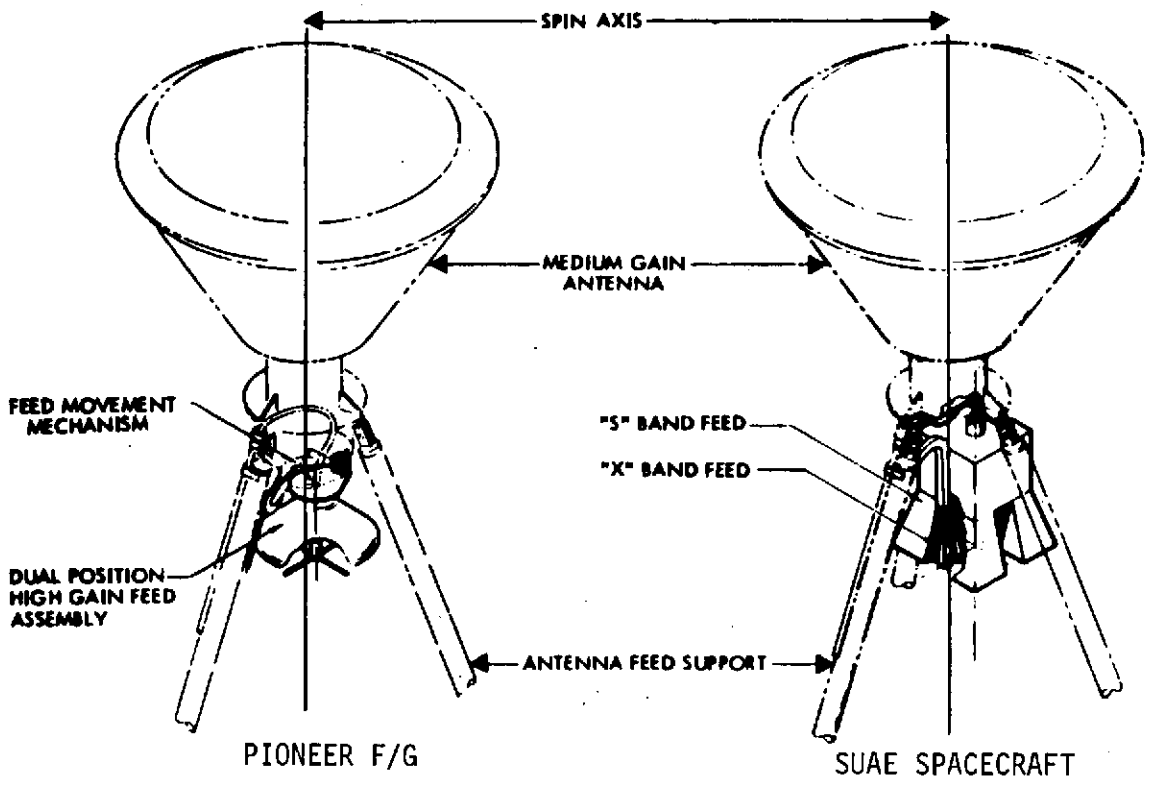

Figure 6-48. Antenna Feed System

The X-band feed will be coupled to the TWTA via waveguide because of the large losses associated with coax at these high frequencies. This waveguide would run parallel to and be supported by one leg of the tripod support. The effect of this waveguide adjacent to the strut on the mechanical stability of the feed system warrants further study, careful design, and development testing. The waveguide must be loosely coupled to the TWTA to permit relative motion between the equipment compartment and the feed. This may be accomplished with a flexible waveguide section or perhaps by a waveguide-coax transition. The attachment of the waveguide to the struts and the induced lateral vibration loads as well as the potential thermal loading of the strut ("hot dog" effect) should be verified by tests.

6.6.6 Conscan Signal Processor

The conscan signal processor (CSP) is a digital implementation of a maximum likelihood estimator, and is shown in block diagram form in Figure 6-49. The CSP estimates the phase (θ) and amplitude (A) of the

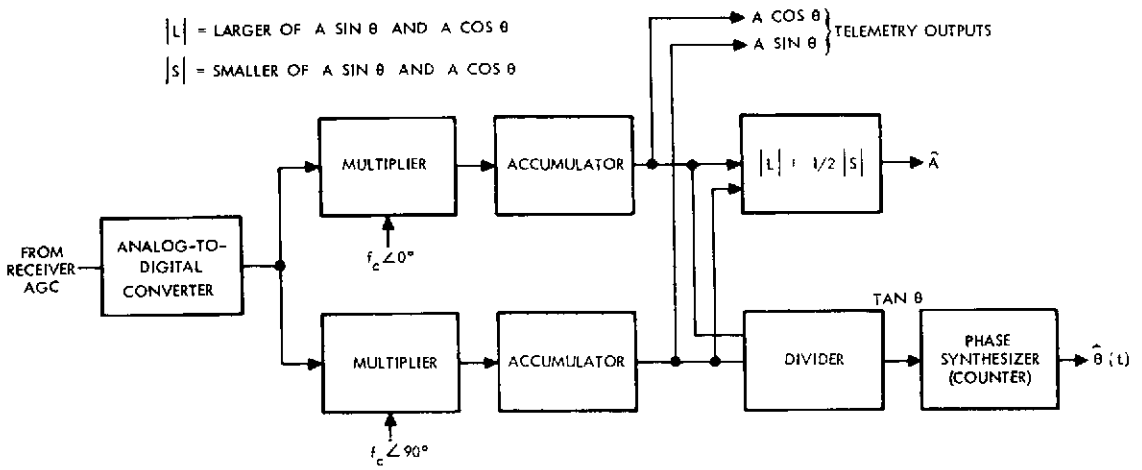

Figure 6-49. Digital Implementation of the Amplitude and Phase Estimation Process

distorted sine wave output from the receiver AGC loop. The phase information is used to time the precession thruster firing so that the pointing error is reduced with the minimum expenditure of propellant. The amplitude information is used to terminate thruster firing when the deadzone has been reached. The reference frequency (f_c) used in the CSP is provided by the spin period sector generator (SPSG). Figure 6-50 is a functional timing diagram for the processor.

The principal outputs of the CSP are:

1) Firing pulses to ACS control the time at which precession thrusters are fired. The thruster firing pulse may be selectively biased prior to flight using the CSP program plug so as to compensate for phase shift in the antenna, receiver, CSP, and one-half the thruster pulsewidth.

2) A firing enable signal to ACS indicates that the conscan signal amplitude is above the predicted threshold. When the amplitude drops below the predicted threshold level, the enable signal level switches to the false state and precession firing or conscan is terminated. If threshold is indicated even momentarily, conscan must be re-enabled by command CNS5 in order to continue.

3) Telemetry of the A sin θ and A cos θ parameters are in the form of two 8-bit telemetry words. From these parameters and the calibration curve the pointing error angle magnitude and phase can be

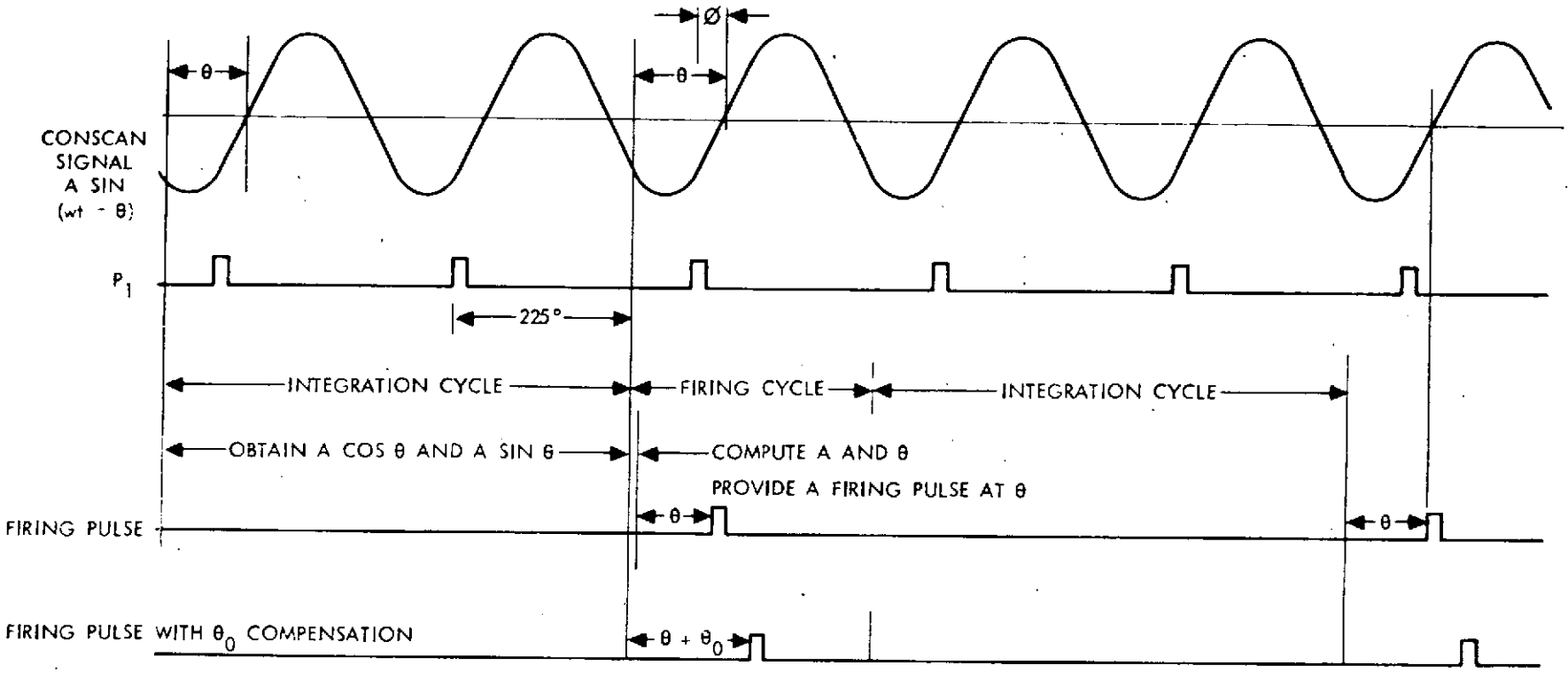

Figure 6-50. Conscan Signal Processor Functional Timing Diagram

computed on the ground for the purpose of establishing spacecraft orientation. In addition, the parameters A sin θ and A cos θ can be used for partial checkout of the CSP before the closed-loop operation is commenced.

Conscan operation can be automatic (closed-loop) in which case outputs 1 and 2 above are used, or it may be utilized open-loop in which case the ground station must provide a program for thruster firings.

6.6.7 Miscellaneous Components

As shown in Figure 6-36, the communication subsystem requires a number of minor components; switches, coax, diplexers, and waveguide to interconnect the receivers, transmitters, and antennas. For the SUAE mission, the only additions to the Pioneer F/G complement are the X-band transmitter transfer switch (similar to the Pioneer F/G unit) and the X-band waveguide runs from the TWTA's to the switch and from the switch to the feed assembly.

6.6.8 Link Power Budgets

Figures 6-51 and 6-52 show the anticipated performance for the uplink transmission and the two downlink transmissions (S- and X-band).

6.6.8.1 Uplink

Figure 6-51 indicates a receiver threshold level of -149 dBm for the received carrier. However, for a carrier modulated at a level of 1.1 radians (the level for uplink commanding) the total signal level at the reciever must be at least -146.2 dBm for the DDU command decoding to reach specified levels of performance — false command suppression and correct command receipt.

At the range of Uranus this signal level cannot be attained via the aft low-gain spacecraft antenna by any ground station combination available. Thus commands can be sent to the spacecraft only via the medium-gain horn and the high-gain antenna. If the medium-gain horn is used the ground station would have to use a 64-meter antenna at the 400 kW level, and the spacecraft would point as far as 10 degrees from the earth. If the high-gain antenna is used, the ground station could use a 64- or 26-

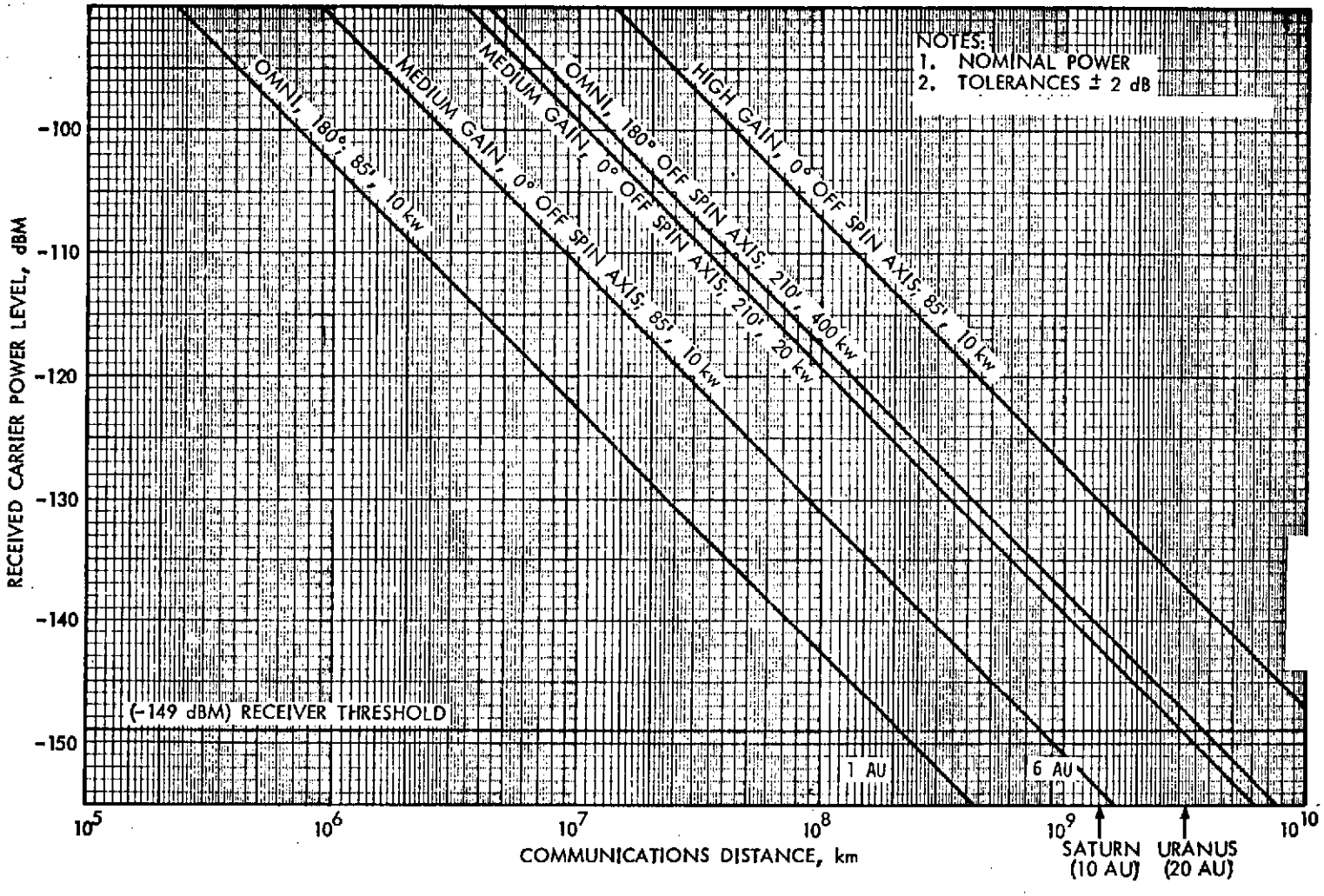

Figure 6-51. Uplink Received Carrier Power Level vs Communications Distance

26-meter antenna, and the transmitted power could be down to 10 kW, but the spacecraft has to point within about 1.0 degrees of the earth.

6.6.8.2 Downlink

Figure 6-52 shows downlink performance using nominal values of all link parameters, and using the spacecraft high-gain antenna at S- or X-band. It indicates that the downlink data rate capability drops off faster than $1/R^2$ because of receiver detection degradation at the lower bit rates. The solid circles represent points for which explicit calculations are made in Table 6-13. The open circles at 32 bps are based on extrapolation of receiver loss measured at higher bit rates — no measured data were available below 64 bps. The open circles at 16 bps in Figure 6-52 indicate range limitation due to insufficient carrier power, a condition that applies anywhere on the vertical line shown.

Carrier Power Limitation. For a given link, the carrier power limitation is a function of the modulation index, the carrier loop threshold bandwidth ($2B_{LO}$), and the carrier loop signal-to-noise ratio (SNR) threshold. The critical link, in this regard, is the S-band transmission to the 64-meter ground station from near Uranus, used primarily as a backup to the X-band link. Table 6-13 indicates $2B_{LO} = 3.0$ Hz, a capability indicated by JPL to be available at 64-meter stations. The carrier loop SNR threshold is shown at 10.0 dB, a value confirmed for use at higher values of $2B_{LO} - 10$, 30 Hz, etc. These values and the 1.15-radian modulation index lead to the carrier power-limited range of 24.2 AU. However it is possible that greater carrier loop SNR threshold is required at the 3.0 Hz bandwidth. ARC has suggested (in Document PV-1006.03) that the 5.2 dB improvement in $2B_{LO}$ when it is decreased from 10 to 3.0 Hz be offset by a 2.2 dB degradation in carrier loop SNR threshold, i.e., increasing it from 10.0 to 12.2 dB.

This 2.2 dB degradation reduces the carrier power-limited range by a factor of 1.29, or from 24.2 to 18.8 AU, inadequate for the 20 AU communication range from Uranus at encounter.

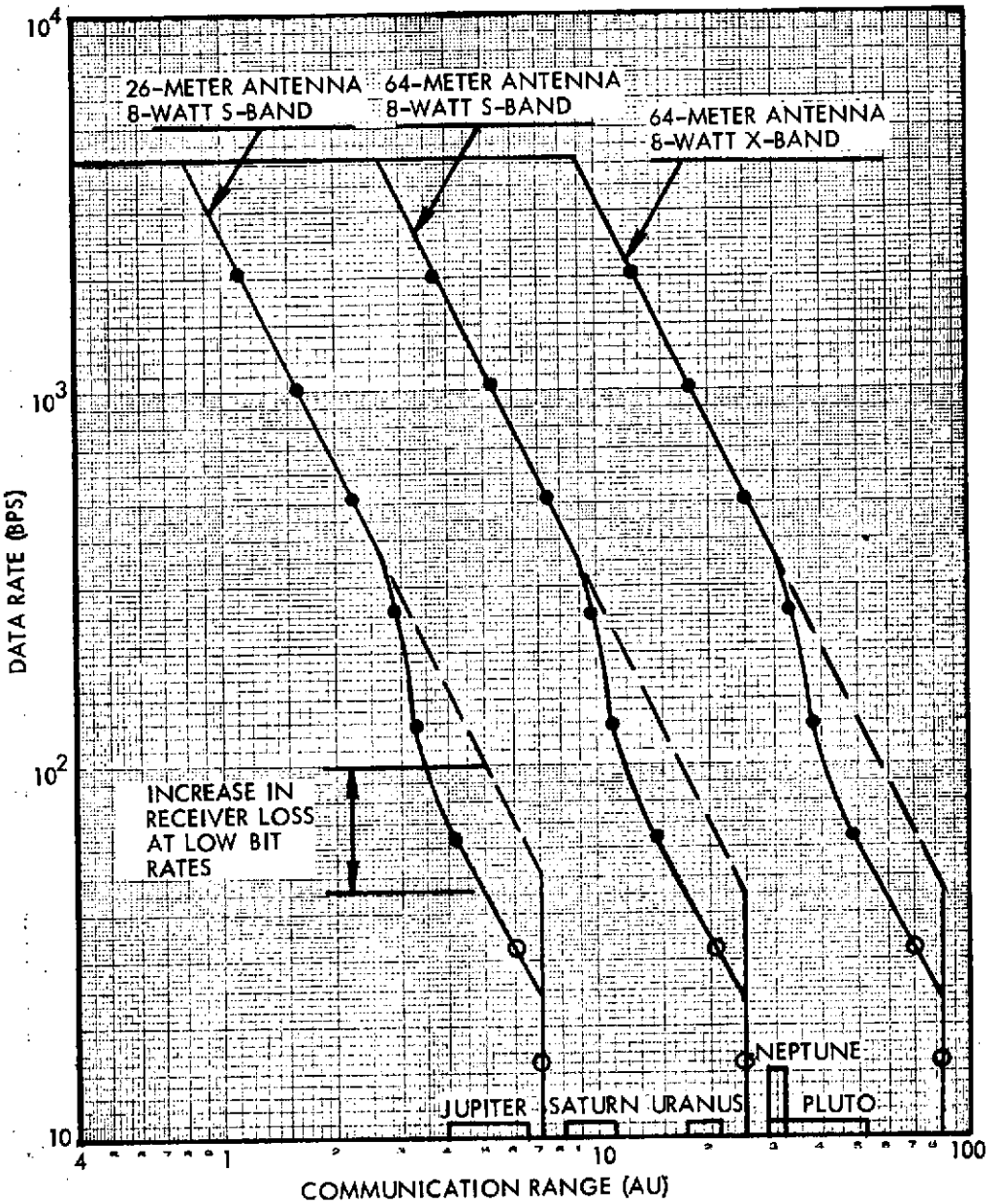

Figure 6-52. Telemetry Bit Rate vs Range Profile

Table 6-13. SUAE Link Power Budget

PARAMETER	NOMINAL VALUE 26 METER S-BAND	NOMINAL VALUE 64 METER S-BAND	NOMINAL VALUE 64 METER X-BAND	NOTES
1. Frequency (MHz)	2300.0	2300.0	-	
2. Spacecraft transmitter power (dBm)	39.0	39.0	39.0	
3. Spacecraft coupling loss (dB)	-2.0	-2.0	-1.5	S-Band: Pioneer F measured values X-Band: Waveguide with 5.5 dB/100 feet loss (eight feet); no diplexer; coax switch with 0.4 dB loss; plus allowance (0.7 dB) for couplings and VSWR loss
4. Spacecraft antenna gain (dBi)	32.8	32.8	44.1	Nine-foot parabolic reflector S-Band: Pioneer F and G measured value X-Band: Scaled from S- to X-Band
5. Antenna pointing loss (dB)	-2.2	-2.2	-0.9	S-Band pointing error: 1.4 degree X-Band pointing error: 0.25 degree
6. Polarization loss (dB)	-0.2	-0.2	-0.2	Spacecraft antenna axial ratio: 3 dB (measured) DSS antenna (210-foot) axial ratio: 1.4 dB (JPL 810-5)
7. Space loss (dB)	-277.1	-277.1	-288.3	Communication range: 5 AU
8. Atmospheric attenuation (dB)	0.0	0.0	-0.2	Per JPL document 810-5
9. Ground station antenna gain (dB)	53.3	61.4	71.5	Referenced to Maser input Per JPL document 810-5 Includes antenna elevation angle sag
10. Total received power (dBm)	-156.4	-148.3	-136.5	
11. Ground station system noise temperature (°K)	41.0	25.0	27.0	S-Band: per ARC document PC-222 X-Band: per JPL document 810-5
12. Relative increase in system noise temperature losses (°K)	0.0	0.0	6.0	Per JPL document 810-5
13. Ground station noise spectral density (dBm/Hz)	-182.2	-184.6	-183.4	
14. Total received power to noise spectral density ratio (dB-Hz)	25.8	36.3	46.9	
Carrier Loop Performance (5 AU)				
15. Carrier modulation loss (dB)	-7.8	-7.8	-7.8	Modulation index: 1.15 radians
16. Carrier power to noise spectral density ratio (dB-Hz)	18.0	28.5	39.1	
17. Carrier loop threshold bandwidth (dB)	4.8	4.8	4.8	$2B_{LO}$ = 3.0 Hz per JPL document 810-5
18. Carrier loop SNR threshold (dB)	10.0	10.0	10.0	See Text
19. Carrier performance margin (dB)	3.2	13.7	24.3	
20. Range for zero carrier margin (AU)	7.0	24.2	82.0	Modulation index: 1.15 radians

Table 6-13. SUAE Link Power Budget (Continued)

PARAMETER		NOMINAL VALUES 26 METER S-BAND	NOMINAL VALUES 64 METER S-BAND	NOMINAL VALUES 64 METER X-BAND	NOTES
1. Telemetry signal to noise spectral density at 1 AU (dB-Hz)		39.8	50.3	60.9	
2. Telemetry modulation loss (dB)		-0.8	-0.8	-0.8	Modulation index = 1.15 radians
3. E_b/N_o required (dB) for a 10^{-3} deletion for a data rate of	1024 bps	3.6	3.6	3.6	Unpublished report by Dale Lumb NASA/ARC
	512 "	3.3	3.3	3.3	
	256 "	3.0	3.0	3.0	
	128 "	2.8	2.8	2.8	
	64 "	2.6	2.6	2.6	
4. Receiver loss (dB) above E_b/N_o for	1024 bps	1.4	1.4	1.4	Line 5 - line 3
	512 "	1.9	1.9	1.9	
	256 "	2.7	2.7	2.7	
	128 "	4.7	4.7	4.7	
	64 "	5.7	5.7	5.7	
5. E_b/N_o required plus receiver loss (dB). Sum of 3 and 4 for	$\geq$1024 bps	5.0	5.0	5.0	Measured @ JPL CTA-21, Experiments F/G NASA/ARC per D. Lumb.
	512 "	5.2	5.2	5.2	
	256 "	5.7	5.7	5.7	
	128 "	7.5	7.5	7.5	
	$\leq$ 64 "	8.3	8.3	8.3	
6. Telemetry signal to noise spectral density required for	2048 bps	38.92	38.92	38.92	Bandwidth in dB plus line 2 and 5.
	1024 "	35.9	35.9	35.9	
	512 "	33.1	33.1	33.1	
	256 "	30.6	30.6	30.6	
	128 "	29.4	29.4	29.4	
	64 "	27.2	27.2	27.2	
7. Maximum communication range R(x) in AU at information rates x.	R(2048)	1.11	3.7	12.6	
	R(1024)	1.56	5.25	17.8	
	R(512)	2.21	7.24	24.6	
	R(256)	2.88	9.65	32.7	
	R(128)	3.3	11.1	37.5	
	R(64)	4.25	14.3	48.4	

Modulation Index. Performance to 24 AU can be restored, notwithstanding the 12.2 carrier loop SNR threshold, if the modulation index is decreased from 1.15 to 1.02 radians. By this means the fraction of power in the carrier is raised from 0.167 to 0.277, while the power in the modulation is lowered from 0.833 to 0.723, a decrease of only 0.6 dB. Thus, with small loss in data power, the range limit could be restored, using a single modulation index of 1.02 radians from S-band.

On the other hand, better performance is available and there is greater tolerance of uncertainties if two modulation indexes are available, commandable in flight. One would be 1.15 radians to maximize data rates when the range is below 18 AU. The other would be about 0.95 radians, giving a nominal maximum range of 26.8 AU, assuring performance at 20 AU. Modulation power is down 1.0 dB at the lower modulation index.

The modulation index change is effected within each S-band driver, as indicated earlier in this section.

The X-band modulation index is retained at a single value of 1.15 radians, established in each X-band driver. There is no need to have this value switchable, because the mission range does not approach the carrier power-limited value of 82 AU.

Antenna Pointing Errors. The link budgets of Table 6-13 are based on relatively small antenna pointing errors and losses (line 5). For the X-band link the loss is 0.9 dB and the pointing error 0.25 degrees. These pointing errors have the following components, in degrees:

Component	S-Band	X-Band
Antenna actual electrical axis relative to intended axis*	0.1	0.05
Antenna intended axis relative to spacecraft body Z axis	0.9	0
Spacecraft body Z axis relative to spacecraft spin axis*	±0.09	±0.09
Spacecraft spin axis relative to the earth line	0.4	0.15
Total pointing error	1.44	0.25

*These two quantities root-sum-squared.

The first entry indicates the X-band antenna pattern would be favored in adjusting the feed position with respect to body axes during installation and alignment, but its narrow beamwidth would permit such fine adjustment by pattern measurements. The second entry shows the intended 0.9-degree permanent offset of the S-band pattern for conical scanning.

The third entry indicates a range encompassing predictable and unpredictable principal axis tilts due to mass properties effects. (The predictable component is reduced from Pioneer F/G because the propellant tank is now on the center of mass.)

The bottom entry represents the offset of the spin axis from the earthline. For X-band this component has been reduced about as much as possible. To get it to 0.15 degree requires careful measurements with the conscan signal processor, and correction by open-loop pulses as well as closed-loop homing, as it represents residual error less than

the closed-loop threshold setting. The 0.4 degree for S-band tolerates a less accurate earth-pointing procedure, and several days' drift of the spacecraft-earthline (0.05 degree/day at Uranus) since the last earth-pointing.

The first and third entries, being essentially random and equally distributed in X and Y directions are combined by root-sum-squaring. Otherwise, all entries are added algebraically, to be applicable at the worst point in the spin cycle.

Admittedly, the pointing error for X-band performance requires careful honing of the orientation procedures, and is not representative of what would actually transpire during the bulk of the cruise portion of the mission. On the other hand, X-band data rates are comfortably high, and an additional 1 or 2 dB drop due to excessive pointing error could be tolerated without hurting the mission. Also note that the table and figure are based on 8 watts transmitted power, whereas the spacecraft DC power budget permits 10 or 12 watts to be transmitted.

6.7 DATA HANDLING

The data handling subsystem (DHS) for the SUAE mission (see Figure 6-53) is virtually identical to the Pioneer F/G configuration. The major change in this subsystem is the expanded storage required to support the SUAE mission. The data handling subsystem accepts digital and analog data, arranges these data into a selected format, and generates a coded digital bit stream for subsequent transmission to the earth. The data handling subsystem has three C-MOS data storage units (DSU's), each of which can store 245, 760 bits of data. The subsystem also provides various timing and control signals to scientific instruments, to the probe data buffer, and to various other subsystems.

The subsystem has three basic modes of operation: real time, telemetry store, and memory readout (Figure 6-54). 23 data formats (A, B, C, and D plus various combinations) are available via ground command (Figure 6-55). Binary bit rates available range from 16 to 2048 bps. Formatted digital data in NRZ format (uncoded or coded as selected by ground command) is biphase modulated onto a 32.768 kHz subcarrier which is then used to modulate the S- and/or X-band transmitters.

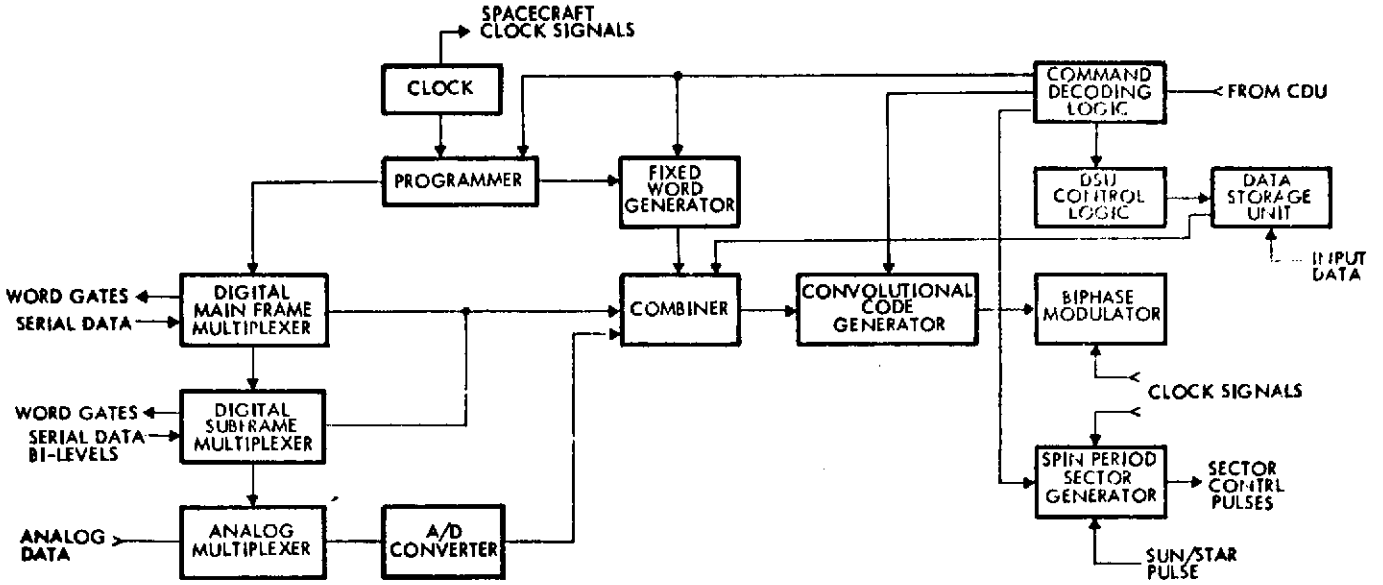

Figure 6-53. Data Handling Subsystem Block Diagram

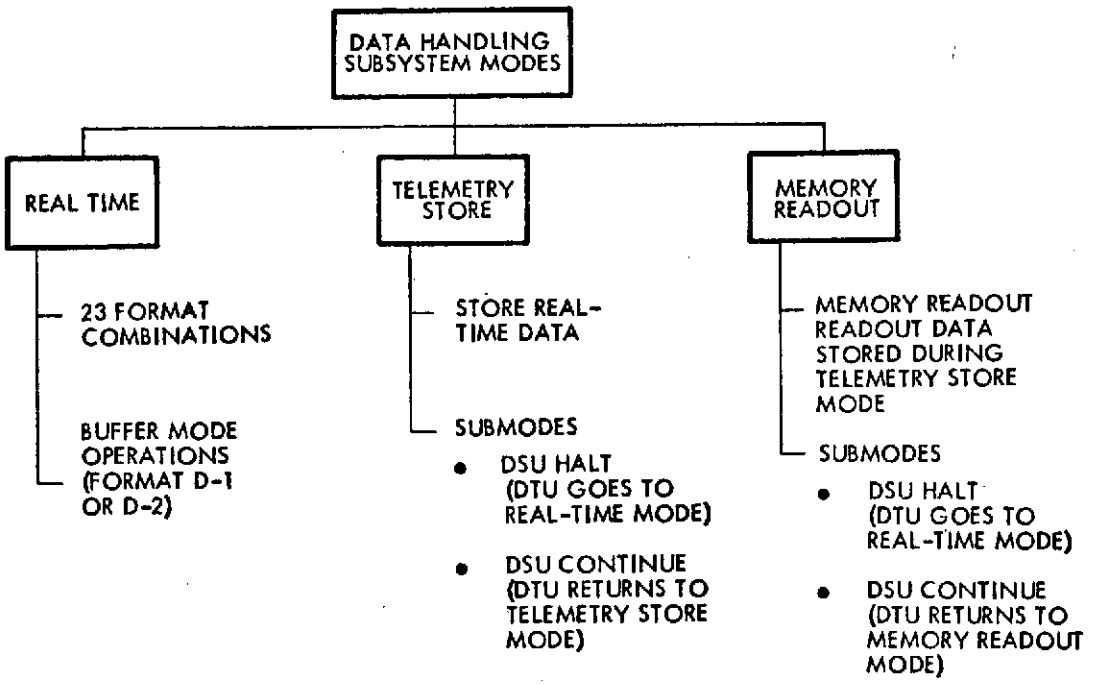

Figure 6-54. Data Handling Subsystem Modes

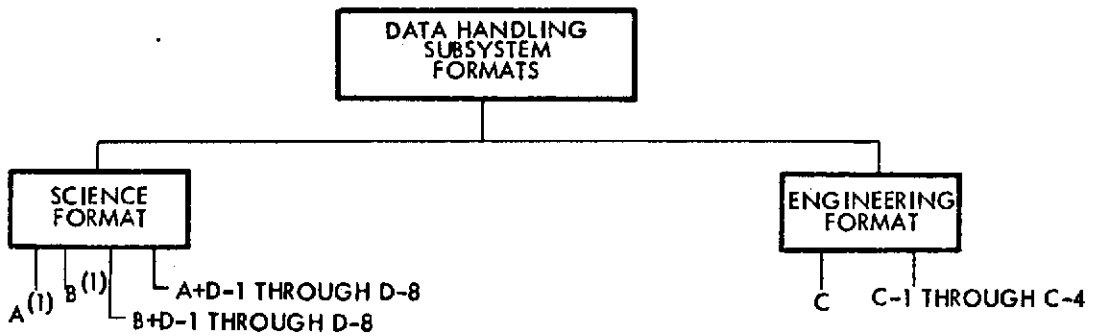

(1) FORMATS A AND B CONTAIN A 64-WORD SCIENCE SUBCOMMUTATOR AND A 128-WORD ENGINEERING SUBCOMMUTATOR.

Figure 6-55. DHS Formats

6.7.1 Subsystem Requirements

6.7.1.1 Functional Requirements

The principal functions of the data handling subsystem are:

a) Analog-to-digital data conversion

b) Analog and digital signal multiplexing

c) Structuring data into the desired format

d) Data storage

e) Generating various clock or timing signals

f) Convolutionally encoding the final data stream prior to transmission.

These are the same requirements as existed on the Pioneer F/G mission.

6.7.1.2 Input Data Rates

The total telemetry data rate will be comprised of three major components: probe data, bus science data, and general engineering or state-of-health data. The SUAE mission, as defined by the statement of work, has identified the bus science data rate as 64.4 bps (see Section 4 for details). The probe data rate has been established as 88 bps. The sum of these two inputs (64.4 + 88 bps) is 152.4 bps. The bit rates available from the DTU are 16, 32, 64, 128, 256, 512, 1024, and 2048 bps. Thus, the minimum or lowest possible bit rate for this mission is 256 bps if simultaneous probe data and bus science data are mandatory. However, by sacrificing real-time transmission of some bus science data (these data could be stored), it would be possible to reduce the required bit rate to 128 bps. Based on the proposed X-band system performance with the 64-meter dish (see Section 6.6), this link will handle data rates up to 512 bps at communication ranges up to 24.6 AU or well beyond the maximum range of Uranus. Of course much higher bit rates are possible at the range of Saturn with the X-band system; up to 2048 bps.

As noted in Section 6.6, the S-band system cannot wholly replace the X-band link at Uranus. It is, however, a credible backup to the X-band system at Saturn at bit rates up to 256 bps. This bit rate of 256 bps has been selected as the baseline or nominal Uranus mission requirement. It should be noted that one candidate bus experiment, identified as a multispectral line-scan camera, could make good use of higher bit rates. However, no specific data rate requirements have been identified for this experiment. Any bit rates from 16 to 2048 bps can be selected by ground command.

6.7.1.3 Telemetry Formats

The Pioneer F/G offers a total of 23 different formats which must be configured prior to launch, but which can be selected by command. Each format variation is identified with the structure of the telemetry main frame.

Each main frame is composed of 64 words, and each word is 3 bits long. Status or bilevel data is also restricted to subframe words like the analog data, and only 1 bit is allocated per channel. Spacecraft generated words are transmitted with the most significant bit first. The main frame organization for all format types except the D formats is shown in Figure 6-56. Bits 1 through 24 and 97 through 120 are reserved for

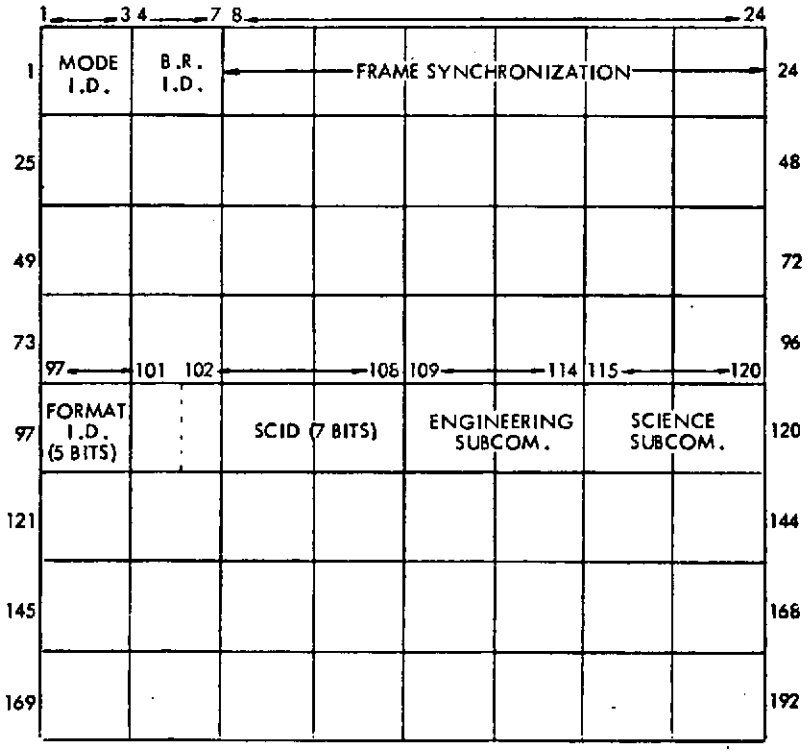

NOTES:

1. FORMATS A AND B ARE THE BASIC SCIENTIFIC FORMATS WITH A WORD SIZE OF 3 BITS.
2. SCID = SUBCOMMUTATOR IDENTIFICATION
3. EACH BLANK WORD SLOT DENOTES A SERIAL DIGITAL WORD SLOT. FORMATS A AND B ARE BOTH INDEPENDENTLY PATCHABLE IN THE DATA PORTION OF THE MAIN FRAME. EACH OF THESE TWO FORMATS HANDLE A MAXIMUM OF 12 DIGITAL INPUT CHANNELS.
4. EACH MAIN FRAME WORD SLOT IS SAMPLED AT A RATE OF B.R/192, WHERE B.R. = BIT RATE.

Figure 6-56. Main Frame Organization

fixed words. In the case of the D formats, all 192 bits are assigned to a single input (two inputs may be shared with format D-2). The D format can only be used in conjunction with the A or B format. That is, one main frame can be any D format, but the next or alternate main frame must be either A or B.

Formats C-1 through C-4 are used to accelerate portions of the engineering subcommutator channel to the main frame (Figure 6-57). The normal organization of the engineering subcommutator is shown in Figure 6-58. The science subcommutator also utilizes 6 bit words, but it is only 64 words long (Figure 6-59).

1	MODE AND B.R. I.D.	FRAME SYNC.						8
9								16
17	FORMAT AND SCID		ENGR. SUBCOM	SCIENCE SUBCOM				24
25								32

NOTES:

1. THE FOLLOWING PORTIONS OF THE ENGINEERING SUBCOMMUTATOR ARE ACCELERATED TO THE MAIN FRAME RATE.
   - C1 = # 1 32
   - C2 = #33 64
   - C3 = #65 96
   - C4 = #97 128
2. BLANK WORD SLOTS DENOTE DATA WORDS ACCELERATED TO A NOMINAL RATE OF B.R./192, WHERE B.R. = BIT RATE (BPS). EIGHT OF THE 6-BIT DATA WORDS ARE INHIBITED BY THE MAIN FRAME FIXED WORDS AS INDICATED.

Figure 6-57. Accelerated Subcommutator Format C1, C2, C3 or C4

1	A/D Low	Calib. Med.	Volt High	Ext. SCID	A	A	A	B	8	C1
9	A	A	A	X	A	A	A	X	16	
17	A	A	A	B	A	A	A	B	24	
25	A	A	A	B	A	A	A	B	32	
33	A	A	A	A	A	A	A	A	40	C2
41	A	A	A	A	A	A	A	A	48	
49	A	A	A	A	A	A	A	A	56	
57	A	A	A	A	A	A	A	A	64	
65	A	A	A	A	D	D	D	B	72	C3
73	A	A	A	A	D	D	D	B	80	
81	A	A	A	A	D	D	D	B	88	
89	A	A	A	A	D	D	D	B	96	
97	B	A	D	D	X	X	X	X	104	C4
105	B	D	D	D	D	D	D	D	112	
113	B	A	D	D	D	D	D	D	120	
121	D	D	D	D	D	D	D	D	128	

Notes:

1. The engineering subcommutator is located in word slot Nos. 37 and 38 of the main frame, Format A or B, with a 6-bit word size.
2. Each subframe is sampled at a nominal rate of BR/24, 576 where BR = bit rate (bit/sec), when this subcommutator is used in Format A or B.
3. A = analog data input.
4. D = 6-bit serial digital word.
5. B = six bilevel inputs.
6. X = words supplied by the fixed word generator:
   a. Roll attitude timing: Word Nos. 12 and 16, 12 bits.
   b. Spin rate and phase indicator: Word Nos. 101 thru 104, 24 bits.
   The first 5 bits of word 104 contains phase and bit 6 contains the sign bit.
7. Word Nos. 1 through 4 have internally hardwired multiplexed data information as indicated (three analog and 6 bilevel channels).
8. Bit No. 1, word No. 32,represents an internally wired bilevel channel for convolutional coder ON/OFF indication.
9. Bit Nos. 1 thru 3, word 113 contain spin period sector generator status bits.

Figure 6-58. Engineering Subcommutator

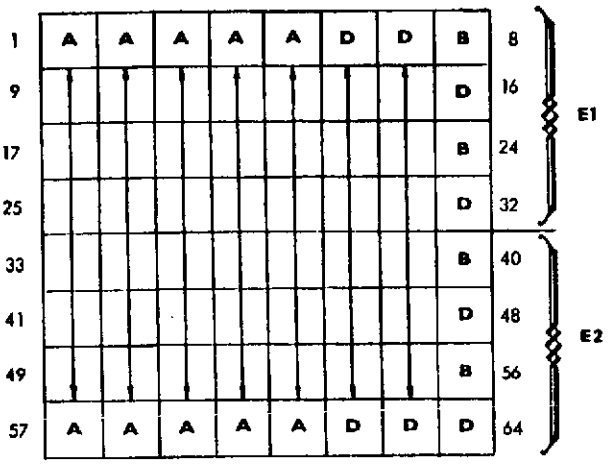

NOTES:

1. THE SCIENCE SUBCOMMUTATOR IS LOCATED IN WORD SLOT #39 AND #40 OF THE MAIN FRAME, FORMAT A OR B, WITH A 6-BIT WORD SIZE.
2. EACH SUBFRAME IS SAMPLED AT A NOMINAL RATE OF B.R./12,288, WHERE B.R. = BIT RATE (BIT/SEC), WHEN THIS SUBCOMMUTATOR IS USED IN FORMAT A OR B.
3. A = ANALOG DATA INPUT.
4. D = 6-BIT SERIAL DIGITAL WORD.
5. B = 6 BILEVEL INPUTS.

Figure 6-59. Science Subcommutator

A possible assignment of scientific formats for the SUAE spacecraft is as follows:

	Format			
	A	B	D-3	D-4
Fixed words	48 bits	48 bits	0	0
Bus science (excluding imaging)	105	0	0	0
Real-time probe data	24	144	0	0
Imaging data	0	0	192 bits	0
Probe stored data	0	0	0	192 bits
Spare	15	0	0	0
Total	192 bits	192 bits	192 bits	192 bits

Format A (Figure 6-60a) would be used for all bus science in cruise and in encounter phases, except for imaging, and would meet the 64.4 bits/sec requirement for these instruments collectively whenever the downlink bit rate is 128 bits/sec or greater (256 bits/sec or greater if in one of the A-D formats). Format A also devotes 24 bits to real-time probe data. The 88 bits/sec at which real-time probe data is received and can be completely accommodated in Format A if the downlink bit rate is 1024 or 2048 bits/sec (2048 bits/sec if in one of the A-D formats).

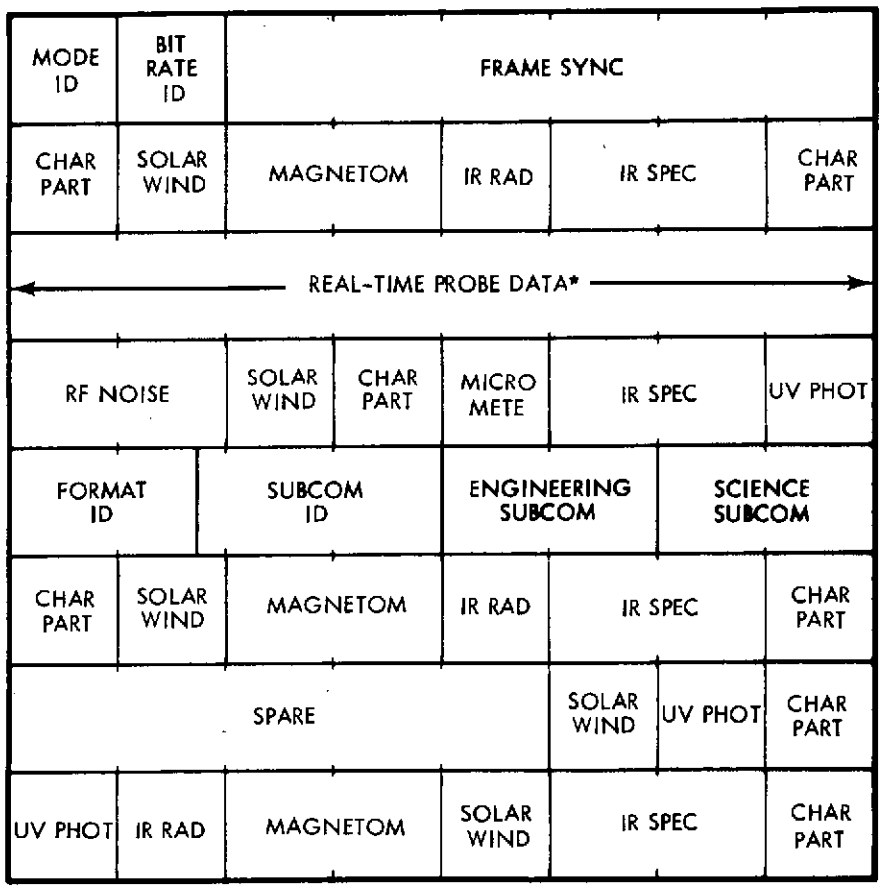

AT 128 BPS NOMINAL

*MUST BE AT 1024 OR 2048 TO UTILIZE FOR PROBE REAL TIME

Figure 6-60a. A Format

Format B (Figure 6-60b) devotes all non-fixed words to real-time probe data. The 88 bits/sec of probe data will be completely accommodated by Format B if the downlink bit rate is 128 bits/sec or greater (256 bits/sec or greater if in one of the B-D formats).

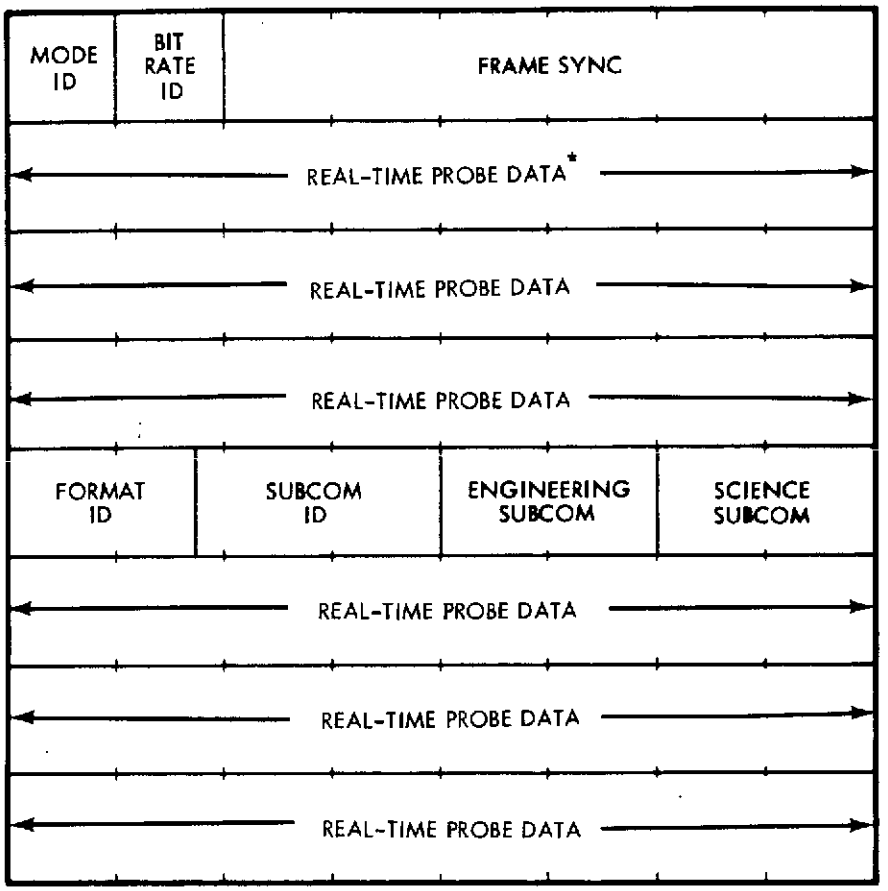

*INCLUDES 132 BITS FROM PROBES, 8 MESSAGE LENGTH BITS, AND 4 FILL BITS, NOMINAL AT 128 BITS/SEC

Figure 6-60b. B Format

Format D-3 is exclusively for imaging data, and Format D-4 exclusively for stored probe data. All critical spacecraft operations (midcourse maneuvers, precession maneuvers, etc.) will utilize the engineering (C) formats. Checkout of the attached probe will use A or B formats.

For a mission delivering the probe to Saturn, interplanetary cruise science will be obtained via Format A. This will satisfy the nominal bus science bit rate requirement at 128 or more bits/sec downlink data rate. From Section 6.6, this rate can be achieved on S-band to 26-meter stations out to 3 AU, on S-band to 64-meter stations beyond Saturn, and on X-band beyond Uranus.

Near Saturn, when imaging data may be obtained, Format A-D3 would be used. The X-band data rate of 2048 bits/sec will provide

1024 bits of imaging data per second. Other bus science is obviously satisfied. When probe data are to be received by the bus and relayed Format A-D4 will be used, both for real-time probe data relay and for later replay of stored probe data. In the event X-band transmission fails Format B-D4 will handle real-time and stored probe data at the S-band rate of 256 bits/sec, although full replay of the stored data will take longer, probably until after the spacecraft crosses the ring plane.

Beyond Saturn bus science would again be transmitted in Format A, but after about 11 AU range, downlink transmission on S-band to 64-meter stations would be at 64, 32, or 16 bits/sec, and would not support nominal bus science data rates. X-band will probably support a 1024 bits/sec downlink rate from Uranus (possibly only 512 bits/sec), easily accommodating all bus science in Format A. When imaging data are desired, approaching Uranus, Format A-D3 will devote 512 bits/sec to imaging data and 512 bits/sec to fixed words and other bus science. Thus a 250,000-bit image can be transmitted in 8 minutes, a 750,000-bit image in 24 minutes. If the X-band link has failed, S-band transmission from Uranus is probably at 16 bits/sec, which gives only one-eighth the nominal bit rate for non-imaging bus science. Imaging data could comprise no more than 8 bits/sec, so that a 250,000-bit image would require 9 hours to transmit, a 750,000-bit image 26 hours. Without X-band at Uranus, imaging would be severely limited, probably consisting of one image, stored, and transmitted later in Format A-D3.

For a mission delivering the probe to Uranus, again interplanetary cruise science will utilize Format A, changing to Format A-D3 near Saturn and approaching Uranus, when imaging data are desired. At Uranus, if X-band provides 1024 bits/sec telemetry, Format A will handle real-time probe data as well. However, if 512 bits/sec is the rate, Format B will be necessary. Format B-D4 will accommodate both real-time and stored probe data. In the event X-band transmission fails, the S-band link will probably only support 16 bits/sec from Uranus, and no format can keep up with real-time probe data. The storage mode using Format A-D4 or B-D4 would then be the only way to bring probe data from Uranus to the earth.

6.7.1.4 Storage Requirements

Storage of data during various phases of the SUAE may be desirable to support certain experiments such as the multispectral line-scan camera, to acquire data during the period when the spacecraft is occulted by the target planet, or to increase the probability of acquiring all of the probe data transmitted to the spacecraft. It is this last capability, which has the highest priority, that will be used to size the memory capacity.

Probe data will emerge from the data synchronizer at a nominal bit rate of 88 bps, and in a continuous stream. These data must be temporarily stored (buffered) prior to entry into the DTU. For long-term storage, they will also be sent directly to the memory unit, for later transmission. The total storage required for probe data may be calculated as the product of probe bit rate and probe transmission time. For this study, the maximum quantities and product are:

$$\text{Storage} = \text{probe bit rate} \times \text{transmission time}$$

$$= 88 \text{ bps} \times 4575 \text{ seconds}$$

$$= 402,600 \text{ bits}$$

If the baseline (nominal) trajectories are used, the elapsed time from 600 km to the 10-bar level drops to about 2700 seconds at either Saturn or Uranus and now the required memory capacity is only 240,000 bits.

The multispectral line-scan camera as defined in the study RFP does not identify sufficient camera characteristics to calculate its required storage. However, some preliminary analysis indicates that a memory size of 300,000 to 400,000 bits would be a reasonable compromise, but as much as 10^5 bits could be utilized by a line scan imager.

The third memory requirement, recording during periods of occultation, can be bounded by evaluating the potential operable bus science experiments during eclipse to establish a nominal bit rate and multiplying this number by the eclipse period. With the current experiment complement, a reduced data storage rate of 32 bps is feasible,

althouth less than the nominal data rate of all non-imaging instruments. At Uranus, the eclipse period is about 2.8 hours in duration. Hence, occultation data would use 320,000 bits of storage. These data could be read out to earth after occultation in slightly over 5 minutes, at 1024 bits/sec.

From the above, we have identified three separate demands for a memory with a capacity of roughly 300,000 bits. Ideally, if these three users could use the same memory, it would be most efficient to use only one storage unit. Unfortunately, the demands for data storage overlap as illustrated by Figure 6-61. Here we see that all three data sources could demand storage throughout the occultation phase. But they do not have equal priority, and at the time of probe entry, probe data has first priority. It is reasonable to assume that no camera image would be transmitted after probe entry and hence only the occultation and probe data would be competing for memory. If a third memory unit is carried for reliability purposes, and if all three units survive, then the camera data could also be preserved throughout the occultation period. Alternately, it may be required that the probe data be simultaneously loaded into two of the three memory units in which case the camera data would be eliminated as above.

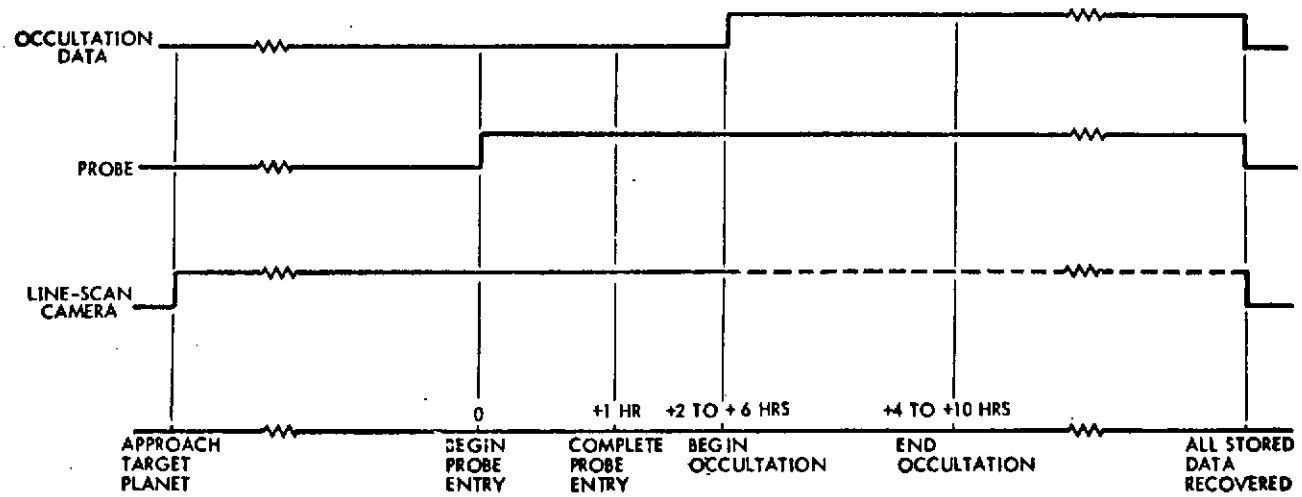

Figure 6-61. Data Storage Timeline

6.7.2 Digital Telemetry Unit

The DTU for the SUAE mission is identical to the unit used for Pioneer F/G. There will obviously be changes in inputs and outputs and changes in data formats. These changes will not require any significant changes in the physical configuration of this unit. As with all Pioneer equipment, this unit must be evaluated in terms of its ability to meet the seven-year mission life in an operable state. Subsequent analyses may require that total redundancy rather than partial redundancy be employed in which case the unit packaging would have to be redesigned. For this study, the unaltered Pioneer F/G unit is used as the baseline design. Figure 6-62 identifies the major DTU interface with the spacecraft.

6.7.2.1 Functional Characteristics Summary

Table 6-14 lists the basic characteristics of the DTU; Table 6-15 tabulates the sampling rates for mainframe and subframe words versus format and bit rate. The DTU processes analog, digital and bilevel (discrete) inputs into a serial time-multiplexed PCM signal which modulates the telemetry transmitter. The DTU operates in 8 bit rates, three modes, and 23 format combinations to process 290 data inputs. The DTU provides 20 timing and operational status signals to the instruments. The unit converts analog inputs into a 6-bit digital code, convolutional codes formatted data and provides a biphase modulated 32 kHz squarewave, NRZ-L output to the communication subsystem. The unit is fully redundant except for the extended frame counter, the inflight calibration voltage generator, and the subframe multiplexer which is partially redundant. The redundant DTU can be selected by ground command.

6.7.2.2 Inputs

The DTU accepts the following types of input signals:

a) Digital and analog data from other spacecraft subsystems and the scientific instruments

b) Operational status (bilevel) signals from other spacecraft subsystems and the scientific instruments

c) Analog signals from the spacecraft engineering instrumentation sensors

d) Digital data from the DSU

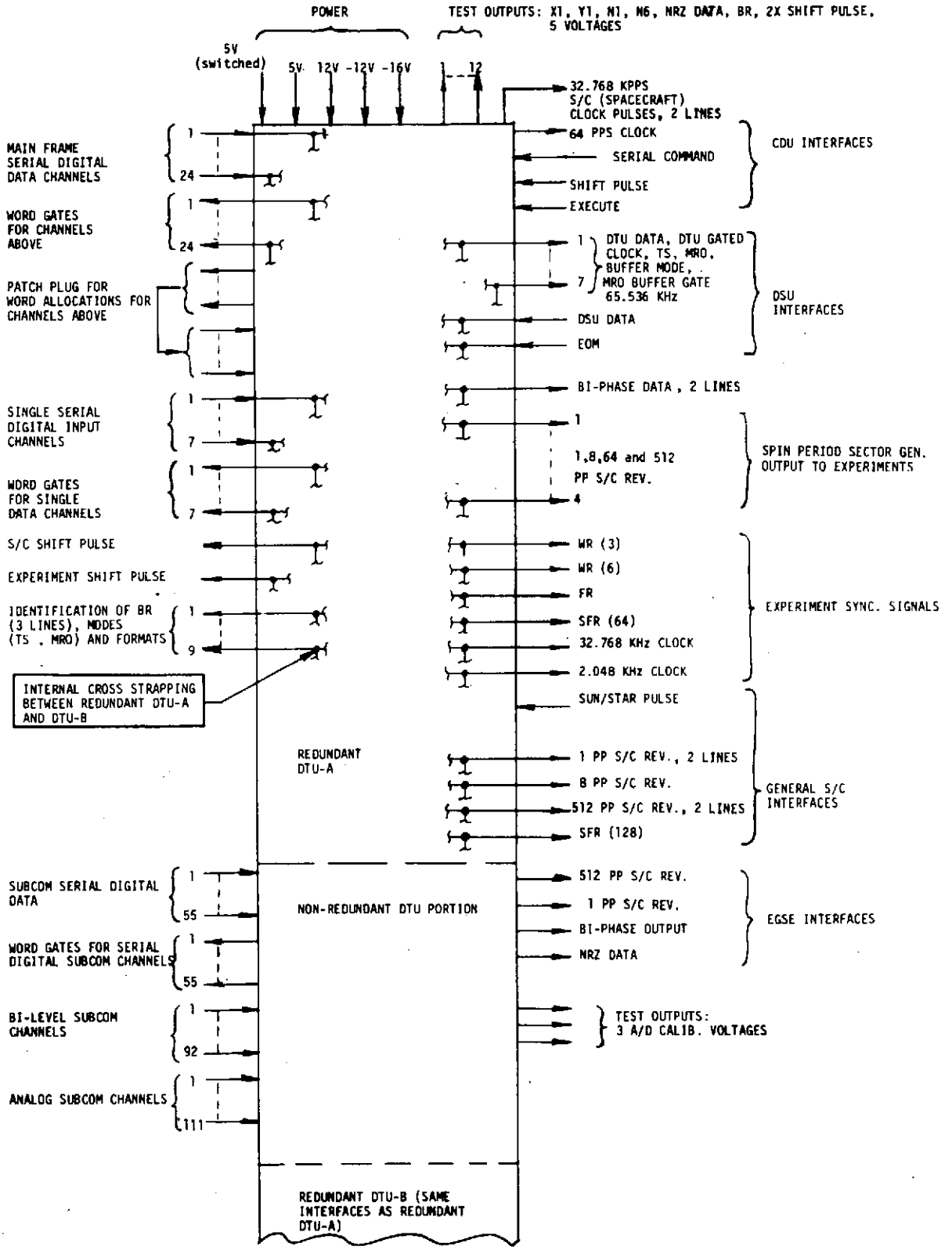

Figure 6-62. Data Handling Unit Interfaces

Table 6-14. DTU Characteristics

	Characteristics
Basic clock frequency	4.194304 MHz Stability = 0.02%
Type	PCM
Bit rates	2048, 1024, 512, 256, 128, 64, 32, 16 bps
Data input channels Mainframe	32 digital channels 24 basic science format A&B 8 special science formats D-1 through D-8
Subframe	55 digital 92 bilevel 111 analog
Input voltage range	0 to +3 volts analog Digital and bilevel comparator threshold +2.0 volts
A/D accuracy	6 bits (±48 mv)
Data output	Biphase modulated NRZ-L
Subcarrier frequency	32.768 KHz ±0.02% squarewave
Data coding	Convolutional coded data output upon command
Operating modes	Real time Telemetry store Memory readout
Data formats, science (selected by ground command)	A (Patchable), B (Patchable), D-1 through D-8, E-1 and E-2 64-word science subframe (not selectable by ground command)
Engineering (selectable by ground command)	C - accelerate formats C-1 through C-4 as four 32-word main frames in sequence C-1 accelerate only C-1 in main frame C-2 accelerate only C-2 in main frame C-3 accelerate only C-3 in main frame C-4 accelerate only C-4 in main frame
Frame size Main frame Subframe	192 bits, 3 bit-word groups Science: 64, 6-bit words; Engineering: 128, 6-bit words
Mainframe length Science	Format A&B: 192 bits Format D-1 through D-8: 384 bits
Engineering	Format C: 768 bits Format C-1 through C-4: 192 bits
Extended frame counter	Identifies 8192 unique data frames

Spin period sector generator

a) Divide spacecraft revolution into 512 sectors to within 150 μs

b) Operate over spacecraft spin rate from 2 to 7 rpm

c) Outputs

1) 1 pulse per revolution - when in averaging mode time between any two adjacent pulses equal to within 150 μs within the same set of 64 spacecraft revolutions.

2) 8 pulses per revolution: Accuracy = spin period/8 to within 150 μs

3) 64 pulses per revolution: Accuracy = spin period/64 to within 150 μs

4) 512 pulses per revolution: Accuracy = spin period/512 to within 150 μs

d) Modes: Averaging, nonaveraging, ACS

e) 1 PPR pulse 0 or 180 degrees upon command

f) Phase error readout: to within 2 ms

g) Configuration at power turn-on: ACS mode
1 PPR Pulse = 0 degree

Power requirements	3.86 watts

Table 6-15. Data Sampling Rate

MAIN FRAME WORDS

Bit Rate	Format		
	A, B, C-1, C-2, C-3, C-4	D-1 thru D-8	C
2048	0.094 sec	0.188 sec	0.375 sec
1024	0.188	0.375	0.750
512	0.375	0.750	1.500
256	0.750	1.500	3.000
128	1.500	3.000	6.000
64	3.000	6.000	12.000
32	6.000	12.000	24.000
16	12.000 sec	24.000 sec	48.000 sec

SCIENCE SUBCOMMUTATOR WORDS

Bit Rate	Format		
	A, B, C-1, C-2, C-3, C-4, C	D-1 thru D-8	
2048	0.10 min	0.20 min	
1024	0.20	0.40	
512	0.40	0.80	
256	0.80	1.60	
128	1.60	3.20	
64	3.20	6.40	
32	6.40	12.80	
16	12.8 min	25.6 min	

ENGINEERING SUBCOMMUTATOR WORDS

Bit Rate	Format		
	A, B, C-1, C-2, C-3, C-4, C	D-1 thru D-8	
2048	0.20 min	0.4 min	
1024	0.40	0.8	
512	0.80	1.6	
256	1.60	3.2	
128	3.20	6.4	
64	6.40	12.8	
32	12.80	25.6	
16	25.6 min	51.2 min	

e) An 8-bit serial command from the CDU for changing modes, formats, and bit rates

f) Spacecraft roll pulses from the attitude control subsystem for the generation of spin period sector pulses

g) Power from the power subsystem.

6.7.2.3 Outputs

The DTU furnishes the following output signals:

- 32.768 kHz PCM NRZ-L biphase modulated squarewave
- 65.536 kHz clock to DSU
- 32.768 kHz clock to ACS, DDU, conical scan unit and scientific instruments
- 2048 Hz clock to scientific instruments
- 64 Hz clock to CDU
- Digital word gates to spacecraft subsystems and scientific instruments
- Main frame and subframe rate pulses to scientific instruments
- Bit shift pulses to spacecraft and scientific instruments
- Format and bit rate status signals to scientific instruments
- Roll index pulse to spacecraft and scientific instruments
- Spin period sector pulses (512, 64, and 8) to spacecraft and scientific instruments
- Commands and control signals to DSU
- Digital data to DSU.

6.7.2.4 Circuit Blocks

The DTU contains the following basic circuit blocks:

- Crystal controlled oscillator
- Programmer
- Multiplexers
- Digital comparator
- A/D converter
- Fixed-word generator
- Combiner
- Convolutional coder
- Biphase modulator
- Command decoder logic

- DSU control logic
- Spin period sector generator
- Roll attitude timing counter
- Interface buffers
- In-flight A/D calibration voltages
- Extended frame counter.

Figure 6-63 shows interconnections between the basic blocks. An 8-bit serial command is received from the command decoder unit; six of these are used to command the DTU. The first 2 bits shifted into the DTU are not used. The command decoding logic generates outputs to the programmer to control bit rate, format and mode. The command logic sends outputs to the DSU control logic to control DSU operation and to the convolutional coder to select coded or uncoded data.

6.7.2.5 Multiplexers

The data multiplexer selects each data input, one at a time, in accordance with the data format and provides a connection for the selection input to the A/D converter (analog inputs) or digital comparator (digital and bilevel inputs).

The main frame multiplexer is redundant and accepts only digital inputs. The subframe multiplexer is nonredundant and accepts analog, bilevel and digital inputs.

Each digital input has a corresponding word gate output which is used by the data source to gate data to the DTU. The DTU accepts digital data only during the period in which the corresponding word gate is true.

6.7.2.6 Digital Comparator

The digital comparator compares the serial digital and bilevel channel inputs with a fixed-reference point selected midway between the minimum true and the maximum false input levels (approximately 2 volts). If the input level is higher than the threshold voltage, the digital comparato gives a binary 1 output to the combiner, or a binary zero output, if the data input level is lower than the comparison reference voltage.

6.7.2.7 A/D Converter

The A/D converter encodes the selected analog input to a 6-bit

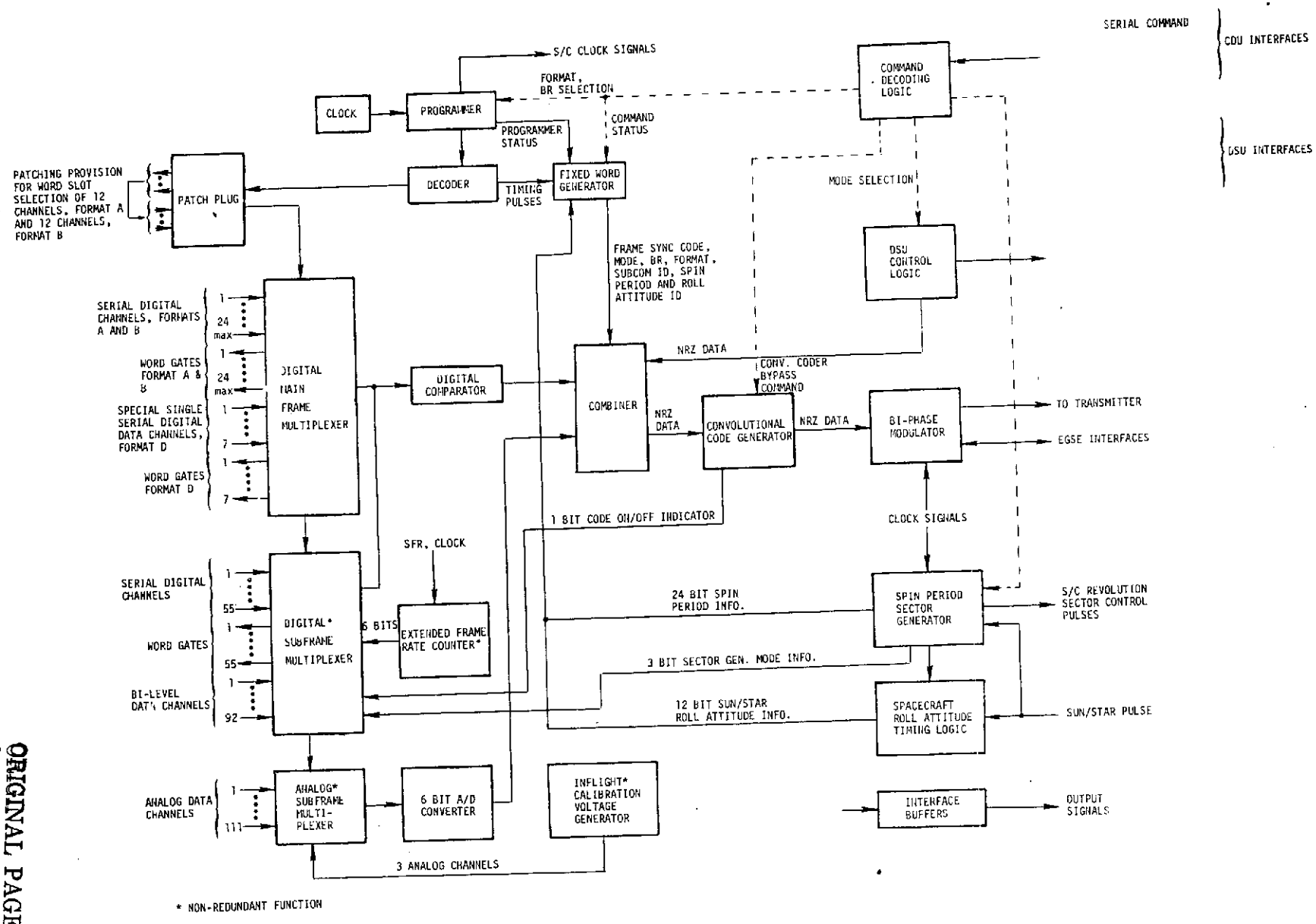

Figure 6-63. DTU Functional Diagram

binary word. The maximum encoding error due to all processes associated with the conversion of data from analog to a 6-bit digital word is less than ±1.6 percent of full scale or ±1 full least significant bit over th full qualification temperature range. The A/D is a ramp type converter where the analog input is compared with a linear ramp. Pulses are accu ulated within a register at a 1 MHz rate from the time a start signal is received to the time the linear ramp voltage equals the analog input. Th accumulated counts are then scaled to a 6-bit word for telemetry.

The accuracy of the A/D is continually checked by encoding three reference voltages and telemetering the results within three engineering subframe words. Analog data is telemetered most significant bit first.

6.7.2.8 Combiner

The combiner collects selected input data sources, fixed words (frame sync, mode and BR ID, etc.), DSU data and internal DTU status signals and combines these data into one serial output bit stream to the convolutional coder. Figure 6-64 illustrates the basic combiner logic a the system for bypassing the convolutional coder when uncoded data is required.

The convolutional coder is bypassed with logic gates as shown in Figure 6-64 to provide uncoded data output. As shown, two independent sources (DTU A and DTU B) can modulate the transmitter. Cross-strapping is provided to allow either DTU to drive either transmitter driver for fail-safe operation.

6.7.2.9 Biphase Modulator

This modulator modulates the serial PCM bit stream into a squar wave biphase data output. The modulating frequency is 32.768 kHz.

An example of the modulation is given in Figure 6-65. The modulated 32 kHz can be in phase for a "1" bit and 180 degrees from phase f a "0" bit or vice versa. The initial phase is determined by the state th biphase modulator flip-flop happens to assume during DTU power turn-(In Figure 6-65, an in-phase condition represents a "0" and an out-of-ph condition represents a "1" bit. The phase change is delayed 1-bit time plus one-half subcarrier cycle as indicated in the figure.

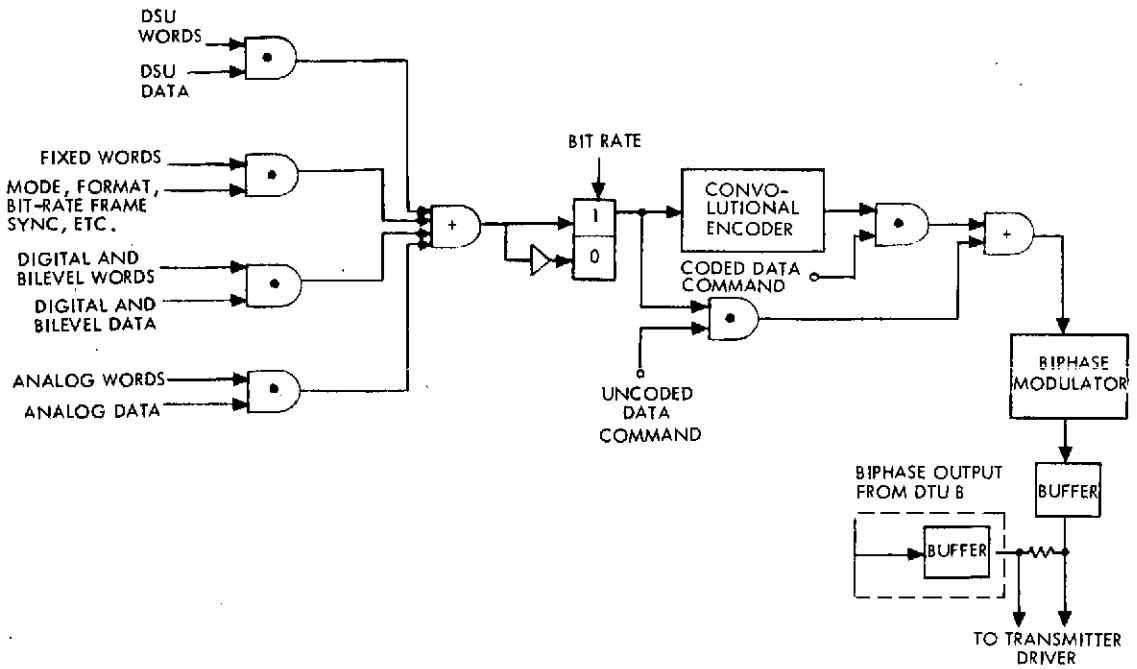

Figure 6-64. Combiner

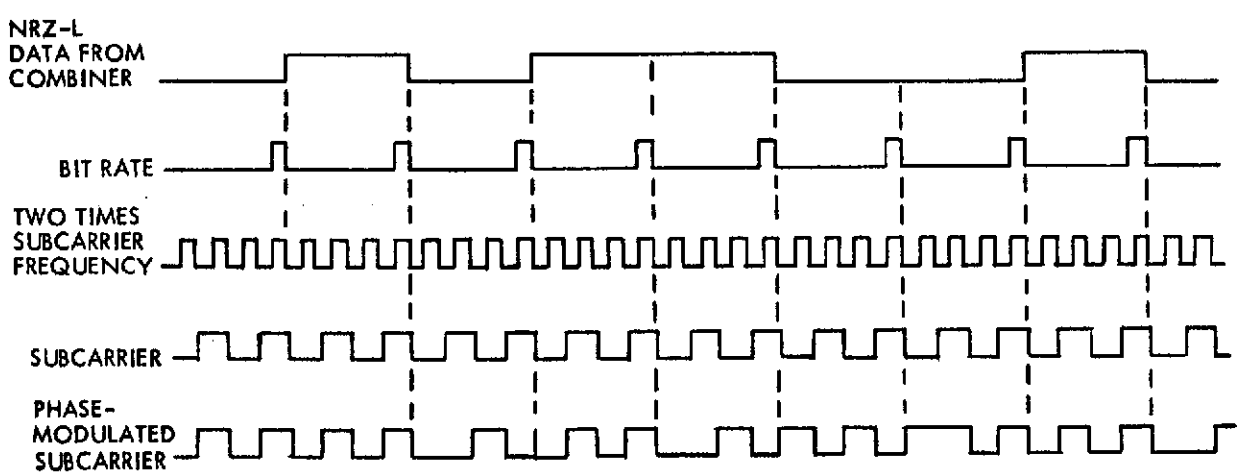

Figure 6-65. Biphase Modulator Timing Diagram

Figure 6-66 illustrates the biphase output interface with the transmitter driver. The circuit is designed such that either DTU can drive either driver. Furthermore, either output line can be shorted to the ground, and the other DTU will still drive the unshorted driver. A modification will permit the DTU's to drive either of the two S-band drivers and either of the two X-band drivers.

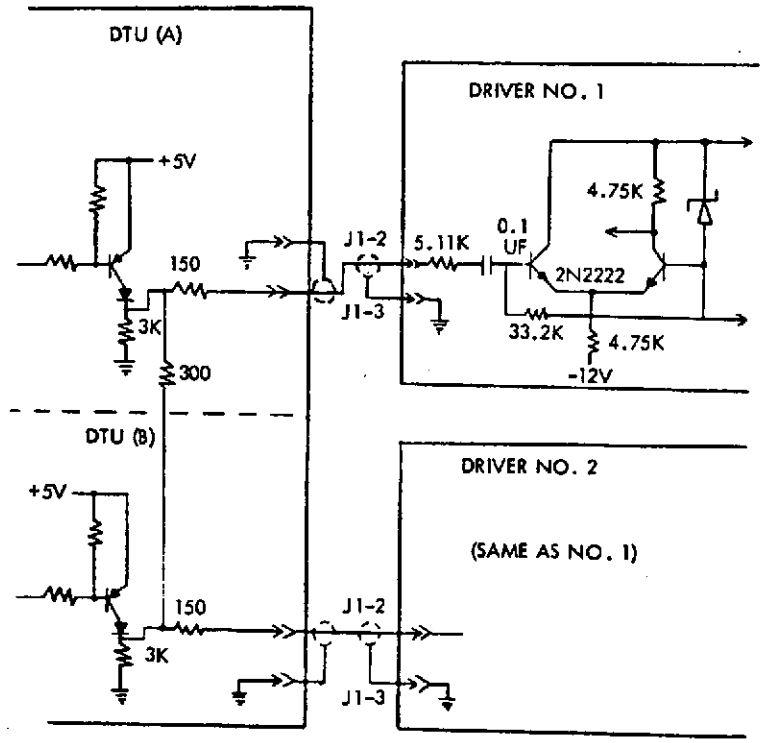

Figure 6-66. Circuit for Biphase Modulator Output

6.7.2.10 Command Operations

The DTU receives an 8-bit binary coded message from the CDU of which only the last six bits are processed. Since the spacecraft command message is eight bits long and the DTU requires only six bits for all of the data handling subsystem commands, each DTU command will respond to at least four 8-bit command numbers.

Figure 6-67 illustrates the command decode logic within the DTU. The first two bits (bits 3 and 4) determine the command type and the remaining four bits contain the select message. All commands are processed immediately except the mode commands which are synchronized with frame rate.

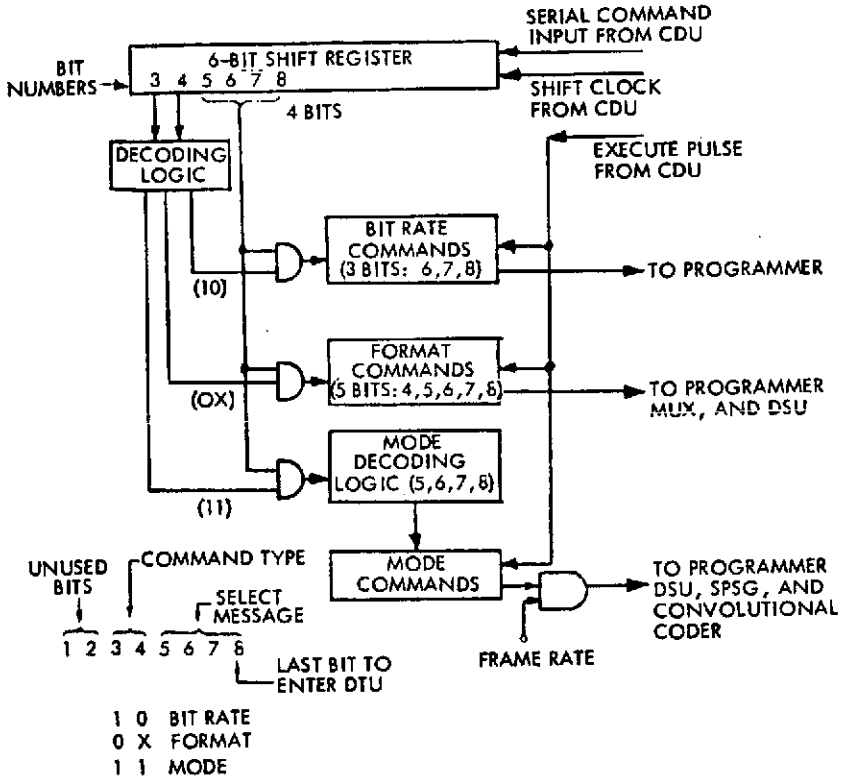

Figure 6-67. Command Decode Logic

The following commands can be detected and processed by the DTU:

1) 8 bit rate commands: 16, 32, 64, 128, 256, 512, 1024, and 2048 bps

2) 23 format command combinations: Formats A, B, C, C1, C2, C3 C4; D1 through D8 interleaved with Format A, and D1 through D8 interleaved with Format B

3) 3 basic modes: Real time, telemetry store and memory readout

   9 secondary modes: Memory halt, memory continue, 0 degree roll index, 180 degree roll index, coded data, uncoded data, spin averaging, non-spin averaging. ACS nonspin averaging.

The commands to select DTU redundancy A and B are decoded directly in the CDU. These commands operate relays within the power subsystem to turn DTU power on. The DTU upon power turn-on will operate in the realtime mode, in format C at a bit rate of 512 bps, with coded data and 0 degree roll index pulse output and SPSG in ACS mode.

6.7.2.11 Spin Period Sector Generator (SPSG)

Definition of terms.

1) P_R Pulse – Roll pulse
A pulse generated by the attitude control subsystem each time the spacecraft Y axis crosses the ecliptic plane.

2) P_f Pulse – Roll index pulse
A filtered roll pulse generated by the SPSG which occurs once per spacecraft revolution.

3) P_8 Pulse – Spin sector pulse
A pulse generated by the SPSG which occurs eight times between each P_f pulse.

4) P_{64} Pulse – Spin sector pulse
A pulse generated by the SPSG which occurs 64 times between each P_f pulse.

5) P_{512} Pulse – Spin sector pulse
A pulse generated by the SPSG which occurs 512 times between each P_f pulse.

Basic Operation. From the roll reference pulse provided by the attitude control subsystem, the spin period sector generator generates for the scientific instruments and spacecraft subsystems a roll-index pulse and spin period sector pulses corresponding to 512, 64, and 8 sectors per spacecraft revolution. The SPSG is fully redundant but requires commanding to the redundant DTU to operate the redundant SPSG. The function of the SPSG is to produce for roll reference a roll-index pulse which has less jitter than the roll pulse (up to $\pm$0.5 degree with Canopus as the source and up to $\pm$1.25 degrees with the sun as the source) and provide accurate spin period sector pulses. The SPSG generates an 18-bit spin period measurement which is telemetered in engineering subcomm words C-405, C-406, and C-407 with the MSB first. The SPSG also generates a phase error measurement between the roll pulse and the roll-index pulse with up to a maximum of 60 msec of phase error. This information is telemetered in bits 1 through 5 of engineering subcomm word C-408 with the MSB first. Bit 6 of work C-408 contains the sign bit where a 1 means the roll pulse has occurred

before the roll-index pulse and a 0 means the roll-index pulse has occurred before the roll pulse. The counters and registers of the SPSG are sized to allow normal operation with spin periods as long as 30 seconds.

Operating Modes. In establishing the period between roll-index pulses, the SPSG can operate in one of three modes:

1) Nonspin-averaging
2) Spin averaging
3) ACS.

At power turn-on the SPSG will automatically enter the ACS mode. The three modes are mutually exclusive and are selectable by ground command only. The commands that select the modes also synchronize the roll-index pulse following receipt of the command by the SPSG with the roll pulse irrespective of the operating mode in effect at the time of command reception; e.g., if the system is operating in the spin-averaging mode and it is determined that the phase error between the roll pulse and the roll index pulse is too large and that it is desirable to synchronize the two pulses (0 degree phase error), a spin-averaging mode command can be transmitted to the spacecraft which will synchronize the roll-index pulse with the roll pulse without interrupting the existing SPSG operating mode. The operating mode of the SPSG is identified in bits 2 and 3 of engineering subcomm word C-417. The operational concepts associated with each SPSG mode are as follows:

a) Nonspin Averaging Mode. In the nonspin averaging mode, the period between a pair of roll-index pulses, P_F, (at the beginning and end of a spacecraft revolution) is equal to the period between the pair of roll pulses, P_R, occurring during the previous revolution to within 150 μsec. In this mode a phase error can build up between the roll pulse and the roll-index pulse because of changes in the spacecraft spin rate. If there are no P_R pulses for an extended period of time, the generator will continue to provide P_F pulses based upon the period of the last two P_R pulses; however, upon receipt of the first P_R after the extended period of no P_R pulses, the P_F period is undefined until receipt of the second P_R pulse.

b) Spin-Averaging Mode. The spin-averaging mode operates in a similar fashion as the nonspin-averaging mode except that the SPSG measures the period of a block of 64 spacecraft revolutions instead of

each revolution. In this mode, the period between a pair of roll-index pulses is equal (to within 150 μsec) to the average period between pairs of roll pulses measured during the previous block of 64 revolutions. At constant spin rates, the spin-averaging mode is better than the nonspin-averaging mode since the change in phase error from revolution to revolution is smaller and is constant during a block of 64 revolutions. For changing spin rates, the non-spin-averaging mode is better than the spin-averaging mode to make the period between any adjacent pair of roll-index pulses or sector pulses the same as that between any other pair within the same block of 64 revolutions to within 150 μsec. If there are no P_R pulses for an extended period of time, the generator will continue to provide R_F pulses based upon this previous block of 64 P_R pulses; however, upon reinstatement of P_R pulses and completion of a block of 64 P_R pulses, the P_F period will be undefined for the next block of 64 P_R pulses.

c) ACS Mode. The ACS mode is provided to accommodate the constraints of the attitude control subsystem during times of high rate of change of spin rate, such as precession or velocity changes, when the acquisition of scientific data is not the primary spacecraft mode of operation. The ACS mode is exactly like the non-spin-averaging mode in operation except that there will be no phase error buildup between the roll pulse and the roll-index pulse since they will be essentially resynchronized with each roll pulse. In this mode, greater or fewer than 512-sector pulses can occur depending upon the phase difference between the roll pulse and the roll-index pulse from revolution to revolution. If there are no P_R pulses for an extended period of time, the generator will continue to provide P_F pulses based upon the period of the last two P_R pulses, however, upon receipt of the first P_R pulse after the extended period of no P_R pulses, the P_F period is undefined until receipt of the second P_R pulse.

Roll-index Phase Change. Since the spin axis of the spacecraft can point to either side of the sun during a year, the roll pulse can occur either when the reference line ascends through the reference plane or when it descends through the reference plane. Therefore, the SPSG can be commanded to change the phase of the roll-index pulse by 180 degrees at those times when the roll pulse occurs when the reference line descends through the reference plane. Bit 1 of engineering subcommutator word C-417 identifies whether the roll-index pulse is in phase with the roll

pulse (0) or whether the roll-index phase is 180 degrees out of phase with the roll pulse (1).

6.7.2.12 Convolutional Code Generator

The DTU has the capability of convolutional coding the output data bit stream (before biphase modulation) by means of redundant encoders. The coding or noncoding of the digital output data is controllable by ground command only. However, the DTU will assume the coded mode when electrical power is applied to the DTU. When the data subsystem is operating in the coded mode, the encoder will replace each data bit generated with two parity bits designated P and Q. The value of each parity bit is based on the values of selected data bits previously generated in a 32-bit shift register. The encoding cycle begins at the end of the last bit of each frame synchronization word at which time the shift register is reset to zero. The encoder shift register is reset for each 192-bit frame except when the DTU is operating in one of the D formats, in which case the shift register is reset every 384 bits since the frame synchronization word occurs in the interleaved Format A or B. If the convolutional coder is inputted with more than 33 consecutive 0's, its output will be a series of alternating 1's and 0's. Conversely, if the input is more than 33 consecutive ones, the output will also be a series of all 1's. The convolutional on/off condition, is telemetered in bit 1 of the engineering subcommutator word C-132 where a 1 indicates that the coding is on. To operate the redundant coder requires that the redundant DTU be commanded on.

It is possible to reconstruct the information without going through the sequential decoding process. Since the taps for the 2-parity bits P and $\bar{Q}$ are identical except for the second stage, the original data sequence, D, can be reconstructed by module 2 adding the 2-parity streams except for a 1-bit delay, i.e., $D_n = P_{n+1} + \bar{Q}_{n+1}$. This process will recover the complete information stream except for the second to the last data bit received just before resetting the registers. The state of this bit cannot be predicted. However, since the bit in question is the second to the last bit of the frame synchronization word, this bit of frame synch can be ignored when operating in the convolutional coded mode.

6.7.3 Data Storage Unit

Various storage techniques (core, plated wire, solid state) are available for application to the SUAE mission. The DSU used on the Pioneer F/G spacecraft, while off-the-shelf and fully compatible with the DTU, is too small (49, 152 bits), and would be much too heavy if expanded for this application. A preliminary tradeoff (Table 6-16) led to the selection of the static C-MOS as yielding the lowest cost, best performance, at reasonable weight.

Table 6-16. Data Storage Unit Tradeoff

MEMORY TYPE	CAPACITY (BITS)	WEIGHT* (LB)	TOTAL COST* ($K)	POWER* (WATTS)	REMARKS
CORE					
PIONEERS 10 AND 11	49 152	3.5	N/A	0.4 TO 1.2	OFF THE SHELF. HAS DTU INTERFACE. INSUFFICIENT CAPACITY. NEEDS THREE VOLTAGES.
EMI	1 100 000	14.0	630	2.0 TO 5.5	OFF THE SHELF. REQUIRES MAJOR MODIFICATION OR NEW INTERFACE UNIT. NEEDS THREE VOLTAGES.
HELIOS	524 288	10.3	?	3.0 TO 5.7	ADVANCED DEVELOPMENT. REQUIRES NEW INTERFACE UNIT. GERMAN MADE. NEEDS THREE VOLTAGES.
PLATED WIRE					
MINUTEMAN	580 000	16.2	644	1.5	OFF THE SHELF. REQUIRES NEW INTERFACE UNIT. NEEDS THREE VOLTAGES.
VIKING	500 000	9.5	655	1.5	ADVANCED DEVELOPMENT. REQUIRES NEW INTERFACE UNIT. NEEDS THREE VOLTAGES.
MOTOROLA	768 000	38	650	1.5 TO 2.5	REQUIRES NEW INTERFACE UNIT. NEEDS TWO VOLTAGES.
HONEYWELL	544 000	36	560	5	REQUIRES NEW INTERFACE UNIT. NEEDS POWER SWITCHING ADDED. NEEDS FOUR VOLTAGES.
SOLID STATE					
DYNAMIC P-MOS (MULTI-CHIP)	491 520	2.7	460	4.3	NEW DESIGN USING PROVEN TECHNOLOGY. BECAUSE OF TIMING PROBLEMS SPECIAL BUFFER MODES CANNOT BE SUPPLIED. NEEDS THREE VOLTAGES.
STATIC C-MOS (MULTI-CHIP)	491,520	2.7	415	0.4 TO 3.0	NEW DESIGN USING PROVEN TECHNOLOGY. GIVES SPECIAL MODES TO SCIENCE. NEEDS ONE VOLTAGE.
STATIC C-MOS (MULTI-CHIP)	737 280	4.0	465	0.6 TO 4.5	NEW DESIGN USING PROVEN TECHNOLOGY. GIVES SPECIAL MODES SIMULTANEOUSLY TO SCIENCE AND PROVIDES RECONFIGURABLE REDUNDANCY. OPERATIONALLY VERY FLEXIBLE. NEEDS ONE VOLTAGE.

*WEIGHT, COST, AND POWER COLUMNS INCLUDE DELTAS TO COVER INCREASED ELECTRONICS REQUIRED FOR ADDED INTERFACE MODULES. COSTS OF POWER REGULATION ALSO INCLUDED.

The DSU is comprised of three separate memory units (MU) as shown in Figure 6-68. Each memory unit is composed of two identical modules. Each module contains 122, 880 bits of storage. These modules can be used serially to yield a total capacity of 245, 760 bits per MU, or they can be used separately to accommodate many possible input sources.

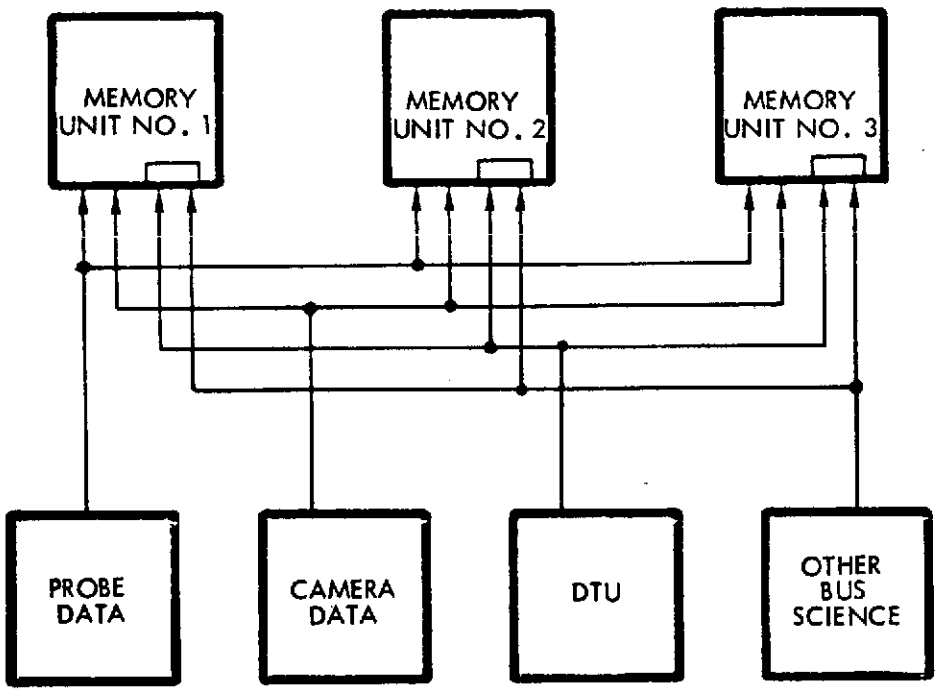

Figure 6-68. Data Storage Unit

The proposed memory is built around a 256-bit CMOS chip (RCA CD4061A). This chip is currently undergoing product development. The chips would be packaged in a 24-pin package, 10 chips per package. A total of 480 chips are required per module, 960 per MU, or 2880 chips per DSU. A block diagram of a module is given in Figure 6-69. Note that each module has independent data and clock gates which are enabled through the timing and control circuitry by ground command. The memory is organized around a 12-bit word to fit comfortably around the 192-bit telemetry format.

During memory load, data are shifted serially into the buffer register. On the 12th clock the contents of the buffer register are strobed into the memory at the address pointed to by the address counter. If the memory is operating in the half-mode and the address counter overflows, and end-of-memory (EOM) signal is generated which places the memory

in the idle mode and resets the device sending data to the memory. In full-mode operation an address counter overflow causes data to be switched automatically to the next memory module in line.

This type of memory is volatile, that is, data stored is lost if power is removed. Readout is nondestructive. The only way, other than via power interrupt, to destroy data in memory is to write over it. Other characteristics of the memory unit are given in Table 6-17.

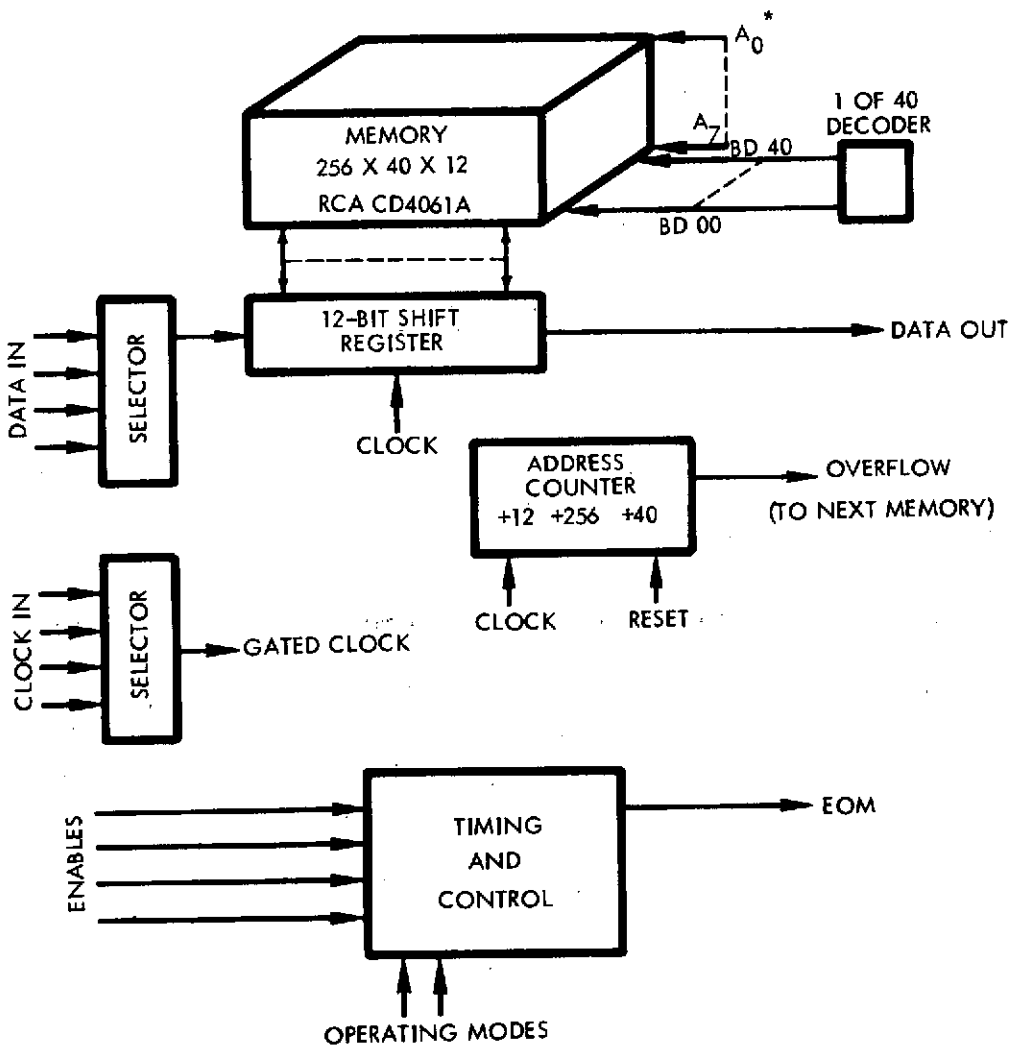

*ON CHIP DECODING SELECTS 1 OF 256.

Figure 6-69. Memory Unit Module Block Diagram

Table 6-17. Memory Unit Characteristics

- 245, 760 bits
- 1.3 pounds
- 1.5 watts
- Parts
  - 102 TTL IC
  - 96 CMOS packages (RCA CD 4061A, 256 bits memory chips - 10 chips per package)
  - 80 discretes
- Operation
  - Interfaces with two experiments and DTU to facilitate cross-strap redundancy
  - Operates at up to 1 MHz data rates
  - 0.2W standby power (memory saved)
  - Half and full memory operation
- Tradeoff
  - No memory hybrid - 5 pound weight increase
  - PMOS shift register memory
    - 0.5 pound weight increase
    - 4.0 watt power increase

The typical operation during the probe entry phase of the mission may be described as follows. Some time prior to entry, a ground command is sent to select the "probe data" input for memory units numbers 1 and 2 (four modules). The units would be operating in the full mode. Memory unit no. 3 would be supporting the acquisition of camera data. When the "signal present" threshold on the probe data receiver (see Section 6.9) is exceeded, the data clock input to the memory is gated on and the contents of the 12-bit shift register is strobed into the memory. These data will remain in the memory until a ground command selects a new data input. Memory unit no. 3 will be switched via ground command from the camera to the DTU input to acquire occultation data.

6.7.4 Digital Decoder Unit

The DDU consists of two completely redundant decoders each of which has the capability of demodulating the FSK modulated subcarrier signal from the receiver and verifying the validity of the command. Each decoder is capable of receiving FSK signals from either receiver. The units are connected by a resistance cross-strap network to protect against a single failure in either decoder or receiver from totally disabling the processing of commands (see Figure 6-70). No changes in this unit are required for the SUAE mission.

6.7.4.1 Functional Characteristics Summary

The DDU functional characteristics summary is given in Table 6-18.

6.7.4.2 Command Format

The bit structure of the command format is shown in Figure 6-71. The first four bits are the preamble and consist of all 0's. These four bits are required to deactivate the squelch in each decoder and establish a condition that will recognize the 1 bit which follows. This 1 bit is used to establish data bit synchronization.

The decoder address bits follow the sync bit and are used to select one of the two decoders. Two bits are used for the decoder address. The address for decoder A is 01 and the address for decoder B is 10. Only the addressed decoder executes the command.

The routing address and the command message comprise the next two groups of bits in the command format. These bits are the usable data in the format. The 3-bit routing address is utilized by the CDU to determine the type of command received and to which user the command message is to be routed. The 8-bit command message contains the actual information required by the user.

The remaining four bits of the command format are parity check bits. These parity bits are used to check the integrity of the routing address and the command message bits. The code is capable of detecting all possible 1- and 2-bit error patterns. Each parity check bit is equal to the modulo-2 summation of selected data bits as shown by the equations in Figure 6-71. Even parity is used in each case.

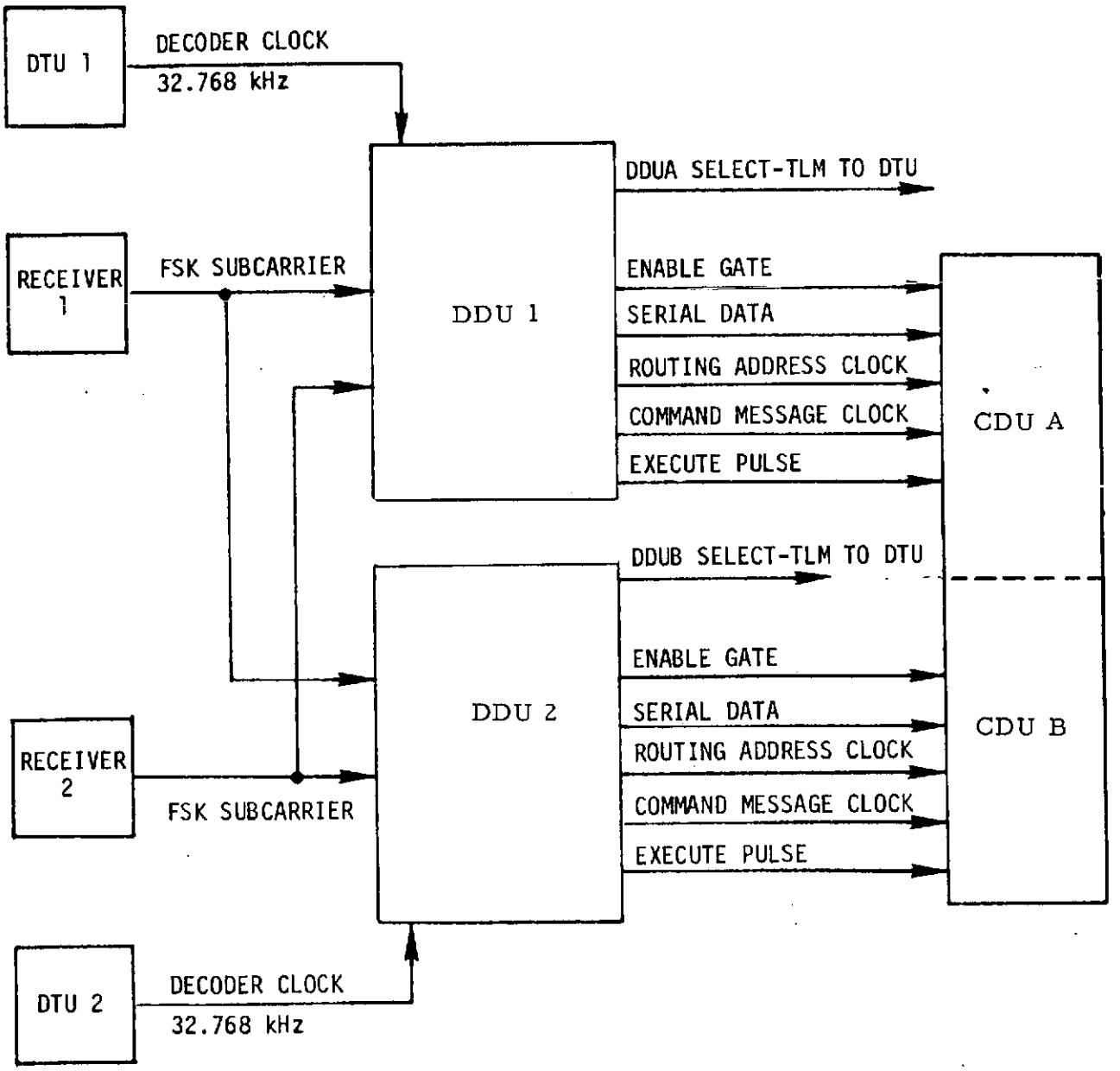

Figure 6-70. DDU Interface Diagram

Table 6-18. DDU Characteristics

	Characteristics
Modulation	FSK
Type	Active twin "T" filter-demodulator
Bit rate	1 bps
Command structure	4-bit preamble (0's) 1-bit sync (1) 2-bit decoder address 3-bit routing address 8-bit command message 4-bit parity
Output interface (serial)	3-bit routing address 8-bit command message Command message clock Routing address clock Command execute
Command authentication	4-bit parity, block hamming code
Tone frequency	1 = 204.8 Hz 0 = 128.0 Hz
Performance	Probability of executing false command is 1.1×10^{-9} with input signal-to-noise ratio of 17.3 dB (performance requirement)
Input signal	Strong signal-to-noise 9.4 ±1.5V P-P (signal only) Threshold signal-to-noise 1.90 ± 0.3V P-P (signal only) Threshold signal-to-noise 10.6 ± 1.7V P-P (signal plus noise)

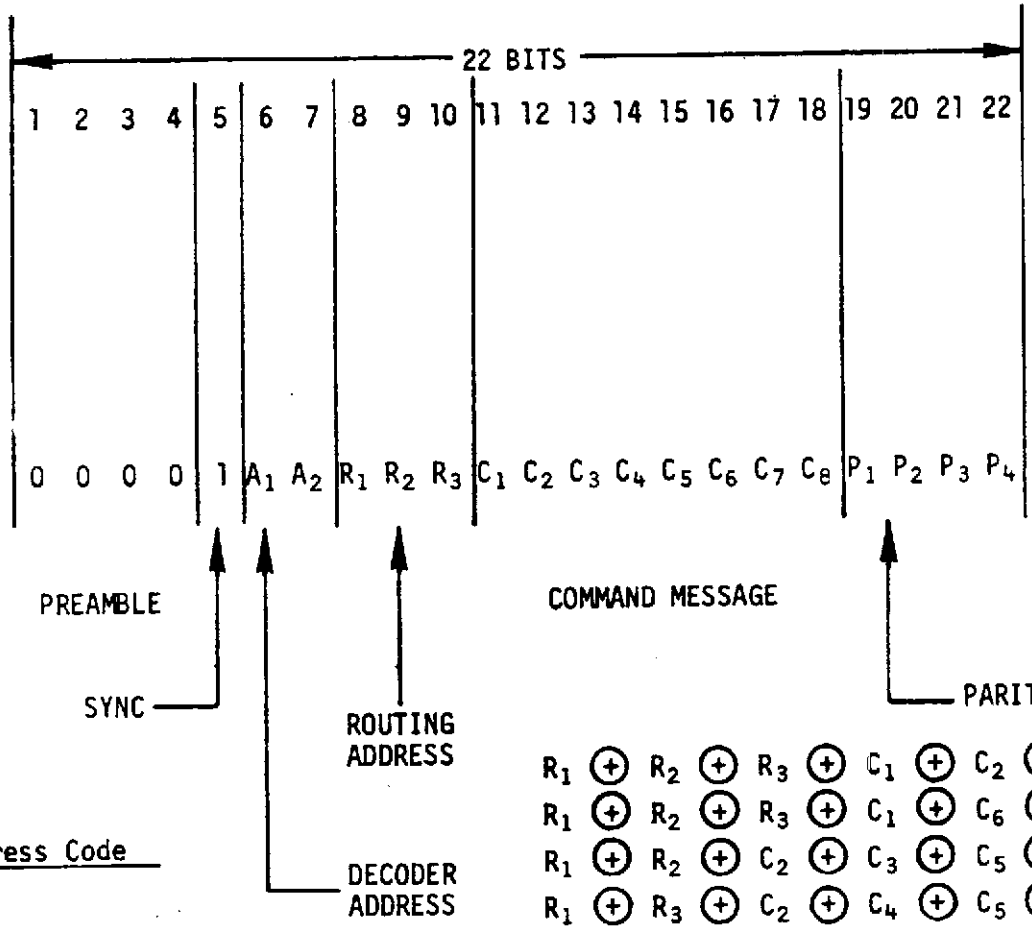

$R_1 \oplus R_2 \oplus R_3 \oplus C_1 \oplus C_2 \oplus C_3 \oplus C_4 = P_1$

$R_1 \oplus R_2 \oplus R_3 \oplus C_1 \oplus C_6 \oplus C_7 \oplus C_8 = P_2$

$R_1 \oplus R_2 \oplus C_2 \oplus C_3 \oplus C_5 \oplus C_6 \oplus C_7 = P_3$

$R_1 \oplus R_3 \oplus C_2 \oplus C_4 \oplus C_5 \oplus C_6 \oplus C_8 = P_4$

Routing Address Code

R_1 R_2 R_3	
000	Not Used
001	CDU Command Processor (Discrete Command)
010	CDU Command Memory, Command
011	CDU Command Meory, DTU Serial Command
100	DTU Serial Command Data (8 Bits)
101	ACS Serial Command
110	CDU Command Memory, Time
111	Not Used

Figure 6-71. Command Format

6.7.4.3 Demodulation

Upon receipt of an FSK signal modulation by tone frequencies of 128 Hz and 204.8 Hz at a 1 bps rate, each decoder will demodulate the data into a digital form. The 128 Hz tone is assigned to represent a logical 0 and the 204.8 Hz tone represents the logical 1 (see Figure 6-72).

These tones are first separated into their respective data channels by bandpass filters. The filters convert the wideband input signal into two signals. These signals are fed into and compared in a comparator circuit which decides whether the current bit is a 1 or a 0 based on which output is largest.

Bit synchronization is achieved when the output of the 1 filter exceeds the output of the 0 filter for the first time in the command. Upon acquiring bit synchronization, the remainder of the command word is bit sampled to convert it into a digital word.

6.7.4.4 Squelch

To conserve power, the digital logic portion of each decoder is not turned on until the FSK input signal is present. The detected signals from both channels are summed and filtered to produce a DC signal for deactivating the squelch. When this occurs power is then applied to the logic. This is shown in the block diagram of Figure 6-72. Because of the long time constants associated with the squelch circuit, it is required that at least five seconds be allowed between "successive commands", otherwise accurate resynchronization cannot be achieved. If a shorter time between commands is desired, a continuous string of 0's must be transmitted between the completion of one command and the start of another. Note that "successive commands", as used above, means separate successive commands not contiguous (back-to-back) commands.

6.7.4.5 Digital Logic

When power is first applied to the digital logic, the logic is reset to an initial state. The programmer is synchronized by the first 1 in the data, the sync bit, and begins generating the clock and timing signals required for processing the data (Figure 6-72).

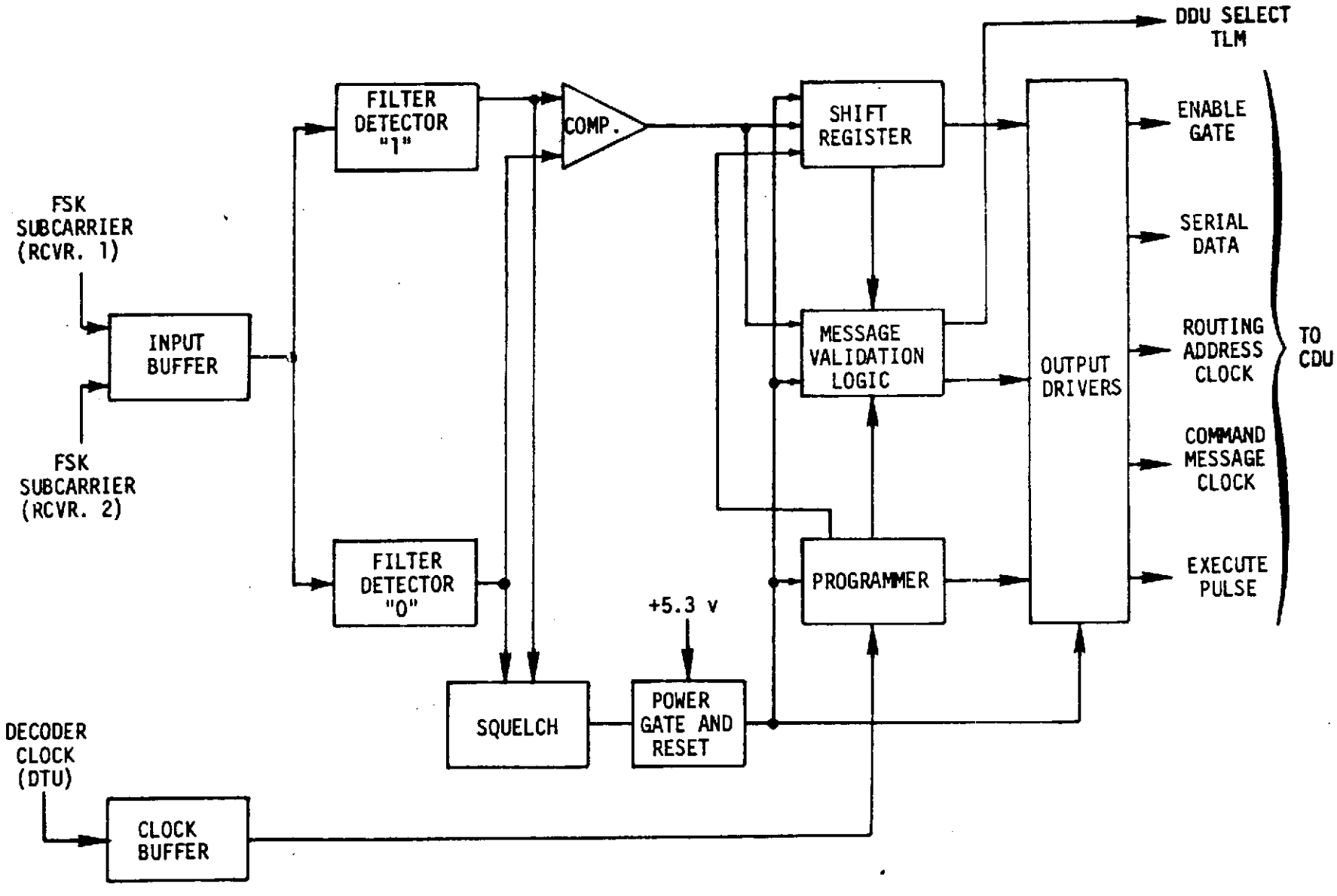

Figure 6-72. DDU Power Gating Schematic

The decoder address is first checked by each decoder. Both decoders will continue to process the command but only the addressed decoder will generate an enable signal. The selected decoder then generates the following output signals to the CDU in the time sequence shown below:

- Enable gate
- Serial data
- Routing address clock
- Command message clock
- Execute pulse

Another output signal, equivalent to the enable gate, is sent to the DTU for telemetry to indicate which decoder is supplying the output signals. If any one or 2 bits in the 15 bits comprised of routing address, command message, and parity are in error, the parity checks will detect the error and inhibit the generation of the execute signal.

6.8 ELECTRICAL DISTRIBUTION SUBSYSTEM

The electrical distribution subsystem consists of the CDU and spacecraft harness. The purpose of the CDU is to process, store, and route to other subsystems and experiments, ground commands which are provided to the CDU via the spacecraft antenna, receiver and DDU. The purpose of the spacecraft harness is to distribute required electrical power, data signals and commands among spacecraft units and experiments. The total spacecraft harness is made up of many individual harnesses. These include:

- The main interconnection harness of spacecraft units and experiments.
- The ordnance harness.
- The +Y outrigger harness to the sun sensor, thruster-cluster and propellant line heaters.
- The -Y outrigger harness to two thruster-clusters, and the propellant line heaters.
- The shunt regulator cable.
- Two ordnance inflight jumpers to provide test panel access to ordnance circuitry.
- A rapid command, inflight jumper to allow speedup of commands to the spacecraft during test.
- The RTG power cables to carry the DC power from the RTG's to the PCU.
- The magnetometer boom harness to carry signals and power from magnetometer electronics to the sensor.
- The probe cable.

Due to the changes in the equipment compartment layout, and because of the new and modified units identified for the SUAE mission, most of the Pioneer F/G cables will require modification or redesign.

The CDU must also be modified to meet the new mission requirements. These modifications include:

- Addition of radial thruster pulse counters
- Addition of ordnance firing circuitry to support probe activation and separation.

6.8.1 CDU Functions

The CDU is designed to perform the following functions:

- Accept, process, and distribute command signals from/to various units of other interfacing subsystems (real-time command processing).
- Provide for the storing of up to five commands to be executed at precise time intervals (also stored) after the unit receives an "initiate" ground command signal (command memory).
- Provide a sequencer operation which activates a sequence of commands at preset time intervals after the unit receives a signal upon separation of the spacecraft (sequencer).
- Provide means of sequentially turning off power to various subsystems in the event of an undervoltage condition of the primary bus (overload control).
- Provide for a signal present detector to automatically switch spacecraft receiver inputs when the signal is not present at the receiver outputs (signal present detection).
- Provide for a thruster firing counter to detect and store the number of firings of a thruster engine, and to route the stored information to the DTU (thruster firing counter).
- Provide for the firing of the spacecraft ordnance devices (ordnance firing operation).
- Provide for bilevel and analog signal conditioning of telemetry signals not compatible with DTU input requirements (telemetry signal conditioning).
- Provide "OR-ing" and overvoltage sensing capabilities of the redundant +5 VDC power input voltages (+5.3V OR switching and overvoltage sensing).

- Provide initialization of the bistable functions during initial application of power to the unit and during momentary outage of the power input (power reset).

The CDU functional block diagram is presented in Figure 6-73. Each function as listed above is depicted in a simplified functional block form and will be discussed in detail in the following paragraphs.

A brief description of the functions' mode of operation is given in Table 6-19. The primary purpose of this table is to present each function's operating time and show their independence of operation from each other. Except for the command memory, thruster firing counting, signal conditioning, and +5.3V OR switching and overvoltage sensing functions, the circuits are power gated and only dissipate the power listed when operating.

6.8.1.1 Real-Time Command Processing

The real-time command processing is shown in Figure 6-74. The function of the real-time command processor is to decode, process, and distribute real-time commands upon receiving signals from the DDU. The signals from the DDU consist of the following (see Figure 6-75 for the timing diagram).

- Enable pulse
- Routing address clock
- Command data clock
- Command data (serial NRZ signal)
- Execute signal

The command processor decodes, processes, and distributes real-time commands of three types. They are:

- Serial commands (routed to the DTU, ACS, and command memory).
- Discrete pulse commands
- Discrete state commands.

Real-time command processing is first initiated by the receipt of the enable pulse (see Figure 6-75). The enable pulse activates the power gating switch which supplies power to the rest of the command processor

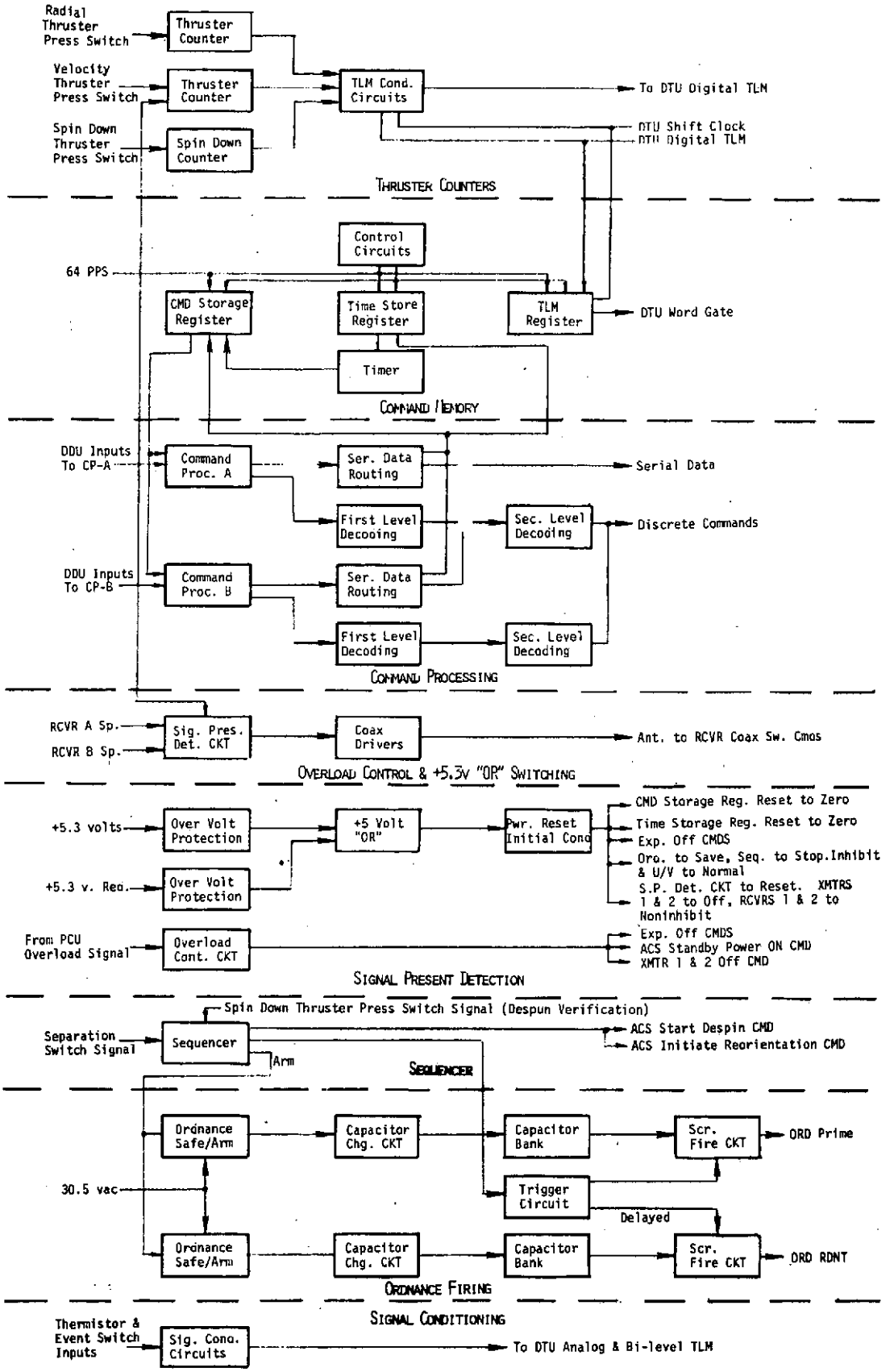

Figure 6-73. CDU Functional Block Diagram

Table 6-19. CDU Operating Modes

Function	Initiation	Operating Time	Operation +5.3V Power (mw)	Remarks
Command processing	Upon receipt of command signal from DDU via command link	15.2 seconds maximum	650	Only one command processor operating at any time when ground commanding
Command memory	Via command processor A or B (ground command "execute stored sequence")	Depend on total of five time delays stored in time registers	1660	Command memory circuits are always "on". Added power is due to command processor executing each command for 70 ms maximum and execution control function
Sequencer	Separation signal from third stage/ spacecraft separation	2560 seconds maximum	180	Sequencer automatically turns itself off
Overload control	Signal from primary bus sensor in PCU	420 seconds	38.4	Operating time will be shorter if bus returns to normal voltage
Signal present detection	Absence of the two receiver inputs indicating loss of lock	36.4 hours	150	Detection of ground transmission presence will terminate timing operation
Thruster firing counting	Thruster pressure switch closure	Continuous	340	Operating power is for total of four VPT's and two SCT's
Ordnance firing	Via sequencer signals or ground commands	During armed period till receipt of safe command ordnance firing pulse ~5 ms capacitor delay	+5.3V=4.3 +28V=3000 30.5VAC=500	+5.3V power is continuous. +28V power during arm and ordnance firing only. 30.5VAC power during arm only
Signal conditioning	Continuous monitoring	Continuous	28	Circuits powered from +5.3V power input
+5.3V OR switching and overvoltage sensing	+5.3V OR switching via ground command. Overvoltage sensing is automatic	+5.3V OR switching, 70 ms maximum overvoltage sensing continuous	+5.3V=198 +28V=808	+5.3V OR switching done only upon a failure of power input being used

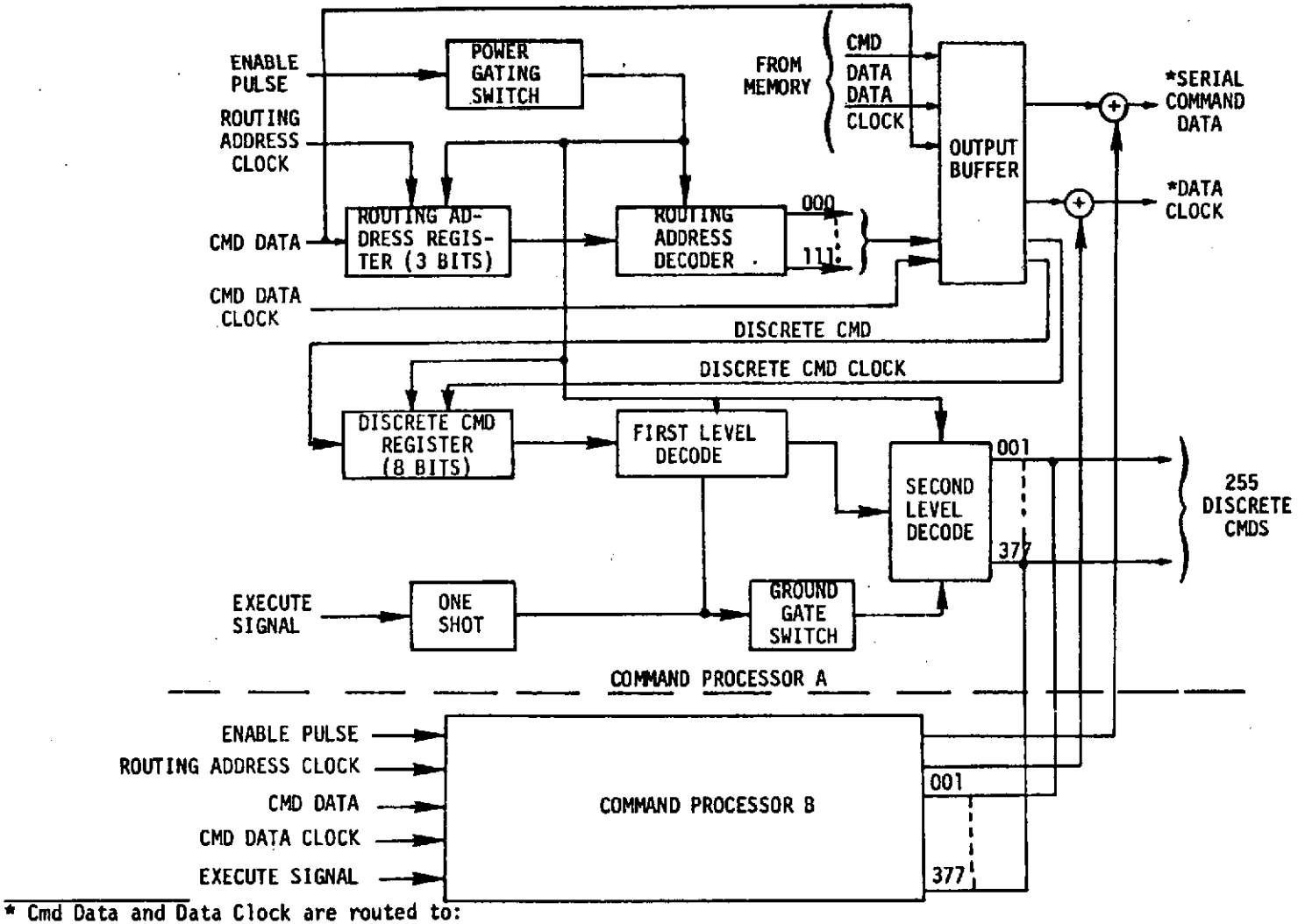

* Cmd Data and Data Clock are routed to:

- Cmd Storage DTU Serial (Memory--CDU)
- Cmd Storage Discrete (Memory--CDU)
- Time Storage (Memory--CDU)
- ACS
- DTU

Figure 6-74. Command Processing Block Diagram

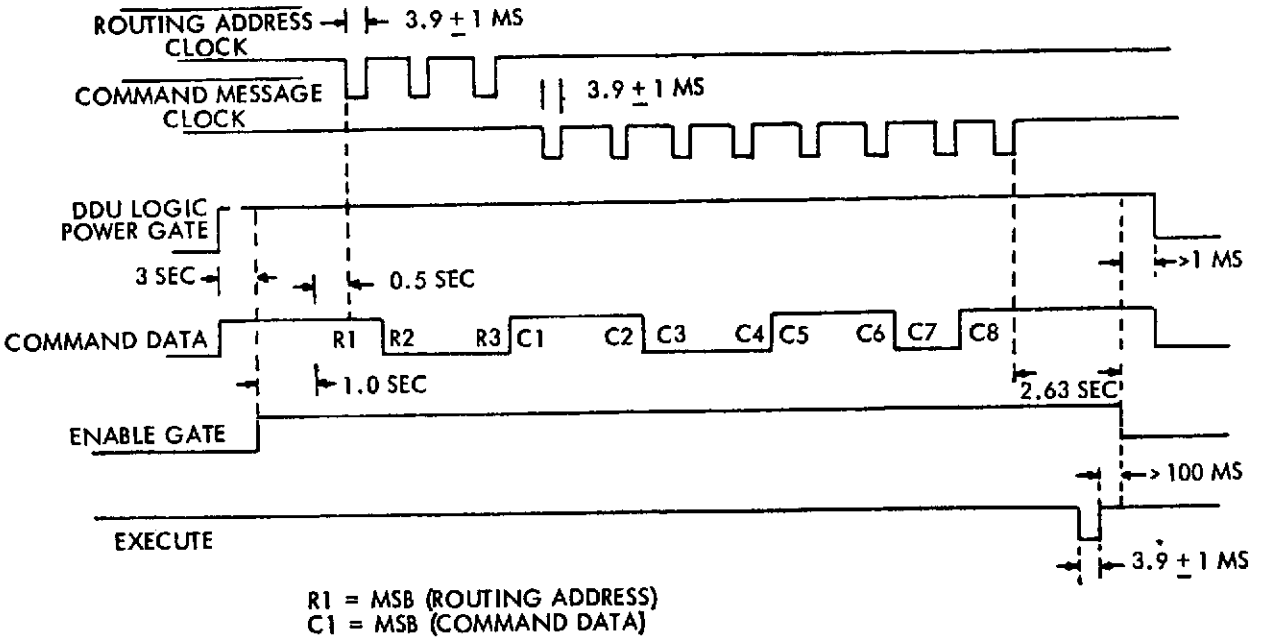

Figure 6-75. DDU Output Timing Diagram

decoding circuits. Following the leading edge of the enable pulse, the first three command data units are clocked into the routing address register by the routing address clock. The information stored in the routing address register is decoded by the routing address decoder which selects one of eight routing destinations.

In the event of a failed command processor (A or B), the alternate command processor must be addressed (through the digital decoder unit) to obtain a serial and/or a discrete command out of the CDU.

During the execution of the memory stored sequence of commands, the CDU is still commandable via ground commands. It is important to note that ground commands during this mode must be sent through the command processor not being used by the memory circuits; otherwise, if during the sending of the ground command the processing becomes coincident with an execution of a command from the memory, an erroneous command may occur.

6.8.1.2 Command Memory

The function of the command memory is to provide the spacecraft with the capability to store commands for execution at a later time. The execution of the stored command is initiated by an "execute stored

sequence" command sent from earth. A "stop stored sequence" command is provided to halt the command memory execution operation at any time in the sequence.

The command memory (Figure 6-76) has the capability of storing up to five command messages and their associated time delay periods for later sequential execution. The command message shall be stored in five registers and the time delay period (time message) in another five registers. The registers utilize flip-flops as storage elements. Each command message register consists of nine flip-flops, eight for the command message and one to identify whether or not the command is a CDU discrete command or a DTU serial command data output. Each time message register consists of seven flip-flops.

Verification of the contents of the stored command messages and associated stored time delay periods is provided by means of a serial digital telemetry readout to the DTU. Continuous telemetry readout is provided even during the stored command execution period, and is interrupted only if coincident with an actual command message readout to the command processor or time message readout to the coincidence counter or if coincident with ground command loading of the command and/or time register.

The CDU stored command capacity of five commands is not being increased in this definition of the SUAE spacecraft design, because there is no clear requirement for an increase. However, by currently available technology it can be increased to 16 or 32 commands with no increase in the size, weight or power of the CDU (due to this change), significantly increasing operational flexibility. Such improvement is contemplated for near-term uses of the CDU design on related programs.

6.8.1.3 Sequencer Description

The sequencer provides an automatic time sequenced commanding function (Figure 6-77). The function is initiated after the separation of the spacecraft from the third stage. The sequencer consists of a binary

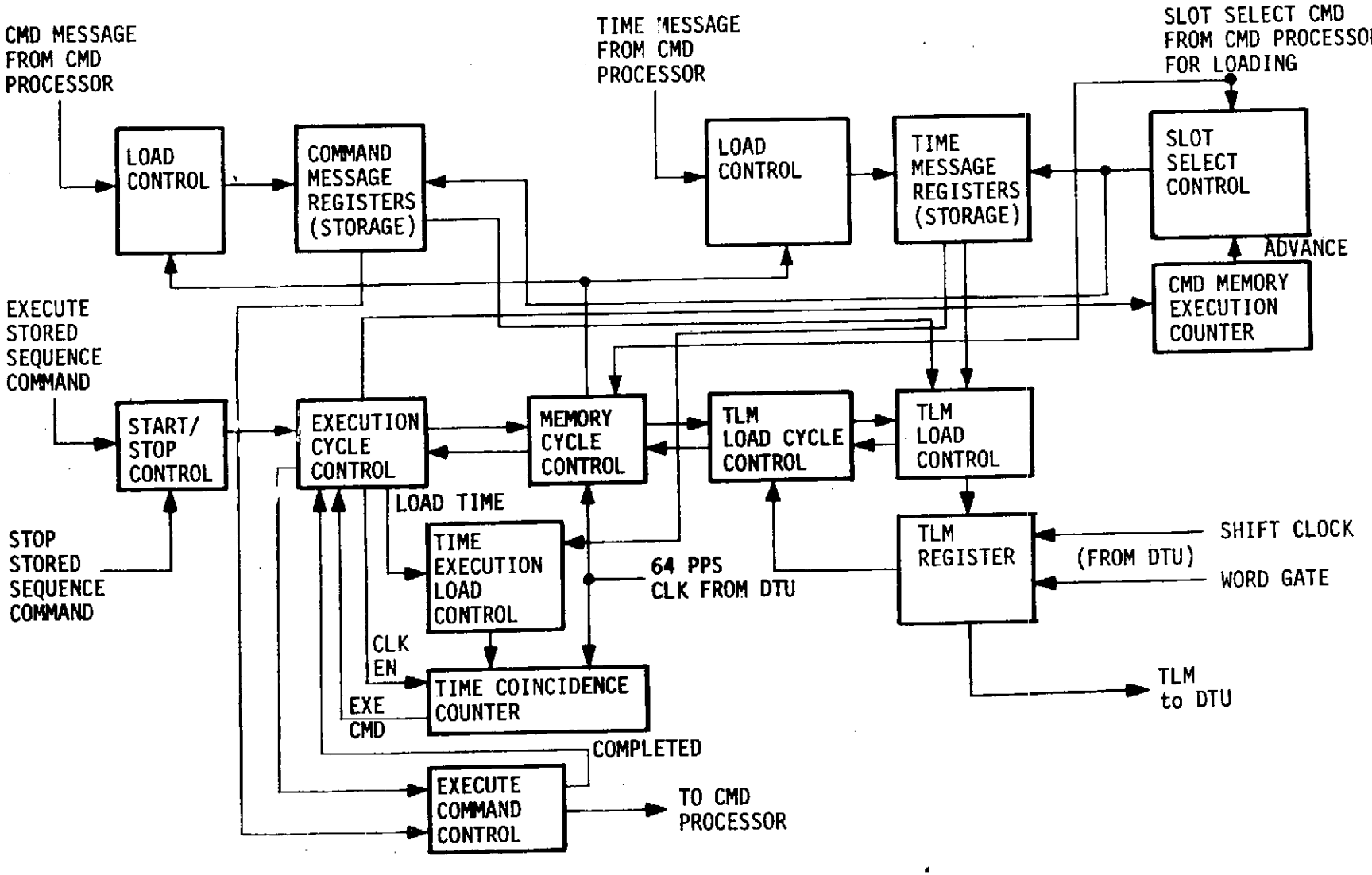

Figure 6-76. CDU Command Memory Block Diagram

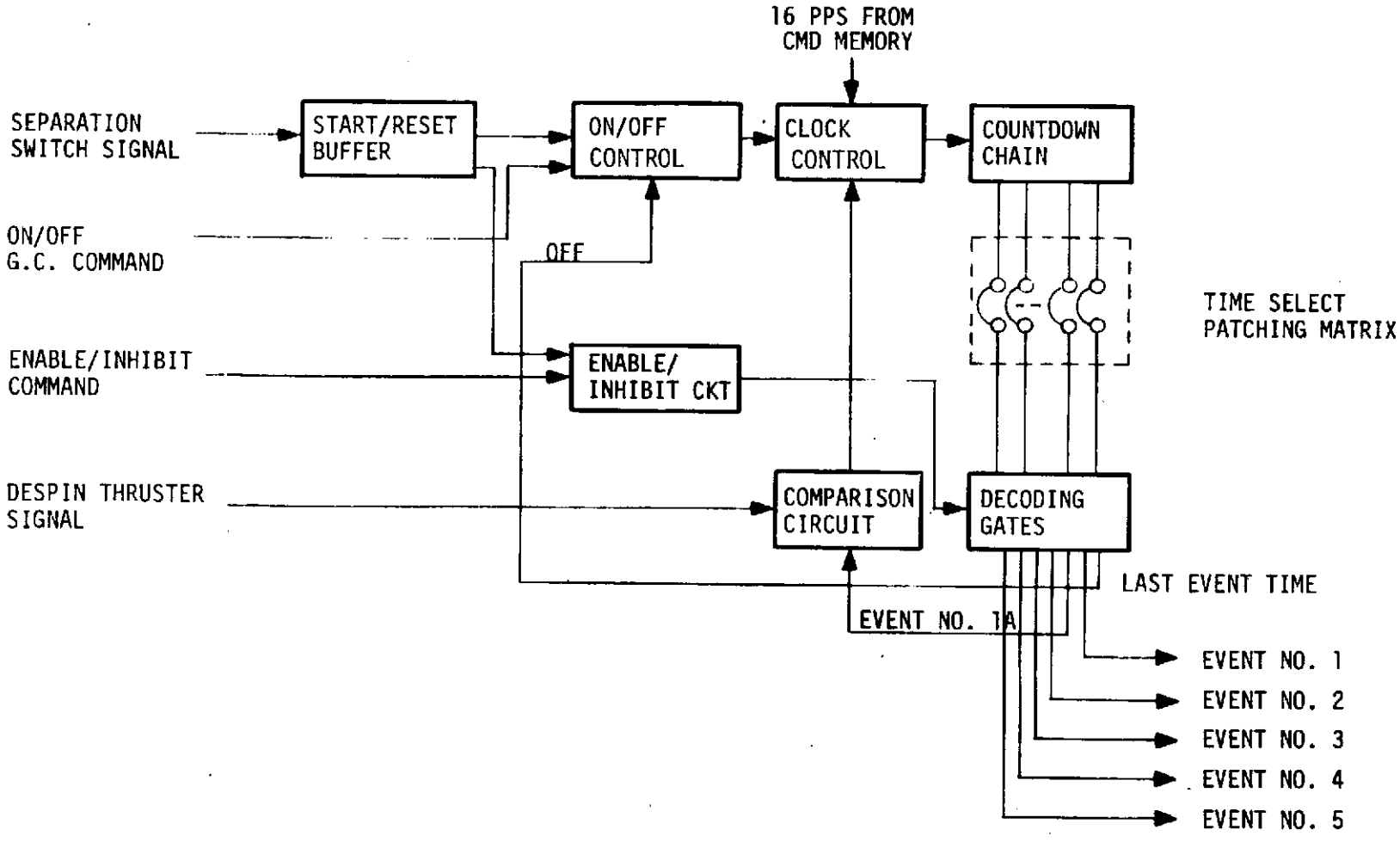

Figure 6-77. Sequencer Block Diagram

countdown chain, decoding gates, and various controlling circuits. The timing sequence is driven from a 16 pps clock signal which is derived from the 64 pps clock in the command memory circuits.

Upon receipt of a separation signal, the CDU initiates the operation of the sequencer, through the start/reset buffer. The start/reset buffer sends a signal to the on/off control which enables a 16 pps clock signal to be fed into a binary countdown chain. The buffer also sends an enable signal to the enable/inhibit circuit to remove the inhibit clamp from the output decoding gates.

The outputs of the countdown chain are decoded by the decoding gates for the event times. The event time intervals are selectable by means of the time select patching matrix.

To ensure that the RTG and magnetometer booms are not deployed at an improper spinning rate of the spacecraft during the despin period, a despin verification check is made at 112 seconds after separation. The check is made by sampling the despin thruster pressure switch signal at that time. If the indication is that the spacecraft is in a despinning mode, then the deployment sequence is enabled and sequencing continued. If the indication is that the spacecraft is not in the despinning mode, then the clock to run the countdown chain is halted. In the event of a sequencer malfunction, the operation can be terminated by the "sequencer inhibit" ground command. The RTG and magnetometer boom deployment and initiate reorientation functions can be completed by ground commands.

The following telemetry sequencer status indications are brought out from the circuits:

- Separation switch signal presence
- Start/stop status
- Enable/inhibit status
- Despin/thruster pressure switch signal indication.

6.8.1.4 Overload Control

The overload control performs the function of turning off certain spacecraft loads in the event of an overload condition to the spacecraft

main power bus. The loads are turned off in the following sequential order:

1) Scientific instruments
2) ACS to standby power
3) Transmitters.

The sensing of an overload condition is performed within the PCU. An overload condition is established when the DC bus voltage falls to 26.5 ±0.5VDC for a length of time of at least 200 ± 100 milliseconds. Upon detection of an overload condition, the PCU sends a signal to the CDU to start the sequential turnoff process. If, during the turning off of any particular load, the DC bus voltage returns to its normal voltage condition and the PCU overload signal returns to its normal state, the control circuit will not continue turning off the remaining loads. The loads already turned off will continue to be off until commanded back on via ground command.

6.8.1.5 Signal Present Detection

The signal present detection provides for the automatic switching of the medium-gain and high-gain antenna inputs to the two spacecraft receivers. The automatic switching takes place if the receivers have lost lock with the ground station for a 36.4-hour time period. The operation starts in the signal present detection circuit when signal present signals from both receivers disappear. If either receiver is activated before the time delay period then the circuit will reset itself.

6.8.1.6 Thruster Firing Counting

The function of the thruster counters is to provide indication of the number of firings performed by the four spacecraft velocity precession thrusters (VPT), two spin control thrusters (SCT), and the two radial velocity thrusters (RVT). The VPT counters have the capability of counting up to 64 firings before recycling back to 0 and starting over again. The SCT counters have the capability of counting up to two firings. The RVT counters have the capability of counting up to 1024 firings before being reset to 0. In addition to the counting capability, the counters provide the real-time telemetry indication of when the thrusters are firing.

The counting circuitry is activated when a pressure switch tied to the thrust chamber is closed, indicating a firing condition. When the pressure switch again opens, the thruster counter steps by one. A block diagram of this circuitry for the VPT's is shown in Figure 6-78.

6.8.1.7 Ordnance Firing

A block diagram of the ordnance firing system is shown in Figure 6-79. It consists of a capacitor discharge-SCR trigger firing scheme. The ordnance devices ignited by the CDU ordnance firing system are:

- RTG ordnance
- Magnetometer boom ordnances
- Vent RTG's
- Uranus decision
- Probe clock activation
- Probe cable cutter
- Probe separation

The last five of these are new in the SUAE mission. One Pioneer F/G ordnance firing (the feed movement mechanism release) is not needed. Thus four new ordnance firing circuits are needed. This change raises the CDU weight from 8.8 to 9.9 pounds.

Redundant capacitor charging and capacitor storage bank circuits are provided such that the prime ordnance devices are ignited from one circuit and the redundant ordnance devices from the other. The redundant firing circuit is designed to trigger approximately 50 milliseconds after the prime side to ensure the bolts holding the RTG's have ample time to pass the redundant bolt cutter after being cut by the first cutter. Possibilities exist that if the redundant bolt cutter starts cutting the same time as the first, the bolt will hang up.

The SCR switches are turned on by triggering circuits which have inputs from the CDU sequencer and CDU command processors. The sequencer inputs trigger the SCR switches automatically when each

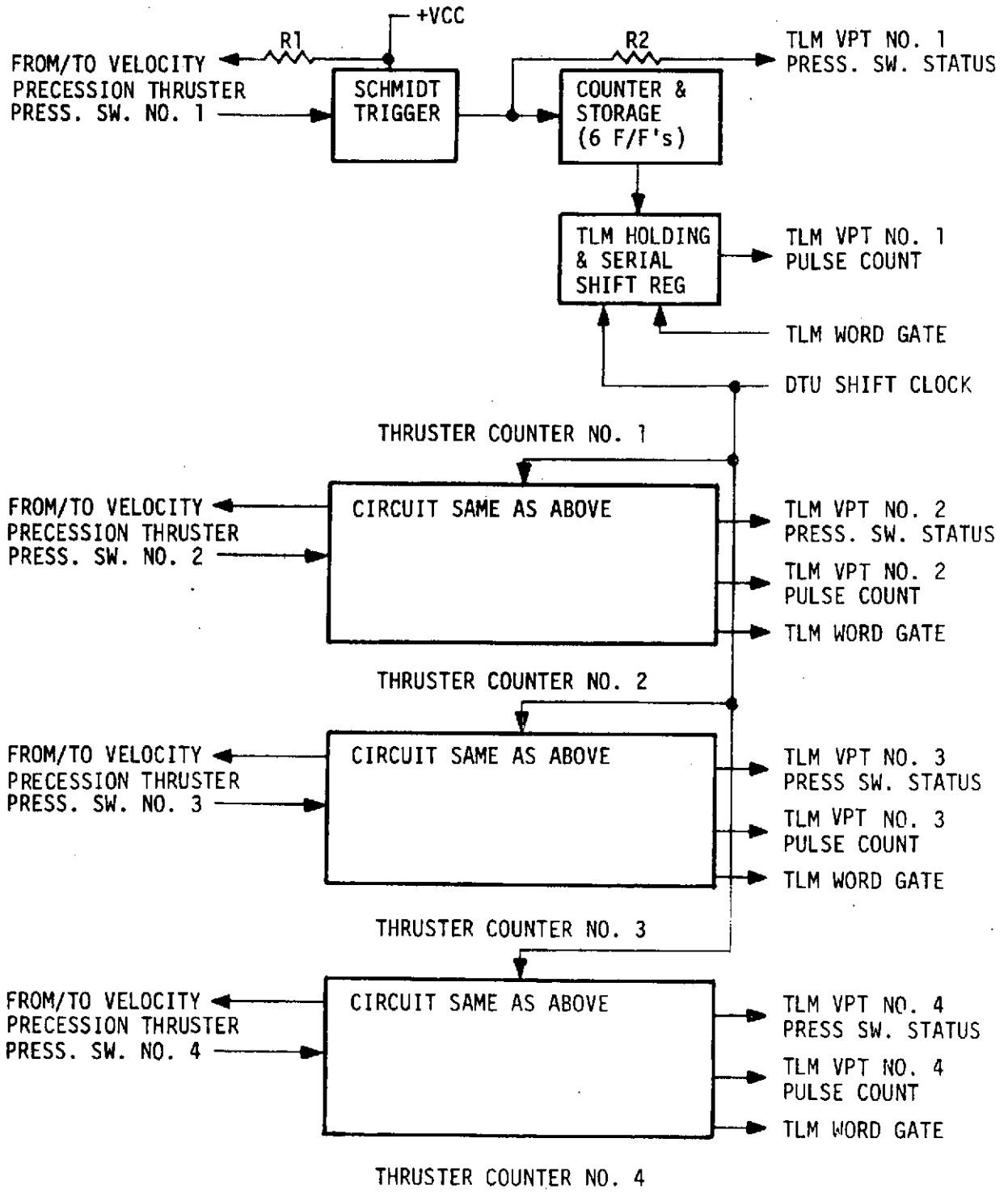

Figure 6-78. Velocity Precession Thruster Counters

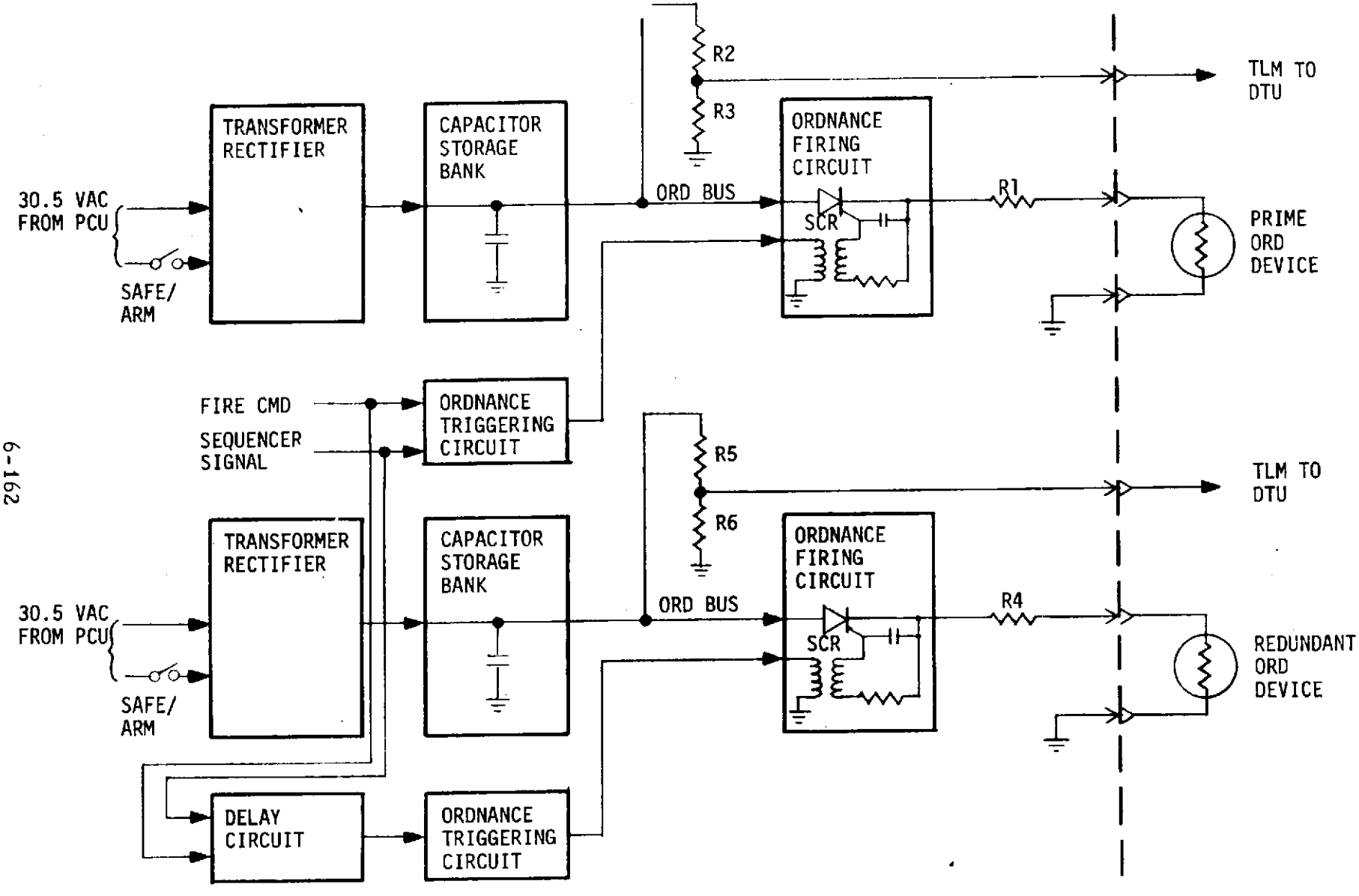

Figure 6-79. Ordnance Firing System

ordnance fire-timed event occurs in a ripple fire mode. The command processor input provide the ground command backup capability to fire ordnance also in a ripple fire mode. In the ripple fire mode a discrete ground command or sequencer signal is received and the primary set of ordnance is fired first. After a set time delay a secondary set of ordnance is fired automatically.

Resistors R2, R3, R5, and R6 provide a voltage divider circuit so that the voltages on the capacitor storage banks are monitored for telemetry readout to the DTU. The telemetry readout indicates a positive SAFE/ARM status. In addition, the SAFE/ARM switch status is monitored for telemetry.

6.9 PROBE DATA LINK

The data acquired by the probe must be transmitted to the bus for subsequent retransmission to the earth. Direct transmission of these data from the probe to the earth is not feasible within the established program constraints. Elements of this link which are located on the bus include an antenna, receiver, data synchronizer, and data buffer. These components are shown interconnected in Figure 6-80.

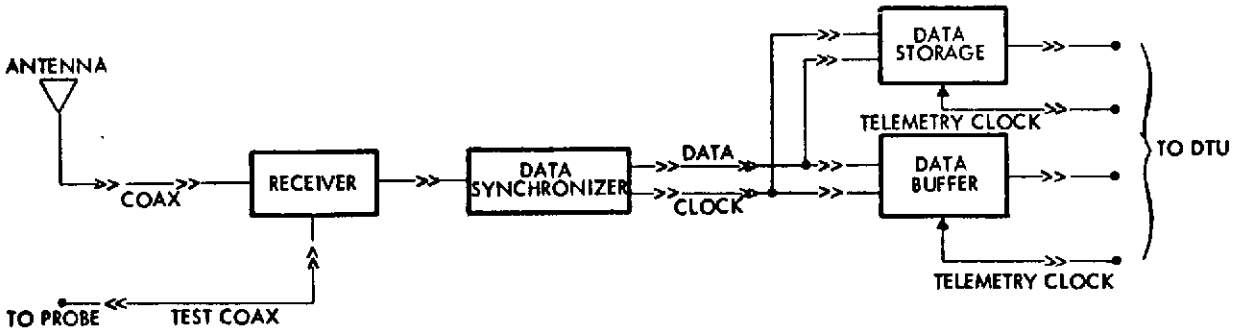

Figure 6-80. Probe-Bus Data Link Block Diagram

6.9.1 Antenna

Various approaches were investigated to select an optimum antenna design for the probe-to-bus RF data link. This included despun antennas of several varieties, an axially symmetric antenna which could be switched to optimize coverage at either Saturn or Uranus, and an axially symmetric antenna which was broad enough in beamwidth to accommodate both planets without switching. The latter approach was selected as described in Appendix A. The selected design, known as the loop vee antenna, is described below.

6.9.1.1 Mechanical Description

The antenna (see Figure 6-81) consists of four loop elements approximately one-quarter wavelength long (one wavelength, λ, is roughly 30 inches). The loop elements are supported and excited by four stubs also approximately $\lambda/4$ in length and tied together at a common feed junction. The loop elements and stub supports are fabricated of tubular aluminum. The loop elements are structurally tied together in a continuous ring by means of a dielectric spacer. A single step

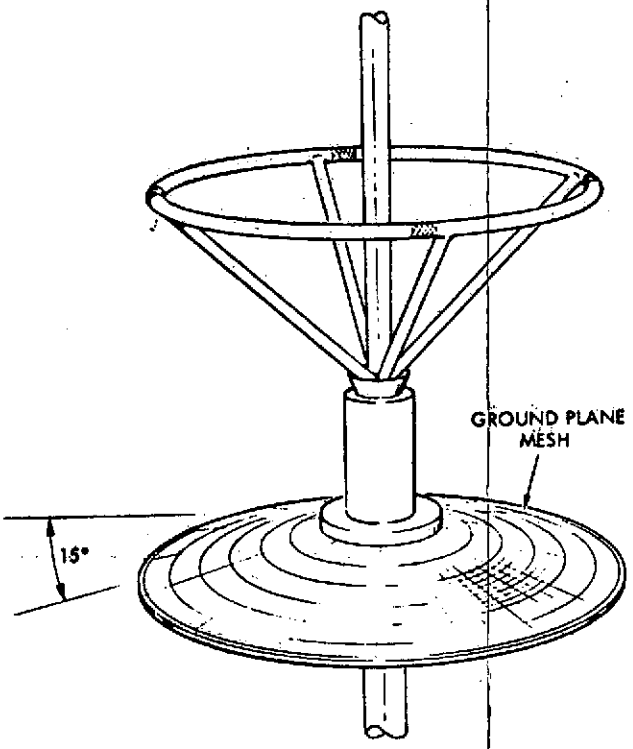

Figure 6-81. Loop-Vee Antenna

quarter-wave transformer is incorporated in the choke sleeve to provide an impedance match to a 50 ohm line. The entire assembly is mounted on a fiberglass strut which also serves as a mount for the S-band omni antenna. The structural details of the common installation are shown in Figure 6-82.

The coaxial feed cables for both antennas are routed internal to the hollow support strut. Note that the antennas are mounted on the -X side of the equipment compartment to minimize cable losses between the antennas and their respective receivers. Two stabilizing struts attached to the cylindrical interstage ring are required to provide support during the high-vibration boost environment. A small ground plane is located at the base of the choke sleeve.

Two clearance angles are implied in Figure 6-82 (and shown explicitly in Figure A-14, Appendix A). The 10-degree angle represents the clearance available before the attached stage adapter begins to occlude the line-of-sight to the probe. The probe nose does intrude into the 10-degree clearance line, but the probe will always be separated when this antenna is in use. The 18-degree clearance angle between the antenna and the third stage adapter should insure that the adapter will not contact the antenna when it is separated.

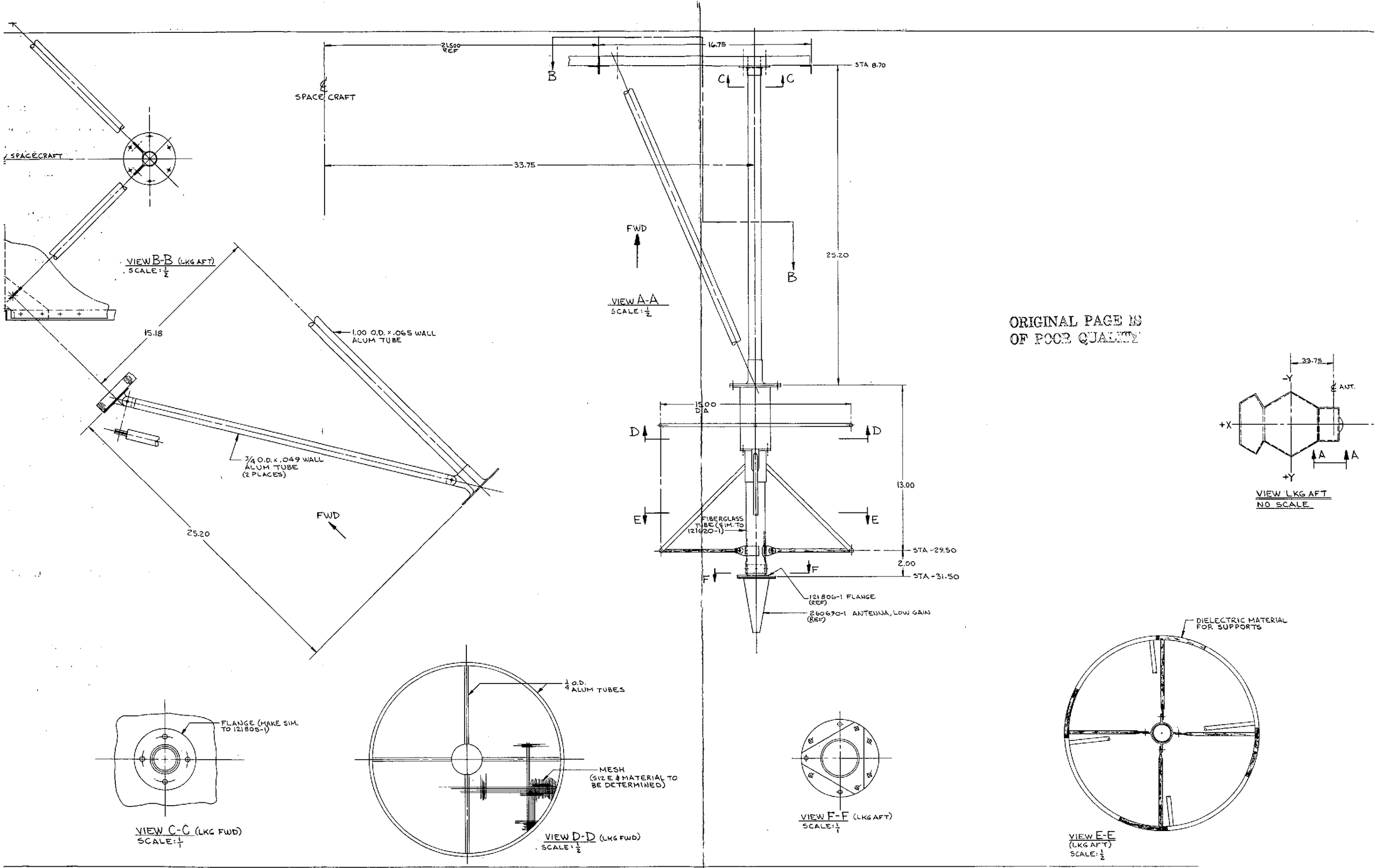

ORIGINAL PAGE IS OF POOR QUALITY

Figure 6-82. Probe-to-Spacecraft and Low-Gain Antenna Arrangement

A lightweight mesh ground plane is located below the choke sleeve to improve forward directivity and to eliminate interference from the body of the spacecraft.

6.9.1.2 Electrical Description

The loop-vee is an extremely simple antenna. Like the helix, it utilizes the geometry of its elements to provide circular polarization. A typical free space pattern for this type of antenna is shown in Figure 6-83. The VSWR of such an antenna will be less than 1.8 and the axial ratio at a cone angle of 90 degrees should be less than 2 dB. Other pertinent parameters are listed below.

- 3 dB beamwidth — 50 degrees
- Efficiency — 80 percent
- Peak gain — 3.8 dB
- Beam edge gain — 0.8 dB
- Polarization loss — 0.2 dB
- Azimuthal ripple — ±0.5 dB
- Worst case gain — 0.1 dB

The peak gain is at 65-degree aspect angle. Some small variations in design parameters have produced peak gain at an aspect anble of 50 to 55 degrees, so this parameter may be varied somewhat to meet more precise mission requirements.

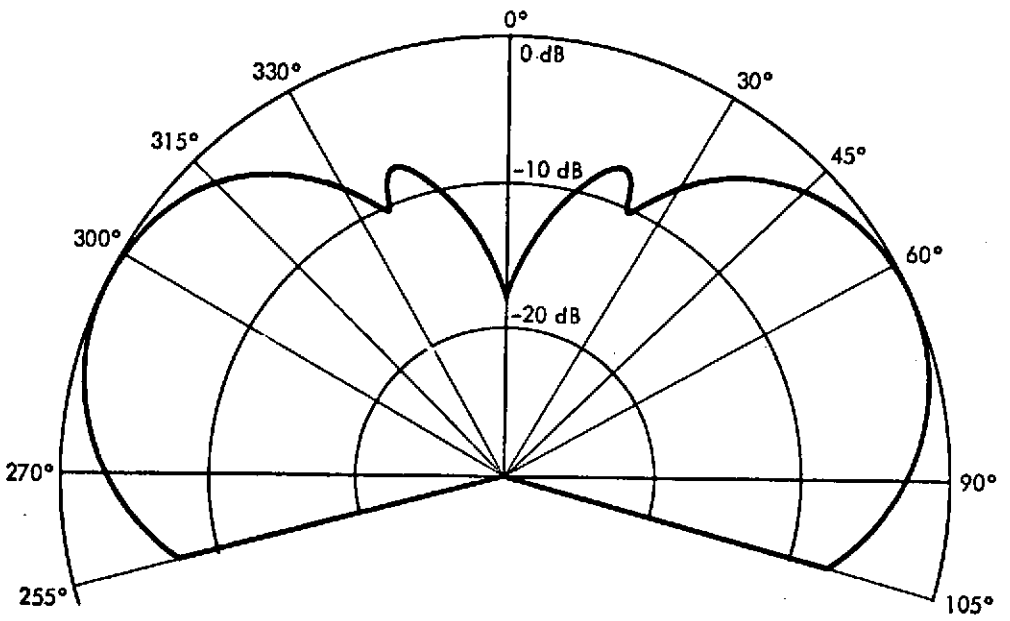

Figure 6-83. Typical Loop-Vee Pattern

6.9.2 Receiver/Data Synchronizer

This portion of the probe data link will be supplied by the probe contractor. Functionally, it receives an RF signal at 400 MHz from the antenna and converts this to a digital bit stream at 88 bps. The principal interface characteristics of this unit are given in Figure 6-84.

6.9.3 Data Buffer

Probe data leaves the data synchronizer at 88 bps. These data must be merged with the DTU bit stream which may operate at any binary bit rate from 256 to 1024 bps during probe data acquisition. To accommodate this asynchronous operation, some form of buffer storage is required. This data buffer allows data to enter at 88 bps and leave at any arbitrary bit rate so long as the average bit rate leaving is at least 88 bps. Otherwise, the data buffer would continue to accumulate bits and would overflow.

Several factors may influence the design of the data buffer. These include anticipated bit rate variations or uncertainties (both input and output) as well as the format of the DTU as it extracts data from the buffer. Referring to the sample formats shown in Figure 6-60, the buffered data is assigned the total 144 available bits in the B format and 24 bits in the A format.

There are several possible mechanizations for the data buffer, one of which is illustrated in Figure 6-85. During a DTU frame period (1.5 seconds at 128 bps) a nominal 132 probe data bits will be received. However, due to the asynchronous operation, any given sample could be 131, 132, or 133 bits. If a 136-bit register is supplied, the total sample will always be received. However, the remaining "fill" bits will not be discernible from the actual data. A counter is provided to count the number of actual data bits received (8 bits provides the 133 necessary count). In this manner simple software on the ground can determine the number of non-data fill bits and perform a stripping operation. At data rates greater than 128 bps, the amount of probe data would be less and the resulting number of fill bits would increase. A data buffer sequence is then:

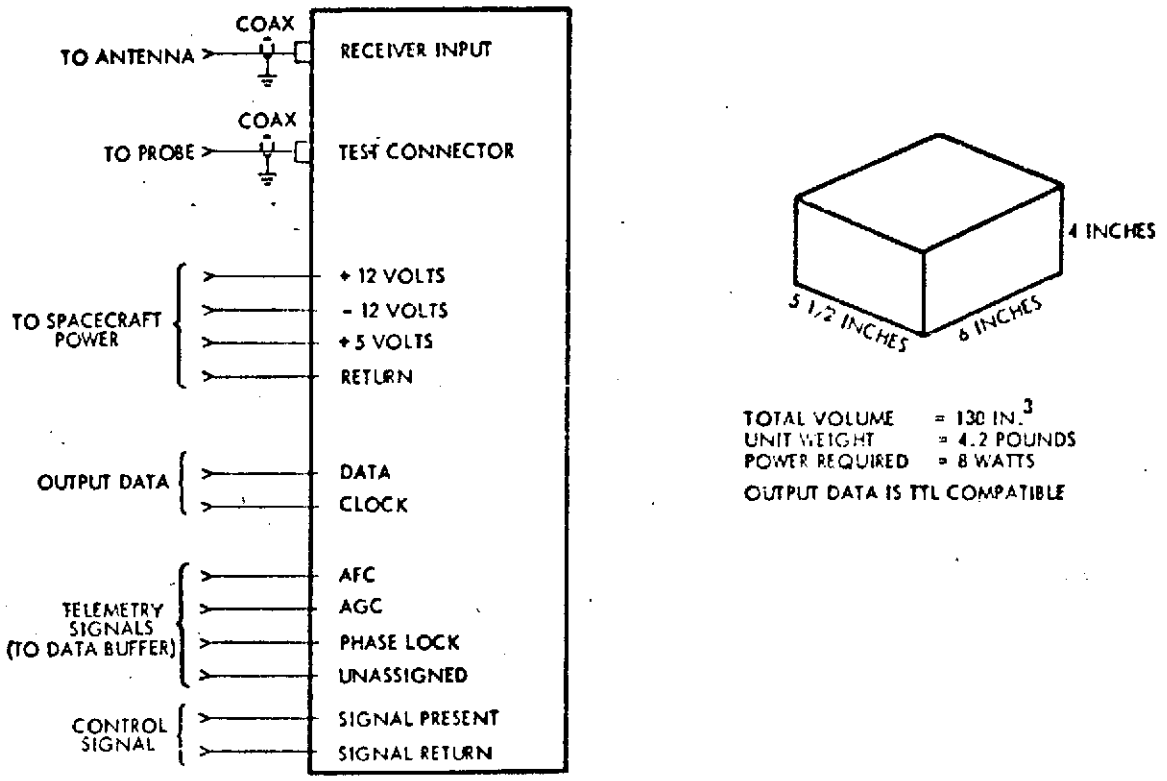

Figure 6-84. Probe Receiver/Data Synchronizer Characteristics

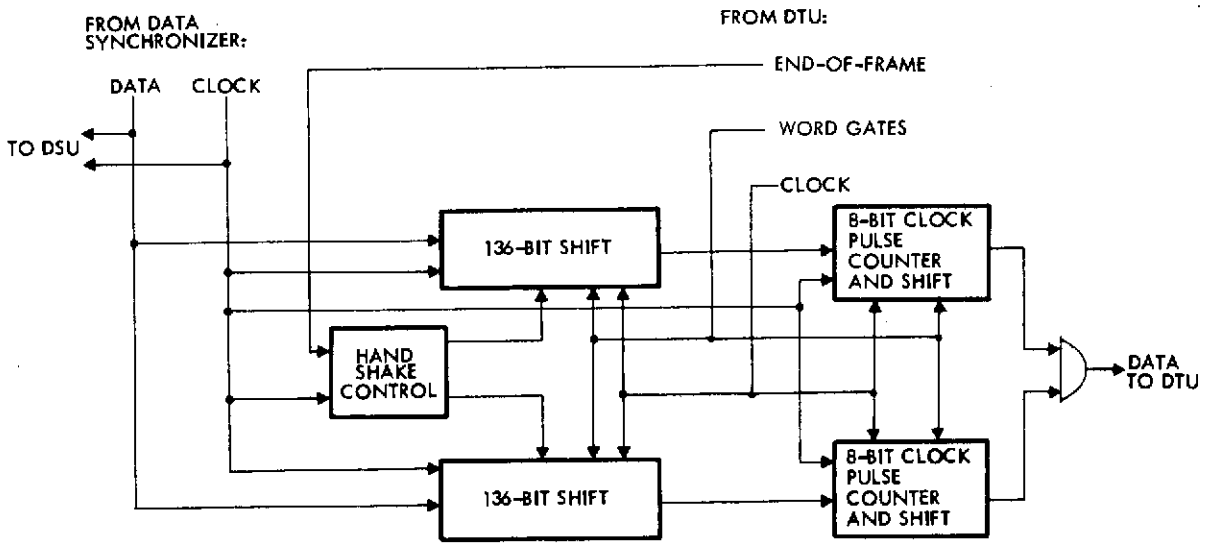

Figure 6-85. Probe Data Buffer Schematic

- Receive a nominal 132 probe data bits and store in a 136-bit shift register.
- Count the number of received pulses
- Transfer the 136-bit register and the 8-bit counter into a single 144-bit output shift register and transmit to the ground
- Receive and count on the opposite set of circuits.

This is done under handshake control. That is, gating is provided to assure that transfer of circuitry roles from input to output and reverse coincides with data bit transition times as well as proper DTU intervals. The combination of handshaking, fill bits, and bit counting allows a buffer process that will neither gain or lose data.

The data buffer will occupy 7.5 inches^3, weigh 0.15 pound, and use 150 mW.

7. DESIGN ALTERNATIVES AND TRADEOFFS

7.1 RTG OPTIONS

As in the Pioneer F/G mission to Jupiter, the only feasible power source for the spacecraft is the use of RTG's.

Solar arrays would entail a significant weight penalty beyond Jupiter, and are more susceptible to degradation in a cosmic dust or nuclear-particle environment. Nuclear power can be considered in other forms. A reactor produces more thermal power per pound of fuel than mere radioactive decay, but is not competitive at the low power levels typical of this mission. Heat-engine converters exploiting the thermodynamic properties of a working fluid are more efficient than thermoelectric converters, but their early state of development (with nuclear heat sources) precludes consideration at this time.

Stored-energy sources (batteries, fuel cells, etc.) are entirely inadequate for missions with duration measured in years, and can be considered only as a secondary source to supply transient loads.

Therefore we will review power source candidates in terms of available RTG power systems.

7.1.1 RTG Source Criteria

The principal criteria for evaluating RTG systems as power sources are:

- Power output (initial)
- Power output (at end of mission)
- Operating voltages
- Weight
- Mechanical interface with the spacecraft
- Thermal interface with the spacecraft
- Radiation effect on the spacecraft
- Nuclear safety conformance
- Variation from Pioneer F/G required of the spacecraft design
- Developmental status
- Cost

The last three criteria are closely related, in that the cost of the RTG system is likely to depend on its developmental status, and the cost of the spacecraft is likely to depend on the extent to which it must be changed from the Pioneer F/G design to accommodate the RTG's.

Preliminary estimates of power required for the SUAE mission came to about 170 watts, assuming it is supplied from the RTG's at 28 VDC. (The required power, measured at the RTG's, will vary according to the voltage at which it is supplied. At low voltages, such as the 4.2V operation of the SNAP-19 RTG's of Pioneer F/G, there are increased cable losses and regulation losses, and the inverters, which invert all the RTG power rather than only that which is to be furnished at other than 28 VDC, have greater losses. The power requirement for a low-voltage source could be increased by possibly 20W to account for these effects. For an intermediate-voltage source, the penalty would be less.)

Thus a design point for the RTG system for the SUAE mission was established at 190 watts at seven years after launch. This encompasses the projected Uranus encounter 6.9 years after launch, and the Saturn flyby about 3.4 years after launch.

7.1.2 RTG System Candidates

The RTG system candidates fall into two classes, those based on the SNAP-19 approach, evolved from lead-telluride converter technology, and those based on the multi-hundred watt (MHW) approach, utilizing silicon-germanium converter technology.

In general, the lead-telluride converters operate at lower temperatures and lower voltages, and are more advanced in development status, with units having flown on the Nimbus and Pioneer F/G programs. In the past they have had lower power conversion efficiency and have produced less power per unit weight than the MHW developments have promised. However, recent development based on SNAP-19 evolution (which has moved from lead-telluride alloys to new alloys for the p-material) and development problems which have forced the MHW to retreat somewhat from design goals have overcome these two disadvantages.

Now the comparison of current units (SNAP-19 and MHW) shows them about equal in power efficiency, with the MHW superior in watts per pound. Projected applicable units for the SUAE mission (SNAP-19 HPG and modified MHW) shows the SNAP-19 HPG superior in both respects, although the margin would be much smaller if we applied a penalty for operation at low voltages.

The two approaches use the same fuel form, $Pu^{238}O_2$, and have comparable radiation effects on the spacecraft and its complement of instruments. The conformance of the two approaches with nuclear safety requirements (pertaining to accidents and aborts between liftoff and escape from the earth) are probably comparable. The SNAP-19 required design modifications for this purpose prior to the Pioneer 10 launch, while the MHW fuel capsule technology faces the handicap of higher operating temperatures within the RTG.

The candidate RTG systems reviewed are the following:

- Four SNAP-19 units, same as those of Pioneer F/G
- Two SNAP-19 HPG units
- Two modified MHW "short stack" units
- Two MHW units, as being developed for LES 8, 9 launches in 1974.

A summary comparison of the characteristics of these RTG systems is given in Table 7-1.

A plot of anticipated power for the systems as a function of time from launch is given in Figure 7-1.

7.1.3 SNAP-19 (Pioneer F/G)

The SNAP-19 RTG system (four units) of the Pioneer F/G spacecraft design is inadequate for the SUAE mission. It is included for review for two purposes, to provide a point of reference and comparison, and for consideration for an atmospheric entry mission to the planet Saturn only (see Appendix D).

It also shows a performance in flight which is significantly better than the performance predicted at the inception of the SNAP-19 (Pioneer)

Table 7-1. RTG Systems

RTG POWER SOURCE	SNAP-19	SNAP-19 HPG	MODIFIED MHW "SHORT STACK"	MHW
NUMBER OF UNITS IN SYSTEM	4	2	2	2
THERMAL LOADING (W)	2600	3040	4000	4800
WEIGHT (LB)	120	100-120	150	170
POWER OUTPUT (W)				
AT LAUNCH (L)				
IN AIR	166	210-230	125[5]	160[5]
IN VACUUM	166	210-230	240	300
AT SATURN (L+3.5YR)	130+4[1]	200-210	210	265
AT URANUS (L+7.0YR)	96 ±10[1]	190	188	233
VOLTAGE FOR MAX POWER	4.2	32[2]	25[3]	30[2]
DIMENSIONS (ONE UNIT)				
LENGTH (INCHES)	11	14 17[4]	21	23
DIAMETER (INCHES)	20	24 20[4]	15.7	15.7
CONVERTER (ONE UNIT)				
NUMBER OF COUPLES	90 (2 x 45)	372 (1 x 372)	264 (2 x 132)	312 (2 x 156)
THERMOELECTRIC MATERIAL (P/N)	TAGS 85/2N	TPM 217/3N	Si 80 Ge 20	Si 80 Ge 20
TEMPERATURE				
HOT JUNCTION	530°C	535°C	963°C	1000°C
COLD JUNCTION	160°C	160°C	285°C	265°C
FUEL CAPSULE	T111	PAD	FSA'S	FSA'S
BASIS OF DATA	PIONEER 10 EXPERIENCE	AEC-ISOTOPES STUDIES	AEC-GE STUDIES	UNDER DEVELOPMENT FOR LES 8,9 LAUNCH, 1974

(1) EXTRAPOLATION OF FLIGHT PERFORMANCE 3/72 TO 5/73.
(2) CAN BE OPERATED AT 28V
(3) CAN BE OPERATED AT 28V WITH HOT JUNCTION <1000°C
(4) DIMENSIONS IF PIONEER-TYPE T111 FUEL CAPSULE IS USED.
(5) ARGON FILL GAS

PAD = PLUTONIA AERODYNAMIC DISC
SFA = SPHERICAL FUEL ASSEMBLY ($100W_T$)
FSA FUELED SPHERE

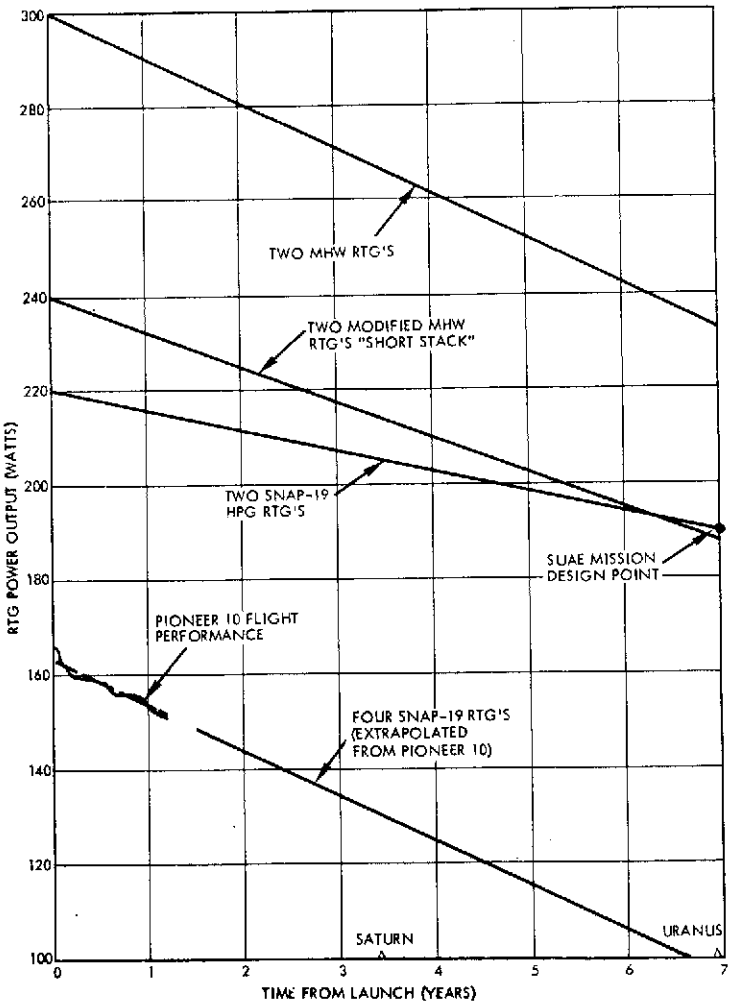

Figure 7-1. RTG System Power vs Time from Launch

procurement. This prediction was for a system output (measured at the RTG terminals) of 151 watts at launch, decreasing linearly to 124 watts 2.5 years later. Flight data show an output of 166 watts at launch, decreasing to 151 watts 14 months later (Figure 7-1). Linear extrapolation of the last 12 months data would show a drop to 124 watts at 4.0 years after launch, and about 96 watts after 7.0 years. This is excellent performance based on the expectation for the Pioneer F/G program. However, for the longer Saturn Uranus mission, it would take eight such units to meet the requirements, and the weight and space for physical accommodation would be prohibitive.

The SNAP-19 generator is cylindrical in shape, with six cooling fins, with overall dimensions 20.0 inches in diameter and 11.1 inches in length. A drawing of this generator is given in Figure 7-2, and its location in pairs on the Pioneer F/G spacecraft may be seen in the spacecraft drawing in Section 2.1.1.

Like all generators using lead telluride for the n-material of the couples, the SNAP-19 is sealed and maintains positive internal pressure to minimize sublimation of the material. The pressurant, a helium-argon mixture, is gradually supplanted by helium released by plutonium decay.

The fuel source consists of plutonia molybdenum cermet (PMC) discs in a cylindrical capsule using T111 as a strength member, and graphite for aerodynamic entry protection. The generator temperatures are maintained by the transfer of heat from the outer casing. In vacuum, the heat is radiated from conducting fins, with the casing temperature at an equilibrium of about 160°C. In air at room temperature convection reduces this to about 90°C. The 90 thermocouples are arranged two in parallel by 45 in series, leading to an operating voltage of 4.2 volts.

7.1.4 SNAP-19 HPG*

The SNAP-19 HPG RTG system (two units) identified for the SUAE mission overcomes several shortcomings of the present SNAP-19's. The specific power (power per unit weight) and the power conversion efficiency are improved markedly at the beginning of the mission, and a lower

*HPG = high power generator.

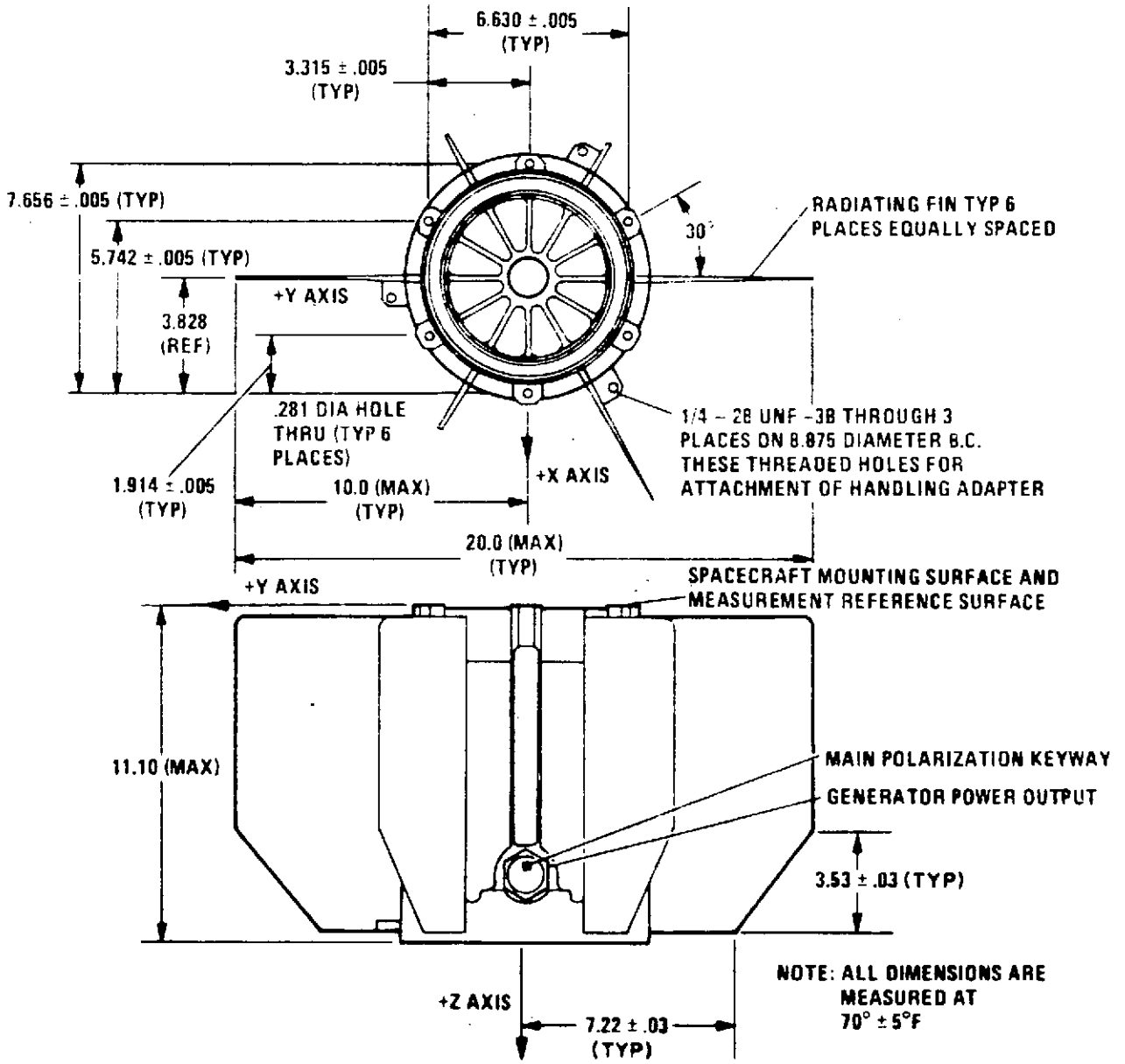

Figure 7-2. SNAP-19 RTG Unit for Pioneer F/G

degradation rate makes the improvement even greater at seven years. The larger units and the greater number of thermocouples permit operation at 28 volts, although internal redundant protection against internal open circuits may have been sacrificed to attain this voltage.

The most significant design changes which lead to the improved performance are the use of a new thermoelectric material, a fuel capsule which has greater volumetric efficiency, and water heat pipes to improve the heat rejection capability of the fins.

The thermoelectric p-material is TPM 217, a copper selenide system which has been tested to 20,000 hours by the 3M Corporation, and which exhibits very low degradation rates, and tolerance to temperatures up to 800°C. In fact, the 565°C hot junction temperature is now limited by the n-material, a doped lead telluride.

The water heat-pipe fin has been developed by Teledyne Isotopes, and is presently being used on an electrically-heated generator to be delivered to JPL for test.

The fuel capsule, stacked plutonia aerodynamic discs (PAD), is a new concept in satisfying nuclear safety requirements, and is receiving limited AEC investigation. This approach leads to a more compact generator, which could save 5 to 10 pounds of weight in the system. However, the change to the PAD fuel capsule approach is not critical to the SNAP-19 HPG concept, and dimensions are given which apply if the T111 fuel capsule approach of the Pioneer F/G RTG's is used.

7.1.5 MHW .

The multihundred watt system (two units) uses converter elements made of 80 percent silicon, 20 percent germanium. This material can tolerate significantly higher temperatures, of the order of 1000°C. It must be operated at these high temperatures to achieve its potential conversion efficiency, and this leads to a requirement for the use of high-temperature technology throughout, from the heat source to the converter and the outer case.

The fuel capsule, a 7.2-inch diameter by 16.9-inch high cylinder, contains 24 spherical fuel assemblies, each of which generates 100 watts of heat from 0.56 lb of $Pu^{238}O_2$ contained within iridium and graphite shells. The 24 FSA's are in six layers of four each, with each layer rotated 45 degrees relative to adjacent layers for optimum nesting.

The fuel capsule is located within a cylindrical array of 312 thermocouples using a 80 percent silicon 20 percent germanium material. The insulation used with the converter to channel heat flow through the

thermoelectric elements is a high-temperature molybdenum multifoil system. To avoid oxidation of this insulation the generator must be sealed when it is operated at high temperature in atmosphere. This is done, filling with an inert gas — argon or xenon — for ground operation. After launch the seal is broken by command from the spacecraft, the inert gas escapes, and the generator then provides full vacuum performance. Because the inert gas, when it is in the generator, permits heat to bypass the thermocouples, the power produced by the generator operating in air during prelaunch and launch phases is reduced to 50 to 80 percent of the power after the generator is vented in flight. Xenon is a heavier gas and a poorer thermal conductor than argon, and would provide the greater fraction of rated power for ground operations.

The data describing MHW characteristics in Table 7-1 are based on the anticipated performance of units to be delivered in 1974 for the LES 8, 9 flights. A drawing of this unit is given in Figure 7-3.

7.1.6 Modified MHW

A modification of the MHW system has been proposed which would employ two units, each of which is reduced in size, weight, and power generating capacity from the MHW unit described above. The term "short stack" has been applied, because the length of the heat source and the generator has been cut down. The heat source now contains 20 rather than 24 of the 100-watt FSA's, so overall length is reduced approximately two inches.

The reduction in weight is due in part to the scaling down of dimensions, and in part to the expectation of design improvements which are considered feasible but cannot be incorporated into the LES 8, 9 units because of schedule constraints. These improvements affect both the heat source and the converter.

The reduction in converter length can proceed so as to accommodate fewer thermocouples of the same size, or an equal number of thermocouples of a smaller size. The first approach, assumed in Table 7-1, reduces thermocouples from 312 to 264, and would lower the voltage of maximum power output from 30 to about 25 volts. The hot junction

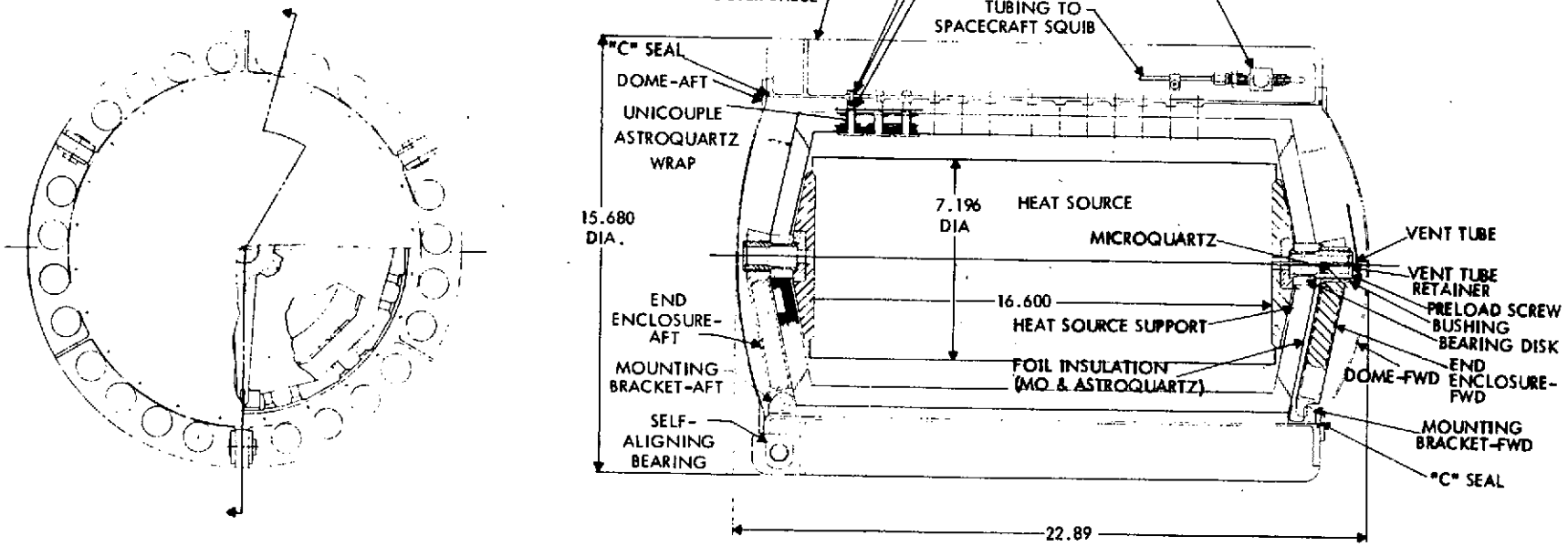

Figure 7-3. Multihundred Watt RTG

temperature drops from 1000°C to 963°C, as end effects are proportionally greater. However, the shortened generator can be operated at 28 volts by the spacecraft voltage regulator; the consequent increased hot junction temperature is not expected to exceed 1000°C, and the power loss (for being off the optimum voltage) about 1 percent. Alternatively, more thermocouples of a smaller size could be used, to maintain a 28-volt output. The 125 watt output before venting (Table 7-1) assumes argon fill gas. Xenon would give about 190 watts.

7.1.7 Selection

The SNAP-19 system, as employed on the Pioneers 10 and 11, is inadequate for the seven-year Saturn Uranus mission. To satisfy the 190-watt requirement seven years after launch, eight units — double the Pioneer F/G complement — would be required on the spacecraft.

The MHW RTG under development for LES 8, 9 has excess power capability for the SUAE mission, and is also heavier than desired.

Thus, two candidate systems were envisioned, scaling the SNAP-19 approach up, and scaling the MHW units down, and in each case anticipating certain technology improvements which are in the test stages now, but which are appropriate to consider in view of the lead time available.

The SNAP-19 HPG system (referring to Table 7-1) has an advantage over the modified MHW system in weight (100-120 pounds vs 150 pounds), in power conversion efficiency (3040 W_t versus 4000 W_t, and in cost. The modified MHW system has 28 volt output, which the SNAP-19 HPG achieves only if parallel redundancy is sacrificed. The modifications envisioned for the MHW system represent less of a technology development program than the SNAP-19 HPG, when measured from the base of current procurement of RTG's for flight spacecraft. Primarily for this last reason that Ames Research Center and TRW have chosen to configure the SUAE spacecraft to accommodate the modified MHW generator system.

However, the SNAP-19 HPG is an attractive candidate for the mission, and could easily be found to satisfy all necessary requirements when a hardware selection is made.

7.1.8 Integration Into Spacecraft Design

There are several aspects of the spacecraft design and its interface with the modified MHW RTG power sources which will be changed in comparison with the Pioneer F/G design.

The stated power requirement of 190 watts after seven years has some flexibility in it. The X-band transmitter has been sized primarily according to data rate requirements, but with an eye on excess power availability. Thus, rather than the transmitter power (the largest single use of electric power on the spacecraft) determining absolutely the RTG power requirement, we have the reverse situation that the RTG power availability can influence the selection of the transmitter. Considering lead times, this is reasonable, because final transmitter selection can be made some time after the RTG performance requirements are made firm.

It is also desirable to include in the power budget enough margin so that pulse or transient loads can be handled within the capability of the RTG sources. This is particularly true for this mission, where the duration of seven years makes it prudent to avoid relying on a battery. As a consequence the battery has been omitted from the design, and the primary source of power for pulse loads will be from the power margin between RTG supply and steady loads. The backup source of power for pulse loads, if this margin were inadequate, would be obtained by turning off steady loads (e.g., experiment loads) at such time that pulse loads must be imposed.

Pulse loads expected for this mission are tallied in Section 5, and include the operations of thruster firing, RF switch activation, and possibly stepper motor actuation for gimballed instruments. For ordnance actuated events, the pulse power is delivered by the discharge of capacitors, as in the Pioneer F/G design. The capacitors are charged slowly from the 28 volt line, and do not constitute an appreciable transient load on the RTG sources.

It is intended that power supplied to the probe from the bus can be supplied with no additional increase in RTG power requirements. Early in the cruise period of the mission, the probe requirements are very low,

and can be met by the extra margin the RTG's must have to allow for their gradual degradation in power output during the long mission. Late in the mission, particular probe power requirements occur – notably, to charge the probe battery – for a duration of several days. For this occasion, the scientific instruments aboard the bus will be turned off to the extent necessary.

A point of change from Pioneer F/G is the increase in RTG supply voltage from 4.2 to 28 Vdc, as discussed earlier. Together with the deletion of the battery, this considerably simplifies the spacecraft's electric power subsystem, resulting in a saving of weight, power, and recurring cost. The design of this subsystem is discussed in Section 6.5.

The physical interface with the RTG's is changed. Instead of a pair of RTG's there is now a single unit on each side of the spacecraft. It is cantilevered from a mounting plate on the inboard end, and held to it by three bolts. The electrical cable which brings RTG power and sensor leads to the spacecraft is pulled out of a slack box when the RTG is deployed. It, too, is simplified, as it serves only one unit. Because it carries power at 28 volts (3.5 to 4.0 amperes per unit) instead of 4.2 volts (7.5 to 9.5 amperes per unit) the optimum cable cross section – reflecting the appropriate tradeoff between weight and power – will be reduced.

The thermal interface with the RTG's is changed somewhat because of the higher RTG case temperatures. The effect on spacecraft design should be minimal, however. Before launch, the temperature of the RTG external surfaces is determined more by convective than radiative characteristics, and it remains much cooler than the vacuum equilibrium temperature. When attached to the spacecraft on the launch vehicle forced air cooling will reduce the RTG temperature below that resulting from natural convection, and will also maintain adjacent spacecraft components at satisfactorily low temperatures.

Several minutes after liftoff the ambient pressure is effectively reduced to the vacuum environment of the remainder of the mission, and from then until RTG deployment is started (about 35 minutes on Pioneer G – possibly 60 to 80 minutes on the SUAE Pioneer because of increased coast time in parking orbit) we reach the period of maximum

radiative and conductive thermal interaction. This interaction is two-way: the RTG heating up adjacent spacecraft components as its outer case temperature increases, and the blockage of radiation paths imposed by the proximity of the spacecraft causing the RTG to rise toward a higher temperature equilibrium.

The portions of the spacecraft most affected during this period are the adjacent side panels of the equipment compartment, the 9-foot dish, the RTG power cables, and the RTG support structure: mounting plate, guide rods, deployment restraint cable, and explosive bolt fittings. It is anticipated that the same design approach used in Pioneer F/G will suffice, although in some instances materials may have to be selected to withstand the higher temperatures they are exposed to.

After deployment the thermal interaction between RTG's and spacecraft again becomes minimal.

The radiation levels from the RTG's are comparable, with the MHW's cleaner fuel form offsetting a 50 percent increase in inventory, so any interference effects, e.g., gamma ray photons interfering with optical instruments or scientific particle counters, will be increased accordingly. The greater mission duration (7 years versus 2.5) means the integrated exposure of the spacecraft to damaging radiation, primarily neutrons in the 1 to 5 MeV range, will be up a factor of three. Even so, this exposure is not significant in affecting the design of any spacecraft components.

7.2 ATTITUDE CONTROL OPTIONS

The subsystem trades performed were limited in scope by the basic ground rule requiring direct adaptation of Pioneer 10/11 hardware wherever possible. Changes in the configuration are determined by requirements of increased sun-spacecraft distance, terminal navigation and retargeting after probe deployment at planetary encounter, and by increased lifetime requirements. To satisfy these constraints and requirements, the following major trade areas were encountered.

7.2.1 Thruster Configurations

The important considerations for the thruster configuration trades were that earth pointing must be maintained for significant ΔV executions required perpendicular to the earthline. The original proposed design

was composed of a single thruster on the equipment compartment with the line of action through the nominal c.g. after probe deployment. Error analysis showed that for nominal c.g. uncertainties and thruster misalignments, up to 22 degrees precession and 3 rpm of spin coupling could occur for a 46-meter/sec ΔV. Since this worst case ΔV maneuver is only one of several required, spin coupling downward with this thruster could be disastrous in the event of a spin thruster failure.

A redundant spin control thruster-cluster would be difficult to locate and would not provide the minimum precession coupling necessary. The selected design, using two thrusters which bracket the nominal c.g., provide not only a minimum coupling configuration, but also provide redundancy for spin control if fired individually, and provide a decrease in the ΔV execution time. This configuration does not improve the coupling problem (22-degrees precession and 3-rpm coupling remain about the same) but the design is compatible with the existing PSE and DSL designs for Pioneer F/G with little modification.

7.2.2 Roll Pulse

Roll reference pulses must be provided out to 20 AU. These could be provided one of three ways: modify the present sun sensor channel 1 to operate at 20 AU, provide a new sun sensor design, or use a star roll reference. The first method was deemed unsuitable since Uranus encounter would probably occur with a sun aspect angle of about 1.5 degrees. The inherent accuracy of the Pioneer design is such that the roll reference accuracy would be at best, inadequate.

A new sun sensor design could be made. The one likely candidate is an image dissector such as that designed for ROARS which observes the sun for the entire revolution about the spin axis. The system contains an optical system and significant electronics that yield a weight penalty on the order of 6 to 7 pounds.

The third possibility for providing the roll reference is from the star mapper. If the sun sensor does not provide a reference at 20 AU, then the star mapper should be redundant. This leads to the next trade item.

7.2.3 Star Mapper Redundancy

Terminal navigation for probe deployment is a mission critical function. With the selected star mapper basic design, redundancy in the terminal navigation function would also satisfy redundancy in the roll pulse as described above.

Three choices were considered for terminal navigation redundancy; none, partial redundancy, or complete redundancy. Complete redundancy would imply two sensors with separate optics, gimbals and electronics, but the penalty is great (each sensor weight would be about 13 pounds). Partial redundancy seemed the better alternative to no redundancy or redesigning the sun sensor. Common optics could be used with a single partially redundant gimbal and of course, a single stray light shade. Bearings in the gimbal could not be made redundant, however, stepper motor windings, and gimbal resolvers can be redundant. The PMT can also be redundant by using an image splitting fiber optics design between a single mask and the two PMT's. All electronics and pulse measurement and control logic must be made redundant since this is the major failure source.

7.2.4 Long-Life Considerations

The nominal 2.5-year Pioneer F/G design life cannot be extended to the required seven years simply by increasing redundancy at all levels as weight constraints do not permit it. Selective redundancy must be considered, and has been for the CEA. In particular, redundancy in the star logic of the SPC and PSE subassemblies were examined. The functional criticality of the various systems was the deciding factor in each case.

Star sensor logic was selected for redundancy, since the roll reference could be lost beyond 6 AU with a single failure otherwise. The PSE on the other hand, was selected as nonredundant because its functions can be performed by the SDL's and the direction of a lateral ΔV can be performed via the fixed-angle logic and the proper delay in the star roll pulse such that the precise roll angle for ΔV execution can be selected.

Although precession and spin coupling still present an operational difficulty, significant ΔV can be performed in reasonble times by making

use of the stored command programmer in the CDU to shorten the command sequence (repeated execution of the stored commands). Furthermore, by using the reduced bit rate of S-band communication, the resulting increase in beamwidth permits a larger range in precession pointing error accumulation between corrections.

7.3 OTHER SUBSYSTEM OPTIONS

In addition to the alternatives discussed above in Sections 7.1 and 7.2, there were many alternate approaches investigated in every subsystem area. Most of these design options have been discussed to some extent in Section 6. For this reason they will not be repeated here except in tabular form.

Table 7-2 summarizes the key subsystem design alternatives which were encountered during the study. The over-riding criteria in selecting alternatives was the desire to use Pioneer F/G hardware. Where new hardware was required, every attempt was made to utilize existing, flight-qualified items. In several instances this was not possible or desirable, and new or customized designs have been recommended. This was true in the case of the third stage adapter, the conical interstage separation, and the shunt regulator. All of these items represent new hardware designs.

Table 7-2. Summary of Principal Design Decisions and Tradeoffs

Subsystem	SUAE Requirement	Major Alternatives	Reason for Selection	Reason for Rejection	Reference
Propulsion	Lateral ΔV for Saturn flyby correction and for spacecraft deflection	Off earth-line maneuvers		Operational risk	Appendix E
		Use existing spin control thrusters		Inefficient and operationally complex	Appendix E
		Add radial thrusters	Simple to implement and relatively efficient		Appendix E
	Increased propellant capacity	Transtage tank (MMC)		Heavy; requires modification	-
		P-95 tank (LMSC)	Lightweight		-
Structure	Accommodate probe separation	Retain standard third stage adapter		Heavy; operationally complex	Section 6.1
		Design custom third stage adapter	Simple and lightweight		Section 6.1
	Probe separation mechanism	One central spring		Heavy; probe aft heat shield deformation	Section 6.1
		Multiple springs	Simple and lightweight		
	Separate probe-spacecraft cable	Zero entry or lanyard connector		Tipoff errors; weight; life; thermal closure	
		Cable cutter	No tipoff errors; lightweight		
Thermal Control	Dissipate excess RTG power	Regulator inside equipment compartment		Complicates thermal design	Section 6.2
		External regulator	Minimize compartment load variations		Section 6.2
Electrical Power	Provide probe battery charging	Provide power only - probe carries charger		Charger is dead weight after separation	-
		Install charger and control logic on bus	Best system design		-
	Accommodate pulse loads	Use a battery		Weight; reliability	-
		Power margin + load control	Minimum weight and cost		-
Communications	Provide probe-to-bus data link antenna	Despun antenna		Heavy; complex; costly; reliability	Appendix A
		Axisymmetric antenna	Minimum weight and cost		Appendix A
	Provide bus-to-earth S-band link	Use solid state transmitter		Not used on Pioneer F/G	-
		Use TWTA	Existing Pioneer F/G unit		-
Command Distribution	Fire probe ordnance after 7 years	Use batteries		Weight; reliability; cost	
		Capacitor discharge	Existing Pioneer F/G design		

8. TEST PROGRAM

The test programs considered in this section pertain to two different periods in the SUAE Pioneer program, before and after the award of contracts for the development, design, and construction of flight hardware. The objective of the test programs in these two periods are somewhat different.

8.1 TEST PROGRAM OBJECTIVES

8.1.1 Interim Test Program

The interim test program refers to the period after the completion of the present study, but before the award of flight hardware contracts for the SUAE program. The objectives of tests during this period is to validate the feasibility of the mission by means of the conceptual designs generated for the spacecraft and probe in the present studies, and the compatibility of spacecraft and probe designs with each other.

This does not mean the spacecraft and probe designs need to be proven in the sense of a qualification program, because that would go much further than validation of feasibility. Where there is no question of feasibility but only of the design details, it is not necessary to conduct any test; the reasonability of proposed design parameters is of concern only to the extent that they impinge in a critical way on overall design constraints such as weight or power.

For example, there is no question that the magnetometer boom deployment restraint cable and damper can be made strong enough to withstand the tensile load they are subjected to, even though this load is greatly increased compared with Pioneer F/G, because of the simultaneous RTG and magnetometer deployments and because of the counterweight carried on the magnetometer boom. Furthermore the effect on weight of making these components twice as strong as necessary is only a few tenths of a pound. Therefore it is neither necessary nor appropriate to perform a detailed test of this component before the hardware phase, when it will be subjected to deployment tests conducted at the system level.

However other spacecraft components, particularly those which operate in conjunction with interfacing elements of the probe are appropriately subjected to engineering model and pre-engineering model tests for both feasibility and compatibility. These include components relating to the structural support of the probe, the separation of the probe, the thermal control of the probe is maintained by the spacecraft, the electrical interface with the probe while it is attached to the spacecraft, and the RF probe-bus communication link.

The purpose of including a discussion of this interim test program in this report is to identify areas where model and test activity are appropriate in future months to provide experimental verification of the design concepts generated in the study.

8.1.2 Test Program of Phase C/D

The objectives of test programs during Phases C and D are to develop engineering designs (developmental) or engineering tests), to prove the validity of the detailed design (qualification tests), and to certify flight hardware for launch (acceptance tests). These are the normal objectives associated with the hardware phase of a spacecraft contract.

The purpose of outlining this test program in this report is to establish the basis for the implementation of the hardware execution phase. This basis is in terms of the number of test and flight articles to be built, the extent of testing operations, and the overall schedule to be followed.

8.2 INTERIM TEST PROGRAM IMPLEMENTATION

The following discussion pertains to feasibility validation tests of an interim test program, prior to hardware phases.

Figure 8-1 indicates the scheduling contemplated for such tests. With the completion of the current system definition studies for the SUAE spacecraft and probe by TRW and McDonnell-Douglas, conceptual designs are being created, pertinent tests are identified, designating generally the units or test models to be employed, and necessary design information for constructing test articles will be furnished at least partially.

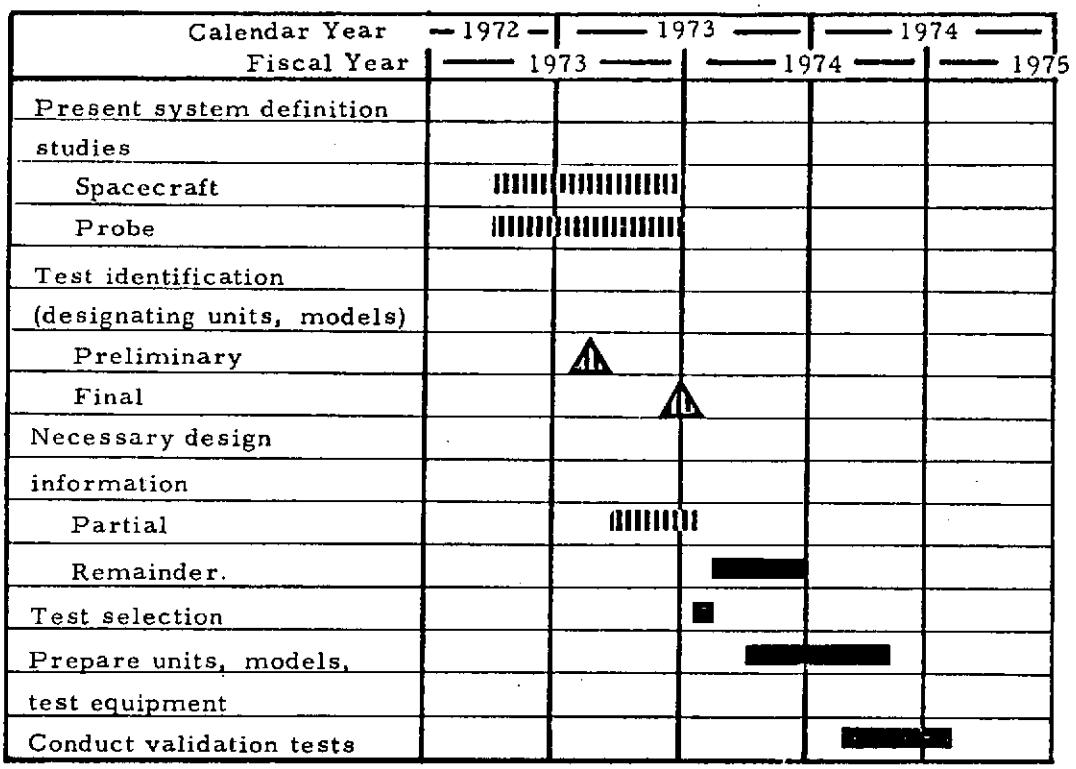

Figure 8-1. Interim Test Program Scheduling

It is anticipated that Ames Research Center will select tests to be performed from among those which have been identified. From approximately September, 1973, to April, 1974, would be occupied by the generation of remaining necessary design information and the preparation of test articles, test equipment and test facilities. Test articles will be produced by modifying existing hardware, by simulating spacecraft or probe units with commercial hardware, or by building up breadboards of circuitry as required.

The conduct of validation tests may then take place during calendar year 1974.

8.2.1 Mechanical Tests

Mechanical tests, covering structural response to launch vehicle-induced vibration and ordnance-induced shock, deployment dynamics, and the separation of the probe, are considered in Table 8-1.

Table 8-1. Mechanical Tests

Test	Models Employed	Objectives	Discussion	Recommendation
Appendage deployment tests (system)	(See discussion.)	Determine predictability of deployment dynamics, effect of mismatching restraint dampers, wobble induced by transient c. g. excursion.	The pertinent factors differing from Pioneer F/G are not amenable to physical system tests. Therefore rely on individual deployment tests and on analytical methods.	No
Appendage deployment tests (individual)				
RTG deployment	(See discussion.)	Verify ability to deploy to latch up, with variations in initial spin rate and physical parameters. Verify that components are not overstressed.	Not enough difference from Pioneer F/G to warrant a test.	No
Magnetometer boom deployment	Magnetometer boom model. Application of varying forces (centrifugal and Coriolis) by simulation. Test table.	Verify ability to deploy to latch up, with variations in initial spin rate, spin rate vs time, and physical parameters. Verify that components are not overstressed.	Because of deployment counterweight (24 lbs) and increased initial spin rate, this is a desirable test for the SUAE spacecraft. System deployment analyses should be performed in advance to provide realistic spin rate vs time profiles.	Yes
System vibration, acoustics, and shock tests	Modified structural model of spacecraft, modified adapter, mass models of RTG's, spacecraft experiments, and spacecraft units. Probe may be a mass model or a structural model, mating at structural interface points in either case.	1. Verify ability of structure to withstand stresses induced by launch environment. 2. Determine amplification factors at various locations in spacecraft and probe. 3. Verify compatibility of bus and probe at interface.	This is an appropriate test to demonstrate structural compatibility of spacecraft and probe. Other objectives depend on the extent to which test articles represent final flight hardware design.	Qualified Yes
Probe separation test	Spacecraft structural model is appropriate, but lesser model may suffice. Same with probe. Separation bolts, springs, and ordnance.	1. Verify reliability of separation mechanization. 2. Determine tipoff rates. 3. Determine flyout angles and necessary clearances.		Yes

8.2.2 Thermal Tests

Thermal tests are considered in Table 8-2. These tests verify the ability of the spacecraft's thermal control system to satisfy probe temperature requirements and to accommodate the changed requirements of the spacecraft equipment compartment.

Table 8-2. Thermal Tests

Test	Models Employed	Objectives	Discussion	Recommendation
Thermal control of the probe when attached to the spacecraft	Thermal model of the probe, with heat sources (simulated) and external insulation. Thermal model of the spacecraft, or at least of that portion of the spacecraft adjacent to the probe.	Verify ability of spacecraft to maintain probe below 32°F in interplanetary cruise (shaded from sun). Determine probe temperatures for partial and full side sun.	Requires thermal vacuum chamber, with solar illumination.	Yes
Thermal control of the spacecraft	Thermal model of the spacecraft. Probe effects may be simulated.	Verify spacecraft thermal control of its own subsystems.	Significant to account for thermal changes from Pioneer F/G: fewer louvers, external shunt amplifier, partial obstruction of louvers by probe, X-band transmitter.	Yes

8.2.3 RF Tests

RF tests are considered in Table 8-3. The recommended tests all pertain to verifying the patterns of antennas to be developed or to be located differently with respect to the spacecraft structure.

8.2.4 Electrical Tests

Electrical tests, pertaining primarily to the electrical interface between spacecraft and probe, are proposed in Table 8-4. Life tests for ordnance-firing circuitry of the spacecraft and for the ordnance devices are recommended. These ordnance devices, which may be used near the end of the seven-year mission, include a cable cutter and separation ball-lock bolts on the spacecraft (but serving the probe), and squibs to initiate events on the probe.

8.2.5 Data Interface Tests

The major new interfaces of data-generating systems (the probe and the line-scan camera) with the spacecraft data handling components are examined in Table 8-5.

Table 8-3. RF Tests

Test	Models Employed	Objectives	Discussion	Recommendation
S-X band high gain antenna	New dual S-X band feed and prototype 9-foot reflector.	1. Verify performance and pattern of dual S-X band feed at both frequencies. 2. Verify pattern of antenna at both frequencies.	The dual feed concept is a key element in the extension of Pioneer F/G to advanced missions	Yes
S-band combined medium/low-gain antenna pattern	One-third scale model of spacecraft with medium-gain horn, aft omni in new location. Probe adapter on spacecraft.	Determine composite pattern, particularly changes in the region of interference nulls.		Yes
Probe-spacecraft RF link			(Not TRW's jurisdiction in this study.)	
Probe link-antenna pattern tests	One-third scale model of loop-vee antenna, used with S-band scale model (above).	Verify pattern (cone angle and clock angle) of link antenna.	An element of the probe-spacecraft link analysis.	Yes
X-band driver, transmitter, switches	Components	Verify development-status of components other than antenna to comprise X-band downlink capability.	These tests are logically performed at the component level only. Not essential now to verify feasibility.	No

Table 8-4. Electrical Tests

Test	Models Employed	Objectives	Discussion	Recommendation
Probe-bus cable separation test	Ordnance actuated cable cutter. Model of adjacent cable geometry.	Verify cable-cutter operation.	The cable cutter is important to mission success, but feasibility is not in question.	Low Priority
Ordnance-firing circuitry life tests	Ordnance-firing circuitry of CDU: capacitor banks and silicon controlled rectifiers.	Verify ability to fire ordnance devices after 3 to 7 years space storage.	Critical to mission. This test program should be formulated and initiated soon. Means should be sought to accelerate life test. This is primarily a test of components; the basic circuitry has been proven on Pioneer F/G, but for short life.	Yes
Pyrotechnic life tests			Same as above, but for the pyrotechnic devices.	Yes
Spacecraft-probe compatibility tests: Ordnance-firing (squibs on probe) Commands to probe Probe battery charging Hardlined probe data to spacecraft Electro-magnetic interference	Unit models or breadboards for both probe and spacecraft.	To verify the compatibility of interfacing electrical circuitry.		Yes

Table 8-5. Data Interface Tests

Test	Models Employed	Objectives	Discussion	Recommendation
Probe data compatibility test	Unit models or bread-boards of receiver - bit synrhrnoizer, data buffer, DTU, DSU.	Verify that data from the probe can be received and processed by the spacecraft.		Yes
Line-scan camera data compatibility test	Camera simulator, models or breadboards of camera data generator and processor, DTU, DSU.	Verify that line-scan camera data can be processed by the spacecraft.		Low Priority

8.2.6 Optical Instruments

Two optical instruments are aboard the spacecraft, each being a significant revision of a previous instrument and performing new functions on the spacecraft. In each case, the appropriate tests to demonstrate feasibility of the instruments to perform their functions are currently underway as the subject of separately-funded test programs, supported by Ames Research Center.

The line-scan camera, part of the complement of scientific instruments, will produce an image in a small portion of a single spin revolution, by sweeping linear array of solid-state sensors across the field of view. This is a significant enhancement of the imaging capability of the photopolarimeter on Pioneers 10 and 11. The ability of the new instrument to operate at the outer planets, Saturn and Uranus, with the light levels to be found there and at Pioneer spacecraft spin rates is what is being subjected to verification tests.

The V-slit star mapper performs the roll-indexing function of the stellar reference unit on Pioneers 10 and 11, but in addition is designed to serve as a navigation sensor for the SUAE mission as well as other planetary and small-body missions. In the navigation role it must be able to determine the direction in celestial coordinates from the spacecraft to targets (specifically, the satellites of Saturn and Uranus) as faint as magnitude 4. It is this ability which is being subjected to feasibility tests.

8.3 IMPLEMENTATION OF PHASE C/D PROGRAM

This section treats the implementation of a Phase C/D program for the design, development, fabrication, assembly, and test of hardware for the SUAE mission. The purposes are:

- To indicate the schedule of major events for this program.
- To outline a minimum-cost program of hardware development and test, subject to satisfying product assurance objectives.
- To indicate the need dates for major interfacing elements of the flight spacecraft, i.e., RTG's, probes, experiments.
- To establish ground rules which may be used in estimating program costs.

The C/D phase of the entire program is considered to start with the award of the contract for spacecraft hardware and to end with the launch of the third flight vehicle. This span is from January 1, 1977 to December, 1980.

8.3.1 System Test Matrix

Table 8-6 gives a matrix for the principal tests to be combined at the system level, involving both the spacecraft and the probe. From left to right are the development tests of the spacecraft structural and thermal subsystems, engineering tests of the electrical subsystems, qualification tests of the prototype spacecraft, and acceptance tests of flight vehicles. "Combined" means the spacecraft and probe are to be tested together, and "separate" means the tests may be done at different times or places for the spacecraft and probe.

8.3.2 Multiple Use of Test Hardware

One means of keeping program costs low is to minimize the creation of dead-end hardware. In the implementation of this program, it is proposed to attain this in several ways, illustrated in Figure 8-2.

Table 8-6. SUAE Mission System Test Matrix

TEST	SPACECRAFT/PROBE MODEL				
	STRUCTURAL	THERMAL	ENGINEERING	PROTOTYPE	FLIGHT
VIBRATION	COMBINED	—	—	COMBINED	COMBINED
THERMAL VACUUM	—	COMBINED	—	COMBINED	COMBINED
RADIATION SENSITIVITY	—	—	—	COMBINED OR SEPARATE	COMBINED OR SEPARATE
MAGNETIC FIELD	—	—	—	COMBINED OR SEPARATE	COMBINED OR SEPARATE
RF (400 MHZ)	—	—	COMBINED	COMBINED	COMBINED
RFI/EMC	—	—	COMBINED	COMBINED	—
ELECTRICAL COMPATIBILITY	—	—	COMBINED	COMBINED	COMBINED
INTEGRATED SYSTEM TEST	—	—	COMBINED	COMBINED	COMBINED
MECHANICAL INTERFACE	COMBINED	—	—	COMBINED	COMBINED
SEPARATION	COMBINED	—	—		
MASS PROPERTIES	—	—	—	COMBINED OR SEPARATE	COMBINED OR SEPARATE
ANTENNA	—	—	—	SEPARATE	SEPARATE
RF SYSTEM	—	—	—	COMBINED	COMBINED
DEPLOYMENT	SPACECRAFT	—	—	SPACECRAFT	SPACECRAFT
ACOUSTIC	COMBINED	—	—	COMBINED	—
SPIN		—	—	SEPARATE	—

The spacecraft structure which is used in structural model testing and in thermal model testing will also be used as the structure of the prototype spacecraft and as the structure of one of the flight spacecraft. After structural and thermal model testing the structure will be repaired refurbished, and modified as necessary, such modifications being under full configuration control and applicable to the other flight spacecraft structures when they are built.

After prototype spacecraft tests units will be removed from the structure, and it is again refurbished where necessary. It is refitted with new subsystem units, new scientific instruments and a new probe, acceptance tested, and launched as one of the three flight vehicles.

In general, subsystem units will be built for four flight ship sets. One set will be used to qualify the units and to be on the prototype spacecraft for system qualification. This set will be removed after prototype spacecraft system qualification, refurbished, acceptance tested at the unit level, and made available as flight spare units. The other three

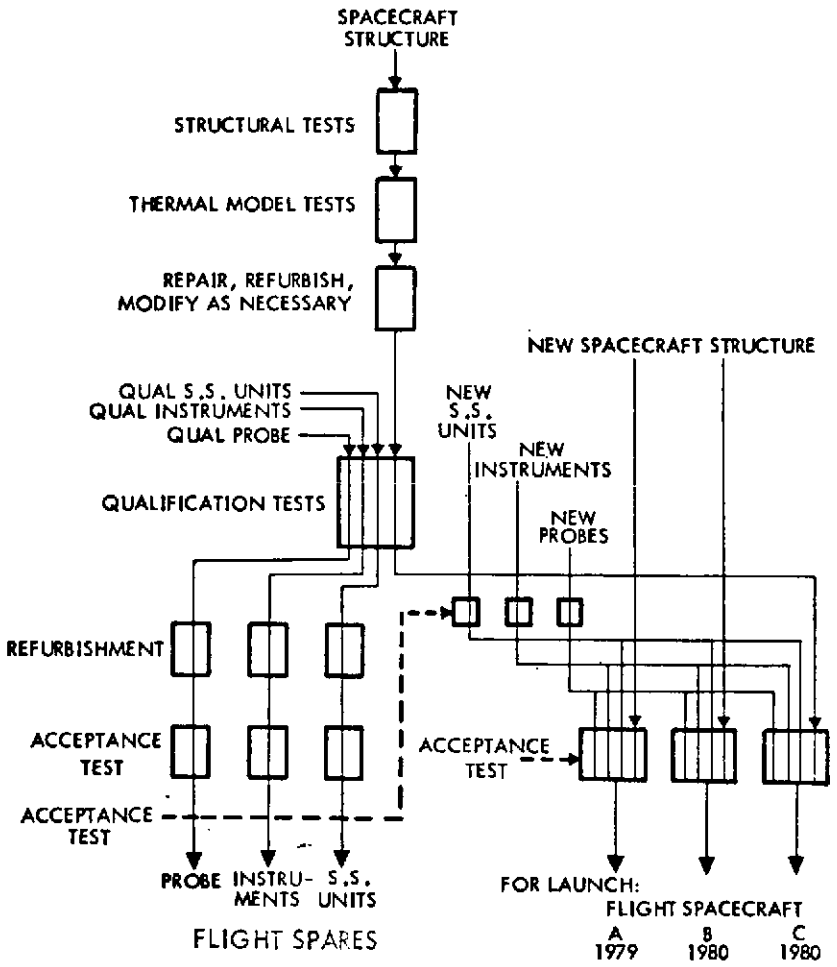

Figure 8-2. Multiple Use of Spacecraft Hardware

ship sets will follow the normal course of manufacture: they will be acceptance tested at the unit level, integrated onto a flight spacecraft, acceptance tested at the system level, and launched. Where a ship set includes identical units, the spare set may have fewer of such units than a full ship set.

We suggest that it is appropriate for probe flight hardware to follow this same course: one probe which has been qualified by the probe contractor is delivered for integration onto the prototype spacecraft. After combined system qualification tests this probe is returned to the probe contractor for refurbishment, retested to acceptance levels, and redelivered to serve as a spare probe for the third flight vehicle launch. The other three probes would be acceptance tested at the probe level by the probe contractor, delivered for integration to flight spacecraft, tested at combined system acceptance test levels, and launched.

(The above assumes that the sparing level for probes is the entire probe. If the probe is more appropriately spared at the unit level, the above sequence would be modified.)

8.3.3 Phase C/D Schedule

Figure 8-3 shows the schedule for Phase C/D of the SUAE spacecraft. The program starts on January 1, 1977, and culminates in the launch of one flight spacecraft in November, 1979, and two flight spacecraft in the opportunity of November-December, 1980.

The schedule is paced by the integration and test program, which starts with structural model tests at the end of 1977. The schedule is consistent with the hardware flow outlined in Figure 8-2.

8.3.4 Government Furnished Equipment

The following classes of equipment are assumed to be furnished by the government:

1) All instruments and instrument electronics of the spacecraft's scientific payload.
2) The RTG power sources.
3) The probes and all equipment mounted within the probe, including the probe's scientific payload.
4) The receiver – bit synchronizer for the probe – bus communication link, which is to be mounted on the spacecraft.
5) The launch vehicle adapter, a modification of the standard 37 x 31D adapter for the TE-364-4 stage.

For these items, all necessary test models and qualification units are assumed GFE, as well as flight hardware.

8.3.5 Hardware Need Dates

Consistent with the Phase C/D schedule, the following need dates are outlined for government furnished equipment for initial use on integration with the spacecraft.

8.3.5.1 Probe Hardware Requirements

Based on the test matrix of Table 8-6 and the schedule of Figure 8-3, requirements for probe hardware including probe scientific instruments (both test and flight models) and the need dates are given in Table 8-7.

8.3.5.2 Other GFE Hardware Requirements

The requirements for test and flight hardware of the bus scientific instruments, RTG power sources, receiver – bit synchronizer, and launch vehicle adapter parallel those of the probe. All are given in Table 8-8.

The RTG power sources do not need radioisotope heaters until the prototype test. The prototype RTG's would serve without refurbishment as flight spares for the 1979 Earth-Saturn launch, but may require refurbishment to serve as spares for the Flight C launch to Saturn and Uranus.

A single test launch vehicle adapter can satisfy spacecraft assembly and acceptance vibration tests for all three flight spacecraft. The flight adapters are furnished with the launch vehicles at the launch site.

8.3.5.3 EGSE Computer

The computer of the Pioneer F/G EGSE is considered to be an appropriate constituent of the Pioneer SUAE spacecraft EGSE. It would have to be available in August 1977.

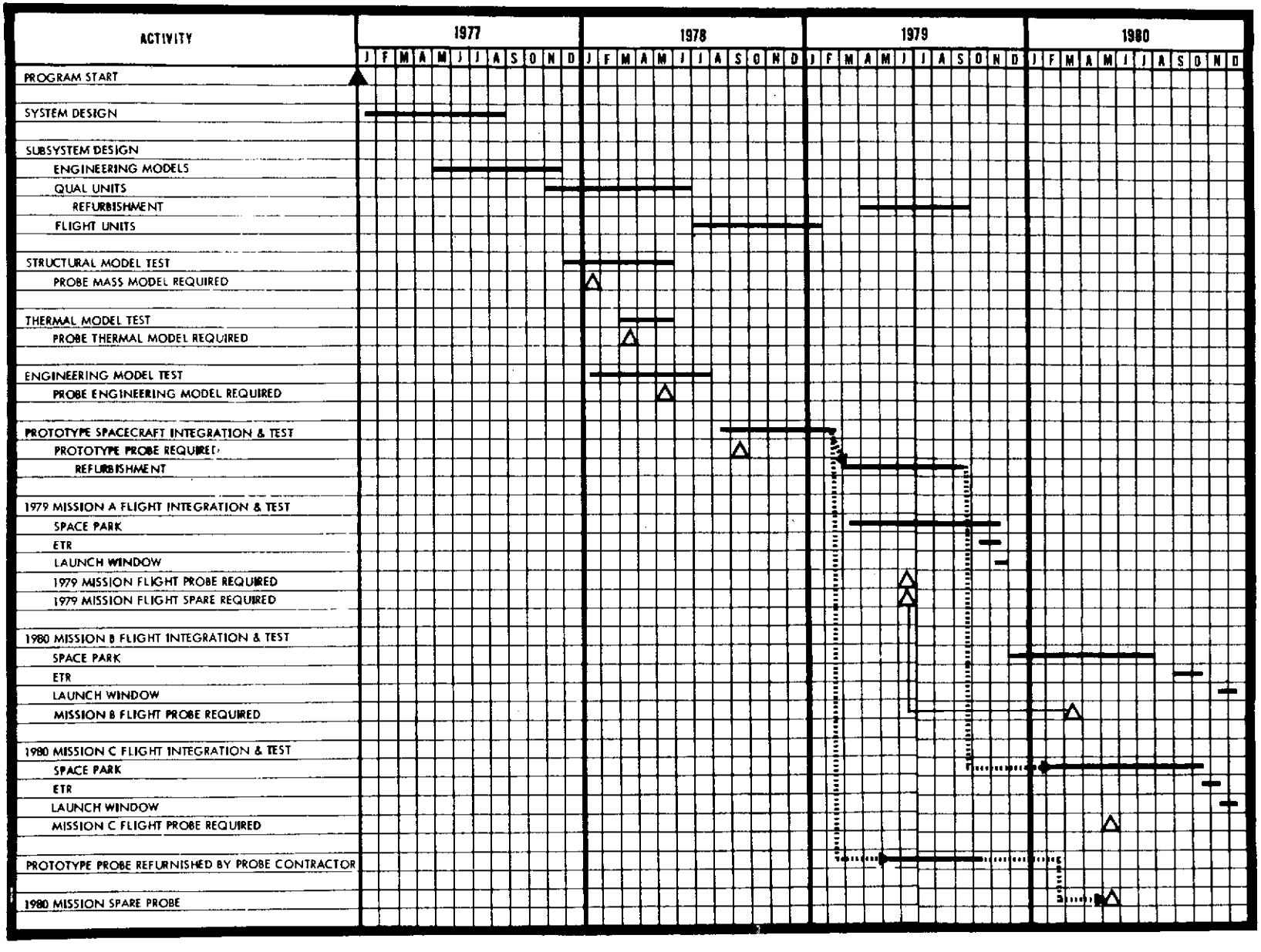

Figure 8-3. SUAE Spacecraft Phase C/D Schedule

Table 8-7. SUAE Probe Hardware Requirements

MODEL TYPE	QUANTITY	DESCRIPTION	NEED DATE
MASS	1	MUST DUPLICATE MASS AND CG OF FLIGHT CONFIGURATION AND DUPLICATE MECHANICAL INTERFACE WITH THE SPACECRAFT/PROBE INTERSTAGE. MOMENT OF INERTIA DUPLICATION IS REQUIRED. DUPLICATION OF EXTERIOR GEOMETRY IS NOT REQUIRED.	JANUARY 1978
THERMAL	1	MUST DUPLICATE MASS AND CG OF FLIGHT CONFIGURATION AND DUPLICATE MECHANICAL INTERFACE WITH THE SPACECRAFT/PROBE INTERSTAGE. THE EXTERNAL GEOMETRY AND EXTERNAL SURFACE FINISH MUST BE THE SAME AS FLIGHT. INTERNAL HEAT SOURCES MUST BE SIMULATED.	MARCH 1978
ENGINEERING	1	MUST DUPLICATE TO THE GREATEST EXTENT POSSIBLE ALL ELECTRICAL COMPONENTS WHICH INTERACT WITH THE SPACECRAFT. MECHANICAL CONFIGURATION MUST BE THE SAME AS FLIGHT ONLY TO THE EXTENT NECESSARY TO PROVIDE FLIGHT-LIKE GROUNDING, SHIELDING, RFI/EMC AND BONDING CHARACTERISTICS	MAY 1978
PROTOTYPE*	1	MUST DUPLICATE THE FLIGHT DESIGN CONFIGURATION IN ALL RESPECTS. DEVIATIONS FROM FLIGHT CONFIGURATION WILL BE APPROVED ON AN INDIVIDUAL BASIS IF IT CAN BE SHOWN THAT INTERACTION WITH THE SPACECRAFT WILL NOT BE AFFECTED.	SEPTEMBER 1978
FLIGHT		FULL FLIGHT CONFIGURATION	
ONE	1		JUNE 1979
TWO	1	(SERVES AS FLIGHT SPARE FOR 1979 LAUNCH)	JUNE 1979
THREE	1		MAY 1980
SPARE*	1	FULL FLIGHT CONFIGURATION (IF THIRD LAUNCH REQUIRES A FLIGHT SPARE)	MAY 1980

*PROTOTYPE PROBE IS RETURNED TO PROBE CONTRACTOR FOR REFURBISHMENT TO SERVE AS A FLIGHT SPARE.

Table 8-8. Hardware Need Dates

Spacecraft Model	Bus Scientific Instruments	RTG Power Sources	Probes, Including Probe Scientific Instruments	Receiver — Bit Synchronizer	Launch Vehicle Adapter
Structural test model	Mass models January 1978	Mass models January 1978	Mass models January 1978	Mass models January 1978	Structural model January 1978
Thermal test model	(Represented by simulated heat sources)	Thermal models March 1978	Thermal model March 1978	(Represented by simulated heat sources)	(Same as above)
Engineering model	Design verification units February 1978	(None)	Engineering model May 1978	Engineering model May 1978	(None)
Prototype	Prototype September 1978	Prototype (4) November 1978	Prototype September 1978	Prototype September 1978	Prototype structure September 1978
Flight A	Flight April 1979	Flight September 1979	Flight June 1979	Flight June 1979	Test (2) April 1979
Flight B	Flight (3) April 1979	Flight May 1980	Flight (3) June 1979	Flight (3) June 1979	(Same as for Flight A)
Flight C	Flight March 1980	Flight August 1980	Flight May 1980	Flight May 1980	(Same as for Flight A)
Flight spare	Spare (1) March 1980	Spare (1) August 1980	Spare (1) May 1980	Spare (1) May 1980	Spare October 1980 at launch site

(1) Spares for Flight C are refurbished units removed from prototype spacecraft.
(2) Test adapter required for acceptance vibration test; flight adapters are furnished with launch vehicles at launch site.
(3) Serves as spare for Flight A.
(4) Also serves as spare for Flight A.

APPENDIX A

PROBE-LINK ANTENNA TRADEOFFS

1. INTRODUCTION

This appendix describes two separate tradeoff analyses regarding the spacecraft terminal antenna for the probe-to-spacecraft communications link. The first analysis (occupying Sections 2 to 7) leads to a choice between a despun antenna and an axisymmetric (non-despun) antenna. Several types of despun antennas were considered — both mechanically and electrically despun — and, for this analysis, the axisymmetric antenna was assumed to be an array of three Lindenblad elements. As a result of this analysis and a corresponding analysis by the probe study contractor the axisymmetric antenna approach was selected.

The second analysis (Section 8) compares two implementations of the axisymmetric approach: the Lindenblad antenna and a simpler loop-vee antenna. As a result of this analysis the loop-vee antenna was selected by Ames Research Center.

1.1 Study Requirements

Bus Aspect Angle. Candidate antennas must accommodate probe communications with the probe delivered to either Saturn or Uranus, although commandable (in-flight) changes are allowable. Nominal trajectories were derived by Ames Research Center mission analysts (see reference cited in Section 1.5), with encounter geometries as described in Figures 3-12 and 3-14. The bus aspect angle ranges are shown in Figure 3-13. Variations in bus encounter phasing and targeting influence these angle ranges. For the antenna tradeoff analyses, the ranges are as shown in Figure A-1: 60 to 90 degrees during the probe descent at Saturn; 40 to 70 degrees at Uranus. Bus aspect angle is measured on the spacecraft from the -Z axis — i.e., spin axis in anti-earth direction — to the descending probe.)

Two approaches of covering this range are considered, for both despun and axisymmetric antennas. An antenna with a single fixed cone angle should have its beam centered at 65 degrees, and have a beamwidth of 50 degrees, in a plane parallel to the spin axis. The antenna may cover

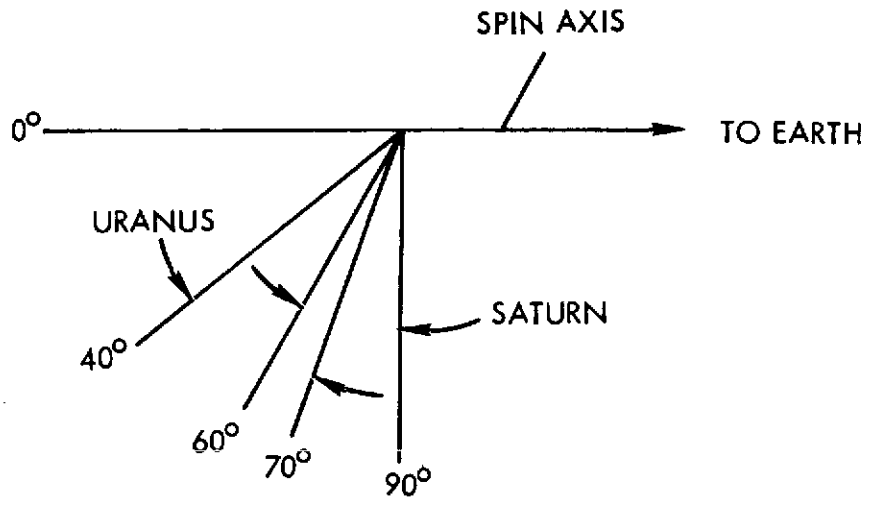

Figure A-1. Bus Aspect Angle Ranges

the range with a two-position switchable cone-angle control. In this case a 30-degree beamwidth suffices. The beam center is at 75 degrees for Saturn, and at 55 degrees for Uranus.

Checkout. Probe-to-bus checks prior to separation are via a coax hardline, not via either the probe or spacecraft antenna.

Frequency. Frequencies utilized are 1000 MHz for despun antennas, and 400 MHz for axisymmetric antennas.[1] A circularly polarized probe antenna is assumed.

Bus Dynamics. Criteria for minimizing the dynamic effects of a mechanically despun antenna on the bus were derived (Section 7 of this appendix). Without detailed analysis it is felt that resulting nutation effects will be kept small (less than one degree total) by reasonable design approaches.

2. CONFIGURATION OPTIONS (DESPUN ANTENNA TRADEOFF)

The bus antenna configuration options covered by this trade study vary from low-gain (0.3 dBi) to medium-gain (12-16 dBi) configurations.

[1] TRW letter 8140.8.10-15 from W. J. Dixon to H. F. Matthews, dated December 27, 1972, "Despun Antenna Analysis, Saturn Uranus Probe Mission."

High-gain antennas (such as retro-directive arrays or other tracking antennas) have not been included as candidate designs. For the configurations considered, several options were examined. These are listed below.

Despin Technique. There are basically two ways to implement a despun antenna; electrically or mechanically. An electrically-despun antenna consists of multiple radiating elements plus some type of switching mechanism or commutator to sequentially excite the element matrix. The mechanically-despun antenna consists of a single radiating element which is physically rotated in a direction opposite to the spacecraft body. Each despin technique has many variations in configuration.

Despin Control. Despin control is to be open-loop rather than closed-loop; the latter would involve tracking a signal from the descending probe, and would involve difficulties in detecting the signal to establish the initial lock-up. The open-loop control requires an external roll reference. The spacecraft's star mapper would serve in this role, and is assumed to do so in this tradeoff study, although the possibility of loss of control due to optical interference from the proximity of the sunlit planet is one disadvantage.

2.1 Mechanically Despun Configurations

A wide variety of configurations are possible for the mechanically despun antenna (MDA). These include designs which:

a) Have a fixed-feed (no rotary joint) and a despun reflector

b) Despin both the reflector and the RF feed (requires a rotary joint)

c) Despin both the antenna and the receiver (requires slip rings)

The first option (fixed-feed plus a despun reflector) is illustrated below as the cylindrical reflector (Figure A-2). Because of the difficulties involved in changing cone angle with this configuration, only one design covering the total cone angle variation is considered.

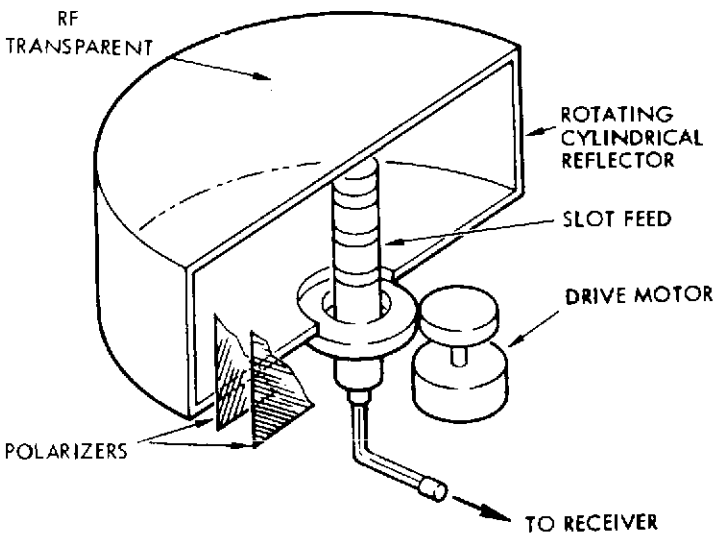

Figure A-2. Cylindrical Reflector

Since the feed radiates uniformly in all directions, this antenna is less efficient than other despun configurations. For example, the periscope reflector (Figure A-3) is an alternate technique for providing a despun reflector with a fixed-feed. In this design, all the energy from the feed is focused by the reflector. With the periscope reflector it is possible to consider varying the cone angle coverage although it is still a difficult design problem.

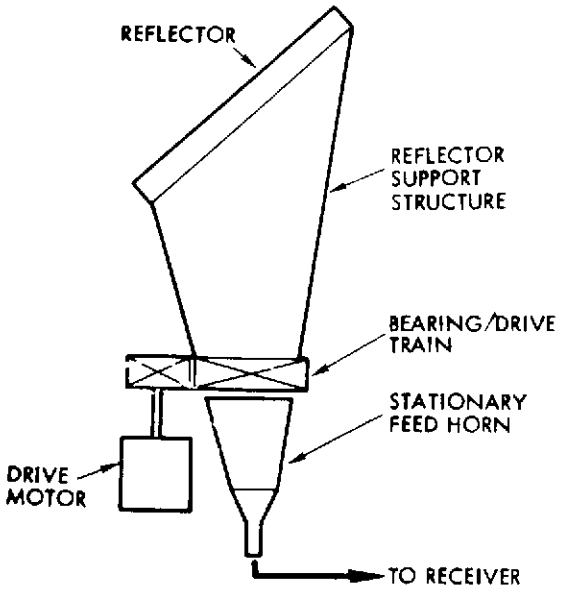

Figure A-3. Periscope Reflector

Despinning the reflector and the RF feed will generally require more drive power as well as requiring a rotary joint in the RF line. One possible implementation of this approach is the shaped parabolic dish shown in Figure A-4.

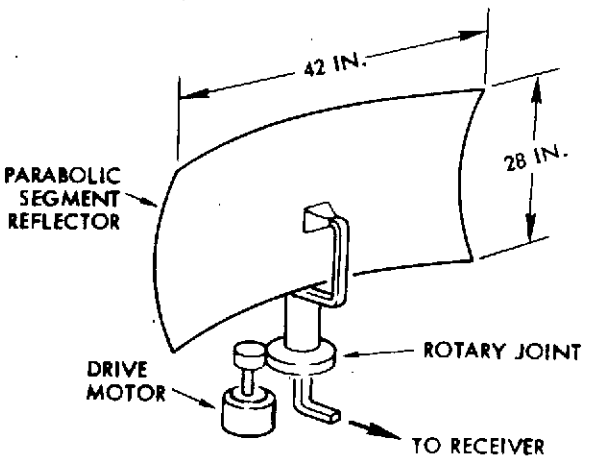

Figure A-4. Parabolic Reflector

An alternate configuration involves the use a a planar array instead of a reflector and feed. This design is a variation of option (b) since it also requires a rotary joint as shown in Figure A-5.

Typical installations of these antenna designs on the Pioneer spacecraft are given subsequently in this appendix.

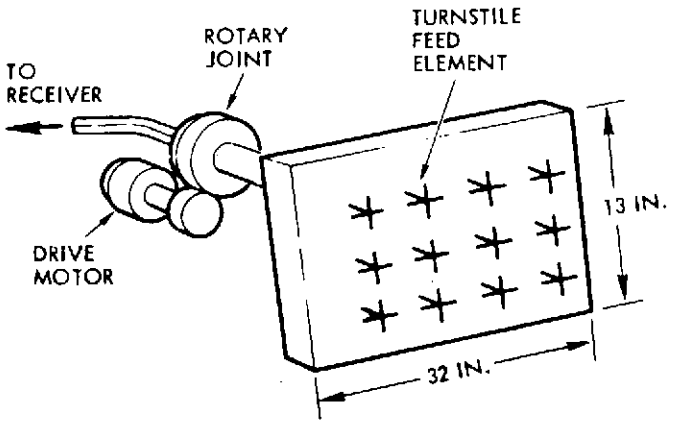

Figure A-5. Planar Array

Antenna Despin Control System. Figure A-6 is a block diagram of the antenna despin control system. The upper part of the figure

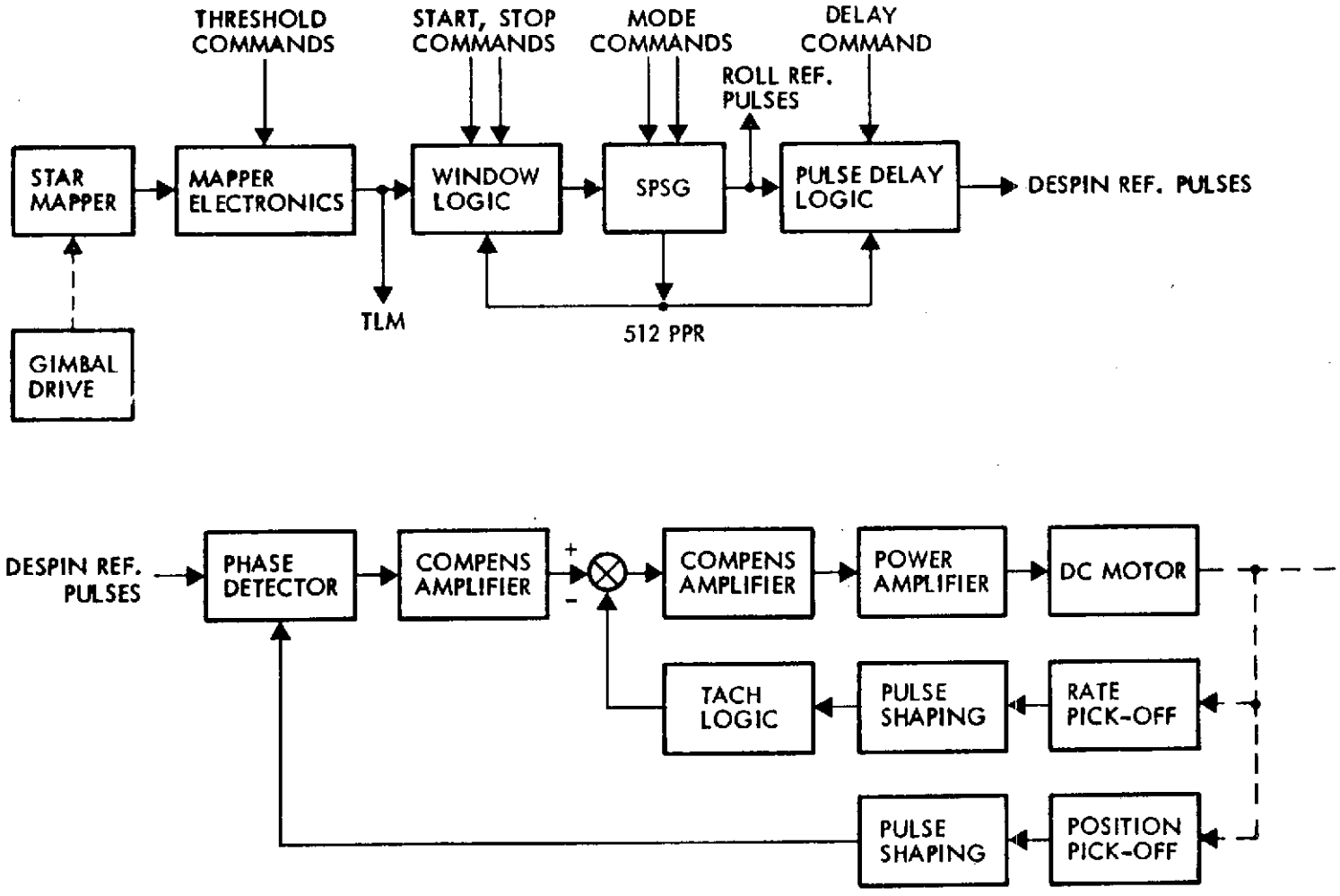

Figure A-6. Antenna Despin Control System Block Diagram

illustrates the process by which despin reference information is derived from the star mapper output. The lower part of the figure shows the loops providing the despin function.

The star mapper consists of a photodetector, optics, and V-type slit mask. The mapper electronics provides amplification and includes an adjustable (by command) threshold detector for reducing (or eliminating) background noise. Thresholded mapper signals are time-tagged and telemetered to the ground for star identification and attitude determination data processing. The window logic allows selection of a particular star for roll and despin references and provides interference rejection capability. The spin period sector generator (SPSG) provides the same functions as in Pioneer F and G, except for an additional holding mode (in which the contents of the spin-period measuring register are not updated until a command to exit the holding mode is issued). The pulse delay logic provides an adjustable (by command) delay of the reference pulses from the spin period sector generator.

A typical drive for antenna despin consists of a brush type DC motor, an RF coupler, and position and rate pickoffs. The rate pickoff generates a sequence of 32 pulses per revolution which, after shaping, is used in the tach logic to provide a measure of relative velocity between antenna and spacecraft. The rate loop is closed through a compensation amplifier, which drives the motor by means of a pulse-width-modulated power stage. Fine position control is exercised by a position loop operating on the despin reference pulses and a 1-PPR sequence provided by the position pickoff. The phase detector is an up-down counter providing a once-per-revolution measure of the antenna pointing error (relative to the ideal reference defined by the pulse delay logic output).

Typical despin/performance data are summarized in Table A-1.

Table A-1. Despin Data Summary

Spin speed range	0-10 rpm
Minimum motor stall torque	100 in.-oz
Minimum rate loop bandwidth	1.25 Hz (at 5 rpm)
Offset pointing range	0-360 degrees
RMS pointing error	0.5 degree
Power (at 5 rpm)	5 watts

2.2 Electrically Despun Configurations

Two different implementations of an electrically-despun antenna (EDA) were studied. One design created a single rotating beam with sufficient beamwidth to cover the full range of aspect angles (40 to 90 degrees). The second approach was a 30-degree beam which could be moved (switched) to accommodate either planet.

For the single beam design, a high gain element is proposed. To simplify the circuitry and scan losses, sixteen (16) equally-spaced radiating elements are sequentially switched to produce a rotating beam. To center the beam at the nominal aspect angle of 65 degrees, the elements are located on a conical section as shown in Figure A-7. The pattern of an individual element is given in Figure A-8.

Both EDA concepts would require reference pulses from a controller such as the one previously described in Figure A-6. The operation of the despun helix array is shown pictorially in Figure A-9. In this diagram, the clock angle uncertainty is postulated to be ± 10 degrees around the nominal. The coverage of this zone of uncertainty by a single element is shown from the time it is switched in (Position 1) to the time it is switched out (Position 3). Note that there is considerable margin for controller clock error in this design.

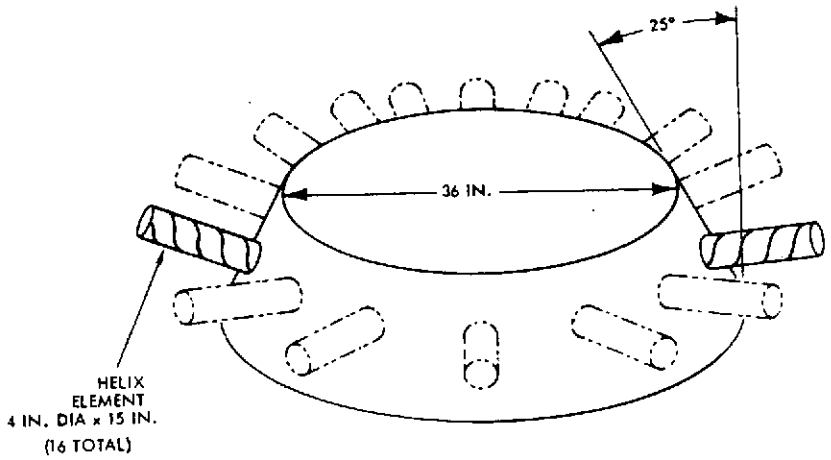

Figure A-7. Helical EDA

The net gain and weight estimates for the helical EDA are given in Table A-2.

Table A-2. Helical EDA Characteristics

Gain		Weight	
Helix Gain	+9.5 dB	16 Elements @ 4 oz	64 oz
Coax Loss	0.9 dB	5 Diode Switches @ 5 oz	25 oz
Switch Loss	0.6 dB	Coax	32 oz
Net Gain	+8.0 dB		121 oz
		or 7.6 pounds	

The higher gain EDA is shown in Figure A-10. The array arrangement and and circuit configuration is given in Figure A-11. The feed network, which includes a 4-port transfer switch for Saturn/Uranus beam selection, is shown in Figure A-12. This antenna is expected to have a net gain on the order of 10 - 12 dB.

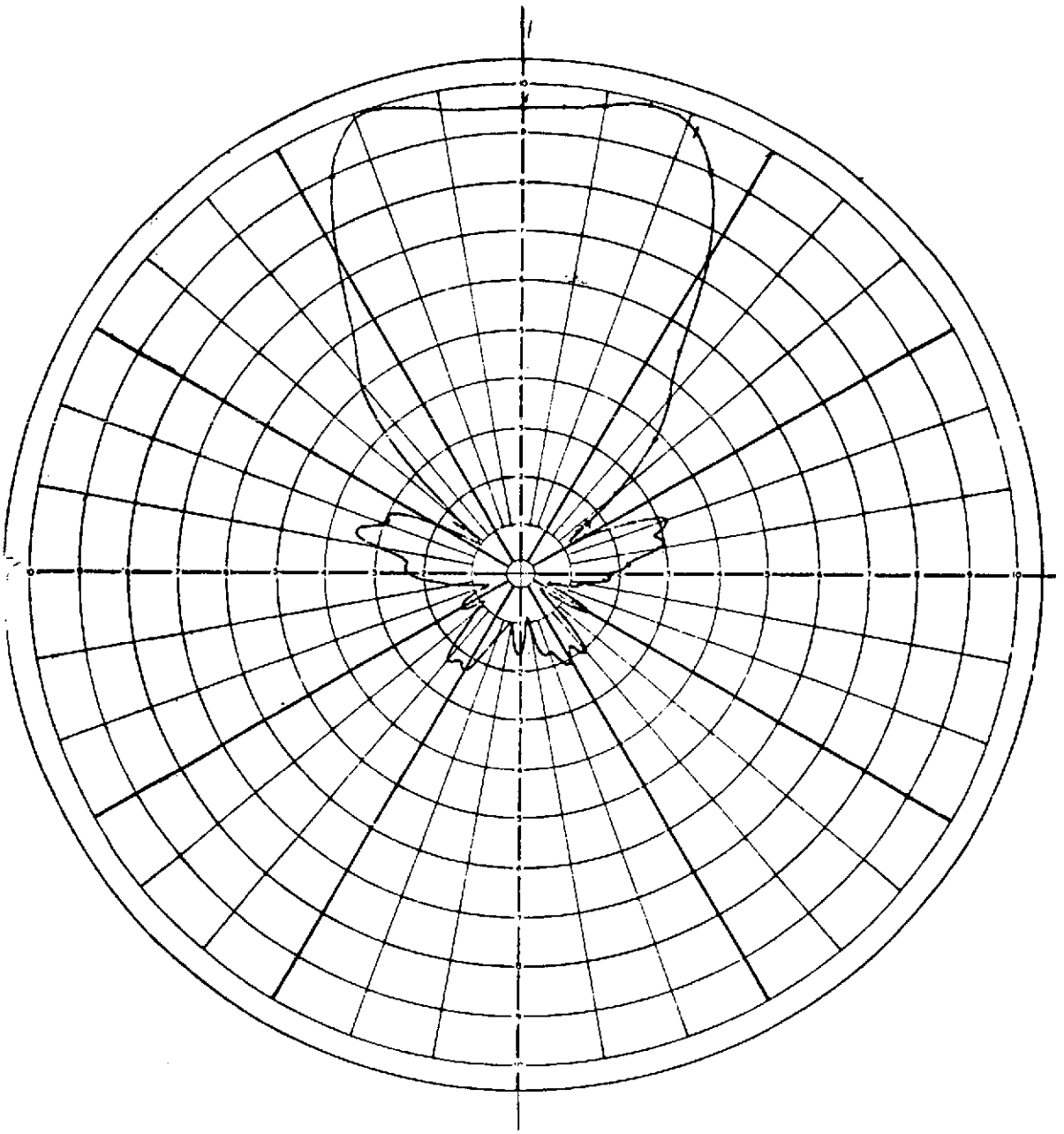

Figure A-8. Pattern of One Element of Helical EDA

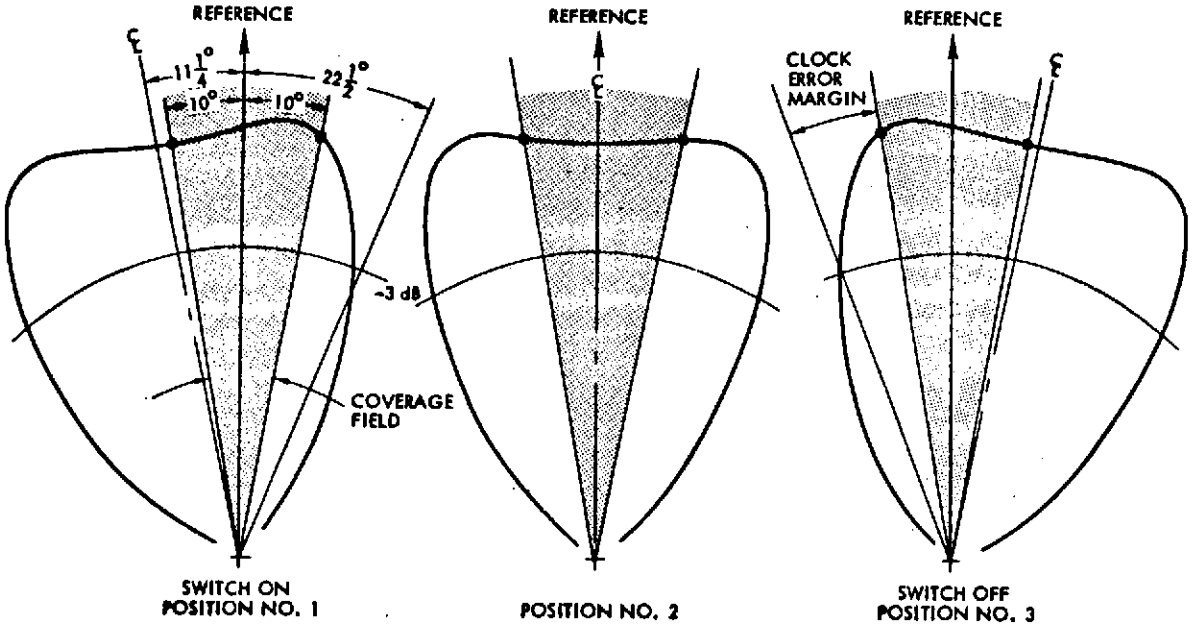

Figure A-9. Electrically Despun Antenna Operation

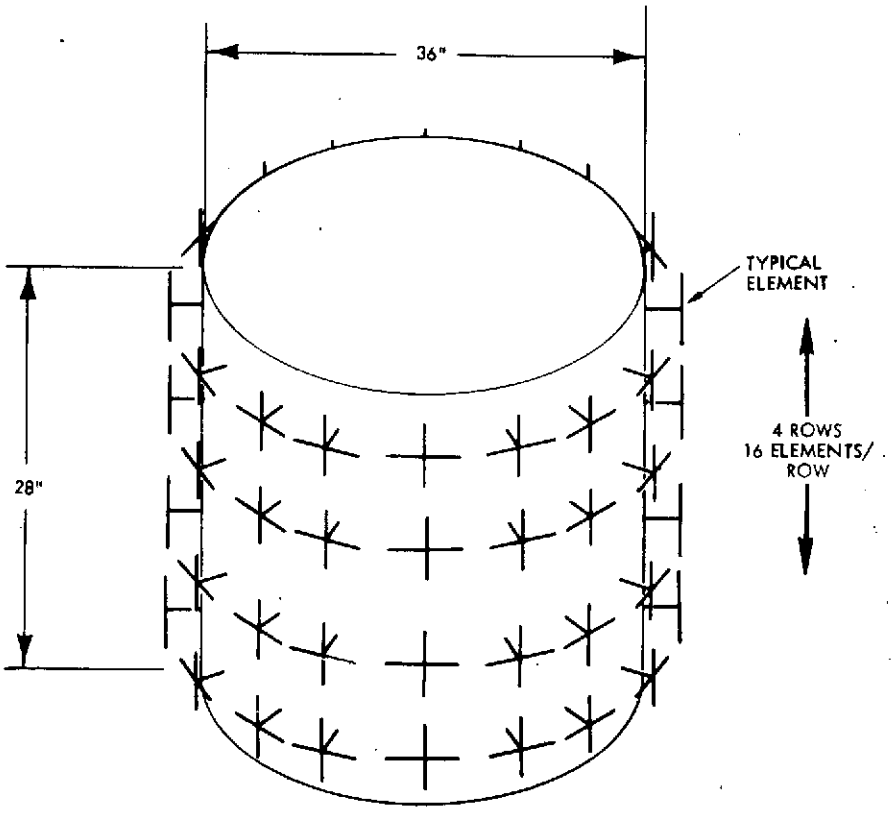

Figure A-10. Stacked Dipole EDA

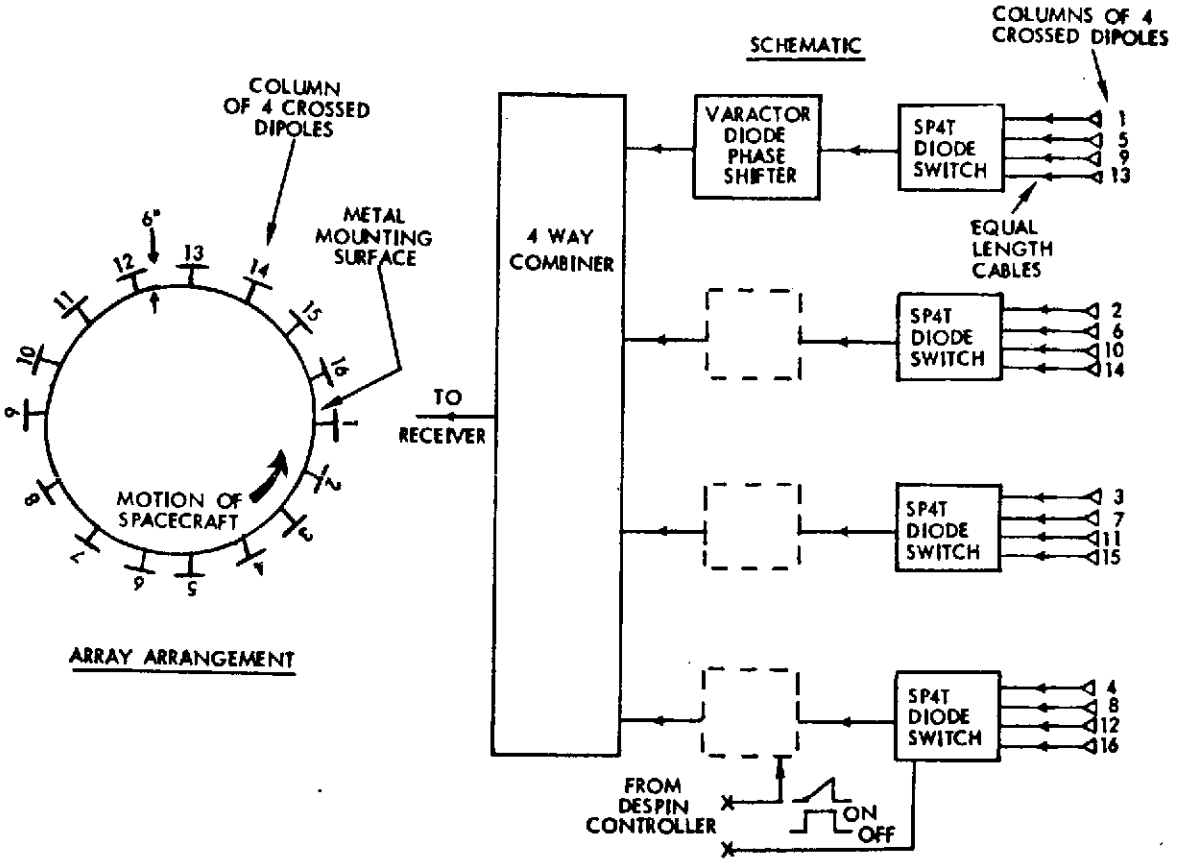

Figure A-11. Electrically Despun Antenna, High-Gain Configuration

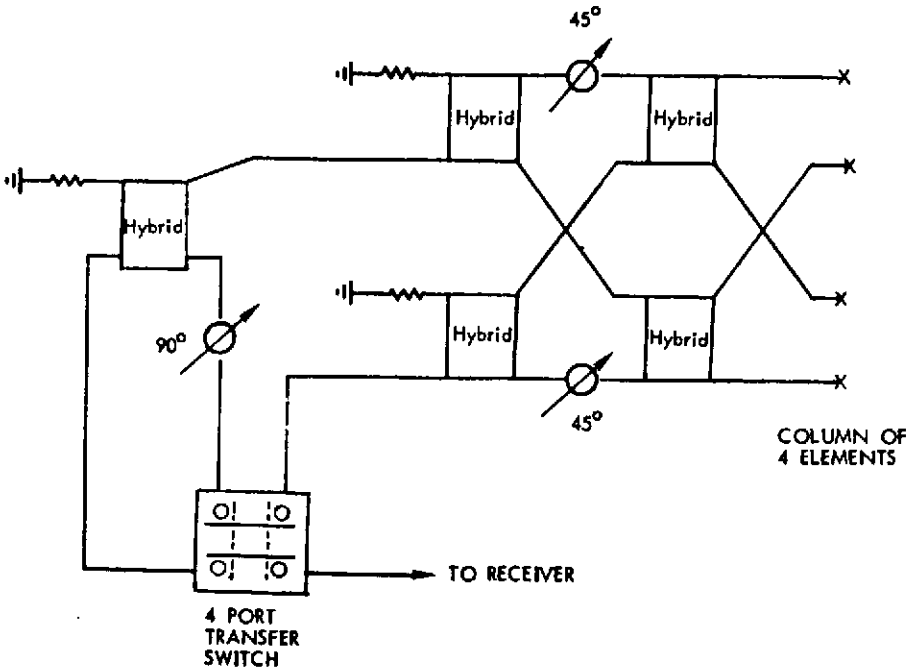

Figure A-12. Electrically Despun Antenna, Butler Feed Network

3. SUMMARY OF DESPUN ANTENNAS

Table A-3 summarizes the main characteristics of the various despun designs examined in this study. One method of comparing the merits of designs from this matrix is illustrated by Figure A-13. Thus, if we utilize antenna performance per pound of system weight (Table A-4 reflects the derivation of system weight) as a measure of design efficiency, the selected design would be either the helix EDA or the planar array MDA. This criteria was used to derive the rank order shown in Table A-3.

Table A-3. Despun Antenna Configuration Comparison

CONFIGURATION CHARACTERISTICS	MECHANICALLY DESPUN					ELECTRICALLY DESPUN	
	PARABOLOID		CYL.	PLANAR ARRAY			
	OPTION A	OPTION B	B	A	B	DIPOLE	HELIX
APERTURE SIZE	42 x 28	42 x 14	42 x 21	32 x 22	32 x 13	50 x 26	40 x 6
FEED TYPE	SLOT DIPOLE	SLOT DIPOLE	3 SLOTS	CROSSED DIPOLE	CROSSED DIPOLE	BUTLER	P.I.N.
FEED SIZE	11 x 3.5	11 x 3.5	11 x 3.5	N/A	N/A	N/A	N/A
ROTARY JOINT	YES	YES	NO	YES	YES	NO	NO
SLIP RINGS	YES	NO	NO	YES	NO	NO	NO
POWER (WATTS)	6	6	6	6	3	0	0
SYSTEM WEIGHT (LB)	55.3	41.3	44.8	42.3	30.2	52.5	17.5
INTEGRATION	HIGH	HIGH	HIGH	MOD	MOD	HIGH	MOD
NET GAIN (DBI)	13.1	10.5	9.8	14.1	12.3	11.3	7
RANK ORDER	3	3	4	2	1	4	1

NOTES:

1. OPTION A HAS TWO BEAM POSITIONS - INCLUDES DIPOLE EDA
2. OPTION B HAS ONE BEAM POSITION
3. NET GAIN IS BEAM EDGE PLUS ALL LOSSES
4. INTEGRATION DIFFICULTIES INCLUDE BALANCING, ACCESS, THERMAL CONTROL, FOV INTERFERENCE

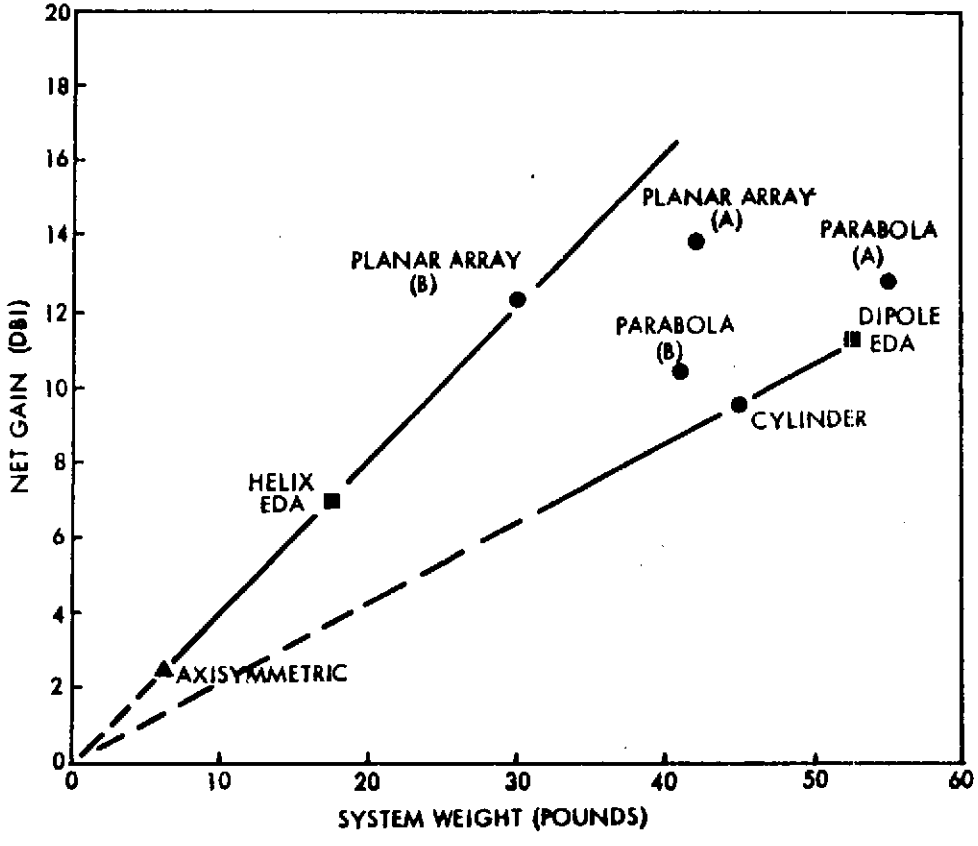

Figure A-13. Antenna Comparison - Weight Versus Gain

Table A-4. Despun Antenna Weight Breakdown

(Pounds)	Configuration						
	Mechanically Despun					Electrically Despun	
	Paraboloid Dish		Parabolic Cylinder Reflector	Planar Array		Large 64-Element Array	16-Element Helix Array
	A 2-Position	B 1-Position	B	A 2-Position	B 1-Position	A 2-Position	B 1-Position
Despun Portion							
Antenna	15	11	15	12	9	-	-
Structure	6	4	5	3	3	-	-
Aspect Angle Control	3	-	-	3	-	-	-
Mass Balancing	6	4	2	3*	3*	-	-
Total	30	19	22	21	15	-	-
Non-Despun Portion							
Antenna	-	-	2.5	-	-	28	7
Structure	7	4	2.0	3	2	21	7
Despin Mechanical Assembly	14.3(1)	14.3(1)	14.3(1)	14.3(1)	4.7(2)	-	-
Despin Electrical Assembly	4(1)	4(1)	4(1)	4(1)	8.5(2)	3.5	3.5
Total	25.3	22.3	22.8	21.3	15.2	52.5	17.5
SYSTEM WEIGHT	55.3	41.3	44.8	42.3	30.2	52.5	17.5

* Assumes Better Balanced Design

(1) Helios DMA and DEA
(2) Skynet DMA and DEA

4. AXIALLY SYMMETRIC ANTENNAS

The alternative to a despun antenna is an antenna which has a beam pattern of sufficient width and symmetric about the spin axis. The resulting pattern is similar to a doughnut in form and, like the despun antenna, it is possible to devise a single beam or a two-position beam configuration.

The single (unswitched) beam axisymmetric antenna selected for study comparison is the loop-vee design shown in Figure A-14. This antenna is estimated to weigh 4 pounds and have a beam-edge gain of approximately 0 to 1 dBi. (See Section 8 of this appendix.)

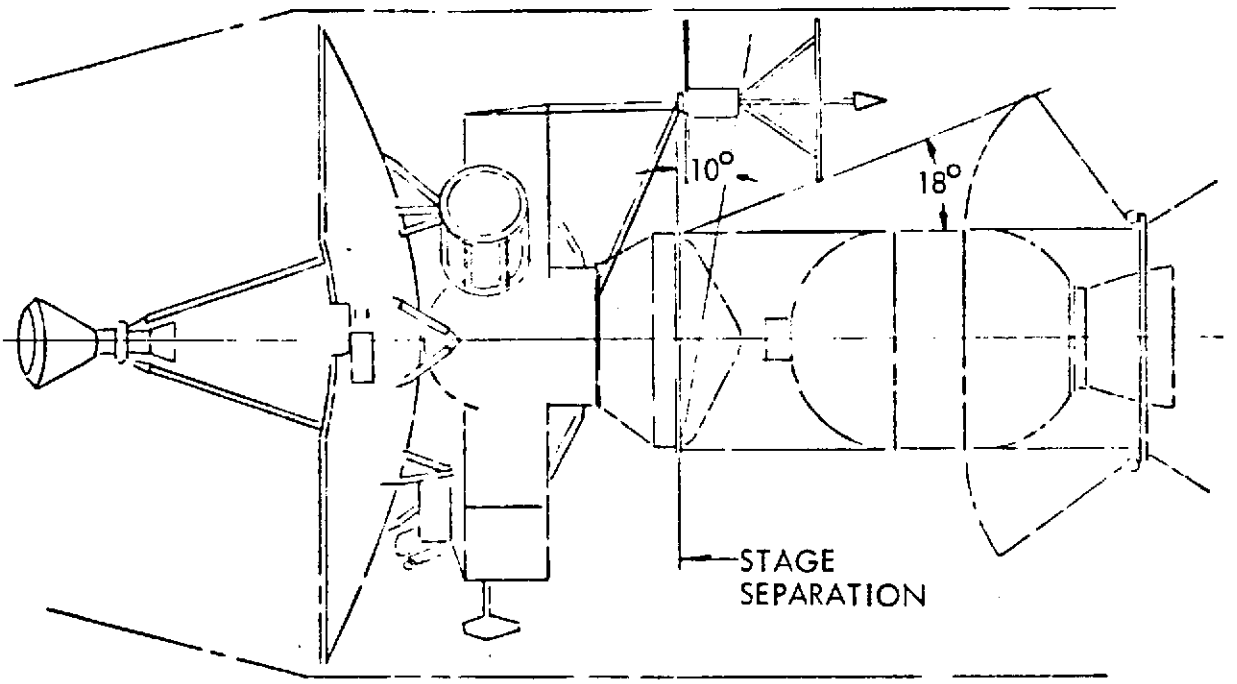

Figure A-14 Pioneer SUAE Loop-Vee Antenna Concept

The higher gain design utilizes a three-tiered array of Lindenblad elements as shown in Figure A-15. This antenna is estimated to weigh 7 pounes with a beam-edge gain of 2 to 3 dBi. See Table A-6 for the derivation of the two antenna gain figures. (Both weights include support structure.) In each case there is provision for the S-band low-gain an antenna at the extremity of the probe link antenna.

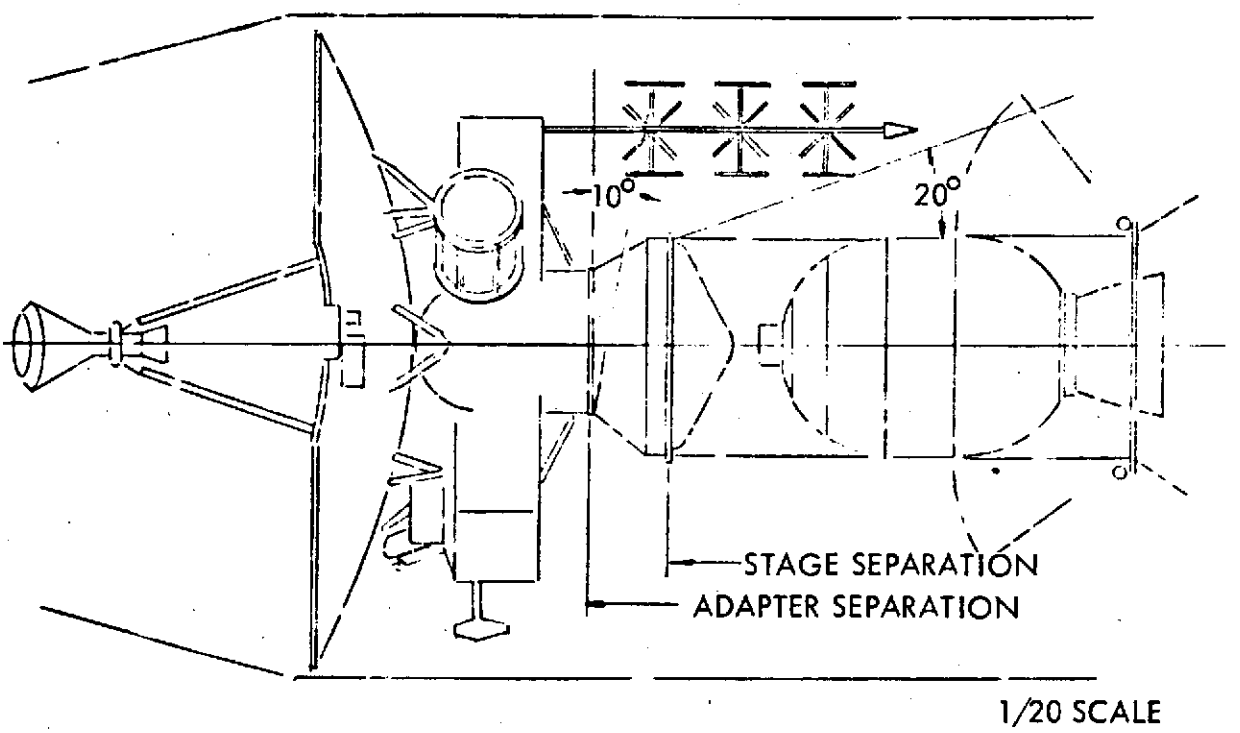

Figure A-15 Pioneer SUAE Lindenblad Antenna Concept

5. COMPARISON OF DESPUN AND AXISYMMETRIC ANTENNAS

Table A-5 reflects the major difference between the three principal antenna options considered to be the best of their particular design. This table clearly shows (qualitatively) the penalties associated with the higher gain despun antenna configurations. On the basis of the results presented above, TRW recommended the axisymmetric antenna as exemplified by the Lindenblad array (Reference 2) as the baseline probe-to-bus link antenna for this phase of the study.

It is possible that the lower axisymmetric antenna gain may cause problems in probe design and that the question of a despun antenna on the bus will be reopened. Transition to a low-gain helix EDA could be made with the least perturbation to the bus design or program cost,

---

[2]See TRW memorandum 8140.8.10-30 dated 28 February 1973, "Performance Data on the Lindenblad Array."

Table A-5. Comparison of Despun and Axisymmetric Antennas

TRADE FACTOR	AXISYMMETRIC LINDENBLAD	ELECTRICALLY DESPUN HELIX	MECHANICALLY DESPUN ARRAY PLANAR
WEIGHT (POUNDS)	7	17.5	30.2
NET GAIN (DBI)	2.5	7	12.3
RELIABILITY	HIGH	LOW	VERY LOW
DEVELOPMENT RISK	NO	YES	YES
INSTALLATION PROBLEMS	SMALL	MINOR	MAJOR
OPERATIONAL PROBLEMS	SMALL	MAJOR	MAJOR

schedule, and risk. However, the impact of a mechanically-despun antenna on the probe design would be substantial and more quantitative details on programmatics as well as technical factors (stability, testing, integration, etc.) would have to be developed.

6. INSTALLATION DRAWINGS

The various concepts discussed above are shown in Figurea A-16 through A-24 for reference.

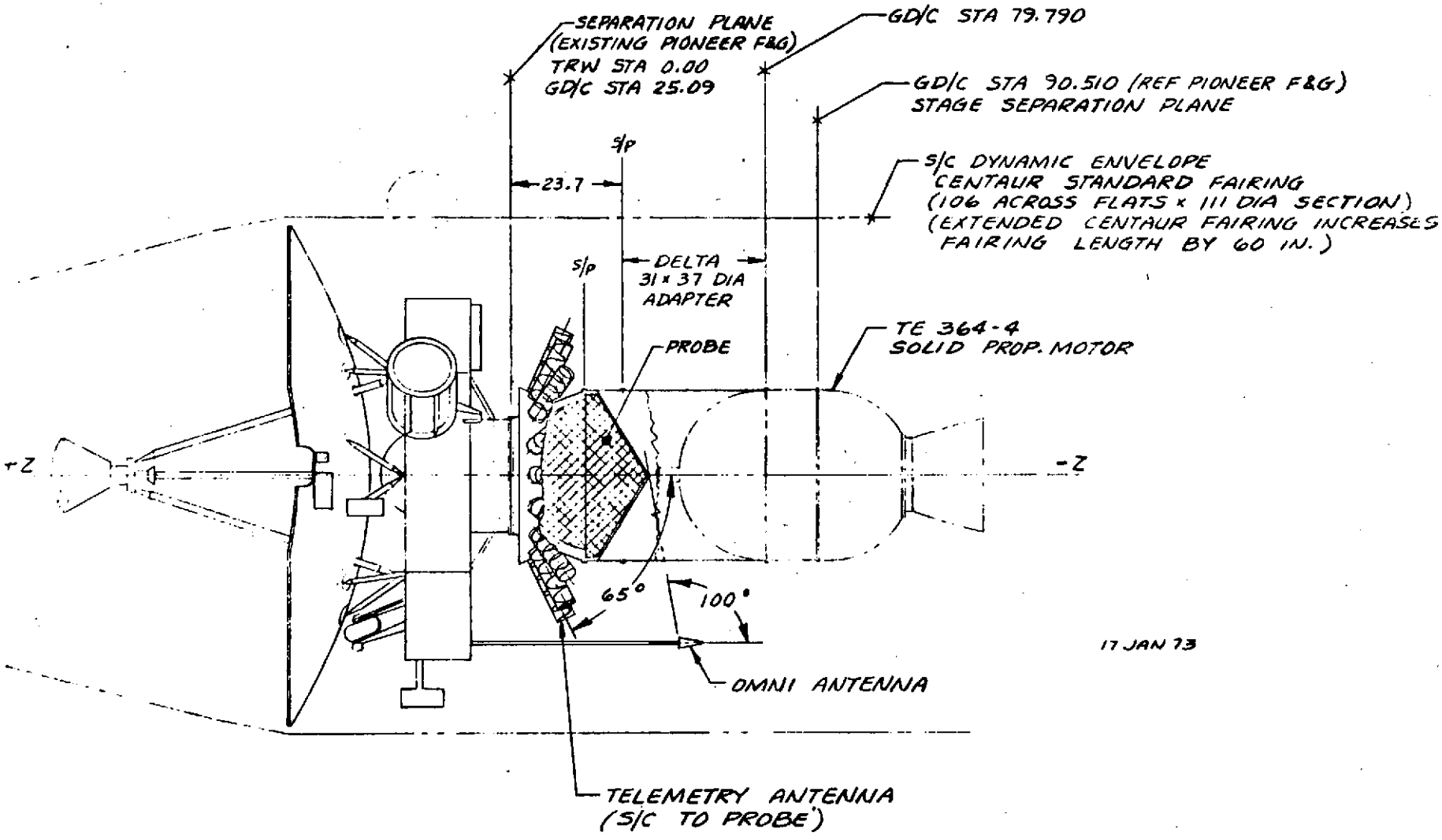

Figure A-16. Helix Array SUAE Probe Study (AD42-44)

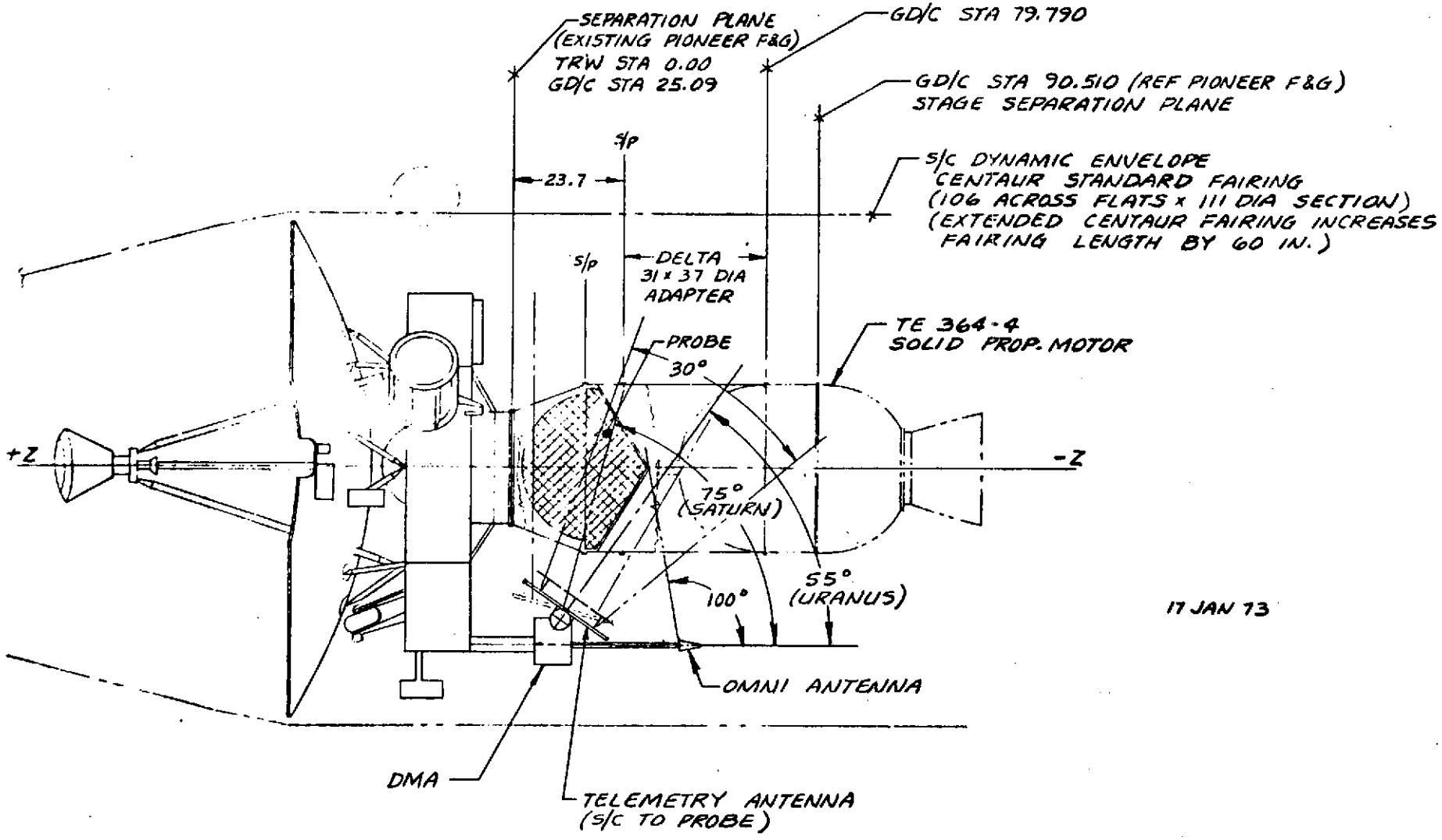

Figure A-17. Two-Position Planar Array SUAE Probe Study (AD42-45)

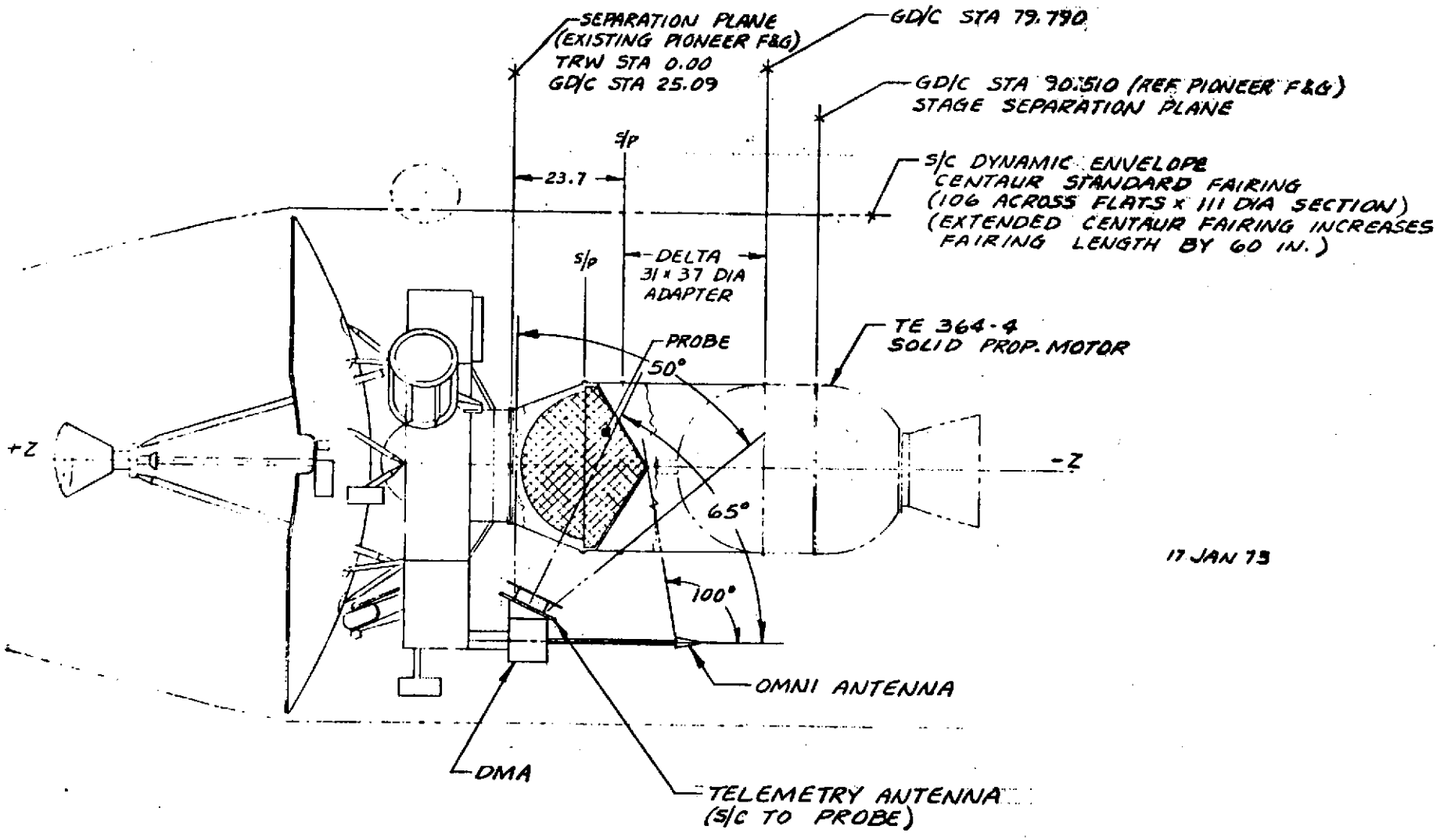

Figure A-18. Fixed-Position Planar Array SUAE Probe Study (AD42-46)

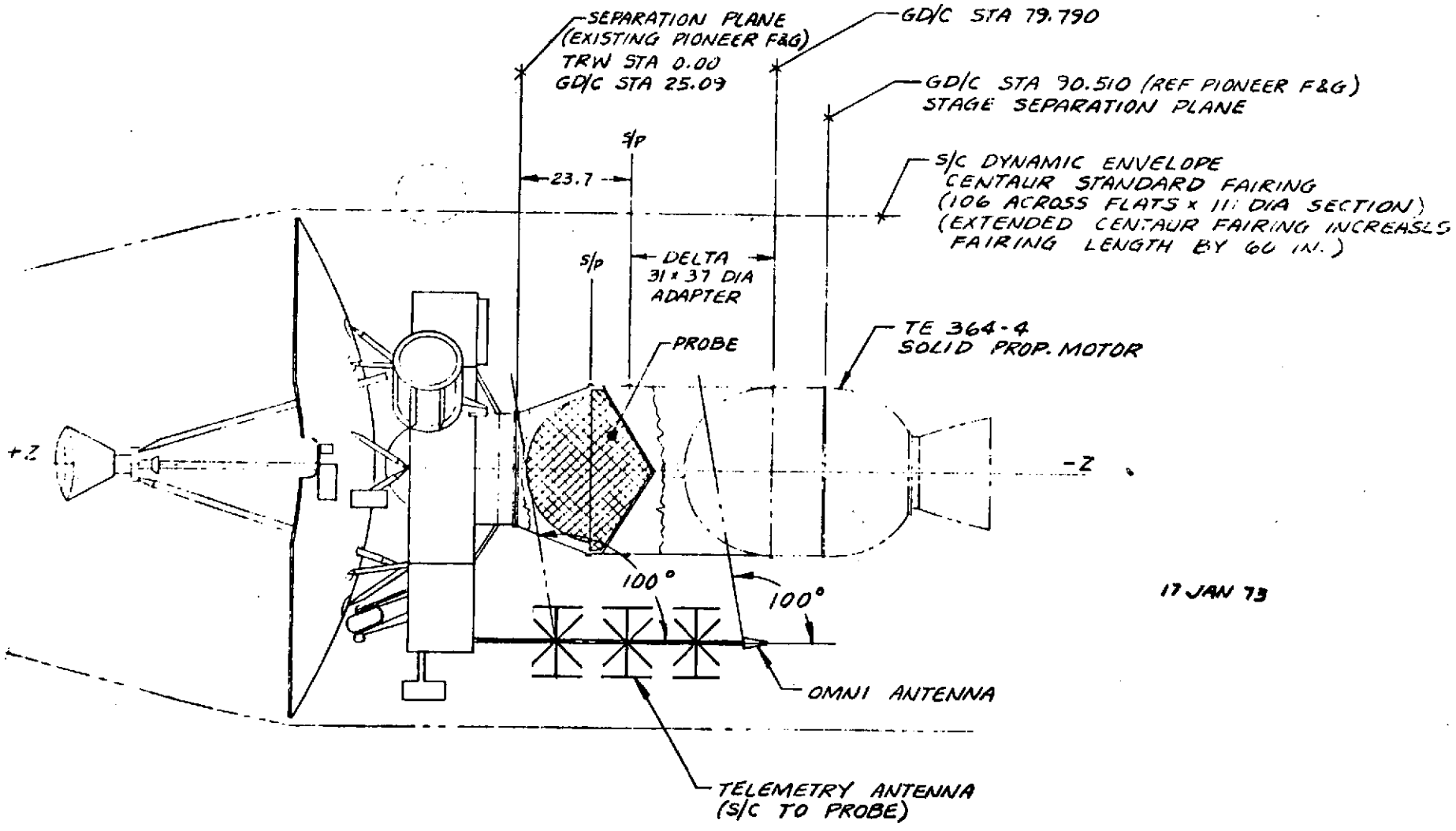

Figure A-19. Lindenblad Array - SUAE Probe Study (AD42-47)

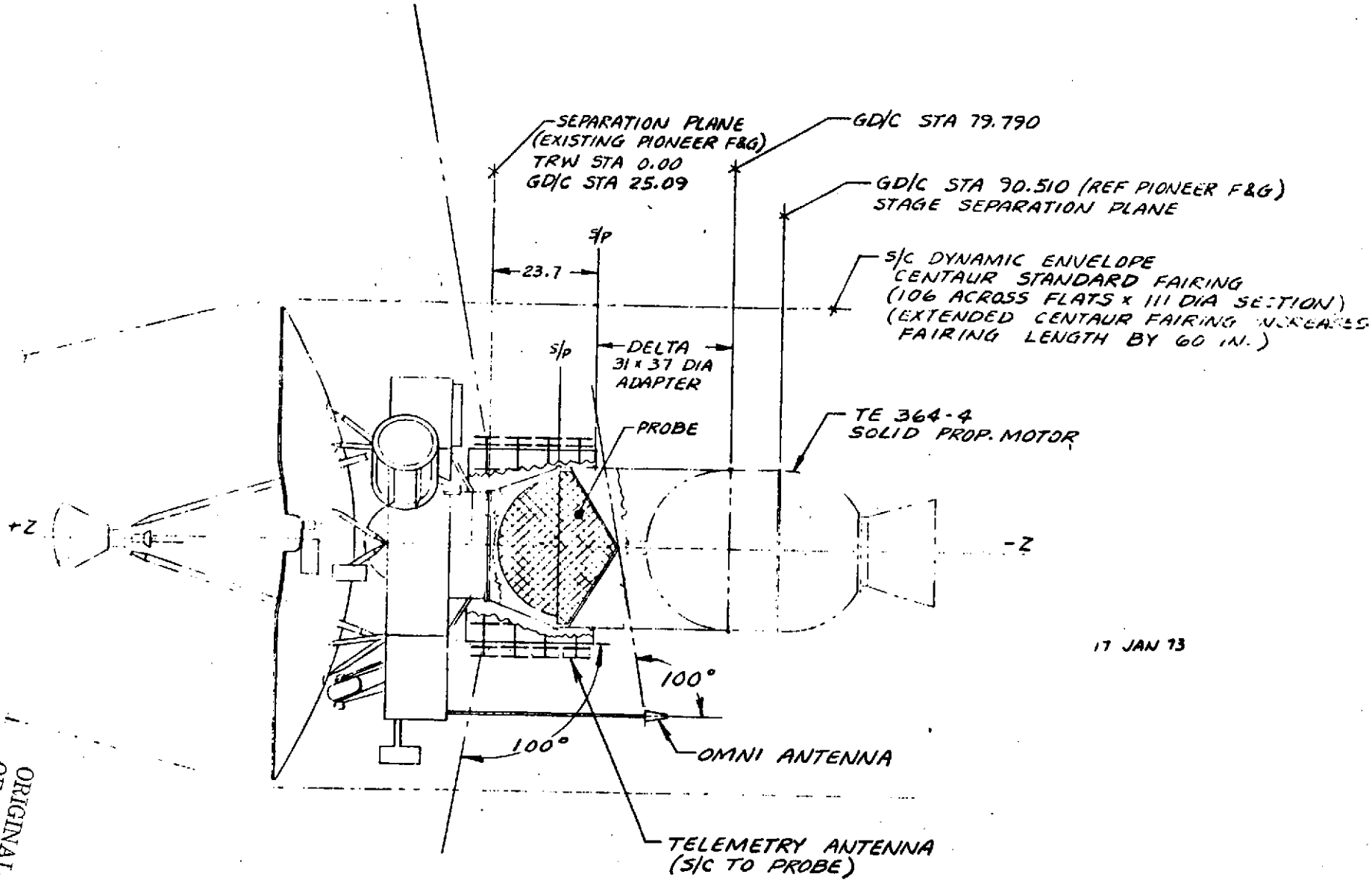

Figure A-20. Cylindrical Array - SUAE Probe Study (AD42-48)

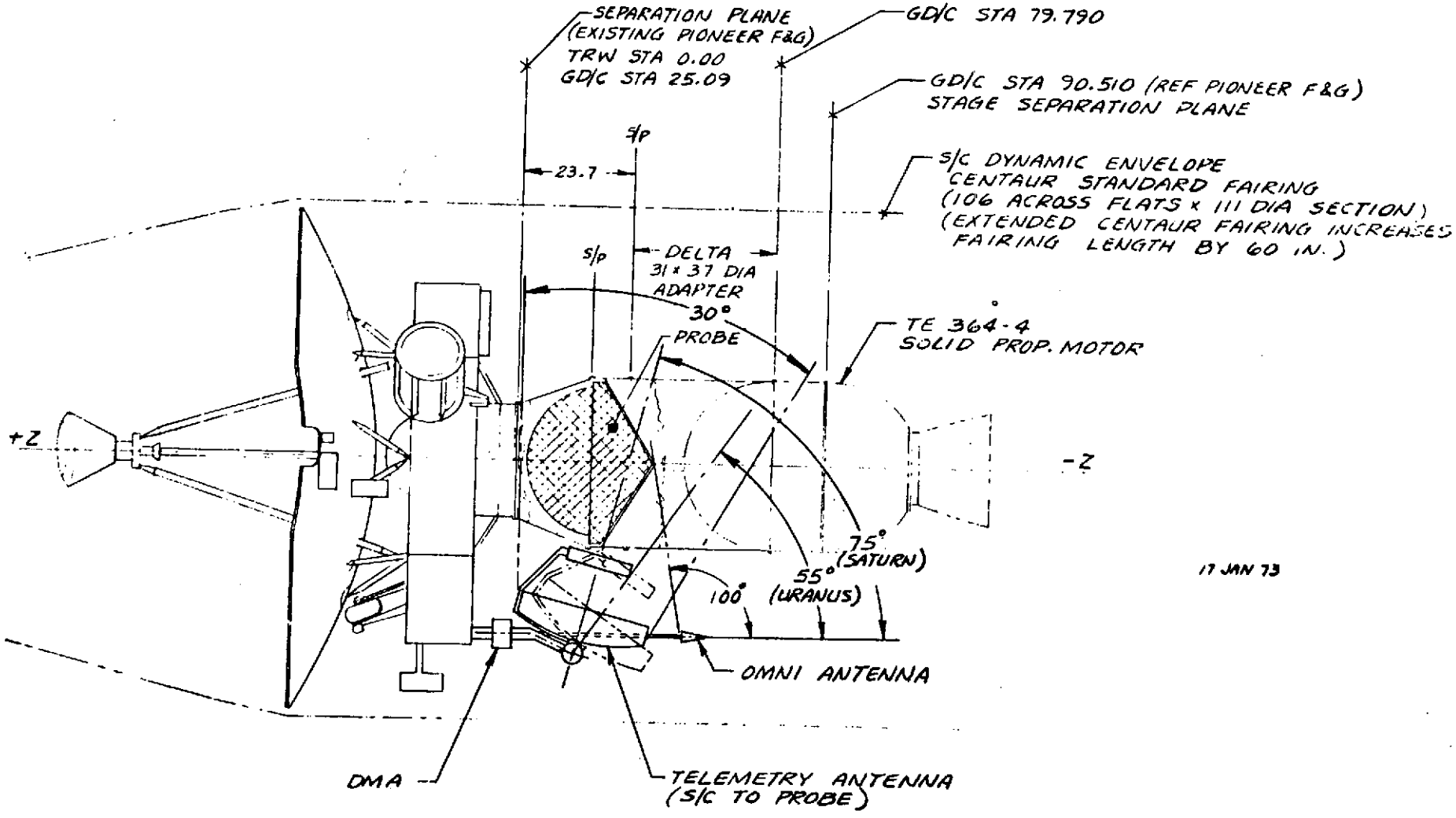

Figure A-21. Two-Position Parabolic Reflector - SUAE Probe Study (AD42-49)

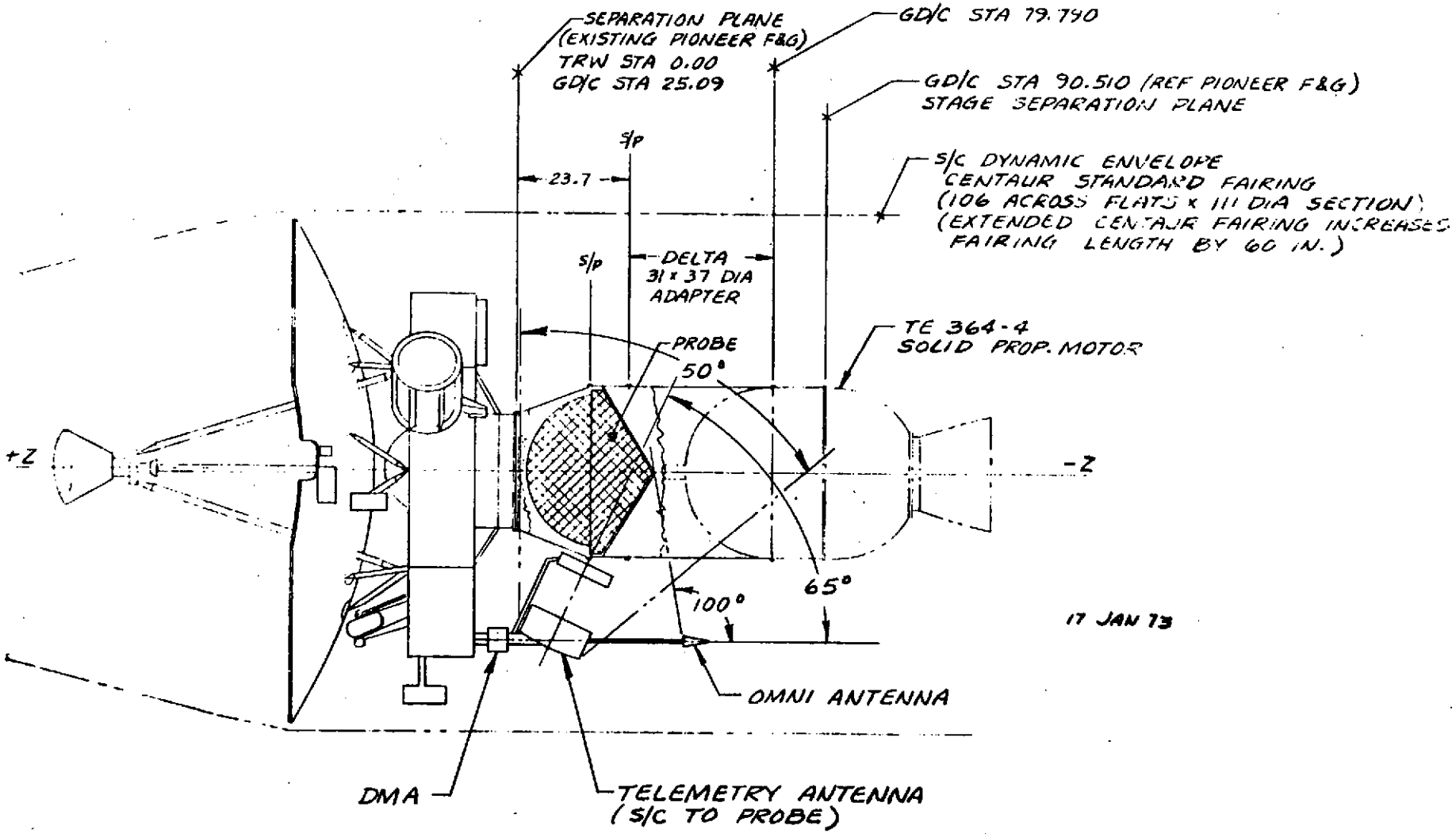

Figure A-22. Fixed-Position Parabolic Reflector - SUAE Probe Study (AD42-50)

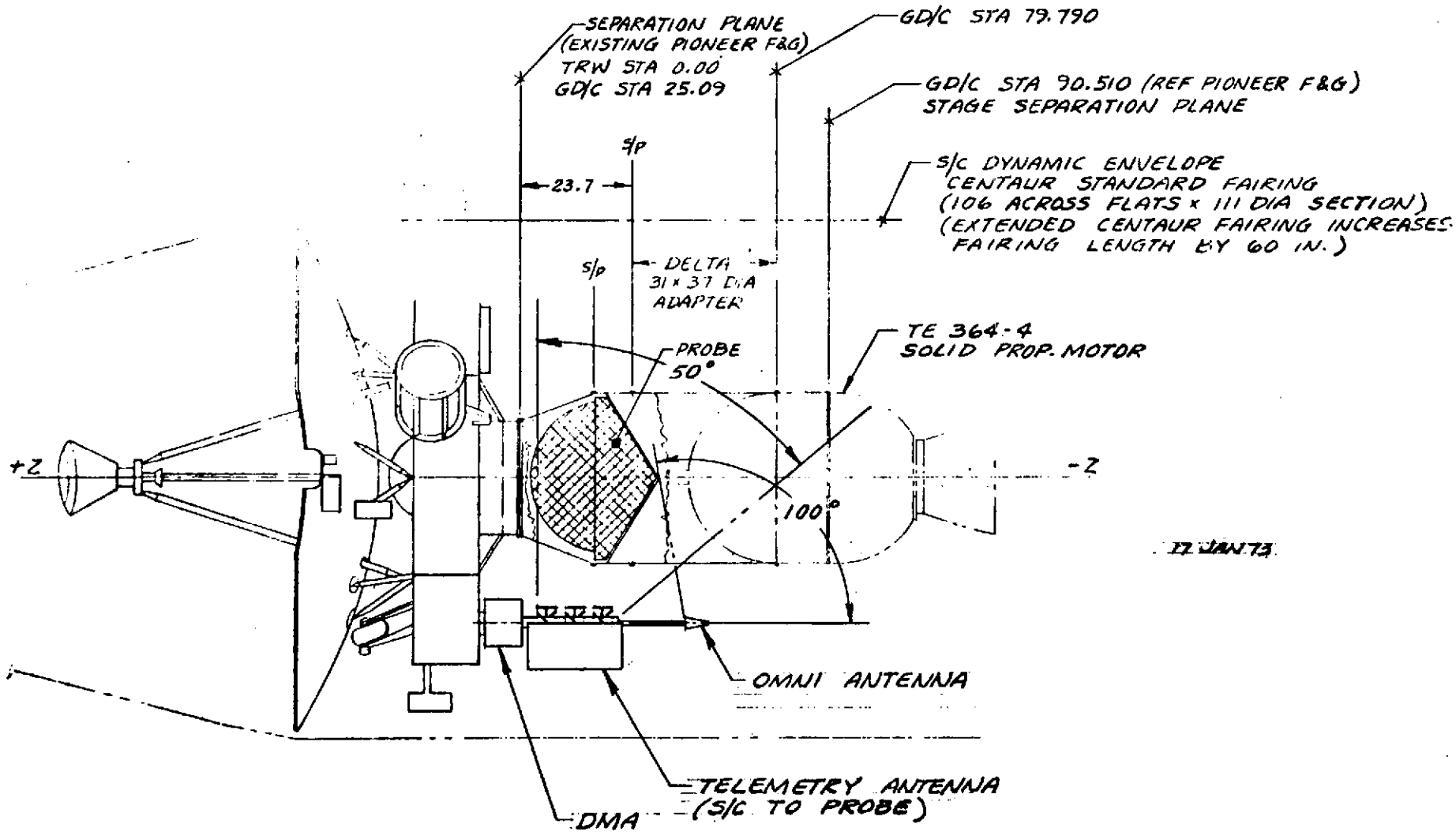

Figure A-23. Cylindrical Reflector Array - SUAE Probe Study (AD42-51)

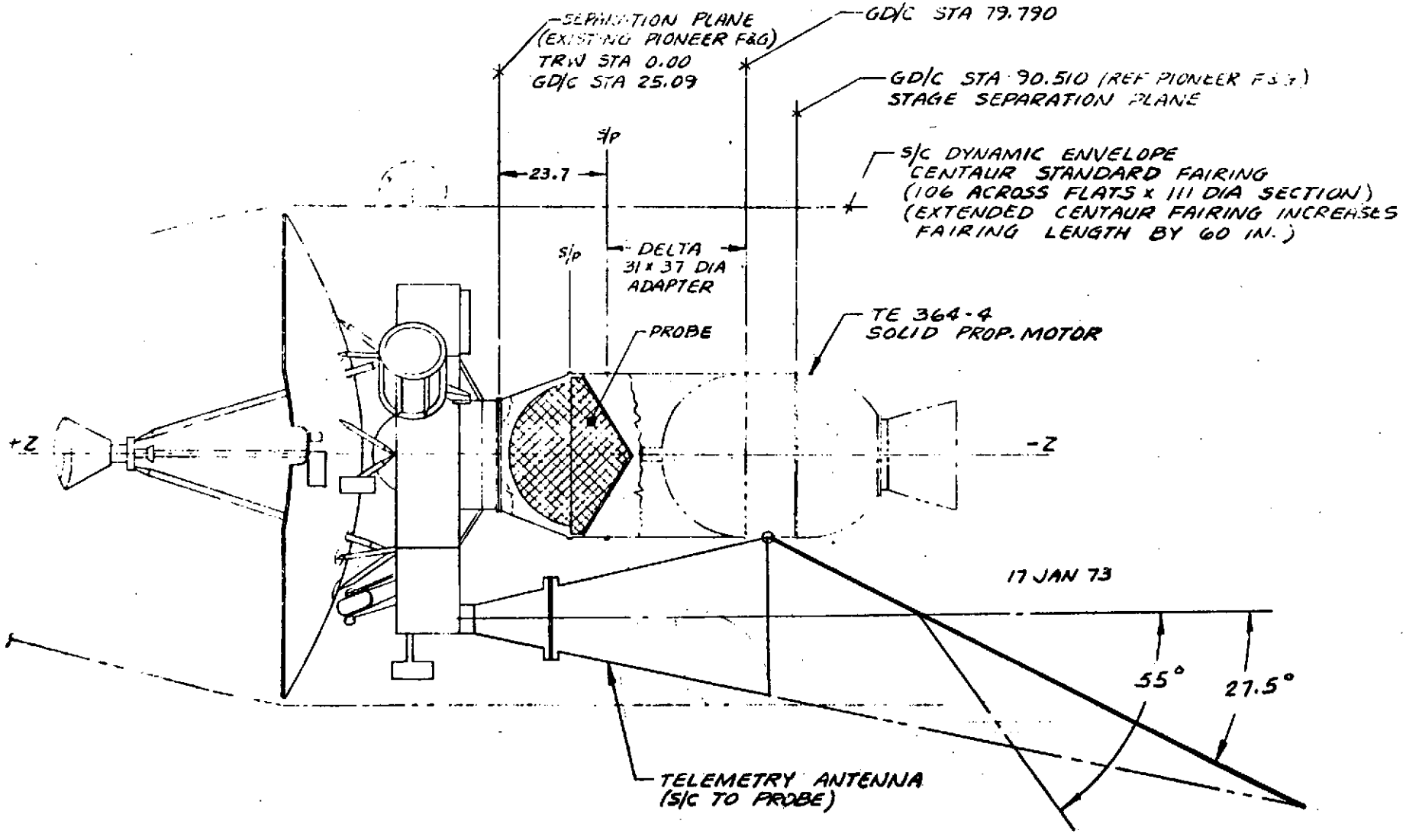

Figure A-24. Periscope Reflector - SUAE Probe Study (AD42-52)

7. DYNAMICS REQUIREMENTS ON DESPUN ANTENNA

The following lists requirements on a Pioneer spacecraft despun antenna and its installation which are derived from dynamics considerations.

7.1 Static Balance

The center of mass of the despun section should lie on the despin axis. If this criterion is not met,

a) the despin drive mechanism will carry a torque which varies sinusoidally at a one-per-revolution rate,

b) this torque will cause variations in the spacecraft spin rate at a one-per-revolution rate, with the per unit peak spin rate change being

$$\left.\frac{\delta \dot{\Theta}_z}{\omega_o}\right|_{o\text{-}pk} = \frac{M_d l r}{M k_r^2},$$

c) assuming the despin mechanization is at a constant relative angular velocity, the despun section will waver in its pointing direction, with a peak angular pointing error of

$$\left.\delta \Phi\right|_{o\text{-}pk} = \frac{M_d l r}{M k_r^2} \quad \text{radians}$$

d) if the z-coordinate of the despun section's c.m. differs from the z-coordinate of the rotating section's c.m., a coning of the rotating spacecraft's angular momentum vector will take place, tilting it an angle of

$$\epsilon = \frac{M_d h l}{M k_r^2} \quad \text{radians}$$

This tilt is always in the plane containing the despin axis and the c.m. of the rotating section. The spacecraft z axis will nutate about the coning momentum vector and its maximum excursion from the nominal angular momentum vector will be 2.46ϵ.

7.2 Dynamic Balance

The despun section should be dynamically balanced about the despin axis. If this criterion is not met, the rotating spacecraft's angular momentum vector will cone as in effect 1 d), with a tilt at an angle of $\epsilon = P/I_{zr}$ radians. (It is assumed that the entire spacecraft is dynamically balanced, with despin drive locked.) Again, the excursion of the spacecraft z axis may be up to 2.46ϵ.

7.3 Equality of Transverse Moments of Inertia

There is no requirement that $I_x = I_y$ for the despun section. I_x and I_y are moments of inertia about principal axes transverse to the despin axis.

Nomenclature

In the above expressions:

P	=	Maximum product of inertia of the despun section with respect to its despin axis and any transverse axis
I_{zr}	=	$M_r k_r^2$ = moment of inertia of the rotating section about an axis through its center of mass and parallel to the spin axis
M_r	=	Mass of rotating section
M_d	=	Mass of despun section
M	=	$M_r + M_d$ = mass of the spacecraft
k_r	=	Spin radius of gyration of rotating section
$\dot{\theta}_z$	=	Actual spin rate (accounting for cyclic variations)
ω_o	=	Nominal or average spin rate
l	=	Despun section's c.m. offset from despin axis
r	=	Distance from rotating section's c.m. to despin axis
h	=	z-coordinate separation of c.m.'s of despun and rotating sections.

8. LOOP-VEE VS. LINDENBLAD ANTENNA

In the choice of an axisymmetric antenna the loop-vee is typical of relatively low-gain, lightweight and simple antennas. The Lindenblad offers somewhat higher gain, but is somewhat heavier and larger, and requires the added complexity of switchable phase shifting networks to set the beam for the Saturn or Uranus mission.

8.1 Antenna Gain

The estimated gain of the two axisymmetric antennas are derived in Table A-6. The gain at the beam edge is 2 dB greater, in the case of the Lindenblad antenna. Part of the superiority comes from the greater directivity; part from the fact that (with the switchable feature) the gain drops off less than 3 dB at the beam edge.

Table A-6. Gain of Axisymmetric Antennas

	LINDENBLAD	LOOP-VEE
3 DB BEAMWIDTH, DEG	40	50
DIRECTIVITY, DBI	5.5	4.8
EFFICIENCY LOSS (80%), DB	1.0	1.0
PEAK GAIN, DBI	4.5	3.8
BEAM-EDGE GAIN	2.8 AT $\pm 15^{\circ}$	0.8 AT $\pm 25^{\circ}$
POLARIZATION LOSS, DB	0.2	0.2
AZIMUTHAL RIPPLE	± 0.5	± 0.5
NET GAIN:		
ON BEAM CENTER	3.8 TO 4.8	3.1 TO 4.1
AT BEAM EDGE	2.1 TO 3.1	0.1 TO 1.1

8.2 Mechanical Considerations

Installation of the loop-vee antenna can be readily accommodated, assuming the probe adapter separated from the bus after probe separation, as was proposed in the midterm briefing. Alternatively, by lengthening the main strut, the loop-vee can be utilized without requiring that the probe adapter be separated; this configuration is presented in Figure A-14. It is shown in detail in Section 6.9 of the body of this report, as the selected configuration.

Eliminating the probe adapter separation system has several beneficial effects. First, there is a significant weight reduction – at least 5 and perhaps as much as 10 pounds. Second, there is the associated reduction in cost. Third, there is the increase in spacecraft reliability. Retaining the probe adapter does not appear to have any disadvantage or penalties, with the use of the loop-vee antenna.

Installation of the Lindenblad antenna can also be accommodated with the adapter removed (see Figure A-15). The antenna is somewhat heavier than the loop-vee due to the four coaxial cables which run up through the mast and due to the longer mast length required. The additional length and mass of the antenna in turn call for additional bracing of the antenna (not shown). Note that this antenna does protrude well beyond the third-stage motor separation plane. This is undesirable since it creates the possibility that the expended and separated motor case could strike the antenna and damage or destroy it and hence abort the spacecraft mission. Preliminary analysis indicates that a minimum 18-degree clearance angle should be maintained to insure a clean motor separation. The installation shown satisfies this criterion.

But attempting to install the Lindenblad antenna while retaining the probe adapter is awkward. Two approaches were considered. For the antenna to be fixed, it projects so far toward the Centaur that it must be moved radially outward to avoid conflicting with the unfolding petals of the spin table at third stage separation from the second stage. Even then, it is not clear that the infringement on space for third stage access is tolerable.

Another possibility is a Lindenblad antenna assembly which is deployable from a stowed position after launch. However, here one is accepting an antenna deployment mechanization to avoid a probe adapter separation mechanization. Furthermore, the performance of the S-band low-gain antenna during the powered flight phase and immediately after is prejudiced.

Additionally, the Lindenblad antenna requires phase switching to change the beam direction from the Saturn to the Uranus geometry. This takes a mechanical switch comprising two poles and two throws;

thus a new mechanical component is introduced with a consequent slight reduction in overall reliability.

8.3 Recommendation

Feeling that the comparative simplicity and compactness of the loop-vee antenna is a greater advantage than the greater gain of the Lindenblad antenna, TRW recommended that the loop-vee antenna be used and the probe adapter not be jettisoned after probe separation. The technical monitor concurred in this recommendation for the baseline configuration.

APPENDIX B

BUS-PROBE INTERFACE SPECIFICATION

FOREWORD

The Bus-Probe Interface Specification which follows is submitted as a "pro-forma" document rather than a completed/coordinated specification. The contents reflect those interface areas which did receive some degree of attention during the study as well as some areas which were ignored. Where definitive agreements were reached, these agreements have been included.

This specification reflects many of the governing specifications which were part of the Pioneer F/G program. These referenced documents should be reviewed and updated for the SUAE mission.

This interface specification is not complete. However, it should form the basis for the development of a document which can be used in future efforts related to the SUAE mission.

APPENDIX B

BUS-PROBE INTERFACE SPECIFICATION

1. SCOPE

This specification establishes the interface constraints and design requirements which the Saturn Uranus Atmospheric Entry Probe (hereafter referred to as "the probe") must meet to insure compatibility with the modified Pioneer F/G vehicle (hereafter referred to as "the bus"). The combination of the probe and the bus is referred to as the Saturn Uranus flight vehicle.

2. APPLICABLE DOCUMENTS

The following documents of the latest issue in effect form a part of this specification to the extent specified herein.

	SPECIFICATIONS
SR 4-1	General Specification for Pioneer F/G Equipment
SR 1-8	EMI/RFI Requirements
EV 2-24	Unit Environmental Test Specification
D 00212	System Safety Design Criteria for Pioneer F/G Project
EQ 13-34A	Performance/Design, Qualification and Acceptance Requirements for a Single Bridge-wire Cartridge Pioneer F/G
EV 1-33	Environmental Qualification and Acceptance Test Requirements for the Pioneer F/G Spacecraft
PC-221	Pioneer F Spacecraft/Launch Vehicle Interface Specification
PC-223	Spacecraft/RTG Interface Specification
	DRAWINGS
ICD-(B-6)*	Bus-Probe Interface Control Drawing

3. REQUIREMENTS

3.1 GENERAL

This section includes those general requirements which are applicable to all spacecraft elements.

---

*B-6 is also used as Figure 5-3 in Section 5.2.9

3.1.1 Margin of Safety

The design margin of safety, as defined as:

$$\frac{\text{allowable stress}}{\text{applied stress}} - 1$$

shall be 1.2 or greater for all load carrying structure based on the powered flight environment defined below in Section 3.1.6.4. Factors of safety for pressure vessels must conform to the applicable Range Safety Standards.

3.1.2 Parts and Materials

Parts, materials, and processes which have been qualified for spaceflight shall be used for all spacecraft components. Use of commercial grade hardware must be specifically approved prior to use and must not compromise other spacecraft requirements (reliability, life, magnetic cleanliness, outgassing contamination, etc.).

3.1.3 Failure Modes

The probe shall be designed so that no single failure shall compromise the primary mission objective. Where redundancy is used to meet this criteria, and where such redundancy is not automatic (i.e., requires a ground command), appropriate telemetry signals will be required to establish operating status.

3.1.4 Ground Operations

The sequence and flow of the flight probe and the flight spacecraft is anticipated to be as follows:

a) Probe completes acceptance test
b) Probe shipped to bus contractor
c) Probe and bus integrated and acceptance tested as the spacecraft
d) Spacecraft shipped to launch site; test for shipping damage
e) Spacecraft mated to launch vehicle; tested prior to launch while on stand.

3.1.5 Launch Vehicle

The flight vehicle will be launched by a vehicle consisting of a Titan TIIIE, Centaur, TE-364-4 combination further defined in the Program Specification.

3.1.6 Environments

3.1.6.1 Pre-launch

The pre-launch (on stand) environment will be controlled as follows:

Cleanliness	As provided by a filter rated at not greater than 0.3 microns with 99.7% efficiency
Relative Humidity	55% maximum
Temperature	$60^{\circ} \pm 5^{\circ}F.$

3.1.6.2 Qualification

Environmental levels and test procedures for qualification of the probe are contained in Specification EV2-24. Spacecraft levels are noted in Specification EV1-33.

3.1.6.3 Acceptance

Environmental levels and test procedures for acceptance testing the probe are contained in Specification EV2-24. Spacecraft acceptance test levels are defined in EV1-33.

3.1.6.4 Powered Flight

The powered flight environment is defined in PC-221 and is summarized below:

Acceleration	+22.5 g longitudinal ± 2.6 g lateral
Vibration	.02 g^2/Hz 150 - 2000 Hz $\pm$ 1.5 G 8.5 - 200 Hz
Acoustic	142 dB overall
Spin Rate	80 RPM maximum
Pressure	0 PSID (Shroud is fully vented)
Fairing Temperature	$275^{\circ}F$ - $390^{\circ}F$

3.1.6.5 Cruise Environment

During the extended cruise period from earth to the target planet, the flight vehicle will be subjected to the natural environment as defined in PC-210.02

In addition, the probe will be exposed to the radiation environment generated by the Radioisotope Thermoelectric Generators (RTGs) as defined in PC-223.

3.1.6.6 Shipping

The spacecraft shall be transported to the range by aircraft in a sealed container and shall be controlled to the following limits:

Temperature	TBD
Pressure	TBD
Humidity	TBD

3.1.7 Ground Support Equipment

The probe contractor will provide all necessary mechanical ground support equipment for the probe prior to mating with the bus as well as to accommodate probe removal from the bus.

3.1.8 Access

Access to the probe following mating with the bus shall be limited as shown on ICD (B-6). This access must accommodate mating/demating, thermal closeout of the probe, and all ground testing of the probe after installation on the bus.

3.1.9 Safety

The probe shall be designed to minimize hazards to personnel. All hazards to the unit shall be identified in accordance with the System Safety Design Criteria for Pioneer F/G Project D00212.

3.1.10 Coordinate Systems

3.1.10.1 Body Coordinates

Spacecraft body coordinate axes are as defined in Figure B-1. The probe shall have a corresponding set of coordinate axes as shown in Figure B-2. The alignment of these axes shall be accomplished as shown on ICD-(B-6).

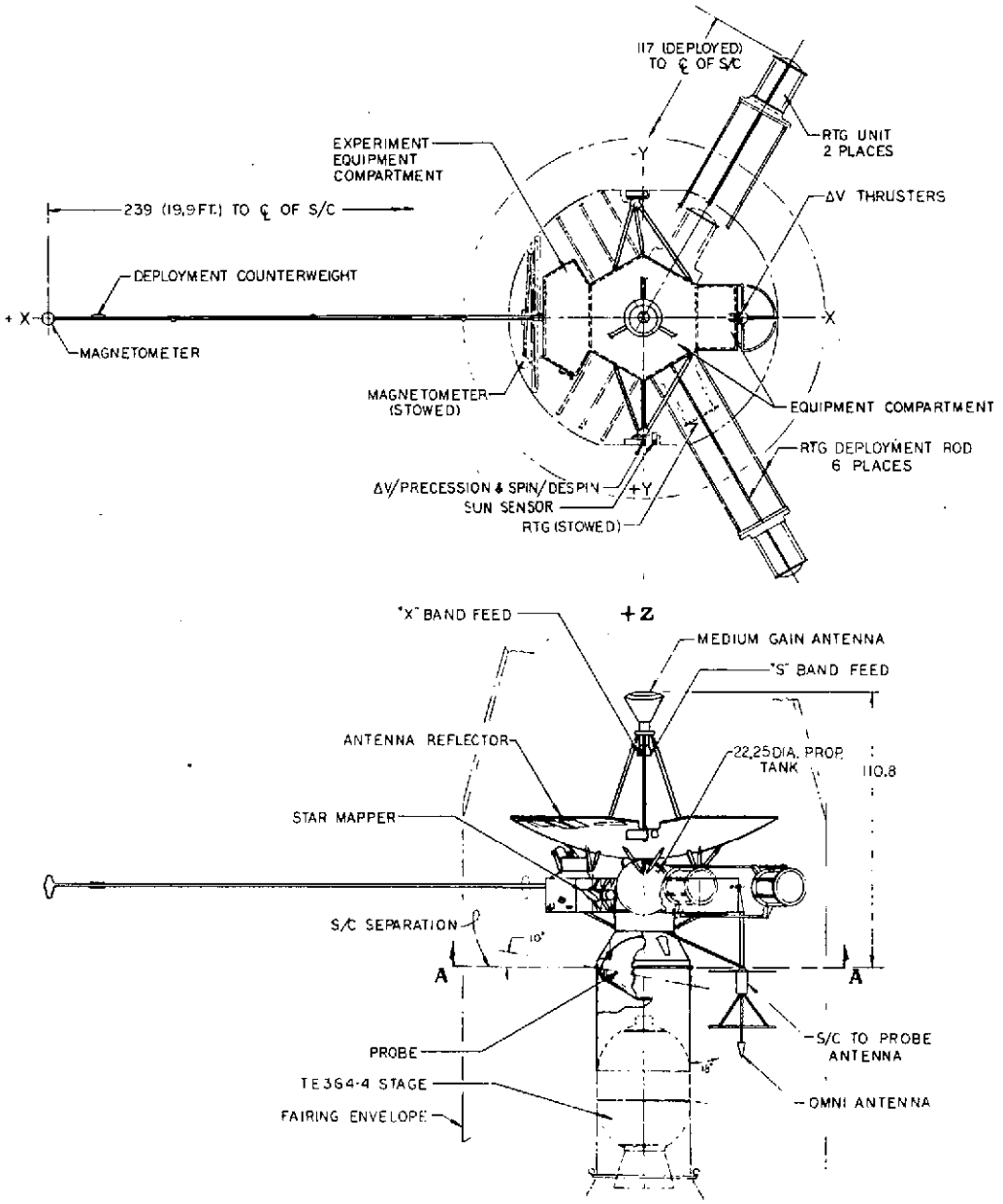

Figure B-1. Spacecraft Body Coordinate Axes

TO BE SUPPLIED

Figure B-2. Probe Coordinate Axes

3.1.10.2 Navigation Coordinates

The instantaneous coordinates of the spacecraft will be established by means of a ranging transponder plus appropriate star/planet sensor(s). These measurements in turn provide the angles shown in Figure B-3.

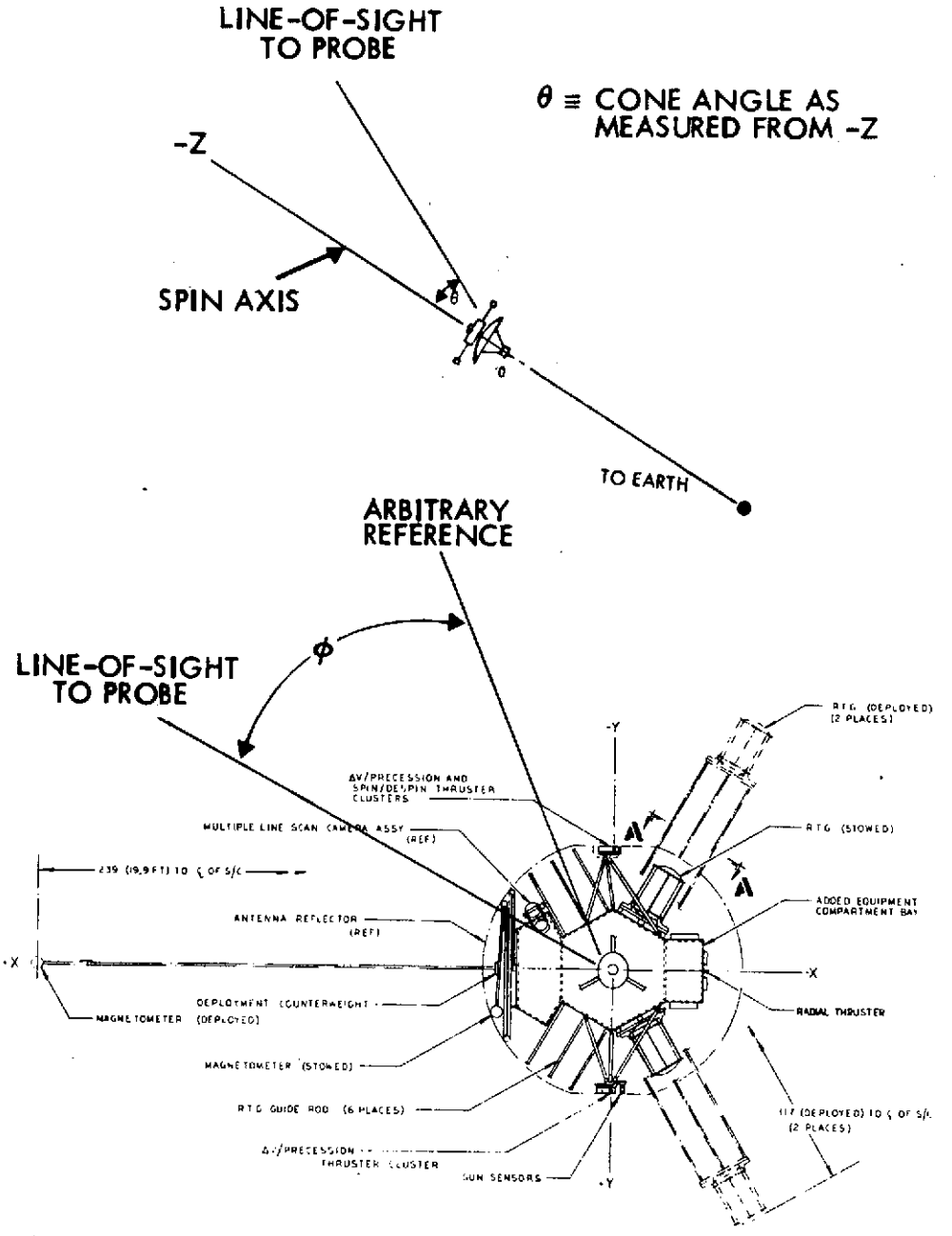

Figure B-3. Spacecraft-Probe Look Angles

3.2 MISSION REQUIREMENTS

This section defines those general mission requirements which directly influence the bus-probe interface.

3.2.1 In-flight Operations

Subject to the limitations in power, weight, volume, thermal control, and other parameters defined elsewhere in this specification, the in-flight operations will consist of six distinct phases as follows:

Phase 1	Powered Flight
Phase 2	Cruise
Phase 3	Pre-Separation
Phase 4	Separation/Deflection
Phase 5	Approach Trajectory
Phase 6	Planetary Entry

Specific operations of interest during these phases are identified below.

3.2.1.1 Powered Flight

No operations involving the bus-probe interface are anticipated.

3.2.1.2 Cruise

During this phase of flight, the spacecraft will be spinning slowly (5 RPM) and earth pointing. The cone angle to the sun will vary early in the mission as shown in Figure B-4. The spacecraft may be required to make one or more mid-course corrections during the cruise phases. Upon ground command, the probe may be energized and exercised to establish state of health.

3.2.1.3 Pre-Separation

Prior to separation, the spacecraft position, attitude, and velocity relative to the target planet will be determined. Under ground command, the bus will provide power to the probe to charge the probe batteries. Other signals as necessary to prepare the probe for separation will be provided via the bus command system.

3.2.1.4 Separation/Deflection

At a pre-determined time, the probe will be physically separated from the bus with the following constraints:

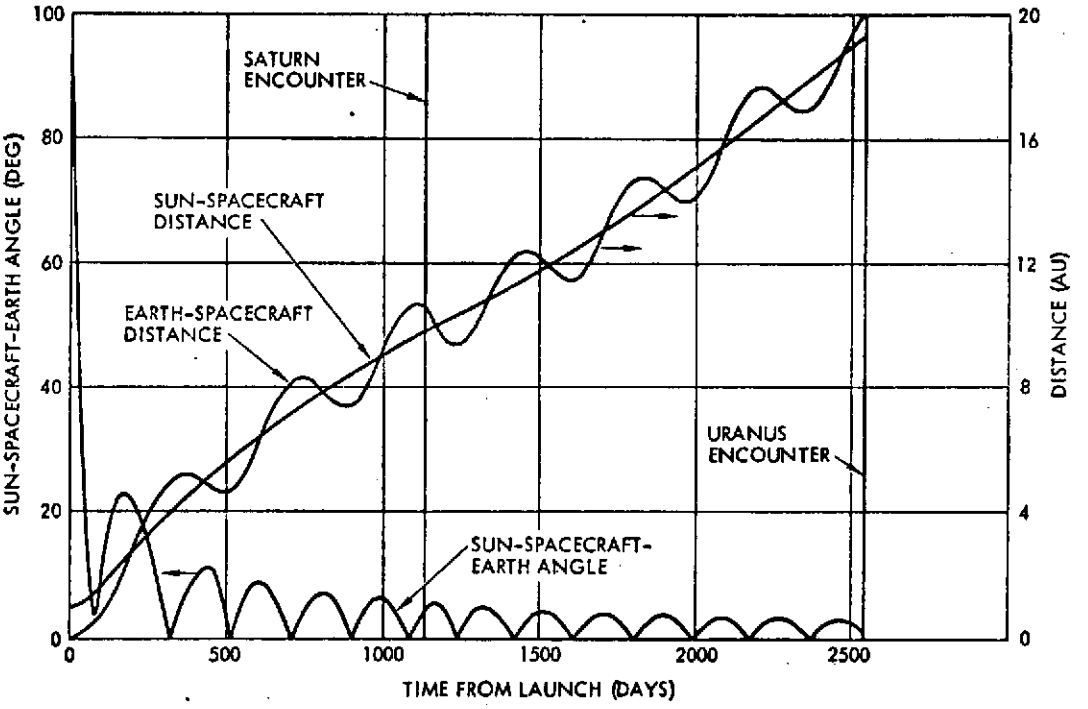

Figure B-4. Sun-Spacecraft-Earth Angle Versus Time

Tipoff Angle	less than 2.0 deg
Tipoff Rate	less than 1.6 deg/sec
Separation Velocity	0.1 ± 0.01 meters/sec

Under ground command, the bus will provide power to the probe to charge the probe batteries. Other signals as necessary to prepare the probe for separation will be provided via the bus command system.

3.2.1.5 Approach Trajectory

No bus-to-probe interfaces exist during this phase of flight.

3.2.1.6 Planetary Entry

During the probe descent through the target planet atmosphere and for 70 minutes after entry (to at least 10 bars), the bus shall receive data from the probe and relay such data to earth in real time as well as store su data for subsequent retransmission to earth.

3.2.2 Launch Plan

Three (3) probe-dedicated missions are considered for this program as follows:

Flight 1	Launched in 1979; dedicated to Saturn
Flight 2	Launched in 1980; backup to Flight 1; may be retargeted to Uranus
Flight 3	Launched in 1980; dedicated to Uranus via Saturn.

3.2.3 Life

The anticipated trip time (mission life) for the two target planets in accordance with the above plan is as follows:

Earth-Saturn (1979)	3.4 years
Earth-Saturn (1980)	3.1 years
Earth-Uranus (1980)	6.9 years

3.3 PHYSICAL INTERFACES

3.3.1 Envelope

The physical dimensions of the probe, excluding any connectors or umbilicals, shall not exceed the envelope shown on ICD-(B-6) .

3.3.2 Mass Properties

The total weight of the probe in its flight configuration shall not exceed 250 pounds. The center of gravity of the probe shall be located within the tolerances shown on ICD-(B-6). The moments of inertia of the probe shall be measured and maintained within 200 lbm in.^{2}. The products of inertia of the probe shall be limited to

P_{xy}	$\leq$200 lbm in.^{2}
P_{xz}, P_{yz}	$\leq$50 lbm in.^{2}

3.3.3 Mounting

The probe shall be attached to the bus by means of three (3) ball-lock pin devices spaced 120 degrees apart as shown on ICD-(B-6). The probe shall provide whatever additional mountings are required to allow

mating with the bus. The three mounting surfaces (or separate jumper straps) must be designed to insure a good thermal as well as a good electrical bond between the probe and the bus. The ball-lock devices will be preloaded to TBD pounds.

3.3.4 Separation Mechanism

Separation of the probe from the bus shall be accomplished by means of three matched separation springs mounted as shown on ICD-(B-6). Total spring travel shall be 0.5 inch. The (compressed) spring force from any one spring shall not exceed 6 pounds.

3.3.4 Umbilical Connector

The probe shall be connected to the bus by means of a single umbilical connector located as shown on ICD-(B-6). Prior to probe separation, the bus shall insure separation of the umbilical by means of a guillotine device located as shown on ICD-(B-6).

3.4 THERMAL INTERFACES

The bus shall maintain the probe adapter temperature within acceptable thermal limits during the cruise phase of powered flight, but not including transient conditions which may occur during pre-launch, powered flights, or pre-separation phases.

3.4.1 Probe Thermal Characteristics

The probe shall have the following thermal characteristics:

Internal power (continuous)	$\leq$ 4 watts
Checkout power (TBD hrs max.)	$\leq$ TBD watts
External covering (continuous except for attachments) with ϵ = TBD α = TBD	TBD layers of MLI
Probe bus conductance (Total)	$\geq$ 0.2 watts/^{o}F
Probe thermal capacity TBD	$\frac{^{o}F}{joule}$

3.4.2 Side Sun

During those periods early in the flight when the sun angle may be between ~60 degrees and 90 degrees from the spin axis, the bus shall

maintain the probe adapter temperature below 70 degrees F. This period of side sun conditions can be avoided by moving the spin axis off the earth line, but will not persist beyond the first 50 days of flight.

3.4.3 Nominal Sun Illumination

Once the sun has moved to within 28 degrees of the spin axis, the probe adapter is no longer illuminated by the sun. Under these conditions, the bus will maintain the probe adapter temperature within the range of -20 degrees F to +20 degrees F, excepting those checkout periods or battery charging periods when bus power is being consumed by the probe.

3.4.4 Probe Adapter

The probe adapter is coupled conductively as well as radiatively coupled to the probe as shown on ICD-(B-6). The adapter consists of four principal thermal elements--a conductive coupling to the primary probe structure, multilayer insulation, a radiator area, and a heater element.

3.5 ELECTRICAL INTERFACES

3.5.1 Electrical Power

Electrical power furnished by the bus to the probe shall be at 28 V DC $\pm$2 percent. The minimum amount of such power available to the probe shall be as follows:

	Ground Power Supply
Prelaunch	
Before RTGs installed	20 W
After RTGs installed	20 W
Powered flight	
Cruise	
Continuous	2 W
Checkout and test periods less than two hours	10 W
Preceding probe separation with spacecraft science instruments off	
Continuous	30 W

3.5.1.1 Inrush Current

The duration of instantaneous load current of each instrument is a function of fuse size and instrument load characteristics. Upon application of the 28 V dc primary power to the instrument's primary power circuit, and upon application of the power control state signal to the instrument's secondary converter control circuit, the instrument's load current surge shall not exceed the following limit envelope:

a) Above 500 mA for total elapsed time of 10 microseconds

b) Up to 500 mA for up to 50 milliseconds, total elapsed time

c) Up to 200 mA for up to 200 milliseconds, total elapsed time

d) Up to 120 percent of nominal steady state (average) load current for the balance of the first second

e) Nominal load current thereafter.

3.5.2 Probe-Bus Telemetry

All continuous telemetry signals from the probe to the bus shall be hardlined via the separable connector (see ICD-(B-6). Hardlined signals from the probe shall be analog voltages with a maximum level of 3.0 volts dc from a source impedance no greater than 5000 ohms. The bus can provide up to TBD command lines are available. All commands telemetry capacity at the lowest usable data rate (TBD bits per second at Uranus).

3.5.3 Commands

The bus will provide command signals to the probe via hardline (see ICD-(B-6). Up to TBD command lines are available. All commands (excepting pyrotechnic firing) will be function commands as defined by Figure B-5. Pyrotechnic devices must conform to Specification EQ13-34. The bus will provide up to TBD pyrotechnic firing signals from a capacitor circuit.

3.5.4 Electromagnetic Compatibility

The probe shall conform to the EMC requirements as defined in Specification SR 1-8 except as noted below:

To be determined.

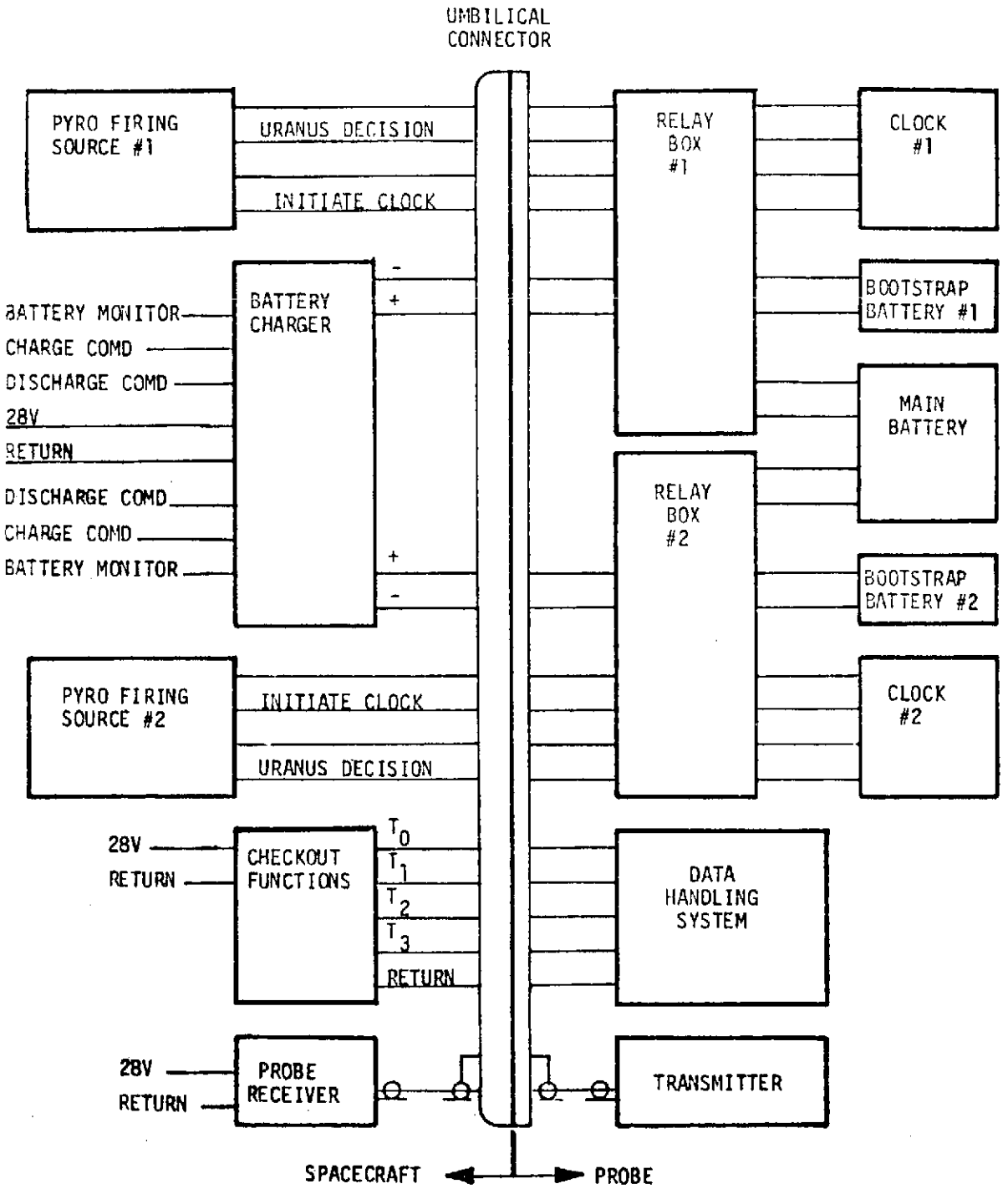

Figure B-5. Umbilical Interface.

3.5.5 Probe-Bus RF Link

The bus shall act as a relay between the probe and earth during the probe's travel through the planetary atmosphere. The bus shall provide a receiving antenna with a minimum of TBD dB gain based on a 400 MHz RHCP received signal. This gain will be provided for all clock angles when the cone angle of the source is between TBD and TBD degrees. The probe shall provide the output from the receiving antenna via a 50 ohm coax line to a *receiver; the minimum gain noted above includes losses in this coaxial line.

3.5.5.1 Test Signal

To be determined

3.5.6 Probe Data

Probe data from a *data synchronizer will be received by the bus as a continuous digital bit stream with the following characteristics:

True level	TBD ± volts dc
False level	TBD ± volts dc
Bit rate	TBD ± bits/second
Message duration	TBD seconds maximum

The bus will buffer these data (as required) and will relay data to earth via the following methods:

a) Direct (real-time) transmission, or

b) Delayed transmission from a Data Storage Unit (DSU), or

c) Simultaneous transmission of direct and stored data.

* These units to be carried on the bus but designed by the probe contractor.

3.5.7 Battery Charging

The bus shall provide power to the probe for periodic charging and conditioning of redundant NiCad batteries. The charger will have the following characteristics:

- V_{in}: 28 VDC $\pm$2 percent
- V_o: Limited to 8.0 VDC $\pm$1 percent at charger terminals
- I_o: Limited to 0.2A$\pm$10 percent
- Discharge: By command through a 22 ohm resistor
- Vd: Discharge terminated at 4.5 VDC
- Commands: Charger on
  Charger/discharger off
  Discharger on
- Telemetry: Charger output voltage

Charge time (approximately 14 hours) will be determined by ground command only and no state-of-charge sensing will be required.

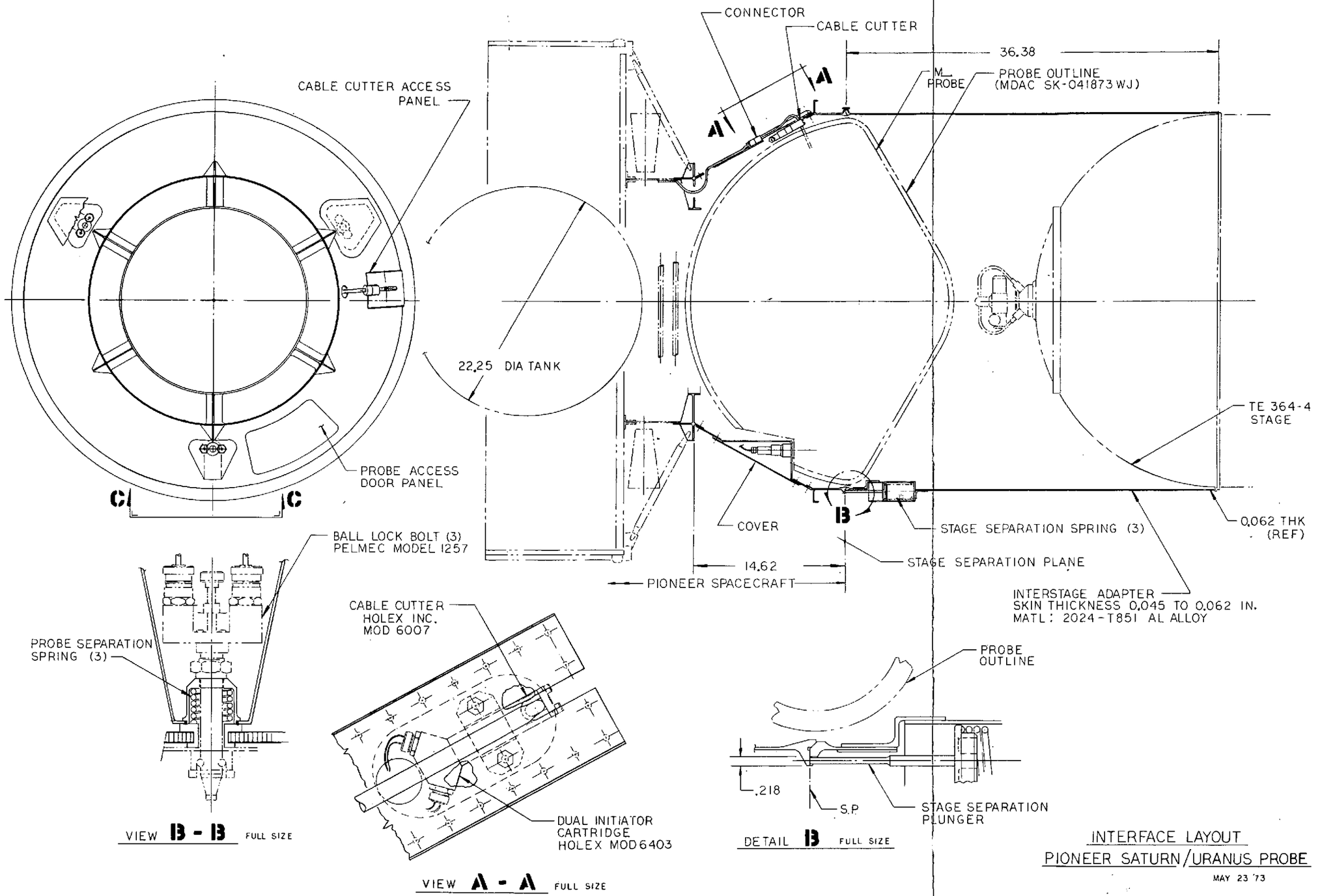

Figure B-6. Interface Layout Pioneer Saturn-Uranus Probe

APPENDIX C

SUPPLEMENTARY MISSION ANALYSIS DATA

Results of transfer trajectory and encounter trajectory computations for the nominal 1979 Earth-Saturn and 1980 Earth-Saturn-Uranus missions are included in this Appendix. These data are supplementary to the material presented in Section 3. Departure and arrival conditions of these trajectories are summarized in Table C-1.

Figures C-1 through C-6 show the heliocentric characteristics of the 1979 Earth-Saturn mission, Figures C-7 through C-12 those of the 1980 Earth-Saturn-Uranus mission.

Figures C-13 through C-28 show the encounter characteristics at Saturn and Uranus, including the bus deflection maneuver components along the earthline and perpendicular to it.

Table C-1. Nominal Trajectory Data (In Planetocentric Equatorial Coordinates)[1]

	1979 Mission		1980 Mission				
	Depart Earth 11-22-79	Arrive Saturn 4-15-83	Depart Earth 11-25-80	Arrive Saturn 1-4-84		Depart	Arrive Uranus 11-9-87
V_∞ (km/sec)	11.62	10.55	11.97	10.52			13.79
RA of V_∞	149.8	180.3	171.3	193.2		281.8	25.0
Declination of V_∞	32.7	-2.3	26.94	8.6		-29.1	-67.8
RA of planet's axis[2]		38.4		38.4			76.8
Declination of planet's axis[2]		83.3		83.3			14.9
Aim angle[3]		-18.25		-28.7			-64.2
Probe entry angle		-30.0					-40.0
Bus periapsis radius		$2.25R_S$		$2.73R_S$			$4.0R_U$

All quantities (except V_∞) in degrees).

NOTES:

1) These coordinates (introduced by JPL) are analogous to celestial coordinates at earth, making use of a redefined planetary "vernal equinox" as reference.

2) RA and declination of planet's rotation axis are given in conventional, earth celestial coordinates.

3) Aim angle is orientation of aim point vector $\bar{B}$ in R, T plane, measured clockwise from T-axis.

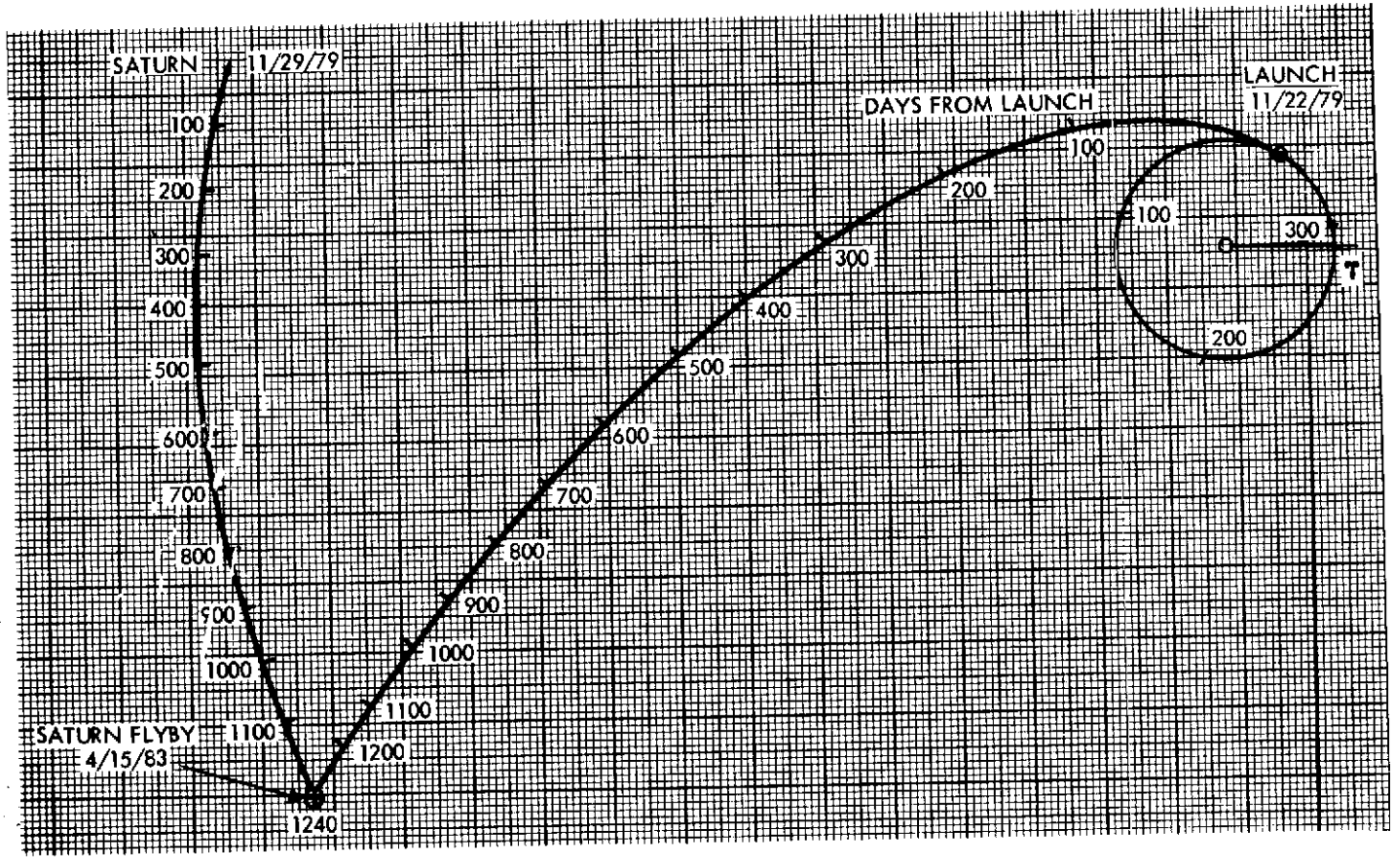

Figure C-1. Nominal 1979 Earth-Saturn Trajectory

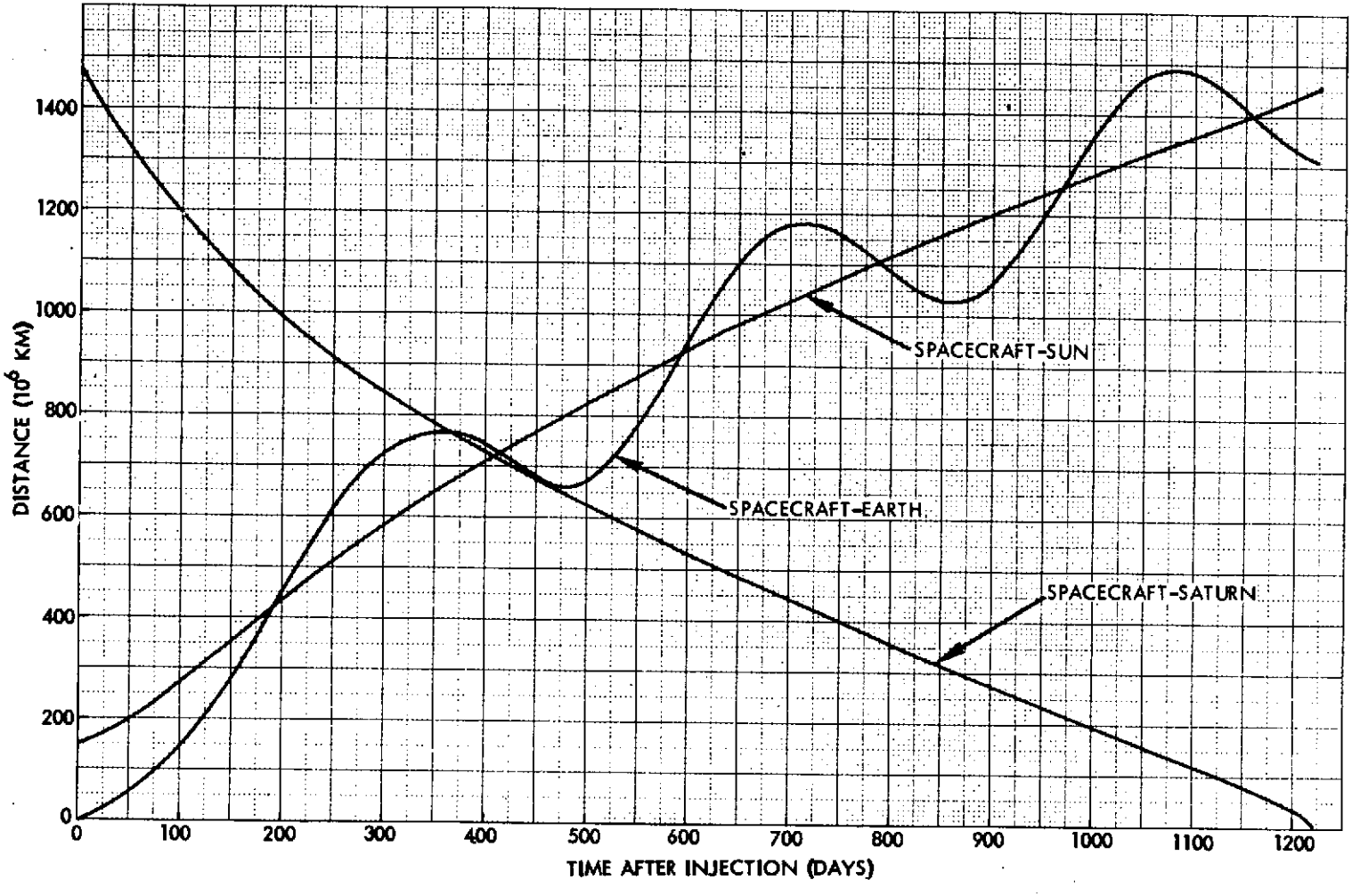

Figure C-2. Spacecraft-Earth, Spacecraft-Sun and Spacecraft-Saturn Distances in Nominal 1979 Earth-Saturn Mission

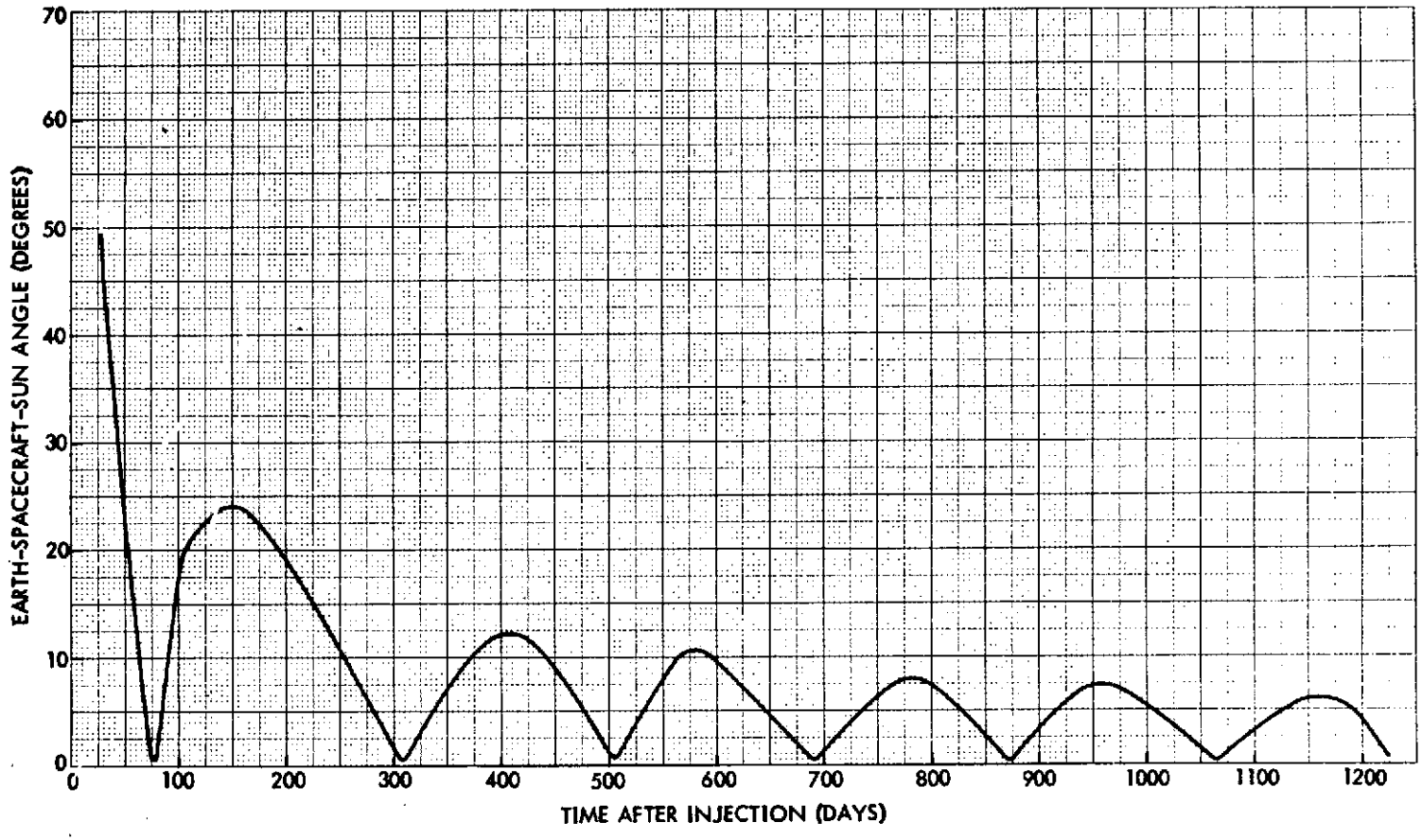

Figure C-3. Earth-Spacecraft-Sun Angle in Nominal 1979 Earth-Saturn Mission

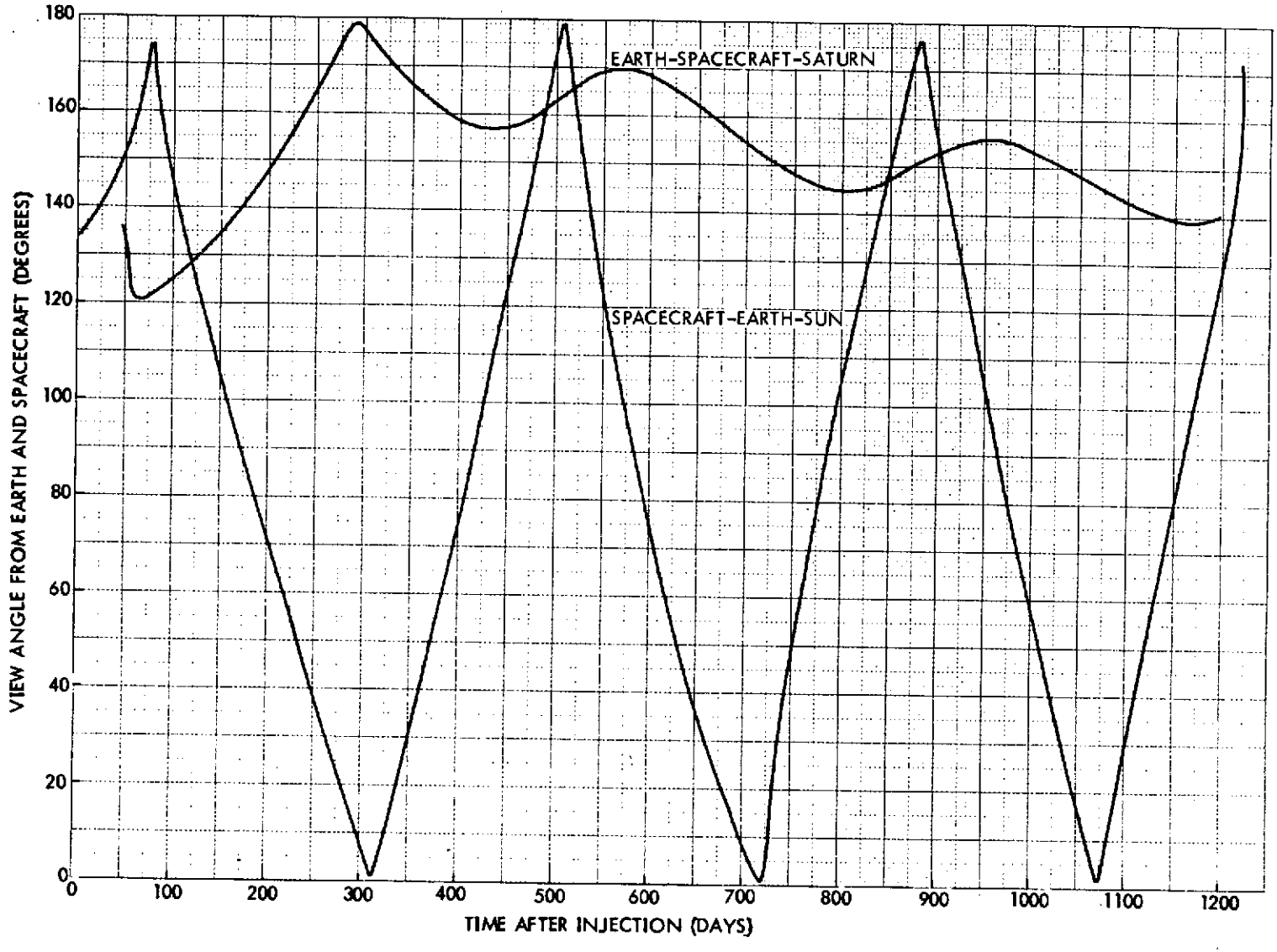

Figure C-4. Spacecraft-Earth-Sun and Earth-Spacecraft-Saturn Angles in Nominal 1979 Earth-Saturn Mission

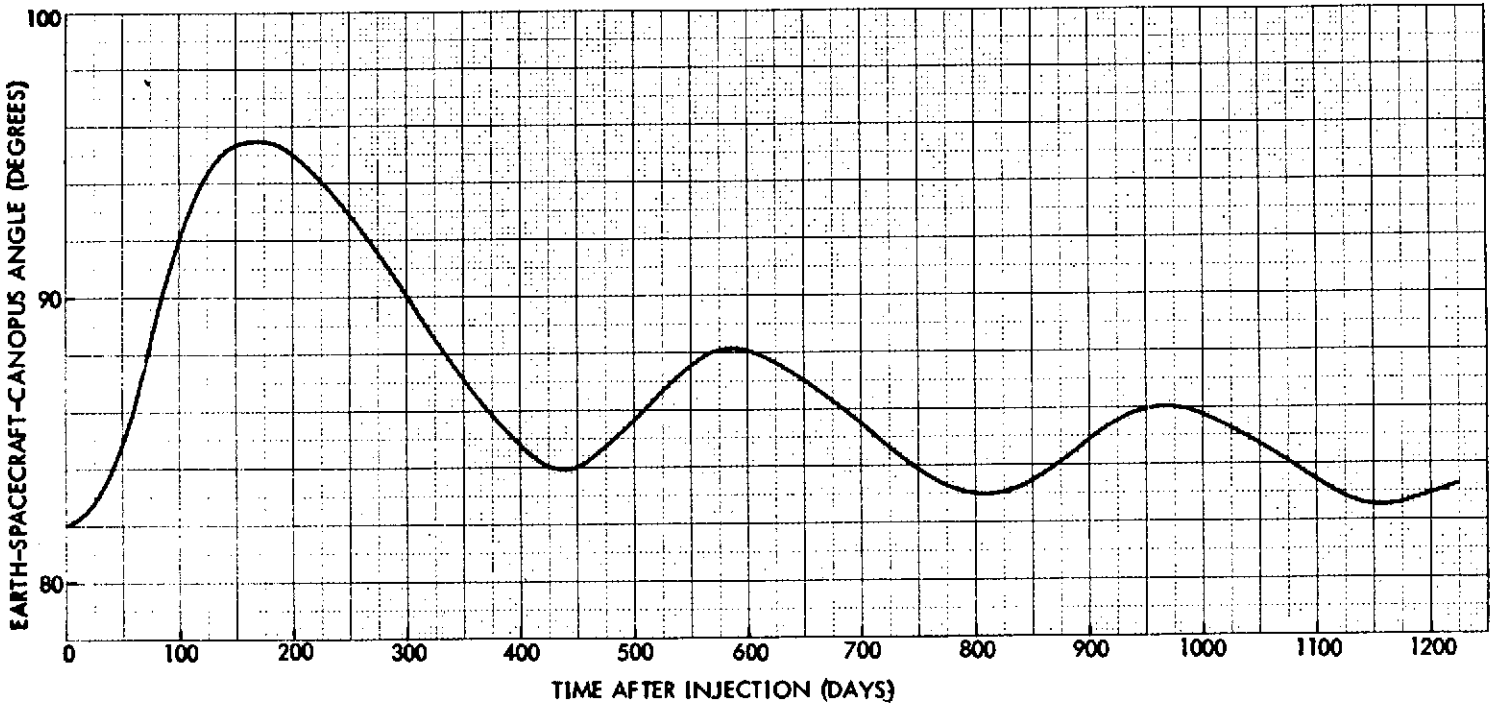

Figure C-5. Earth-Spacecraft-Canopus Angle in Nominal 1979 Earth-Saturn Mission

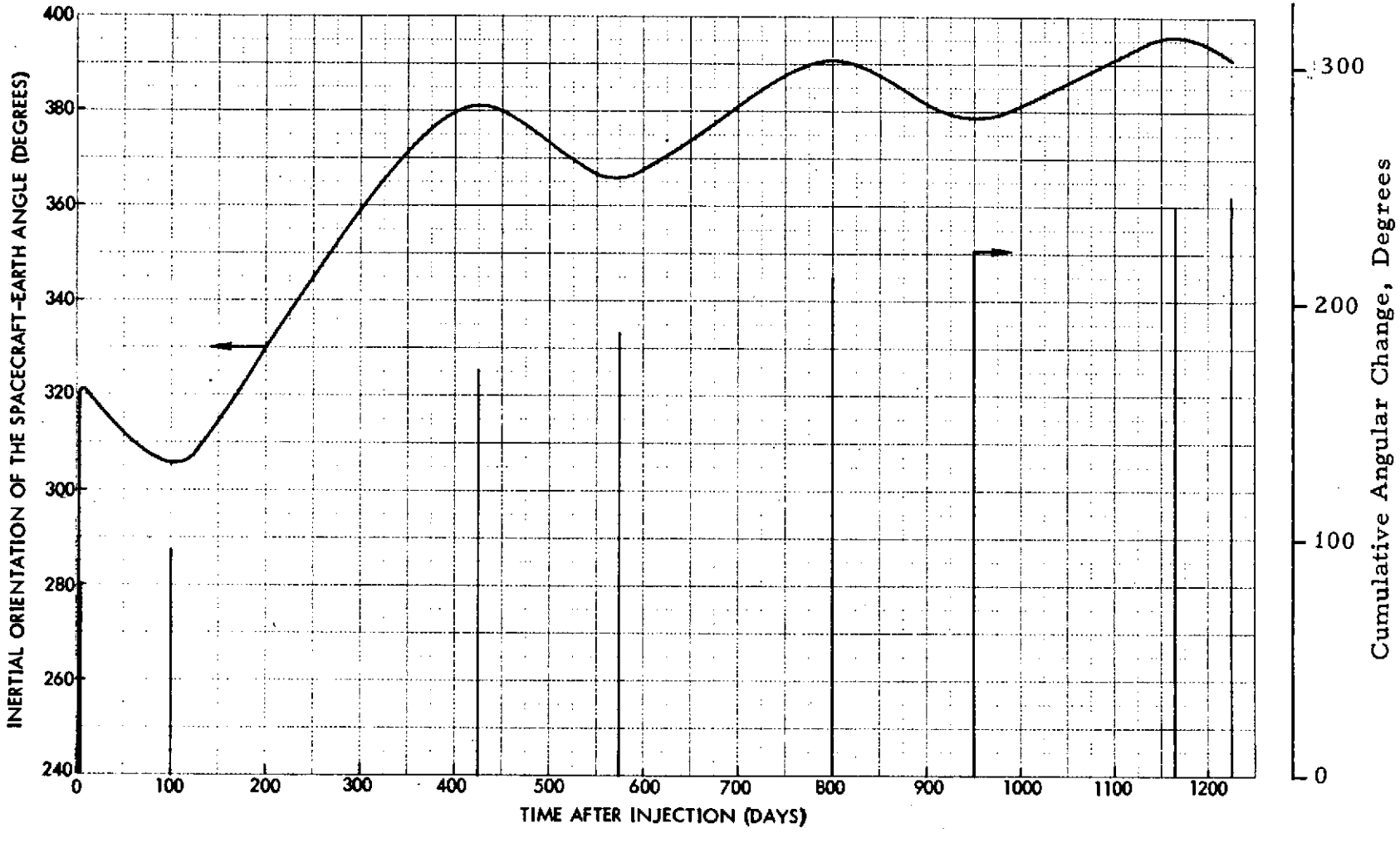

Figure C-6. Inertial Orientation and Cumulative Angular Change of Spacecraft-Earth Angle in Nominal 1979 Earth-Saturn Mission

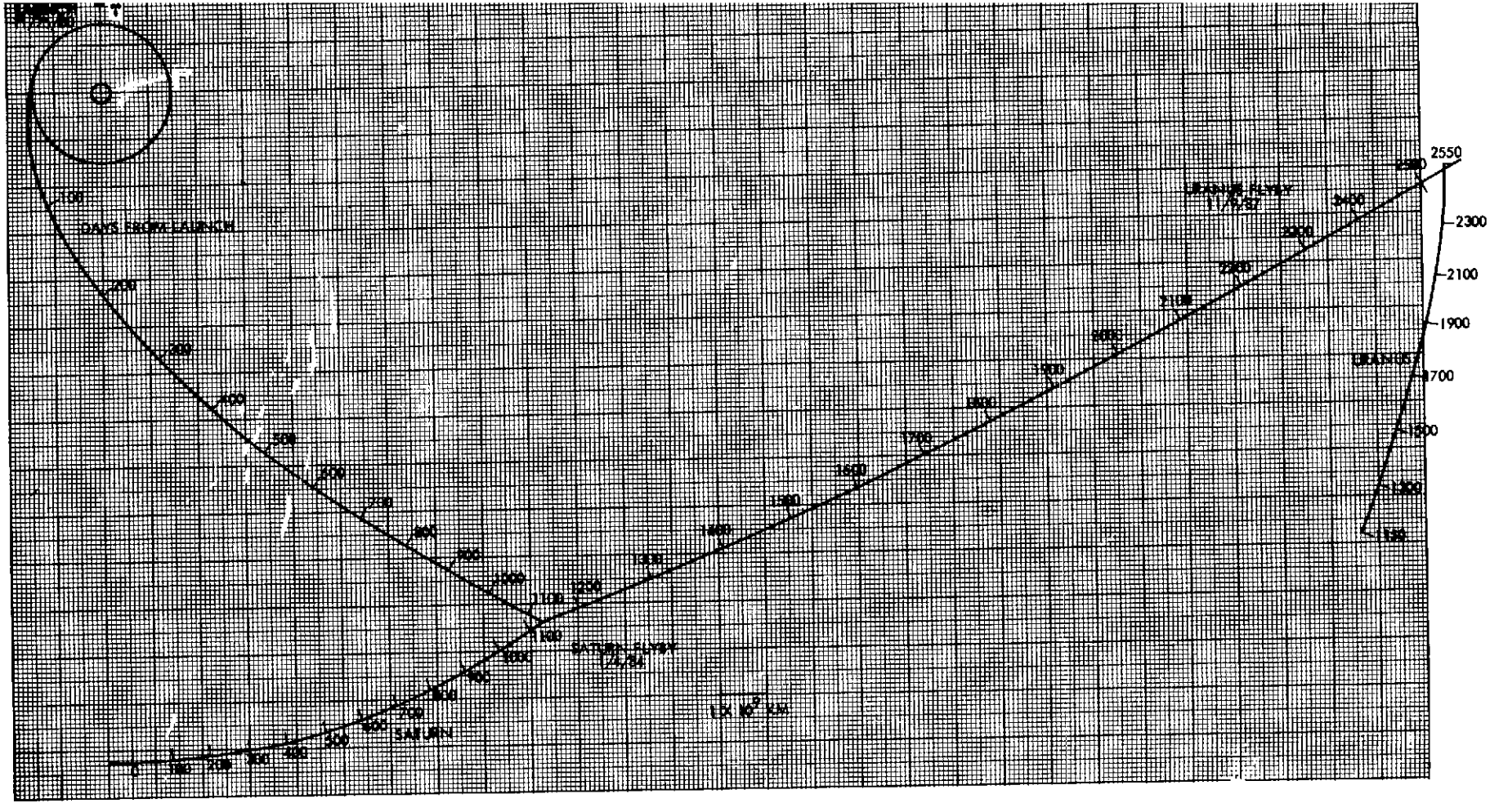

Figure C-7. Nominal 1980 Earth-Saturn-Uranus Trajectory

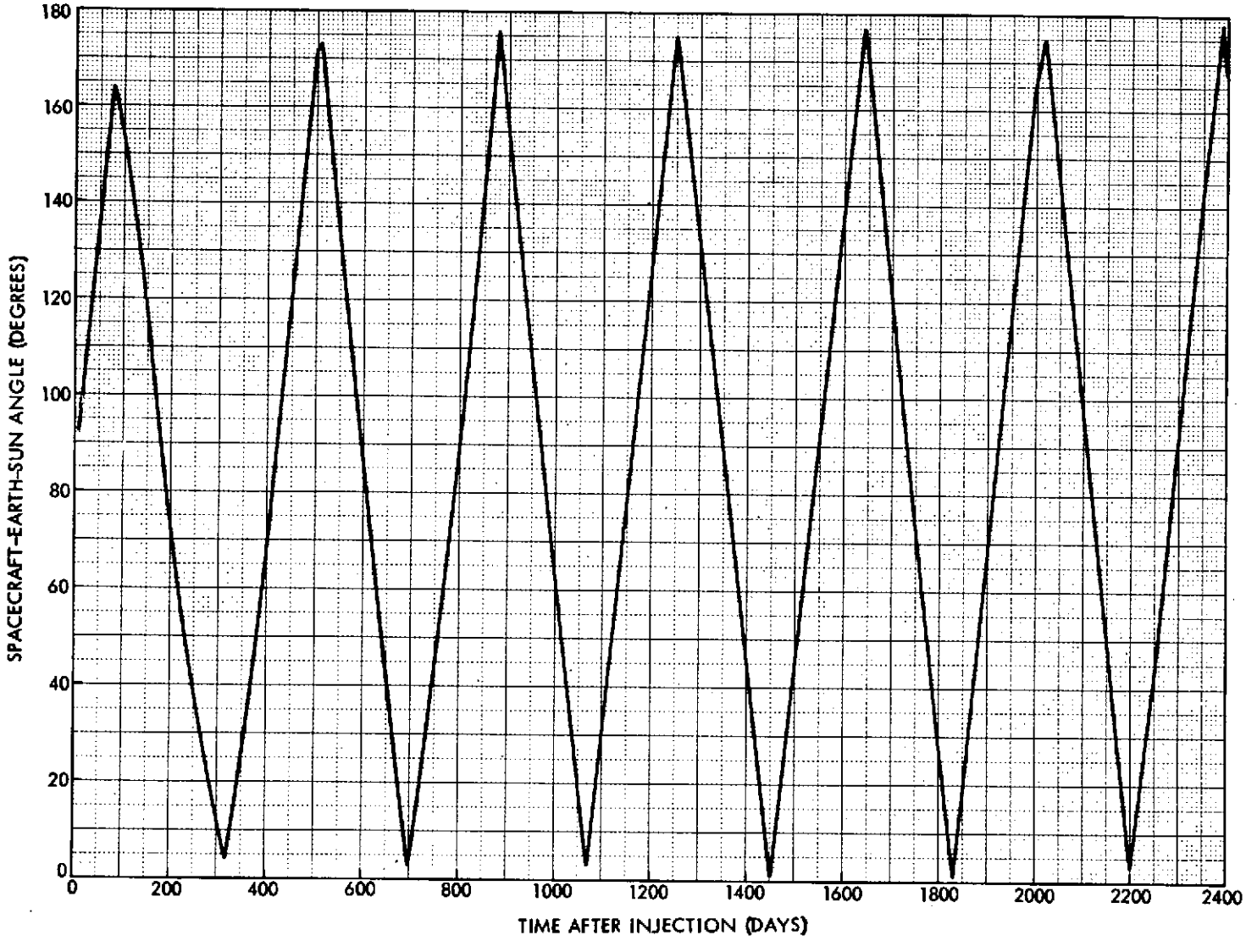

Figure C-8. Spacecraft-Earth-Sun Angle

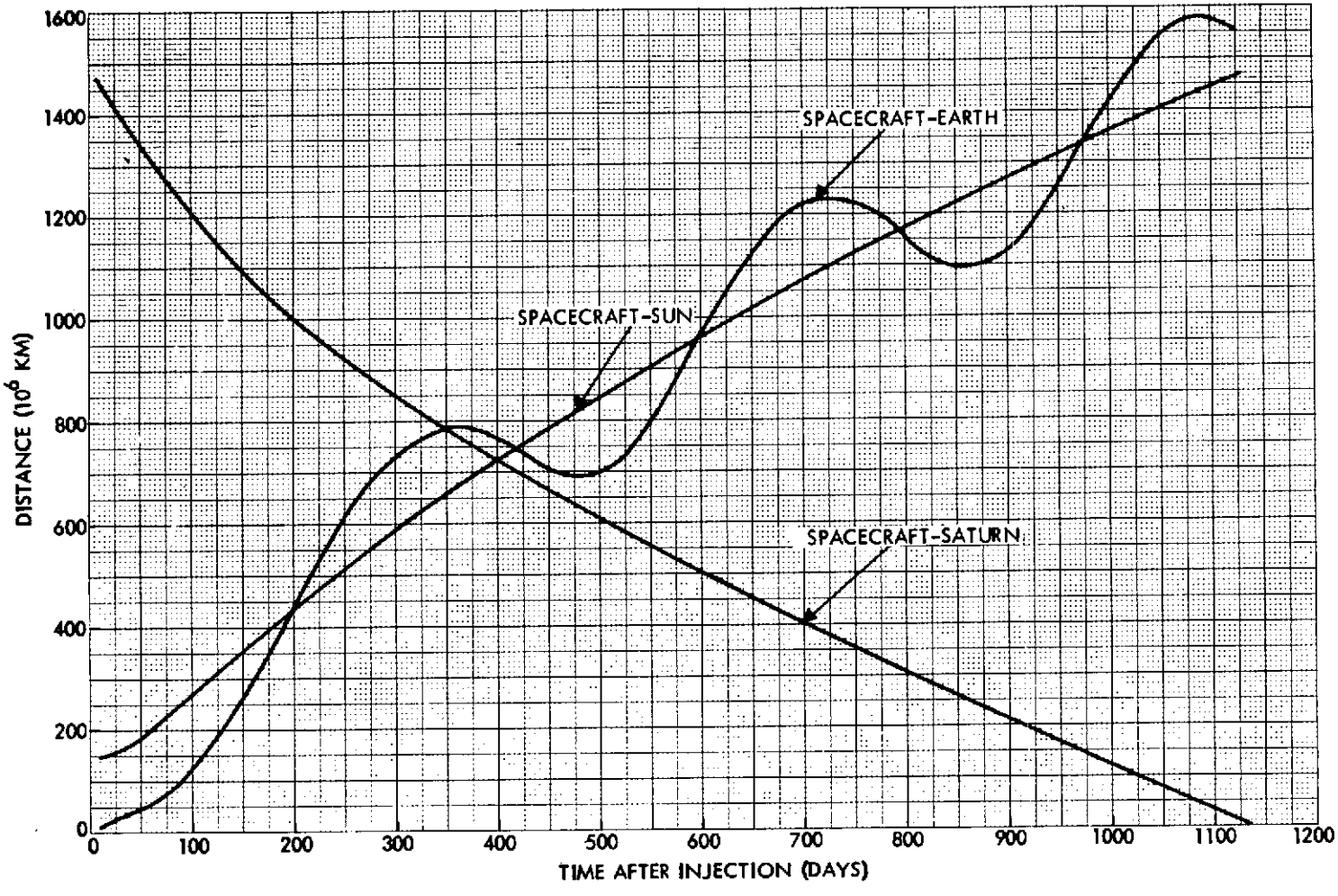

Figure C-9. Spacecraft Distances to Earth, Sun, and Saturn

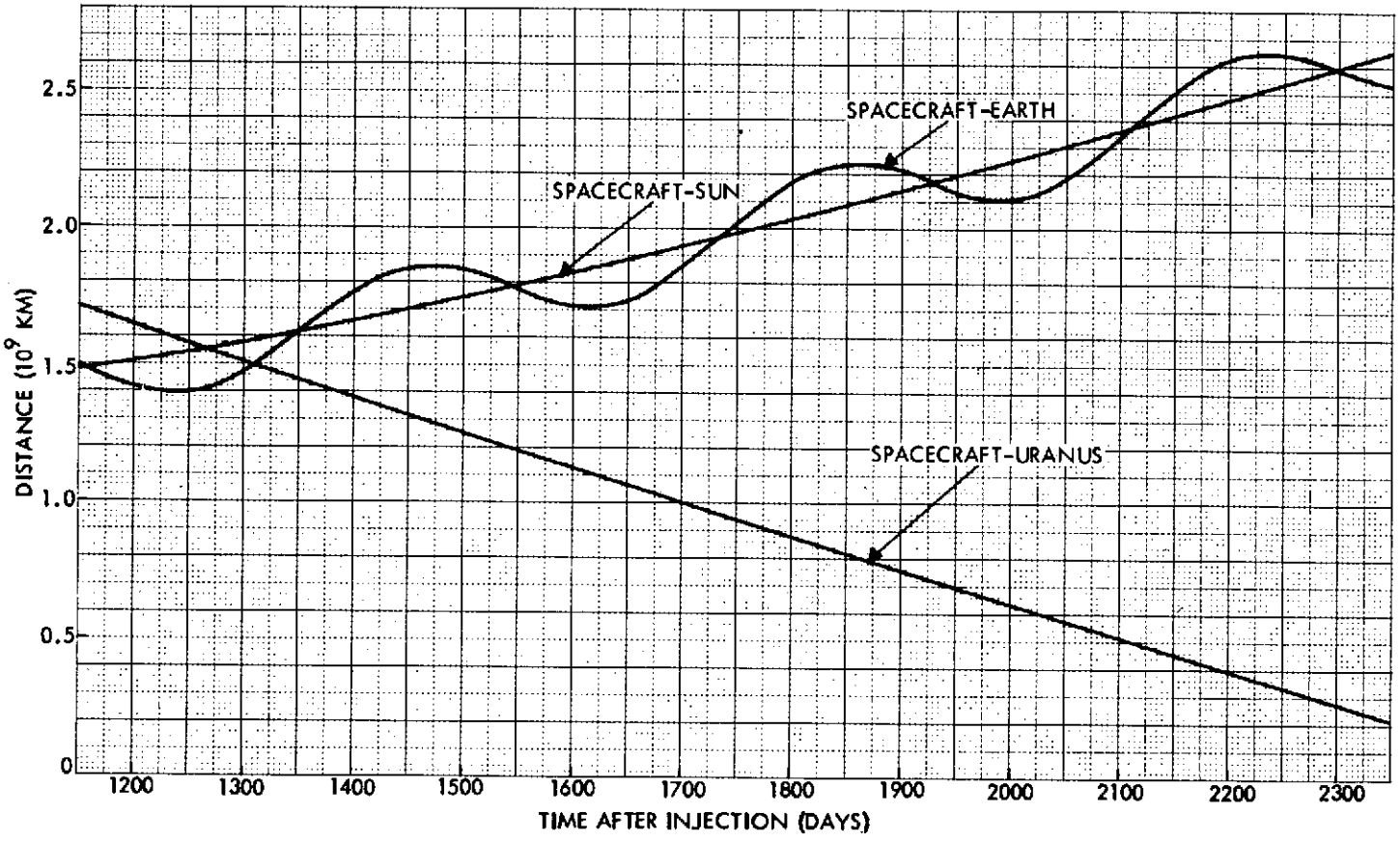

Figure C-10. Spacecraft Distances to Earth, Sun, and Uranus

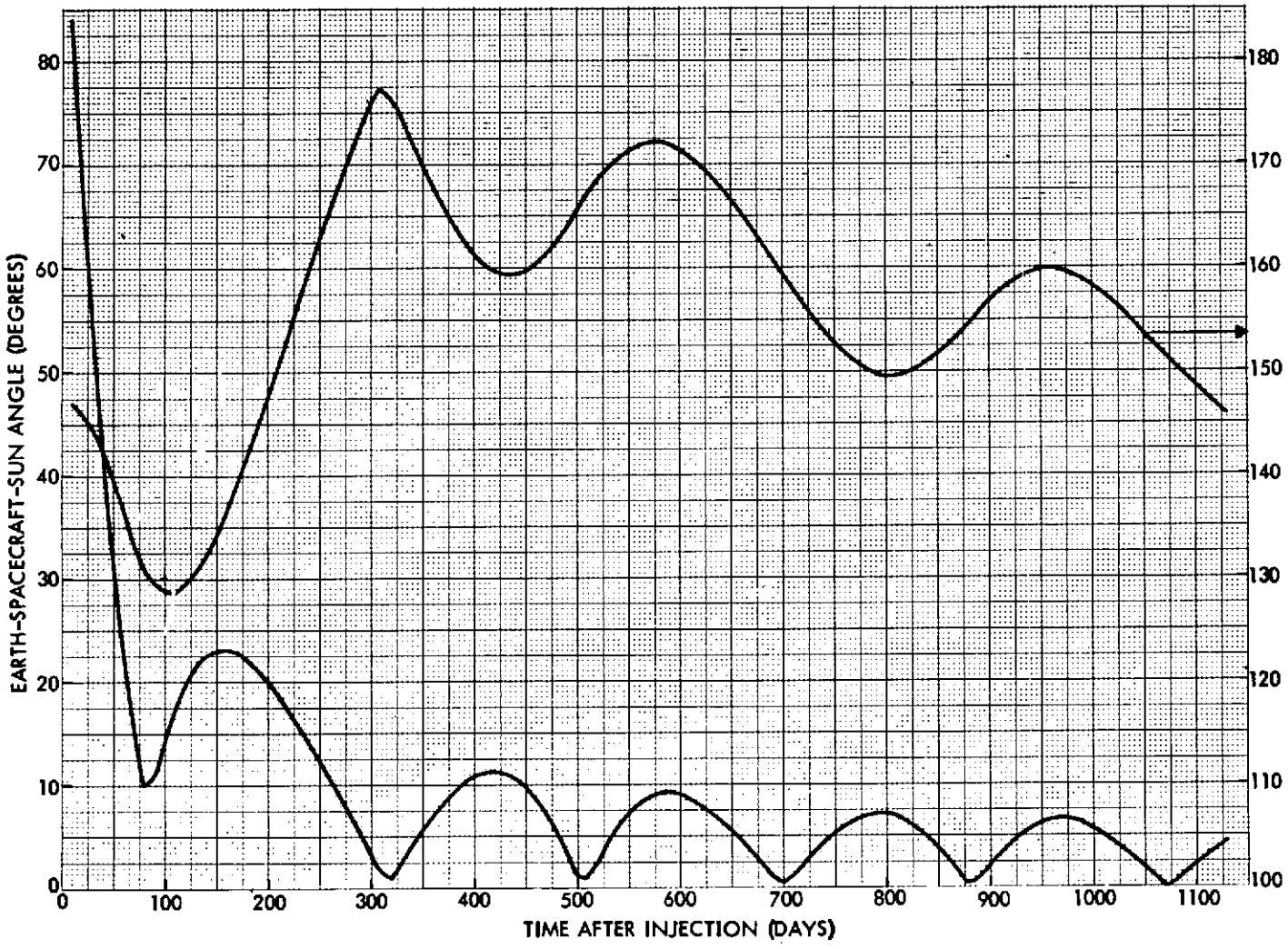

Figure C-11. **Earth-Spacecraft-Sun Angle and Earth-Spacecraft-Saturn Angle**

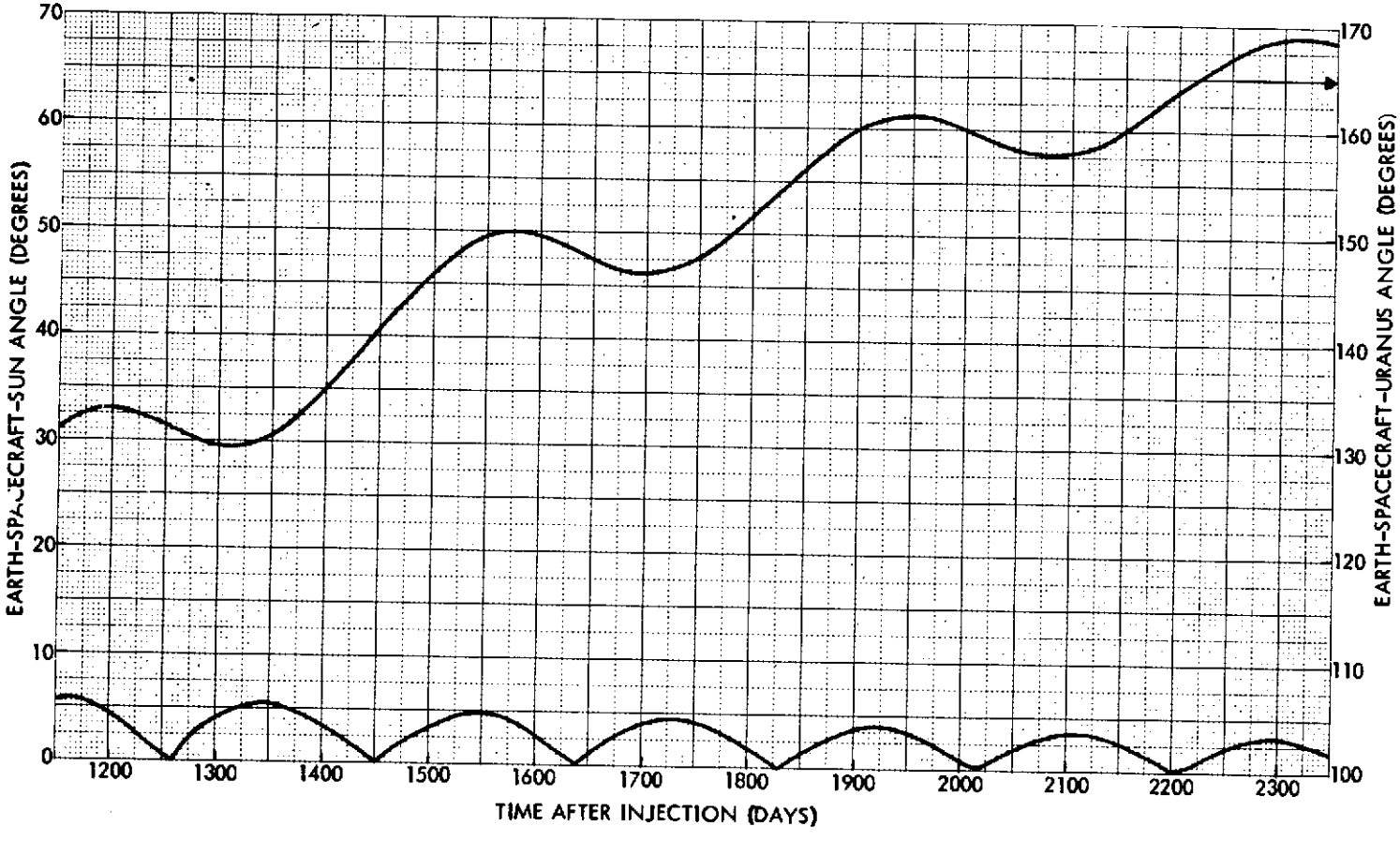

Figure C-12. Earth-Spacecraft-Sun Angle and Earth-Spacecraft-Uranus Angle

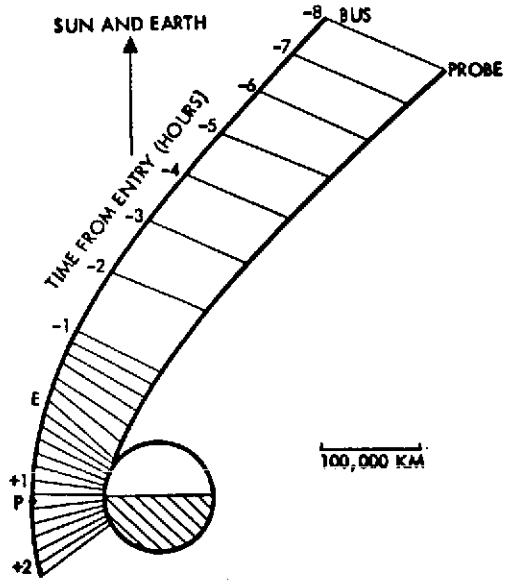

Figure C-13. Approach Geometry for 1979 Saturn Direct Mission

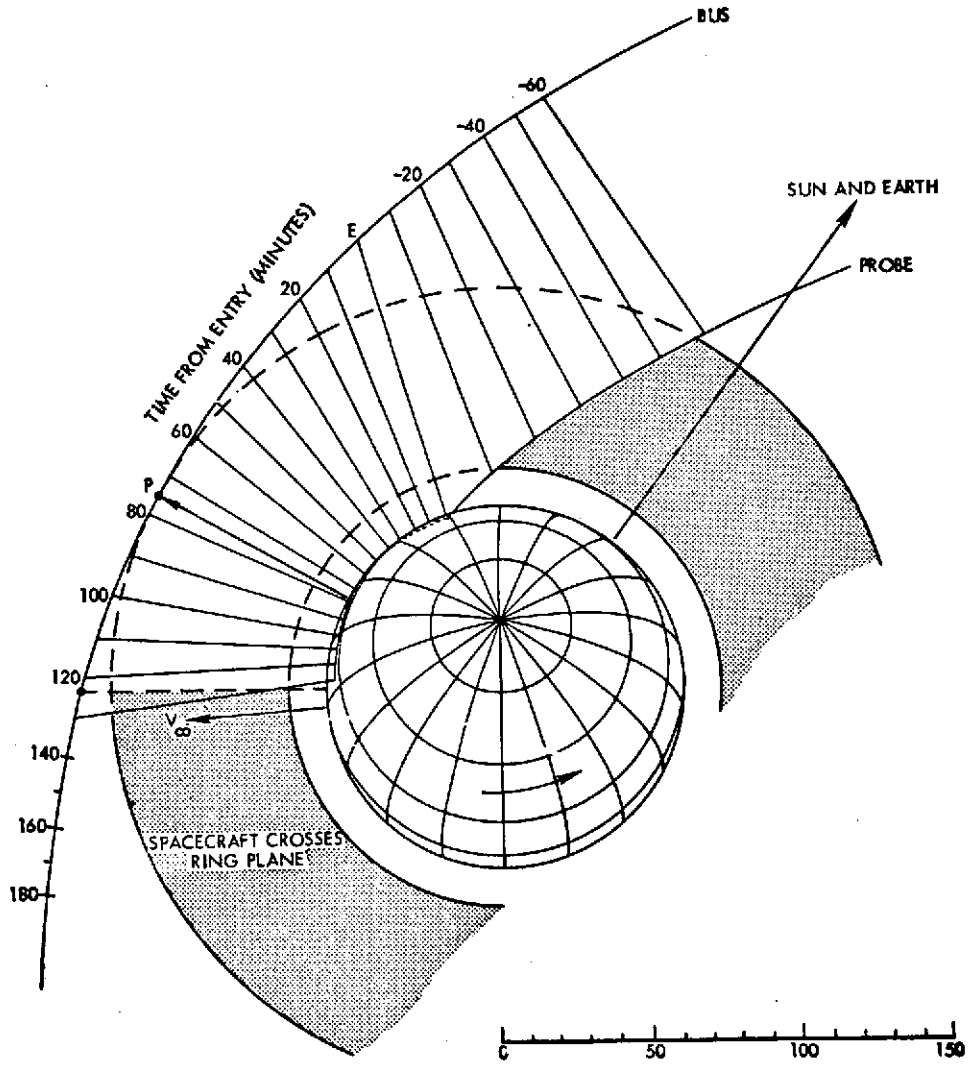

Figure C-14. Approach Geometry for 1979 Saturn Direct Mission (Detail)

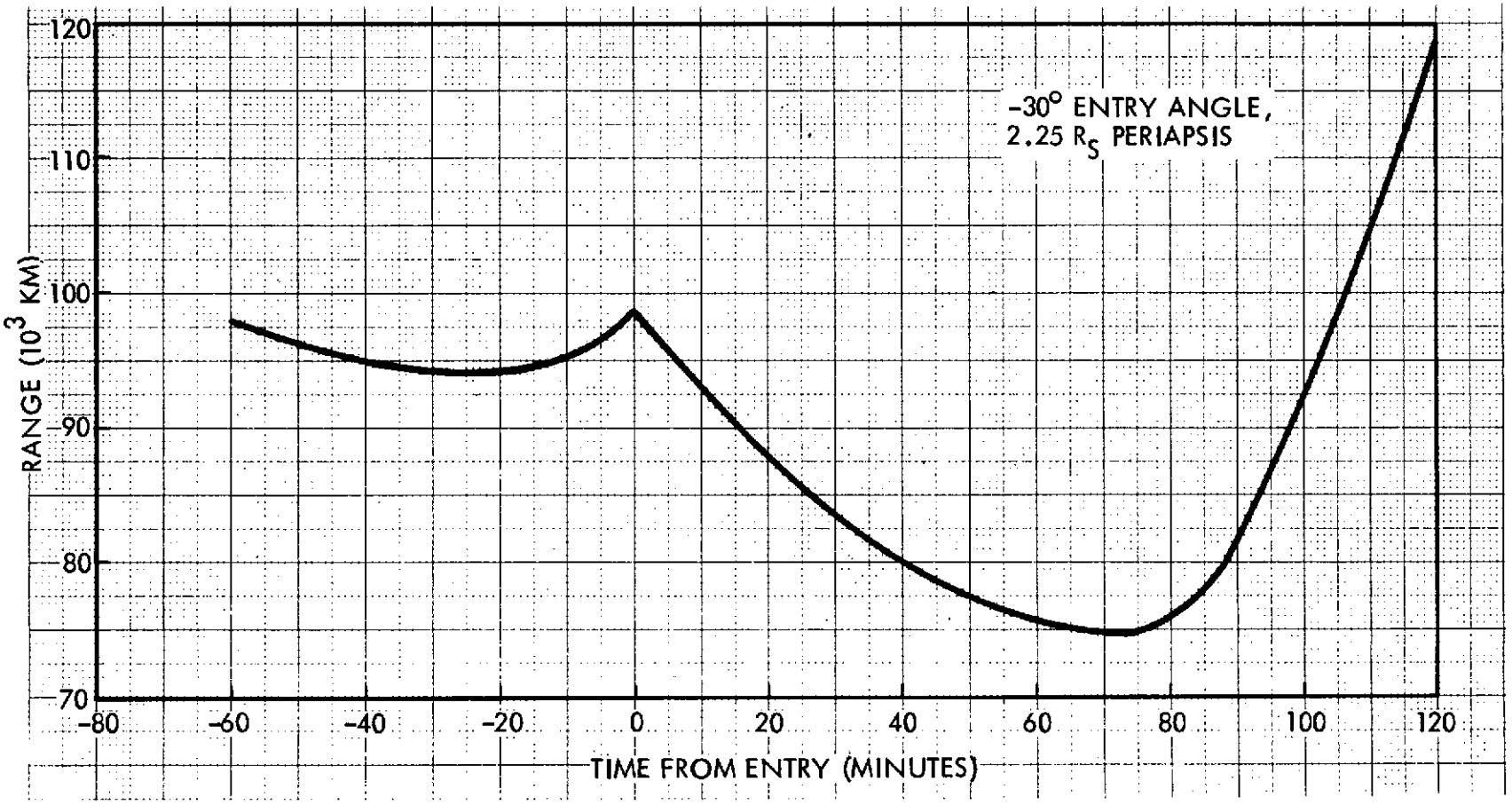

Figure C-15. Bus-Probe Range for 1979 Saturn Direct Mission

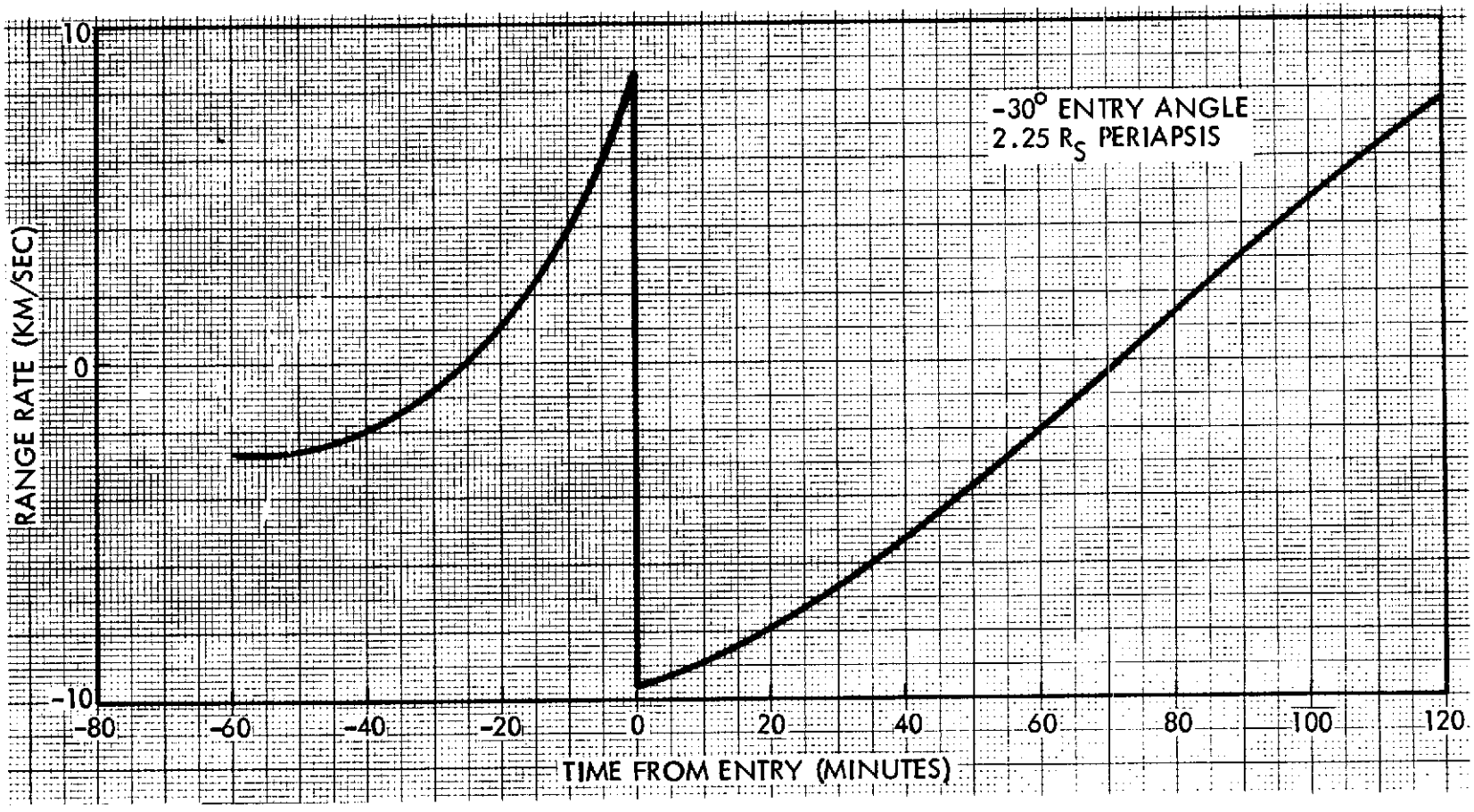

Figure C-16. **Bus-Probe Range Rate for 1979 Saturn Direct Mission**

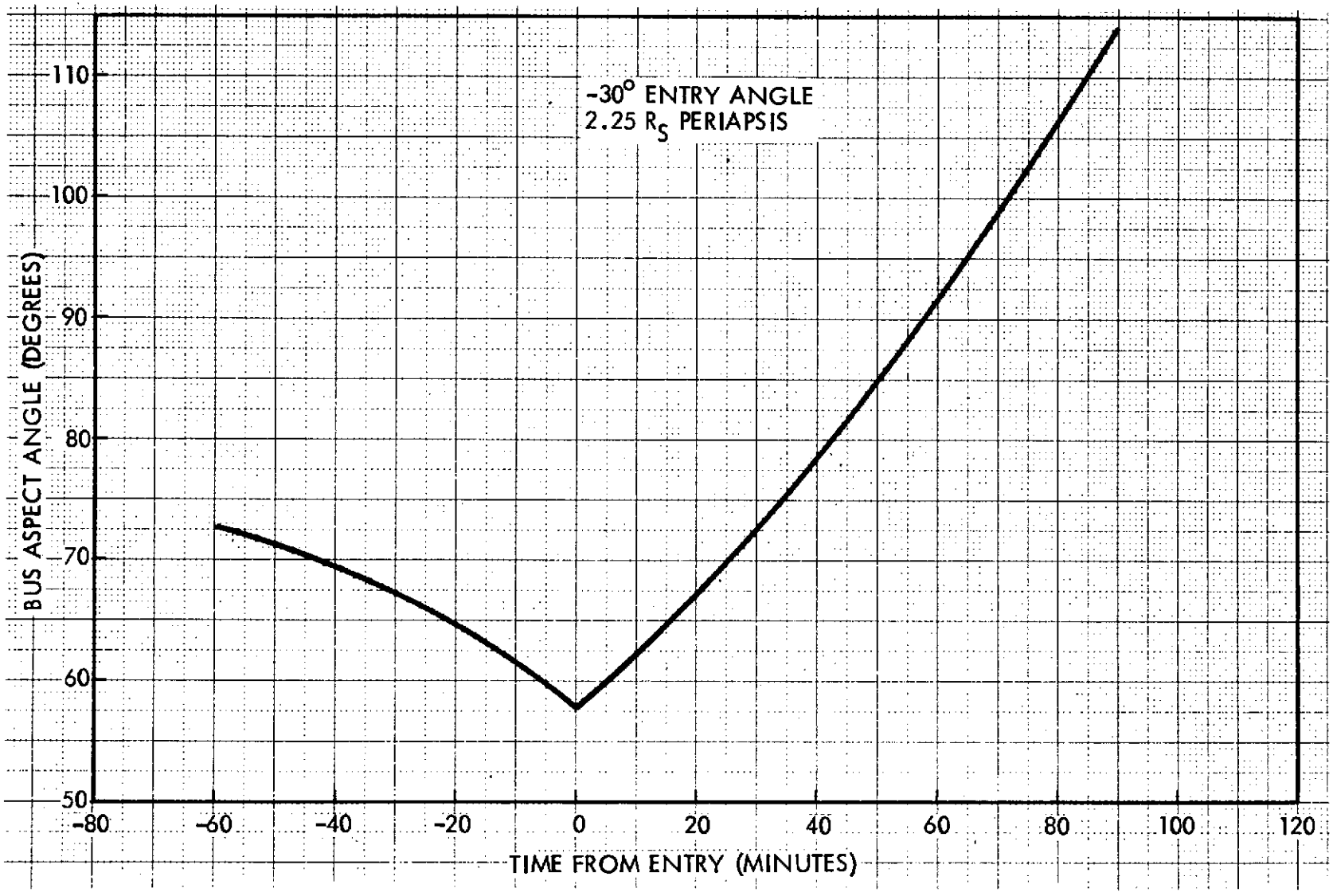

Figure C-17. Bus Aspect-Angle for 1979 Saturn Direct Mission

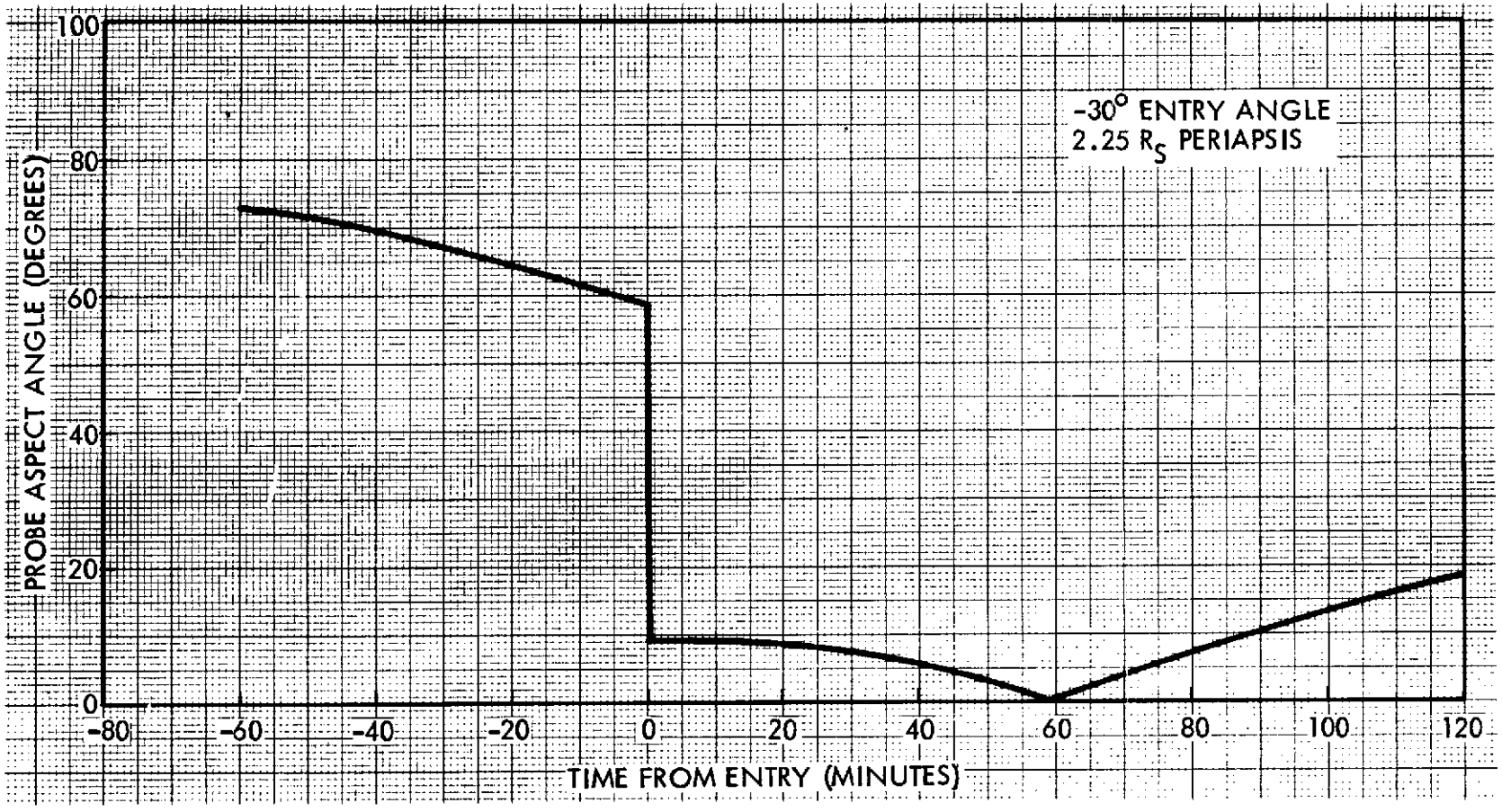

Figure C-18. Probe Aspect-Angle for 1979 Saturn Direct Mission

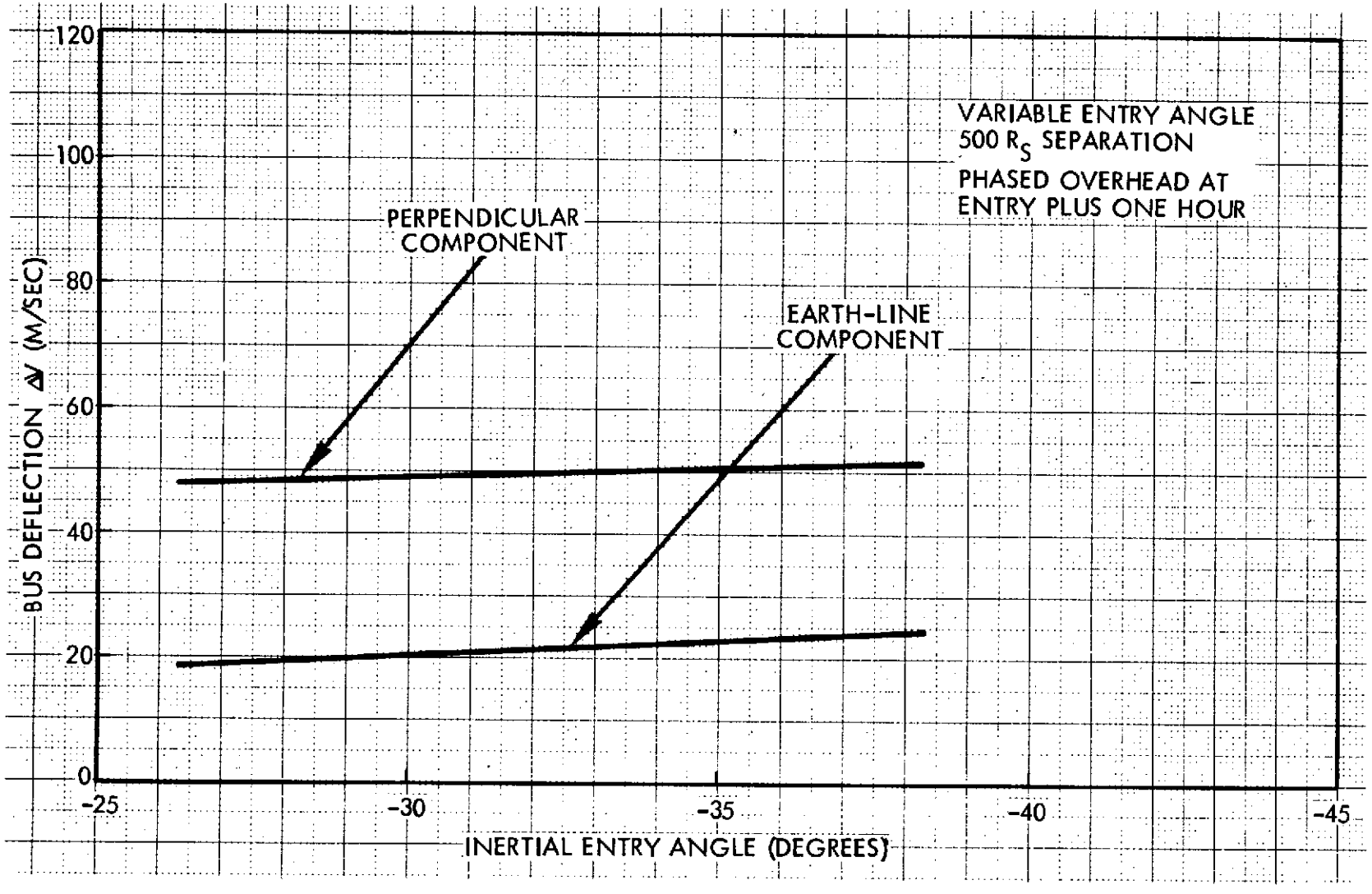

Figure C-19. Deflection/Phasing ΔV for 1979 Saturn Direct Mission

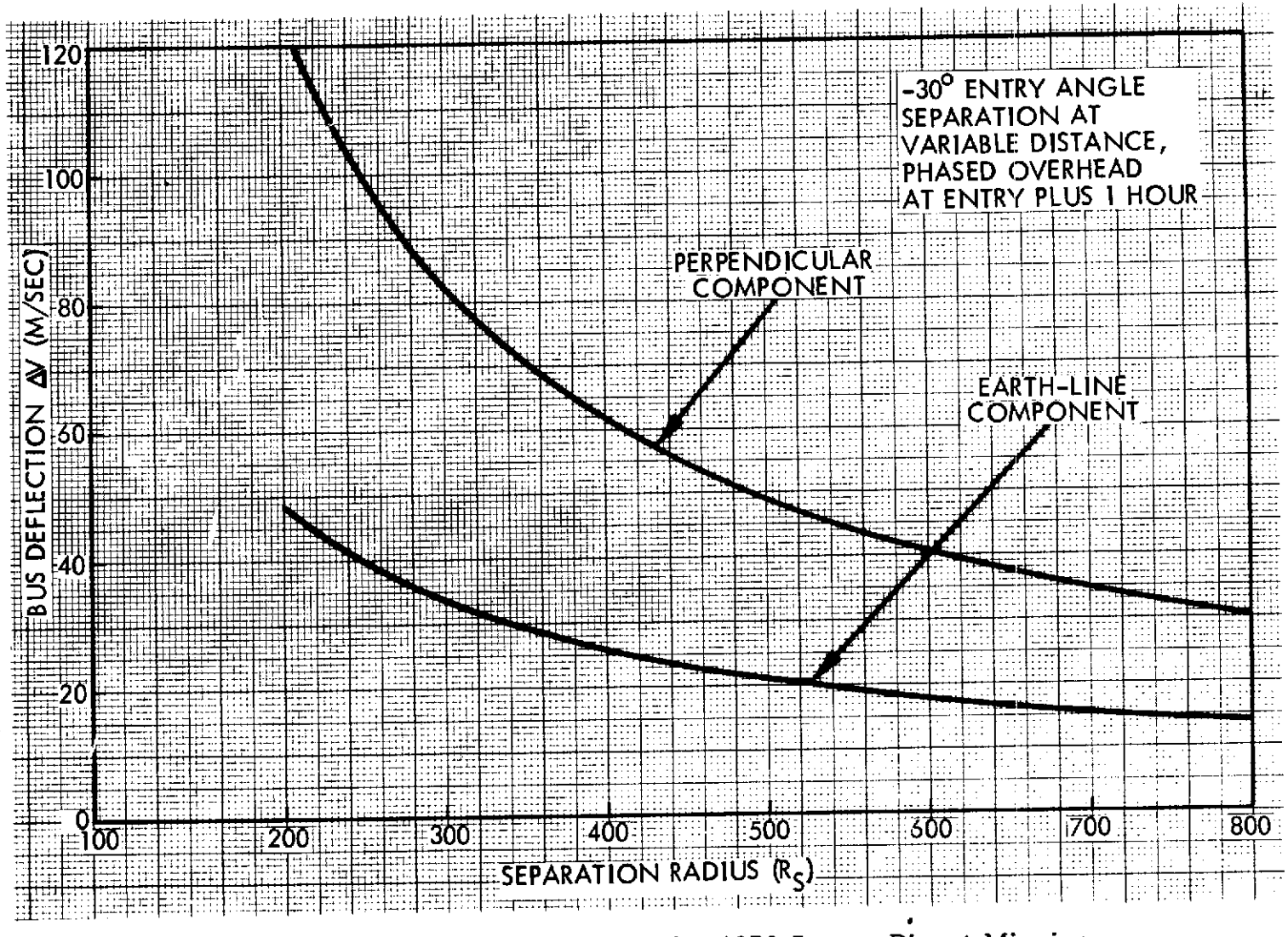

Figure C-20. **Deflection/Phasing ΔV for 1979 Saturn Direct Mission**

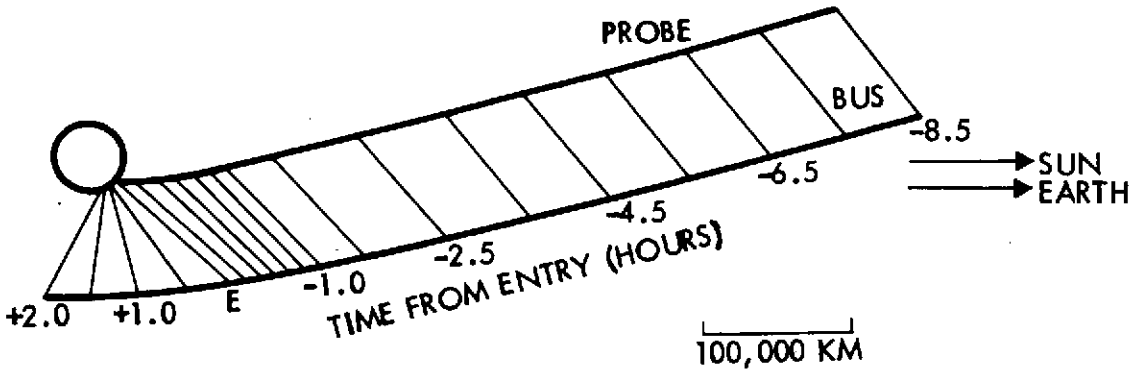

Figure C-21. Approach Geometry for 1980 Saturn-Uranus at Uranus

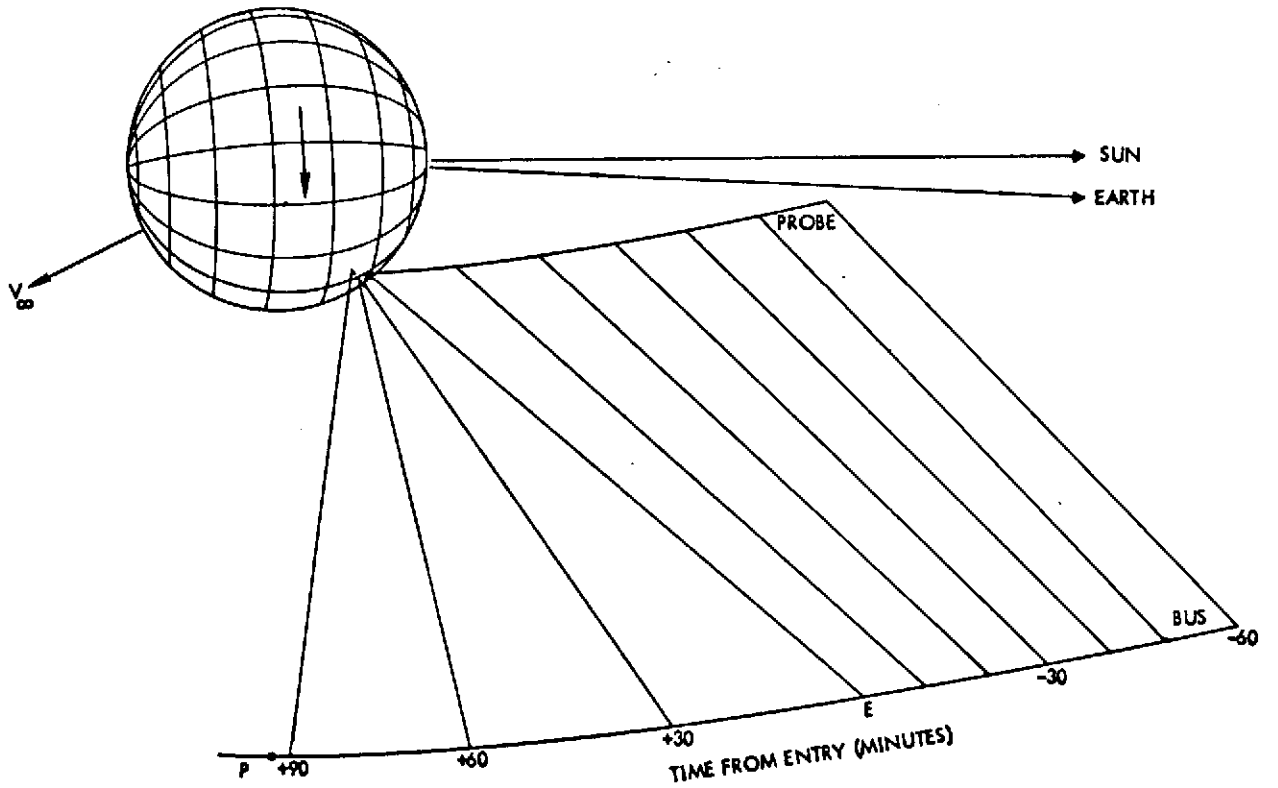

Figure C-22. Approach Geometry for 1980 Saturn-Uranus at Uranus (Detail)

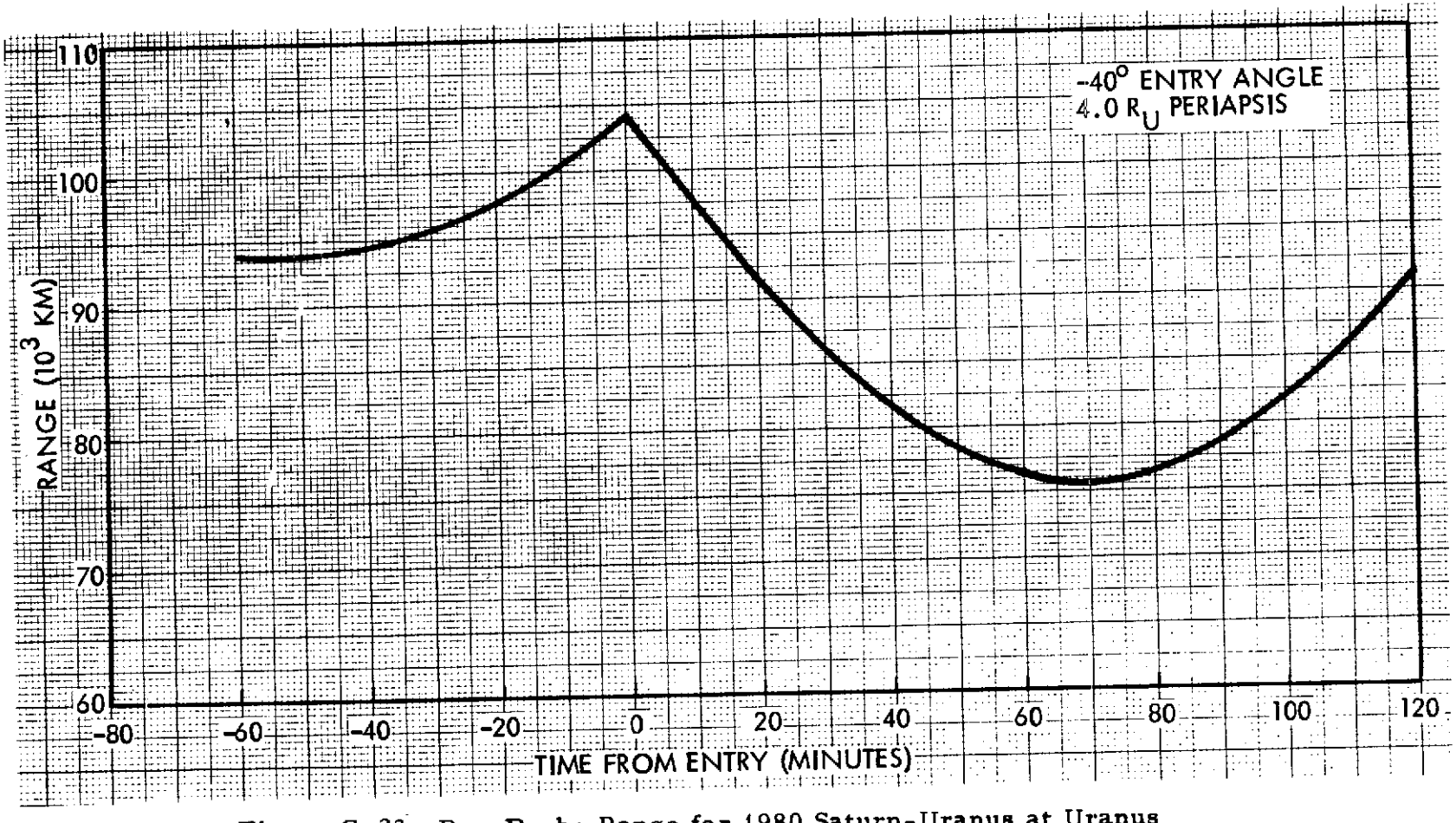

Figure C-23. Bus-Probe Range for 1980 Saturn-Uranus at Uranus

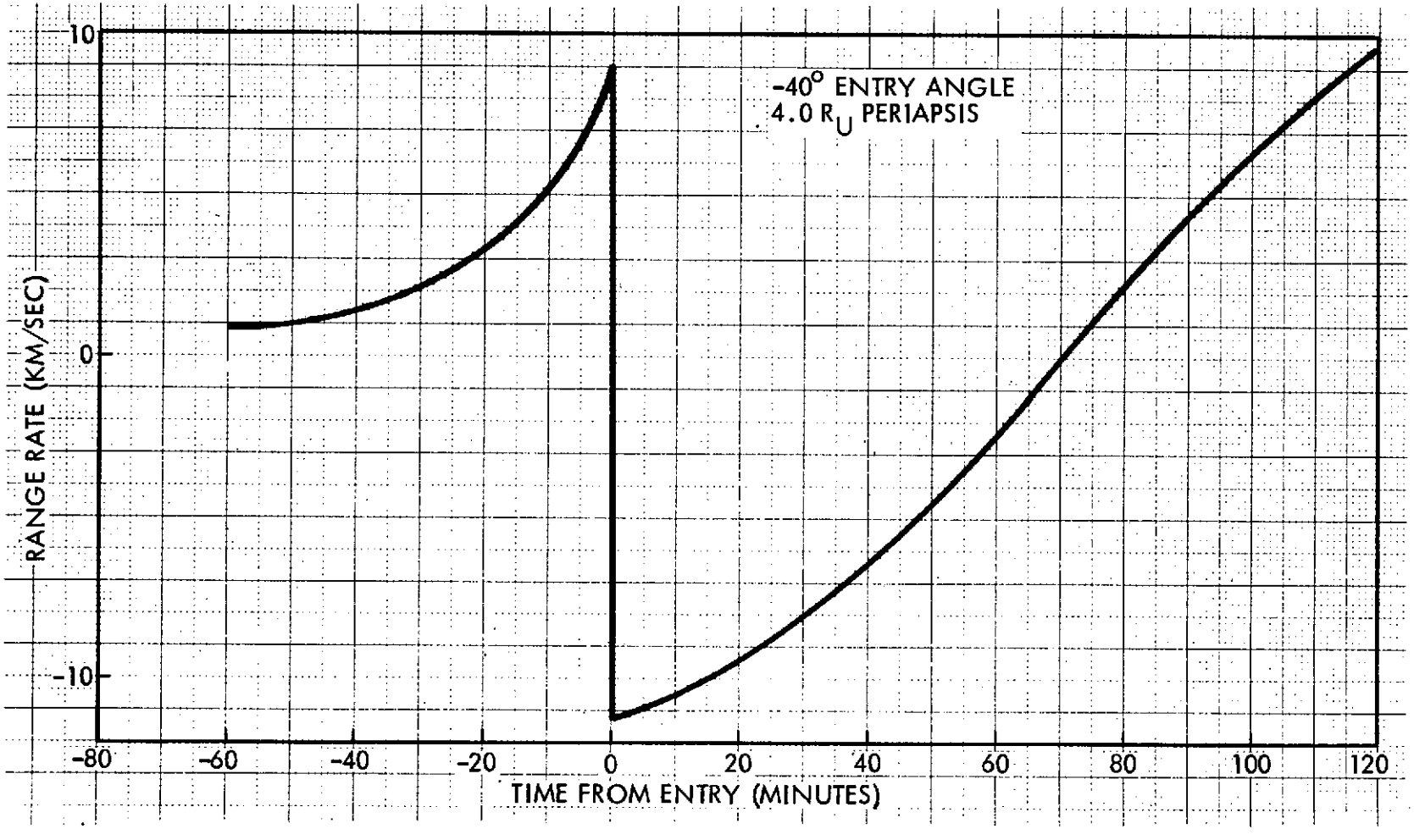

Figure C-24. Bus-Probe Range Rate for 1980 Saturn-Uranus at Uranus

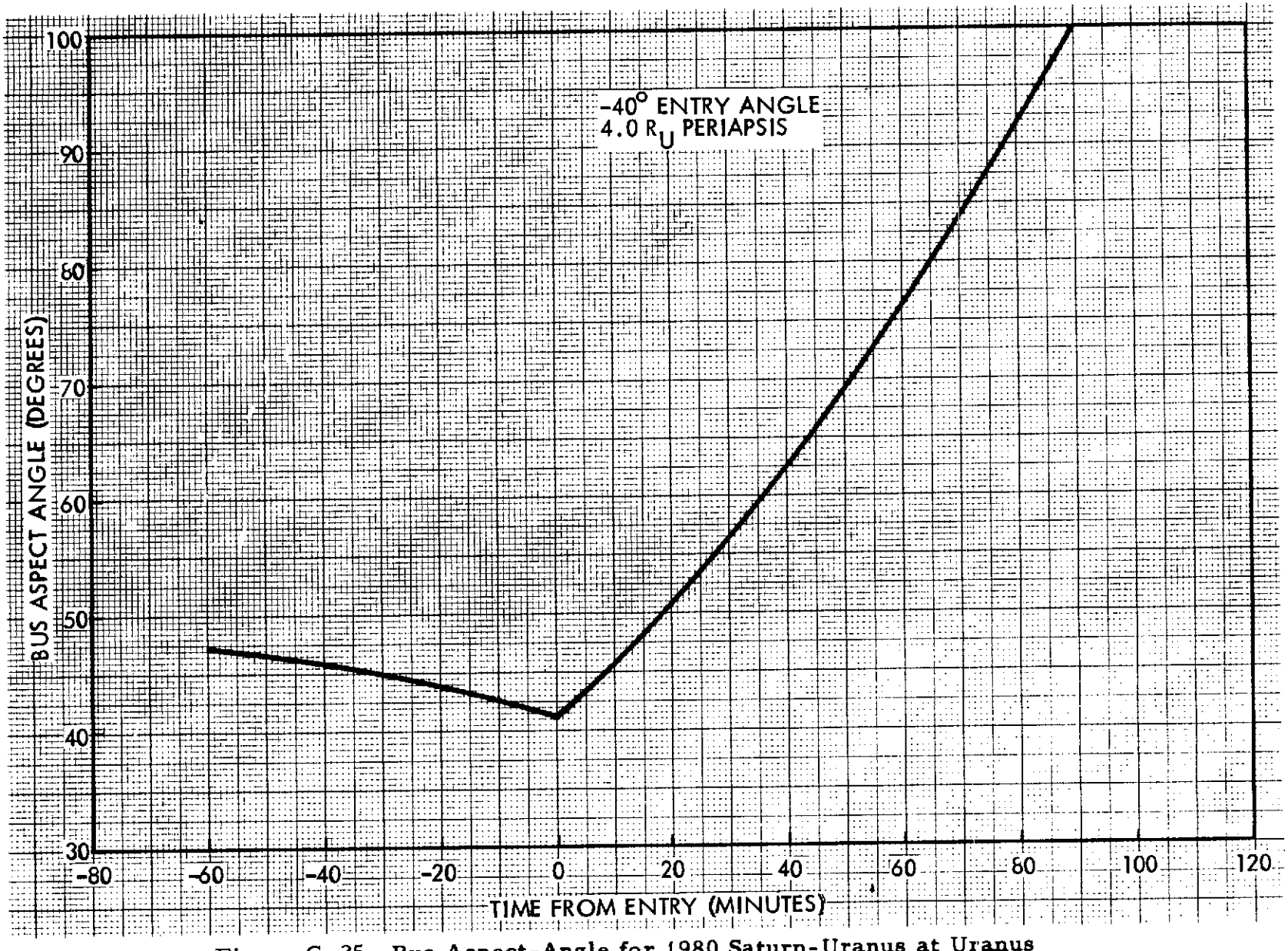

Figure C-25. **Bus Aspect-Angle for 1980 Saturn-Uranus at Uranus**

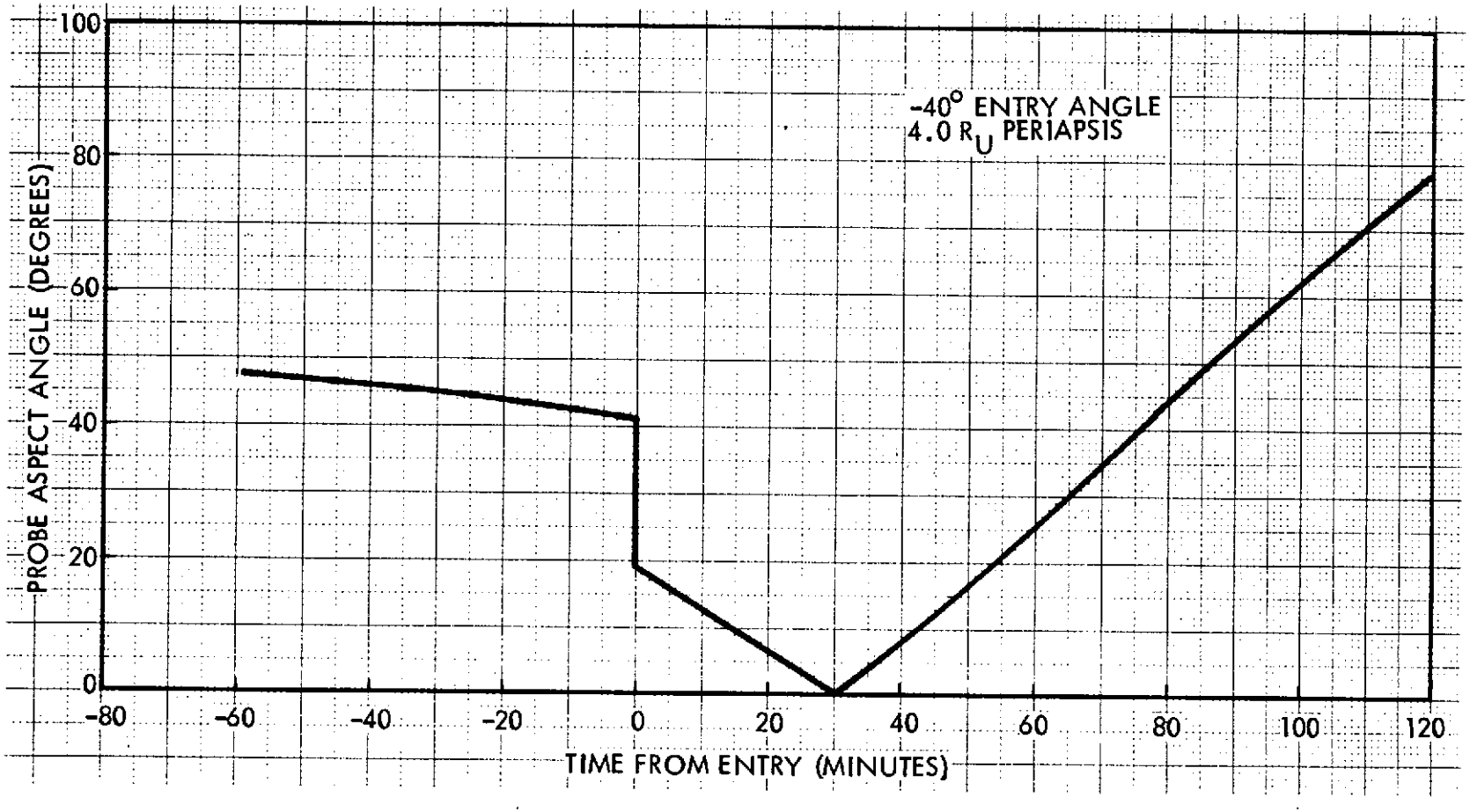

Figure C-26. Probe Aspect Angle for 1980 Saturn-Uranus at Uranus

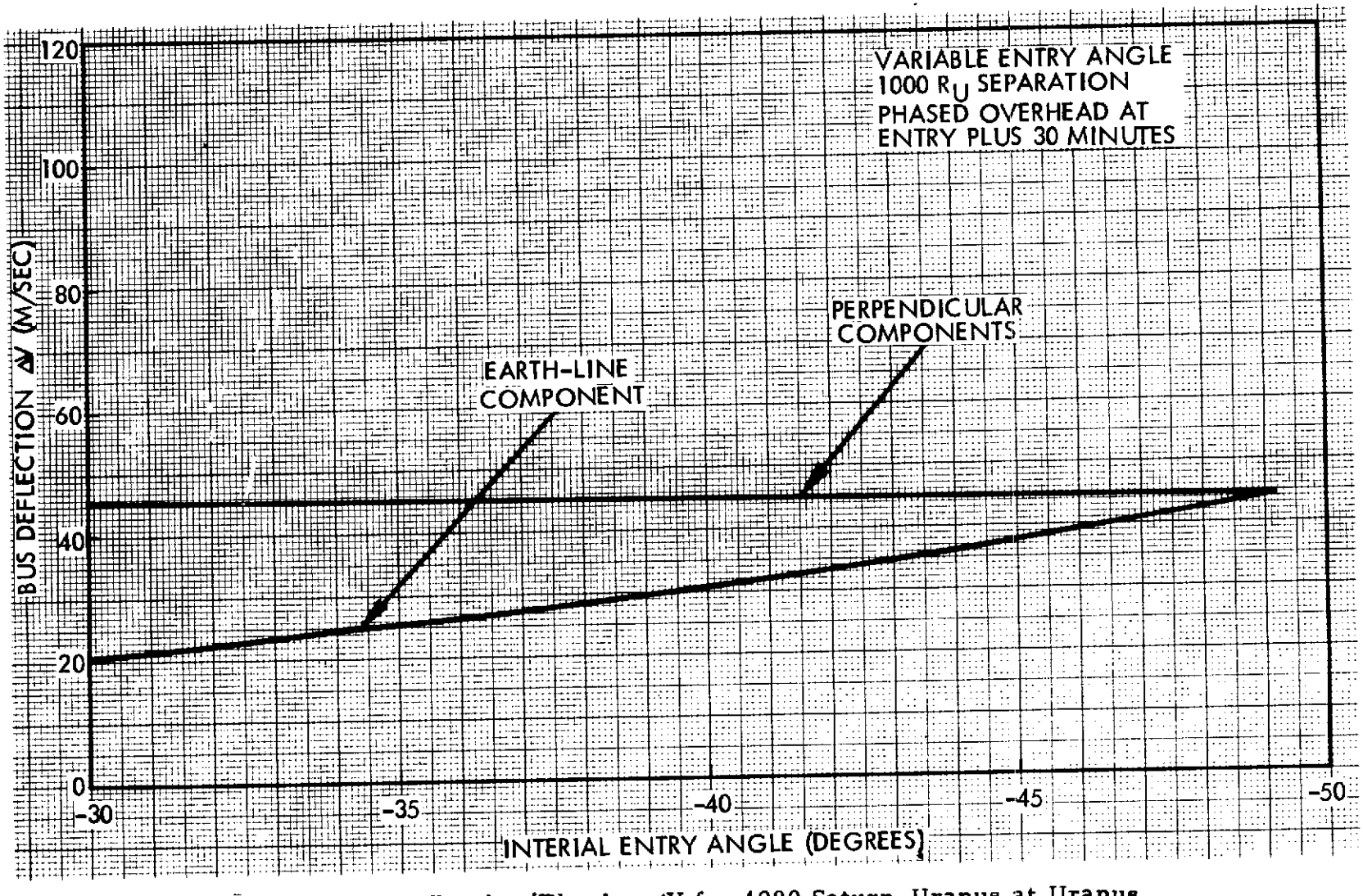

Figure C-27. **Deflection/Phasing ΔV for 1980 Saturn-Uranus at Uranus**

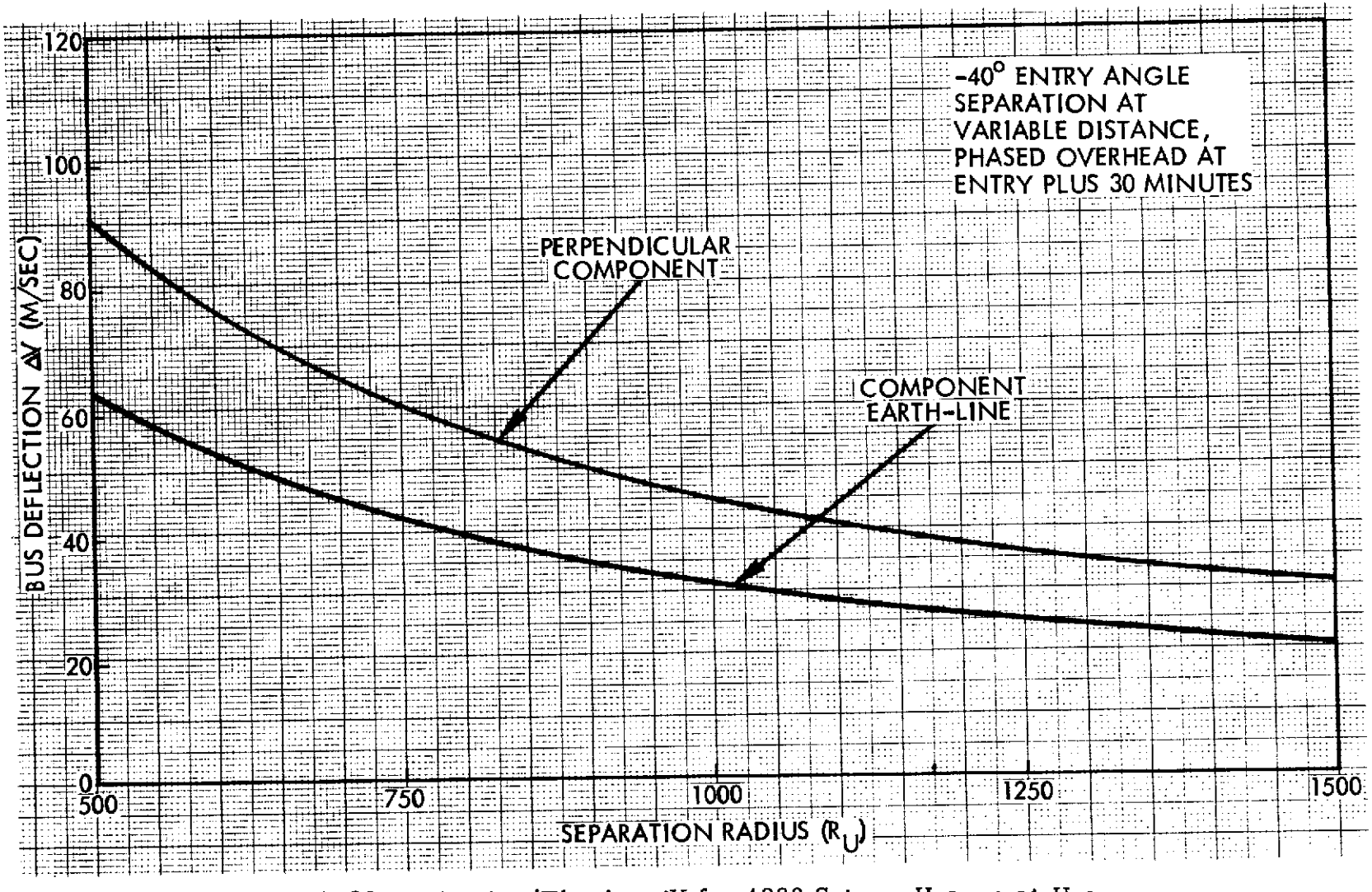

Figure C-28. Deflection/Phasing ΔV for 1980 Saturn-Uranus at Uranus

APPENDIX D

SPACECRAFT FOR A MISSION TO SATURN ONLY

1. MINIMUM-MODIFICATION SPACECRAFT OPTION

Design requirements and performance capabilities of a spacecraft intended only for a Saturn probe mission were briefly evaluated (see Section 1.1) and compared to those of the proposed SUAE spacecraft. Because of the shorter mission life (3.4 years) and lower maximum communication distance (8.7 AU) fewer modifications of the baseline Pioneer F/G configuration are required in this case. That is, maximum program cost economy is achieved by restricting the spacecraft's mission potential.

Specific design features of Pioneer F/G that can be retained essentially without modification for the Saturn-only mission include:

- The SNAP-19 RTG's
- The S-band communication system (without addition of X-band capability)
- The Pioneer F/G equipment bay (without add-on compartment)
- The Pioneer F/G star reference assembly and roll reference logic, since an optical navigation sensor is unnecessary.

The main modifications of Pioneer F/G required for this mission are those necessitated by accommodation of and interfaces with the entry probe and by the change in bus payload instruments. These modifications are essentially the same as in the SUAE spacecraft, as will be discussed below.

The purpose of this design comparison is mainly to identify an alternative, minimum-cost and minimum-development option of extending the Pioneer F/G mission capability to outer-planet atmospheric entry probe delivery. Evaluation of programmatic implication and possible advantages of the cost-economy versus system capability tradeoff is outside the scope of this study.

2. SPACECRAFT MODIFICATIONS FOR SATURN MISSION

Figure D-1 summarizes the design modifications of Pioneer F/G that are required for the Saturn-only mission. The design evolution chart previously shown in Section 2 (Figure 2-8) is used to indicate which of the modifications adopted in the SUAE spacecraft are still necessary. Those features not required for the Saturn-only mission are crossed out.

The following list, also adopted from Section 2, tabulates the modifications of the individual components and units of the Saturn spacecraft.

Propulsion	
a) Propellant tank	Must be enlarged to satisfy the requirement for increased propellant. Increased from 16.5 to 18.0 inches in diameter
b) Thrusters	A pair of radial thrusters is added to the six already present, to permit ΔV maneuver components normal to the spin axis at long distances from the earth
c) Propellant lines and heaters	Modified to accommodate larger tank and added thrusters
Thermal Control	
a) Insulation, louvers, and heaters	New insulation and heaters on probe adapter to control probe temperatures
Structure	
a) Probe adapter	New spacecraft-probe adapter structure to carry spacecraft loads around probe to launch vehicle adapter, and to pick up probe loads
	Modification of spacecraft separation ring

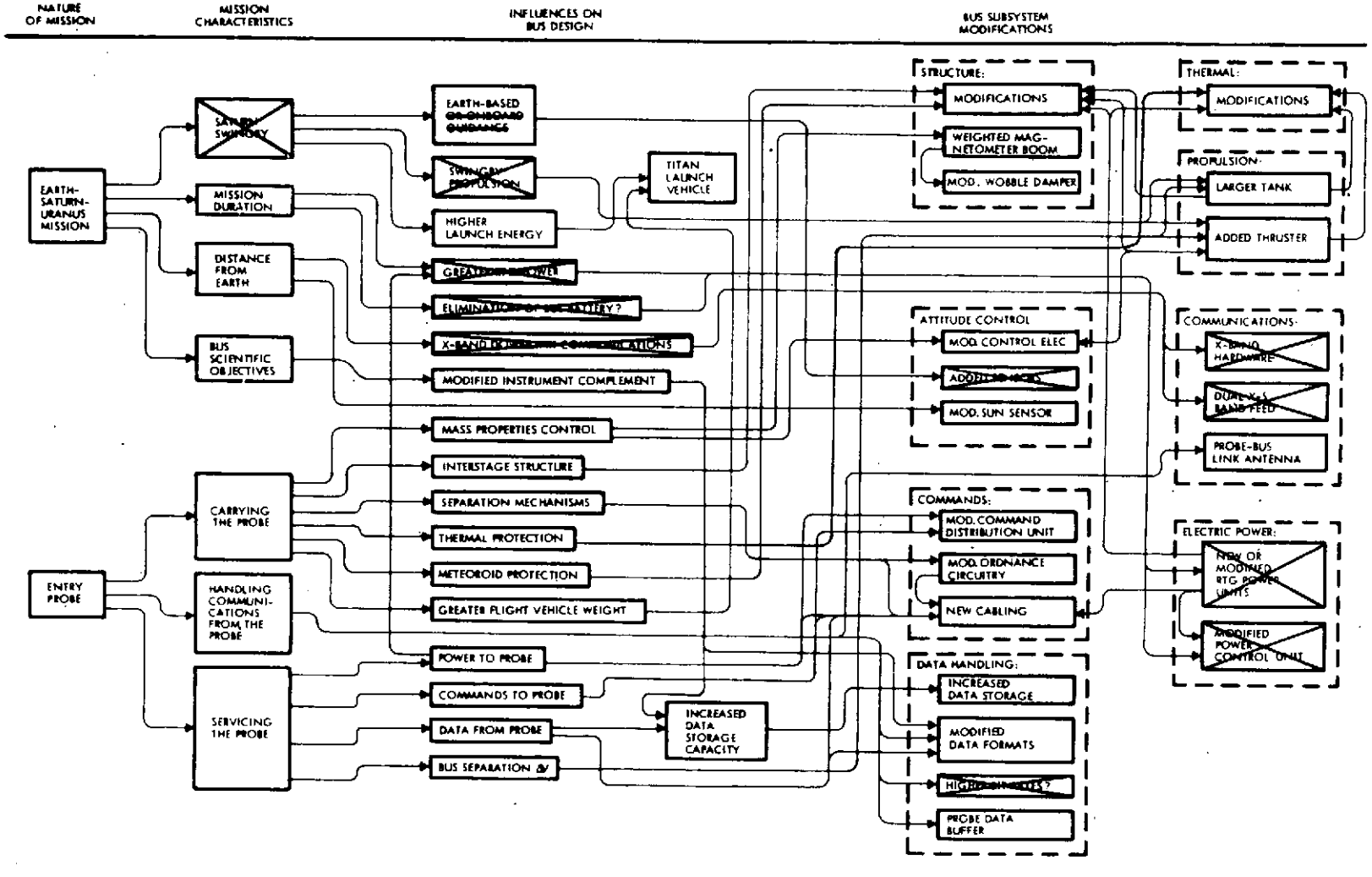

Figure D-1. Elimination of Modifications Not Necessary for Saturn Mission

	New hold-down, release, and separation fittings for the probe
b) Launch vehicle adapter	Modification of standard 37-inch diameter by 31-inch adapter, to allow single separation joint
c) Magnetometer boom	Added deployment counterweight (~20 pounds)
	Modified and strengthened boom and fittings, to accommodate counterweight and simultaneous deployment
	Modified deployment damper
d) Wobble damper	Modified to change damping constant
Attitude Control	
a) Control electronics	Modified to accommodate added thrusters
b) Despin sensors	Relocated to operate at different spin rate
Communications	
a) Low-gain S-band antenna	Remount on new pedestal
b) Probe-bus antenna	New unit, operating at 400 MHz, mounted on same pedestal as S-band low-gain antenna
c) Receiver	Receiver-bit synchronizer unit (furnished by probe contractor) added
Data Handling	
a) Digital telemetry unit	Modified to install new formats to accommodate probe data
b) Data storage unit	Enlarged to accommodate probe data and line-scan imaging data
c) Probe data buffer	New unit to accept probe data into spacecraft data handling system, from probe-link receiver

Command Distribution	
a) Command distribution unit	Modified to accommodate: • commands destined to the attached probe • commands to cut probe cable and to separate the probe • increased ordnance – actuated events • commands associated with the reception of probe data by RF link
b) Cable harness	New
Electrical Power	
a) Power control unit	Modified to include probe battery charge/discharge circuitry

3. PERFORMANCE CHARACTERISTICS

3.1 Communications and Data Handling

With downlink communications restricted to the capability of the unchanged S-band system of Pioneer F/G a bit rate of 256 bps is available at the Saturn encounter distance of 8.7 AU, based on the arrival date on April 15, 1983 of the nominal 1979 earth-Saturn mission profile) with a margin of about 2 dB. This data rate is considered adequate under the constraints of the desired system economy, since entry probe data to be relayed to earth are received nominally at 88 bps. The telemetry data rate analysis in Section 6.6 shows that with 256 bps the use of the DTU B-Format permits telemetry of 66 data bits per cycle (about one-third of the 192 bits per frame). The B-D Format option would transmit 132 data bits per cycle. If under adverse conditions the telemetry bit rate is reduced to 128 bps, the B-Format option would handle 132 bits of probe data per frame.

System economy requires in this case that bus science data be limited to a small percentage of the available channel capacity. We also

note that the RF occultation experiment is limited to a single frequency as in the Pioneer 10/11 Jupiter missions.

Data storage capacity is dictated by probe data relay/storage requirements and must therefore be the same as in the SUAE spacecraft bus, namely 3 DSU's of 245-kbit capacity each. Although mission life is less than half of that of the ESU mission, the redundancy provided by the third DSU is considered essential to assure full probe data playback in the event of failure of one unit. The additional DSU storage capacity also serves the secondary objective of handling bus occultation data in addition to probe data.

3.2 Power Requirements

Elimination of X-band telemetry is the key to confining the total bus spacecraft power requirements to the capability of the four SNAP-19 RTG's of Pioneer F/G. As shown in Section 7.1 the power output of these RTG's can be reasonably extrapolated from Pioneer 10 flight experience to date to a value of about 130 watts at the time of Saturn encounter (see Figure 7-1).

Table D-1 shows that the total power requirements of the Saturn spacecraft at encounter can be met by the projected power output. The (nearly identical) power budget of Pioneer F/G is also shown for comparison. In order to accommodate pulse loads of up to 14 watts it appears that the Pioneer F/G battery must be retained in the Saturn spacecraft, unless continuing favorable RTG flight performance on Pioneers 10 and 11 demonstrates that even a higher power level than 130 watts can be projected for the end of the 3.4-year Saturn mission. The present extrapolation indicates a deficit of at least 6 watts, even with time-sharing of several items in the power budget (see notes at bottom of Table D-1).

3.3 Propulsion

The maneuver requirements for the earth-Saturn mission are summarized in Table D-2.

Table D-1. Electrical Power Requirements of Pioneer F/G and Saturn Spacecraft (Watts)

Load	Pioneer F/G at Jupiter	Saturn-Only Mission
SECONDARY DC POWER		
Communications		
Receivers (2)	3.4	3.4
Driver, S-band	1.3	1.3
Conscan signal processor	1.2	1.2
Attitude Control		
Control electronics assembly	2.7	3.2
Sun sensor assembly	0.2	0.2
Star sensor assembly	0.3	0.3
Command		
Command distribution unit	3.1	3.6
Digital decoder unit	1.3	1.3
Data Handling		
Digital telemetry unit	3.7	4.2
Digital storage unit	0.6	5.0
	17.8	23.7
SECONDARY AC POWER		
CTRF losses (63% efficiency)	10.6	14.1
	28.4	37.8
PRIMARY DC POWER		
Communications		
TWTA, S-band (8W)	27.8	27.8
Attitude Control		
Control electronics assembly	0.4	0.4
Command		
Command distribution unit	0.2	0.2
Propulsion		
Transducers	0.2	0.4
Propulsion heaters	2.0	3.5
Electric Power		
Power control unit	7.7	7.7
Inverter losses (85% efficiency)	13.3	15.4
Experiments		
Experiments	24.0	20.0 (a)
Probe		
Heaters	-	4.0
Data link	-	(b)
Battery charging	-	(c)
Subtotal		110.5
Cable losses (spacecraft)	0.6	0.6
Subtotal (primary bus output)	104.4	117.8
RTG POWER		
RTG cable losses	4.2	4.2
Power margin	15.6	8.0
Total RTG output	124.0 (e)	130.0 (d)

(a) Additional power of 10.0W for image system is time shared.
(b) 10.0W time-shared with experiments.
(c) 6.0W time-shared with experiments.
(d) Extrapolated RTG output after 3.4 years based on Pioneer 10 flight experience.
(e) Total output of Pioneer F/G RTG's after 2.5 years (estimated performance as per interface specification).

Table D-2. Propulsive Maneuver Requirements for Earth-Saturn Mission

A. ΔV Requirements

Time	Maneuver	ΔV (m/sec)	Equivalent ΔV (m/sec)	
E + 5	Launch vehicle correction no. 1	85	85	
E + 20	Launch vehicle correction no. 2	3	3	
S - 26	Saturn approach trim	5	7.5	166.5
S - 24	Spacecraft deflection ΔV			
	∥ Earthline	19	19	
	⊥ Earthline	48	49.5	
S - 10	Saturn approach trim	2	2.5	

B. Spin Control Requirements

Appendages	ΔN (rpm)	I_{sp} (sec)
Stowed	60	225 (continuous)
Deployed	14	160 (pulsed)

C. Precession Requirements

Angle precessed through:	$\Delta\theta$ = 1400 deg
Specific impulse:	I_{sp} = 150 sec
Spin rate	N = 4.8 rpm

The propellant budget (see Table D-3) was derived from these data based on a spacecraft dry weight (minus probe) of 588.3 pounds. The total propellant mass is 30 percent larger than in Pioneer F/G. The required tank size of about 18-inch diameter is compatible with the tank support structure of the baseline Pioneer F/G. However, a new task wou would have to be developed and qualified in this mission.

Table D-3. Summary of Propellant Budget for Earth-Saturn Mission

Assumed Sequence of Maneuvers	Weight (lbm)
Initial weight	918.0
Spin control	2.6
ΔV maneuvers (probe on)	38.5
Precession control	14.3
Probe removal[1]	250.0
ΔV (probe off)	21.3
Final dry weight	588.3
Total propellant weight[1]	79.7
Minimum tank diameter[2] (inches)	17.9

[1]Includes 3 lbm of unusable propellant and pressurant

[2]Assumes the same ratio of usable propellant to ullage volume as for Pioneer F/G propellant tank.

4. WEIGHT SUMMARY

Weight estimates for the Saturn mission flight vehicle are given in Table D-4. Individual weight increments relative to Pioneer G subsystems are listed and sources of the increase are identified in the last column. The total dry weight of the bus spacecraft is 80 pounds greater than in Pioneer G, primarily due to structural changes and the addition of a deployment counterweight. There is ample margin for weight contingency (not included in the tabulated weights).

Table D-4. Saturn Probe Mission Flight Vehicle Weight Estimates

(Pounds)

SUBSYSTEM	PIONEER G*	INCREMENT	S.P. MISSION SPACE VEHICLE	COMMENTS
ELECTRICAL POWER	39.0	0	39.0	
COMMUNICATIONS (BUS-EARTH)	22.5	0	22.5	
COMMUNICATIONS (PROBE-BUS)	0	+4.2	4.2	ADDED RECEIVER AND DEMODULATOR
ANTENNAS	45.5	4.2	49.7	ADDED SPACECRAFT TO PROBE ANTENNA
DATA HANDLING	11.8	1.6	13.4	ADDED PROBE DATA BUFFER AND INCREASED DSU
ELECTRICAL DISTRIBUTION	38.0	5.1	43.1	INCREASED CABLING AND CDU CIRCUITS
ATTITUDE CONTROL	12.6	+0.5	13.1	
PROPULSION (DRY)	24.2	+7.2	31.4	INCREASED TANK (18 INCHES) AND ADDED THRUSTER
THERMAL CONTROL	16.3	+3.1	19.4	ADDED LOUVERS AND INSULATION
STRUCTURE	104.5	+37.1	141.6	
PRIMARY	60.2	+7.0	67.2	ADDED EQUIPMENT BAY
RTG AND MAGNETOMETER SUPPORTS	30.0	7.2	37.2	BOOM INCREASE FOR COUNTERWEIGHT SUPPORT
SECONDARY	14.3	+0.5	14.8	
BUS/PROBE ADAPTER ASSEMBLY	0	+22.4	22.4	ADDED INTERSTAGES
DEPLOYMENT COUNTERWEIGHT	0	+20.0	20.0	ADDED DEPLOYMENT COUNTERWEIGHT
BALANCE WEIGHTS	5.9	+3.1	9.0	INCREASED ALLOWANCE FOR HEAVIER SPACECRAFT
RTG'S	120.4	0	120.4	
SCIENTIFIC EXPERIMENTS	67.0	-5.8	61.5	PER STATEMENT OF WORK
ENTRY PROBE	0	250.0	250.0	PER STATEMENT OF WORK
SPACECRAFT (DRY)	507.7	330.3	838.3	
UNUSABLE PROPELLANT AND PRESSURANT	1.8	12.2	3.0	
USABLE PROPELLANT	59.2	17.5	76.7	
SPACECRAFT GROSS WEIGHT	568.7	350.0	918.0	TARGET WEIGHT 950 POUNDS
LAUNCH VEHICLE ADAPTER	30.0	29.5	59.5	
LAUNCH VEHICLE PAYLOAD WEIGHT	598.7	379.5	977.5	

*REFERENCE: IOC 8524.4-73-04, "PIONEER G MASS PROPERTIES BASED ON FINAL MEASUREMENTS PRIOR TO SHIPMENT," DATED 2-5-73, FROM J. L. PETTY TO W. F. SHEEHAN.

APPENDIX E

PROPULSIVE VELOCITY CORRECTIONS IN THE EARTH-LINE MODE

1. INTRODUCTION

For the spin-stabilized Pioneer spacecraft on an interplanetary trajectory, there are two modes in which propulsive velocity correction maneuvers may be conducted:

a) The normal mode, in which the spacecraft is oriented to an attitude in which the spin axis is parallel to the desired velocity increment ($\Delta\overline{V}$). The velocity correction is attained by continuous firing of thrusters acting parallel to the spin axis. The spacecraft may then be reoriented to its cruise attitude, normally pointing toward the earth. The orientations are achieved by propulsive precession pulses, normally fired at the rate of one pulse pair per revolution.

b) The earth-line mode, in which all velocity corrections are performed with the spacecraft remaining in an earth-pointing attitude. The component of $\Delta\overline{V}$ parallel to the earth line is attained by continuous firing of thrusters parallel to the spin axis, and the component of $\Delta\overline{V}$ perpendicular to the earth line by pulsed firing of thrusters acting in a plane perpendicular to the spin axis. Phasing of the firing pulses relative to the roll index pulses gives this perpendicular component the proper direction in the transverse plane.

This memorandum discusses the need for conducting velocity corrections in the earth-line mode, and examines the potential for the Pioneer F/G spacecraft and future Pioneer-based spacecraft to provide the earth-line mode capability. High-thrust requirements such as orbit insertion maneuvers are not covered.

2. REQUIREMENT FOR EARTH-LINE MODE

The dominating requirement for implementation of the earth-line mode arises from the desire to have downlink communications operational at all times during a critical operation such as a velocity correction maneuver. (For a given spacecraft orientation, uplink communication is always possible at a greater range than downlink.)

With the Pioneer 10 axis pointing within 1.6 degrees of the earth, downlink communication is possible at a range of 20 AU or more at a data

rate of 64 bits per second,* using the spacecraft's high-gain antenna and the 210-ft ground antenna. Using the spacecraft's medium-low gain antenna the maximum range with the spin axis pointed at the earth is about 1.5 AU. With the spin axis 10 degrees away from the earth it is 0.7 AU, and at 30 degrees 0.35 AU. Except for possible interference nulls in the range of 50 to 80 degrees off the spin axis, 64-bps downlink is possible in any spacecraft attitude, out to a range of 0.2 AU.

All velocity correction maneuvers to compensate for launch vehicle injection errors were accomplished before Pioneer 10 exceeded 0.12 AU from the earth. Thus, for these maneuvers, which are expected to comprise the greatest portion of all velocity increments of the Pioneer 10 mission, they could be conducted in any attitude in the normal mode. Even so, it may be desirable to avoid ΔV thrusting while in an attitude where possible interference nulls exist. Indeed, in the case of Pioneer 10, such a region was avoided by resolving the desired ΔV into two components, neither of which required orientation of more than 45 degrees from the earth; this was done at a loss of propulsive efficiency which was quite tolerable because of the very accurate injection.

However, we can see that velocity correction maneuvers conducted later in the mission must be restrained to lower and lower earth look angles, if telemetry is to be maintained during the maneuvers. Beyond 1.5 AU — reached by Pioneer 10 about 140 days after launch — the high-gain antenna must be used, and excursions from earth-pointing must be limited to 1.5 to 2.0 degrees. Thus velocity correction maneuvers are effectively restricted to the earth-line mode, if continuous telemetry is a requirement.

It should be noted that Pioneers 10 and G have the capability to perform velocity correction maneuvers in the normal mode, even if uplink and downlink telemetry is inoperative while the spacecraft points away from the earth. By using the Program Storage and Execution features the propulsive sequence: precession away from earth line, ΔV, precession return to earth line, can be executed autonomously by the spacecraft with all parameters based entirely on quantitative commands which have been

*A lower data rate does not increase the maximum range appreciably.

stored in registers before the start of the maneuver. If the return precession has a residual pointing error, the earth can be "acquired" by closed-loop, conical scan homing using the medium-gain antenna from a 9-degree offset at ranges well beyond Jupiter. Thus the reluctance to employ the normal mode for velocity corrections at ranges where communications will not be continuous stems not so much from a lack of capability of the spacecraft to perform the required maneuvers as from concern over the loss of ability to monitor the maneuver and to intervene in case of abnormal performance. Of course, at long communication ranges, even if communications are unbroken, the ability to monitor and intervene is significantly reduced by the long round trip communication time. So it is really the monitoring and not the intervention which is missed in the normal mode.

Pioneer 10 has had only one small velocity correction maneuver since exceeding 0.2 AU range from the earth, and that ΔV was parallel to the earth line. No additional velocity correction maneuvers are expected. Therefore no requirement has occurred or is expected to occur in which lateral velocity components are exerted in the earth-line mode.

Pioneer G, to be launched in 1973, will have its velocity increment capability of 200 meters/second allocated 100-120 meters/second for midcourse corrections to compensate for injection errors of the launch vehicle, and 60-80 meters/second reserved for a late retargeting maneuver which may be desired if the results of the Pioneer 10 encounter at Jupiter call for a revision in the mission objectives of Pioneer G at its encounter. This retargeting maneuver will have to be done at a range of over 3 AU from the earth. Fortunately thrusting parallel to the earth line gives much of the retargeting capability desired, producing changes in the targeting $\overline{B}$ vector along a line almost parallel to the T axis, or ecliptic plane. But capability for a ΔV component perpendicular to the earth line would be desirable, particularly for out-of-ecliptic changes in targeting (parallel to the R axis).

In other possible future Pioneer missions velocity corrections beyond 1.5 AU from the earth are needed as follows:

Multiple planet flybys	terminal guidance maneuver approaching an intermediate planet (<10 meters/second); trajectory correction maneuver departing from an intermediate planet (<50 meters/second)
Entry probe missions	post-separation maneuver (spacecraft deflection mode) (30-150 meters/second)
Orbiter missions*	orbit trim maneuvers (2-200 meters/second)
Comet intercept missions	trajectory correction after comet orbit is updated (<30 meters/second)
Asteroid flyby missions	terminal guidance maneuver approaching an asteroid (<50 meters/second); retargeting maneuver departing from an intermediate asteroid (<400 meters/second).

As with Pioneer G it is desirable in the case of any planetary mission to retain flexibility for a late retargeting maneuver in response to information received from a preceding spacecraft on a similar mission.

Nearly all of the above maneuvers, possibly excepting comet intercept mission maneuvers, are executed at greater range than 1.5 AU, and if the requirement for continuous communication is in effect, must be done in the earth-line mode.

While some of the $\Delta\overline{V}$'s of these maneuvers may fortuitously lie along the earth line, and while others may be constrained to be along the earth line by accepting some penalty (for example, foregoing control of arrival time while exercising control of the targeting $\overline{B} \cdot \overline{T}$ component), most of these missions have a requirement for ΔV components perpendicular to the earth line.

Thus future Pioneer missions call for significant velocity increments to be attained in the earth-line mode, and significant ΔV components perpendicular to the earth line must be accommodated.

*Orbit insertion maneuvers and major orbit change maneuvers executed at periapsis require high thrust (20-100 pounds) and are not addressed in this memorandum.

3. PIONEER F AND G THRUSTER COMPLEMENT

The thruster complement of the Pioneer F and G spacecraft consists of six one-pound thrusters arranged in three clusters as shown in Figure E-1 The one-pound thrust level is nominal; as a blowdown pressurization system is used, the thrust ranges from 1.2 lbf (full tank) to 0.45 lbf (empty tank). The location of the thrusters with respect to axes through the spacecraft center of mass (appendages deployed) is indicated as follows:

VPT 1, 2, 3, 4	Thrust line displaced from z axis in $\pm$y direction by R = 50.5 inches
SCT 1, 2	Thrust line displaced from x axis: in +z direction by h = 13.0 inches in -y direction by R = 50.5 inches.

The velocity-precession thrusters act parallel to the z axis. They are fired in pairs to give axial velocity increments (VPT 1, 3 or VPT 2, 4) or to produce precession when pulsed at the appropriate time in the spin cycle (VPT 1, 4 or VPT 2, 3). Axial velocity increments are produced by firing the appropriate pair of thrusters in pulses or continuously.

The spin control thrusters act parallel to the x axis. Thruster SCT 1 is fired in pulse pairs with a separation of $(n + \frac{1}{2})$ revolutions to increase the spin rate without accruing precession or lateral ΔV. Thruster SCT 2 is similarly fired in pulse pairs to decrease the spin rate. Thrusters SCT 1 and SCT 2 are fired consecutively in a pulse pair with a separation of $\frac{1}{2}$ revolution to produce a ΔV component perpendicular to the spin axis without accruing a change in spin rate, although a net precession of the spin axis does occur.

4. PRECESSION EFFECTS

This precession of the spin axis, when spin control thrusters are fired consecutively to produce a lateral ΔV component, is illustrated in Figure E-2. This figure shows the location of the spin control thrusters (in inertially-fixed coordinates) at the time of firing each of the two pulses. Because of the lateral and vertical separation of the thrusters from the spacecraft center of mass there is a moment exerted by each pulse which has components parallel to the spin axis producing a spin rate change, and perpendicular to the spin axis producing a precession. Figure E-2 shows

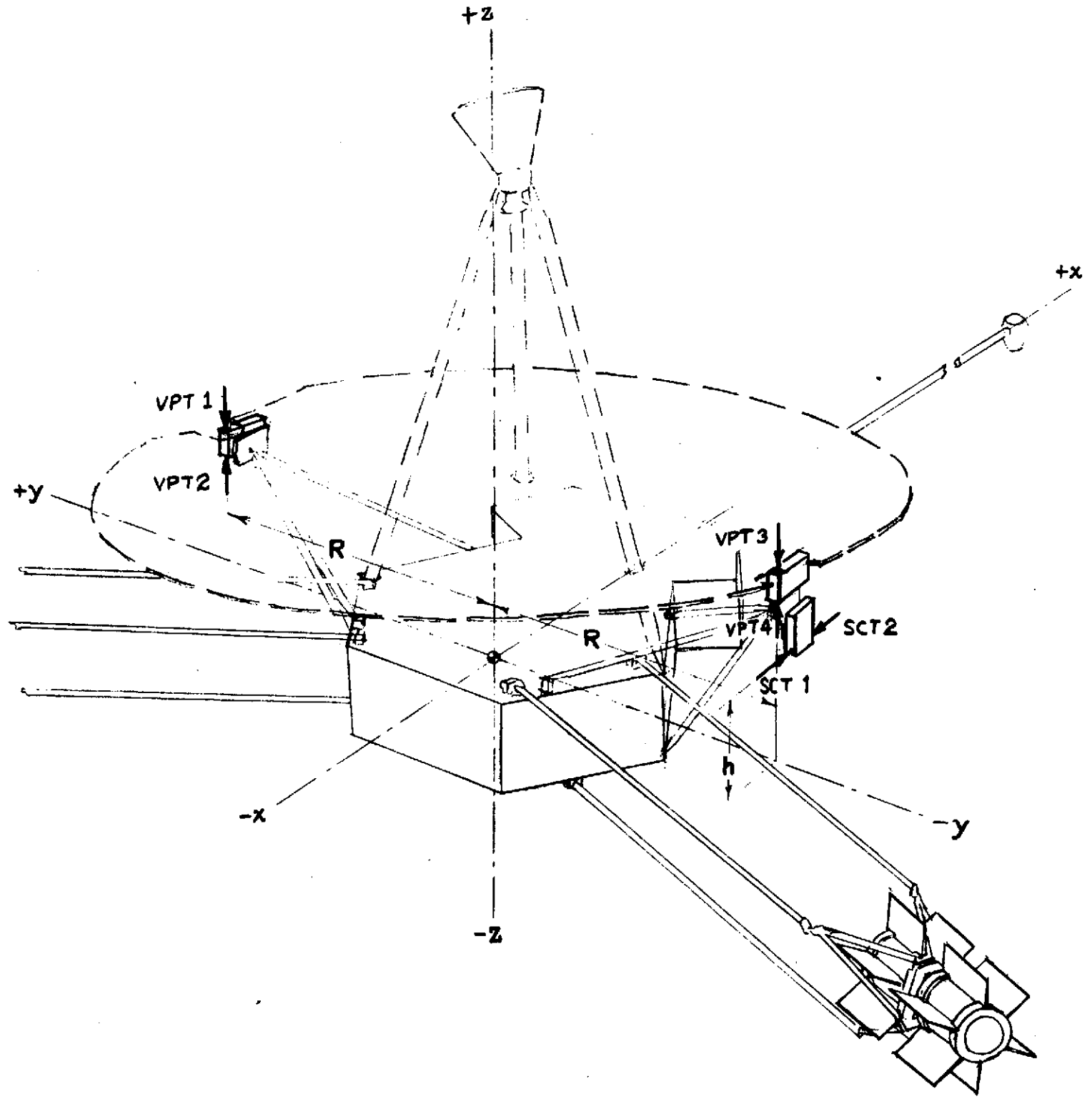

Figure E-1. Pioneer F and G Thruster Complement

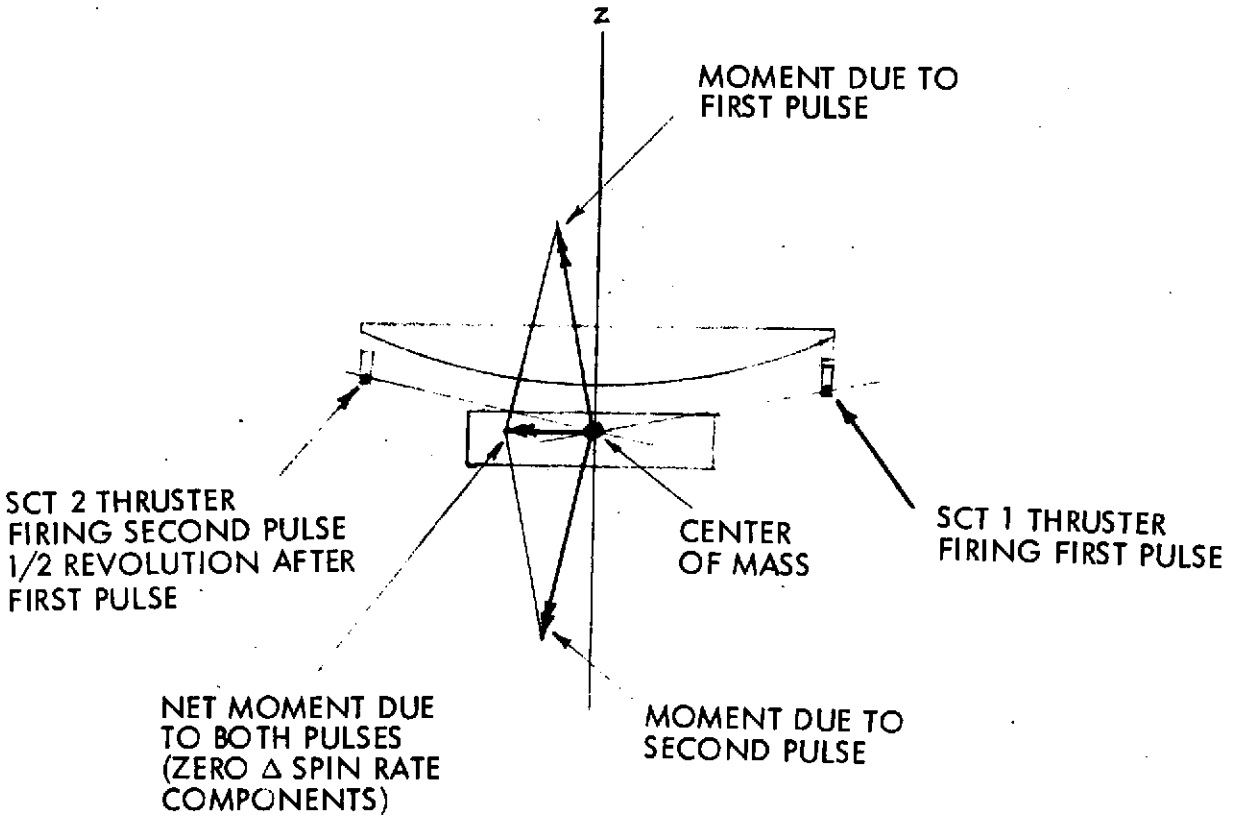

Figure E-2. **Residual Precession Moment from Lateral ΔV Obtained with Spin Control Thrusters**

that after the pair of pulses has been fired giving a net ΔV perpendicular to the spin axis, the combined effect of these moments is to precess the spacecraft, but not change its spin rate.

The magnitude of the precession incurred, in relation to the lateral ΔV effected, is determined from these equations:

$$\Delta\theta_p = C_1 \frac{2 F_1 \Delta t_1 h}{I_s \omega_s} \tag{1}$$

$$\Delta V = C_1 \frac{2 F_1 \Delta t_1}{M} \tag{2}$$

$$\frac{\Delta\theta_p}{\Delta V} = \frac{h M}{I_s \omega_s} = \frac{h}{k_s^2 \omega_s} \tag{3}$$

where

$\Delta\theta_p$ = precession angle displacement due to pulse pair

ΔV = lateral velocity increment effected by pulse pair

C_1 = a constant <1 accounting for the cosine loss due to finite pulse length

F_1 = the force exerted by each thruster when firing

Δt_1 = duration of each firing pulse

h = vertical offset (Figure E-1)

I_s = moment of inertia of spacecraft about spin axis

ω_s = spin angular velocity

M = mass of spacecraft

k_s = radius of gyration of spacecraft about spin axis

Equation (3) can be solved for the ΔV which can be effected by spin control thrusters with $\Delta\theta_p$ restricted to, say, 1.6 degrees which is the half-beamwidth of the high-gain antenna. Using Pioneer F and G values of

$h = 13.0$ in. and $k_s = 61.2$ in. and the nominal spin rate of 4.8 rpm gives

$$\Delta V = \frac{k_s^2 \omega_s \Delta\theta_p}{h} = 0.103 \text{ meters/sec} \qquad (4)$$

We can also solve equation (2) for Δt_1, the accumulated firing time on each of the two thrusters which produces this amount of velocity increment:

$$\Delta t_1 = \frac{M \Delta V}{2 C_1 F_1} = \frac{(560 \text{ to } 505 \text{ lbm})\ (0.103 \text{ m/sec})}{2 \cdot (1.0 \text{ to } 0.955)\ (1.2 \text{ to } 0.45 \text{ lbf})} \cdot \frac{\text{lbf sec}^2}{9.8 \text{ lbm m}}$$

$$\Delta t_1 = 2.40 \text{ to } 6.2 \text{ sec}$$

The range of values of C_1, 1.0 to 0.955 approximates the cosine loss for pulse lengths of 0.125 to 2.0 sec. The major variability in the expression is due to the variation in thrust level with tank pressure.

Suppose an intermediate tank pressure and thrust level leads to $\Delta t_1 = 4.0$ sec. Then after four pulse pairs are fired, each pulse of one second duration, 0.103 meters/sec lateral ΔV will have been achieved, and the spacecraft will have precessed from earth pointing to 1.6 degrees off the earth line.

The correction of this precession is accomplished by firing simultaneously the precession thrusters (for example VPT 1 and VPT 4) at a time in the spin cycle when the thrusters are ±90 degrees away from the positions of Figure E-2. The precession effected in this correction maneuver is given by:

$$\Delta\theta_p = C_2 \frac{2 F_2 \Delta t_2 R}{I_s \omega_s} \qquad (5)$$

where the terms are those given above, except subscript 2 refers to the precession correction maneuver rather than the ΔV maneuver, and R is the radial offset (Figure E-1).

To make this precession cancel the unintended precession which accompanied the ΔV, the firing time is determined by equating (1) and (5):

$$\Delta t_2 = \frac{C_1 F_1 h}{C_2 F_2 R} \Delta t_1 \tag{6}$$

Assume we use equally long pulses at the same tank pressure. Then $C_1 = C_2$ and $F_1 = F_2$. Under these circumstances,

$$\Delta t_2 = \frac{h}{R} \Delta t_1 = 0.257 \, \Delta t_1 \tag{7}$$

Thus, in the example discussed above, after four spin control thruster pulse pairs (one second pulse duration) have been fired to effect a lateral ΔV of 0.103 meters/second, a single one-second pulse pair of the precession thrusters will restore the spacecraft spin axis to its original attitude. (However, to avoid a large nutation, the corrective precession might better be accomplished with a number of shorter precession pulses.)

The precession correction propellant weight is related to the propellant weight used in the lateral ΔV maneuver as follows:

$$\frac{\text{Precession correction propellant}}{\text{Lateral } \Delta V \text{ propellant}} = \frac{\frac{F_2 \Delta t_2}{I_{sp2}}}{\frac{F_1 \Delta t_1}{I_{sp1}}} = \frac{I_{sp1}}{I_{sp2}} \frac{h}{R} \tag{8}$$

Again, if the maneuvers are at the same pulse length and tank pressure, the specific impulses will be equal, and the ratio is $h/R = 0.257$. Thus, for each pound of propellant producing lateral ΔV, another 0.257 pound of propellant must be used to correct the undesired precession. (If the precession correction is done with a larger number of shorter pulses to reduce nutation, I_{sp2} will be reduced, and the penalty is increased somewhat.)

Operationally we have a fairly complex sequence of propulsive maneuvers to be executed, particularly if the lateral ΔV component is

of substantial magnitude, for example, tens of meters per second. We can envision a series of lateral ΔV pulse pairs being commanded, utilizing the spin control thrusters, followed by a series of precession correction pulses, fired by the velocity precession thrusters. This sequence could be repeated a number of times, with faith that the open-loop accuracy of these maneuvers would result in the restoration of the spacecraft attitude sufficiently close to earth pointing. However, ultimately the accrual of errors due to deviations of propulsive performance from the predicted performance would require correction that cannot be done by continuing open-loop propulsive maneuvers.

At this time there would be two options. The first would be to delay sending further commands until the results of the commands already sent could be determined and evaluated. This determination and evaluation would be by means of the pointing direction components determined by the onboard Conscan signal processor and included in the telemetry to the ground. The accrued pointing error would then be known on the ground, and the next train of ΔV pulse sequences and precession correction pulse sequences would incorporate precession pulses necessary to remove these accrued errors. In this way the results of the entire ΔV sequence of propulsive maneuvers are monitored periodically on the ground and any accrued errors can be corrected in the next sequence of commands. Of course, this requires an interruption in the transmission of propulsion commands each time this monitoring is desired, and with a duration at least equal to the round trip light time. This delay is more than 1 hour at the distance of Jupiter and about 2.5 hours at the distance of Saturn.

Another approach to the elimination of accrued pointing errors is to employ the conical scanning or closed-loop precession mode on the spacecraft, to have it home on uplink RF signals from the earth whenever there is concern that the accrued errors may be approaching desired limits. Certainly when this method is first employed to remove accrued precession errors after sequences of open-loop ΔV maneuvers and open-loop precession correction pulses, it will be desirable to monitor the performance on the ground, to ascertain that accrued errors were within predicted limits and

and that the Conscan operation does precess the spacecraft so as to remove these accrued errors. This first monitoring will again entail a time delay of at least a round trip light time. However, after the first use of the Conscan maneuver to remove accrued precession errors is observed and determined to be satisfactory, it may well be feasible to employ this mode at subsequent times in the overall sequence of propulsive maneuvers by sending open-loop commands and without waiting for confirmation by the monitoring of telemetry before proceeding with the next sequence of lateral ΔV pulses.

While the total sequence of commands and monitoring operations is necessarily complex to accomplish a substantial ΔV maneuver by the use of thrusters earth-line mode it is possible, by the means described above, to keep the total time of the operation within bounds.

We will also see that there are design modifications that can be incorporated into future Pioneers which will drastically reduce the precession and other cross-coupling effects which are incurred during the course of lateral ΔV pulses, and therefore result in decidedly simpler operational sequences for ΔV propulsion in the earth-line mode.

5. ALTERNATE THRUSTER COMPLEMENTS

For future Pioneer missions it may be desirable to alter the complement of thrusters to facilitate velocity corrections in the earth-line mode. Possible changes and the corresponding benefits are the following, which may be applied singly or in combination:

Change	Benefits
a) Addition of a fourth Thruster Cluster Assembly (TCA) on the +y side of the spacecraft to provide a second spinup thruster and a second despin thruster (Figure E-3a)	• Adds redundancy and reliability for spin control functions • Adds redundancy and reliability for obtaining the lateral ΔV component in the earth-line mode • By permitting simultaneous firing of two thrusters for the lateral ΔV, the transient spin-rate change of the sequential-pulse method is avoided.

Change	Benefits
b) Lowering of spin control thrusters to the plane of spacecraft center of mass (c. m.), z = 0 in Figure 1. Thus h is reduced to zero. (Figure E-3b)	• Avoids the incurring of precession moment as a result of firing the pulse pair to provide a lateral ΔV component.
c) Addition of a radial thruster, with the thrust line directed from the spacecraft c. m. (Figure E-3c)	• Permits lateral ΔV to be obtained with the firing of single pulses • Avoids transient spin-rate change of the sequential-pulse method • Avoids incurring a precessing moment as a result of the lateral ΔV maneuver.

The elimination or great reduction in precessing moment which results from change (b) or (c) leads to an operationally much simpler lateral ΔV maneuver by eliminating the need for precession corrections. It also avoids the 25. 7 percent propellant penalty to perform the precession corrections.

There are also some disadvantages involved in implementing these changes. Changes (a) and (c) which add one or two thrusters incur the obvious penalties of thruster weight and the requirements to provide structural support, unobstructed exhaust paths, propellant feed lines, and thermal control. Other disadvantages include the necessary increase in complexity of the Control Electronics Assembly for the circuitry to control the added thruster(s) and to accommodate additional commands to implement operational modes utilizing the added thrusters.

In locating new thrusters of changes (a) or (c) or in relocating the thrusters of change (b) additional considerations apply. The new thrusters and their supports should not obstruct the view of any optical (or other) sensors. Furthermore, the exhaust products of the thrusters should not impinge on any components -- such as optical sensors -- which are sensitive to such contamination. These considerations may make the addition of a radial thruster, change (c), the most desirable way to eliminate the precession problem.

For changes (b) and (c) which aim to eliminate the precession effect from the lateral ΔV maneuver, the resultant lateral force must be on a line

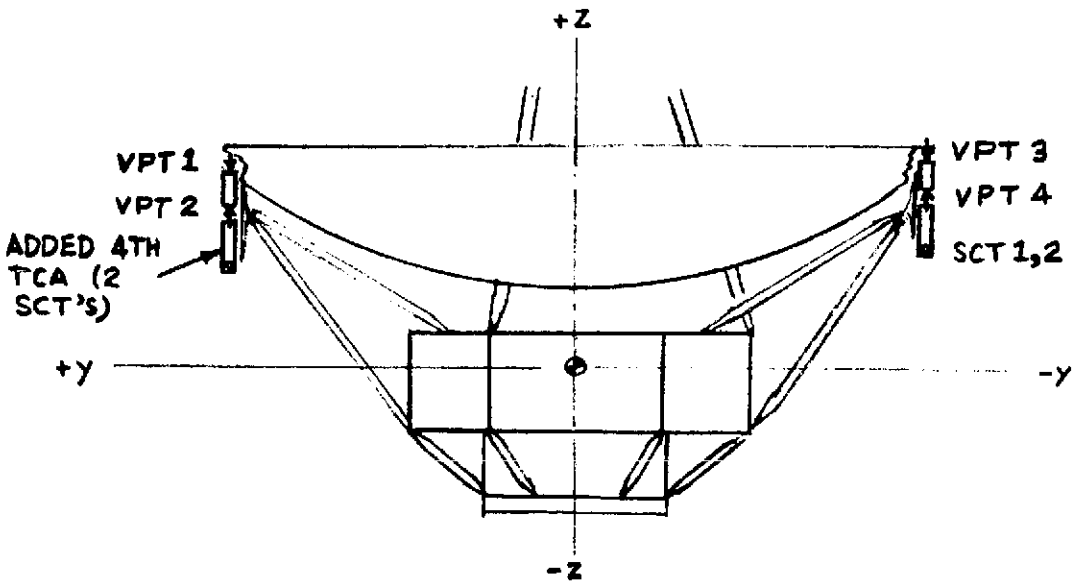

a) ADDITION OF FOURTH TCA

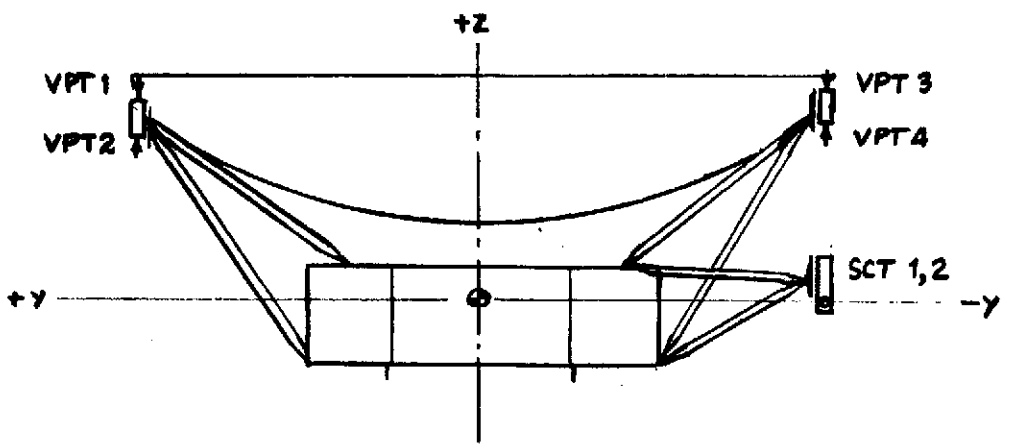

b) LOWERING OF SPIN CONTROL THRUSTERS

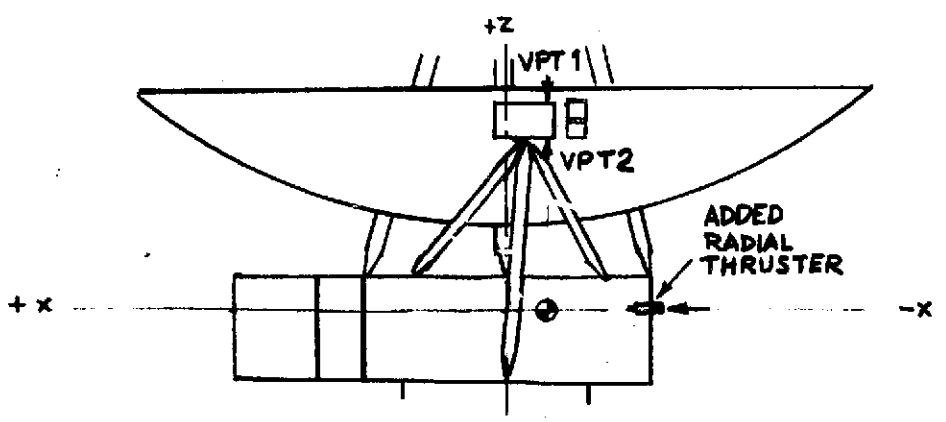

c) ADDITION OF RADIAL THRUSTER

Figure E-3. **Alternate Thruster Complements**

which passes through the spacecraft center of mass. Misalignment or mismatch of the thrusters can mean that this goal is not met precisely, and extensive ΔV firing will lead to the accumulation of spin rate and precession changes. These are examples of cross-coupling terms.

Even if the thruster alignment were perfect, there are both the uncertainty in the location of the c. m. of the spacecraft and the expected excursion of it from its nominal location as appendages are deployed and as propellant is consumed. These characteristics produce similar cross-coupling effects.

In two possible Pioneer configurations -- for atmospheric entry probe missions and for orbiters of the outer planets -- a large mass which is separable (the probe) or depletable (the orbit insertion propellant) is located on the z-axis below the equipment compartment. This causes a significant change in the z-coordinate of the vehicle's c. m. with separation or depletion. Therefore, lateral ΔV thrusters aligned with the c. m. during one phase of the mission will be misaligned and will induce a coupled precession during another phase. For these configurations several options exist:

d) Have more than one (set of) lateral ΔV thruster(s), each one aligned with the c. m. location during one mission phase, e. g., before and after probe separation.

e) With a radial thruster, utilize a hinging mechanism with two or more positions, so that when the c. m. location changes, the thruster can be rotated to change its line of action accordingly.

f) Locate a single fixed (set of) lateral ΔV thruster(s) to cater to the mission phase with the dominant lateral ΔV requirement; in other mission phases, where the c. m. is at a different location, either forego lateral ΔV maneuvers in the earth-line mode, or accept and compensate for the accompanying precession effects.

Figure E-4 illustrates options (d) and (e), assuming the use of a radial thruster, for an atmospheric probe mission.

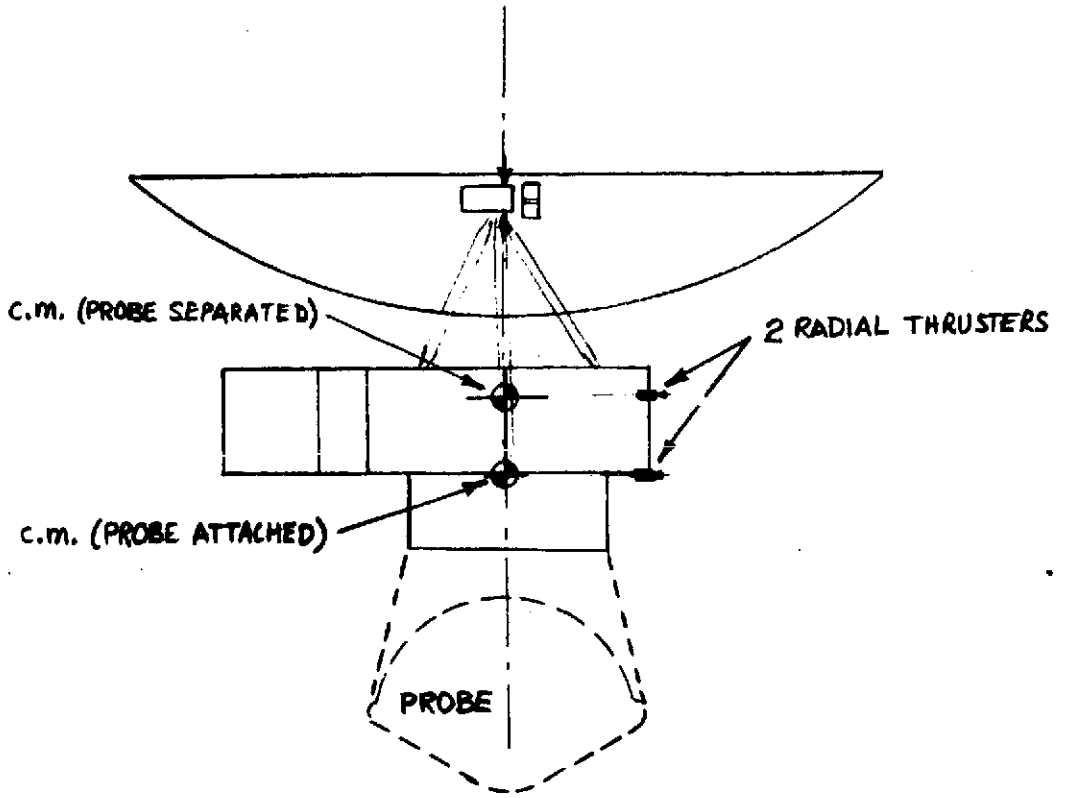

a) TWO RADIAL THRUSTERS

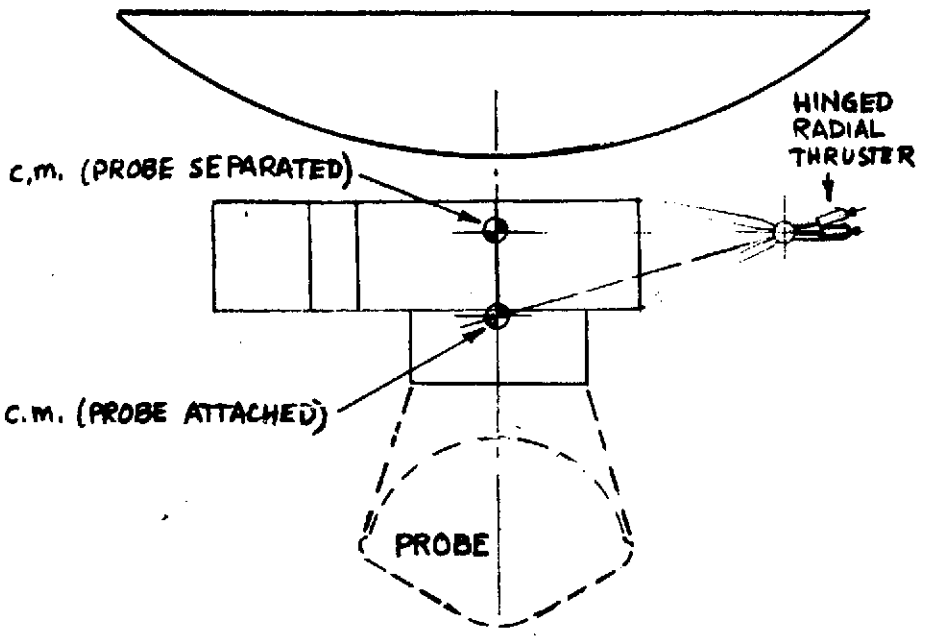

b) ONE RADIAL THRUSTER HINGED

Figure E-4. **Options to Accommodate Longitudinal Displacement of Center of Mass**

6. POSSIBLE CANTING OF THE RADIAL THRUSTER

The spin control thrusters are mounted to act in a plane perpendicular to the spin axis. (Otherwise a spin control maneuver would cause an unwanted longitudinal ΔV component.) However, it is not necessary that a radial thruster, added to give a lateral ΔV component, act perpendicular to the spin axis. It may be canted significantly away from perpendicular without a very great penalty in its use for velocity corrections in the earth-line mode.

One reason for canting the radial thruster was illustrated in the preceding section, where the thruster is hinged so as to act through the spacecraft c. m. which has two distinct locations for two different phases of the mission. At most, only one of the orientations of this thruster will be perpendicular to the spin axis. Another reason, not necessarily related to a variable c. m. location, would be to permit the radial thruster to be at a favorable location on the spacecraft. For example, for the Multiple Asteroid Flyby mission* several optical instruments are located in a bay added to the -x end of the equipment compartment, leading to a conflict with the use of that location for a radial thruster. A compromise location of the radial thruster is at the same region where the axial and tangential thrusters are mounted, below the rim of the antenna dish. At this location the line of action which passes through the spacecraft c. m. must be canted some 12 to 15 degrees above the plane perpendicular to the spin axis.

Figure E-5 shows how a desired ΔV is resolved into components in the instances where the radial thruster acts perpendicular to the spin axis or canted from the perpendicular plane. In this example the desired $\Delta\overline{V}$ has a component in the +z direction, and with the radial thruster canted into the +z hemisphere (and therefore the radial thruster giving a ΔV in the -z hemisphere) more propellant is consumed than in the case of the uncanted radial thruster. However, if the desired $\Delta\overline{V}$ had a component in the -z direction, the use of the radial thruster canted into the +z hemisphere would entail a reduction in propellant.

*See "Study of Multiple Asteroid Flyby Missions," TRW Report 22442-6003-RU-00, 17 November 1972, for NASA Ames Research Center under Contract NAS2-6866.

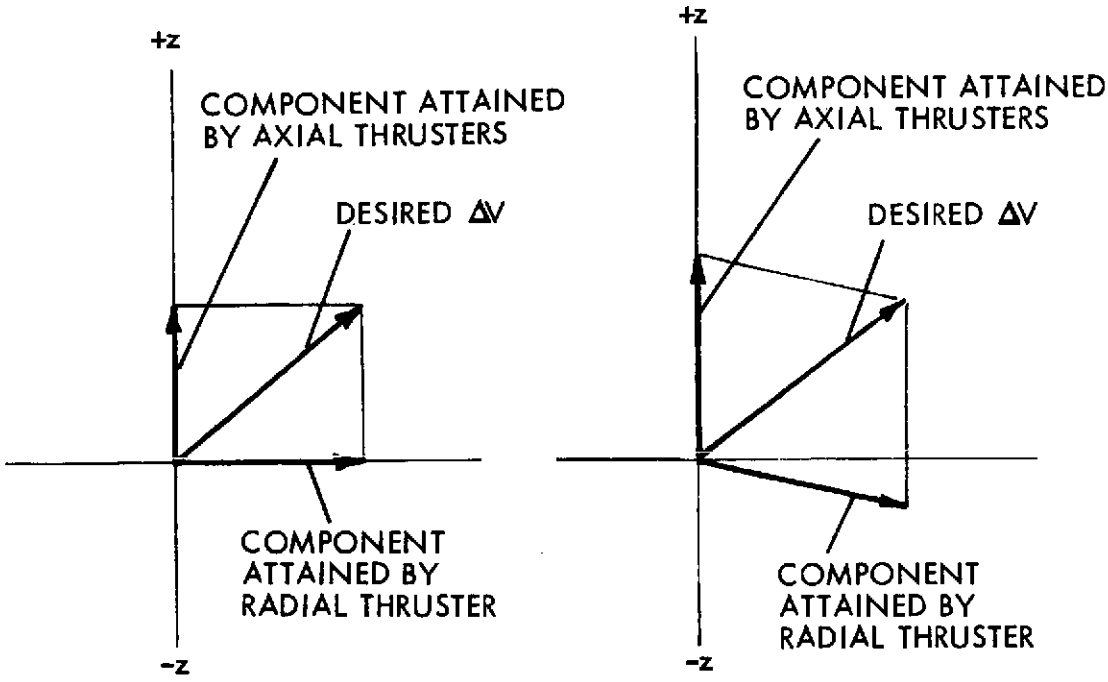

Figure E-5. **Resolution of ΔV into Components**

Another advantage of the canted thruster may be noted. Doppler radio tracking will give immediate confirmation of the execution of a lateral ΔV maneuver, because the proportional longitudinal component is along the earth line.

7. EFFICIENCY OF THE LATERAL ΔV MANEUVER

Three factors cause the efficiency of the lateral ΔV maneuver to be lower than that of the longitudinal component:

a) The precession effect, requiring additional propellant to remove precession accumulated as a result of the lateral ΔV maneuver.

b) The reduced specific impulse (I_{sp}) of firing radial or spin control in a pulsed mode, compared with firing axial thruster continuously.

c) The cosine loss incurred when the firing pulse lasts over a significant portion of a spin revolution, leading to different thrust directions at different portions of the firing pulse.

The first factor is negated by the methods of Section 5 which eliminate the precessing moment by directing the radial force through the spacecraft c. m. Factors (b) and (c) both depend on pulse length, but in contrary ways. The I_{sp} effect, (b), causes a larger penalty when the pulses are shortest, because thruster temperature is low; but the cosine loss, (c), is greatest when the pulses are long, and the spacecraft rotation is appreciable during the pulse. The combination of effects (b) and (c) leads to a broad maximum in efficiency versus pulse length, as indicated in Figure E-6. For this example based on the nominal Pioneer F/G spin rate of 4. 8 rpm, the optimum pulse duration is about 1 second, and the composite efficiency, η, for that pulse length is 0. 97.

This efficiency, η, is the product of two effects. The I_{sp} effect is the ratio of the I_{sp} for a given pulse duration I_{sp} for continuous firing:

$$I_{sp} \text{ effect} = I_{sp}/I_{sp} \text{ (cont.)},$$

and is shown in one curve in Figure E-6. The other curve is the cosine loss effect, determined by integrating the force component in the direction of the mean pulse resultant, over the firing angle ϕ_o:

$$\text{cosine loss effect} = \frac{\int_{-\phi_o/2}^{+\phi_o/2} \cos\phi \, d\phi}{\int_{-\phi_o/2}^{+\phi_o/2} d\phi} = \frac{\sin\frac{\phi_o}{2}}{\frac{\phi_o}{2}}$$

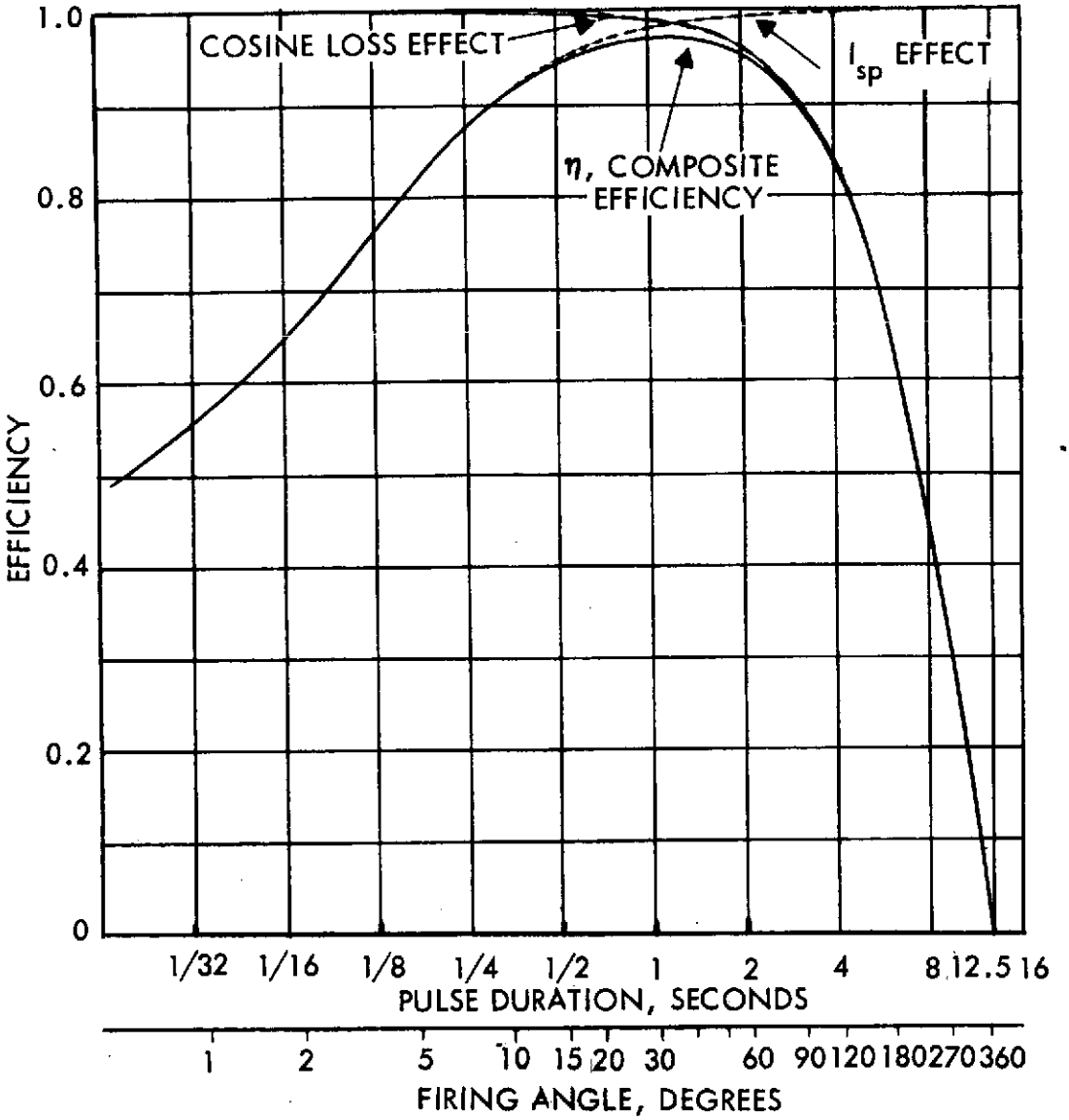

Figure E-6. **Composite Efficiency of Pulsed Lateral ΔV Thrusting**

8. CAPABILITY COMPARISONS

We speak of "capability" as the magnitude of $\Delta\bar{V}$ which can be effected in a particular direction in space by the burning of, say, 1 pound of propellant. This ΔV is normalized with respect to the value which can be effected by burning of 1 pound of propellant by continuous firing of the axial thrusters. Thus, "capability" in any direction, based on firing of longitudinal and lateral components in the earth-line mode, represents the efficiency compared with the normal mode.* (For comparison we assume the same propellant supply pressure and the same spacecraft mass in all cases.)

Thus, "capability" in the earth-line mode accounts for the reduced efficiency, η, of the pulsed lateral ΔV component (as indicated in Figure E-6, including in addition - if appropriate - a penalty for precession correction propellant) and for the penalty incurred in generating the $\Delta\bar{V}$ vector by adding longitudinal and radial components.

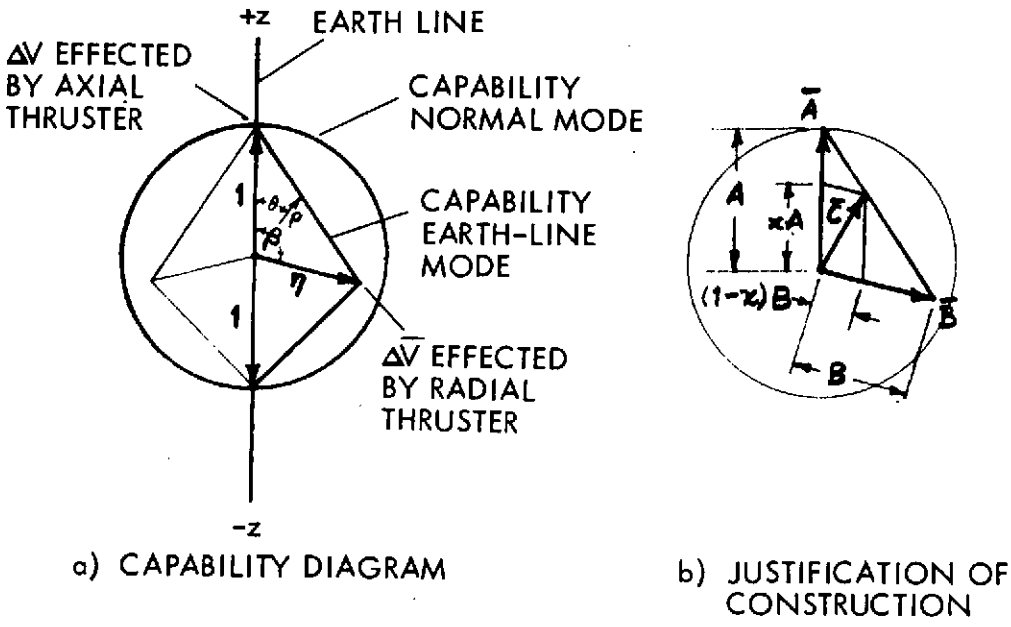

Figure E-7. **Capability of $\Delta\bar{V}$ in the Earth-Line Mode, Compared with Normal Mode**

*The propellant required for precession to and from the $\Delta\bar{V}$ direction in the normal mode is disregarded in this comparison, as it is not proportional to the magnitude of the ΔV.

Figure E-7a shows the combination of these effects. It is in the plane of the $\Delta\overline{V}$ and the earth line, and indicates ΔV capability as a function of $\Delta\overline{V}$ direction, θ. The capability per unit propellant mass in the earth-line mode is indicated by the straight-line segments, and in the normal mode by the unit circle.

Figure E-7b illustrates the construction technique for the earth-line mode, and verifies that the straight-line segments are appropriate. If a given mass of propellant would produce a $\Delta\overline{V}$ of magnitude A with the axial thrusters or B with the radial thrusters, then the same mass apportioned in the ratio x:(1-x) to the axial and radial thrusters produces a $\Delta\overline{V}$ indicated by the vector $\overline{C}$, where:

$$\overline{C} = x\overline{A} + (1 - x)\overline{B} = \overline{B} + x(\overline{A} - \overline{B})$$

Thus the tip of $\overline{C}$ must lie on the line from $\overline{B}$ to $\overline{A}$.

Because the $\Delta\overline{V}$ direction may be in any plane containing the earth line, the complete picture of capability is given by rotating Figure E-7a about the earth line, producing a three-dimensional figure (Figure E-8). The capability of the earth-line mode is given by the two conical surfaces within the unit sphere representing the normal mode.

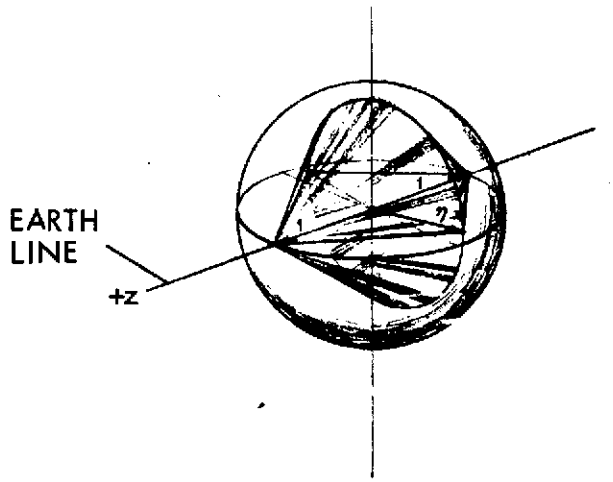

Figure E-8. **Earth-Line Mode ΔV Capability (3 Dimensional)**

The methods shown in Figures E-7 and E-8 can be used directly to determine the propellant efficiency of the earth-line mode if the direction of the $\Delta\overline{V}$ is known relative to the earth line. However, often this direction is not known in advance, or only its statistical distribution, $f(\theta)$, is known.

We may then estimate the expected value of the propellant efficiency, μ, of the earth-line mode:

$$\mu = \frac{\int_0^{\pi} f(\theta)\, \rho(\theta)\, d\theta}{\int_0^{\pi} f(\theta)\, d\theta} \qquad (1)$$

Here,

θ = colatitude of $\Delta\bar{V}$, measured from the earth line

$\rho(\theta)$ = capability, as a function of θ, from Figure E-7 or E-8

$f(\theta)$ = the probability distribution of the $\Delta\bar{V}$ for the maneuver under consideration.

From Figure E-7 we may write

$$\rho(\theta) = \cos \theta_o \sec (\theta - \theta_o) \qquad [0 \leq \theta \leq \beta] \qquad (2)$$

$$\rho(\theta) = -\cos \theta_1 \sec (\theta - \theta_1) \qquad [\beta \leq \theta \leq \pi] \qquad (3)$$

where

$$\tan \theta_o = \frac{1 - \eta \cos \beta}{\eta \sin \beta} \qquad (4)$$

$$\tan \theta_1 = -\frac{1 + \eta \cos \beta}{\eta \sin \beta}. \qquad (5)$$

θ_o and θ_1, define radial lines perpendicular to the two line segments.

If the direction of the ΔV is completely unknown, i. e., it has equal probability in every spherical direction, we may write $f(\theta) = \sin \theta$, recognizing that there are more directions near the equator than near the pole of a sphere. Under these circumstances we can compute the expected efficiency μ by Equations (1) to (5), getting:

$$\mu = \frac{\eta \sin \beta}{(1 + \eta^2)^2 - 4\eta^2 \cos^2 \beta} \left[\frac{\pi}{2} (1 - \eta^2 \cos 2\beta) - \eta(1 + \eta^2) \log \frac{1}{\eta} \sin \beta \right.$$
$$\left. + \eta(1 - \eta^2)\left(\beta - \frac{\pi}{2}\right) \cos \beta \right] \qquad (6)$$

The results of Equation (6) are plotted as contours on a β-η diagram in Figure E-9.

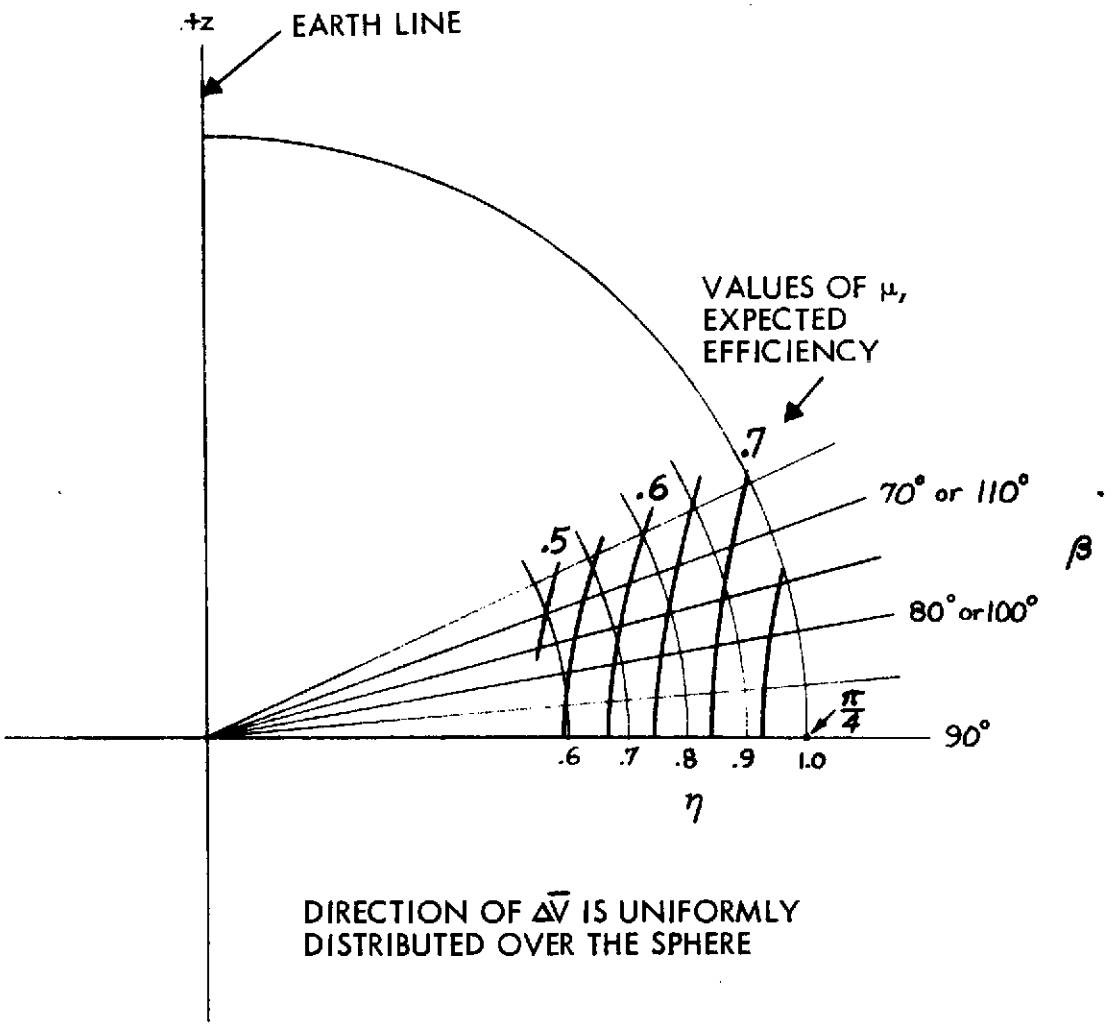

Figure E-9. **Expected Propellant Efficiency in the Earth-Line Mode, Uniform Distribution of $\Delta\bar{V}$ Direction**

Special examples of Equation (6) include these:

- Radial thrusting efficiency, η, = 1:

$$\mu = \frac{\pi}{4} \sin \beta$$

- Radial thruster is not canted; $\beta = 90^{\circ}$:

$$\mu = \frac{\pi \eta}{2(1 + \eta^2)} \left(1 - \frac{2\eta}{\pi} \log \frac{1}{\eta}\right)$$

- $\eta = 1$ and $\beta = 90^{\circ}$:

$$\mu = \frac{\pi}{4}$$

Thus the maximum expected efficiency, with $\Delta\bar{V}$ direction uniformly distributed, is 78.5 percent. With the radial thrusting efficiency η, equal to 97 percent (Figure E-6), $\mu = 0.77$ if the radial thruster is not canted, and $\mu = 0.75$ with the thruster canted 12 degrees ($\beta = 78$ degrees). Thus, the reduction of expected efficiency, μ, below unity is largely due to the penalty of executing the vector components separately.

9. CONCLUSIONS

The Pioneer F and G design can produce propulsive velocity corrections in the normal mode (precessing the spin axis to the $\Delta\bar{V}$ direction), but at large distances from the earth the normal mode causes earth-spacecraft communications to be interrupted during the maneuver. The Pioneer F and G design can also produce velocity corrections in the earth-line mode, maintaining continuous communications, but with disadvantages in operational complexity and propellant efficiency to correct for the precession which accompanies lateral ΔV thrusting. (Longitudinal ΔV is attained routinely with axial thrusters.)

Improvements in the design of future Pioneers can overcome these disadvantages; by relocating the spin control thrusters or adding a radial thruster to act through the spacecraft center of mass. This eliminates the accrual of precession with lateral ΔV. Thus the operation of the maneuver is greatly simplified, as frequent precession correction maneuvers are not needed. Moreover, the propellant efficiency is raised by eliminating the precession correction maneuver. The propellant efficiency is still not as good as in the normal mode, but the primary deficiency is attributable to the penalty of executing the $\Delta\bar{V}$ components separately.

For those missions such as entry probe missions where the spacecraft center of mass undergoes a marked change in longitudinal position, the above improvements apply in only one mission phase; however, they can be extended to all phases by using multiple radial thrusters or a radial thruster which can be commanded into multiple orientations.

Thus, relatively minor modifications to the Pioneer propulsion subsystem will make it suitable for advanced missions requiring $\Delta\bar{V}$'s with extensive lateral components at large distances from the earth.

APPENDIX F

STRESS ANALYSIS

1. STRESS ANALYSIS - CONICAL ADAPTER

1.1 Condition VII - Qualification Vibration (Ref. 1)

Lateral Sta. 11.7

P_L = 1093 (6.8) = 7430 lbs ult.

Rocking moment (M_R) = $\frac{788}{580}$ (24,000) = 32,600

$M = 32,600 + \left[(788)(29.9) + (250)(-5.1)\right] 6.8$

$M = 32,600 + \left[22,350\right] 6.8 = 184,300$ in-lbs ult.

Axial Sta. -11.7

P_Z = (1038)(18.3) = 19,000 lbs ult.

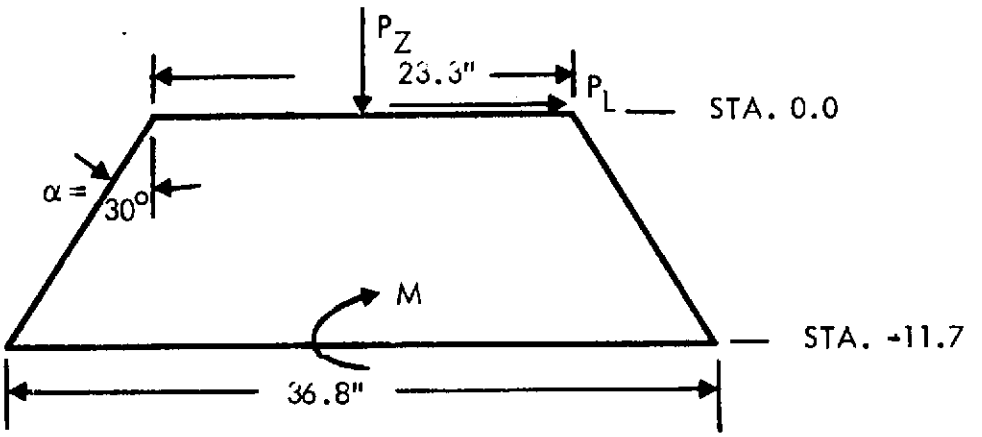

From Reference 2 determine load allowables

$P_U = 11.65 \div \cos 30^\circ = 13.45$

$P_L = 18.4 \div \cos 30^\circ = 21.3$

Assume t = 0.04 in.

$P_{U/t} = 13.45/0.04 = 336$; $C_A = 0.24$, $C_b = 0.30$

$P_{L/t} = 21.3/0.04 = 532$; $C_A = 0.19$, $C_b = 0.26$

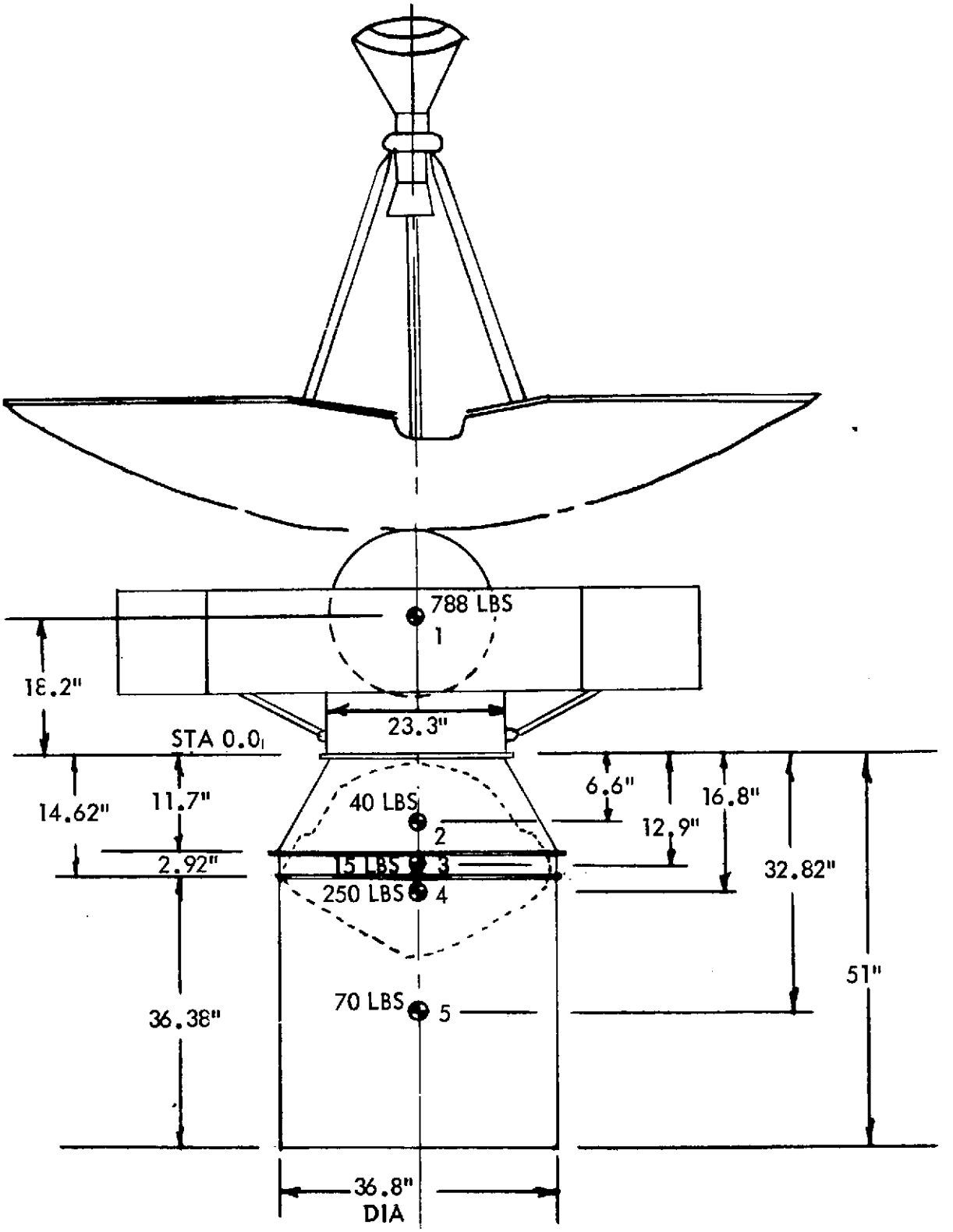

TE-364-4 STAGE

Upper end of conical section (allowable loads)

$$P_{AU} = 0.24(2\pi)(10^7)(0.04)^2(\cos^2 30^\circ) = 18,150 \text{ lbs}$$

$$M_U = 0.30(\pi)(10^7)(11.65)(0.04)^2(\cos^2 30^\circ) = 132,300 \text{ in-lbs}$$

Lower end of conical section (allowable loads)

$$P_{AL} = 0.19(2\pi)(10^7)(0.04)^2(\cos^2 30^\circ) = 14,350 \text{ lbs}$$

$$M_L = 0.26(\pi)(10^7)(18.4)(0.04)^2(\cos^2 30^\circ) = 181,000 \text{ in-lbs}$$

Try t = 0.05 inch

$$P_{U/t} = 13.45/0.05 = 260; \; C_A = 0.270 \; C_b = 0.325$$

$$P_{L/t} = 21.3/0.05 = 425; \; C_A = 0.220 \; C_b = 0.280$$

Upper end allowable loads

$$P_{A_U} = 0.27(2\pi)(10^7)(0.05)^2(\cos^2 30^\circ) = 31,900 \text{ lbs}$$

$$M_U = 0.325(\pi)(10^7)(11.65)(0.05)^2(\cos^2 30^\circ) = 225,000 \text{ in. -lbs}$$

Lower end allowable loads

$$P_{A_L} = 0.22(2\pi)(10^7)(0.05)^2(\cos^2 30^\circ) = 26,000 \text{ lbs}$$

$$M_L = 0.28(\pi)(10^7)(18.4)(0.05^2)(\cos^2 30^\circ) = 305,000 \text{ in. -lbs}$$

1.2 Margins for Lateral Qualification Vibration Condition VII (Ref. 1)

Upper End

$$R_M = 129,100 \div 132,300 = 0.98$$

$$\text{M. S.} = \frac{1}{R_M} - 1 = +0.02$$

Lower End

$$R_M = 184,300 \div 305,000 = 0.60$$

$$\text{M. S.} = \frac{1}{R_M} - 1 = +0.67$$

1.2 Margins for Axial Qualification Vibration Condition VII (Ref. 1)

$$R_A = 14,300 \div 18,150 = 0.78 \text{ (critical upper end)}$$

$$M.S. = \frac{1}{R_A} - 1 = +0.28$$

Material: 2024 T 851 aluminum.

For adequate strength of conical adapter use 0.045 inch at top and 0.050 inch at the bottom (linear taper in between).

2. PROBE TO LAUNCH VEHICLE INTERSTAGE CYLINDER

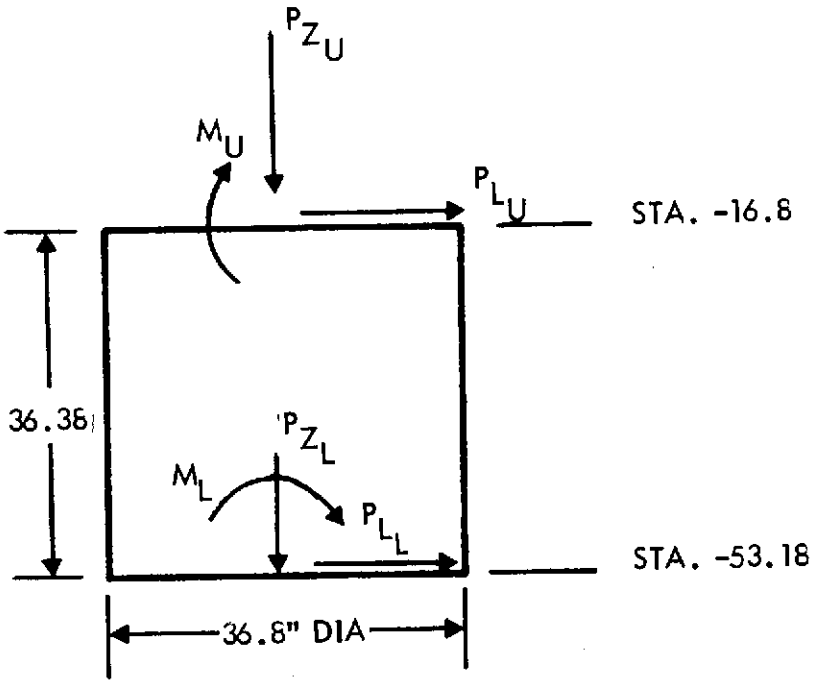

2.1 Station -16.8 Lateral Qualification Vibration Condition VII (Ref. 1)

$$P_{L_U} = \left[788 + 40 + 15 + 250\right] 6.8 = 7430 \text{ lbs ult.}$$

$$M_U = 32,000 + \left[(738)(32.82) + (40)(8.02) + (15)(1.92) + (250)(-2.18)\right] 6.8$$

$$M_U = 207,600 \text{ in.-lbs ult.}$$

2.2 Axial Qualification Vibration Condition VII (Ref. 1)

$$P_{Z_U} = 1093(18.3) = 20,000 \text{ lbs ult.}$$

2.3 Aft End Station -53.18 Lateral Qualification Vibration Condition VII (Reference 1)

$$P_{L_L} = \left[788 + 40 + 15 + 250 + 70\right] 6.8 = 7,906 \text{ lbs ult.}$$

$$M_L = \Big[(788)(69.2) + (40)(44.4) + (15)(38.3) + (250)(34.2) + (70)(18.19)\Big] 6.8 + 32,600$$

$$M_L = 487,600 \text{ in.-lbs ult.}$$

Axial qualification vibration Condition VII (Reference 1)

$$P_{Z_L} = 1163(18.3) = 21,300 \text{ lbs ult.}$$

2.4 Compute Allowables from Reference 2

Assume t = 0.04

$$R/t = 18.4/0.04 = 460 \qquad C_A = 0.205;\ C_b = 0.28$$

$$P_{Allow} = 0.205(2\pi)(10^7)(0.04)^2 = 20,600 \text{ lbs}$$

$$M_{Allow} = 0.28(\pi)(10^7)(18.4)(0.04)^2 = 259,000 \text{ in.-lbs}$$

M.S. on bending at upper end

$$R_b = \frac{207,600}{259,000} = 0.80$$

$$\text{M.S.} = \frac{1}{R_b} - 1 = +0.25$$

M.S. on axial load at upper end

$$R_A = \frac{20,000}{20,600} = 0.97$$

$$\text{M.S.} = \frac{1}{R_A} - 1 = +0.03$$

Use t = 0.045 at upper end.

2.5 Determine Thickness at Aft End of the Cylinder

For $t = 0.062$

$R/t = 18.4/0.062 = 297 \quad C = 0.25; C_b = 0.31$

$$P_A = 0.25(2\pi)(10^7)(0.062^2) = 60,383$$

$$M = 0.31(\pi)(10^7)(18.4)(0.062)^2 = 688,855$$

Check margins of safety

M. S. on bending aft end

$$\text{M. S.} = \frac{688,855}{487,600} - 1 = +0.41$$

M. S. on axial load aft end

$$\text{M. S.} = \frac{60,383}{21,300} - 1 = +1.83$$

Use $t = 0.045$ at forward end and $t = 0.062$ at aft end. Vary thickness linearly between forward and aft ends. Material is 2024 T 851 aluminum.

REFERENCES

1. TRW 8522.2-73-26, "Preliminary Load and Strength Evaluation for Saturn/Uranus Probe," dated 14 February 1973.

2. STL/TR-60-0000-19425, "Final Report on the Development of Design Criteria for Elastic Stability of Thin Shell Structures," dated 18 November 1970.

3. RTG MOUNTING PLATE

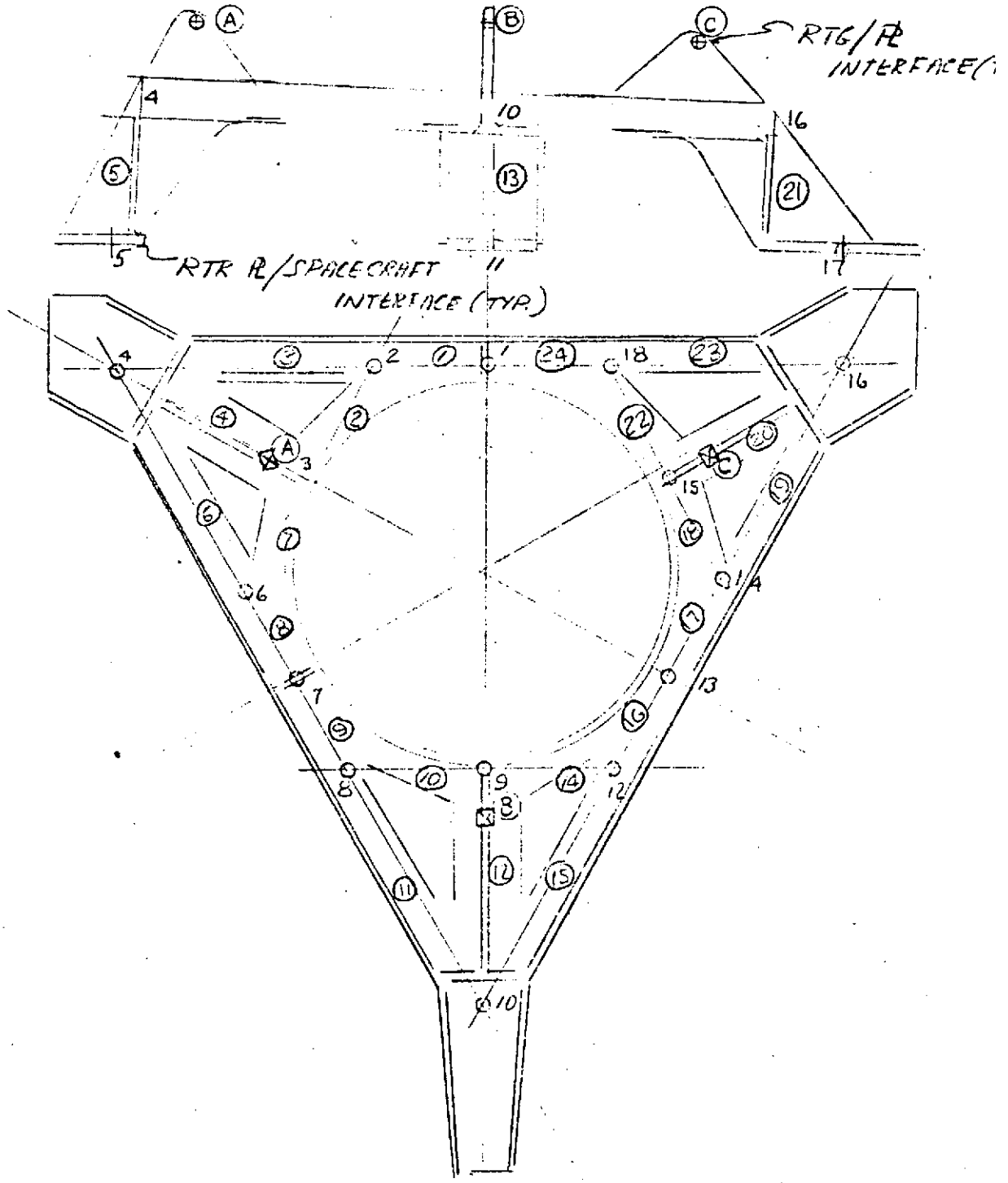

RTG Mounting R Computer Model

RTG / Mounting & Interface loads

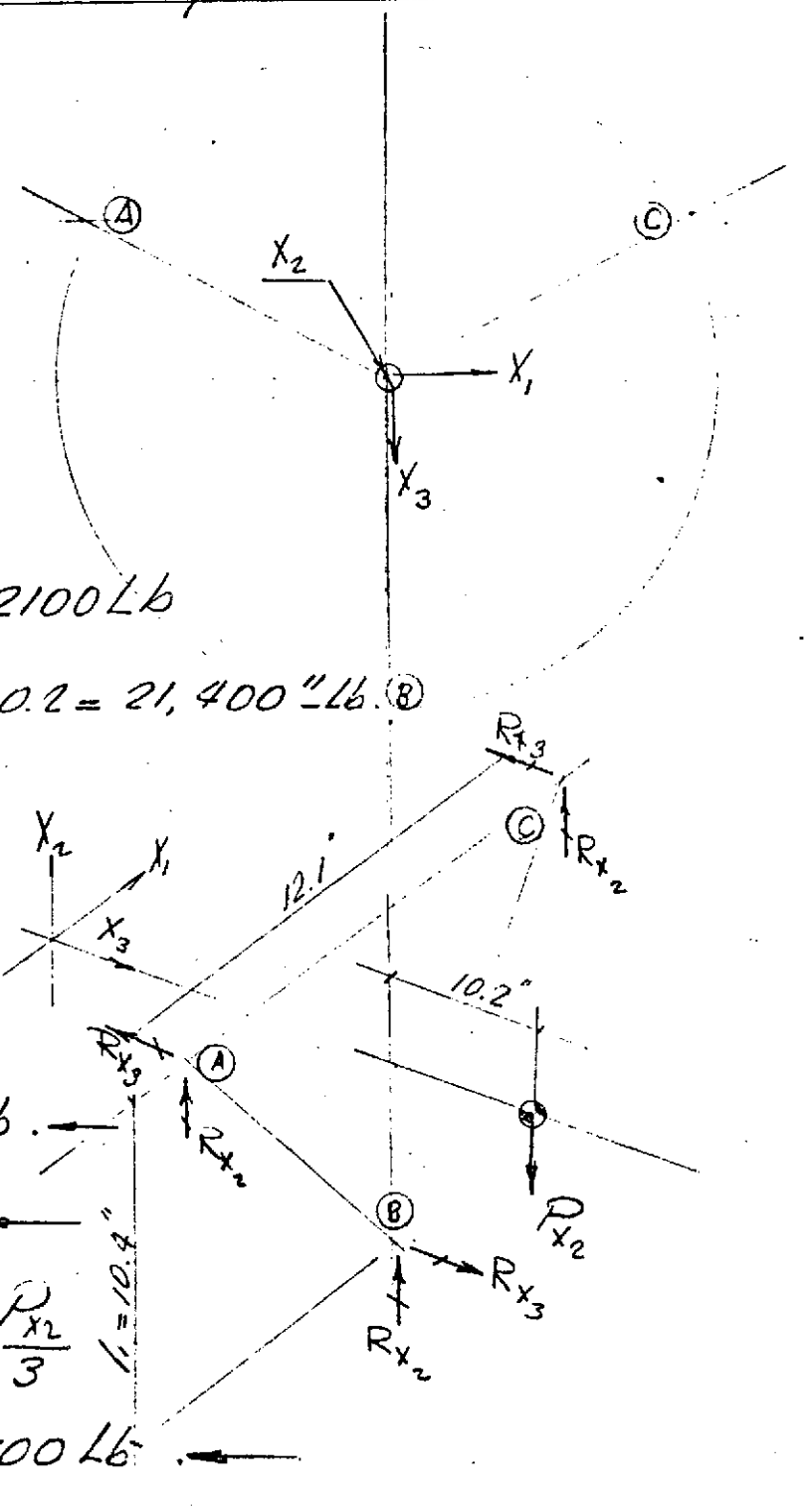

Cond 1.

Axial 30 G's ± X_2

$W = 70$ Lb

$P = G \times W$

$P_{X_2} = 30 \times 70 = 2100$ Lb

$M_{X_1-X_1} = 2100 \times 10.2 = 21,400$ "Lb. (B)

$R^{(A)}_{X_3} = R^{(C)}_{X_3} = \frac{1}{2} M/h$

$R^{(A)}_{X_3} = \frac{1}{2} \frac{21,400}{10.4}$

$R^{(A)}_{X_3} = R^{(C)}_{X_3} = 514$ Lb. ←

$R^{(B)}_{X_3} = 1028$ Lb. ←

$R^{(A)}_{X_2} = R^{(C)}_{X_2} = R^{(B)}_{X_2} = \frac{P_{X_2}}{3}$

$R^{(A)}_{X_2} = \frac{2100}{3} = 700$ Lb ←

ORIGINAL PAGE IS
OF POOR QUALITY

RTG / Mounting & Interface Loads (Cont'd)

Cond II.

Tangential ±20 g's ± X_1

$W = 70$ Lb.

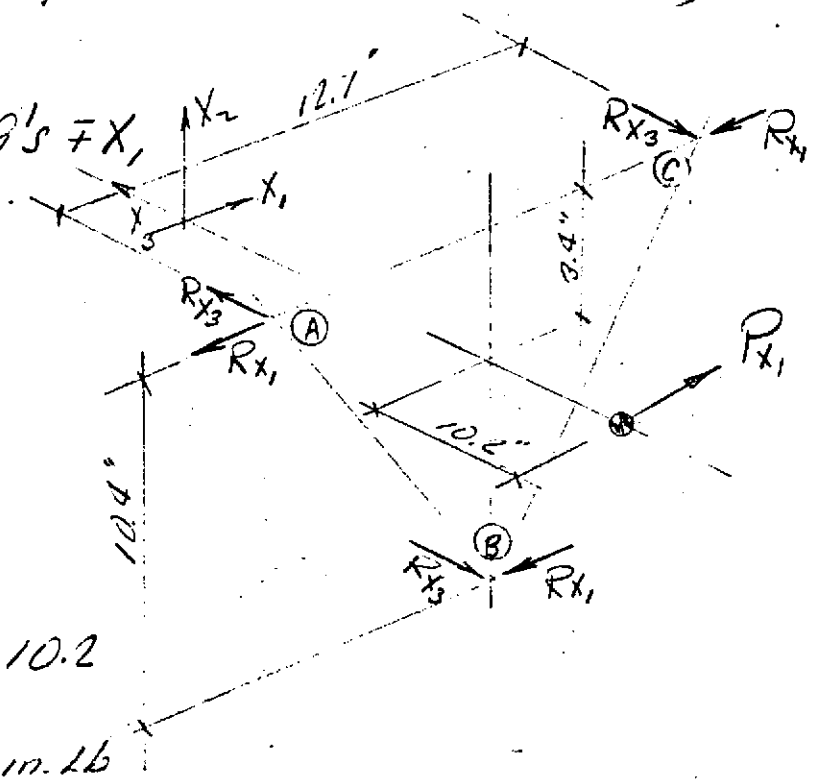

$P_{X_1} = g \times W$

$P_{X_1} = 20 \times 70$

$P_{X_1} = 1400$ Lb

$M_{X_2-X_2} = 1400 \times 10.2$

$M_{X_2-X_2} = 14{,}300$ in. Lb

$R_{X_1}^{(A)} = R_{X_1}^{(C)} = R_{X_1}^{(B)} = P_{X_1}/3 = 1400/3 = 465$ Lb. ←

$R_{X_3}^{(A)} = -R_{X_3}^{(C)} = 14300/12.7 = 1130$ Lb. ←

$R_{X_3}^{(B)} \cong 0$

Cond III.

Radial ± 20 g's in ± direction.

$P_{X_3} = g \times W = 20 \times 70 = 1400$ Lb

$R_{X_1}^{(A)} = R_{X_1}^{(C)} = R_{X_1}^{(B)} = 0$

$R_{X_3}^{(A)} = R_{X_3}^{(C)} = R_{X_3}^{(B)} = P_{X_3}/3 = 465$ Lb. ←

RTG Mounting plate / Spacecraft interface loads

Cond 1.

Load in $\pm X_2$ direction

$W_{RTG} \cong 70$ Lb $W_{IE} \cong 7$ Lb $\Sigma W = 77$ Lb

Axial 30 G's Vibration response. (Ref Ref. 1)

Loads @ Mounting plate

$$P_{X_2} = 30 \times 77 = 2310 \text{ Lb.}$$

$$M_{X_1-X_1} = 30 \times 77 \times 15 = 34600 \text{ in-Lb.}$$

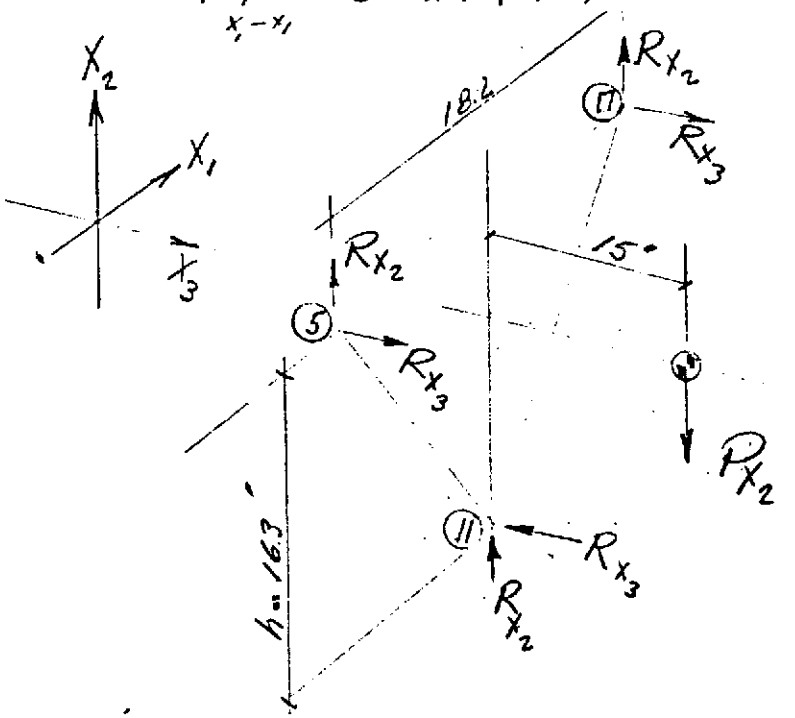

$$R_{X_2}^{(5)} = R_{X_2}^{(11)} \cong R_{X_2}^{(17)} = \frac{P_{X_2}}{3} = \frac{2310}{3} = 770 \text{ Lb}$$

$$R_{X_3}^{(5)} = R_{X_3}^{(17)} = \frac{1}{2}\frac{M_{X-X_1}}{16.3} = \frac{1}{2}\frac{34600}{16.3} = 1060 \text{ Lb.}$$

$$R_{X_3}^{(11)} = 2120 \text{ Lbs.}$$

RTG Mount #1 (Con't)

Cond 2.

Load in ∓ X_1 direction

Tangential 20 G's Vibration response.

Loads @ Mount #1.

$P_{X_1} = 20 \times 77 = 1540$ Lb.

$M = 1540 \times 15 = 23,100$ in-Lb

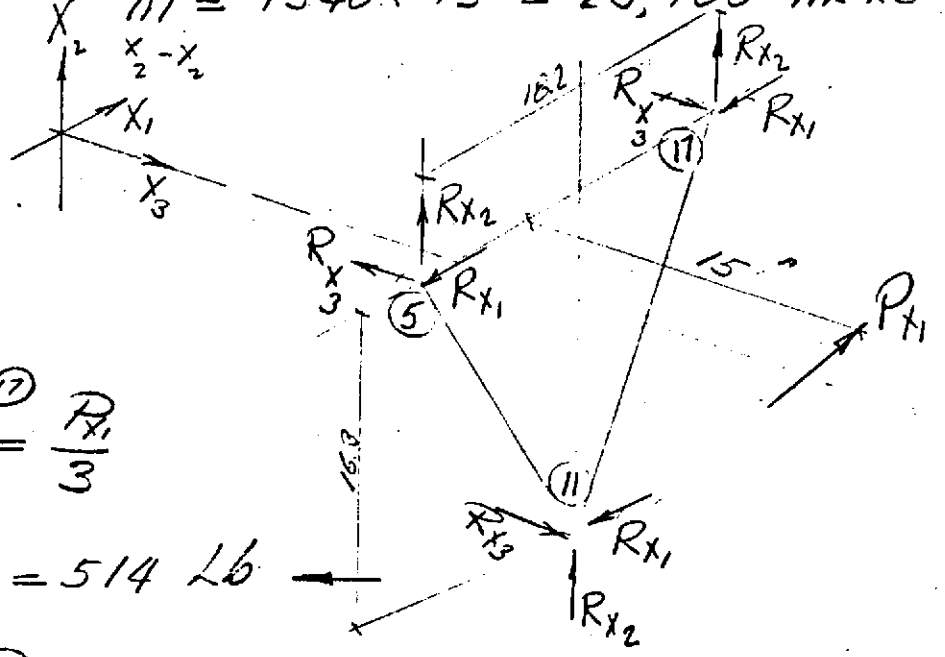

$R_{X_1}^{(5)} = R_{X_1}^{(11)} = R_{X_1}^{(17)} = \frac{P_{X_1}}{3}$

$R_{X_1}^{(5)} = \frac{1540}{3} = 514$ Lb ←

$R_{X_3}^{(5)} = -R_{X_3}^{(17)} = \frac{M_{X_2-X_2}}{h} = \frac{23,100}{18.2} = 1270$ Lb ←

Cond 3

Load in ∓ X_3 direction

Radial 20 g's Vibration response

$P_{X_3} = 1540$ Lb.

$R_{X_3}^{(5)} = R_{X_3}^{(11)} = R_{X_3}^{(17)} = \frac{1540}{3} = 514$ Lb ←

RTG Mounting Pt Lug analysis

Load Cond 1. (Ref. table 1. pp 9.)

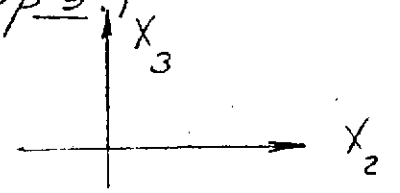

P_{X_3} = 1028 Lb. u/H.

P_{X_2} = 700 Lb u/t

Matl

7079-T652

F_{tu} = 69 KSI

F_{tu} = 53 KSI

$F_{s.u}$ = 41 KSI

F_{brg} = 59 KSI

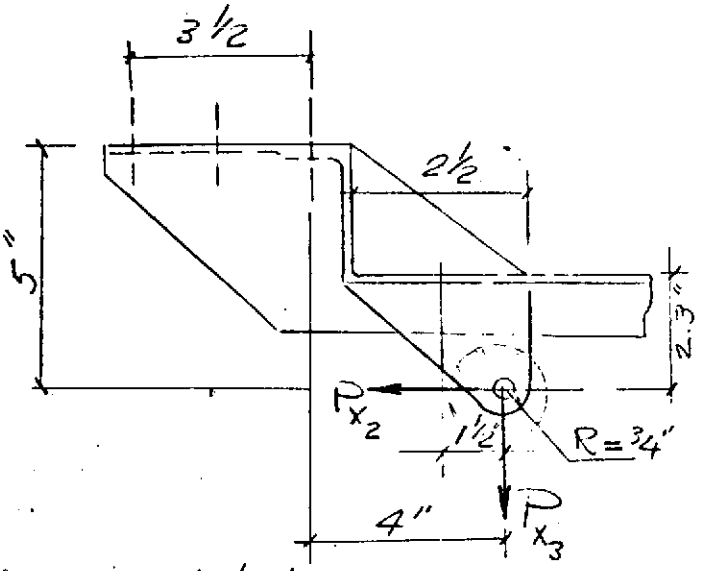

Assume RTG/Lug interface insulated for 390° F temp. and reduction in material strength:

F'_{tu} = .85-80(F_{tu})

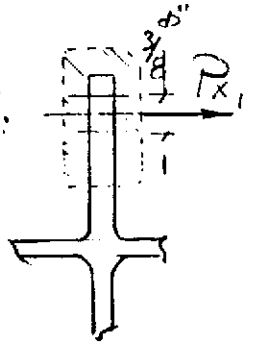

$P = \sqrt{(1028)^2 + (700)^2}$

P = 1240 Lb. ←

Shear out

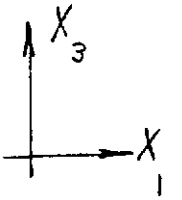

$f_s = \frac{P}{2at}$ $\quad a = \sqrt{R^2 - .1033D^2} - .3330$

$f_s = \frac{1240}{2 \times .58 \times .25}$ = 4280 PSI $\quad F_{s.u} = .80 \times 41 \times 10^3 = 32800$ psi

MS IS HIGH ←

RTG Mounting & Lug analysis (Con't)

Bearing.

$P = 1240$ lb

$$f_{brg} = \frac{P}{t\,D} = \frac{1240}{(.25)(.375)} = 13{,}200 \text{ PSI}$$

$F_{brg} = .80\,(59000) = 4720$ PSI

M.S IS HIGH ←

Tension

$P = 1240$ Lb

$$f_t = \frac{P}{.9\,A_{net}} \cong \frac{1240}{.9 \times (1.5 - .375)(.25)} = 12{,}200 \text{ PSI}$$

$F_t = .80 \times 69000 = 55200$ PSI

M.S IS NOT CRITICAL ←

Cond II. (Ref. Table 1.___.)

Load in X, direction

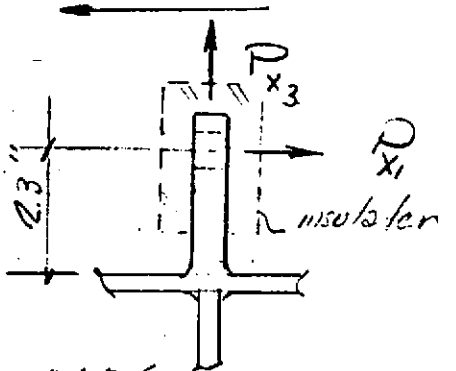

$P_{X_1} = 465$ Lb. $P_X = 1130$ Lb.

$$f_t = \frac{P}{A} + \frac{Mc}{I} = \frac{1130}{(2.5)(.25)} + \frac{465(2.3) \times 6.0}{(2.5)(.25)^2}$$

$f_t = 1810 + 41{,}000 = 42810$ PSI ←

$F_{bu} = .80\,(69{,}000) = 55{,}000$ PSI

M.S $\cong$ 22% ←

RTG Mounting Pt Stress analysis

Cond 1.

The results of computer model analyses indicated that the critically loaded element is the member 10 between joint 8 & 9.

No reduction in material mechanical properties was assumed in these regions

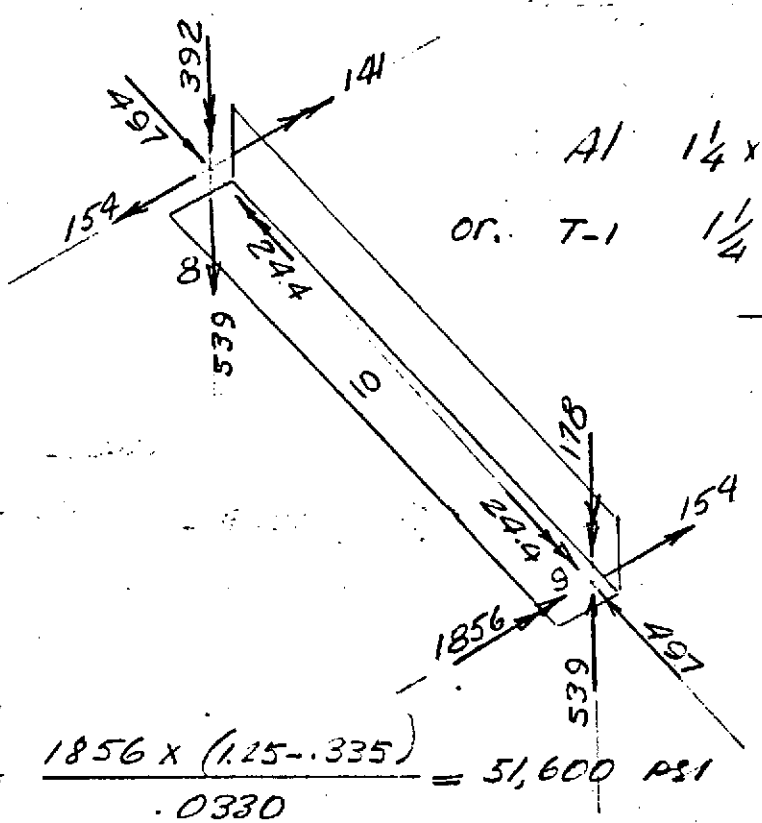

Al $1\frac{1}{4} \times 1\frac{1}{4} \times \frac{1}{8}$

or. T-1 $1\frac{1}{4} \times \frac{1}{4} - .093$

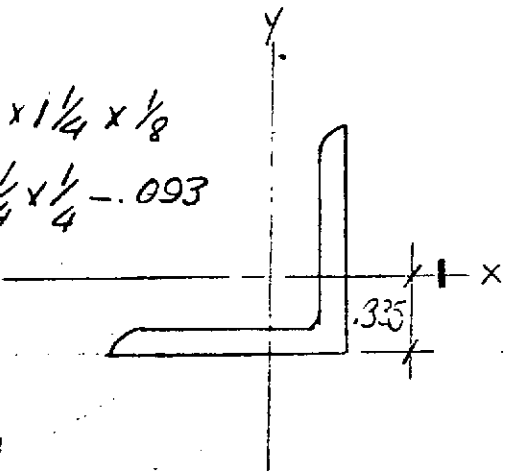

$A = .230 \square''$

$I = .0330\ in^4$

$y-y,\ x-x$

$\rho = .379$

$\frac{b}{t} = \frac{1.15}{.093} = 13.5$

$f_b^{x-x} = \frac{1856 \times (1.25 - .335)}{.0330} = 51,600$ PSI

$f_b^{y-y} = \frac{178 \times .335}{.0330} = 1800$ PSI

$f_a^b = \frac{497}{.230} = 2160$ PSI

$\Sigma f = \underline{58,560}$ PSI

$\sigma_{xy} = \frac{T}{\alpha b t^2} = \frac{24.4}{.333 \times 2.5 \times .093^2} = \underline{3380}$ PSI

$M.S \cong \frac{1}{\sqrt{\left(\frac{58,560}{67,000}\right)^2 + \left(\frac{3380}{41,000}\right)^2}} - 1 \cong 12\%$ ←

RTG Mounting Pt stress analysis (Cont'd)

Cond II.

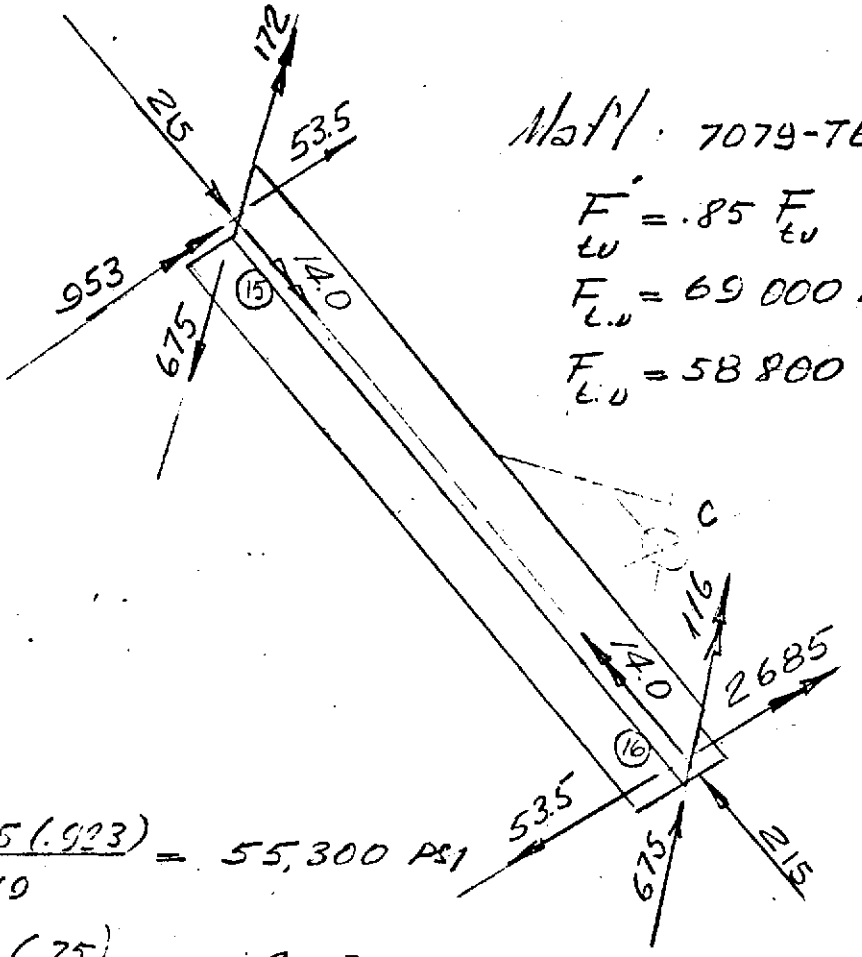

Matl: 7079-T652

$F'_{tu} = .85\ F_{tu}$

$F_{t.u} = 69\,000$ PSI

$F_{t.u} = 58\,800$ PSI

$$f_{b_x} = \frac{2685(.923)}{.0449} = 55{,}300 \text{ PSI}$$

$$f_{b_y} = \frac{116(.75)}{.0319} = \frac{2730}{58030}$$

$$f_c = \frac{215}{.329} = \frac{655}{58{,}685} \text{ PSI}$$

$$J_{xy} = \frac{3M_t}{bt^2}$$

$$J_{xy} = \frac{3 \times 14.0}{2.625(.125)^2} = 1012 \text{ PSI}$$

$$M.S. = \frac{1}{\sqrt{\left[\frac{58.6}{(.85)(68.0)}\right]^2 + \left[\frac{10.1}{(.85)(410)}\right]^2}} - 1 = 1\%$$

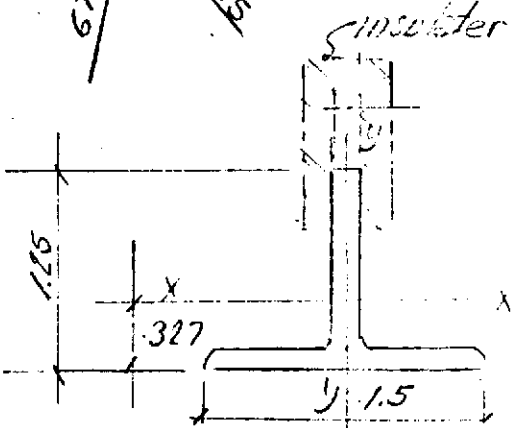

$A = .326\ in^2$

$J = .00163\ in^3$

$I_x = .0449$

$I_y = .0319$

RTG / Mounting R. Interface load

TABLE I.

Int.	A			B			C		
	R_{x_1}	R_{x_2}	R_{x_3}	R_{x_1}	R_{x_2}	R_{x_3}	R_{x_1}	R_{x_2}	R_{x_3}
Cond I. (30 g's in X_2 direction)	0	700	514	0	700	-1028	0	700	514
Cond II. (20 g's in X_1 direction)	465	0	1130	465	0	0	465	0	-1130
Cond III. (20 g's in X_3 direction)	0	0	465	0	0	465	0	0	465

Wt = 70 Lbs

RTG Mounting R / Spacecraft int. Loads.

TABLE II.

Int.	5			11			17		
	R_{x_1}	R_{x_2}	R_{x_3}	R_{x_1}	R_{x_2}	R_{x_3}	R_{x_1}	R_{x_2}	R_{x_3}
Cond I. (30 g's in X_2 direction)	0	770	1060	0	770	-2120	0	770	1060
Cond II. (20 g's in X_1 direction)	514	0	1270	514	0	0	514	0	-1270
Cond III. (20 g's in X_3 direction)	0	0	514	0	0	514	0	0	514

Wt = 77 Lbs.

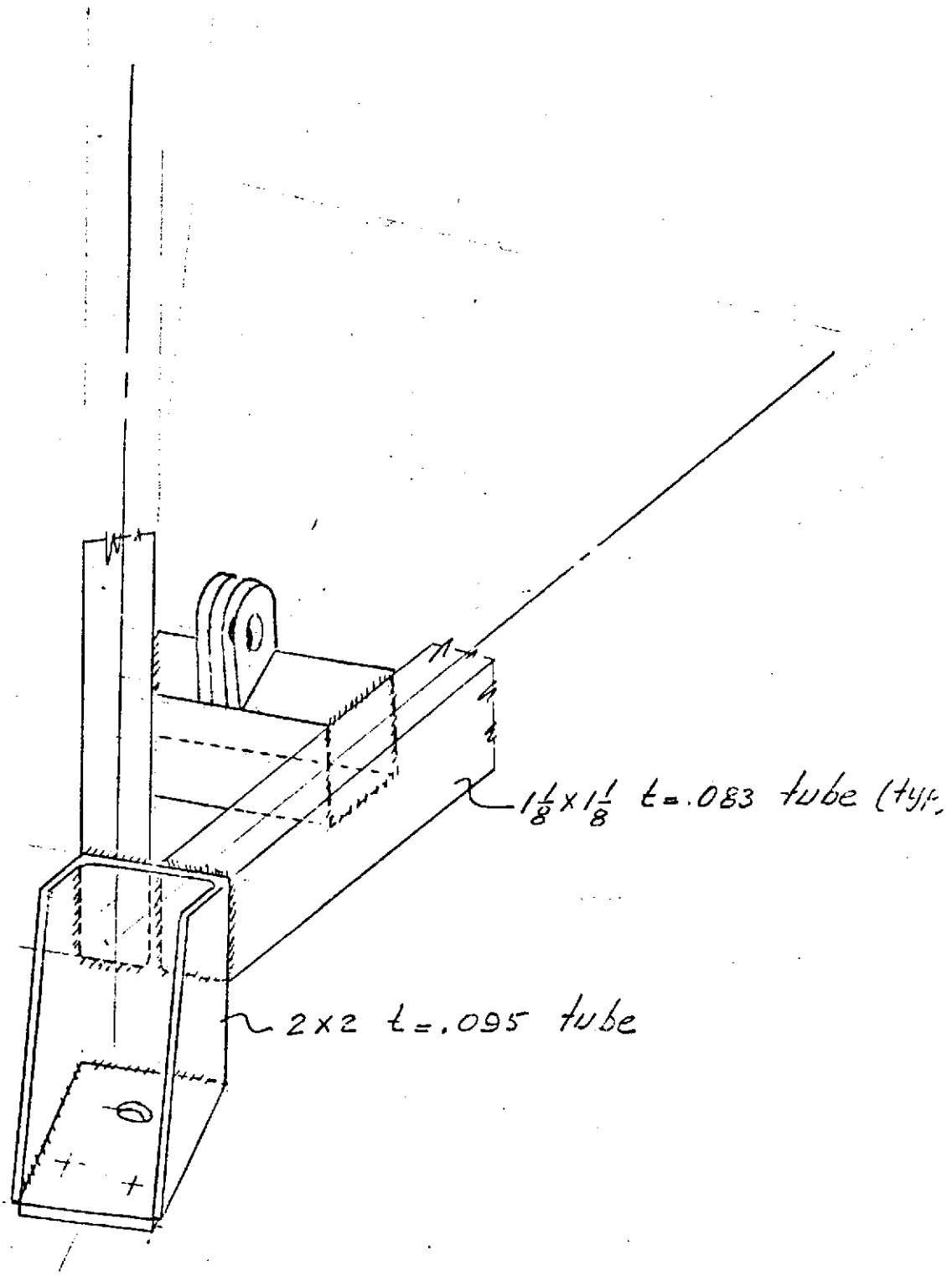

Propellant Tank Support Cone

Loading Cond.

I. 30 g's in $\mp X_2$

II. 44.6 g's in $\mp X_1$

III. 44.6 g's in $\mp X_3$

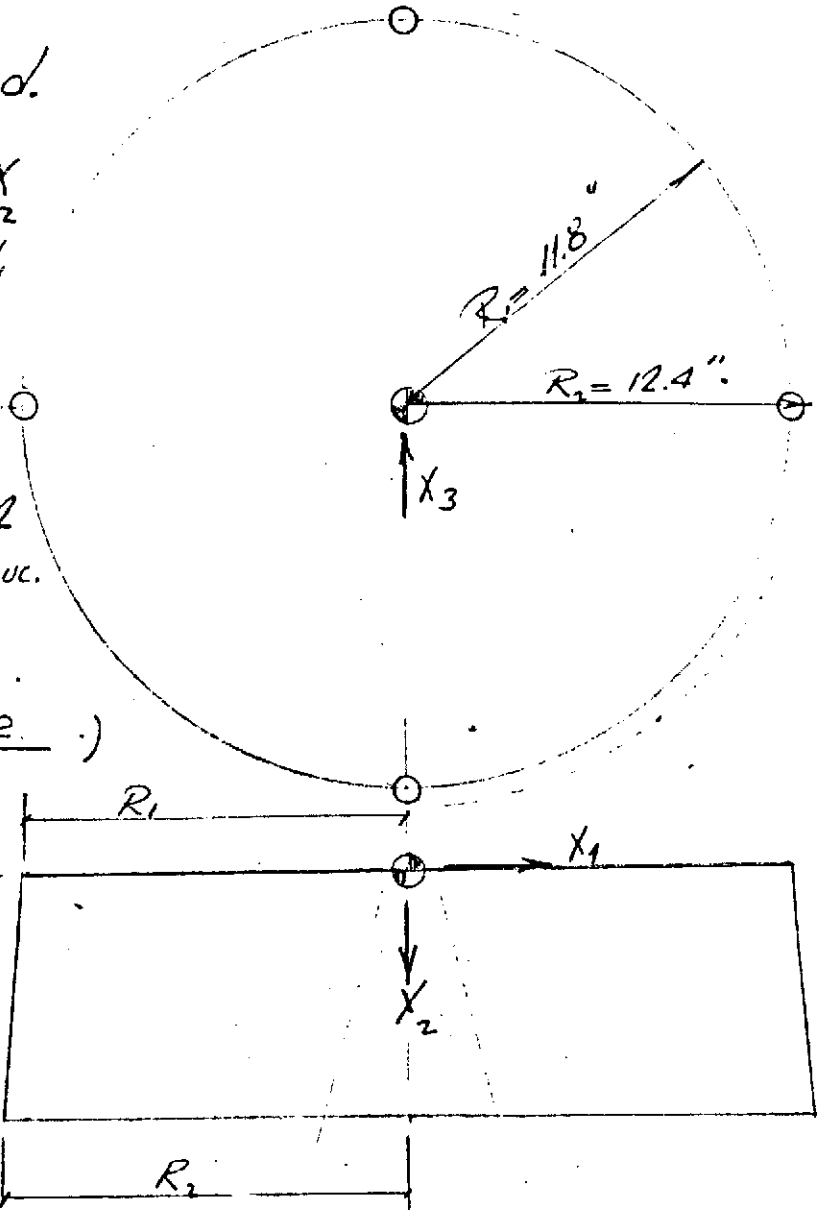

$W = 116.9 + 17.2$

prop. struc.

$W_{tot.} = 134.1$ Lb. (Ref 2.)

Cond i

Load in $\pm X_2$ direction 30 g's

$P_{X_2} = 30(134.1) = 4040$ Lb

Propellant Support Cone (Con't)

Cond II & III

Load 44.6 g's in X_1 & X_3 direction respectively

$$P_{X_1} = 44.6 \times 134.1 = 6000 \text{ Lb.}$$

$$P_{X_3} = 44.6 \times 134.1 = 6000 \text{ Lb.}$$

$P_{X_2} = 4040$ Lb./per condi.

The load at four attachment points of the propellant tank

$$P_{X_2}/4 = 1010 \text{ Lbs. ult.}$$

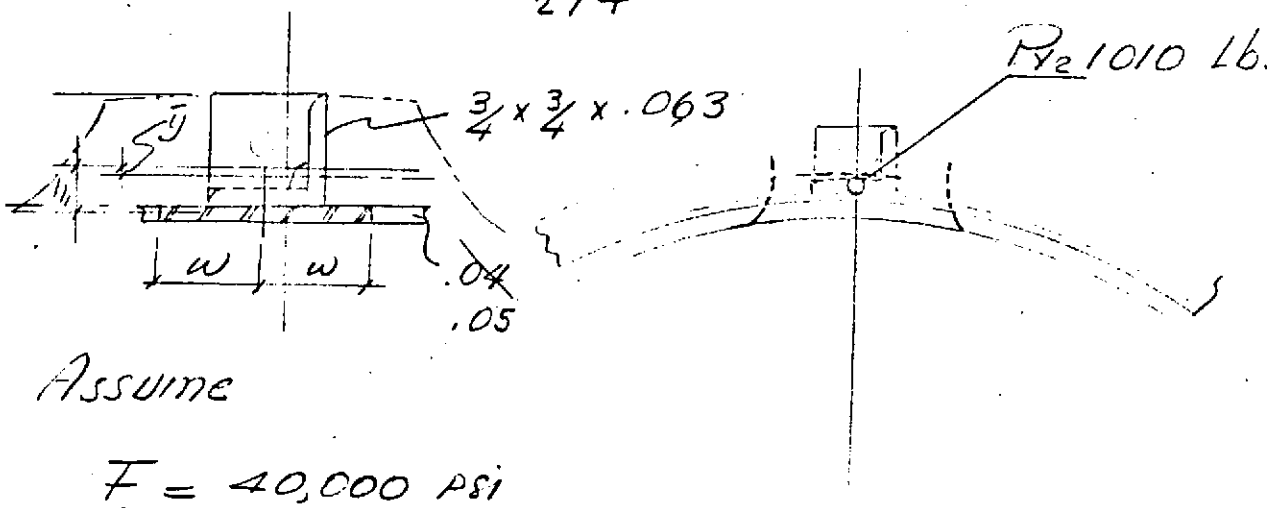

Assume

$$F_{cy} = 40{,}000 \text{ psi}$$

$$w \cong .85\, t \sqrt{E/F_c} = .85(.04)\sqrt{\frac{10 \times 10^6}{40 \times 10^3}} = .535"$$

$$A_{SKIN} = 2 \times .535 \times .04 = .0428 \text{ in}^2$$

$$\bar{y} = \frac{.0428 \times .208}{.0908 + .0428} = .0675$$

Propellant tank Support Cone (Con't)

$$I_{combine} = I_L + A_{SKIN}(h_1)^2 - \Sigma A(\bar{y})^2 \qquad \Sigma A = .0908 + .0428$$

$$= .0047 + .0428(.208) - .1336(.0675)^2$$

$$= .00595\ in^4 \qquad \Sigma A = .1336\ in^2$$

$$\rho = \sqrt{I/A} = \sqrt{\frac{.00595}{.1336}} = .211$$

$$\ell/\rho = 7.83/.211 = 37$$

$$F_c = F_{cc}\left[1 - \frac{F_{cc}(\ell/\rho)^2}{4\pi^2 E}\right]$$

$$F_c = 40\times10^3\left[1 - \frac{40\times10^3(37)^2}{4\times3.141^2\times10\times10^6}\right]$$

$$F_c = 33{,}600\ psi$$

$$P_{allw.} = 33{,}600\times.1336 = 4500\ Lb.$$

$$P = 1010\ Lb.$$

MS IS HIGH

Propellant tank Support Cone (con't)

Cond II

Load 44.6 g's in X_3 direction (Ref ____)

$P_{X_3} = 44.6 \times 134.1 = 6000$ Lb.

$q = \frac{P_{X_3}}{I} \Sigma y A_f$

$A_f = .1336\ in^2$

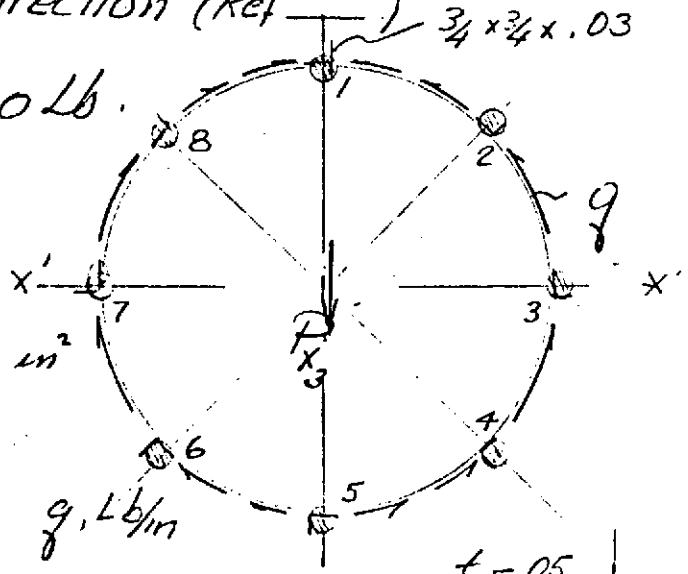

El/m.	y	yAf	$y^2 A_f$	$\Sigma y A_f$	q, Lb/in
1	12	.80	11.5	.80	56.6
2	8.5	1.13	9.7	1.93	137.0
3	~0	0	0	1.93	137.0
4	-8.5	-1.13	9.7	.80	56.6
5	12	-.80	11.5		
			42.4		

$q_{1-2} = \frac{3000}{42.4}(.80) = 56.6$ #/in

$q_{2-3} = \frac{3000}{42.4}(1.93) = 137$ #/in

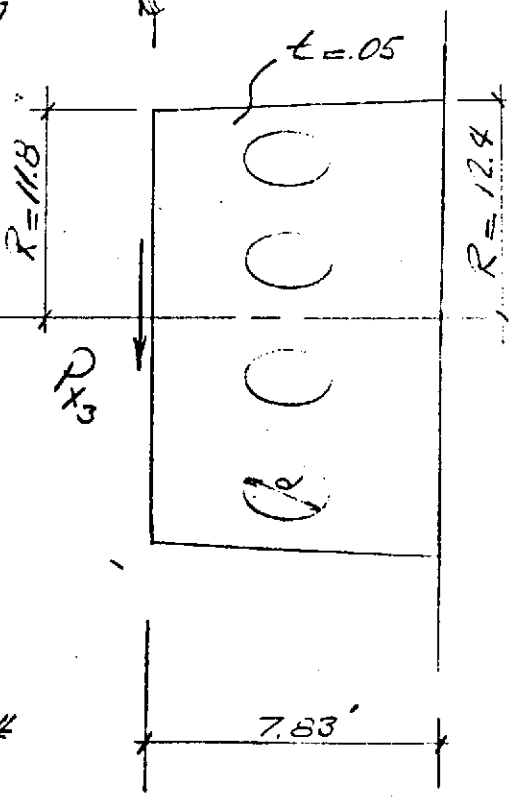

$\Delta V_{2-3} \cong q h_c = 137(8.5) = 1160$ #

$q_{cutout} \cong \frac{1.25 \Delta V}{(h_c - d)} = \frac{1.25 \times 1160}{8.5 - 3.5} = 291$ #/in due to hole cut out in web.

Propellant Tank Support Cone (Con't)

$q = 291$ #/in

critical

$f_s = q/t = 291/.05 = 5840$ PSI

$F_s = K_s E\left(\frac{t}{b}\right)^2$ $\qquad b^2/rt = 7.8^2/(12)(.05) = 101$

$a/b \cong 1.2$

$K_s \cong 15$

$F_s = 15 \times 10 \times 10^6 \left(.05/7.8\right)^2 = 6150$ PSI

$M.S = \dfrac{1}{5840/6150} - 1 = 5\%$

Use 2024-T851 $t = .05$ ~~.04~~

Note: Hole diameter should not exceed ½ of web beam depth.
Load peaking between rivets on web - flange near the hole should be minimized by reducing rivet spacing

5. LOW GAIN ANTENNA SUPPORT

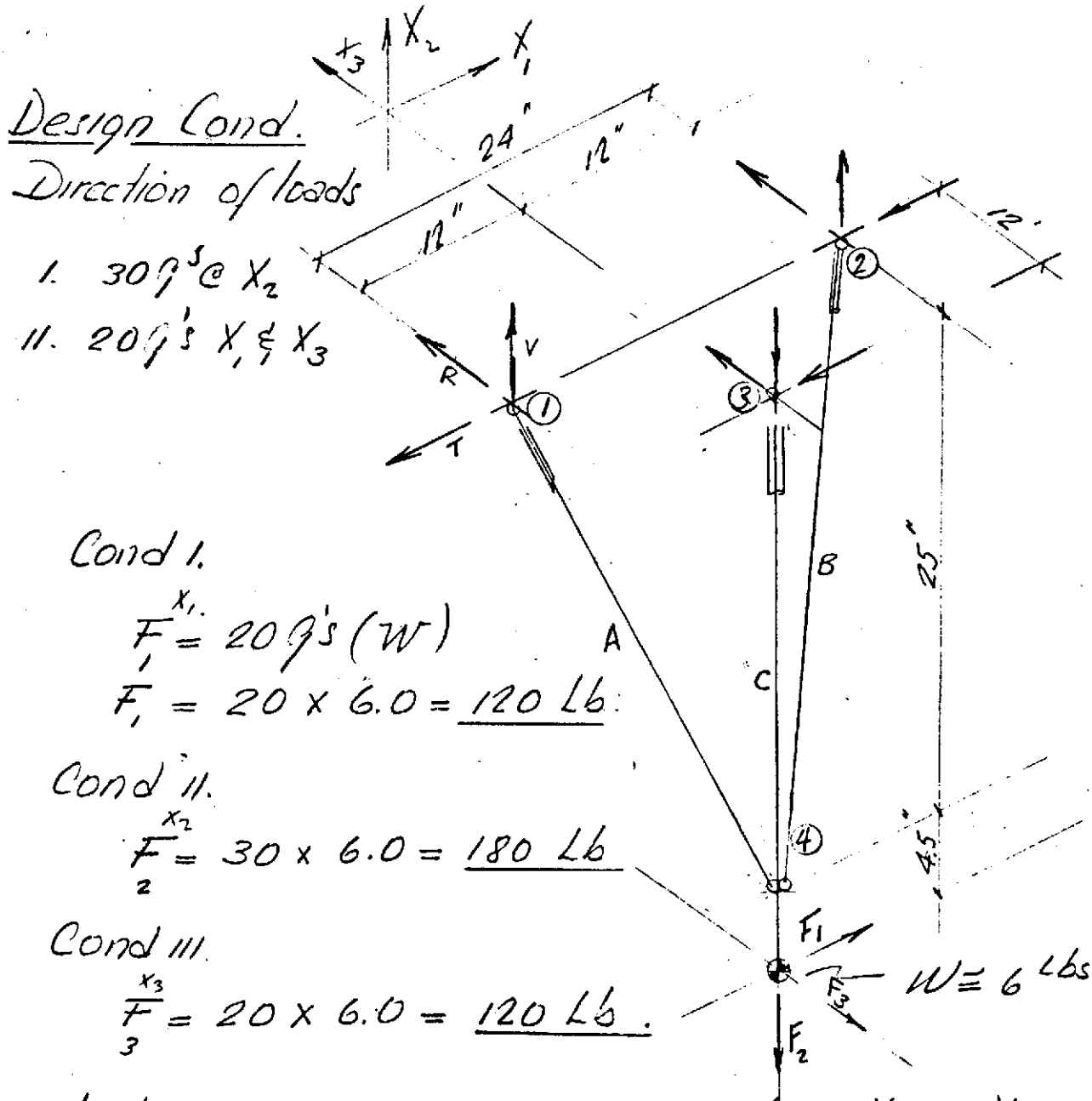

Design Cond.

Direction of loads

I. 30 #'s @ X_2

II. 20 #'s X_1 & X_3

Cond I.

$F_1^{X_1}$ = 20 #'s (W)

F_1 = 20 x 6.0 = 120 Lb.

Cond II.

$F_2^{X_2}$ = 30 x 6.0 = 180 Lb

Cond III.

$F_3^{X_3}$ = 20 x 6.0 = 120 Lb.

Memb.	Jn.	X_2	X_1	X_3	L	X_2/L	X_1/L	X_3/L
A	1-4	25	12	12	30.2	.822	.397	.397
B	2-4	25	-12	12	30.2	.822	-.397	.397
C	3-4	25	0	0	25.0	1.0	0	0

Support/bracing loads

Cond'l. 20g's in ± X_1 direction

Assumed member "A & B" two-force member. Member "C" resists bending but joint 3 is hinged joint (see page 1.)

Loads @ Jt. 4

$$F_{X_1}' = 120 + \frac{120(29.5)}{25} = 134.2 \text{ Lb}$$

$$M_{X_3-X_3}' = 120(4.5) = 540 \text{ IN-Lb}$$

$$\Sigma F_{X_1} = 0$$

$$.397A + .397B = 134.2 \qquad A = B$$

$$2A.397 = 134.2$$

"A" = 170 Lb. ←

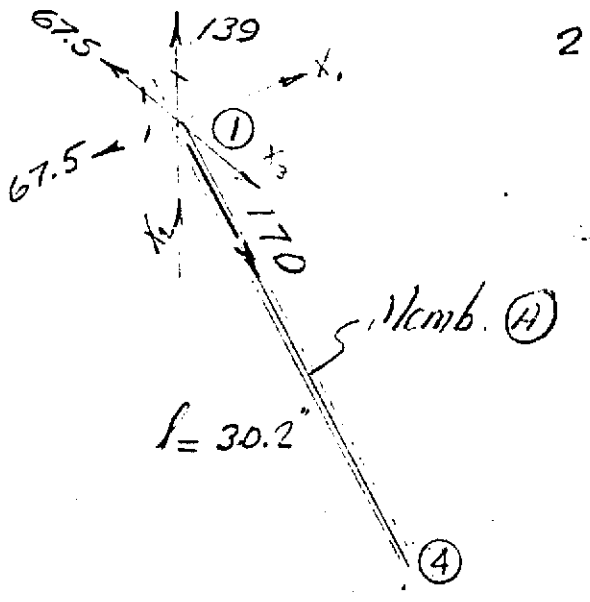

$A_V = .822(170) = 139$ Lb

$A_R = .397(170) \cong 67.5$ Lb

$A_T = .397(170) \cong 67.5$ Lb

"B" = − 170 Lbs

$B_V = -139$ Lb.

$B_R = -67.5$ Lb.

$B_T = -67.5$ Lb.

Support bracing analysis

Member "A" Jt ① - ④

Loading condition 20 g's ⊥ X_3 direction

$P_{ult.} = -170$ Lb. (Ref page 5)

$\ell_{①④} = 30.2$ inch.

Try 2024-T6 $\frac{3}{4}\phi$" $t = .049$"

$A = .1079$

$\rho = .2485$

$I = .0006661$

$D/t = 15.30$ $\gamma = .109\ ^{\#}/_{100}$"

$$f_c = \frac{P}{A} = \frac{170}{.1079} = 1580 \text{ PSI}$$

$$\ell/\rho = 30.2/.2485 = 121 \qquad K = 1.0$$

$$F_c = \frac{\pi^2 E}{\left(\frac{K\ell}{\rho}\right)^2} = \frac{3.141^2 \times 10.3 \times 10^6}{(121)^2} = 6943 \text{ PSI}$$

M.S IS HIGH

Use 2024-T6 $\frac{3}{4}\phi$" $t = .049$ @ 30.2" $\gamma = .36\ ^{\#}$s

Member "B" Jt ④ - ②

Use same tube because of similar loading.

Support bracing Analysis (con't)

Member "c" Joint ③-④

Loading Condition 20 g's in X_3 direction

$F_3 = 120$ Lb

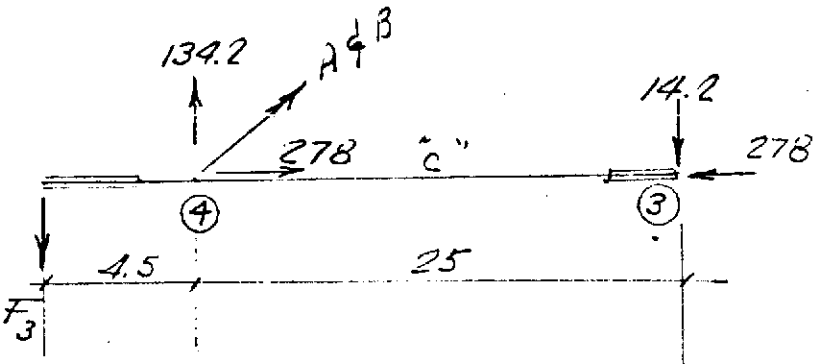

@④

$M = 120(4.5) = 540$ in-Lb

$x_1 - x_1$

$P = 278$ Lb

Try 1 ϕ" $t = .065$" 2024-T6

$A = .1909$ in²

$\rho = .3314$

$I = .02097$ in⁴

$f_c = \frac{P}{A} = \frac{278}{.1909} = 1460$ psi $\quad \frac{\ell}{\rho} = \frac{25}{.3314} = 76$

$f_b = \frac{Mc}{I} = \frac{540 \times .5}{.02097} = 12920$ psi

$F_c = 17500$

$M.S = \frac{1}{\left(\frac{1460}{17500}\right) + \left(\frac{12920}{45,000}\right)} - 1 =$ HIGH

Diagonal Bracing loads

Condi.

Load in ± X_1 direction 20g's

Memb. A = 170 Lb. (ult.)

① - ④

Components $\begin{cases} T_{X_1} = 67.5 \text{ Lb} \\ V_{X_2} = 139.0 \text{ "} \\ R_{X_3} = 67.5 \text{ "} \end{cases}$

Memb B = −170 Lbs

② - ④

Components $\begin{cases} T_{X} = 67.5 \text{ Lb} \\ V_{X_2} = -139.0 \text{ "} \\ R_{X_3} = -67.5 \text{ "} \end{cases}$

Memb C = 0

$M_{X_3 - X_3} = 540$ IN-Lb

$V_{X_1} = 14.2$ Lb.

Cond ii.

Load in ± X_2 direction 30 g's

Memb C = ± 180 Lb (Ult)

" A & B = 0

Diagonal Bracing loads Con't

Cond III.

Load III $\pm X_3$ direction

Memb A = 170 Lb (Ult.)

① - ④ Comp. $\begin{cases} T_{X_1} = \mp 67.5 \text{ Lb} \\ V_{X_2} = \mp 139.0 \text{ "} \\ R_{X_3} = \mp 67.5 \text{ "} \end{cases}$

Memb B = 170 Lb

① - ④ Comp $\begin{cases} T_{X_1} = \mp 67.5 \text{ Lb} \\ V_{X_2} = \mp 139.0 \text{ "} \\ R_{X_3} = \mp 67.5 \text{ "} \end{cases}$

Memb C = 278 Lb.

③ - ④

$T_{X_1} = 0$

$V_{X_2} = 278 \text{ Lb}$

$R_{X_3} = 14.2 \text{ Lb}$

$M_{X_1 - X_1} = 540 \text{ IN-Lb.}$

6. SPACECRAFT PROBE ADAPTER (LOCAL PROBE LOAD CONCENTRATIONS)

Loading Condition

Cond I.

Loading $\pm X_1$ & X_3 direction 6.8 g's

Cond II.

Loading $\pm X_2$ direction 18.3 g's

$W_{probe} = 250$ Lb.

$P_{X_2} = 250 \times 18.3 = 4570$ Lb. ult.

$P_{X_2}/3 = 4570/3 = 1523$ Lb. ult.

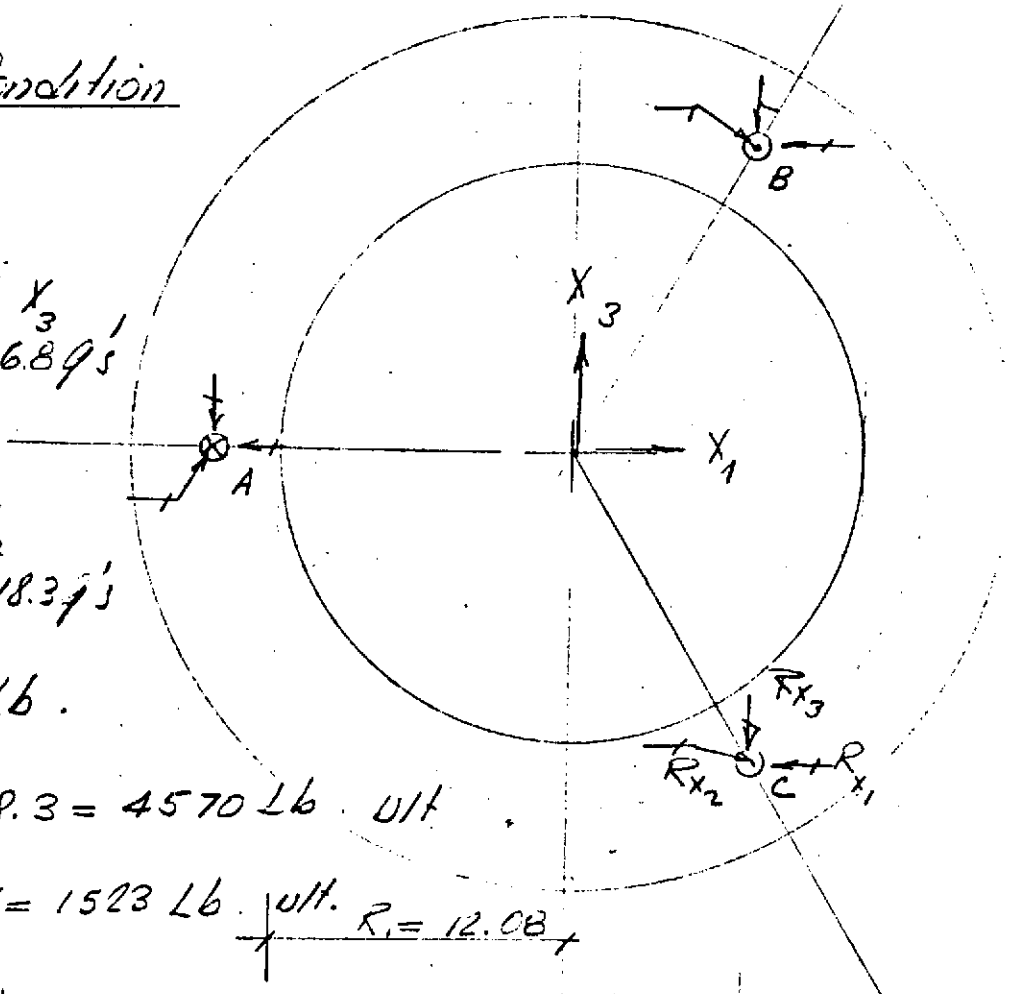

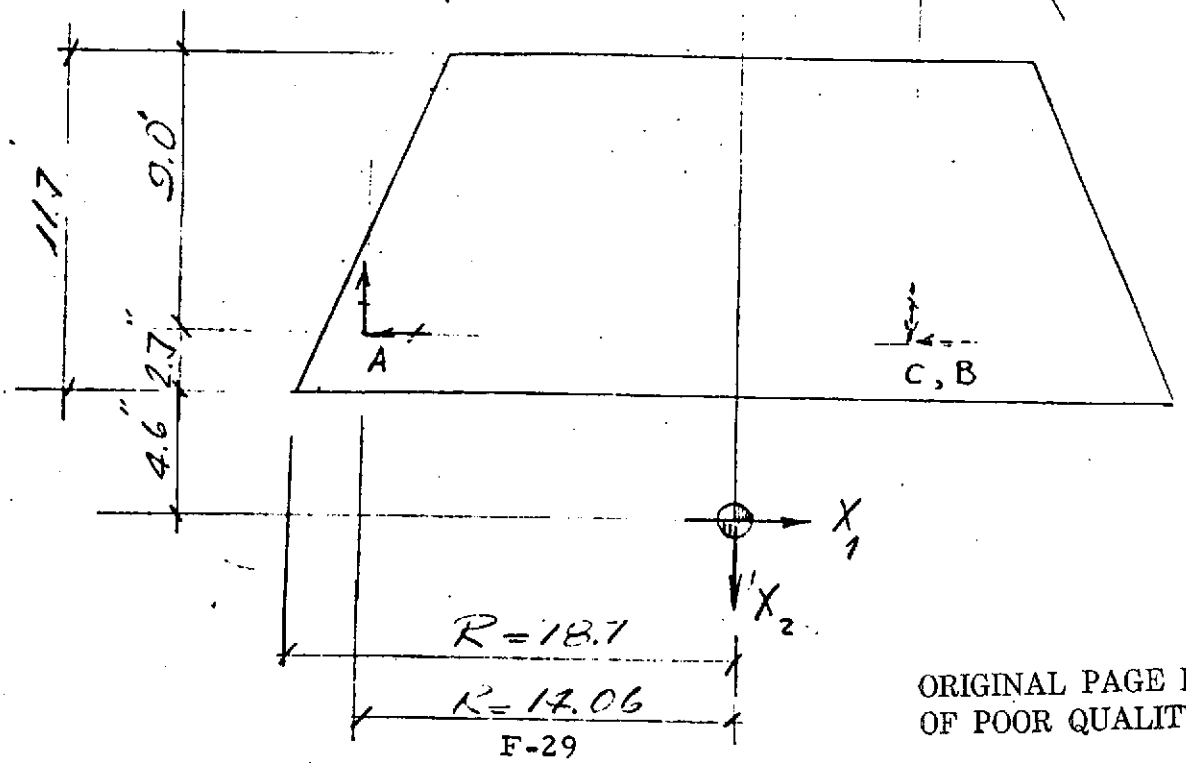

ORIGINAL PAGE IS OF POOR QUALITY

Probe/Cone attachment #2.

Cond II.

$P_{x_2} = 1523$ Lb (ult.)

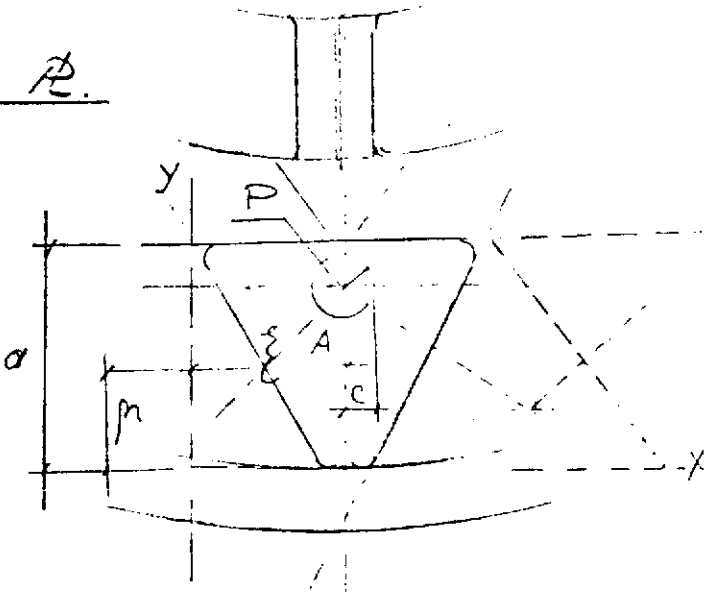

$$M_x = \frac{(1+\nu)P}{4\pi}\left(\log \frac{a\sqrt{3}}{\pi c} - .379\right) + \frac{(1-\nu)P}{8\pi}$$

$t = .25"$

$c = .75$

$a = 5.0"$

$\nu = .3$

$$M_x = \frac{(1+.3)\,1{,}523}{4(3.141)}\left(\log \frac{5\sqrt{3}}{3.141(.75)} - .379\right) + \frac{(1-.3)1523}{8(3.141)}$$

$M_x = 632$ IN-Lb/in

$$f_b = \frac{6 \times 632}{1 \times (.25)^2} = 60600 \text{ psi ult.}$$

Use 7075-T6 Al

$F_{t.u} = 77{,}000$ psi

$F_{t_y} = 66{,}000$ psi

$$M.S = \frac{1}{\frac{60.6}{77.0}} - 1 = +22\ \%$$

Probe/Cone Attachment #2

Cond II.

$P_{X_2} = 1523$ Lb

$P_{II} = 765$ Lb

$P_V = 1320$ Lb

$q_{II} = \frac{765}{10} = 76.5$ #/"

$q_V = \frac{1320}{10} = 132.0$ #/"

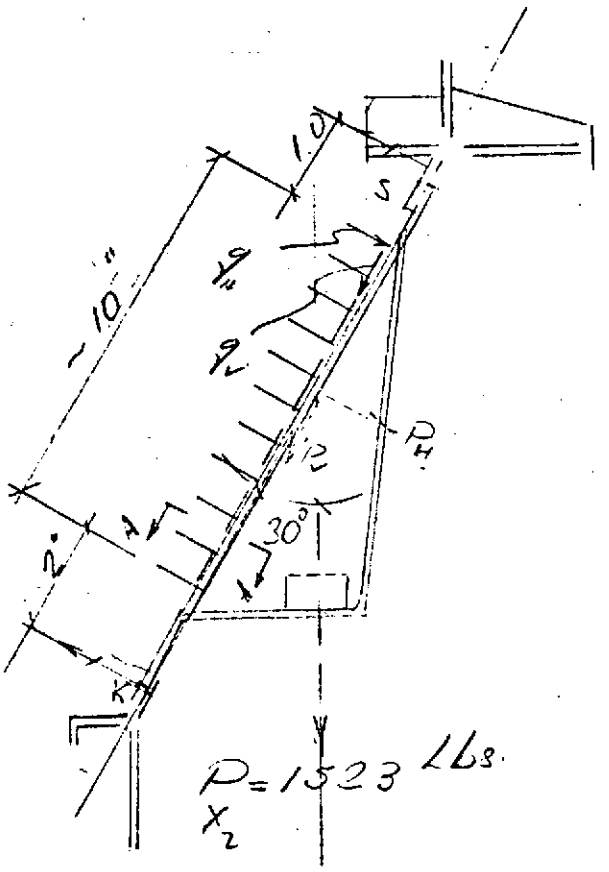

$P_{X_2} = 1523$ Lbs.

$BM \simeq \frac{wl^2}{8}$

$BM = \frac{76.5 \times 10^2}{8} = 956$ in-lb

$BM/side = \frac{1}{2} 956 = 478$ in-lb.

$M_{DESIGN} = 1.2 \times 478 = 575$ in-lb

$f_b = \frac{575 \times .535}{.0063}$

$f_b = 49000$ psi

Use 7075-T73 Al A.

$F_{t.u} = 67,000$

M.S $= \frac{1}{49/67} - 1 = 32\%$

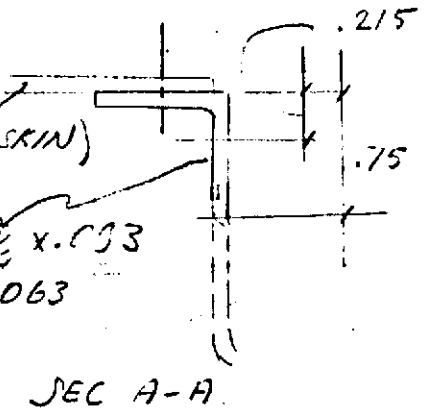

Probe/Cone attachment R

$\gamma_v = 132\ ^{\#}/_{ft}$ @ 1.0 c.c.

Use #6 RH rivet $P_{allow} = 523$ lb.

check inter rivet buckling

$\ell = 10$

c.c $= 1.6' / \ell/\rho = 69.1$ $t = .05$ $\rho = \frac{t}{\sqrt{12}} = \frac{.05}{\sqrt{12}} = .0144$

$\ell/\rho = \frac{1.0}{.0144} = 69.1$

Use 1.0 c c ok ←

check minimum stiffner mom of inertia reqd.

$$\frac{I_s}{t^3} = .321 \left(\frac{\ell}{h_e}\right)^{-5/3}$$

ℓ = spacing = 5

h_e = height = 11

t = cone thickness

$\ell/h_e = 5/11 = .454$

$I_s/h_e t^3 = 1.25$

$I_s = 1.25\,(11)(.05)^3$

$I_s = .002$ in^4 reqd

$I = .0063$ in^4 provided ∴ No general instability expected.

Cond II

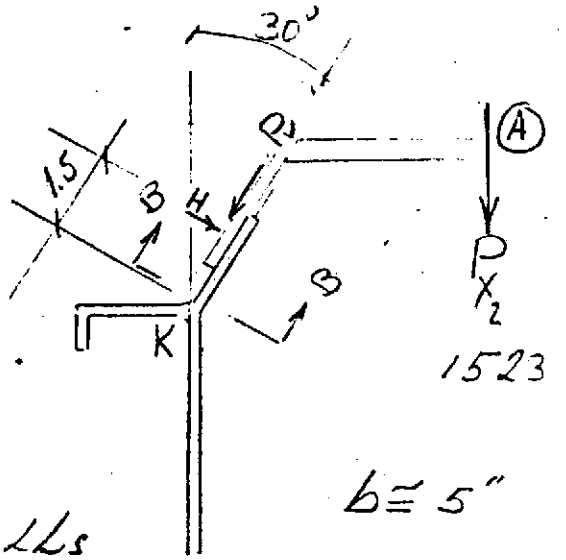

Support ring flange

$P_H = 765$ Lb
$P_V = 1320$ Lb
} Ref pp 3.

$b \cong 5"$

$$H \cong \frac{765\,(5+1)}{13} = 353 \text{ Lbs}$$

$$t_{min}^{B.} = \sqrt{\frac{6M}{6F}} = \sqrt{\frac{6 \times 1.5 \times 353}{5 \times 65{,}000}} = .1"$$

$$t^{C.} = \frac{1320}{5 \times 65000} \cong .004"$$

$t_{min} = .11"$ for Cond II.

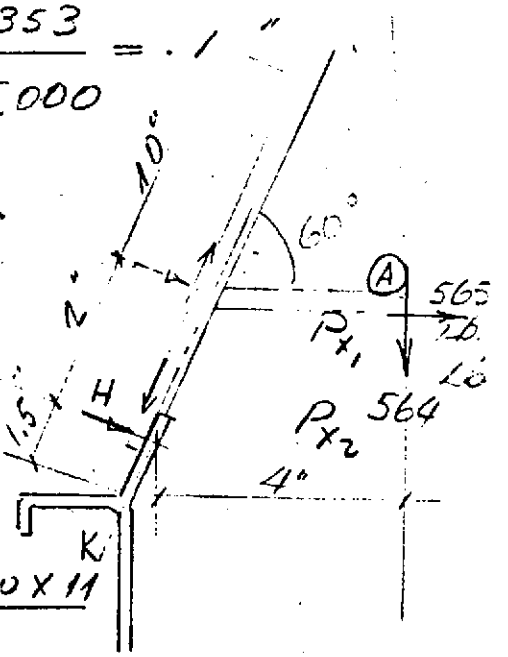

Cond I.

$$H = \frac{564 \sin 30 \times 6 + 565 \cos 30 \times 11}{13}$$

$H = 550$ Lbs.

$$t_{min} = \sqrt{\frac{6M}{b F_b}} = \sqrt{\frac{6 \times 1.5 \times 550}{5 \times 65{,}000}} = .123$$

Use 7075-T652 $t = .13 - .15"$

7. INSTRUMENT BOX

Inst. Box, Platform interface loads

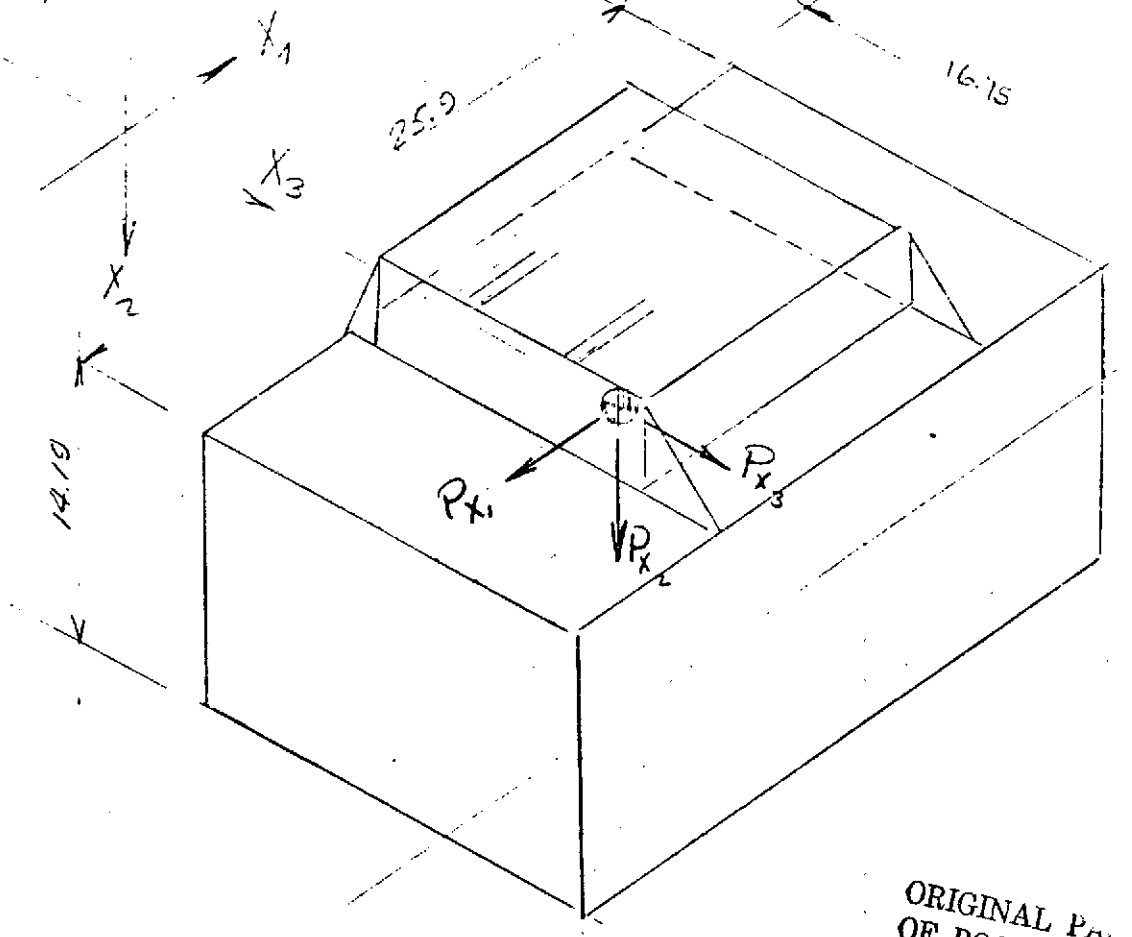

$$W \cong W_{\text{instrument}} + W_{\text{antenna}} + W_{\text{box}}$$

$$W = 20 + 5 + 15 \cong 40 \text{ Lb.}$$

Load in $\pm X_1$ direction

$$F_{X_1} = 40\,(20) = 800 \text{ Lb}$$

Load in $\pm X_2$ direction

$$F_{X_2} = 40\,(30) = 1200 \text{ Lb}$$

Load in $\pm X_3$ direction

$$F_{X_3} = 40\,(20) = 800 \text{ Lb.}$$

Inst. Box / Platform interface loads (cont'd)

Cond 1.

Load in $\pm X_2$ direction

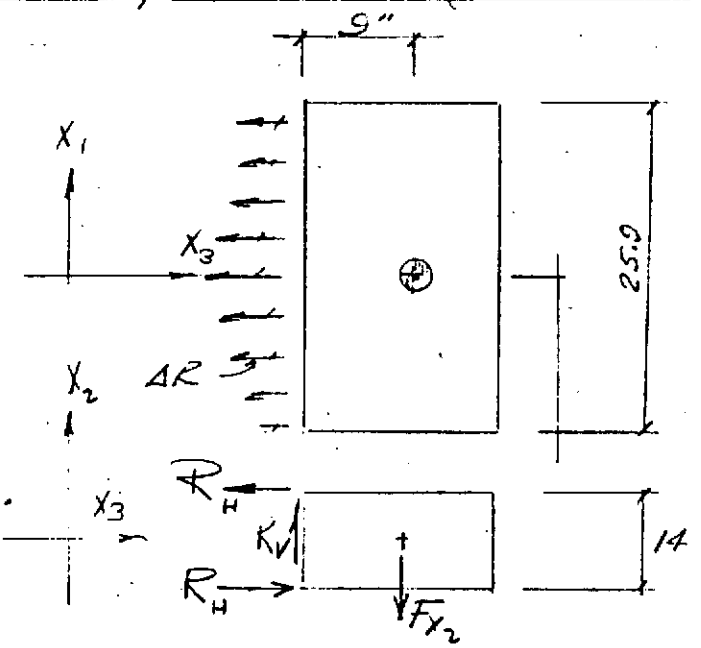

$F_{X_2} = 1200$ Lb

$M_{X_1-X_1} = 1200 \times 9$

$M_{X-Y} = 10,800$ in-Lb.

$$R_H = \frac{M}{11} = 10,800/14 = 770 \text{ Lb}$$

$$R_V = \frac{1}{2} F_{X_2} = 1200/2 = 600 \text{ Lb}$$

Check attachment

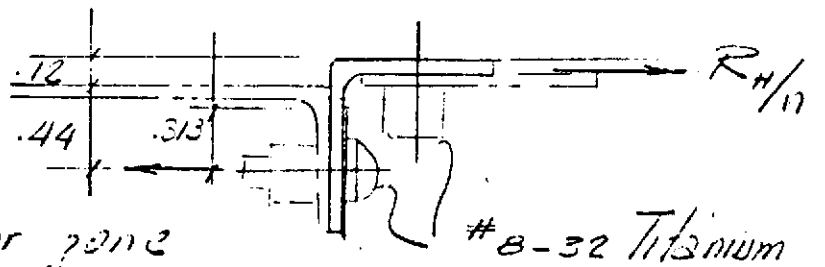

Assume thread in shear zone

$$P_{allw} = .0196/.0211 \times 1922 = 1080 \text{ Lb}$$

$$\Delta R_H = K\left(\frac{R_H}{n}\right) \qquad K \cong 1.4 \text{ Load peaking}$$

$$\Delta R = 1.4\left(\frac{770}{15}\right) = 66.5 \text{ Lb}$$

M.S. IS HIGH

Instrument Box / Platform interface

check attached angle in bending

$\Sigma R_u = 66.5$ Lbs.

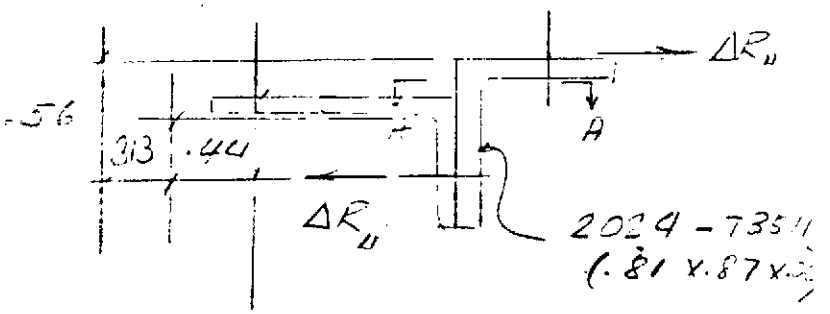

$M_{A-A} = 66.5(.44)$

$M_{A-A} = 29.2$ in-Lb

$f_b = \frac{6M}{bt^2} = \frac{6 \times 29.2}{(2)(.06)^2} = 24{,}300$ psi ult

$f_b = f_b^{ult} / 1.5 = 16{,}200$ psi ←

MS IS HIGH ←

References

I. PIONEER F/G STRESS ANALYSIS
By. T. J. OCKEY dated 18 Nov. 1970
(TRW I.OC. 70.8522.2-157)

II. SATURN URANUS ATMOSPHERIC ENTRY PROBE
MISSION SPACECRAFT SYSTEM DEFINITION STUDY
By. TRW System Group dated June 4, 1973